EMPIRICAL STABILITY CRITERIA FOR HIERARCHICAL MANY-BODY DYNAMICAL SYSTEMS IN CELESTIAL MECHANICS

by

IAN W. WALKER B.Sc.

Thesis
submitted to the
University of Glasgow
for the degree of
Ph.D.

Department of Astronomy,
The University,
Glasgow G12 8QQ.

November 1980

To my wife Linda

"Will the present configuration of the solar system be preserved for some long interval of time? Will the planets eventually fall into the Sun or will some of the planets recede gradually from the Sun so that they no longer belong to the solar system? Will any planet approach another planet and form a binary system revolving around the Sun like the Earth-Moon system or become more eccentric or more inclined to the ecliptic, and break the present configuration of the solar system?..... All these questions are called vaguely as the *stability* in celestial mechanics.

The question has long been an acute problem in celestial mechanics....."

Hagihara (1957)

PREFACE

In this thesis the stability of many-body systems is examined. This is a problem which, although it has been studied by celestial mechanics for over 300 years, still evades general solution. A new approach to the problem is adopted. Instead of seeking a definite "yes or no" answer to the problem we require only that it should be possible in a purely empirical and probabilistic way to predict for how long a time systems will exist before unstable behaviour is manifested i.e. a close approach between bodies occurs (or becomes probable due to orbits crossing over) or one of the bodies escapes the system.

In Chapter 1 a general review of the present status of the problem of the Solar System's stability is given along with brief descriptions of methods by which stability may be investigated. Since Hill's method is used extensively in succeeding chapters of the thesis, Chapter 2 deals with the use of the zero-velocity surfaces of the restricted three-body problem and zero-velocity curves of the planar general three-body problem in studies of stability.

Parameters are sought in Chapter 3 which have a physical significance for the stability of hierarchical dynamical systems, such as the Solar System, triple stellar systems, etc. These ε parameters are a *measure of the disturbance* of the orbits of a hierarchical system by the mutual perturbations of the bodies in the system. The ε parameters are then examined by the use of the zero-velocity curves of the planar general three-body problem to test their applicability to stability considerations (Chapter 4). The analytical stability criterion afforded by the zero-velocity curves is refined in Chapter 5 so that the effect of all the orbital parameters on the Hill stability of coplanar hierarchical three-body systems may be assessed prior to carrying out a numerical investigation.

By using extensive sets of numerical integrations it is demonstrated in Chapter 6 that the ε parameters may be used to predict how stable a three-body system is, in the sense of stating for how long a time systems may be *expected* to continue before instability sets in. The use of the ε parameters as a tool to predict the amplitude of the

variations in semi-major axes and eccentricities of these systems is demonstrated in Chapter 7. The four-body problem is briefly considered in Chapter 8 to show that similar results may be derived for these systems.

The validity of the ε parameters as a true measure of the disturbance, due to perturbation by other bodies in the system, is considered for the planetary case of hierarchical n-body systems in Chapter 9. Also in this chapter a new set of generalised ε parameters are determined which allow consideration of more complex hierarchical systems such as the sextuple Castor system, other multiple stellar systems, hypothetical planets of multiple stellar systems, etc.

Chapter 10 includes a brief review of the work of the thesis and suggests a few interesting lines for future research.

The original work of this thesis is contained in Chapters 3 to 9 and also Appendices A to F. The results of Appendix C have been published in *Celestial Mechanics* . The contents of Chapters 3 and 4 constitute one paper which is in press and is to be published in the same journal. Chapter 5 (along with Appendix A) contains the results of a paper which has been accepted for publication. Of the remaining parts of the thesis Chapter 6, Chapter 9 (along with Appendices E and F) and Appendix D are in preparation as papers.

ACKNOWLEDGEMENTS

The work in this thesis was carried out while the author was a research student in the Department of Astronomy, University of Glasgow. It is a pleasure to thank the staff and fellow students of the department for making my stay here both enjoyable and profitable. In particular I would like to thank Professor P. A. Sweet for giving me ideal facilities within his department for carrying out this research.

My special thanks go to my supervisor, Professor Archie E. Roy, for many hours of fruitful discussion, practical help in the compilation of large amounts of data and guidance in the preparation of this thesis. Various aspects of this work were also discussed or carried out in co-operation with Prof. V. V. Markellos, Dr. A. G. Emslie, Dr. D. B. Taylor and Mr. H. E. Schwarz: I would like to thank each of them.

I would also like to thank Mrs. L. Williamson for her very efficient typing of the thesis (and her patience with some of the most complex equations that I could think up). Also my thanks go to Mr. C. Aspin and Mrs. M. I. Morris for time in preparing several of the diagrams contained in the thesis and to the staff of the Computing Service at the University for the successful execution of several hundred "computer jobs".

Finally, I thank the Science Research Council for providing me with a grant to carry out this research.

Ian W Walker
Department of Astronomy,
The University,
Glasgow G12 8QQ.

CONTENTS

		Page
Preface		iv
Acknowledgements		vi
Summary		xii
Frontispiece		xvi
CHAPTER 1	STABILITY IN DYNAMICAL SYSTEMS	
1.1	The Stability of the Solar System	1
1.2	Definitions of Stability	7
1.3	Resonances and Small Divisors	10
1.4	Periodic Orbits and Linear Stability	13
1.5	The Kolmogorov-Arnol'd-Moser Theory	14
1.6	Special Perturbation Methods	15
1.7	Summary	21
CHAPTER 2	THE EFFECT OF INTEGRALS ON POSSIBLE SOLUTIONS OF THE THREE-BODY PROBLEM	
2.1	Introduction	22
2.2	The Surfaces of Zero-Velocity in the Circular Restricted Three-Body Problem	23
2.3	A Discussion of the Elliptic Restricted Three-Body Problem	32
2.4	Zero-Velocity Curves in the Coplanar General Three-Body Problem	34
2.5	Application of the Zero-Velocity Curves in the General Three-Body Problem to Stability Considerations	43
2.6	Summary	45
CHAPTER 3	STABILITY PARAMETERS FOR HIERARCHICAL DYNAMICAL SYSTEMS	
3.1	Introduction	47
3.2	Lunar Theory-The Disturbing Function	49
3.3	Planetary and Lunar Theory - A Brief Comparison	54
3.4	Stability in Multiple Stellar Systems	56
3.5	The Jacobian Coordinate System	58
3.6	Expansion of the Force Function of a Hierarchical n-Body Dynamical System	62
3.7	Discussion	68

Page

CHAPTER 4 EXAMINATION OF THE EMPIRICAL STABILITY PARAMETERS IN THE THREE-BODY CASE

4.1 Introduction 70
4.2 The Empirical Stability Parameters 72
4.3 The Stability of Coplanar Hierarchical Three-Body Systems - A Review 74
4.4 Determination and Modification of the Critical Stability Surface 77
4.5 Real Systems and the Critical Stability Surface 83
4.6 Discussion and Conclusions 102

CHAPTER 5 REFINEMENT OF THE SUFFICIENT CONDITION FOR THE STABILITY OF COPLANAR HIERARCHICAL THREE-BODY SYSTEMS

5.1 Introduction 112
5.2 An Exact Expression for the Parameter c^2H in Coplanar Hierarchical Three-Body Systems 114
5.3 The General Effects of Orbital Parameters on the Stability 121
5.4 Results for Coplanar Hierarchical Three-Body Systems in General 130
5.5 Comparison of Results with Numerical Integrations 140
5.6 Sun-Jupiter-Saturn System 144
5.7 Earth-Moon-Sun System 148
5.8 Discussion and Conclusions 153

CHAPTER 6 EMPIRICAL STABILITY REGIONS FOR COROTATIONAL COPLANAR HIERARCHICAL THREE-BODY SYSTEMS

6.1 Introduction 159
6.2 Definitions and Description of the Numerical Experiments 161
6.3 The Results 167
6.4 The Effect of Commensurabilities on the Degree of Stability 197
6.5 Discussion and Conclusions 202

Page

CHAPTER 7 THE PREDICTION OF THE AMPLITUDE OF VARIATIONS IN SEMI-MAJOR AXES AND ECCENTRICITIES IN COPLANAR COROTATIONAL INITIALLY CIRCULAR HIERARCHICAL THREE-BODY SYSTEMS

7.1 Introduction 213

7.2 The Numerical Experiments and Results 214

7.3 The Effect of Commensurabilities on the Amplitude of the Variations 236

7.4 Discussion and Conclusions 238

CHAPTER 8 THE EMPIRICAL STABILITY PARAMETERS FOR THE HIERARCHICAL FOUR-BODY PROBLEM AND THEIR APPLICATION IN THE COPLANAR COROTATIONAL INITIALLY CIRCULAR CASE

8.1 Introduction 240

8.2 The Empirical Stability Parameters Defined 241

8.3 The Numerical Experiments 243

8.4 Results - The Stability of Four-Body Systems 246

8.5 Results - The Relationship Between the Empirical Stability Parameters and the Amplitude of Variations in the Eccentricities 252

8.6 Discussion 258

CHAPTER 9 SPECIAL CASES OF HIERARCHICAL DYNAMICAL SYSTEM

9.1 Introduction 261

9.2 The Planetary Case - A Re-evaluation of the "ε" Parameters 262

9.3 A Coordinate System for General Hierarchical Systems 269

9.4 The Expansion of the Force Function in the Case of General Hierarchical Systems 275

9.5 Discussion and Conclusions 288

CHAPTER 10 FUTURE WORK

10.1 Review 292

10.2 The Extension to Non-Coplanar, Co/Counter-Rotational and Initially Non-Circular Orbits in the Hierarchical Three-Body Problem. 292

10.3 The Analytical Determination of the Amplitude of Variations in Semi-Major Axes, Eccentricities and Inclinations in the General n-Body Problem 294

10.4 Numerical Investigation of n-Body ($n \geq 4$) Hierarchical Systems 295

Page

APPENDIX A Ordering of the Masses in Collinear Equilibrium Configurations to Obtain Primary, Secondary and Tertiary Bifurcation Values of c^2H . 298

APPENDIX B The Surfaces of Critical Stability in the Initially Circular Case of the Coplanar, Corotational, Hierarchical, Three-Body Problem 302

APPENDIX C A Description of the Recurrence Relation Scheme Used in the Numerical Integration of the Equations of Motion of the Many-Body Problem - Its application to the Restricted Three-Body Problem and Comparison with Similar Methods Used Previously

C.1 Introduction 310
C.2 Equations and Recurrence Relations 312
C.3 Adjustment of the Integration Step-Length 314
C.4 Computational Results 322
C.5 Discussion and Conclusions 327

APPENDIX D Applications of the Explicit Taylor Series Integration Scheme, Employing Recurrence Relations, and its Comparison with Classical Single-Step and Multi-Step Methods of Numerical Integration (as available on the Glasgow University ICL2976 Computer)

D.1 Introduction 329
D.2 Applications - Equations of Motion and Recurrence Relationships 330
D.3 Numerical Integration Experiments 336
D.4 Machine Time 338
D.5 Errors 342
D.6 Conclusions 349

APPENDIX E Derivation of Expressions for the Force Function in a General Hierarchical Many-Body System in terms of the ρ_{ij} - The Four-Body and Eight-Body Cases 351

Page

APPENDIX F Derivation of the Equations of Motion and Generalised ε Parameters for General Hierarchical Systems - The Four-Body and Eight-Body Cases 373

References 392

EMPIRICAL STABILITY CRITERIA FOR HIERARCHICAL MANY-BODY DYNAMICAL SYSTEMS IN CELESTIAL MECHANICS

by

IAN W. WALKER B.Sc.

Summary

Department of Astronomy,
The University,
Glasgow G12 8QQ.

November 1980

SUMMARY

The question of whether the Solar System is stable or not has been investigated by many researchers since the beginnings of celestial mechanics, with the formulation of the law of gravitation by Newton, up until the present day. As yet, even after some 300 years, celestial mechanics is unable to give a definite answer to this question. However throughout the studies which have been made there are strong indications that, among the major bodies i.e. the planets and (the majority of) satellites, the orbits are stable.

Dynamical systems, such as those occurring in nature, may be broadly classified into two types: (i) those which contain *large* numbers of bodies, the gravitational attraction of the *whole* system dominating the movement of each of the bodies and (ii) those which contain relatively *few* bodies where the *particular* interactions of one body with each of the others is important. This thesis considers only the latter type: these are hierarchical systems where the orbits of the system are arranged so that close approaches of one body to another *may* be prevented e.g. the Solar System, triple stellar systems, etc.

The concept of *stability* which is used in this thesis is that there should be no collisions between bodies within a hierarchical dynamical system, neither should any bodies escape the system. Having fulfilled these conditions a system may be called "stable". In other words we require a maintenance of the *status quo* with the orbits in the system being executed over many revolutions with only periodic changes in the semi-major axes, eccentricities and inclinations defining the osculating orbits; secular changes in these orbital elements should be absent.

To investigate the stability of these systems empirical stability parameters are derived which are representative of the disturbances on the orbits of a hierarchical system due to the other bodies which are present. These parameters are obtained in the following manner. The equations of motion of the masses making up an n-body dynamical system are expressed in the Jacobian coordinate system. An expansion of the force function then gives rise naturally to a set

$(n-1)(n-2)$ dimensionless parameters, the ε parameters, representative of the size of the perturbations on the osculating Keplerian orbits of the various bodies in the system. In the case where there are only three bodies the relationship between these ε parameters and the analytical stability criterion employing the zero-velocity curves of the coplanar general three-body problem is examined. It is shown that the stability, in the sense of the zero-velocity curves of the problem being open or closed and thus whether an exchange between bodies is possible or not, is dependant, in a very simple fashion, on the magnitude of the ε parameters. The analytical stability criterion involving the use of the zero-velocity curves of the general three-body problem is then refined in order to take account of all the orbital parameters relevant to coplanar hierarchical three-body systems prior to a numerical investigation of the coplanar, corotational hierarchical three-body problem with initially circular orbits.

By means of this numerical investigation it is demonstrated that the ε parameters can be used to both predict how stable or unstable a three-body system is, in the sense of the number of orbits it may be expected to execute before instability sets in, and also to predict the variations in semi-major axes and eccentricities of the system's constituent orbits. The effect commensurabilities in mean motion have on the stability of these systems is also demonstrated. It is shown how systems which are unstable can extend their predicted "lifetime" if they are close to a commensurable situation. Stable systems have their variations in semi-major axes and eccentricities greatly magnified by the presence of commensurabilities.

This numerical study was continued into the four-body problem. Although only a brief consideration was given to the problem it is apparent that results, similar to those obtained in the three-body case, may be derived.

The applicability of the ε parameters to the planetary case of the hierarchical many-body problem is also considered by application of another expansion of the force function which takes into account the smallness of the planetary masses with respect to the central mass, namely the Sun. It is thus shown that the ε parameters are

truly representative of the disturbances on the planetary orbits over a sufficiently wide range of the semi-major axes of the hierarchical planetary many-body problem.

Another coordinate system is then developed which is applicable to all types of hierarchical system, including the type exemplified by the sextuple Castor system and similar multiple stellar-systems. Using this coordinate system a more general set of ε parameters are developed and the perturbations on the orbits of a system, such as that of Castor, are considered.

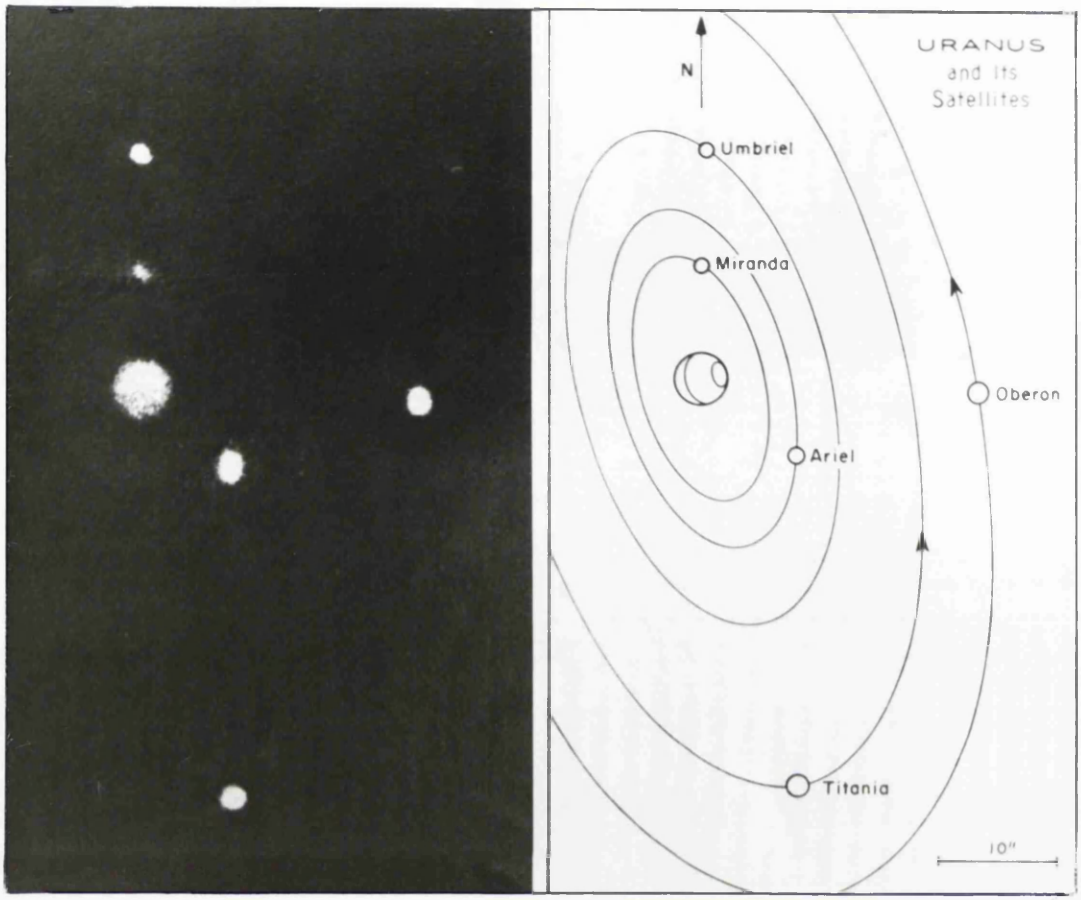

Frontispiece The equator of the planet Uranus is inclined at 97° 53' to its orbital plane. The five satellites - Miranda, Ariel, Umbriel, Titania and Oberon - move in the equatorial plane of the planet. Their orbits, which are nearly circular, are thus presented at various angles to the Earth as the planet revolves about the Sun. In 1966 the system was presented edgewise to us : in 1987 the system will be seen "flat on".

In this view, and the accompanying diagram, we see that the satellites' orbits are well-spaced, are arranged in a definite order and do not cross : this is the *hierarchical structure* typical of many naturally occurring dynamical systems e.g. the Solar System, triple stellar systems, etc.

The photograph above is an infrared composite taken at the Mauna Kea observatory, Hawaii (see Sinton, 1972).

CHAPTER 1 STABILITY IN DYNAMICAL SYSTEMS

1.1 The Stability of the Solar System

The family of bodies associated with the Sun, known to us as the Solar System, consists of many thousands of bodies. The major components, apart from the Sun itself, are the nine major planets and some thirty-odd satellites. Among the lesser components may be found the asteroids, which are largely concentrated between the orbits of Mars and Jupiter, the comets, estimated to exist in millions by some authorities and the uncountable number of meteors which travel round the Sun in swarms. In addition there are also the rings of Jupiter, Saturn and Uranus and the interplanetary medium.

Observation of this system shows it to possess characteristic properties. The planets, without exception, revolve about the Sun in the same direction. The system possesses a hierarchical structure in that the orbits are well-spaced and are arranged in a definite order (Fig.1.1).

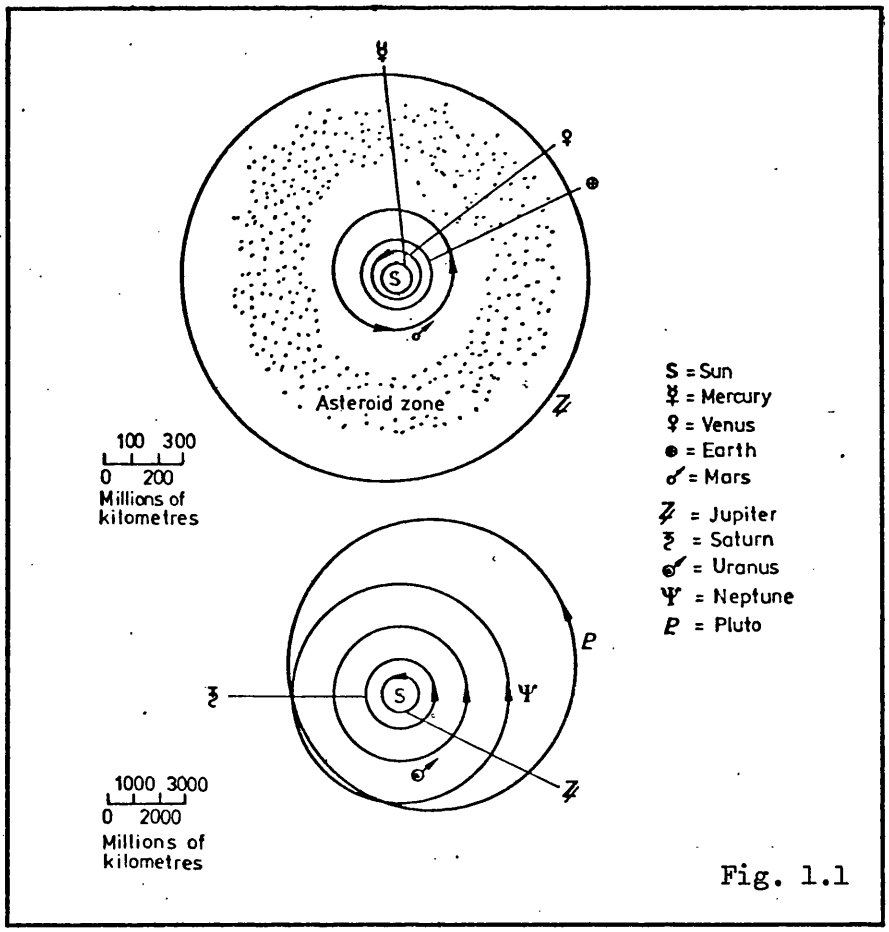

Fig. 1.1

Further, excepting the orbits of Mercury and Pluto, all have small eccentricities and inclinations. In only one instance do the orbits of any two planets cross, this being the case with Neptune and Pluto. However in this exceptional case there is reason to believe (Cohen and Hubbard, 1964, 1965; Williams and Benson, 1971) that there are additional dynamical characteristics which allow these two bodies to avoid close encounters which would otherwise lead to the disruption of the Neptune-Pluto system.

The satellite systems too follow this broad pattern although there are exceptions. The outermost satellites of Jupiter (JXII, JXI, JVIII and JIX) and Phoebe, the outermost satellite of Saturn, move in a retrograde fashion. In the former case there is a strong possibility that these bodies are captured asteroids (Bailey 1971, 1972) and may therefore not be permanent features of the system.

Roy and Ovenden (1954, 1955) pointed out that the occurrence of near commensurabilities in mean motions within the Solar System is greater than one would expect on a purely random basis, suggesting that a mechanism exists able to produce such resonant states. Commensurabilities, such as exist in the solar system, may be divided into two broad types viz. hard and soft. The former is exemplified by the Titan-Hyperion (4:3), Neptune-Pluto (3:2), Enceladus-Dione (2:1) and Mimas-Tethys (2:1) resonances: in such cases a critical argument exists and there are grounds for believing the dynamical situation is one of stability. On the other hand a soft commensurability may be exemplified by Jupiter-Saturn (5:2) and Uranus-Neptune (2:1) where the existence of the commensurability does not seem to be essential for the maintenance of stability.

If we now however turn our attention to the asteroids we find in many cases orbits of certain semi-major axes are avoided. Upon examination it is found that such distances would give rise to mean motions commensurable with that of Jupiter. In Fig.1.2(a) (due to Hagihara, 1957) the distribution of asteroids with respect to their mean motions about the Sun in seconds of arc per day is plotted: The orders of the commensurabilities are marked along the top of the diagram. The notable feature of the diagram is the gaps in the distribution arising at mean motions commensurable with that of Jupiter,

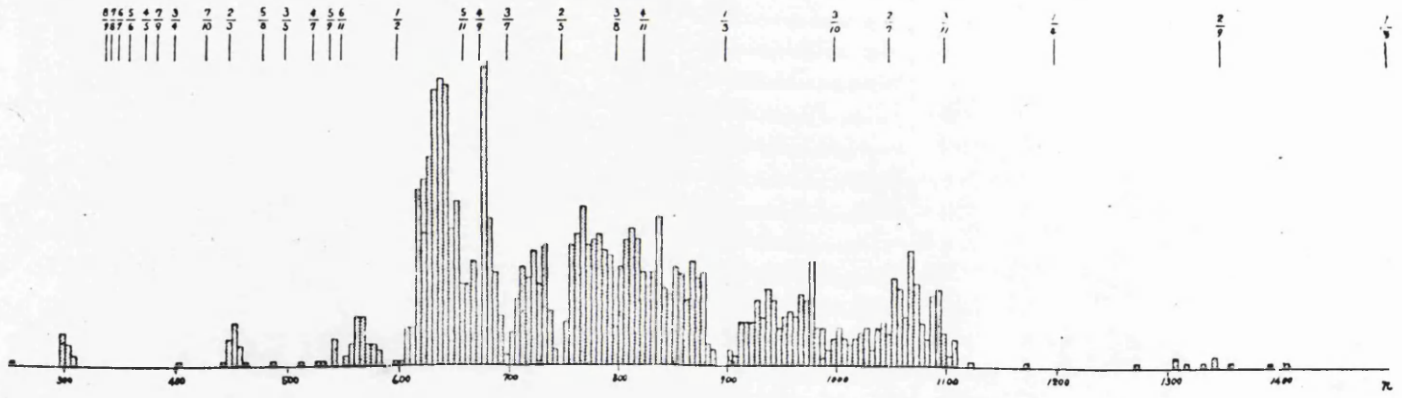

Fig. 1.2(a)

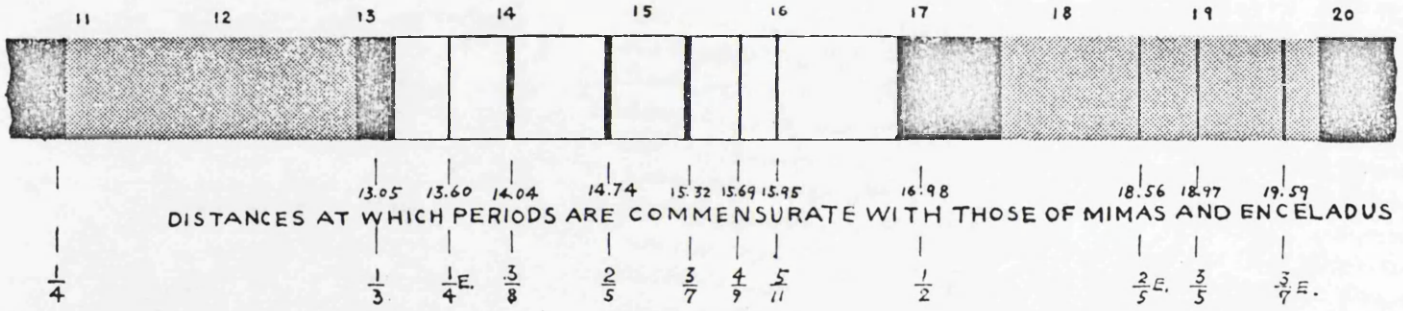

Fig. 1.2(b)

the so-called Kirkwood gaps. Furthermore there is a sharp cut off in asteroid numbers beyond the 2:1 commensurability, the so-called Hecuba Gap and a clustering of asteroids at the 3:2 and 1:1 commensurabilities, respectively the Hilda and Trojan groups. The feature of avoidance of certain commensurable orbits is repeated on a smaller scale in the Saturnian ring system Fig.1.2(b). The three innermost satellites of Saturn are massive enough and close enough to the ring system to disturb its constituent particles. The division between rings A and B - Cassini's division - occurs at distances which offer orbits commensurable with those of Mimas, Enceladus and Tethys in the ratios 2:1, 3:1 and 4:1 respectively. The other boundary between the rings B and C - Encke's division - results in a 3:1 commensurability with Mimas. Further faint divisions have also been observed within rings A and B.

Comets generally follow orbits of high eccentricity and inclination and are, in this respect, different from the planets. There are several occasions on record where cometary orbits have been suddenly and dramatically changed by planetary encounters. For example, Brook's Comet (1889V) had a period of revolution 29.2 years, its orbit lying outside that of Jupiter. After a close approach to Jupiter on 20, July 1886 the period had changed to 7.10 years, the orbit lying wholly within that of Jupiter. Similarly it might be expected that meteors will have their orbits severely changed at planetary encounters, the event however being unobservable, except if the meteor enters the Earth's atmosphere.

It is possible that the interplanetary medium may give rise to temporary features associated with planets. A faint glow, called the *Gegenschein*, is observed in the night sky opposite the Sun: it is possible this glow could be the reflection of sunlight from particles which are trapped at the L_3 collinear equilibrium point of the Earth-Sun system, which is on the far side of the Earth from the Sun. It has been argued that interplanetary and meteoric particles may be temporarily trapped in this position. However, since such particles would be at a position which is essentially a point of unstable equilibrium they would, due to perturbation by the Moon and other planets, gradually be lost from the system, the aggregation of particles having to be continuously supplemented. This case may be contrasted with the Trojan asteroids which are at a position of stable equilibrium namely

the triangular Lagrange configurations with Jupiter.

All the bodies in the Solar System are thus observed to be continually undergoing changes in their orbits due to their mutual gravitational attractions. We have seen that in some cases the body may have its orbit changed drastically, as in the case of some comets. There are grounds for believing that the outermost satellites of Jupiter may be captured asteroids. The asteroids themselves, in certain cases, if they indeed originally formed a uniform distribution between the orbits of Jupiter and Mars, seem to have undergone substantial changes resulting in the avoidance of certain commensurabilities. The explanation of the *Gegenschein* as particles "trapped" at the collinear equilibrium points is another temporary situation. What of the other members of the system? Will the present configuration of the planets in relation to the Sun, and the satellites with respect to their parent planets, be preserved for an astronomically long time? Is there any evidence to suggest the permanance or otherwise of the orbits of the major bodies of the solar system?

Using records from ancient Babylonia circa. 500 B.C. up to the present day it is possible to observe the planets in time as well as in space. Data on the movements of the five anciently-known planets - Mercury, Venus, Mars, Jupiter and Saturn - in the form of cuneiform tablets show that the planetary orbits were not substantially different from the present day ones. By studying the lunar observatories of megalithic man another 2.5 millenia earlier it is seen that the Moon was moving in the orbit lunar theory predicts for this period. The contemporary solar observatories lend weight to our theories which give the changes in the obliquity of the ecliptic.

The three outermost planets - Uranus, Neptune and Pluto - the satellites of the planets and the asteroids are all of much more recent discovery and it may be thought that their history cannot be so well documented as that of the above bodies. However if it is considered that the relevant unit of time is the period of the object about its primary then we see this is by no means the case. In Table 1.1 are presented all the known satellites and planets in the solar system along with the number of periods completed since discovery: in some instances a second figure is given derived from numerical

Table 1.1

OBJECT	YEAR OF DISCOVERY	PERIOD	NUMBER OF ORBITS OBSERVED SINCE DISCOVERY OR COMPUTED *	
		years		
Mercury	Before 2000 BC	0.241	1.7×10^4	
Venus	"	0.615	6.5×10^3	
Earth	"	1.000	4.0×10^3	
Mars	"	1.881	2.1×10^3	
Asteroids	1801	4.6	3.9×10^1	
Jupiter	Before 2000 BC	11.86	3.4×10^2	4.2×10^4 *
Saturn	"	29.46	1.3×10^2	1.7×10^4 *
Uranus	1781	84.01	2.4	6.0×10^3 *
Neptune	1846	164.78	1.0	3.0×10^3 *
Pluto	1930	248.4	0.2	2.0×10^3 *
		days		
Moon	Before 2000 BC	27.32	5.3×10^4	
Phobos	1877	0.319	1.2×10^5	
Deimos	1877	1.262	2.9×10^4	
Jupiter V	1892	0.498	6.3×10^4	
I	1610	1.769	7.6×10^4	
II	1610	3.551	3.8×10^4	
III	1610	7.155	1.9×10^4	
IV	1610	16.69	8.1×10^3	
VI	1904	251	1.1×10^2	
VII	1905	260	1.0×10^2	
X	1938	260	5.6×10^1	
XIII	1975	252	4.3	
VIII	1908	739	3.5×10^1	
IX	1914	745	3.1×10^1	
XI	1938	696	2.1×10^1	
XII	1951	617	1.0×10^1	
Janus	1966	0.749	5.9×10^3	
Mimas	1789	0.942	7.3×10^4	
Enceladus	1789	1.370	5.0×10^4	
Tethys	1684	1.888	5.7×10^4	
Dione	1684	2.737	3.9×10^4	
Rhea	1672	4.518	2.5×10^4	
Titan	1655	15.95	7.4×10^3	
Hyperion	1848	21.28	2.2×10^3	
Iapetus	1671	79.33	1.4×10^3	
Phoebe	1898	550.5	5.3×10^1	
Miranda	1948	1.414	1.1×10^4	
Ariel	1851	2.520	1.8×10^4	
Umbriel	1851	4.144	1.1×10^4	
Titania	1787	8.706	8.0×10^3	
Oberon	1787	13.46	5.2×10^3	
Triton	1846	5.877	8.2×10^3	
Nereid	1949	359	3.0×10^1	

* Cohen, Hubbard and Oesterwinter's numerical integration over 500,000 years

integration experiments by Cohen, Hubbard and Oesterwinter (1967). Inspection of the table reveals that in many cases several thousands of orbits have been observed to be completed. During this time the changes in the orbits have been in accord with general perturbation methods. The semi-major axes, eccentricities and inclinations have undergone periodic variations, secular trends being absent. This lends weight to the idea that sudden, far-reaching changes in the orbits are unlikely, at least within the next few revolutions.

Beyond the data of Table 1.1 there is *no* further observational information on the dynamics of the system which can be put forward in support of the stability of the Solar System. Thus the questions asked earlier remain unanswered.

1.2 Definitions of Stability

The problem of the stability of the Solar System has been studied by many astronomers since the time of Newton. It is therefore not surprising that there are many different definitions of stability which are applicable to dynamical systems. It is conceivable then that *one* particular system may be stable according to one definition but unstable according to another.

Consider the example of an asteroid in orbit about the Sun in the absence of any perturbing bodies. The asteroid will then execute a Keplerian ellipse, described by the usual constant orbital parameters a_1, e_1, i_1, ω_1, Ω_1, τ_1 say, about the Sun and will have a position in this orbit given by the true anomaly f_1. If we then displace the asteroid by a small amount in its orbit resulting in a new set of elements a_2, e_2, i_2, ω_2, Ω_2, τ_2 with the new position given by f_2 we may ask the following question: Given that all the quantities denoted suffix "2" differ by only a small amount from those denoted suffix "1" at some initial time then will that difference remain small for all time? Put another way the question is asking if the two asteroids will always remain close to each other in space? The answer to this question is obviously "no", since at some subsequent time the asteroids will be separated by a distance roughly equal to the major axis of either of their orbits (assuming $a_1 \simeq a_2$ and e_1 and e_2 are small).

However, if we require for stability that the general shape and orientation of the orbits should not differ by much at any time, that is we do not consider f_1, f_2 the positions of the asteroids in the two orbits, then the answer would be "yes" and the system is stable.

It is therefore imperative that a good clear definition of what is meant by stability is given at the outset of any discussion.

"Is the Solar System stable in the sense that no collisions can occur and no major body will escape the system?" is the question around which Laplace formed his definition of stability. Many such qualitative questions may be asked. They all relate to the basic idea that the "status quo" of the dynamical system will be maintained. In the case of the solar system these qualitative definitions of stability preclude the possibility that the ordering of the orbits or hierarchy of the system, can be disrupted. For example, the system may only be called stable if the orbit of Saturn, for example, always lies between the orbits of Jupiter and Uranus. Pluto is, of course, an exceptional case which does not come under the scope of such a definition except inasmuch as Pluto is never found to lie between Neptune and the Sun.

Laplace himself made one of the earliest attempts to study the stability of the Solar System. He found that in the first-order solution of the Lagrange planetary equations governing the motion of a perturbed planet no secular terms appear in the expressions which yield the changes in the semi-major axes. This result implies that each planet is restricted to an annulus about its present orbit. The width of the annulus depends on the magnitude of the periodic variations in the semi-major axis. The main point is of course that no annuli cross and that all are of small width in comparison to the distance between planetary orbits, thus rendering collisions between bodies and escapes impossible. The second-order theorem was considered by Poisson, the third-order theorem by many others and at present the state of the problem, which is still a burning issue in celestial mechanics, is that if the expansions are done in a specific fashion then no secular terms appear to any order (see Message, 1978).

The approach of Laplace was generalized by Newcomb (1876) who showed that purely periodic solutions with secular terms in the angular variables could be found to satisfy the n-body problem where the central

mass is large compared to the others, the others moving in almost circular coplanar orbits about the large mass. Questions of the convergence or divergence of the trigonometrical series obtained were left open until Poincaré at the end of the 19th century showed that in general such series were divergent, thus demonstrating that such approaches were inapplicable to the question of the long-term stability of the solar system.

In any event these results are valid only inasmuch as the assumptions upon which they are based are valid. In the physics of the problem it is assumed that the planets and Sun may effectively be replaced by point masses which exhibit only Newtonian gravitational forces. This is obviously not the case since in many systems the long-term evolution is affected by other factors. For example the Moon's orbit about the Earth is affected by tidal forces, and general relativistic effects play a role in the advance of perihelion of the planets' orbits, these being strongest in the case of Mercury. All these effects are *not* negligible over astronomically long time scales such as the age of the Solar System - 5.10^9 years.

There are many other definitions of stability, a few of which are mentioned below and will be expanded upon in succeeding pages. In Section 1.3 we discuss the part resonances play in maintaining stability where it seems, on a superficial level, that the system is unstable. Section 1.4 is devoted to the brief consideration of the closely related topic of periodic orbits. These have been used extensively, since the recent introduction of fast and efficient computers, to map out regions of phase-space where such orbits are linearly stable. By this means statements may be made about the stability of general orbits which lie in the vicinity of the periodic solutions. In recent years Arnol'd (1963), Kolmogorov (1954), Moser (1973) and Siegel and Moser (1971) have shown that the approach taken by Laplace and Newcomb can, under certain circumstances, give rise to convergent series (see Section 1.5). Again resulting from the advent of computers is the application of special perturbation methods to the stability of dynamical systems (see Section 1.6). In this case a particular set of masses with given initial conditions are integrated numerically over a sufficiently long period of time in order to be able to make statements about the stability of the orbits comprising the system.

Discussion of one particular method of investigating stability, due to Hill (1878), is deferred until Chapter 2 in order to deal with it more fully since the concept will occur in later chapters of the thesis. Hill's original theory was applied by him to the Earth-Moon-Sun system in order to study the stability of the Moon's orbit. Originally applied to the restricted three-body problem, the concept has of late been generalized to allow study of the general three-body problem (cf. Zare, 1976).

1.3 Resonances and Small Divisors

As was mentioned above in Section 1.1 the occurrence of commensurabilities in mean motion in the Solar System is greater than one would expect through random effects (Roy and Ovenden 1954, 1955). Goldreich (1965) proposed a mechanism whereby such commensurabilities could be arrived at from initially non-commensurable states. A pair of satellites under their parent planet's tidal forces will change their semi-major axes so that, even if the ratio of the mean motions was originally irrational, it will not only have a chance to become rational i.e. a commensurability will result but, having attained that state, the commensurability will persist as the orbits continue to evolve.

Given certain assumptions, he showed that if two satellites S_i and S_o are in orbits of semi-major axes a_i and a_o respectively with $a_i < a_o$ about a planet P, tidal forces will act upon S_i to a greater extent than upon S_o. This results in S_i spiralling outwards faster than S_o. The system $P\text{-}S_i\text{-}S_o$ may eventually reach a commensurable situation. Having reached this state the system will be stabilized due to the highly non-linear nature of the gravitational n-body problem. Considering this system of $P\text{-}S_i\text{-}S_o$ let us now take the situation when S_i and S_o are in conjunction on one side of the line passing through the aphelion of the orbit of S_o (see Figure 1.3). Due to the asymmetry of the orbit of S_o with respect to the conjunction line energy will be transferred from S_o to S_i. The net exchange of energy results in the orbital period of each satellite changing so that, supposing they were formerly in exact resonance, they no longer will be. This occurs in a

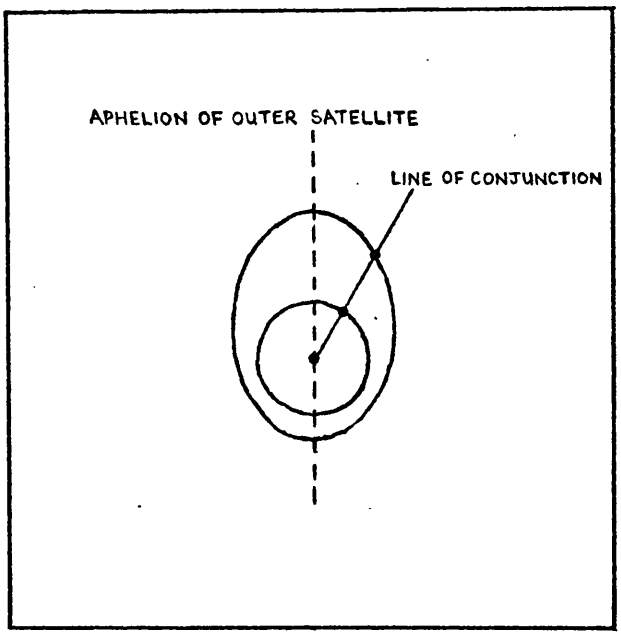

Figure 1.3 If two satellites are in exact resonance, and their conjunction is on the right side of the dashed line in the diagram, energy is transferred from the outer to the inner body.

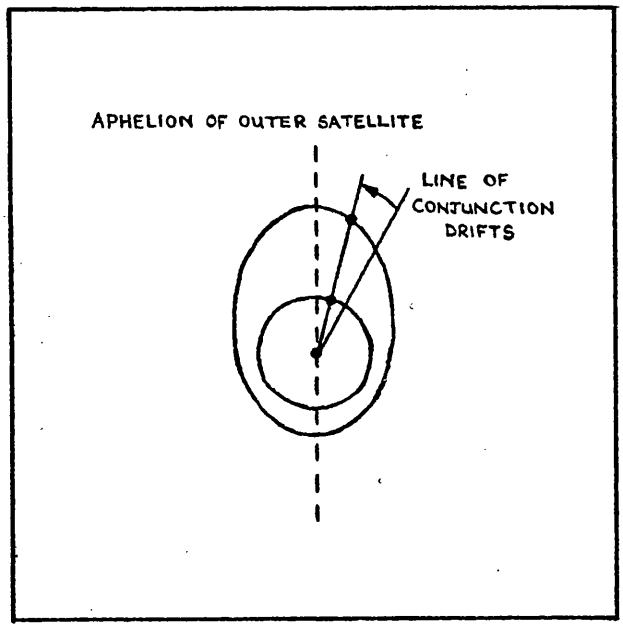

Figure 1.4 Transfer of energy from the outer to the inner body causes the period of the outer to shorten and the inner to lengthen. Therefore, the line of conjunctions drifts to the left. To the left of the dashed line the energy flow is reversed and so the drift of the line of conjunctions is slowed down, halted and reversed.

systematic fashion causing the line of conjunctions to drift in space (Fig.1.4) until it lies on the other side of the apse line of S_o. The process will then be reversed, S_i giving up energy to S_o, and the drift halted. This is repeated until the line of conjunctions drifts back to its original position and the cycle is restarted. The motion of the system is distinctly different from a superimposition of two two-body motions the resonance having changed its character completely.

Although it is clear that resonance plays a large part in the stability of some parts of the Solar System problems do occur in general perturbation theory due to resonances. The trigonometrical series which are used to represent the motion of the planets in general perturbation theory are generally made up of an infinite number of periodic terms. Each of the terms of such series involves a linear combination of the fundamental frequencies of the system. Upon the integration of these terms to obtain a solution, the linear combinations of frequencies then appear as divisors in the terms of the equations. The difficulty arises since all possible linear combinations of the frequencies may appear and thus even if the ratio of any of two fundamental frequencies is *irrational* the ratio may be *closely approximated* by a rational. Hence "small divisors" appear factoring certain terms, greatly magnifying the effect these terms have on the motion of the bodies (see Brown, 1896; Plummer, 1918; Smart, 1953; Brouwer and Clemence, 1961).

For instance suppose n_J and n_S are the mean motions of Jupiter and Saturn about the Sun respectively. Then terms will be continually having multipliers of the form $n_S/(i_1 n_J \pm i_2 n_S)$ or $n_J/(i_1 n_J \pm i_2 n_S)$ produced by the integration (i_1, i_2 are positive integers). In general the greater i_1 and i_2 the smaller will be the coefficient of the term; however if we consider the case of Jupiter and Saturn we see that this is not always the case. The ratio of the fundamental frequencies in this case is 0.40268677 which is approximated to about one half of one per cent by the ratio 2/5 or to about one part in 10^5 by the ratio 60/149. Thus it is found that deviations from the purely elliptic motion of Jupiter and Saturn are greater than we might expect.

1.4 Periodic Orbits and Linear Stability

A further approach to the concept of stability in dynamical systems is that of periodic orbits. Within the last hundred years, in the restricted three-body problem, and more recently in the general problem, many investigators have explored the existence of families of periodic orbits. The reason for such searches is threefold:

(i) The conjecture of Poincaré states that given any solution to the equations of motion of a dynamical system then it is possible to find a periodic solution which is as close as we please to the original for all time. Thus periodic orbits have a possible application as reference orbits.

(ii) Since many dynamical systems are found in nature to exhibit resonances, periodic orbits have, in this instance, a direct relevance to the stability or instability of such systems.

(iii) Finally, it is possible to obtain and classify such periodic solutions since they may be found readily by analytical-numerical or numerical techniques, the integration time required being simply the period of the particular solution sought. In such a way it is possible to obtain a "global picture" of all possible periodic solutions in any given problem and hence through considering the stability of the orbits map out regions of stability or instability.

Since Poincaré (1895) set out his classification of the periodic orbits of the restricted problem into three types many have turned their attention to the search for families of periodic orbits. Amongst early pioneers in this field were Darwin and Strömgren. Since the advent of fast and efficient digital computers in the early 1960's many comprehensive studies of periodic orbits have been made cf. Hénon (1965a,b; 1966a,b), Broucke (1968), Hénon (1969), Rabe (1961,1962), Deprit and Henrard (1965, 1967), Markellos (1974a,b) and many more.

Having obtained a periodic solution its stability may be investigated by the methods of linear stability analysis. Stability, in this sense, may be described rather loosely as the ability of an orbit to resist change if a small alteration is made to the orbit at any time. Poincaré was the first to formalize the method and to introduce characteristic exponents into the description of the stability

of linearized dynamical systems. An important feature of the analysis to note however is that if the linearized system is unstable then likewise the original (non-linearized) system will be unstable. The reverse, unfortunately, is not true. If the linearized system exhibits stability it does not then follow that the original system is stable: it might exhibit unstable behaviour, due to terms of higher order neglected in the linear treatment, when the imposed perturbation is large enough. Second order methods have been devised to try to take account of this; however, this is still not sufficient since the third and higher order terms may produce instabilities.

Thus it is doubtful if the use of periodic orbits can shed light on the long-term stability of the Solar System. Clearly its main relevance lies in the consideration of parts of the Solar System where there exist almost periodic motions. Here conclusions can be drawn if we consider the stability of periodic orbits in the vicinity of the real solution (cf. Wiesel, 1980).

1.5 The Kolmogorov-Arnol'd-Moser Theory

In recent years Kolmogorov and Arnol'd working in the USSR and Moser in the USA made a significant advance in understanding the stability of dynamical systems such as the Solar System (see Arnol'd, 1963; Kolmogorov, 1954; Moser, 1973; Siegel and Moser, 1971). They found that approaches such as those due to Laplace, Lagrange and Poisson could, under certain circumstances, give rise to convergent series. The restrictions on their theory may be briefly summarised as follows:

(i) The perturbations within the system have to be sufficiently small i.e. a large central mass with several *small* planets in revolution about it.

(ii) The natural frequencies of the system have to be such that their ratios are poorly approximated by rational numbers. With these two conditions satisfied the perturbation theory gives rise to convergent series.

Unfortunately however, when we turn out attention to the real Solar System, we find that the planets and satellites have masses which are too large so that the question of the stability of the Solar System is

outwith the scope of KAM Theory. The question of the rationality or otherwise of the ratios of natural frequencies is impossible to answer since they cannot be measured to infinite accuracy. However, it is found that most choices of natural frequencies would fall within the scope of the theory, in the sense that it is unlikely to select at random a set which is unsuitable for its application. This gives us hope that the real values observed in the Solar System also satisfy the requirements.

Although the KAM Theory fails to answer the question of the stability of the Solar System it is nevertheless probable that the theorems are valid for a larger range of perturbations since the limits set are only a sufficient and not a necessary condition.

1.6 Special Perturbation Methods

Having failed to answer the question of the stability of the Solar System through general perturbation methods we now consider what may be gained through the application of special perturbation methods. Special perturbation methods involve the numerical integration of the equations of motion of some dynamical system in one form or another in order to study the variations of the orbital elements of a real system over time scales greater than those for which they have been observed or, alternatively, to set up hypothetical systems which could otherwise not be studied.

Possibly among the most noteable studies done along the former lines were those carried out by Cohen and Hubbard (1965), Cohen, Hubbard and Oesterwinter (1967, 1972). In the first mentioned study the authors numerically integrated the equations of motion for the orbits of the five outer planets. The integration spanned a time of 120,000 years. They discovered a critical argument

$$\theta_N = 3\lambda_P - 2\lambda_N - \varpi_p$$

where λ is the mean longitude, ϖ is the longitude of perihelion and suffices P and N denote Pluto and Neptune respectively. The value of θ_N librates about 180° with an amplitude of 76° in a period of 19670 years resulting in the closest approach of Neptune and Pluto being some

18 astronomical units. Their later study in 1967, when they used improved elements for the orbit of Pluto, resulted in the revision of the amplitude of the libration to 80° with the period being 19440 years.

The latter study involved a numerical integration of the equations of motion for the five outer planets over a span of 10^6 years - the integrations were carried out forward and backwards for 5.10^5 years from the epoch Jan. 6.0 1941. Throughout these integrations it was found that no secular trends were present in any of the orbital elements a, e, i of the outer planets (cf. Fig. 1.5). The 900 year oscillation resulting from the 2:5 commensurability in mean motions of Jupiter and Saturn is evident in the plots. Similarly the plots for Pluto show a strong modulation of the variations in the elements with a period of 19500 years. It was however possible considering the plots of the elements i and e that these two elements had secular trends in the case of Pluto. Williams and Benson (1971) carried out a numerical integration of Pluto only over a period of $4{\cdot}5.10^6$ years, assuming that the remaining four outer planets' orbits were known, in order to resolve this problem. They used the method of Gauss secular variations to eliminate the short period terms, finding that the argument of perihelion librates about 90° with an amplitude of 24° in a period of $3{\cdot}995.10^6$ years.

Although such methods involving the elimination of short period terms are suspect for considering the long term stability of the Solar System it is remarkable to compare such a theory with the actual values obtained by a numerical integration of the exact equations of motion. In Figure 1.6 we see that the results of Brouwer and Van Woerkom (1950) agree well with those of Cohen, Hubbard and Oesterwinter (1972).

This approach while not *proving* the stability of the Solar System is strongly suggestive that major changes in the planetary orbits are at the least very unlikely over the next few revolutions of the bodies.

The stability of the Sun-Jupiter-Saturn system has been studied by Nacozy (1976, 1977). Systems involving the Sun and augmented Jupiter and Saturn masses were integrated numerically. It was found that if the masses of the two planets exceeded about thirty times

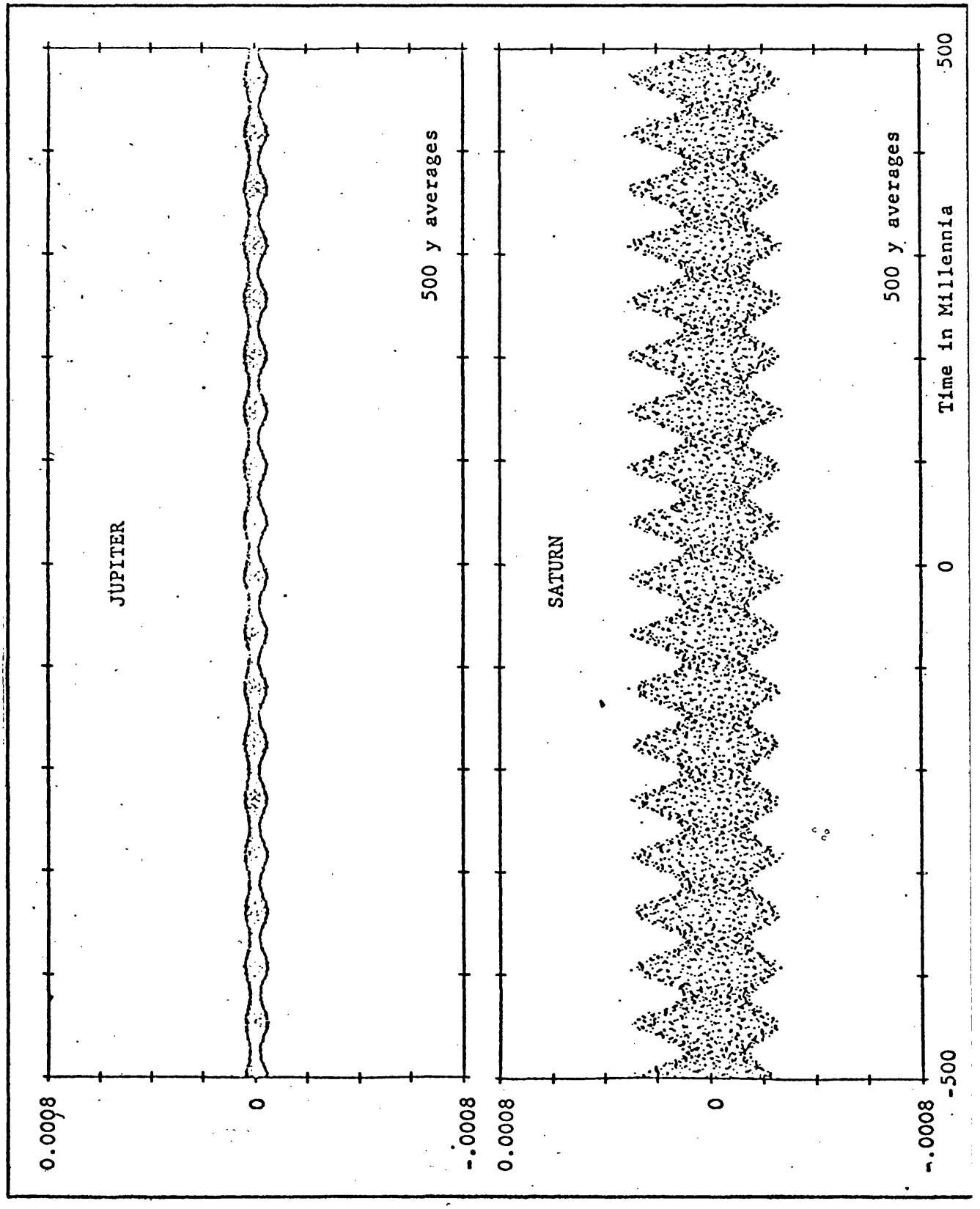

Figure 1.5 Semi-major axis, relative variation $\Delta a/\bar{a}$. For Jupiter, $\bar{a}$ = 5.20257 A.U.; for Saturn, $\bar{a}$ = 9.5549 A.U.

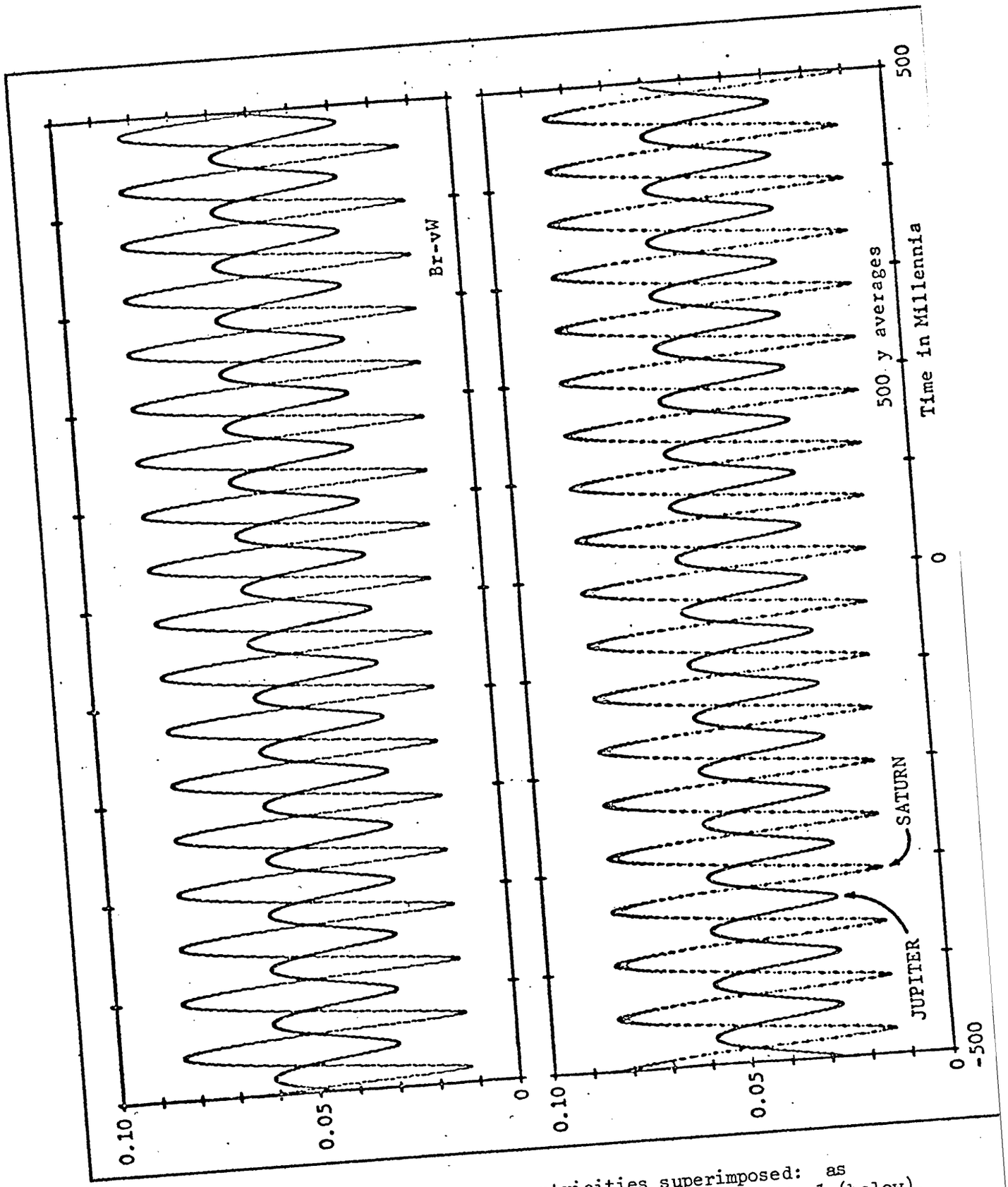

Figure 1.6 Jupiter and Saturn eccentricities superimposed: as calculated by Brouwer and Van Woerkom (above) and Cohen, *et al.* (below).

their present values then secular trends entered the semi-major axes and eccentricities resulting in the escape of Saturn from the system in 10^4 years or less. This result suggests that the present values for these planets' masses lie well within the region required for stability.

As was mentioned above, special perturbation methods allow us to construct and examine hypothetical dynamical systems: for example triple stellar systems (Fig.1.7(a)), inferior planets in double star systems (Fig.1.7(b)) and superior planets in double star systems (Fig.1.7(c)) have been examined by Harrington(1972,1977). (In each of these diagrams the arrows show the direction of motion with respect to the mass-centre of the binary i.e. the point denoted "C".) Harrington found that in general the stability of equal mass triple stellar systems depends on whether the revolution is corotational (Arrow "1" in Fig.1.8) or counter-rotational (Arrow "2" in Fig.1.8) and the ratio of the pericentre distance of the outer orbit to the semi-major axis of the inner orbit (respectively distances AC and BC in Fig.1.8). It was found that this ratio must be at least 3.5 for corotational orbits and at least 2.75 for counter-rotational orbits to ensure that the binary retains its identity and the third mass always remains at a more remote distance from the other two. Inferior and superior planets were found to be stable

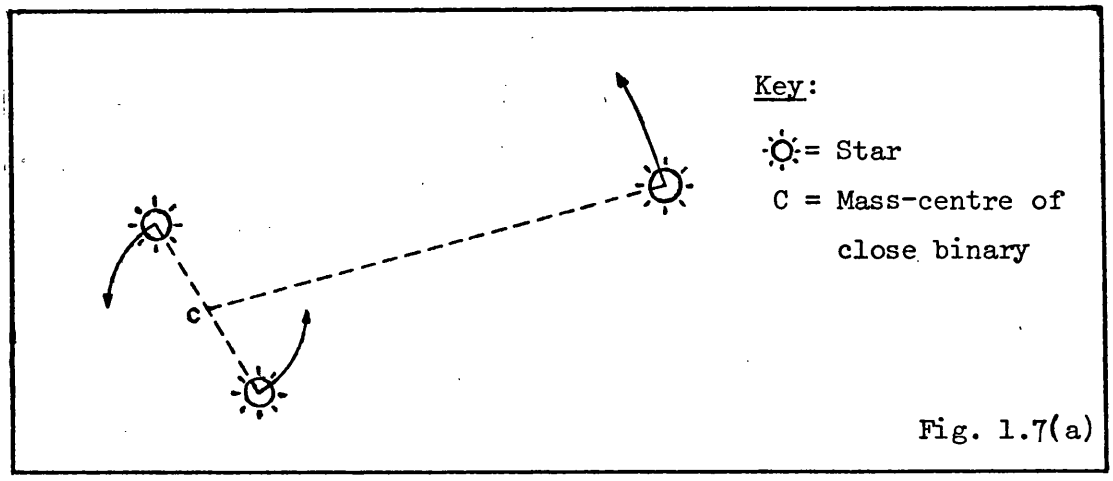

Fig. 1.7(a)

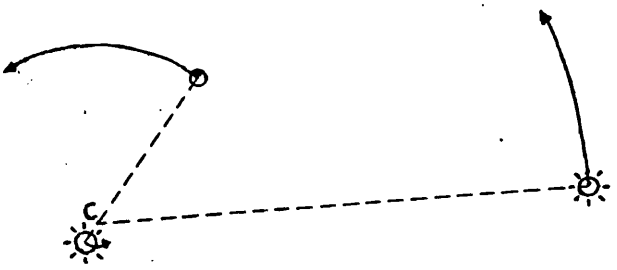

Key:

☼ = Star

◑ = Planet

C = Mass-centre of star and planet

Fig. 1.7(b)

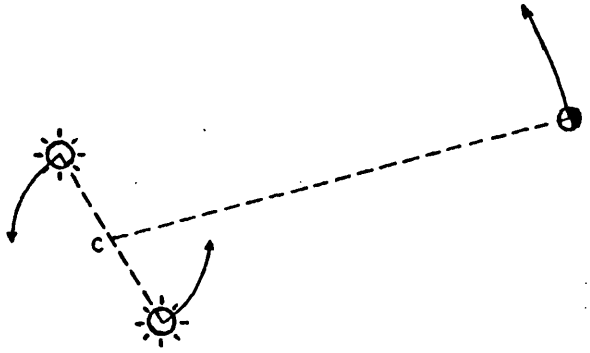

Key:

☼ = Star

◑ = Planet

C = Mass-centre of double star

Fig. 1.7(c)

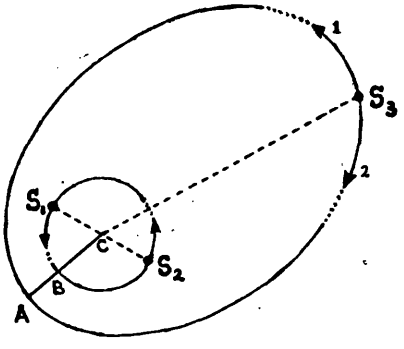

Key:

S_1, S_2, S_3 denote stars

C is the mass-centre of the close binary

A is the position of the pericentre of S_3

Fig. 1.8

in general if the ratio of the semi-major axes of the binary components' orbit to the pericentre distance of the outer component is of the order 1/4 to 1/3 regardless of whether the orbits are corotational or counter-rotational. By studies such as these it is possible to study the likelihood of the existence of what might be termed more "exotic" types of dynamical systems.

1.7 Summary

Despite the vast amount of effort which has been expended in the problem of the stability of the Solar System it is nevertheless a fact that celestial mechanics is still unable today to answer the question in any definite way. There are however strong suggestions through all the methods of considering stability outlined above that the Solar System is stable. It seems extremely unlikely that the Solar System should suffer any dramatic alteration in its main structure, viz. the orbits of the planets and majority of satellites, within any short time scales as indicated, for example, by the work of Cohen, Hubbard and Oesterwinter. However, at the present moment, celestial mechanics can make no comments on the history of the Solar System over the longer time scale of 10^9 years since the beginnings of the system.

CHAPTER 2 THE EFFECT OF INTEGRALS ON POSSIBLE SOLUTIONS OF THE THREE-BODY PROBLEM

2.1 Introduction

General perturbation methods having failed to demonstrate the stability of the Solar System, a valuable advance in the problem was made by Hill (1878). Hill applied his method to the Earth-Moon-Sun system and showed that, under the assumptions that the Moon's mass was negligible and the Earth's orbit about the Sun was circular, the Moon could not escape from the vicinity of the Earth. (A direct corollary of this fact is that the Moon could at no time in the past have been captured by the Earth, excepting for the intervention of another body, gross changes in the mass of the Earth or Sun or the effects of tidal friction). Hill's method is essentially the approach of the circular restricted three-body problem where the Jacobi integral (see for example Danby,1962; Szebehely,1967; Roy,1978) exists giving rise to the concept of zero-velocity surfaces. The technique is equally applicable to the case of a planet of negligible mass in an orbit about both massive bodies or in an orbit about the more massive of the two bodies as well as the case of the satellite in orbit about the less massive of the two bodies.

In recent years use has been made of the integrals of angular momentum and energy in the general problem of three-bodies by a number of authors including Bozis (1976), Golubev (1968), Marchal and Saari (1975), Smale (1970) and Zare (1976, 1977). Essentially the approach is one of bifurcation theory. Zare used the product c^2H, in which c is the angular momentum and H the energy of a coplanar three-body system. He showed that statements could be made about the stability of any given three-body system in terms of the possibility or impossibility of an exchange between bodies i.e. an *interplay* situation (see Szebehely, 1971) by considering the value of c^2H for that system in a fashion similar to the zero-velocity curves of the coplanar restricted three-body problem. (see Szebehely, 1977, 1978; Szebehely and McKenzie, 1977a,b; Szebehely and Zare, 1977). The method is applicable to three-body systems where the bodies are arranged in the following

fashion: two of the masses move in disturbed Keplerian orbits with respect to their common mass-centre while the third mass moves in an orbit *outwith and not crossing* the orbits of the former two masses. For values of c^2H less than a certain critical value it is found that the arrangement of binary and external third mass is assured permanence, it being impossible for the third mass to come between the components of the binary or one of the binary components to recede beyond the external mass. The status quo of the system will then be maintained.

2.2 The Surfaces of Zero Velocity in the Circular Restricted Three-Body Problem

As a step towards understanding the general problem of three-bodies a great deal of study has been devoted to the circular restricted three-body problem. The problem is defined as follows. Two masses - the primaries - move in undisturbed circular orbits about their common mass-centre. A third body - a particle of infinitesimal mass - moves under the influence of these two, its mass however being so small as not to disturb the primaries' orbits. The problem is: given the position and velocity of the particle at any instant, with respect to the primaries, to find its position and velocity at any subsequent time.

The complexity of the problem has thus been reduced from the solution of nine second-order differential equations to the solution of three such equations i.e. a reduction from 18th to 6th order has been effected. (A further reduction to a system of the 4th order may be gained through consideration of the coplanar circular restricted three-body problem which is, as the name suggests, the case when the particle moves in the plane of the primaries' orbits). All the ten previously available integrals of the general problem have been lost in this process. However, Jacobi (1836) showed the existence of an integral of the motion which is of much use in considering the stability of the orbit of the particle. Stability here implies that the particle may not move from the vicinity of one of the primaries to the other i.e. *interplay* is forbidden.

Let the primaries P_1 and P_2 (see Fig.2.1) be in circular orbits

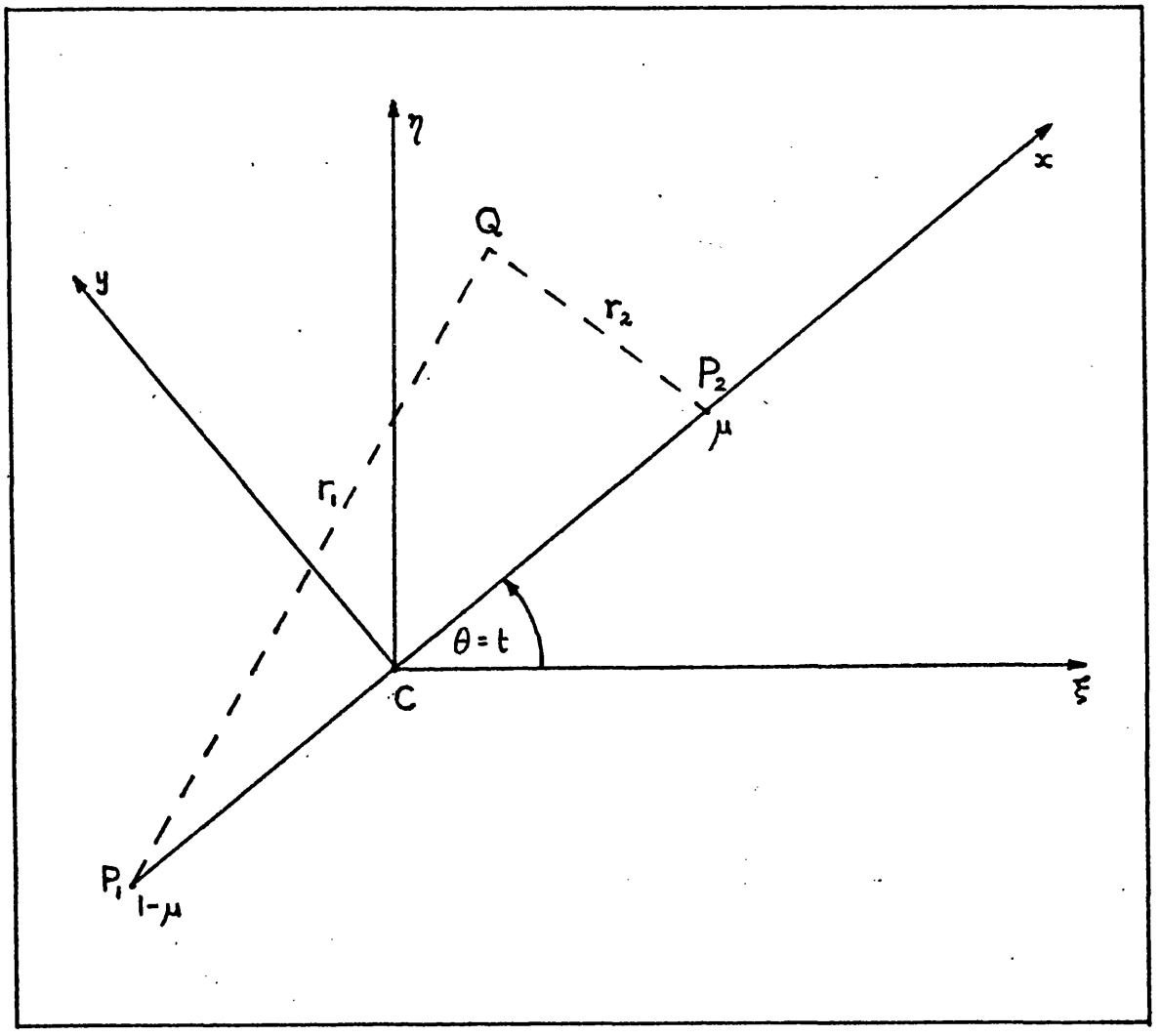

Figure 2.1 The primaries, denoted P_1 and P_2, move in circular orbits with respect to their common mass-centre C. The masses of P_1 P_2 are m_1 and m_2 such that $m_1 : m_2 = 1-\mu : \mu$ where $\mu \leq \frac{1}{2}$. A particle of infinitesimal mass, denoted Q, moves under the influence of the primaries but does not affect their motion. The axes ξ, η, ζ constitute a non-rotating coordinate system with its origin at C. The x,y,z axes rotate about the z-axis such that P_1 and P_2 always lie on the x-axis. The ζ-axis and z-axis are not shown in the diagram but are at "right angles to the page".

about their common mass-centre C and further let the ratio of their masses $m_1 : m_2$ be denoted by $1-\mu : \mu$ where $\mu \leq \frac{1}{2}$. Since they are executing circular orbits their separation is constant, which constant we will take as the unit of distance. Further, let the unit of time be chosen so that G, the constant of gravitation, is unity. Then since we have

$$n^2 a^3 = G(m_1 + m_2) \qquad (1)$$

it follows that the angular velocity of the bodies is also unity.

The equations of motion of a particle Q, under the gravitational forces of P_1 and P_2, are now required. Let P_1 and P_2 have coordinates (ξ_1, η_1, ζ_1) and (ξ_2, η_2, ζ_2) in a *non-rotating* coordinate system with its origin at C. Let the coordinates of Q be (ξ, η, ζ), then the equations of motion are

$$\ddot{\xi} = (1-\mu)\frac{\xi_1-\xi}{r_1^3} + \mu\frac{\xi_2-\xi}{r_2^3} \qquad (2)$$

$$\ddot{\eta} = (1-\mu)\frac{\eta_1-\eta}{r_1^3} + \mu\frac{\eta_2-\eta}{r_2^3} \qquad (3)$$

$$\ddot{\zeta} = (1-\mu)\frac{\zeta_1-\zeta}{r_1^3} + \mu\frac{\zeta_2-\zeta}{r_2^3} \qquad (4)$$

where

$$\left.\begin{aligned} r_1 &= \left[(\xi_1-\xi)^2 + (\eta_1-\eta)^2 + (\zeta_1-\zeta)^2\right]^{\frac{1}{2}} \\ r_2 &= \left[(\xi_2-\xi)^2 + (\eta_2-\eta)^2 + (\zeta_2-\zeta)^2\right]^{\frac{1}{2}} \end{aligned}\right\} \qquad (5)$$

and (ξ_1, η_1, ζ_1) and (ξ_2, η_2, ζ_2) are known functions of time. Without loss of generality we may suppose the motion of the primaries to be wholly in the $\xi\eta$-plane, so that $\zeta_1 = \zeta_2 = 0$.

A new set of coordinates x,y,z is now defined with the same origin C as the previous set and the z-axis coinciding with the ζ-axis, but *rotating* about the z-axis at an angular velocity unity such that the primaries always lie on the x-axis. P_1 then lies at a point $x_1 = -\mu$, $y_1 = z_1 = 0$ and P_2 at $x_2 = 1 - \mu$, $y_2 = z_2 = 0$. The equations of motion of the particle must now be transformed into the new coordinate system.

If θ is the angle ξCx at any time t then the relationship between (ξ,η,ζ) and (x,y,z) is

$$\begin{bmatrix}\xi\\ \eta\\ \zeta\end{bmatrix} = \begin{bmatrix}\cos\theta & -\sin\theta & 0\\ \sin\theta & \cos\theta & 0\\ 0 & 0 & 1\end{bmatrix}\begin{bmatrix}x\\ y\\ z\end{bmatrix} \qquad (6)$$

However it is noted that since $n = d\theta/dt = 1$ in the chosen units then we have $\theta \equiv t$. More exactly, $\theta = t +$ constant, however the constant may be set zero without loss of generality. Using Equation (6) the derivatives $\ddot{\xi}$, $\ddot{\eta}$, $\ddot{\zeta}$ may be obtained in terms of x,y,z, and their first and second derivatives. Substituting the results for these into Equations (2), (3) and (4) we obtain

$$(\ddot{x} - 2\dot{y} - x)\cos t - (\ddot{y} + 2\dot{x} - y)\sin t = \left[(1-\mu)\frac{x_1 - x}{r_1^3} + \mu\frac{x_2 - x}{r_2^3}\right]\cos t + \left[\frac{1-\mu}{r_1^3} + \frac{\mu}{r_2^3}\right]\sin t \qquad (7a)$$

$$(\ddot{x} - 2\dot{y} - x)\sin t + (\ddot{y} + 2\dot{x} - y)\cos t = \left[(1-\mu)\frac{x_1 - x}{r_1^3} + \mu\frac{x_2 - x}{r_2^3}\right]\sin t - \left[\frac{1-\mu}{r_1^3} + \frac{\mu}{r_2^3}\right]\cos t \qquad (7b)$$

and

$$\ddot{z} = -\left[\frac{1-\mu}{r_1^3} + \frac{\mu}{r_2^3}\right]z\ , \qquad (7c)$$

where

$$\left.\begin{aligned} r_1 &= \left[(x_1-x)^2 + y^2 + z^2\right]^{\frac{1}{2}}\\ r_2 &= \left[(x_2-x)^2 + y^2 + z^2\right]^{\frac{1}{2}}\\ x_1 &= -\mu\\ \text{and}\quad x_2 &= 1-\mu\ . \end{aligned}\right\} \qquad (8)$$

Multiplying Equation (7a) by cost and (7b) by sint and adding, Equation (9) is obtained. Similarly Equation (10) may be got by multiplication of (7a) by (- sint) and adding (7b) multiplied by cost. These two together with Equation (7c) comprise the equations of motion of the particle Q in a rotating coordinate frame viz.

$$\ddot{x} - 2\dot{y} = \frac{\partial U}{\partial x} \qquad (9)$$

$$\ddot{y} + 2\dot{x} = \frac{\partial U}{\partial y} \qquad (10)$$

$$\ddot{z} = \frac{\partial U}{\partial z} \qquad (11)$$

where $$U = \tfrac{1}{2}(x^2 + y^2) + \frac{1-\mu}{r_1} + \frac{\mu}{r_2} \qquad (12)$$

$$r_1 = \left[(x_1 - x)^2 + y^2 + z^2\right]^{\frac{1}{2}}$$

$$r_2 = \left[(x_2 - x)^2 + y^2 + z^2\right]^{\frac{1}{2}}$$

$$x_1 = -\mu$$

and $$x_2 = 1-\mu .$$

Multiplying Equations (9), (10) and (11) by $\dot{x}$, $\dot{y}$ and $\dot{z}$ respectively we obtain

$$\dot{x}\ddot{x} + \dot{y}\ddot{y} + \dot{z}\ddot{z} = \frac{\partial U}{\partial x}\cdot\dot{x} + \frac{\partial U}{\partial y}\cdot\dot{y} + \frac{\partial U}{\partial z}\cdot\dot{z} \qquad (13)$$

which is a perfect differential since $U \neq U(t)$. Integrating Equation (13) once we obtain C, *Jacobi's Integral*,

$$C = x^2 + y^2 + 2\frac{(1-\mu)}{r_1} + \frac{2\mu}{r_2} - (\dot{x}^2 + \dot{y}^2 + \dot{z}^2), \qquad (14)$$

or

$$C = 2U - (\dot{x}^2 + \dot{y}^2 + \dot{z}^2). \qquad (15)$$

Since $\dot{x}^2 + \dot{y}^2 + \dot{z}^2$ is clearly positive for real values of $\dot{x}$, $\dot{y}$ and $\dot{z}$ it is obvious that $C \leqslant 2U$ at all times.

Supposing now that the particle's velocity is zero then we have

$$x^2 + y^2 + 2\frac{(1-\mu)}{r_1} + \frac{2\mu}{r_2} = C . \qquad (16)$$

Equation (16) defines a set of surfaces in x,y,z coordinate space for any given constant C. The significance of these surfaces is due to the fact that motion of the particle can only occur in the regions where $2U \geqslant C$ (see Equation (15)). Thus boundaries have been set in x,y,z coordinate space which limit the regions of space within which

the particle, with given Jacobi Integral, C, can be at any time. We now proceed to briefly examine the nature of these surfaces.

If we consider the intersection of the above mentioned surfaces with the x,y-plane a set of curves are obtained giving limits on the regions a particle can occupy in the coplanar case of the circular restricted three-body problem (see Fig. 2.2(a) - (f)). The regions where the particle is forbidden to move are shaded. The reason for the shape of these curves may be explained as follows.

Commencing with $C = C_1 >> 1$ it may be seen from Equation (16) that such a large value of C can be obtained when $x^2 + y^2$ is large *or* either of r_1, r_2 is small. The former of these results in the large external circle of the forbidden region. The latter result in two ovals about the masses m_1 and m_2, the larger oval being around the larger mass (Fig. 2.2(a)).If a particle then has initial conditions resulting in a value of C equal to C_1 then it will be trapped inside one of the ovals or outside the external circle for all time. If C is decreased to C_2 it is found that the two ovals have a common tangent at the point L_2 (Fig.2.2(b)). Further reduction to $C = C_3$ results in the ovals coalescing to form a "dumb-bell" shape (see Fig.2.2(c)). In this situation the particle, if inside the "dumb-bell", is free to move between the primaries; if the particle is outside the external circle then the situation is as before. As C decreases, to C_4 say (Fig. 2.2(d)), then the dumb-bell has a common tangent with the external region at a point L_3. This point is situated to the far side of m_2 away from m_1. When this join at L_3 "breaks" as C is decreased the particle is free to move between the primaries and also to wander into the external region and vice versa. Continuing to C_5 (Fig.2.2(e)) a similar joining occurs at L_1 to the outside of the larger mass m_1 with the neck joining the inner region to the outer via L_3 increasing in size. At $C = C_6$ the size of the forbidden regions has reduced still further leaving only "islands" about the points L_4 and L_5 (Fig. 2.2(f)). These islands will vanish at the L_4 and L_5 points as C is decreased still further. Sections through the zero-velocity surfaces in the xz- and yz- planes are shown in Fig.2.3(a,b) for the same values of Jacobi's integral.

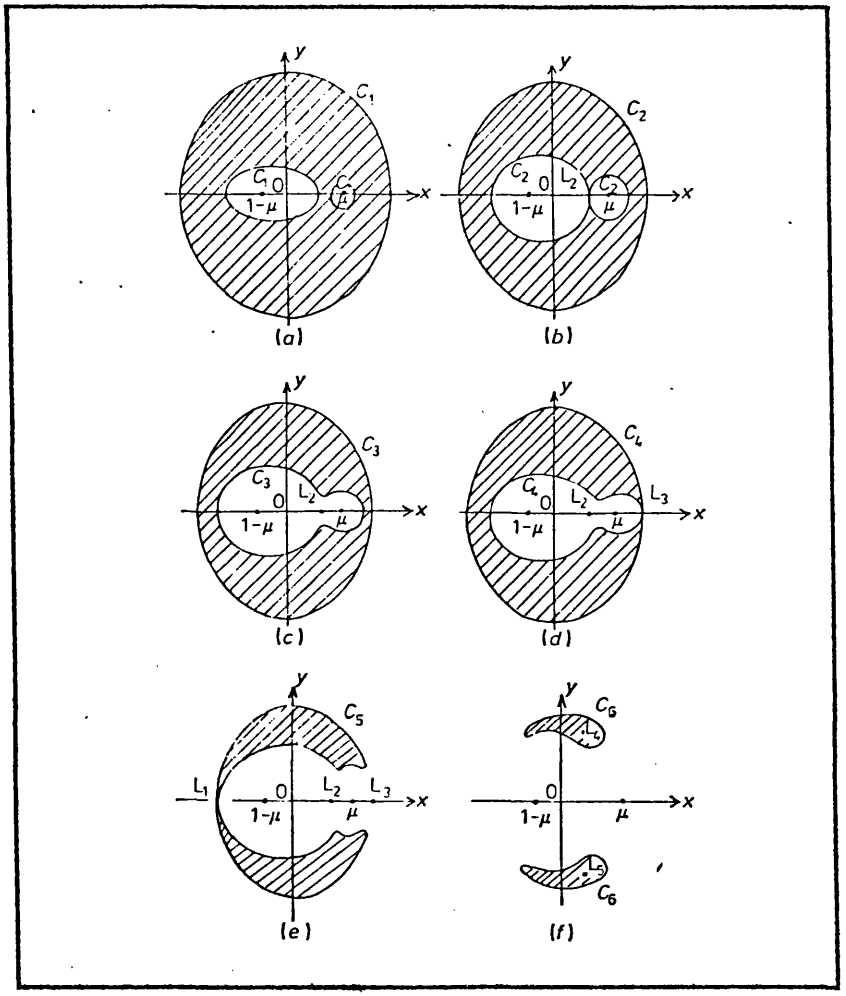

Figures 2.2 The zero-velocity curves of the circular restricted three-body problem.

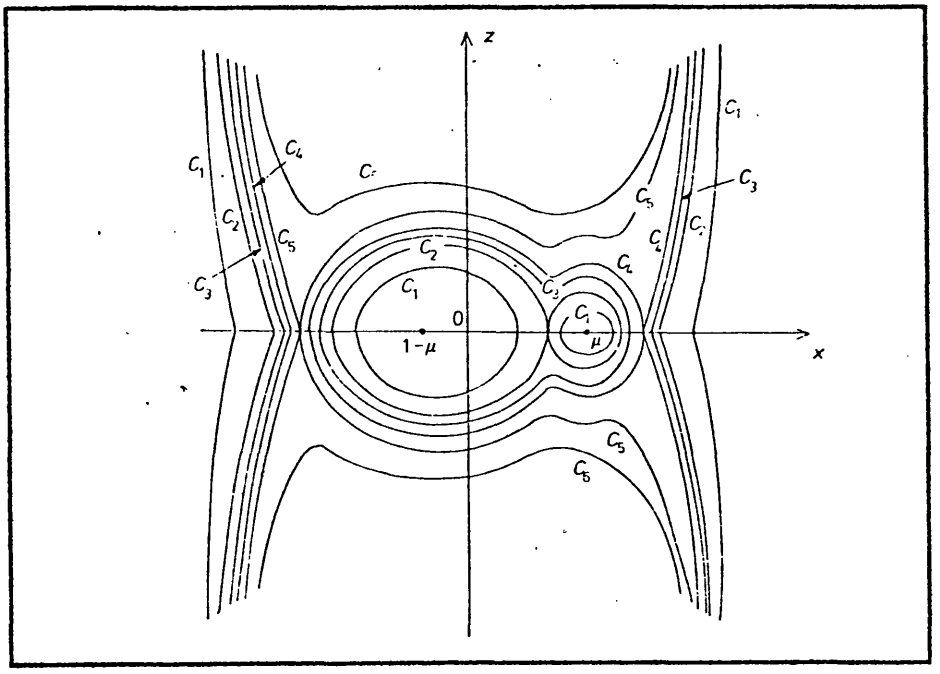

Figure 2.3(a) Section through the zero-velocity surfaces of the circular restricted three-body problem in the xz-plane.

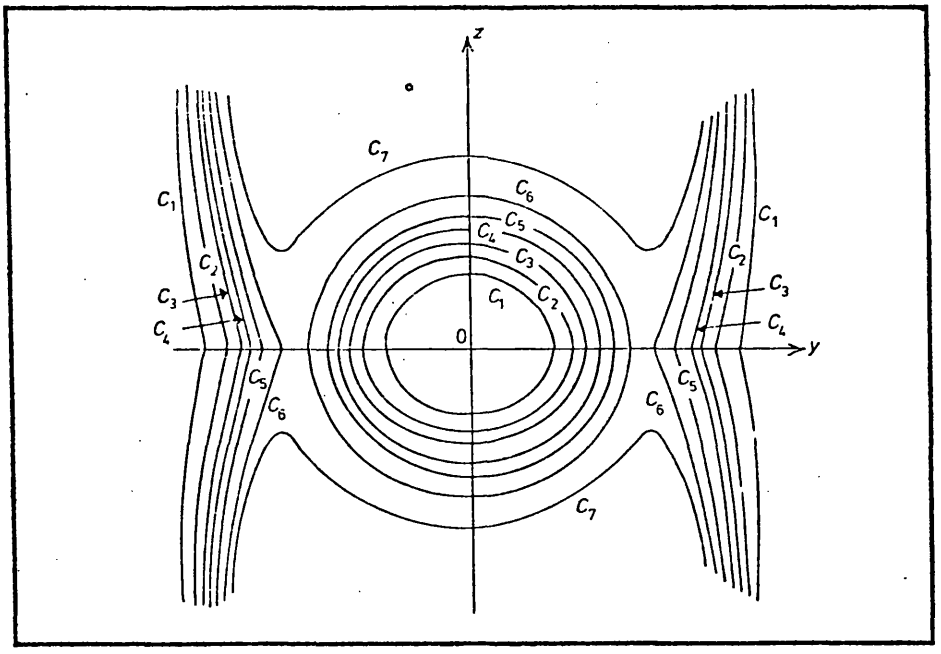

Figure 2.3(b) Section through the zero-velocity surfaces of the circular restricted three-body problem in the yz-plane.

Now the points L_1, L_2, L_3, L_4, L_5 are double points where the partial derivatives of the function

$$f = x^2 + y^2 + 2\frac{(1-\mu)}{r_1} + 2\frac{\mu}{r_2} - C = 2U - C$$

vanish. Hence at these points $\partial U/\partial x = \partial U/\partial y = \partial U/\partial z = 0$ which since $\dot{x} = \dot{y} = \dot{z} = 0$ by definition on the zero velocity curves results through Equations (9), (10) and (11) in $\ddot{x}$, $\ddot{y}$, $\ddot{z}$ being zero. There are no resultant forces on the particle and these points are the familiar Lagrange equilibrium solutions.

The importance of the Lagrange solutions in stability considerations derives from the fact that the values C_2, C_4, C_5 determine whether the zero-velocity curves are open or closed in any given system. There are three cases to consider depending upon whether the particle is in orbit about one or other primary or about both.

(i) $P_1 - Q - P_2$ - This is the case of a (massless) planet in an inferior orbit about the larger star in a double star system ($\mu \lesssim \frac{1}{2}$) or in an inferior orbit, with a disturbing planet, about the Sun ($\mu << \frac{1}{2}$). The particle is orbiting m_1 and if its initial conditions dictate a value of C greater than or equal to C_2 then it is forever trapped within the zero-velocity oval about m_1. If $C_4 \leq C < C_2$ then it could transfer to an orbit about m_2 or an interplay situation could arise whereby the particle alternates between m_1 and m_2. When $C < C_4$ then the particle may escape from the vicinity of the primaries altogether.

(ii) $P_2 - Q - P_1$ - This is the case of a (massless) satellite in orbit about a planet ($\mu << \frac{1}{2}$) or a (massless) planet in orbit about the lesser component of a binary star system ($\mu \lesssim \frac{1}{2}$). The discussion of this case is identical to case (i).

(iii) $P_1 - P_2 - Q$ - Here the (massless) body is in a superior orbit about either a double star system ($\mu \lesssim \frac{1}{2}$) or a Sun-Planet system ($\mu << \frac{1}{2}$). It is only necessary for stability in this case that $C \geq C_4$. Since the particle is outside the external circle it is not important for its stability that the ovals about m_1 and m_2 should be separate. If however $C < C_4$ then the particle may enter the region of the primaries.

It is clearly possible to use the initial conditions $x, y, z, \dot{x}, \dot{y}, \dot{z}$ to determine whether the zero-velocity surfaces are open or closed.

However, if instead we express the rotating coordinates in terms of the elements of some osculating orbit about either m_1 (case (i)), m_2 (case (ii)) or m_1 and m_2 (case (iii)) we may determine limiting values of the semi-major axis of the particles orbit, for particular values of μ and the other orbital parameters e.g. eccentricity and inclination, such that an interplay situation cannot arise.

Clearly then this would give us the opportunity of immediately recognizing whether real three-body systems which included a body of negligible mass were stable in the sense that exchanges (of the particle) between bodies was not possible. This may be applied to many cases apart from the Earth-Moon-Sun system e.g. Jupiter-Satellite-Sun, Sun-Asteroid-Jupiter, etc. In *all* these cases however the eccentricity of the primaries' orbit is neglected.

2.3 A Discussion of the Elliptic Restricted Three-Body Problem

In the previous section it was demonstrated how the zero-velocity surfaces of the circular restricted three-body problem could be used to determine the stability of orbits when one of the masses in a three-body system is negligible. The technique has been used widely in other investigations. Hagihara (1952) applied the Jacobi integral to the satellites in the Solar System other than the Moon. There is a sharp cut-off in asteroid numbers beyond semi-major axes of 4 A.U.: Kuiper (1956) explained this by considering that asteroids within this semi-major axis (given they have orbits of small eccentricity and inclination) are enclosed within the zero-velocity oval about the Sun (cf. Figure 2.2(a)). Hence he concluded that these asteroids must always have been there since the time when the Jovian and Solar masses stabilized at their present values. The stability of planetary orbits in binary star systems has been studied by Huang (1960). The zero-velocity surfaces have been used extensively in the study of the transfer of matter between the components of a close binary star (cf. Kopal, 1956; Strohmeier, 1972; Roy, 1978). Szebehely and Evans (1980), discussing the capture of the Moon by the Earth, concluded, on the basis of a circular restricted three-body model, that a reduction of around 37% in the Solar mass is required to "open" the zero-velocity curves thus allowing capture to occur.

However, all these applications and the results derived therefrom are valid only inasmuch as the circular restricted three-body problem is a valid model of the system under investigation. Since in general real systems exhibit eccentricities in their orbits it might be supposed that a better model would be the elliptic restricted three-body problem. This problem is identical to the circular case excepting that the primaries' relative orbit is now a Keplerian ellipse. Formal expressions for the Jacobi integral and the angular momentum integrals of the elliptic restricted problem were derived by Ovenden and Roy (1960). It was shown that certain functions arose in the expressions for these integrals which were dependant upon time through the coordinates of the infinitesimal particle. Thus although at some initial epoch $t = 0$ a result could be derived showing the system to be stable this result could not be applied over arbitrarily long time scales. At a later time $t = t_1$ the zero-velocity surfaces may bear no similarity to the initial set of surfaces. In summary it may be said that although the initial conditions allow the construction of a set of zero-velocity surfaces which will be little different from the surfaces as obtained through application of the circular case if the eccentricity of the primaries' relative orbit is small, this does not allow one to identify the surfaces of the circular problem with those of the elliptic problem for all time. In order to make the comparison the values of the above-mentioned time dependant functions would have to be known for all time.

Hill in his lunar theory (1905) pointed out that his result on the stability of the Moon's orbit about the Earth rested on neglecting the eccentricity of the Earth's orbit about the Sun. He went on to obtain the actual motion of the Moon from an intermediate orbit - a periodic solution of the circular restricted problem. This is essentially analogous to obtaining the values of the unknown time dependant functions.

No additional information can therefore be gained through the use of the zero-velocity surfaces of the circular restricted three-body model since it is as easy to obtain the positions of the particle at subsequent times as to evaluate the unknown time dependant functions. No rigorous results concerning the satellites of the Solar System may be derived from the circular restricted three-body problem; asteroids

may wander from the asteroid belt due to the eccentricity of Jupiter's orbit; it is not necessary to invoke a loss in solar mass of 37% to allow capture of the Moon since the Earth's orbit is eccentric, etc. Since binary stars have orbits of considerable eccentricity it is therefore necessary to resort to means other than the circular restricted three-body problem to study them.

2.4 Zero-Velocity Curves in the Coplanar General Three-Body Problem

Zare (1976) established regions of possible motion for dynamical systems possessing time-independent Hamiltonians or possessing Hamiltonians reducible to that form by means of integrals of the motion using only extended point transformations. He applied his method to the coplanar general three-body problem and derived zero-velocity curves which may be used to make statements concerning possible configurations of the three-bodies applicable for all time. The parameters found to control the opening and closing of the zero-velocity curves are the masses and the integrals of angular momentum and energy. The derivation of these zero-velocity curves is given in the following pages.

Following Whittaker (1904), the motion of three bodies is supposed to take place in a plane: it is required to reduce the equations of motion of the system to a Hamiltonian system of the lowest possible order.

Let the masses be denoted m_1, m_2, m_3 and let their coordinates with respect to fixed axes in the plane of motion of the bodies be (q_1,q_2), (q_3,q_4) and (q_5,q_6) respectively. The momenta p_i are defined as follows

$$p_i = m_k \dot{q}_i \qquad i = 1,....6 \tag{17}$$

where k denotes the greatest integer in $\frac{1}{2}(i+1)$.
The equations of motion are

$$\dot{q}_i = \frac{\partial H}{\partial p_i} \quad , \quad \dot{p}_i = -\frac{\partial H}{\partial q_i} \qquad i = 1,...,6 \tag{18}$$

where

$$H = \frac{1}{2m_1}(p_1^2 + p_2^2) + \frac{1}{2m_2}(p_3^2 + p_4^2) + \frac{1}{2m_3}(p_5^2 + p_6^2) - \\ - \frac{G\, m_1\, m_2}{r_{12}} - \frac{G\, m_2 m_3}{r_{23}} - \frac{G\, m_3 m_1}{r_{31}} \tag{19}$$

is the Hamiltonian of the system,

$$r_{12} = \left[(q_1 - q_3)^2 + (q_2 - q_4)^2 \right]^{\frac{1}{2}} \qquad (20a)$$

$$r_{23} = \left[(q_3 - q_5)^2 + (q_4 - q_6)^2 \right]^{\frac{1}{2}} \qquad (20b)$$

and

$$r_{31} = \left[(q_5 - q_1)^2 + (q_6 - q_2)^2 \right]^{\frac{1}{2}} . \qquad (20c)$$

Equations (18) are a system of the 12th order. By means of the integrals of motion of the mass-centre the order of the system may be reduced to eight. The extended point transformation defined by the equations

$$q_i = \frac{\partial W}{\partial p_i} \quad , \quad p_i' = \frac{\partial W}{\partial q_i'} \qquad i = 1,\ldots,6 \quad (21)$$

where

$$W = p_1 q_1' + p_2 q_2' + p_3 q_3' + p_4 q_4' + (p_1 + p_3 + p_5) q_5' + (p_2 + p_4 + p_6)\, q_6' \qquad (22)$$

is performed on the variables. In this notation (q_1', q_2') are the coordinates of m_1 relative to axes through m_3 parallel to the original fixed axes, (q_3', q_4') are the coordinates of m_2 with respect to the same axes and (q_5', q_6') are the coordinates of m_3 with respect to the original set of axes. Now (p_1', p_2'), (p_3', p_4') are the components of momentum of m_1 and m_2 respectively, (p_5', p_6') being the components of momentum of the whole system.

On substituting the new variables it is found that q_5' and q_6' do not appear in the expression, they are therefore ignorable coordinates. The corresponding integrals, the components of momentum of the mass-centre of the system, are

$$p_5' = \text{constant} \quad ; \quad p_6' = \text{constant}.$$

Without loss of generality we may assume $p_5' = p_6' = 0$, that is the coordinates and momenta are expressed with respect to the (stationary)

mass-centre of the system. Removing the accents from the new variables the equations of motion become

$$\dot{q}_i = \frac{\partial H}{\partial p_i} \quad , \quad \dot{p}_i = -\frac{\partial H}{\partial q_i} \qquad i = 1,\ldots,4 \tag{23}$$

where

$$H = \left(\frac{1}{2m_1} + \frac{1}{2m_3}\right)(p_1^2 + p_2^2) + \left(\frac{1}{2m_2} + \frac{1}{2m_3}\right)(p_3^2 + p_4^2) + \frac{1}{m_3}(p_1p_3 + p_2p_4)$$

$$- \frac{G\, m_1m_2}{r_{12}} - \frac{G\, m_2m_3}{r_{23}} - \frac{G\, m_3m_1}{r_{31}} \tag{24}$$

$$r_{12} = \left[(q_1 - q_3)^2 + (q_2 - q_4)^2\right]^{\frac{1}{2}} \tag{25a}$$

$$r_{23} = \left[q_3^2 + q_4^2\right]^{\frac{1}{2}} \tag{25b}$$

and

$$r_{31} = \left[q_1^2 + q_2^2\right]^{\frac{1}{2}} \tag{25c}$$

A further extended point transformation defined by

$$q_i = \frac{\partial W}{\partial p_i} \quad , \quad p_i' = \frac{\partial W}{\partial q_i'} \qquad i = 1,\ldots,4 \tag{26}$$

where

$$W = p_1q_1' \cos q_4' + p_2q_1' \sin q_4' + p_3(q_2' \cos q_4' - q_3' \sin q_4')$$

$$+ p_4(q_2' \sin q_4' + q_3' \cos q_4') \tag{27}$$

is performed on the system. The interpretation of the new coordinates is as follows: q_1' is the distance $|\vec{m_1m_3}|$; q_2' and q_3' are projections of $\vec{m_2m_3}$ on and perpendicular to $\vec{m_1m_3}$ respectively; q_4' is the angle between $\vec{m_3m_1}$ and the original x-axis. The new components of momenta are as follows: p_1' is the component of m_1 along $\vec{m_3m_1}$; p_2' and p_3' are the components of m_2 parallel and perpendicular to $\vec{m_3m_1}$; p_4' is the angular momentum of the system.

The equations of motion, when expressed in terms of the new variables are

$$\dot{q}_i' = \frac{\partial H}{\partial p_i'} \quad , \quad \dot{p}_i' = -\frac{\partial H}{\partial q_i'} \quad i = 1,\ldots,4 \qquad (28)$$

where

$$H = \left(\frac{1}{2m_1} + \frac{1}{2m_3}\right)\{p_1'^2 + \frac{1}{q_1'^2}(p_3'q_2' - p_2'q_3' - p_4')^2\} + \left(\frac{1}{2m_2} + \frac{1}{2m_3}\right)(p_2'^2 + p_3'^2)$$

$$+ \frac{1}{m_3}\{p_1'p_2' - \frac{p_3'}{q_1'}(p_3'q_2' - p_2'q_3' - p_4')\} - \frac{G m_1 m_2}{r_{12}} - \frac{G m_2 m_3}{r_{23}}$$

$$- \frac{G m_3 m_1}{r_{31}} \qquad (29)$$

$$r_{12} = [(q_1' - q_2')^2 + q_3'^2]^{\frac{1}{2}} \qquad (30a)$$

$$r_{23} = [q_2'^2 + q_3'^2]^{\frac{1}{2}} \qquad (30b)$$

and

$$r_{31} = q_1' \, . \qquad (30c)$$

Since q_4' is not contained in the expression for H, q_4' is an ignorable coordinate. The corresponding integral is $p_4' =$ constant (c say), which may be interpreted as the angular momentum of the system. Removing the accents on the variables we than have a system of the sixth order viz.

$$\dot{q}_i = \frac{\partial H}{\partial p_i} \quad , \quad \dot{p}_i = -\frac{\partial H}{\partial q_i} \quad i = 1,2,3 \qquad (31)$$

where

$$H = \left(\frac{1}{2m_1} + \frac{1}{2m_3}\right)\{p_1^2 + \frac{1}{q_1^2}(p_3q_2 - p_2q_3 - c)^2\} + \left(\frac{1}{2m_2} + \frac{1}{2m_3}\right)(p_2^2 + p_3^2)$$

$$+ \frac{1}{m_3}\{p_1p_2 - \frac{p_3}{q_1}(p_3q_2 - p_2q_3 - c)\} - \frac{G m_1 m_2}{r_{12}} - \frac{G m_2 m_3}{r_{23}}$$

$$- \frac{G m_3 m_1}{r_{31}} \qquad (32)$$

and r_{12}, r_{23}, r_{31} are as given by Equations (30) removing the accents.

Having followed this procedure Zare (1976) then introduced the variables η and z as follows

$$\eta = x + iy = \frac{q_2}{q_1} + i\,\frac{q_3}{q_1} \qquad (33a)$$

$$z = q_1 \qquad (33b)$$

and $i = \sqrt{-1}$.

This set of variables specifies the scale (z) and configuration (η) of the triangle formed by the three bodies. Zare further stated and proved the following theorem:

"*If* $H(q,p)$ *is a quadratic polynomial in the momenta,* p, *and its Hessian,* $\partial^2 H(q,p)/\partial p^2$, *is positive definite, then there is a unique function* $H^*(q)$ *such that for all* $q \in \mathbb{R}^n$

$$H^*(q) \lesssim H(q,p) \qquad (T1)$$

and the projection of the submanifold of the state of motion for a given value of H on the configuration space is given by

$$M(q) = H - H^*(q) \gtrsim 0. \qquad " \qquad (T2)$$

In this theorem Equation (T1) is analogous to the result in the circular restricted three-body problem that $2U \gtrsim C$ at all times and Equation (T2) is analogous to the result (cf. Equation (15)) that

$$(\dot{x}^2 + \dot{y}^2 + \dot{z}^2) = 2U - C \gtrsim 0 .$$

where C (a constant) takes the place of H (also constant), and 2U the place of $H^*(q)$.

Since the Hamiltonian defined in Equations (32) and (30a,b,c) does not depend on the time explicitly and satisfies the requirements of the above-quoted theorem the equations

$$\frac{\partial H}{\partial p_i} = 0 \qquad i = 1,2,3 \qquad (34)$$

have a unique solution, which may be expressed, in terms of the variables defined in Equations (33), as follows:

$$p_1 = \frac{c\psi y}{z} \quad ; \quad p_2 = -\left(1 + \frac{m_3}{m_1}\right)\frac{c\psi y}{z} \quad ; \quad p_3 = \frac{c\psi}{z}\left(1 - \left(1 + \frac{m_3}{m_1}\right)x\right) \qquad (35)$$

where

$$\psi = \left[\left(1 + \frac{m_3}{m_1}\right)(x^2 + y^2) - 2x + \left(1 + \frac{m_3}{m_2}\right) \right]^{-1} . \qquad (36)$$

By constructing $H^*(q)$ and forming $M(q)$ as given in Equation (T2) it may then be shown that the regions of possible motion are given by

$$Hz^2 + G\, b_o(\eta) z - \frac{c^2 M}{2} c_o(\eta) \geq 0 \qquad (37)$$

where

$$\left.\begin{aligned} M &= m_1 + m_2 + m_3 \\ b_o(\eta) &= m_3 m_1 + \frac{m_2 m_3}{|\eta|} + \frac{m_1 m_2}{|\eta - 1|} \\ c_o(\eta) &= \{ m_3 m_1 + m_2 m_3 |\eta|^2 + m_1 m_2 |\eta - 1|^2 \}^{-1} \end{aligned}\right\} \qquad (38)$$

and it may be noted that $c_o(\eta)$ and $b_o(\eta)$ are both positive functions.

The Equation (37), along with Equations (38), represents regions in the three-dimensional space (x,y,z) where motion is possible. These regions may be projected onto the complex η-plane in order to obtain limits on the possible configurations irrespective of the scale of the system. For a region of possible motion we require that the scale, z , be a real quantity, therefore, forming the discriminant of Equation (37), it is required that

$$\Delta(\eta) = G^2 b_o^2(\eta) + 2M c^2 H c_o(\eta) \geq 0 . \qquad (39)$$

It is in this Equation that the important parameter c^2H first appears.

Considering Equation (39) it may be seen that if $H \geq 0$ then all configurations, η, are possible since $\Delta(\eta) > 0$ in any case. If $H > 0$ then the scale is restricted by

$$z \geq \frac{-G\, b_o(\eta) + \{\Delta(\eta)\}^{\frac{1}{2}}}{2H} , \qquad (40)$$

in the case H = 0 there is a restriction that

$$z \geq \frac{c^2 M c_o(\eta)}{2 G b_o(\eta)} \quad . \tag{41}$$

The interesting cases, as far as stability is concerned, arise when H < 0.. Here all configurations are not possible since $\Delta(\eta)$ may be positive or negative depending on the values of c^2H and the masses. The scale is restricted in the following fashion

$$\left.\begin{aligned} & z_1 \leq z \leq z_2 \ , \\ \text{where} \quad & z_1 = \frac{- G b_o(\eta) + \{\Delta(\eta)\}^{\frac{1}{2}}}{2H} \\ \text{and} \quad & z_2 = \frac{- G b_o(\eta) - \{\Delta(\eta)\}^{\frac{1}{2}}}{2H} \end{aligned}\right\} \tag{42}$$

are the roots of the quadratic Equation (37). It is now possible to plot in the complex η-plane the curves for which $\Delta(\eta) = 0$. It is found that this divides the complex η -plane in a similar fashion to the separation of the x,y-plane of the restricted problem by the zero-velocity curves into regions where motion is or is not possible. There are regions where $\Delta(\eta)$ is negative and consequently such configurations are forbidden and regions where $\Delta(\eta)$ is positive allowing these ranges of configuration.

The Figures 2.4(a-c) reproduced from Zare's paper show how the regions of possible configurations change as c^2H is increased from initially large negative values. As the value of c^2H is increased from $-\infty$ it is found that triply, doubly, simply and un-connected forbidden regions appear. A triply connected region is sufficient to preclude an exchange of bodies occurring and in some cases only a doubly connected region would be necessary. The critical values of c^2H where the zero-velocity curves open or close are those of the collinear equilibrium solutions (asin the case of the restricted problem) and by considering the value of c^2H for a given system it may be demonstrated whether an exchange of bodies is possible or not.

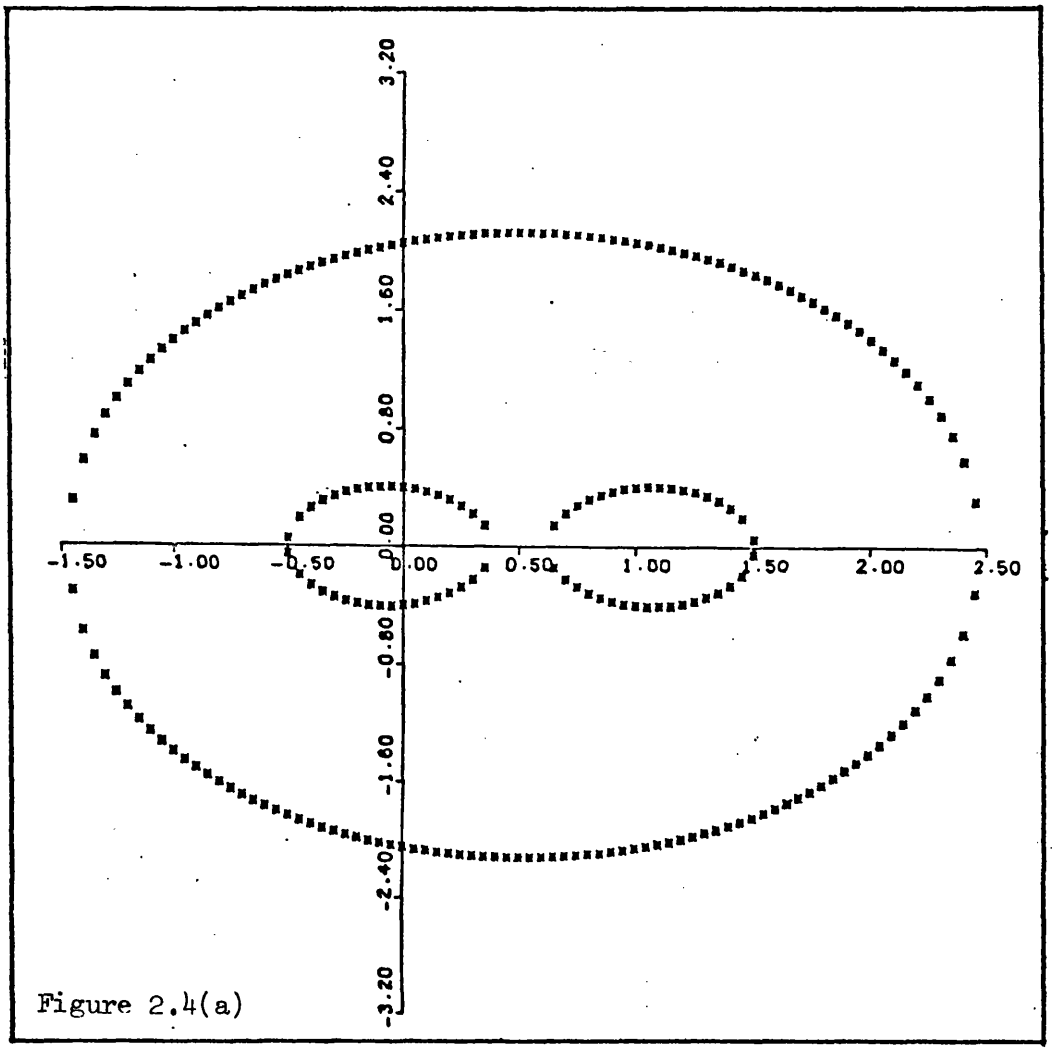

Figures 2.4 Regions of forbidden configurations for G = M = 1, $m_1 = 2m_2 = m_3 = 0.4$, (a) $c^2H = -0.025$, (b) $c^2H = -0.0225$ and (c) $c^2H = -0.0215$.

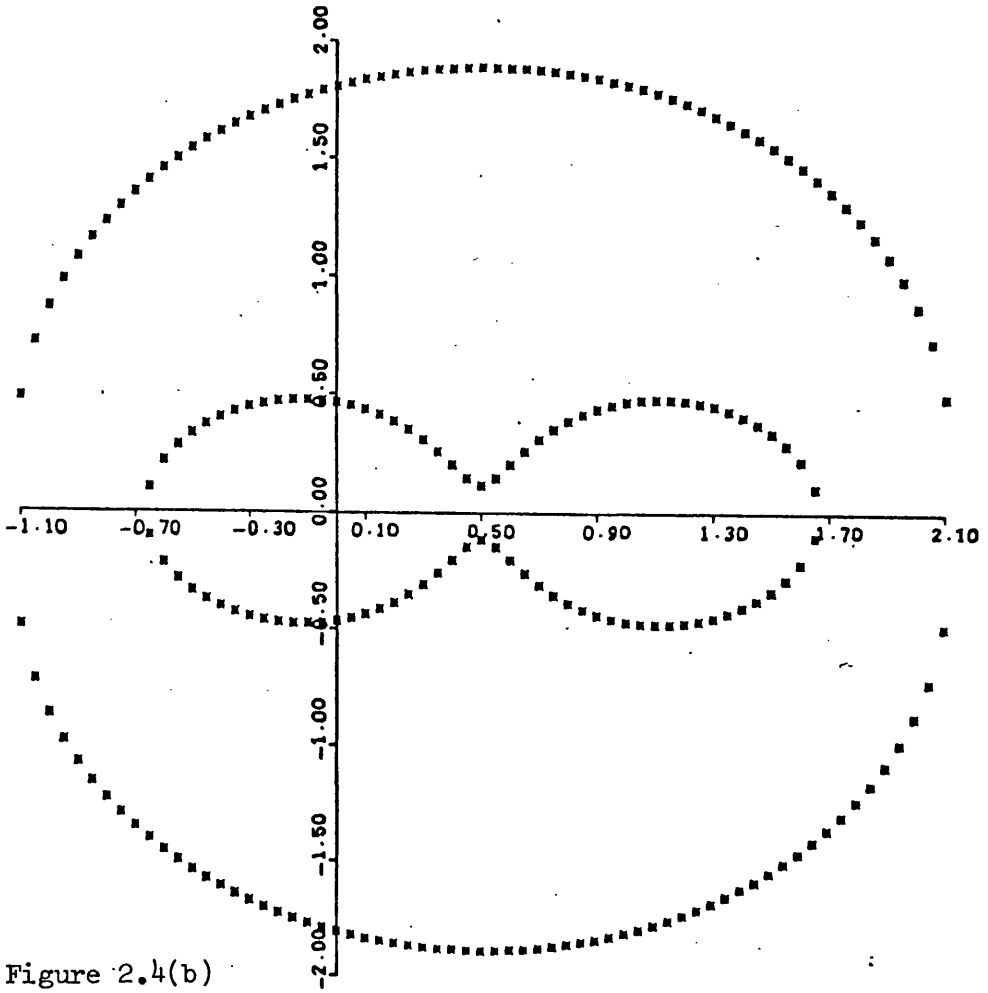

Figure 2.4(b)

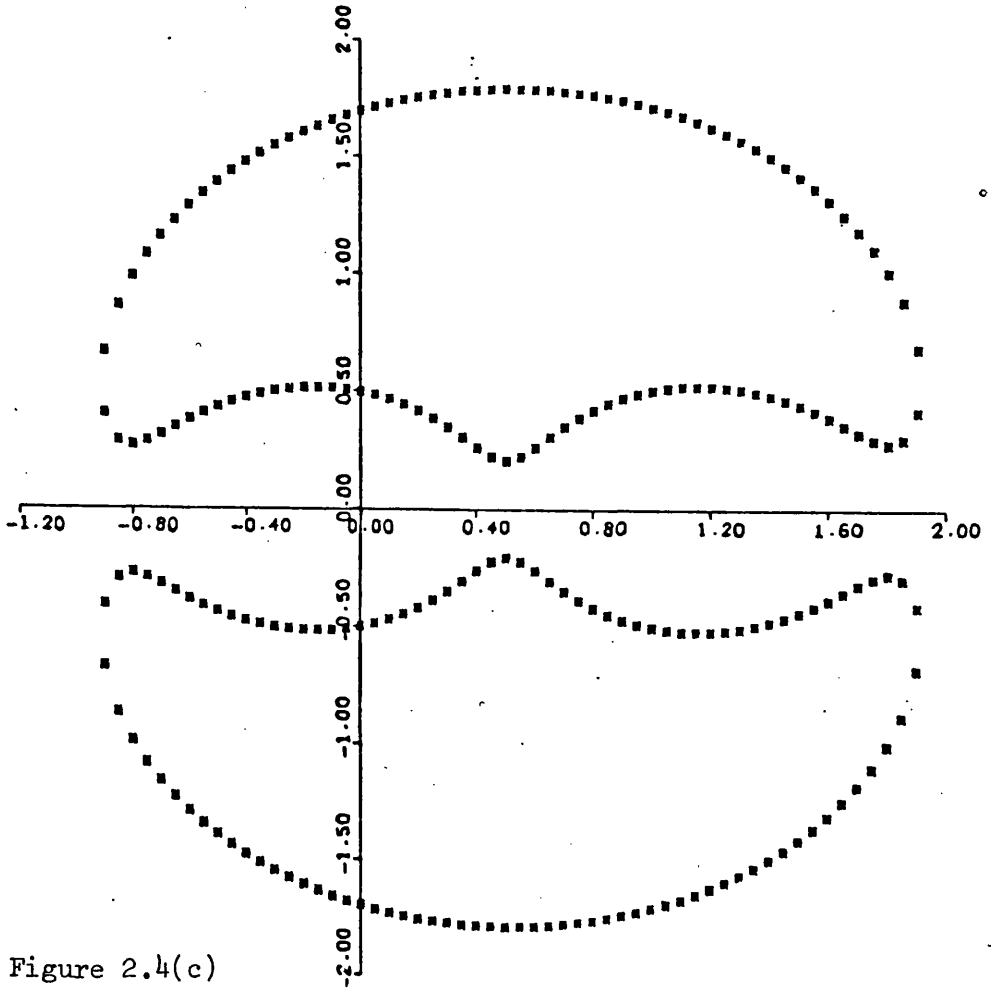

Figure 2.4(c)

2.5 Application of the Zero-Velocity Curves of the General Three-Body Problem to Stability Considerations.

As was shown in the previous section the regions of possible motion are defined by $F(\eta,z) \geq 0$ where

$$F(\eta,z) = Hz^2 + G\, b_o(\eta) z - \frac{c^2 M}{2} c_o(\eta) ,$$

all the quantities retaining their previous meanings. The projection of these regions onto the complex η-plane gives all the possible configurations independant of the scale through the relation

$$\Delta(\eta) = G^2\, b_o^2(\eta) + 2\, M\, c^2 H\, c_o(\eta) \geq 0.$$

The parameter c^2H then controls whether the zero-velocity curves, in the configuration space, are open or closed.

In the same way as the critical values of the Jacobi integral are associated with the Lagrange equilibrium solutions of the circular restricted problem, the critical values of c^2H determining the opening and closing of the zero-velocity curves in the general three-body case may be obtained from the equilibrium solutions of the general problem. The critical values of c^2H are associated with the singularities of the manifold $F(\eta,z) = 0$, corresponding to the equilibrium solutions (cf. the double points $L_1,\ldots,L_5$ in the restricted problem where the partial derivatives of the function $f = 2U - C$ vanish). The singularities are further defined by

$$\frac{\partial F}{\partial z} = 0 \quad \text{and} \quad \frac{\partial F}{\partial \eta} = \frac{\partial F}{\partial x} + i \frac{\partial F}{\partial y} = 0. \qquad (43)$$

From the first of Equations (43) a value $z = z_o$ may be derived where

$$z_o = - \frac{G\, b_o(\eta)}{2H} . \qquad (44)$$

It can then be shown, substituting Equation (44) into Equation (37), that

$$F(\eta, z_o) = - \frac{1}{4H} \Delta(\eta) \qquad (45)$$

and $$\frac{\partial F}{\partial \eta} = -\frac{1}{4H}\ \frac{d}{d\eta}\left[\Delta(\eta)\right] \qquad (46)$$

which demonstrates that the singularities of the manifold $F(\eta,z)$ may be identified with the singularities of its projection on the complex η-plane i.e. the three relations Equations (43) and $F(\eta,z) = 0$ may be replaced through the two Equations (45) and (46) by

$$\Delta(\eta) = 0\ , \qquad \frac{d}{d\eta}\Delta(\eta) = 0. \qquad (47)$$

From the first of Equations (47) we obtain

$$c^2H = -\frac{G^2\ b_o^2(\eta)}{2M\ c_o(\eta)}\ , \qquad (48)$$

which if substituted into the second of Equations (47) results in

$$\begin{aligned}&\left[\ m_3\ (1-|\eta|^{-3}) + m_2(|\eta-1|^{-1} -|\eta\ |^{-3}|\eta-1|^2\ )\right]\eta\ + \\ &\left[\ m_1(1-|\eta-1|^{-3})+ m_2(|\eta|^{-1} -|\eta-1|^{-3}|\eta|^2\ )\right]\ (\eta-1) = 0^*\ .\end{aligned} \qquad (49)$$

In order to find the real roots of Equation (49) which correspond to the collinear equilibrium solutions let $\eta = 1 + \rho$ where ρ is positive and real. Equation (49) then becomes

$$\begin{aligned}&(m_3 + m_1)\rho^5+(3m_3 + 2m_1)\rho^4+(3m_3 + m_1)\rho^3 - \\ &-(3m_2 + m_1)\rho^2-(3m_2 + 2m_1)\rho - (m_2+ m_1) = 0.\end{aligned} \qquad (50)$$

This equation has one positive root ρ where ρ is the ratio

*Clearly $|\eta|= |\eta-1| = 1$ is a solution of this equation. It corresponds to the triangular equilibrium configurations with $c^2H = (c^2H)_4= (c^2H)_5= -\frac{G^2}{2M}\ (m_3m_1 + m_2m_3 + m_1m_2)^3$. If $c^2H > (c^2H)_4 = (c^2H)_5$ then no forbidden configurations exist.

$|\vec{m_1 m_2}| : |\vec{m_3 m_1}|$ when the bodies are in a collinear equilibrium configuration in the order $m_3 m_1 m_2$. Two other values of ρ may be obtained arising from the other distinct orderings of the masses $m_3 m_2 m_1$ and $m_1 m_3 m_2$. Three critical values of c^2H may then be obtained through Equation (48), remembering that $\eta = 1 + \rho$: let these be denoted $(c^2H)_1$, $(c^2H)_2$, $(c^2H)_3$ according as $(c^2H)_1 \leq (c^2H)_2 \leq (c^2H)_3 < (c^2H)_4 = (c^2H)_5$* (where $(c^2H)_4$ and $(c^2H)_5$ are as defined in the above footnote).

Summing up, if c^2H in a real three-body system is less than (or equal to) $(c^2H)_1$ then the forbidden regions are triply connected and under no circumstances can there be an exchange of bodies. If $(c^2H)_1 < c^2H \leq (c^2H)_2$ then the forbidden region is doubly connected; this is a sufficient condition to preclude an exchange of bodies only if one of the three bodies lies outside the central "dumbbell" (cf. Figure 2.4b). If $c^2H > (c^2H)_2$ then an exchange of bodies may take place in any event.

2.6 Summary

Zare (1976, 1977) has shown that an approach similar to that applied in the circular restricted three-body problem can yield regions of possible motion for the coplanar case of the general problem. The opening and closing of the forbidden regions is governed by the critical values of c^2H obtainable from the collinear equilibrium solutions.

If we consider now a hierarchical three-body system, that is, one which consists of a binary component, involving m_1 and m_2, with an external mass m_3 in orbit about the binary at some greater distance than $|\vec{m_1 m_2}|$, then statements may be made about this system's stability. In the case where the value of c^2H for the system is less than (or equal to) $(c^2H)_1$, as obtained by the above procedure, then the system is stable in the sense that the binary will always maintain its identity and m_3 cannot come in between m_1 and m_2. When m_3 is the smallest mass then it is sufficient for such stability that $c^2H \leq (c^2H)_2$.

*The values of c^2H_i, i=1,2,3,4,5 may be identified with the values of the Jacobi integral at the L_2, L_3, L_1, L_4, L_5 equilibrium positions in the restricted problem respectively (see Figs.2.2(a) - (f)).

More detailed consideration will be given to the opening and closing of the zero-velocity curves in later chapters when the work of several authors (Szebehely, 1977; Szebehely and McKenzie, 1977a,b; Szebehely and Zare, 1977; Szebehely, 1978) in the field of stability in hierarchical three-body systems will be briefly reviewed. The method will also be applied to an investigation of the suitability of certain stability parameters to be derived in the next chapter.

CHAPTER 3 STABILITY PARAMETERS FOR HIERARCHICAL DYNAMICAL SYSTEMS

3.1 Introduction

The general problem of celestial mechanics is concerned with the determination of the relative motion of n bodies attracting one another according to the law of gravitation. Since the problem is not soluble certain limitations and assumptions must be made.

The first simplification we make is in treating all the bodies according to the Newtonian law of gravitation and thus neglect any general relativistic effects. Having done this only point masses are then considered i.e. we neglect any effects due to the finite sizes, irregularity of shape or non-uniformities in internal distribution of mass of the bodies. This is reasonable since it is observed that bodies in the solar system, excepting certain satellites and asteroids, deviate little from spheres and in general do not have gross anomalies in the internal distribution of their constituent matter. Bodies with spherically symmetric mass distributions may be *exactly* represented by point masses.

Secondly only systems which exhibit a hierarchical structure are examined. Evans (1968) described the hierarchical arrangement of bodies by means of "mobile diagrams" (see Figures 3.1(a) - (c)). In planetary systems the characteristic hierarchy is demonstrated by each successive member being further from the parent star than its previous neighbour. The orbits are well-spaced and do not cross (Fig.3.1(a)). Similar structure is generally to be observed in satellite systems. They may however be included on the one diagram with the planets (Fig.3.1(b)). Multiple star systems arrange themselves in a variety of hierarchies: there are the binary and triple star systems, as well as quadruple systems allowing two possible arrangements (Fig.3.1 (c)). Notice that the quadruple star system, may be arranged in a fashion similar to planetary systems (Evans' Hierarchy (3)) or can form into two binaries which are in orbit about their common mass-centre (Evans' Hierarchy (2)). Star systems of higher multiplicity may be made up in successively more complex forms.

Due to the arrangement of the bodies of the Solar System in a

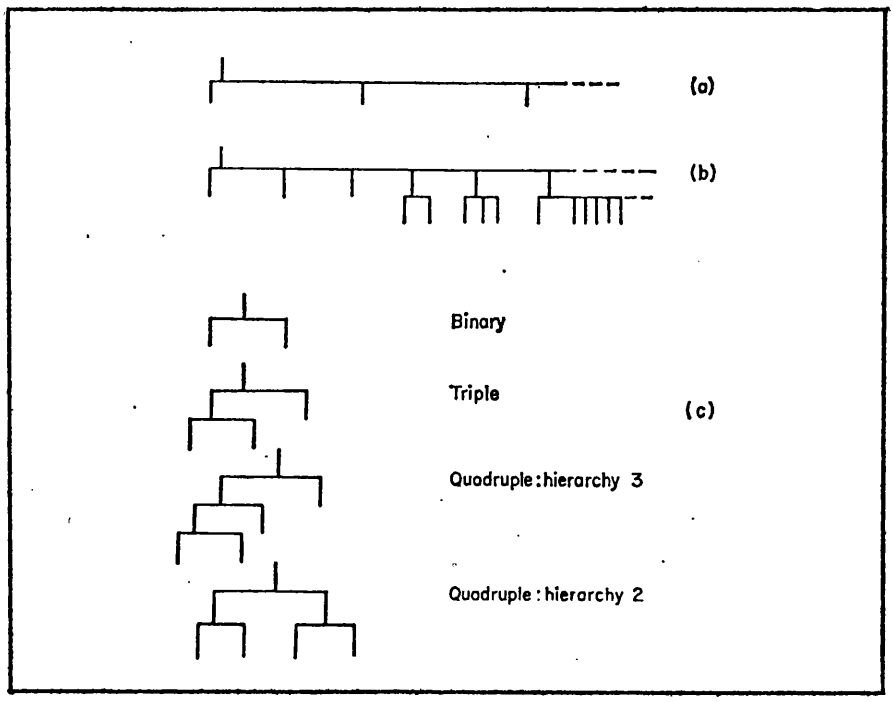

Figure 3.1 Evans mobile diagrams for (a) planets (b) planets and satellites and (c) multiple stellar systems.

hierarchy it is possible to subdivide this many-body system into two main classes of problem. These may be individually treated by the problem of three (or more) bodies. The lunar theories are particular examples of the three-body problem where the motion of the Moon about the Earth is examined, *including* the disturbing effect of the Sun but *neglecting* the effect due to the other planets. Planetary theories have been evolved to examine the motion of several small bodies about a large central mass as is the case with the planets and the Sun. Here the mutual perturbations of the small bodies are taken into account.

These two problems are both cases of the three (or more) body problem; the division is only made on the grounds of observational evidence and the convenience of analysis of the problem. In the remaining sections of this chapter a set of parameters are sought for,

which it is felt have a physical meaning for the stability of hierarchical dynamical systems. Stability in this sense requires that the system does not undergo any exchange of bodies, escapes or collisions. This is essentially the maintenance of the "status quo" as mentioned in Section 1.2.

3.2 Lunar Theory - The Disturbing Function

Following Brown (1896) we consider the forces present in the problem of three-bodies in the case of the Earth-Moon-Sun system. Two methods are adopted: the accelerations due to the forces acting on the Sun and Moon relative to the Earth are found first, secondly the accelerations due to the forces acting are obtained relative to the Earth, for the Moon, and relative to the mass-centre of the Earth-Moon system for the Sun.

(i) *The Forces Relative to the Earth*

Let E, M, S and C be the positions of the Earth, Moon, Sun and mass-centre of the Earth-Moon system respectively (see Fig.3.2).

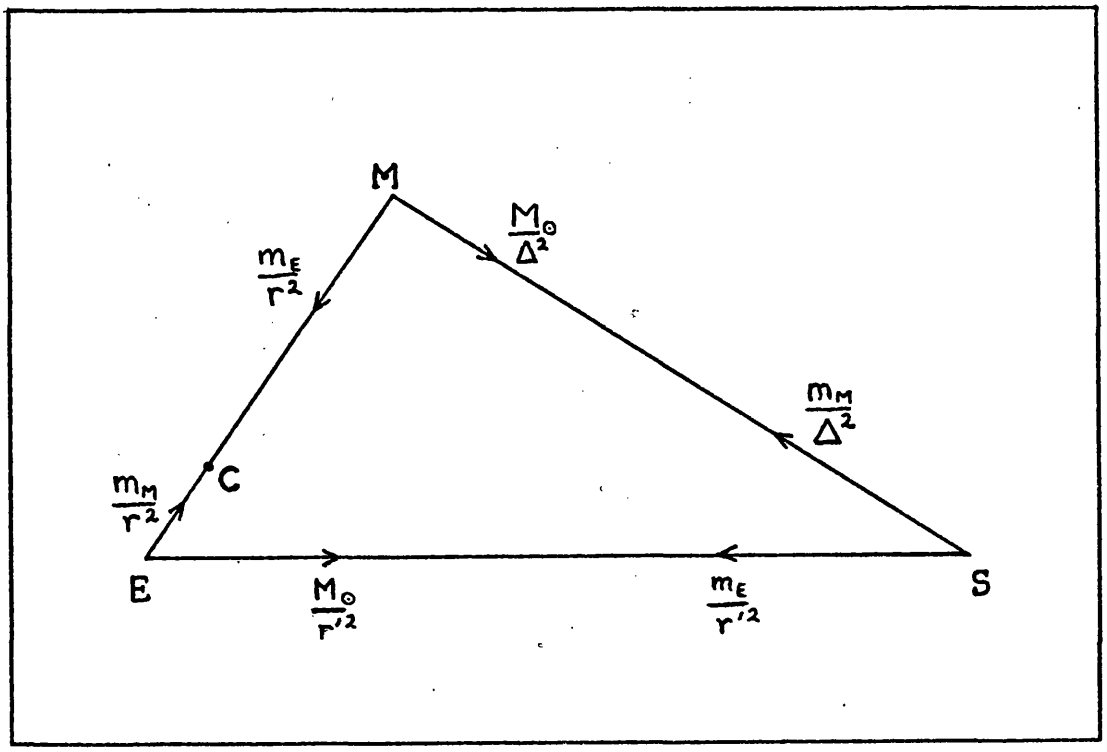

Figure 3.2 Forces acting in the Earth-Moon-Sun system.

Further, let the masses of the Earth, Moon and Sun be m_E, m_M and $M_\odot$ respectively, and the mutual distances ME, SE and SM be denoted r, r' and Δ. The forces acting are as shown on the diagram and hence the accelerations due to the forces, relative to the Earth, are as follows:

On the Moon		On the Sun	
$\frac{m_E + m_M}{r^2}$	in the direction ME	$\frac{m_E + M_\odot}{r'^2}$	in the direction SE
$\frac{M_\odot}{\Delta^2}$	" " " MS	$\frac{m_M}{\Delta^2}$	" " " SM
$\frac{M_\odot}{r'^2}$	" " " SE	$\frac{m_M}{r^2}$	" " " ME

If we consider the Earth as the origin of a set of rectangular axes and let (x,y,z) be the coordinates of the Moon and (x', y', z') the coordinates of the Sun and L, M, N, L', M', N' the accelerations acting on the Moon and Sun relative to the Earth referred to these coordinate axes then

$$L = -\frac{m_E + m_M}{r^2}\cdot\frac{x}{r} - \frac{M_\odot}{\Delta^2}\cdot\frac{x - x'}{\Delta} - \frac{M_\odot}{r'^2}\cdot\frac{x'}{r'} \qquad (1)$$

and $$L' = -\frac{M_\odot + m_E}{r'^2}\cdot\frac{x'}{r'} - \frac{m_M}{\Delta^2}\cdot\frac{x'-x}{\Delta} - \frac{m_M}{r^2}\cdot\frac{x}{r} \qquad (2)$$

with similar expressions for M, M' and N,N'.

Putting

$$F = \frac{m_E + m_M}{r} + \frac{M_\odot}{\Delta} - \frac{M_\odot}{r'}\cdot\frac{\underset{\sim}{r}.\underset{\sim}{r}'}{r'^2} \qquad (3)$$

and $$F' = \frac{M_\odot + m_E}{r'} + \frac{m_M}{\Delta} - \frac{m_M}{r}\cdot\frac{\underset{\sim}{r}.\underset{\sim}{r}'}{r^2} \qquad (4)$$

where $\underset{\sim}{r}.\underset{\sim}{r}' = xx' + yy' + zz'$,

we have

$$L = \frac{\partial F}{\partial x} \quad , \quad M = \frac{\partial F}{\partial y} \quad , \quad N = \frac{\partial F}{\partial z} \quad ;$$

$$L' = \frac{\partial F'}{\partial x'} \quad , \quad M' = \frac{\partial F'}{\partial y'} \quad , \quad N' = \frac{\partial F'}{\partial z'} \quad . \qquad (5)$$

F and F' are the force functions for the motions of the Moon and Sun with respect to the Earth. These expressions for F and F' are general in nature and are applicable to any system of three masses. We now proceed, in the light of certain observations, to simplify the solution of this problem.

To find the motion of the Moon about the Earth it is assumed that the motion of the Earth about the Sun is known i.e. x', y', z' are known functions of time. Equation (4) giving the functional form of F' demonstrates that the motion of the Sun is dependent upon the coordinates of the Moon as we would indeed expect. Considering only the first term in the expression for F' viz. $(M_\odot + m_E)/r'$ would result in the motion of the Earth about the Sun being an undisturbed Keplerian ellipse. Of the other two terms clearly $m_M \, \underset{\sim}{r}.\underset{\sim}{r}'/r^3$ is the larger since $r \ll \Delta$, Δ and r' being the same magnitude. This term arises from the force m_M/r^2 acting on E and if the motion of the Sun were referred to C this term would not have appeared. Thus we consider:

(ii) *The Forces acting on the Sun relative to C and the Moon Relative to the Earth*

Clearly $$EC = \frac{m_M}{m_E + m_M} \cdot EM$$

and therefore the acceleration of C relative to E is $m_M/(m_E + m_M)$ times that of M relative to E. Hence the force on theSun relative to C parallel to the x-axis is $L' - m_M L/(m_E + m_M)$ which by Equation (2) is equal to

$$- \frac{M_\odot + m_E + m_M}{m_E + m_M} \cdot \left(\frac{m_E}{r'^2} \cdot \frac{x'}{r'} + \frac{m_M}{\Delta^2} \cdot \frac{x' - x}{\Delta} \right). \qquad (6)$$

Let ξ, η, ζ be the coordinates of the Sun referred to a set of axes, origin at C, which are parallel to the original set x, y, z. Let SC = ρ. Then

$$\left.\begin{aligned} \xi &= x' - \frac{m_M}{m_E + m_M} \cdot x, \\ \eta &= y' - \frac{m_M}{m_E + m_M} \cdot y, \\ \text{and } \zeta &= z' - \frac{m_M}{m_E + m_M} \cdot z. \end{aligned}\right\} \qquad (7)$$

Therefore $x' - x = \xi - \frac{m_E}{m_E + m_M} \cdot x$, etc. (8)

and $$r'^2 = \left(\xi + \frac{m_M}{m_E + m_M} \cdot x\right)^2 + \left(\eta + \frac{m_M}{m_E + m_M} \cdot y\right)^2 + \left(\zeta + \frac{m_M}{m_E + m_M} \cdot z\right)^2 \qquad (9)$$

$$\Delta^2 = \left(\xi - \frac{m_E}{m_E + m_M} \cdot x\right)^2 + \left(\eta - \frac{m_E}{m_E + m_M} \cdot y\right)^2 + \left(\zeta - \frac{m_E}{m_E + m_M} \cdot z\right)^2 . \qquad (10)$$

Putting $$\Phi' = \frac{M_\odot + m_E + m_M}{m_E + m_M} \cdot \left(\frac{m_E}{r'} + \frac{m_M}{\Delta}\right) \qquad (11)$$

where r' and Δ are expressed in terms of x, y, z, ξ, η, ζ. The partial derivatives $\partial\Phi'/\partial\xi$, $\partial\Phi'/\partial\eta$, $\partial\Phi'/\partial\zeta$ will be the forces acting on the Sun relative to C in the directions ξ, η, ζ.

Again replacing x', y', z' in Equation (1) by their values given by Equations (8) we obtain

$$L = -\frac{m_E + m_M}{r^2} \cdot \frac{x}{r} + \frac{M_\odot}{\Delta^3}\left(\xi - \frac{m_E}{m_E + m_M} \cdot x\right) - \frac{M_\odot}{r'^3}\left(\xi + \frac{m_M}{m_E + m_M} \cdot x\right) \qquad (12)$$

again with similar expressions for M and N. The forces L, M, N may therefore be derived by partial differentiation with respect to x, y, z of the force function

$$\Phi = \frac{m_E + m_M}{r} + \frac{M_\odot}{\Delta} \cdot \frac{m_E + m_M}{m_E} + \frac{M_\odot}{r'} \cdot \frac{m_E + m_M}{m_M} \qquad (13)$$

where $\Delta = \Delta(x,y,z,\xi,\eta,\zeta)$ and $r' = r'(x,y,z,\xi,\eta,\zeta)$.

It is a relatively simple exercise to show that Φ' differs little from $(M_\odot + m_E + m_M)/\rho$. We have

$$r'^2 = \rho^2 + \frac{2m_M}{m_E + m_M} r\rho \cos\theta + \left(\frac{m_M}{m_E + m_M} \right)^2 r^2 \qquad (14)$$

where θ is the angle $M\hat{C}S$,

whence

$$\frac{1}{r'} = \frac{1}{\rho} - \frac{m_M}{m_E + m_M} \cdot \frac{r}{\rho^2} \cos\theta + \left(\frac{m_M}{m_E + m_M} \right)^2 \frac{r^2}{\rho^3} P_2(\cos\theta) + \ldots . (15)$$

where $P_n(x)$ is the Legendre polynomial of order n in x: in this case

$P_2(x) = \frac{1}{2}(3x^2 - 1)$.

Similarly

$$\frac{1}{\Delta} = \frac{1}{\rho} + \frac{m_E}{m_E + m_M} \cdot \frac{r}{\rho^2} \cdot \cos\theta + \left(\frac{m_E}{m_E + m_M} \right)^2 \frac{r^2}{\rho^3} P_2(\cos\theta) + \ldots . (16)$$

and therefore

$$\Phi' = \frac{M_\odot + m_E + m_M}{\rho} \cdot \left[1 + \frac{m_E m_M}{(m_E + m_M)^2} \frac{r^2}{\rho^2} P_2(\cos\theta) + \ldots . \right] . \qquad (17)$$

Now the ratio $r:\rho$ differs little from 1:400 at any time and the ratio $m_M:m_E$ is approximately 1:80 resulting in the ratio of the first to second terms being approximately 10^7:1. Thus the second term is negligible and the motion of the mass-centre of the Earth-Moon system relative to the Sun is very closely approximated by an undisturbed Keplerian ellipse.

With the assumption that the motion of C about S is elliptic and therefore a known function of time the force function Φ may then be used to obtain the motion of the Moon. In practice however it is easier to use the function F, the corrections required to relate F and Φ are

easily obtainable to sufficient accuracy and need not concern us here.

It may be seen in Equation (17) that the term $m_E m_M/(m_E + m_M)^2 . r^2/\rho^2$ is a measure of the "disturbance" of the Moon on the orbit of the mass-centre of Earth-Moon system about the Sun normalized to the two-body forces acting between the Earth-Moon system and the Sun. This measure is very small and consequently the actual orbit will not deviate far from an undisturbed Keplerian ellipse. It would clearly be possible to operate on Φ in a manner similar to that done on Φ' and obtain a measure of the disturbance of the Sun on the Moon's orbit about the Earth. The measure of disturbance in this case would obviously be found to be much larger than the effect of the Moon on the Sun's orbit about C.

3.3 Planetary and Lunar Theory - A Brief Comparison

As was mentioned above the division between the planetary and lunar theories is one of convenience only, both being examples of the n-body problem ($n \geq 3$). The need for different analytical procedures arises through the distinct differences between the arrangement of the two types of system.

On considering the Moon in revolution about the Earth (or indeed any satellite about its parent planet) disturbed by the Sun it is immediately apparent that the ratio of the semi-major axis of the lunar orbit to that of the Earth-Moon system about the Sun is very small. Therefore, when expanding the disturbing function, we should clearly expand first in terms of this small ratio in order to reduce the number of terms we require to take in the expansion. Having done this we would then expand in terms of the (small) eccentricities and inclinations.

The case of two mutually perturbing planets in orbit about the Sun is different. Here the ratio of the semi-major axes of the planetary orbits may be close to unity; for example in the case of the Earth and Venus this ratio is 0.723. Therefore since the orbits of the planets are generally of small eccentricity and inclination - generally even smaller than in the case of satellites - the expansion in terms of these quantities is done first. The functions Φ and Φ', derived

in the previous section, may be directly carried over to the planetary case if we allow m_E to be the mass of the Sun (M), m_M the mass of the inner planet (m_i) and M_O the mass of the outer planet (m_o). Making these alterations and including the term in r^3/ρ^3 Equation (17)* becomes

$$\Phi' = \frac{M + m_i + m_o}{\rho} \left[1 + \frac{Mm_i}{(M + m_i)^2} \frac{r^2}{\rho^2} P_2(\cos\theta) + \right.$$

$$\left. + \frac{Mm_i (M - m_i)}{(M + m_i)^3} \frac{r^3}{\rho^3} P_3(\cos\theta) + \ldots\ldots \right] \quad (18)$$

where r, ρ, θ and $P_n(x)$ have their previous meanings.

Now $M >> m_i$, thus we see that the coefficients consisting of combinations of the masses are equal to a high degree of accuracy to the first order in m_i/M, this would also be found to hold true for the higher order terms involving the P_4, P_5, etc. terms. The quantities $(r/\rho)^n$ in the expansion will be decreasing as n increases. However, as was noted above, r/ρ may be almost unity, therefore a relatively large number of terms will be required in the expansion to give sufficient accuracy - as opposed to the lunar case where r/ρ is small. It may similarly be shown that the expansion of Φ is similar, terms involving $(r/\rho)^n$ appearing in conjunction with coefficients of the order m_o/M. This is not carried out here since it will be dealt with more fully in Section 3.6.

It is therefore apparent that in lunar theory the expansion will involve few terms of rapidly decreasing magnitude whereas in planetary theory large numbers of terms will be retained all being of similar magnitude - excepting, of course, for the modifications due to *small*

* This expression implies that forces acting on the outer planet are expressed relative to the mass-centre of the Sun-Inner Planet system and not relative to the Sun itself as is more usually the case. The difference between the two ways of expressing these forces is less than in the lunar case since the position of the Sun is very close to the mass-centre of the Sun-Inner Planet system due to the smallness of the planetary mass as compared to that of the Sun.

divisors as mentioned in Chapter 1. However even in the planetary case the leading term in Equation (18) is the largest and is a measure of the disturbance of the inner planet* on the orbit of the outer planet. Thus through such expansions - as exemplified in Equations (17) and (18) - it is possible to derive parameters which characterize the "size" of the disturbance of one body on another in a hierarchical system.

3.4 Stability in Multiple Stellar Systems

The remaining case of the hierarchical three-body system not yet accounted for by the lunar and planetary cases is that of the triple stellar system. This is the case when the three masses are of nearly equal magnitude. There are many observed cases of triple stellar system. It is estimated that half of all stars occur in multiple systems i.e. binary, triple, etc: of these a proportion considered to lie between 1/4 and 1/3, are triple systems (or higher multiplicity). The same ratio seems to hold when comparing the number that are quadruple or higher with those which are triple or more, and so on (see Batten, 1973). In triple systems it is generally found that there is a (relatively) close binary component with a third more remote component. The binary components execute disturbed Keplerian ellipses about their common mass-centre with the third star following a disturbed Keplerian orbit with respect to that mass-centre. The ratios r/ρ can vary greatly in this case: the system may consist of a spectroscopic binary with the third mass in orbit about them resulting in a small value for r/ρ, or r/ρ may be as large as 1/3, this being a rough upper limit beyond which the system may exhibit instability (Harrington, 1972). Eccentricities and relative inclinations of the orbits in the stellar three-body case will in general not be small therefore the formulations of any general perturbation theory would be facilitated

* More precisely it is the disturbance on the outer planet due to the Sun and inner planet not being found at their common mass-centre.

by a "lunar-type" development as in Section 3.2. The place of the Earth and Moon would be taken by the binary, the third component 'acting' as the Sun. If we set $M_\odot = m_E = m_M = m$ in Equation (17), thus implying equal masses, we obtain

$$\Phi' = \frac{3m}{\rho}\left[1 + \frac{1}{4}\cdot\frac{r^2}{\rho^2}P_2(\cos\theta) + \ldots\ldots\ldots\right]. \qquad (19)$$

Thus it is seen taking $r/\rho \simeq 0.2$ as a typical value that the coefficient of the P_2 term in Equation (19) is 10^{-2}. This is a measure of the disturbance of the binary components on the orbit of the third mass about their common mass-centre. Clearly it is again possible to obtain the expression for Φ in order to estimate a measure of the disturbance of the third mass on the binary components' relative orbit.

There are no cases observed where the ratio r/ρ is very small. This is probably due to two factors. Firstly if ρ is very large in comparison to r then the period of the third mass about the mass-centre of the binary would also be large therefore it is unlikely such a system would have had a chance to be observed to be a triple system in the time since such observations began. Secondly, there is obviously an upper limit to the separation of a binary star due to the disruptive effect of the "central bulge" of the galaxy. In a similar fashion the third component of a triple stellar system may be removed from the system if ρ is very large.

There are systems in existence of higher multiplicity. One of the best examples is the Castor system which consists of six stars. These are arranged in three pairs, as close binaries, their periods of revolution being 9.2, 2.9 and 0.8 days. The two closer binaries revolve about each other with a period of about 500 years. The third binary is placed further out and revolves relative to the mass-centre of the first two binaries in a period of several thousand years. The situation is shown schematically as a "mobile diagram" in Fig. 3.3. The orbits in the system are all well-spaced and therefore the disturbance on the relative Keplerian orbits is kept to a minimum.

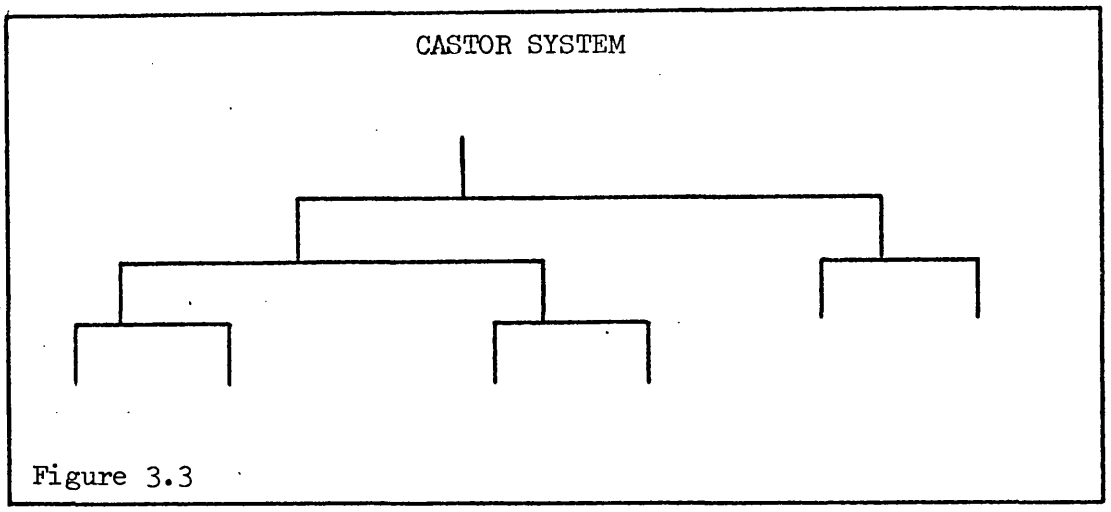

Figure 3.3

3.5 The Jacobian Coordinate System

A form of the equations of motion of the general n-body problem is introduced which is of use when considering naturally occurring systems. The method was originated by Jacobi and Lagrange (see Plummer, 1918). The equations are applicable to systems which exhibit a hierarchical structure and consist of relatively few bodies: examples of such would be the triple stellar systems (or indeed stellar systems of any multiplicity which exhibit the arrangement of bodies as in Evans' Hierarchy (3) for the four-body case), planetary systems, and satellite systems including or excluding the Sun. Systems which are excluded, or rather where no substantial gain is forthcoming from the use of such a coordinate system, are loose aggregates of stars such as open clusters and many-body systems such as globular clusters. These however are not considered in this work.

Consider the equations of motion of an n-body system with respect to an inertial reference frame origin O (see Figure 3.4). In the usual notation

$$m_i \ddot{\underset{\sim}{R}}_i = \underset{\sim}{\nabla}_i U \qquad (i = 1,2,\ldots,n) \qquad (20)$$

where $$U = \frac{1}{2} G \sum_{k=1}^{n} \sum_{\ell=1}^{n} \frac{m_k m_\ell}{r_{k\ell}} \quad (k=1,\ldots,n;\ \ell=1,\ldots n;\ k\neq\ell) \qquad (21)$$

is the force function

$\underset{\sim}{\nabla}_i$ is the gradient operator associated with $\underset{\sim}{R}_i$

m_i is the ith mass

$\underset{\sim}{R}_i$ is the position vector $\overrightarrow{Om_i}$

$r_{k\ell} = |\underset{\sim}{r}_{k\ell}| = |\underset{\sim}{R}_\ell - \underset{\sim}{R}_k|$

G is the gravitational constant

and a dot denotes differentiation with respect to time.

Let us consider that the bodies lie in a hierarchical arrangement as shown in Figure 3.4, so that successive bodies m_i $(i = 2,\ldots,n)$ lie at greater and greater distances from m_1 such that their orbits, taken with respect to the mass-centre of the previous (i-1) bodies $m_1, m_2, \ldots, m_{i-1}$, do not cross (at least in some initial phase).

We now define the vectors $\underset{\sim}{\rho}_i$ as follows: $\underset{\sim}{\rho}_i$ is the vector from the mass-centre of the masses $m_1, m_2, \ldots, m_{i-1}$ to the mass m_i as shown in the diagram. It is then required to express the motion of the bodies with respect to these new coordinates $\underset{\sim}{\rho}_i$. Notice that whereas there were n position vectors $\underset{\sim}{R}_i$ there are only (n-1) vectors $\underset{\sim}{\rho}_i$.

Now the mass centre of the first j masses $m_1,\ldots,m_j$ is at a position given by

$$\underset{\sim}{\bar{R}}_j = \frac{1}{M_j} \sum_{k=1}^{j} m_k \underset{\sim}{R}_k \qquad (22)$$

where

$$M_j = \sum_{k=1}^{j} m_k . \qquad (23)$$

Thus

$$\underset{\sim}{\rho}_i = \underset{\sim}{R}_i - \underset{\sim}{\bar{R}}_{i-1}$$

and

$$\underset{\sim}{\rho}_i = \underset{\sim}{R}_i - \frac{1}{M_{i-1}} \sum_{k=1}^{i-1} m_k \underset{\sim}{R}_k \qquad (24)$$

giving

$$\ddot{\underset{\sim}{\rho}}_i = \ddot{\underset{\sim}{R}}_i - \frac{1}{M_{i-1}} \sum_{k=1}^{i-1} m_k \ddot{\underset{\sim}{R}}_k \qquad (25)$$

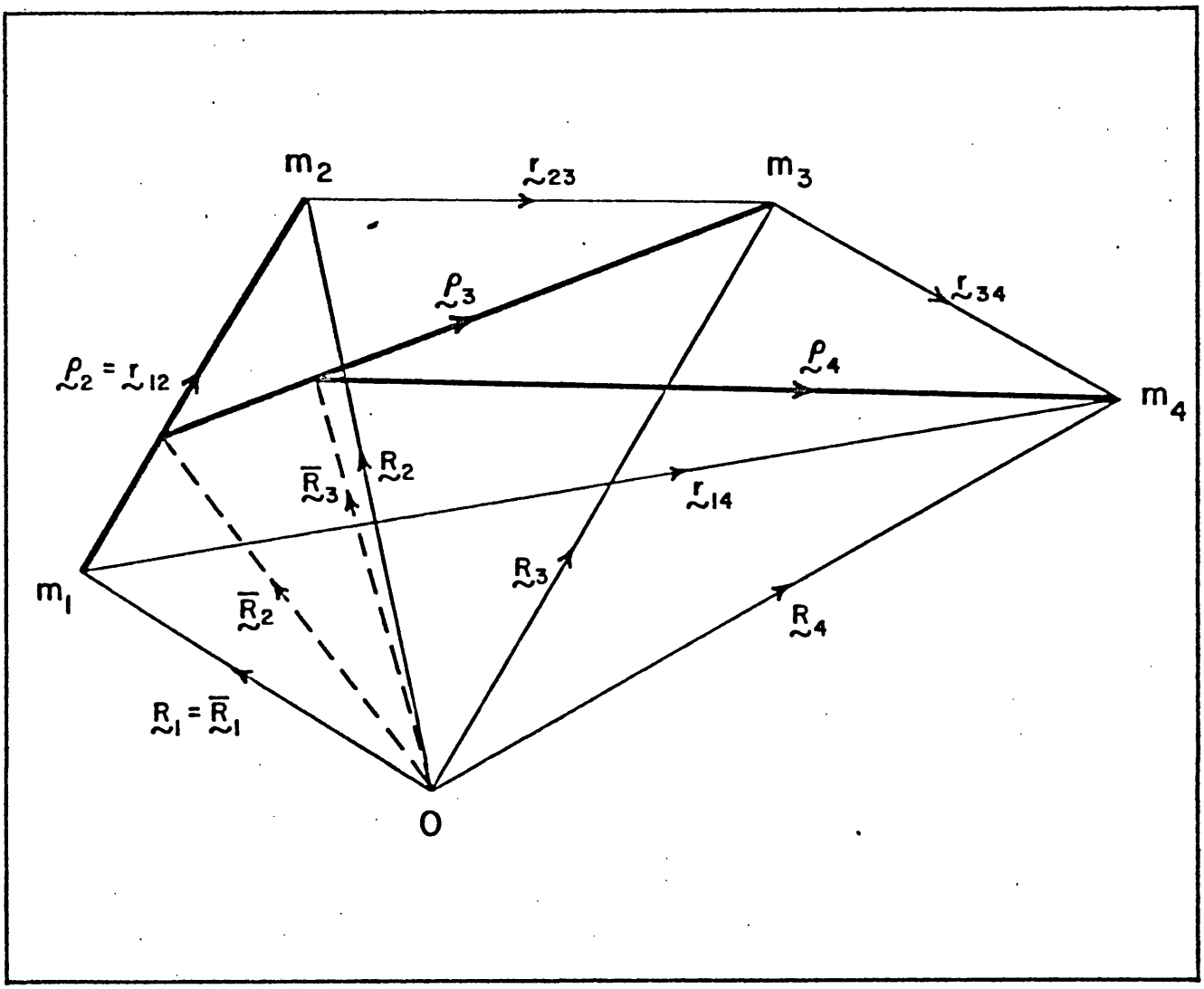

Figure 3.4 A particular case of the Jacobian coordinate system where n = 4. (See text for definition of symbols used).

Multiplying Equation (25) by m_i and substituting from Equation (20) we obtain

$$m_i \ddot{\underset{\sim}{\rho}}_i = \nabla_{\underset{\sim}{i}} U - \frac{m_i}{M_{i-1}} \sum_{k=1}^{i-1} \nabla_{\underset{\sim}{k}} U \quad (i=2,\ldots,n). \qquad (26)$$

Supposing $\underset{\sim}{R}_i = (X_i, Y_i, Z_i)$ and $\underset{\sim}{\rho}_i = (\xi_i, \eta_i, \zeta_i)$ in the inertial reference frame, consider the x-component of Equation (26) viz.

$$m_i \ddot{\xi}_i = \frac{\partial U}{\partial X_i} - \frac{m_i}{M_{i-1}} \sum_{k=1}^{i-1} \frac{\partial U}{\partial X_k} .$$

This may be rewritten as

$$m_i \ddot{\xi}_i = \frac{\partial U}{\partial \xi_i} \frac{\partial \xi_i}{\partial X_i} - \frac{m_i}{M_{i-1}} \sum_{k=1}^{i-1} \frac{\partial U}{\partial \xi_i} \frac{\partial \xi_i}{\partial X_k} . \qquad (27)$$

By Equation (24), noting that k is a dummy suffix,

$$\frac{\partial \xi_i}{\partial X_i} = 1$$

and

$$\frac{\partial \xi_i}{\partial X_k} = -\frac{m_k}{M_{i-1}}$$

thus

$$m_i \ddot{\xi}_i = \frac{\partial U}{\partial \xi_i} \left[1 + \frac{m_i}{M_{i-1}^2} \sum_{k=1}^{i-1} m_k \right] . \qquad (28)$$

Now $\sum_{k=1}^{i-1} m_k = M_{i-1}$ thus we have, after applying the same procedure to the y and z components

$$\frac{m_i M_{i-1}}{M_i} \ddot{\underset{\sim}{\rho}}_i = \frac{\partial U}{\partial \underset{\sim}{\rho}_i} \quad (i=2,\ldots,n) \qquad (29)$$

These are the equations of motion of an n-body dynamical system in Jacobian coordinates and are thus applicable to hierarchical systems. Equations (29) form a $(6n-6)^{th}$ order system, the reduction from the original $6n^{th}$ order system being effected by the use of the six centre-of-mass integrals. We proceed, in the next section, by means of an

expansion of the force function U in terms of the ratios ρ_i/ρ_j ($i=2,\ldots, j-1$; $j=3,\ldots,n$) to carry out an analysis similar to Section 3.2 in the case where there are n bodies.

3.6 Expansion of the Force Function of a Hierarchical n-Body Dynamical System

As was seen in the previous section the form of the equations of motion of an n-body dynamical system is as follows (cf. Roy (1978, 1979)).

$$\frac{m_i \, M_{i-1}}{M_i} \ddot{\underset{\sim}{\rho}}_i = \underset{\sim}{\nabla}_i U \qquad (i=2,\ldots,n) \qquad (30)$$

where
$$U = \frac{1}{2} G \sum_{k=1}^{n} \sum_{\ell=1}^{n} \frac{m_k \, m_\ell}{r_{k\ell}} \qquad (31)$$

is the force function of the problem. In these equations the definitions of m_i, $\underset{\sim}{r}_{k\ell}$ and $r_{k\ell}$ are as previously given. Now $M_i = \sum_{j=0}^{i} m_j$, with $m_o = 0$ being defined, $\underset{\sim}{\nabla}_i$ denotes the gradient operator with respect to $\underset{\sim}{\rho}_i$ with $\underset{\sim}{\rho}_i$ being defined as the vector $\overrightarrow{M_{i-1}\, m_i}$ (M_{i-1} being the position of the mass-centre of the first (i-1) masses).

Clearly the force function U, can be rewritten in the form

$$U = G \sum_{\ell=2}^{n} m_\ell \, B_\ell \, , \qquad (32)$$

where
$$B_\ell = \sum_{k=1}^{\ell-1} \frac{m_k}{r_{k\ell}} \qquad (33)$$

Let the vectors $\underset{\sim}{R}_g$ ($g=1,\ldots,n$) be the position vectors of the n masses $m_1,\ldots,m_n$ in an inertial reference frame; then clearly, if we let $\underset{\sim}{\bar{R}}_j$ be the position vector of the centre of mass of the subsystem $m_1,\ldots,m_j$ in the same coordinate system we have

$$M_j \bar{\underset{\sim}{R}}_j = \sum_{g=1}^{j} m_g \underset{\sim}{R}_g . \qquad (34)$$

Using Equation (34) and the equivalent equation involving $\bar{\underset{\sim}{R}}_{j-1}$ and subtracting them we derive

$$\bar{\underset{\sim}{R}}_j - \bar{\underset{\sim}{R}}_{j-1} = \frac{m_j}{M_j} (\underset{\sim}{R}_j - \bar{\underset{\sim}{R}}_{j-1}). \qquad (35)$$

Summing over j, between the limits k and $\ell-1$ ($k < \ell-1$), in Equation (35) yields

$$\bar{\underset{\sim}{R}}_{k-1} - \bar{\underset{\sim}{R}}_{\ell-1} + \sum_{j=k}^{\ell-1} \frac{m_j}{M_j} (\underset{\sim}{R}_j - \bar{\underset{\sim}{R}}_{j-1}) = \underset{\sim}{0}. \qquad (36)$$

Now clearly

$$\underset{\sim}{r}_{k\ell} = \underset{\sim}{R}_\ell - \underset{\sim}{R}_k$$

which upon application of Equation (36) can be rewritten as

$$\underset{\sim}{r}_{k\ell} = \underset{\sim}{R}_\ell - \bar{\underset{\sim}{R}}_{\ell-1} - \underset{\sim}{R}_k + \bar{\underset{\sim}{R}}_{k-1} + \sum_{j=k}^{\ell-1} \frac{m_j}{M_j} (\underset{\sim}{R}_j - \bar{\underset{\sim}{R}}_{j-1})$$

whence, noting that $\underset{\sim}{\rho}_i = \underset{\sim}{R}_i - \bar{\underset{\sim}{R}}_{i-1}$, we have

$$\underset{\sim}{r}_{k\ell} = \underset{\sim}{\rho}_\ell - \underset{\sim}{\rho}_k + \sum_{j=k}^{\ell-1} \frac{m_j}{M_j} \underset{\sim}{\rho}_j . \qquad (37)$$

where we *define* $\underset{\sim}{\rho}_1 = \underset{\sim}{0}$.

Thus on constructing $(\underset{\sim}{r}_{k\ell} \cdot \underset{\sim}{r}_{k\ell})^{-\frac{1}{2}}$ we obtain

$$\frac{1}{r_{k\ell}} = \frac{1}{\rho_\ell} \cdot \left[1 + \alpha_{k\ell}^2 + \sum_{j=k}^{\ell-1} \sum_{h=k}^{\ell-1} \left(\frac{m_j m_h}{M_j M_h} \alpha_{j\ell} \alpha_{h\ell} C_{jh} \right) - 2\alpha_{k\ell} C_{k\ell} + 2 \sum_{j=k}^{\ell-1} \frac{m_j}{M_j} \alpha_{j\ell} (C_{j\ell} - \alpha_{k\ell} C_{jk}) \right]^{-\frac{1}{2}}$$

where

$$\left.\begin{aligned} \alpha_{ij} &= \frac{\rho_i}{\rho_j} \\ C_{ij} &= \frac{\underset{\sim}{\rho_i} \cdot \underset{\sim}{\rho_j}}{\rho_i \ \rho_j} \\ \text{and} \qquad \rho_i &= |\underset{\sim}{\rho_i}| \end{aligned}\right\} \quad (i < j) \qquad (38)$$

Applying the binomial expansion for $(1 + x)^{-\frac{1}{2}}$, assuming that

$$\left(\frac{r_{k\ell}}{\rho_\ell}\right)^2 - 1 < 1 \quad \forall\, k,\ell \ \ (k < \ell),^*$$

we obtain, correct to the second order in the α's,

$$\begin{aligned} \frac{1}{r_{k\ell}} = \frac{1}{\rho_\ell} \Bigg[& 1 - \frac{1}{2}\,\alpha_{k\ell}^2 - \frac{1}{2} \cdot \sum_{j=k}^{\ell-1} \sum_{h=k}^{\ell-1} \left(\frac{m_j}{M_j} \frac{m_h}{M_h}\, \alpha_{j\ell}\, \alpha_{h\ell}\, C_{jh} \right) + \\ & + \alpha_{k\ell}\, C_{k\ell} + \sum_{j=k}^{\ell-1} \frac{m_j}{M_j}\, \alpha_{j\ell} \left(\alpha_{k\ell}\, C_{jk} - C_{j\ell} \right) + \frac{3}{2}\, \alpha_{k\ell}^2\, C_{k\ell}^2 + \\ & + \frac{3}{2} \sum_{j=k}^{\ell-1} \sum_{h=k}^{\ell-1} \left(\frac{m_j}{M_j} \cdot \frac{m_h}{M_h} \cdot \alpha_{j\ell}\, \alpha_{h\ell}\, C_{j\ell}\, C_{h\ell} \right) - 3\alpha_{k\ell}\, C_{k\ell} \cdot \\ & \cdot \sum_{j=k}^{\ell-1} \frac{m_j}{M_j}\, \alpha_{j\ell}\, C_{j\ell} \Bigg] \end{aligned} \qquad (39)$$

Lemma 1:
$$\sum_{k=1}^{\ell-1} \frac{m_k}{\rho_\ell} \left[\alpha_{k\ell}\, C_{k\ell} - \sum_{j=k}^{\ell-1} \frac{m_j}{M_j}\, \alpha_{j\ell}\, C_{j\ell} \right] \equiv 0$$

Proof:

Now
$$\sum_{k=1}^{\ell-1} \frac{m_k}{\rho_\ell}\, \alpha_{k\ell}\, C_{k\ell} - \sum_{k=1}^{\ell-1} \sum_{j=k}^{\ell-1} \frac{m_k}{\rho_\ell} \cdot \frac{m_j}{M_j}\, \alpha_{j\ell}\, C_{j\ell},$$

*This condition is clearly satisfied for hierarchical systems within which the bodies are numbered from 1 to n in the above mentioned systematic fashion (see Section 3.5). The central mass [e.g. the Sun in the case of the Solar System, the larger component of the binary in a triple stellar system, the planet in a satellite system (either including or excluding the Sun as a disturber), etc.] is denoted m_1 and the outermost $m_n : m_2$ is constrained to be less than m_1 the remaining masses being free to assume any values. Note also that $\alpha_{ij} < 1$ $(i < j)$ i.e. $\rho_i < \rho_j$ where $j = 3,\ldots,n$; $i = 2,\ldots, j-1$.

on reversing the order in the double summation (see Fig.3.5), is given by

$$\sum_{k=1}^{\ell-1} \frac{m_k}{\rho_\ell} \cdot \alpha_{k\ell}\, C_{k\ell} - \sum_{j=1}^{\ell-1} \left[\frac{1}{\rho_\ell} \cdot \frac{m_j}{M_j}\, \alpha_{j\ell}\, C_{j\ell} \sum_{k=1}^{j} m_k \right] .$$

Observing that $\sum_{k=1}^{j} m_k = M_j$ (since $m_o = 0$ is defined) and that k and j are dummy suffices, the result trivially follows. We may note finally that this result is independent of the definition of the α_{ij} and C_{ij} terms, and relies only upon the definition of M_j, which fact will be made use of in Lemma 2 below.

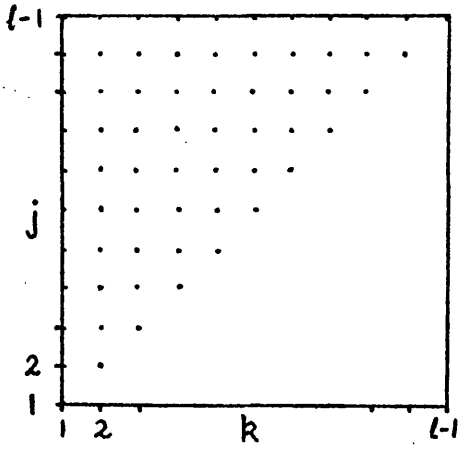

Figure 3.5

Lemma 2:

$$\sum_{k=1}^{\ell-1} \frac{m_k}{\rho_\ell} \left[\frac{1}{2} \sum_{j=k}^{\ell-1} \sum_{h=k}^{\ell-1} \frac{m_j}{M_j} \cdot \frac{m_h}{M_h}\, \alpha_{j\ell}\, \alpha_{h\ell}\, E_{jh\ell} - \sum_{j=k}^{\ell-1} \frac{m_j}{M_j}\, \alpha_{j\ell} \alpha_{k\ell}\, E_{jk\ell} \right]$$

$$= -\frac{1}{\rho_\ell} \sum_{j=1}^{\ell-1} \frac{m_j^2}{M_j}\, \alpha_{j\ell}^2\, P_2\,(C_{j\ell})$$

where P_2 is the Legendre polynomial of order two in $C_{j\ell}$ and

$$E_{ij\ell} = 3\, C_{i\ell}\, C_{j\ell} - C_{ij} .$$

Proof: By considering the symmetry of the region of (j,h) summation, the L.H.S. of the above expression can be rewritten as

$$\sum_{k=1}^{\ell-1} \sum_{j=k+1}^{\ell-1} \sum_{h=k}^{j-1} \frac{m_k}{\rho_\ell} \cdot \frac{m_j}{M_j} \cdot \frac{m_h}{M_h}\, \alpha_{j\ell} \alpha_{h\ell}\, E_{jh\ell} - \sum_{k=1}^{\ell-1} \frac{m_k^2}{M_k} \frac{\alpha_{k\ell}^2}{\rho_\ell}\, E_{kk\ell}$$

$$+ \tfrac{1}{2} \sum_{k=1}^{\ell-1} \sum_{j=k}^{\ell-1} \frac{m_k}{\rho_\ell} \left(\frac{m_j}{M_j} \right)^2 \alpha_{j\ell}^2\, E_{jj\ell} - \sum_{k=1}^{\ell-1} \sum_{j=k+1}^{\ell-1} \frac{m_k}{\rho_\ell} \cdot \frac{m_j}{M_j}\, \alpha_{j\ell}\, \alpha_{k\ell}\, E_{jk\ell}$$

Consider, firstly, the second and third terms in this expression. Reversing the order of the double summation in the second of these (as in Fig.3.5) we obtain

$$\frac{1}{2}\sum_{j=1}^{\ell-1}\left[\frac{1}{\rho_\ell}\left(\frac{m_j}{M_j}\right)^2\alpha_{j\ell}^2\,E_{jj\ell}\sum_{k=1}^{j}m_k\right]-\sum_{k=1}^{\ell-1}\frac{m_k^2}{M_k}\cdot\frac{\alpha_{k\ell}^2}{\rho_\ell}\,E_{kk\ell}$$

Upon noting $\sum_{k=1}^{j} m_k = M_j$, the fact that k and j are dummy suffices and that $E_{ii\ell} = 2\,P_2(C_{i\ell})$, these may be seen to contribute a term

$$-\frac{1}{\rho_\ell}\sum_{j=1}^{\ell-1}\frac{m_j^2}{M_j}\,\alpha_{j\ell}^2\,P_2(C_{j\ell})\,.$$

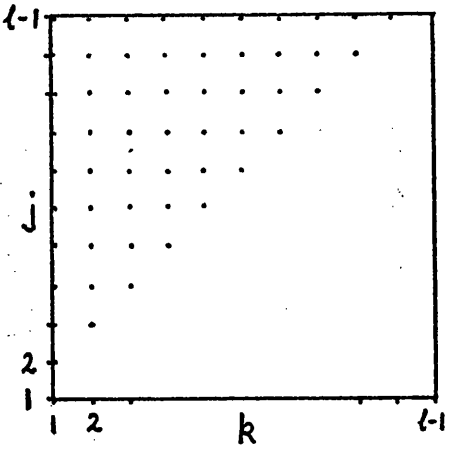

Fig.3.6

Next, considering the first and fourth terms above the order of (k,j) summation is changed (see Fig.3.6) yielding a contribution

$$\frac{1}{\rho_\ell}\sum_{j=2}^{\ell-1}\frac{m_j}{M_j}\,\alpha_{j\ell}\left[\sum_{k=1}^{j-1}\sum_{h=k}^{j-1}m_k\,\frac{m_h}{M_h}\,\alpha_{h\ell}\,E_{jh\ell}-\sum_{k=1}^{j-1}m_k\,\alpha_{k\ell}\,E_{jk\ell}\right],$$

which is identically zero by Lemma 1. Hence the required result is obtained. Q.E.D.

Using Equation (39) in conjunction with the results of Lemmas 1 and 2 we have the following simple expression for the B_ℓ, correct to the second order in the α's,

$$B_\ell = \frac{1}{\rho_\ell}\sum_{k=1}^{\ell-1}\left[m_k + m_k\,\alpha_{k\ell}^2\,P_2(C_{k\ell}) - \frac{m_k^2}{M_k}\,\alpha_{k\ell}^2\,P_2(C_{k\ell})\right],$$

which, on substitution into Equation (30), using Equations (31), (32) and (33), and noting that we defined $m_o = 0$ and $\underset{\sim}{\rho}_1 = \underset{\sim}{0}$, gives

$$\frac{m_i}{M_i}\frac{M_{i-1}}{}\,\ddot{\underset{\sim}{\rho}}_i = G\underset{\sim}{\nabla}_i\left[\sum_{\ell=2}^{n}\frac{m_\ell}{\rho_\ell}\left[M_{\ell-1}+\sum_{k=1}^{\ell-1}\frac{m_k\,M_{k-1}}{M_k}\,\alpha_{k\ell}^2\,P_2(C_{k\ell})\right]\right].$$

Noting that all the $\underset{\sim}{\rho}_i$ are independent we thus obtain

$$\ddot{\underset{\sim}{\rho}}_i = G M_i \nabla_{\underset{\sim}{i}} \left[\frac{1}{\rho_i} \{1 + \sum_{k=1}^{i-1} \epsilon^{ki} P_2(C_{ki}) + \sum_{\ell=i+1}^{n} \epsilon_{\ell i} P_2(C_{i\ell})\} \right] \quad (40)$$

where

$$\left.\begin{aligned} \epsilon^{ki} &= \frac{m_k M_{k-1}}{M_k M_{i-1}} \cdot \alpha_{ki}^2 \\ \epsilon_{\ell i} &= \frac{m_\ell}{M_i} \cdot \alpha_{i\ell}^3 \end{aligned}\right\} \quad (i = 2,\ldots,n). \quad (41)$$

It may be noted that if i = 2 there is no term contributed from the first summation; in addition if i = n there is no term contributed from the second summation as would be expected in the light of the comments below.

On examination, it can be seen that the first term on the right hand side of Equation (40) represents the undisturbed elliptic motion of the ith mass about the mass-centre of the subsystem of masses $m_1, m_2 \ldots, m_{i-1}$, while the $\epsilon^{ki}, \epsilon_{\ell i}$ provide a measure of the disturbance of the elliptic motion by the remaining masses. Note that ϵ^{ki} (a superscripted ϵ) denotes the disturbance of the ith body by the kth (inferior) body i.e. one closer to the central mass, while $\epsilon_{\ell i}$ (a subscripted ϵ) denotes the disturbance of the ith body by the ℓth (superior) body i.e. one further from the central mass. Furthermore, the disturbances in terms of the ϵ's are all normalised with respect to the central "two body" force i.e. the undisturbed Keplerian motion due to the force between the mass-centre at M_{i-1} and the mass m_i.

For example in the case of the Earth-Moon-Sun system the disturbance of the Moon on the orbit of the Sun relative to the Earth-Moon mass-centre is characterised by ϵ_{32} which is approximately 7.94×10^{-8} (as noted in Section 3.2). The disturbance of the Sun on the Earth-Moon system's orbit is characterised by ϵ^{23} which is 5.65×10^{-3}. Thus it is seen that the disturbance of the lunar orbit is greater than that of the solar orbit.

3.7 Discussion

The ε parameters derived in the previous section are thought to have a physical meaning for the stability of hierarchical dynamical systems. If we consider stability to be the situation wherein a system does not undergo an exchange of bodies, no body escapes the system and no collisions occur, then it may be conjectured that stability will be assured if the ε parameters are sufficiently small. In other words, small ε's will result in small perturbations to the orbits and the orbits may then be constrained to annuli about their initial positions for very long time scales, that is, it would be extremely unlikely that the mutual perturbations, characterised by the ε's, would be large enough to result in the disruption of the system.

For instance we see that the disturbance of the Moon on the orbit of the Sun relative to the mass-centre of the Earth-Moon system is negligible ($\varepsilon^{23} \simeq 8.10^{-8}$) inasmuch as any changes it will bring about in the orbit will be very small. However in the case of the disturbance of the relative orbit of the Earth and Moon by the Sun ($\varepsilon_{32} \simeq 6.10^{-3}$), this is not so clear. The question arises "Is the ε parameter small enough to ensure stability of the system?" Clearly, in the case of the Earth and Moon, the system has been observed to be stable for a long time and it therefore seems probable that the ε_{32} parameter is small enough.

In a many-body situation, such as the planetary and satellite systems, the ε-parameters may be considered jointly. The question may then be asked, if we neglect the effect of the P_2 factors, "Is the sum of the magnitudes of the ε parameters small enough for each body such that each orbit, described by the $\underset{\sim}{\rho}_i$ (i=2,...,n), will not be sufficiently perturbed so as to cause instability of the system?" Obviously if the ε's were zero then we could pack the bodies as close as we please in the hierarchy, i.e. taking large values for the α's approaching unity, and the system would remain stable in any case. However supposing the ε's are greater than zero, then there will be a limit to how closely the bodies may be packed. Packing them any closer than this limit would result in the perturbation on the orbits being so large as to allow instability of the system to set in. A case may also be envisaged where

the ε parameters are so large, approaching unity, that even a very loosely packed system cannot be stable i.e. the ratio of the disturbing force to the central "two-body" force is too great to allow stability.

With these considerations in mind the ε parameters are examined in the next chapter with reference to three-body systems which may also be examined by the analytical technique of the zero-velocity curves (see Chapter 2).

CHAPTER 4 EXAMINATION OF THE EMPIRICAL STABILITY PARAMETERS IN THE THREE-BODY CASE

4.1 Introduction

When the equations of motion of the general n-body problem are expressed in the Jacobian coordinate system an expansion of the force function, as was shown in Chapter 3, gives rise to a set of (n-1)(n-2) dimensionless parameters denoted ε^{ki}, $\varepsilon_{\ell i}$ { i=2,...,n; k = 2,...,i-1 ($i \geq 3$); ℓ=i + 1,...,n ($i \leq n-1$) }. These parameters characterise the size of the disturbance on the various two-body Keplerian orbits of the system and therefore appear suitable for the discussion of the stability of hierarchical systems, such as the solar system or triple stellar systems. The general case of n bodies is particularized, in Section 4.2, to n = 3 resulting in only two parameters ε^{23}, ε_{32}. The first parameter characterises the disturbance that the bodies m_1 and m_2 impose on the Keplerian orbit of m_3 relative to the mass-centre of the m_1, m_2 system due to their not being positioned at their common mass-centre; the second parameter characterises the disturbance of m_3 on the Keplerian orbit of m_2 relative to m_1. We then proceed in successive sections of this chapter to assess the suitability of these parameters for a discussion of stability.

The application of zero-velocity surfaces in the *restricted* three-body problem as a tool in investigating the stability of orbits is well known (e.g. Tisserand, 1889; Szebehely, 1967; Roy, 1978). The similar result for the general problem, due to Zare (1976, 1977), was described in Chapter 2. Recently several authors (Szebehely, 1977; Szebehely and McKenzie, 1977 a,b; Szebehely and Zare, 1977) have used this concept in dealing with the stability of hierarchical triple systems so that the finite mass of each body may be taken into account. These authors employ the technique of expressing general three-body motion as a superposition of two two-body motions in order to calculate c^2H values for the real system. The c^2H value thus obtained is then compared to the critical values in order to assess stability. Their analysis was shown to be quite consistent with available numerical studies (Harrington, 1972; Nacozy, 1976).

In Section 4.3 the work of Szebehely and Zare (1977) is therefore briefly reviewed. From this we obtain a stability criterion $\alpha_{act} < \alpha_{cr} = \alpha(\mu, \mu_3)$ where $\alpha_{act} = a_2/a_3$ is the ratio of the semi-major axes of inner (m_1, m_2) and outer (mass-centre of m_1 and m_2, m_3) two-body orbits, and μ and μ_3 specify the mass ratios of the system (m_1: m_2: m_3 = 1-μ: μ: μ_3). It may be noted here that $\alpha_{cr} = \alpha(\mu, \mu_3)$ defines a surface in the $O\mu\mu_3\alpha$ parameter space - this is called the *critical stability surface* (see Section 4.4). The derivation of this surface involves the lengthy and repeated solution of a number of high-order polynomial expressions and therefore tends to obscure the underlying physical processes. Therefore the parameters ε^{23} and ε_{32} are introduced and the *critical stability surface* is transformed from $\alpha_{cr} = \alpha(\mu, \mu_3)$ to $\alpha_{cr} = \alpha'(\varepsilon^{23}, \varepsilon_{32})$: it is then found that this latter surface has a particularly simple shape which permits a simple stability/instability criterion, based on the sizes of ε^{23} and ε_{32} to be employed. The dependance of the stability on α still remains but it is probable that this will be less for a fixed (ε^{23} , ε_{32}) pair, than for a fixed (μ, μ_3). If this is so, then the original three dimensional problem (in $O\mu\mu_3\alpha$ space) has effectively been reduced to a two dimensional one (in the $O\varepsilon^{23}$ ε_{32} plane).

Having established the stability criterion of Szebehely and Zare in $O\varepsilon^{23}\varepsilon_{32}\alpha_{23}$ parameter space we then proceed, in Section 4.5, to compare it with data on "real" triple systems, both actual (e.g. known triple stellar systems, triple subsystems*) and numerically simulated (see Harrington, 1977; Horedt, *et al.*, 1977; Hunter, 1967). Excellent agreement is obtained, providing justification that the ε parameters are meaningful for stability. In Section 4.6 some general conclusions are derived and the extension of the criterion to n(> 3) body systems is discussed.

*A triple sub-system or subset of a many-body system ($n \geq 4$) is defined as being any group of three bodies whose mutual gravitational forces constrain the motion so that the system can be considered as two disturbed binaries e.g. (1) Earth and Moon in rotation about each other and the Earth-Moon system in rotation about the Sun, (2) Jupiter in rotation about the Sun and Saturn in rotation about the mass-centre of the Sun-Jupiter system. Excluded would be combinations such as the Earth-Moon system being disturbed by Jupiter.

4.2 The Empirical Stability Parameters

The Equations (3.40) and (3.41) are now specialized to the case of the three-body problem in order to examine the empirical stability parameters in the light of the work of Szebehely and Zare (1977). With n=3, the case of hierarchical three-body systems (see Fig.4.1), the set of Equations (3.40) and (3.41) reduce to

$$\ddot{\underset{\sim}{\rho}}_2 = G M_2 \underset{\sim}{\nabla}_2 \left[\frac{1}{\rho_2} \{ 1 + \varepsilon_{32} P_2 (C_{23}) \} \right] \qquad (1)$$

$$\ddot{\underset{\sim}{\rho}}_3 = G M_3 \underset{\sim}{\nabla}_3 \left[\frac{1}{\rho_3} \{ 1 + \varepsilon^{23} P_2 (C_{23}) \} \right] \qquad (2)$$

where $$\varepsilon^{23} = \frac{m_2 M_1}{M_2^2} \cdot \alpha_{23}^2 \qquad (3a)$$

$$\varepsilon_{32} = \frac{m_3}{M_2} \cdot \alpha_{23}^3 \cdot \qquad (3b)$$

and all the symbols have their usual meaning. It may be noted that the ε^{23} term is exactly that derived by Brown in his lunar Theory (1896). In terms of the individual masses we have

$$\varepsilon^{23} = \frac{m_1 m_2}{(m_1 + m_2)^2} \cdot \alpha_{23}^2 \cdot \qquad (4a)$$

and

$$\varepsilon_{32} = \frac{m_3}{(m_1 + m_2)} \cdot \alpha_{23}^3 \cdot \qquad (4b)$$

The physical significance of the $(\varepsilon^{23}, \varepsilon_{32})$ is now obvious. ε^{23} is a measure of the disturbance of the third mass by the other two (the close binary): it must be symmetrical in the masses m_1 and m_2 and contains α_{23} raised to the second power as a direct consequence of the Newtonian gravitational force law. ε_{32}, on the other hand, which measures the disturbance of the binary by the outside mass, contains only m_3 and α_{23} raised to the *third* power, the disturbance being in the nature of a differential gravitational force across the orbit of m_2 relative to m_1.

It is worthwhile noting that if m_2 is moving in a disturbed Keplerian orbit about m_1 we may define at any instant a set of elements for an

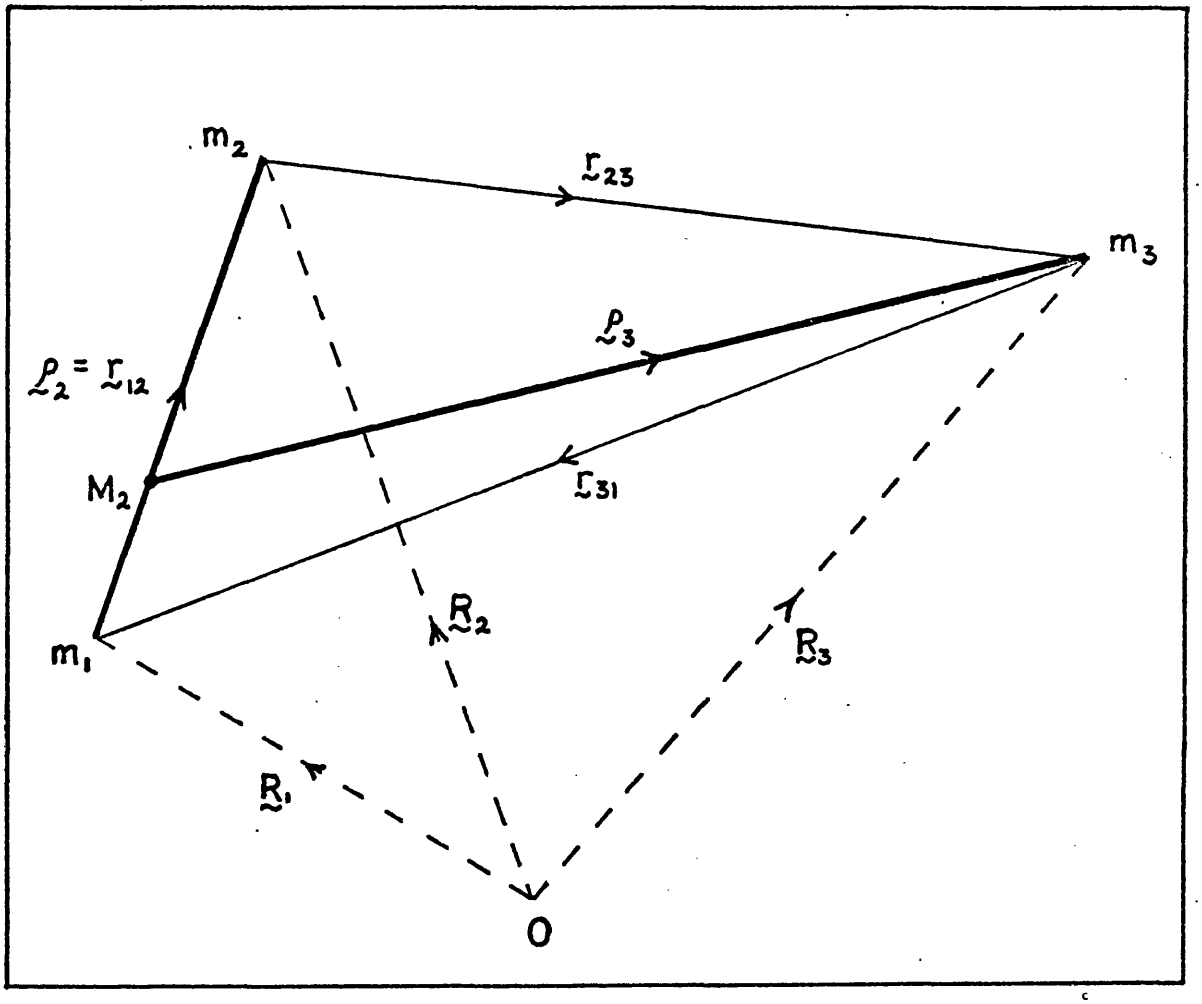

Figure 4.1 Definitions of quantities in the Jacobian Coordinate system in the case n = 3.

osculating orbit viz. a_2, e_2, i_2, Ω_2, ω_2, τ_2 with the position in this orbit being given by the true anomaly f_2 so that the expression for ρ_2, at any instant, in terms of these quantities is

$$\rho_2 = \frac{a_2 (1 - e_2^2)}{1 + e_2 \cos f_2} . \qquad (5a)$$

Similarly for the orbit of m_3 about the mass-centre of m_1 and m_2 we have

$$\rho_3 = \frac{a_3 (1 - e_3^2)}{1 + e_3 \cos f_3} . \qquad (5b)$$

4.3 The Stability of Coplanar Hierarchical Three-Body Systems - A Review.

The study of regions of possible motion (for given initial conditions) in the coplanar general three-body problem by Zare (1976, 1977) has shown that the stability - as previously defined in Chapter 2 - is controlled by the parameter c^2H, where c is the total angular momentum and H the total energy of the system. Outlined below are the basic steps of the procedure given in Szebehely and Zare (1977).

That c^2H should enter naturally into the problem follows from dimensional considerations. Any stability parameter must be dimensionless and be a function only of the force coupling constant G (dimensions $L^3 T^{-2} M^{-1}$), the angular momentum c (dimensions $ML^2 T^{-1}$), the energy H (dimensions $ML^2 T^{-2}$), and the total mass M (these latter three quantities being constants of the motion). From this it follows that stability is controlled by the parameter c^2H/G^2M^5 (cf. Szebehely and Zare, 1977).

Zare (1977) stated the problem as follows

"..... *If the value of* c^2H *is smaller than the value corresponding to the* primary bifurcation point $(c^2H)_1$, *two of the bodies form a binary and the configuration cannot be disturbed by the third mass.*

If $(c^2H)_1 < c^2H < (c^2H)_2$, *where* $(c^2H)_2$ *corresponds to the* secondary bifurcation point, *there will be no exchange between the bodies if the smallest mass is outside.....*".

The primary bifurcation point may be identified as that value of c^2H $[= (c^2H)_1]$ when the forbidden regions change from being triply to doubly connected. The secondary bifurcation occurs at $c^2H = (c^2H)_2$ when the transition from doubly to simply connected forbidden regions takes place. Thus we require to determine the primary or secondary bifurcation point depending upon certain conditions. Considering the well-known collinear equilibrium configurations: in general there are three possible arrangements of the masses m_1, m_2, m_3, each of which will determine the primary, secondary or tertiary bifurcation points - depending on the relative sizes of the masses. However, since m_1 and m_2 are constrained to move about each other with the mass m_3 outside, we have only two remaining possibilities: if m_3 is not the smallest mass we determine the primary bifurcation point and the masses assume the order m_3, min (m_1,m_2) max(m_1,m_2). If the masses are then in the order m_3, m_2, m_1 i.e. $m_1 > m_2$, $m_3 \not< \min(m_1,m_2)$ and we define $\mu = m_2/(m_1 + m_2)$, $\mu_3 = m_3/(m_1 + m_2)$ we require to solve the following quintic equation for ρ:

$$(\mu+\mu_3)\rho^5+(2\mu+3\mu_3)\rho^4+(\mu+3\mu_3)\rho^3-(3-2\mu)\rho^2-(3-\mu)\rho-1 = 0 \quad (6)$$

where, if we define $|\overrightarrow{m_3\ m_2}| = 1$, then $|\overrightarrow{m_1\ m_2}| = \rho$.
If m_3 is the smallest mass we again solve Equation (6) for ρ, this time however obtaining the secondary bifurcation point.

The critical value of c^2H is then obtained from

$$(c^2H)_{cr} = -\frac{G^2 f^2(\rho)\, g(\rho)}{2(1+\mu_3)} \quad (7)$$

where G is the constant of gravitation

$$f(\rho) = \mu\mu_3 + \frac{\mu_3(1-\mu)}{1+\rho} + \frac{\mu(1-\mu)}{\rho} \quad (8)$$

and

$$g(\rho) = \mu\mu_3 + \mu_3(1-\mu)(1+\rho)^2 + \mu(1-\mu)\rho^2 \quad (9)$$

(cf. Equations (2.38) and (2.48)). It is now possible to define a *measure of stability*

$$\beta = \frac{c^2H - (c^2H)_{cr}}{(c^2H)_{cr}} \quad (10)$$

where c^2H is the actual value for any given system such that if $\beta \geq 0$ then the triple system is stable (equality implying *critical stability*), whereas if $\beta < 0$ then exchange between bodies may occur. The value of c^2H is obtained from the two-body approximation to the three-body motions (see Szebehely and Zare, 1977) through

$$-\frac{(c^2H)}{G^2} = \mu^2(1-\mu)^2\mu_3\left[\frac{1-e_2^2}{2}\right]\alpha \pm \frac{\mu(1-\mu)\mu_3^2}{(1+\mu_3)^{\frac{1}{2}}}\left\{(1-e_2^2)(1-e_3^2)\right\}^{\frac{1}{2}}\alpha^{\frac{1}{2}}$$
$$+\left[\frac{1-e_2^2}{2}\right]\mu^3(1-\mu)^3 + \left[\frac{1-e_3^2}{2}\right]\frac{\mu_3^3}{1+\mu_3} \pm \frac{\mu^2(1-\mu)^2\mu_3}{(1+\mu_3)^{\frac{1}{2}}}\cdot$$
$$\cdot\left\{(1-e_2^2)(1-e_3^2)\right\}^{\frac{1}{2}}\alpha^{-\frac{1}{2}}$$
$$+\left[\frac{1-e_3^2}{2}\right]\frac{\mu(1-\mu)\,\mu_3^2}{1+\mu_3}\,\alpha^{-1} \qquad (11)$$

where $\alpha = a_2/a_3$,

(a_2, e_2) refer to the orbit of m_2 about m_1, (a_3, e_3) refer to the orbit of m_3 about the mass-centre of (m_1, m_2) and + or - refers respectively to co-rotational and counter-rotational motion (although we consider only the former in the remainder of the chapter).

Thus, from given values of μ, μ_3 and e_2, e_3, a value for α, α_{cr}, can be determined such that $c^2H(\alpha,\mu, \mu_3, e_2, e_3)$ as derived through Equation (11) is identically equal to $(c^2H)_{cr}$ as obtained by solution of Equation (6) and application of Equations (7), (8) and (9) i.e. $\beta = 0$. This is interpreted as a *critical stability surface* in the parameter space $0\mu\mu_3\alpha$ such that $\alpha_{cr} = \alpha(\mu, \mu_3)$ - for a given pair e_2, e_3 - is the value of α which results in critical stability for the system with mass parameters μ, μ_3. If $\alpha \leq \alpha_{cr}$ then the system is stable (equality again implying critical stability) and exchange between bodies cannot occur, whereas if $\alpha > \alpha_{cr}$ then exchange *may* occur. Although these surfaces are of interest in themselves (various cross sections have been presented, see Szebehely and Zare,1977), we proceed in the light of physical considerations to modify the problem slightly (in the next section) and translate the critical stability surface into

the $0\varepsilon^{23}\ \varepsilon_{32}\alpha_{23}$* parameter space.

4.4 Determination and Modification of the Critical Stability Surface

Referring to Equations (4) it is easily seen that the $\varepsilon^{23},\varepsilon_{32}$ parameters, in terms of the dimensionless mass parameters μ and μ_3 become

$$\varepsilon^{23} = \mu(1-\mu)\ \alpha_{23}^2 \qquad (12a)$$

and

$$\varepsilon_{32} = \mu_3\ \alpha_{23}^3 \ . \qquad (12b)$$

These may be taken respectively as a measure of the disturbance of (i) the elliptic motion of the mass μ_3 about the mass-centre of the binary $(1-\mu,\mu)$ by the masses μ and $1-\mu$ not being found at their common mass-centre and (ii) the elliptic motion of the masses $(1-\mu,\mu)$ about their common mass-centre by the mass μ_3. Thus, it is clearly reasonable to expect that if the values of ε^{23}, ε_{32} are sufficiently small then the elliptic motion will continue largely undisturbed for an astronomically long period of time. This is essentially the approach that Brown took in his Lunar Theory: he neglected the very small term $m_E\ m_M/(m_E + m_M)\ r^2/\rho^2$ in the expansion of the disturbing function and took the motion of the Sun relative to the mass-centre of the Earth-Moon system to be exactly elliptic since any disturbances to that motion would be very small. It is therefore contended that the values ε^{23}, ε_{32} will throw light on the possible stability or instability of hierarchical triple systems, and therefore we proceed to find the critical stability surface $\alpha_{cr} = \alpha'(\varepsilon^{23},\varepsilon_{32})$ in place of $\alpha_{cr} = \alpha(\mu,\mu_3)$, where as arguments for the function α' we take initial values of $\varepsilon^{23},\varepsilon_{32}$ viz.

$$\varepsilon^{23} = \mu(1-\mu)\ \alpha^2 \qquad (13a)$$

and

$$\varepsilon_{32} = \mu_3\ \alpha^3, \qquad (13b)$$

the orbits being considered (at least initially) to be circular so that $\rho_2 = a_2$ and $\rho_3 = a_3$.

*Note that the initial value of α_{23} is being considered here as equivalent to α, which, considering Equations (5), is certainly true for circular orbits with which we deal here.

As a preliminary to the determination of the α_{cr} surface we examine the behaviour of the surface in $0\mu\mu_3\alpha$ parameter space as $\mu, \mu_3 \to 0$. If $\mu, \mu_3 << 1$ then we can choose the dominant terms in Equation (6) and derive the expression

$$(\mu + \mu_3)\rho^3 - 3 \simeq 0 \qquad (14)$$

which has the solution

$$\rho = \left[\frac{3}{\mu + \mu_3}\right]^{1/3} . \qquad (15)$$

Thus it can be seen that for small μ, μ_3 $\rho >> 1$.

If we then consider Equations (8) and (9), neglect terms involving products of μ, μ_3 and approximate $1 + \rho \simeq \rho$ (since $\rho >> 1$), then by Equation (7), on putting $\mu_3 = k\mu$, we obtain

$$\frac{-2(c^2H)_{cr}}{G^2 \mu^3} = (k + 1)^3 \qquad (16)$$

and similarly Equation (11) (on setting $e_2 = e_3 = 0$ and taking the + sign for co-rotational motion) can be rewritten, upon neglect of terms of order μ and higher

$$\frac{-2(c^2H)}{G^2 \mu^3} = k\alpha + 2k^2\alpha^{\frac{1}{2}} + k^3 + 1 + 2k\alpha^{-\frac{1}{2}} + k^2\alpha^{-1}. \qquad (17)$$

Equating (16) and (17) then yields the equation for α_{cr}

$$\alpha_{cr}^2 + 2k\,\alpha_{cr}^{3/2} - (3 + 3k)\alpha_{cr} + 2\alpha_{cr}^{\frac{1}{2}} + k = 0, \qquad (18)$$

which has one physical solution, $\alpha_{cr} = 1$. Thus it is seen that as $\mu, \mu_3 \to 0$, $\alpha_{cr} \to 1$. It can readily be seen by examination of Equations (13) that $\alpha_{cr} \to 1$ as $\varepsilon^{23}, \varepsilon_{32} \to 0$ also.

Since the expression for the ε-parameters involve α it is clear that, for calculation of the surface $\alpha_{cr} = \alpha'(\varepsilon^{23}, \varepsilon_{32})$, an iterative procedure is required, commencing with some estimated value. We use the fact that for small $(\varepsilon^{23}, \varepsilon_{32})$ $\alpha_{cr} \simeq 1$ and commence calculation of the surface from these small values working towards the larger values, using previously calculated values of α_{cr} as the first

approximation in successive calculations. A suitable method of iteration was found to be as follows:

(i) calculation of values of μ and μ_3 from approximate value of $\alpha = \alpha_{cr}$ through Equations (13);

(ii) solution of Equation (6) by the Newton-Raphson method to obtain the only root, ρ, for the above calculated values of μ, μ_3 thus yielding, through application of Equations (7), (8) and (9) a value of $(c^2H)_{cr}$;

(iii) solution of Equation (11), again by Newton-Raphson procedure - taking care to choose the "correct" root by considering the continuity of the surface - to obtain a new approximation to $\alpha_{cr} = \alpha'(\varepsilon^{23}, \varepsilon_{32})$. This process was repeated to yield sufficient accuracy in α_{cr}.

Considering the expression for ε^{23} - Equation (13a) - we find the value of α is restricted by the condition that $\mu \in \mathbb{R}$.

Now

$$\varepsilon^{23} = \mu(1-\mu)\alpha^2$$

may be recast in the form

$$\mu^2 - \mu + \frac{\varepsilon^{23}}{\alpha^2} = 0 \qquad (19)$$

which is a quadratic in μ which may be solved for given values of ε^{23} and α. The solution is

$$\mu = \frac{1 \pm \left[1 - \frac{4\varepsilon^{23}}{\alpha^2}\right]^{\frac{1}{2}}}{2} \qquad (20)$$

where the " - " sign is applicable since $\mu \leq \frac{1}{2}$. It is thus required for μ to be real that

$$\alpha \geq 2(\varepsilon^{23})^{\frac{1}{2}} . \qquad (21)$$

Setting $\alpha = 2(\varepsilon^{23})^{\frac{1}{2}}$ defines the surface $\mu = \frac{1}{2}$ in the $0\varepsilon^{23}\varepsilon_{32}\alpha$ parameter space. Above this surface, i.e. $\alpha > 2(\varepsilon^{23})^{\frac{1}{2}}$, μ is less than $\frac{1}{2}$ and below this surface where $\alpha < 2(\varepsilon^{23})^{\frac{1}{2}}$ it is found that μ is in fact complex thus precluding the existence of any real systems in this

region. This condition leads to the critical stability surface being *cut off* beyond certain values of $(\varepsilon^{23},\varepsilon_{32})$ outwith which α_{cr} would not comply with inequality (21). This implies the existence of regions in the $\varepsilon^{23},\varepsilon_{32}$-plane where no physically meaningful value of α_{cr} exists for such ε values and therefore any *real* system of three masses, defined by $\mu = \mu(\varepsilon^{23},\alpha)$, $\mu_3 = \mu_3(\varepsilon_{32}, \alpha)$ and α, has its α value greater than $\alpha_{cr} = \alpha(\mu,\mu_3)$, and *may* therefore undergo an exchange of bodies. This is a consequence of the fact that no system may change from one side of the critical stability surface to the other during the transformation from $\alpha_{cr} = \alpha(\mu, \mu_3)$ to $\alpha_{cr} = \alpha'(\varepsilon^{23},\varepsilon_{32})$: this point is discussed further in the next section.

As a first step the critical stability surface $\alpha_{cr} = \alpha(\mu, \mu_3)$ (see Figure 4.2) was obtained, the eccentricities e_2 and e_3 being zero. The equivalent critical stability surface $\alpha_{cr} = \alpha'(\varepsilon^{23},\varepsilon_{32})$ (e_2 and e_3 again both zero) is shown in Fig.4.3 - the diagram demonstrating the effect of the cut off of the surface due to inequality (21).

The main difference between these two diagrams may be put as follows. In Fig.4.2, which shows the critical stability surface in $0\mu\mu_3\alpha$ parameter space, it is clear that for all values of μ,μ_3 it is possible, with sufficiently small α, to arrange that a system with those mass parameters be stable since the surface extends in μ_3 from $10^{-\infty}$ to $10^{+\infty}$ and from $10^{-\infty}$ to $10^{\log(0.5)}$ in μ. However, upon examination of Fig.4.3 we see that the new critical stability surface in the $0\ \varepsilon^{23}\varepsilon_{32}\alpha$ parameter space is more restricted. The values of ε^{23} and ε_{32} can both be very small, i.e. down to $10^{-\infty}$, however, if any possibility of stability is to remain (in the sense of $\alpha \leqslant \alpha_{cr}$), the ε values of any system must be less than the *cut off values*. The cut off values are defined as those values of $\varepsilon^{23},\varepsilon_{32}$ where the critical stability surface, $\alpha_{cr} = \alpha'(\varepsilon^{23},\varepsilon_{32})$ intersects with the surface $\mu = \frac{1}{2}$ (as shown in Fig.4.3). This intersection if projected onto the $\varepsilon^{23},\varepsilon_{32}$ -plane will form a line which is the boundary between the region where stability is possible (towards smaller values of ε^{23} and ε_{32}) and stability is impossible (towards higher values of ε^{23} and ε_{32}); we stress here again that stability here implies closure of the zero-velocity surfaces and therefore an exchange between bodies is precluded. Thus

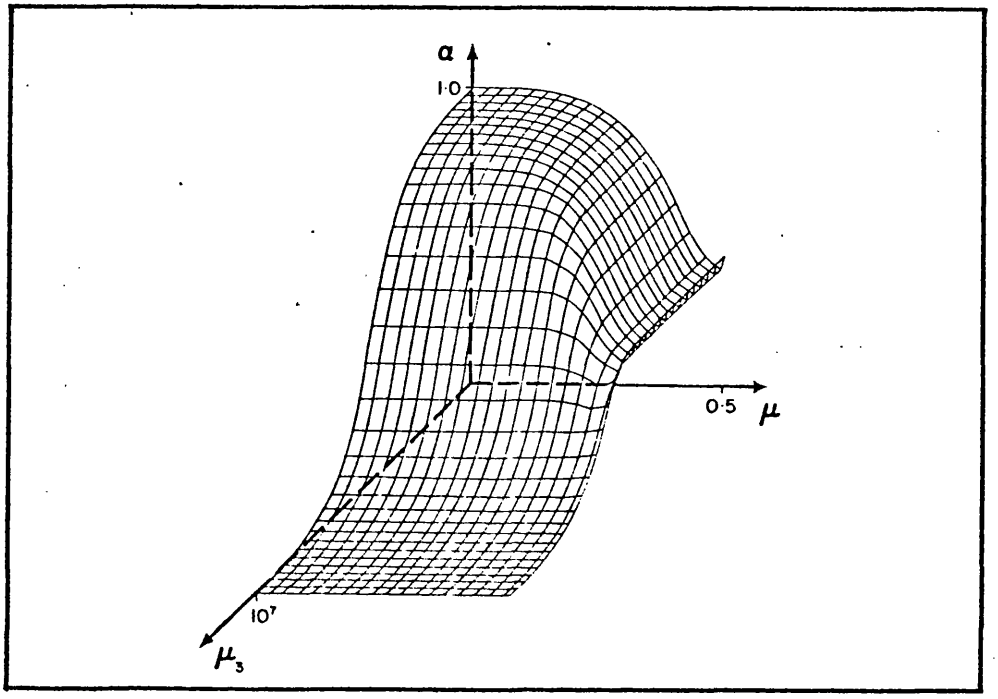

Figure 4.2 The critical stability surface in $O\mu\mu_3\alpha$ parameter space. (n.b. Origin situated at $\mu = 10^{-9}$, $\mu_3 = 10^{-9}$ and $\alpha = 0$ and $O\mu$ and $O\mu_3$ axes' scales are logarithmic).

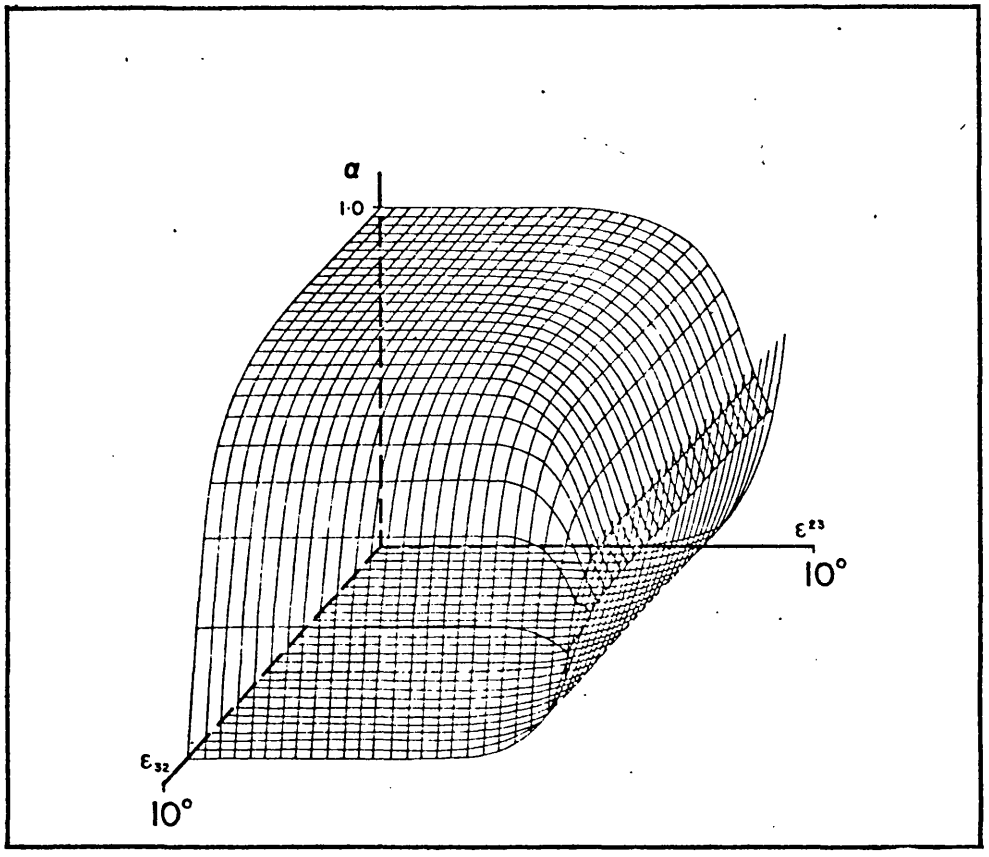

Figure 4.3 The critical stability surface in $O\varepsilon^{23}\varepsilon_{32}\alpha$ parameter space. (n.b. Origin situated at $\varepsilon^{23} = 10^{-9}$, $\varepsilon_{32} = 10^{-9}$ and $\alpha = 0$ and the $O\varepsilon^{23}$ and $O\,\varepsilon_{32}$ axes' scales are logarithmic).

regions in the $\varepsilon^{23},\varepsilon_{32}$ - plane are determined where it is possible to state *a priori*, without recourse to numerical solution of several equations, that the zero-velocity curves in a system found in this region are open and the system *may* be unstable.

4.5 Real Systems and the Critical Stability Surface

In this section, in order to demonstrate the benefits of the alternative calculation of the critical stability surface in the form $\alpha_{cr} = \alpha'(\varepsilon^{23},\varepsilon_{32})$, a change in the presentation of the surfaces is effected: they are represented as contours of equal α_{cr} in either the μ, μ_3-plane or the $\varepsilon^{23},\varepsilon_{32}$-plane. Tabulated below are all the triple systems considered in this section (see pp. 84 - 93).

The systems which we have tabulated may be divided into three categories, according to their origin, as follows:

Category A - The Solar System

Category B - Simulated Planetary Systems - from numerical investigation by other authors

Category C - Triple Stellar Systems

Categories A and B can be further subdivided into the following groups:-

Group A1. - The Planetary System - planet disturbing planet

Group A2. - The Satellite Systems - satellite disturbing satellite

Group A3. - The Satellite Systems - Sun disturbing satellite

Group A4. - The Asteroid System - planet disturbing asteroid

and

Group B1. - Superior planet of binary star system

Group B2. - Inferior planet of binary star system

Group B3. - Planetary Systems - planet disturbing planet.

Table 4.1

Group A1

System Number	Name	μ	μ_3	α_{23}	α_{cr}	ε^{23}	ε_{32}
1	Sun - Mercury - Venus	1.680E-07	2.453E-06	5.353E-01	9.676E-01	4.814E-08	3.763E-07
2	- Earth	1.680E-07	3.003E-06	3.871E-01	9.656E-01	2.517E-08	1.742E-07
3	- Mars	1.680E-07	3.243E-07	2.539E-01	9.813E-01	1.083E-08	5.308E-09
4	- Jupiter	1.680E-07	9.550E-04	7.438E-02	7.999E-01	9.294E-10	3.930E-07
5	- Saturn	1.680E-07	2.859E-04	4.052E-02	8.588E-01	2.758E-10	1.902E-08
6	- Uranus	1.680E-07	4.384E-05	2.018E-02	9.203E-01	6.842E-11	3.603E-10
7	- Neptune	1.680E-07	5.195E-05	1.288E-02	9.160E-01	2.787E-11	1.110E-10
8	- Pluto	1.680E-07	2.703E-06	9.815E-03	9.667E-01	1.618E-11	2.556E-12
9	- Venus - Earth	2.450E-06	3.003E-06	7.233E-01	9.589E-01	1.282E-06	1.136E-06
10	- Mars	2.450E-06	3.243E-07	4.746E-01	9.670E-01	5.518E-07	3.467E-08
11	- Jupiter	2.450E-06	9.550E-04	1.390E-01	7.997E-01	4.734E-08	2.565E-06
12	- Saturn	2.450E-06	2.859E-04	7.571E-02	8.584E-01	1.404E-08	1.241E-07
13	- Uranus	2.450E-06	4.384E-05	3.771E-02	9.190E-01	3.484E-09	2.351E-09
14	- Neptune	2.450E-06	5.195E-05	2.406E-02	9.148E-01	1.418E-09	7.236E-10
15	- Pluto	2.450E-06	2.703E-06	1.834E-02	9.597E-01	8.241E-10	1.667E-11
16	- Earth - Mars	3.000E-06	3.243E-07	6.562E-01	9.650E-01	1.292E-06	9.163E-08
17	- Jupiter	3.000E-06	9.550E-04	1.922E-01	7.997E-01	1.108E-07	6.781E-06
18	- Saturn	3.000E-06	2.859E-04	1.048D-01	8.583E-01	3.295E-08	3.291E-07
19	- Uranus	3.000E-06	4.384E-05	5.214E-02	9.187E-01	8.156E-09	6.214E-09
20	- Neptune	3.000E-06	5.195E-05	3.327E-02	9.145E-01	3.321E-09	1.913E-09
21	- Pluto	3.000E-06	2.703E.06	2.535E-02	9.583E-01	1.928E-09	4.403E-11

Table 4.1 (contd.)

Group A1

System Number	Name		μ	μ_3	α_{23}	α_{cr}	ε^{23}	ε_{32}
22	- Mars	- Jupiter	3.240E-07	9.550E-04	2.729E-01	7.999E-01	2.413E-08	1.941E-05
23		- Saturn	3.240E-07	2.859E-04	1.596E-01	8.587E-01	8.253E-09	1.162E-06
24		- Uranus	3.240E-07	4.384E-05	7.944E-02	9.202E-01	2.045E-09	2.198E-08
25		- Neptune	3.240E-07	5.195E-05	5.069E-02	9.159E-01	8.325E-10	6.766E-09
26		- Pluto	3.240E-07	2.703E-06	3.863E-02	9.661E-01	4.836E-10	1.559E-10
27	- Jupiter	- Saturn	9.540E-04	2.859E-04	5.454E-01	7.816E-01	2.835E-04	4.638E-05
27N		- Saturn †	2.730E-02	8.405E-03	5.454E-01	5.131E-01	7.899E-03	1.364E-03
28		- Uranus	9.540E-04	4.384E-05	2.713E-01	7.940E.01	7.015E-05	8.754E-07
29		- Neptune	9.540E-04	5.195E-05	1.731E-01	7.935E-01	2.856E-05	2.694E-07
30		- Pluto	9.540E-04	2.702E-06	1.317E-01	7.963E-01	1.653E-05	6.172E-09
31	- Saturn	- Uranus	2.860E-04	4.384E-05	4.973E-01	8.509E-01	7.071E-05	5.392E-06
32		- Neptune	2.860E-04	5.195E-05	3.173E-01	8.499E-01	2.879E-05	1.660E-06
33		- Pluto	2.860E-04	2.702E-06	2.415E-01	8.565E-01	1.668E-05	3.806E-08
34	- Uranus	- Neptune	4.380E-05	5.195E-05	6.381E-01	8.981E-01	1.783E-05	1.350E-05
35		- Pluto	4.380E-05	2.702E-06	4.856E-01	9.183E-01	1.033E-05	3.094E-07

† Nacozy's unstable system with masses of Jupiter and Saturn increased by a factor of about 30

Table 4.2
Group A2

Number	System Name			μ^*	μ_3^*	α_{23}	α_{cr}	ε^{23}	ε_{32}
41	Jupiter	- Io	- Europa	3.817E-05	2.481E-05	6.289E-01	9.104E-01	1.510E-05	6.172E-06
42			- Ganymede	3.817E-05	8.197E-05	3.940E-01	8.909E-01	5.925E-06	5.013E-06
43			- Callisto	3.817E-05	5.102E-05	2.240E-01	9.003E-01	1.915E-06	5.734E-07
44		-V	- Io	1.000E-15	3.817E-05	4.289E-01	9.239E-01	1.840E-16	3.011E-06
45		- Callisto	-Vl,Vll,X,Xlll	5.102E-05	1.000E-15	1.590E-01	9.161E-01	1.290E-06	4.020E-18
46		- Europa	- Ganymede	2.481E-05	8.197E-05	6.265E-01	8.948E-01	9.739E-06	2.016E-05
47			- Callisto	2.481E-05	5.102E-05	3.562E-01	9.053E-01	3.148E-06	2.306E-06
48		- Ganymede	- Callisto	8.197E-05	5.102E-05	5.685E-01	8.871E-01	2.649E-05	9.374E-06
49	Saturn	- Janus	- Mimas	1.000E-15	6.667E-08	8.548E-01	9.903E-01	7.307E-16	4.164E-08
50			- Enceladus	1.000E-15	1.429E-07	6.681E-01	9.875E-01	4.464E-16	4.260E-08
51			- Tethys	1.000E-15	1.099E-06	5.390E-01	9.757E-01	2.905E-16	1.721E-07
52			- Dione	1.000E-15	2.041E-06	4.206E-01	9.702E-01	1.769E-16	1.518E-07
53			- Rhea	1.000E-15	4.000E-06	3.017E-01	9.629E-01	9.102E-17	1.098E-07
54			- Titan	1.000E-15	2.410E-04	1.301E-01	8.660E-01	1.693E-17	5.306E-07
55		- Mimas	- Enceladus	6.667E-08	1.429E-07	7.815E-01	9.859E-01	4.072E-08	6.819E-08
56			- Tethys	6.667E-08	1.099E-06	6.305E-01	9.752E-01	2.650E-08	2.754E-07
57			- Dione	6.667E-08	2.041E-06	4.921E-01	9.699E-01	1.614E-08	2.432E-07
58			- Rhea	6.667E-08	4.000E-06	3.529E-01	9.627E-01	8.303E-09	1.758E-07
59			- Titan	6.667E-08	2.410E-04	1.522E-01	8.658E-01	1.544E-09	8.496E-07
60		- Enceladus	- Tethys	1.429E-07	1.099E-06	8.068E-01	9.747E-01	9.299E-08	5.771E-07
61			- Dione	1.429E-07	2.041E-06	6.296E-01	9.695E-01	5.663E-08	5.093E-07
62			- Rhea	1.429E-07	4.000E-06	4.516E-01	9.625E-01	2.913E-08	3.684E-07
63			- Titan	1.429E-07	2.410E-04	1.948E-01	8.658E-01	5.421E-09	1.781E-06

Table 4.2 (contd.)

Group A2

System Number	Name		μ^*	μ_3^*	α_{23}	α_{cr}	ε^{23}	ε_{32}
64	Saturn - Tethys	- Dione	1.099E-06	2.041E-06	7.804E-01	9.657E-01	6.693E-07	9.700E-07
65		- Rhea	1.099E-06	4.000E-06	5.598E-01	9.599E-01	3.444E-07	7.017E-07
66		- Titan	1.099E-06	2.410E-04	2.414E-01	8.656E-01	6.404E-08	3.390E-06
67	- Dione	- Rhea	2.041E-06	4.000E-06	7.173E-01	9.576E-01	1.050E-06	1.476E-06
68		- Titan	2.041E-06	2.410E-04	3.093E-01	8.654E-01	1.952E-07	7.130E-06
69	- Rhea	- Titan	4.000E-06	2.410E-04	4.313E-01	8.651E-01	7.441E-07	1.933E-05
70	- Titan	- Hyperion	2.410E-04	2.000E-07	8.251E-01	8.641E-01	1.640E-04	1.123E-07
71		- Iapetus	2.410E-04	3.333E-06	3.431E-01	8.636E-01	2.836E 05	1.346E-07
72		- Phoebe	2.410E-04	1.000E-15	9.429E-02	8.642E-01	2.142E-06	8.383E-19
73	Uranus - Miranda	- Ariel	1.000E-06	1.493E-05	6.458E-01	9.422E-01	4.171E-07	4.020E-06
74		- Umbriel	1.000E-06	5.882E-06	4.644E-01	9.558E-01	2.157E-07	5.892E-07
75		- Titania	1.000E-06	5.000E-05	2.831E-01	9.165E-01	8.015E-08	1.134E-06
76		- Oberon	1.000E-06	2.941E-05	2.112E-01	9.290E-01	4.461E-08	2.771E-07
77	- Ariel	- Umbriel	1.493E-05	5.882E-06	7.191E-01	9.368E-01	7.718E-06	2.187E-06
78		- Titania	1.493E-05	5.000E-05	4.384E-01	9.098E-01	2.869E-06	4.213E-06
79		- Oberon	1.493E-05	2.941E-05	3.271E-01	9.199E-01	1.597E-06	1.029E-06
80	- Umbriel	- Titania	5.882E-06	5.000E-05	6.096E-01	9.140E-01	2.186E-06	1.133E-05
81		- Oberon	5.882E-06	2.941E-05	4.549E-01	9.255E-01	1.217E-06	2.769E-05
82	- Titania	- Oberon	5.000E-05	2.941E-05	7.462E-01	9.037E-01	2.784E-05	1.222E-05
83	Neptune - Triton	- Nereid	1.332E-03	3.333E-07	6.355E-02	7.764E-01	5.370E-06	8.555E-11

* where values of masses are too small to be known accurately a mass of 10^{-15} is assumed (in units of the planetary mass).

Table 4.3

Group A3

System Number	Name		μ^*	μ_3	α_{23}	α_{cr}	ε_{23}	ε_{32}
84	Sun - Earth	- Moon	1.218E-02	3.330E+05	2.570E-03	4.478E-03	7.944E-08	5.653E-03
85	- Mars	- Deimos	1.000E-14	3.083E+06	1.031E-04	2.163E-03	1.063E-22	3.378E-06
86		- Phobos	1.000E-14	3.083E+06	4.124E-05	2.163E-03	1.700E-23	2.162E-07
87	- Jupiter	-VIII,IX,XI,XII	1.000E-14	1.047E+03	2.923E-02	3.020E-02	8.544E-18	2.615E 02
88		-VI,VII,X,XII	1.000E-14	1.047E+03	1.522E-02	3.020E-02	2.316E-18	3.692E-03
89		- Callisto	5.102E-05	1.047E+03	2.420E-03	3.020E-02	2.988E-10	1.484E-05
90		- Ganymede	8.197E-05	1.047E+03	1.376E-03	3.020E-02	1.552E-10	2.728E-06
91		- Europa	2.481E-05	1.047E+03	8.621E-04	3.020E-02	1.844E-11	6.710E-07
92		- Io	3.817E-05	1.047E+03	5.422E-04	3.020E-02	1.122E-11	1.669E-07
93		- V	1.000E-14	1.047E+03	2.325E-04	3.020E-02	5.406E-22	1.316E-08
94	- Saturn	- Phoebe	1.000E-14	3.498E+03	9.082E-03	2.018E-02	8.248E-19	2.620E-03
95		- Iapetus	3.333E-06	3.498E+03	2.496E-03	2.018E-02	2.077E-11	5.439E-05
96		- Hyperion	2.000E-07	3.498E+03	1.038E-03	2.018E-02	2.154E-13	3.910E-06
97		- Titan	2.409E-04	3.498E+03	8.563E-04	2.018E-02	1.766E-10	2.196E-06
98		- Rhea	4.000E-06	3.498E+03	3.693E-04	2.018E-02	5.455E-13	1.762E-07
99		- Dione	2.041E-06	3.498E+03	2.649E-04	2.018E-02	1.432E-13	6.502E-08
100		- Tethys	1.099E-06	3.498E+03	2.067E-04	2.018E-02	4.695E-14	3.089E-08
101		- Enceladus	1.429E-07	3.498E+03	1.668E-04	2.018E-02	3.975E-15	1.623E-08
102		- Mimas	6.667E-08	3.498E+03	1.303E-04	2.018E-02	1.132E-15	7.738E-09
103		- Janus	1.000E-14	3.498E+03	1.114E-04	2.018E-02	1.241E-22	4.836E-09

Table 4.3 (contd.)

Group A3

System Number	Name			μ*	μ_3	α_{23}	α_{cr}	ε^{23}	ε_{32}
104	Sun	- Uranus	- Oberon	2.941E-05	2.281E+04	2.046E-04	1.096E-02	1.231E-12	1.953E-07
105			- Titania	5.000E-05	2.281E+04	1.526E-04	1.096E-02	1.164E-12	8.105E-08
106			- Umbriel	5.882E-06	2.281E+04	9.305E-05	1.096E-02	5.093E-14	1.838E-08
107			- Ariel	1.493E-05	2.281E+04	6.691E-05	1.096E-02	6.682E-14	6.832E-09
108			- Miranda	1.000E-06	2.281E+04	4.322E-05	1.096E-02	1.868E-15	1.841E-09
109		- Neptune	- Nereid	3.333E-07	1.925E+04	1.239E-03	1.161E-02	5.117E-13	3.661E-05
110			- Triton	1.332E-03	1.925E+04	7.872E-05	1.161E-02	8.240E-12	9.390E-09
111		- Jupiter	- Satellite Direct †	1.000E-14	1.047E+03	3.000E-02	3.020E-02	9.000E-18	2.827E-02
112			- Satellite Retrograde†	1.000E-14	1.047E+03	4.500E-03	3.020E-02	2.025E-19	9.543E-05

* where the mass of the body is too small to be known accurately a value of 10^{-14} ia assumed (in units of the planetary mass)

† Numerical experiments with Jovian satellites see Hunter, 1967.

Table 4.4

Group A4

System Number	Name	μ	μ_3	α	α_{cr} *	ε^{23}	ε_{32}
36	Sun - Mars - MD† Asteroid	3.240E-07	1.000E-10	5.442E-01	9.836E-01	9.595E-08	1.612E-11
37	- MD† Asteroid - Jupiter	1.000E-10	9.550E-04	5.382E-01	7.999E-01	2.897E-11	1.489E-04
38	- Saturn	1.000E-10	2.859E-04	2.935E-01	8.588E-01	8.614E-12	7.228E-06
39	- OL† Asteroid - Jupiter	1.000E-10	9.550E-04	6.650E-01	7.999E-01	4.422E-11	2.808E-04
40	- Saturn	1.000E-10	2.859E-04	3.627E-01	8.588E-01	1.316E-11	1.364E-05

* The exact value is dependant on the mass of the asteroid - we have assumed a mass of 10^{-10} solar masses.

† MD Asteroid - body situated at the mean distance of the asteroid belt
OL Asteroid - body situated at the outer limit of the asteroid belt

Table 4.5

Groups B1 and B2 - Numerical experiments taken from Harrington, 1977.

Number	System Type† and Group		μ	μ_3	α_{23}	α_{cr}	ε^{23}	ε_{32}
RD11	Double Star A - D Planet	(B2)	1.000E-03	1.000E 00	2.500E-01	2.436E-01	6.244E-05	1.563E-02
RD12	- D Planet	(B2)	3.300E-06	1.000E 00	2.500E-01	2.437E-01	2.062E-07	1.563E-02
RD21	- D Planet	(B1)	5.000E-01	5.000E-04	5.000E-01	4.390E-01	6.250E-02	6.250E-05
RD22	- D Planet	(B1)	5.000E-01	1.600E-06	5.000E-01	4.393E-01	6.250E-02	2.000E-07
RR11	- R Planet	(B2)	1.000E-03	1.000E 00	3.333E-01	2.436E-01	1.110E-04	3.704E-02
RR12	- R Planet	(B2)	3.300E-06	1.000E 00	2.500E-01	2.437E-01	2.062E-07	1.563E-02
RR21	- R Planet	(B1)	5.000E-01	5.000E-04	3.333E-01	4.390E-01	2.778E-02	1.852E-05
RR22	- R Planet	(B1)	5.000E-01	1.600E-06	5.000E-01	4.393E-01	6.250E-02	2.000E-07
R1	Double Star B - D Planet	(B1)	5.000E-01	0.000E 00	5.000E-01	4.433E-01	6.250E-02	0.000E 00
R2	- Venus	(B1)	5.000E-01	0.000E 00	2.500E-01	4.433E-01	1.563E-02	0.000E 00
R3	Double Star C - Mercury	(B2)	0.000E 00	1.000E 00	7.463E-02	2.448E-01	0.000E 00	4.156E-04
R4	- Venus	(B2)	0.000E 00	1.000E 00	1.429E-01	2.448E-01	0.000E 00	2.915E-03
R5	- Earth	(B2)	0.000E 00	1.000E 00	2.000E-01	2.448E-01	0.000E 00	8.000E-03
R6	- Mars	(B2)	0.000E 00	1.000E 00	3.077E-01	2.448E-01	0.000E 00	2.913E-02

† Double Star A - Both components have mass equal to one solar mass

Double Star B - Both components have mass equal to one half solar mass

Double Star C - Both components have mass equal to one solar mass, one being positioned in an orbit equivalent to that of Jupiter

D Planet - Planet in corotational motion with the double star system

R Planet - Planet in counter-rotational motion with respect to the double star system

Table 4.6

Group B3 - Numerical experiments taken from Horedt *et al.*,1977.

System Number	Type† and Comments¶	μ	μ_3	α_{23}	α_{cr}	ε^{23}	ε_{32}
H 1	R4BTS - Break up in 300 Periods	0.000E 00	1.000E-04	8.300E-01	8.972E-01	0.000E 00	5.718E-05
H 2		1.000E-04	0.000E 00	7.950E-01	8.962E-01	6.320E-05	0.000E 00
H 3	- No break up in 2500 Periods	0.000E 00	1.000E-05	8.300E-01	9.502E-01	0.000E 00	5.718E-06
H 4		1.000E-05	0.000E 00	7.950E-01	9.499E-01	6.320E-06	0.000E 00
H 5	G4BTS - Break up in 16000 Periods	1.000E-04	1.000E-04	7.690E-01	8.723E-01	5.913E-05	4.548E-05
H 6		1.000E-04	1.000E-04	7.690E-01	8.723E-01	5.913E-05	4.548E-05
H 7		1.000E-04	1.000E-04	5.920E-01	8.723E-01	3.504E-05	2.075E-05
H 8	- No break up in 40000 Periods	1.000E-04	1.000E-04	7.140E-01	8.723E-01	5.097E-05	3.640E-05
H 9		1.000E-04	1.000E-04	7.140E-01	8.723E-01	5.097E-05	3.640E-05
H10		1.000E-04	1.000E-04	5.100E-01	8.723E-01	2.601E-05	1.327E-05
H11	- No break up in 50000 Periods	1.000E-05	1.000E-05	8.330E-01	9.377E-01	6.939E-06	5.780E-06
H12		1.000E-05	1.000E-05	8.330E-01	9.377E-01	6.939E-06	5.780E-06
H13		1.000E-05	1.000E-05	6.940E-01	9.377E-01	4.816E-06	3.343E-06

† R4BTS - Triple sub-sets obtained from the restricted four-body problem

G4BTS - Triple sub-sets obtained from the general four-body problem

¶ The period understood here is the period of revolution of mass m_3 about m_1, where the masses are arranged in the order m_1, m_2, m_3, m_4 and $m_2=m_3=m_4=10^{-4}.m_1$ *or* $m_2=m_3=m_4=10^{-5}.m_1$.

Table 4.7

Group C

System Number	Name	μ	μ_3	α	α_{cr}	ε^{23}	ε_{32}
S 1	ε Hyd	4.480E-01	9.575E-01	5.236E-02	2.633E-01	6.780E-04	1.374E-04
S 2	ADS 3358	4.580E-01	4.576E-01	1.229E-01	3.105E-01	3.749E-03	8.495E-04
S 3	$-30^{\circ}529$	5.000E-01	3.086E-01	1.190E-01	3.416E-01	3.540E-03	5.200E-04
S 4	ζ Cnc	4.700E-01	9.626E-01	1.111E-01	2.656E-01	3.075E-03	1.320E-03
S 5	ξ U Maj	2.700E-01	8.070E-01	8.065E-02	2.569E-01	1.282E-03	4.233E-04
S 6	ζ Aqr	1.800E-01	8.197E-01	7.692E-02	2.519E-01	8.733E-04	3.731E-04
S 7	λ Tau	2.090E-01	5.814E-02	2.381E-01	3.716E-01	9.372E-03	7.848E-04
S 8	Algol	1.860E-01	3.721E-01	2.347E-02	2.956E-01	8.340E-05	4.811E-06

It may be noted here that some of these groups are essentially the same. For instance A3 and B2 are essentially similar in arrangement with a small mass in orbit about a larger mass being disturbed by a large mass at a greater distance. The difference between the two arises in the values of μ, μ_3 and α one would expect for each system. In the former case μ is small (say $\lesssim 10^{-3}$), μ_3 being very large (greater than 10^3) and α ($\sim 10^{-3}$) small in order that the satellite can be stable. The latter case would have a similar μ value but μ_3 would be of order unity resulting in $1 - \mu \simeq \mu_3 \simeq 1$, a double star, with α being somewhat larger, say 0.1. Thus the divisions given above do not indicate any essential difference between the systems: the divisions are made solely for clarity of presentation and from consideration of real systems.

Further, it is possible, given ranges of the mass parameters, μ and μ_3, to map out regions of the $\varepsilon^{23}, \varepsilon_{32}$-plane where particular types of system may be found. Considering Equations (13), we have the following expressions for α, in terms of $\varepsilon^{23}, \varepsilon_{32}$, μ and μ_3:

$$\alpha = \left[\frac{\varepsilon^{23}}{\mu(1-\mu)} \right]^{\frac{1}{2}} \qquad (22a)$$

and

$$\alpha = \left[\frac{\varepsilon_{32}}{\mu_3} \right]^{1/3} . \qquad (22b)$$

Equating these two expressions, a relationship between the ε-parameters, in terms of the mass-parameters, is found viz.

$$\log \varepsilon_{32} = \frac{3}{2} \log \varepsilon^{23} + \log \left[\frac{\mu_3}{\{\mu(1-\mu)\}^{3/2}} \right] . \qquad (23)$$

If we then consider a particular type of system and assume that in such a system $\mu_L \leqslant \mu \leqslant \mu_u$ and $\mu_{3L} \leqslant \mu_3 \leqslant \mu_{3u}$, where subscripts "U" and "L" denote upper and lower limits, we may write

$$\log \varepsilon_{32} = \frac{3}{2} \log \varepsilon^{23} + \log \left[\frac{\mu_{3L}}{\{\mu_u(1-\mu_u)\}^{3/2}} \right] \qquad (24a)$$

$$\text{and} \quad \log \varepsilon_{32} = \frac{3}{2} \log \varepsilon^{23} + \log \left[\frac{\mu_{3u}}{\{\mu_L(1-\mu_L)\}^{3/2}} \right]. \qquad (24b)$$

These are the equations of two lines in the $\varepsilon^{23}, \varepsilon_{32}$-plane and any given system which falls into the group defined by the above limits on μ and μ_3 will occupy a position on the $\varepsilon^{23}, \varepsilon_{32}$-plane between these lines.

For instance if we consider triple stellar systems then we may suppose, in general, that $\mu_L = 5.10^{-2}$, $\mu_u = \frac{1}{2}$, $\mu_{3L} = 5.10^{-2}$ and $\mu_{3u} = 10$, resulting in Equations (25) viz.

$$\log \varepsilon_{32} = \frac{3}{2} \log \varepsilon^{23} - 0.398 \qquad (25a)$$

and

$$\log \varepsilon_{32} = \frac{3}{2} \log \varepsilon^{23} + 2.985. \qquad (25b)$$

Thus all triple stellar systems, included in the above range of mass parameters, will be found in the region of the $\varepsilon^{23}, \varepsilon_{32}$-plane shown shaded in Fig.4.4(a).

In a similar way we may treat the case of planet disturbing planet (Groups A1 and B3): here $\mu_u = \mu_{3u} = 10^{-3}$ and $\mu_L = \mu_{3L} = 0$. The lower limits for μ and μ_3 will cause infinities to appear in Equations (24) and we therefore recast these equations as

$$\log \varepsilon^{23} = \log \mu_u(1-\mu_u) + \frac{2}{3} \log \left[\frac{\varepsilon_{32}}{\mu_{3L}} \right] \qquad (26a)$$

$$\text{and} \quad \log \varepsilon_{32} = \log \mu_{3u} + \frac{3}{2} \log \left[\frac{\varepsilon^{23}}{\mu_L(1-\mu_L)} \right]. \qquad (26b)$$

The first of these may then be rewritten as

$$\log \varepsilon^{23} = \log \mu_u(1-\mu_u) + 2 \log \alpha$$

which results in, applying the limiting case of $\alpha = 1$,

$$\log \varepsilon^{23} = \log \mu_u(1- \mu_u) , \qquad (27)$$

a vertical line in the $\varepsilon^{23},\varepsilon_{32}$-plane. In a similar fashion we may rewrite Equation (26b) as

$$\log \varepsilon_{32} = \log \mu_{3u} + 3 \log \alpha$$

to obtain, in the limit $\alpha = 1$,

$$\log \varepsilon_{32} = \log \mu_{3u} , \qquad (28)$$

which is a horizontal line in the $\varepsilon^{23},\varepsilon_{32}$-plane. The two lines given by Equations (27) and (28) provide boundaries in the $\varepsilon^{23},\varepsilon_{32}$-plane within which any planetary system with $\mu \leqslant 10^{-3}$ and $\mu_3 \leqslant 10^{-3}$ will be found (see Fig.4.4 (b)). Here it may be noted that systems consisting of the Sun, a planet and an asteroid will, by virtue of the small mass of the asteroid, occupy positions in the directions shown by arrows (i) and (ii) in Fig.4.4 (b). The case of an asteroid in a superior orbit with respect to the planet where ε_{32} is small occupies the region in the direction of arrow (i), the inferior case lying in the region indicated by arrow (ii).

The remaining types of system, the planet in an inferior or superior orbit in a binary star system and the case of satellites disturbing each other or being disturbed by the Sun, are given in Figs. 4.4 (c) - (f).

It may be noted from the tables that we have included in Table 4.1 all possible combinations of triple sub-systems in the solar system. Not only are those which might be termed the dominant systems included e.g. Sun-Jupiter-Saturn, but also those which at first glance would appear to have very little bearing on the overall stability of the system e.g. Sun-Mercury-Mars. This is done partly for the sake of completeness but also to give an indication of the size of the total perturbation from all the other bodies on any one given body in the system. It may be remarked at this point that Jupiter has the largest influence, in terms of disturbance as measured

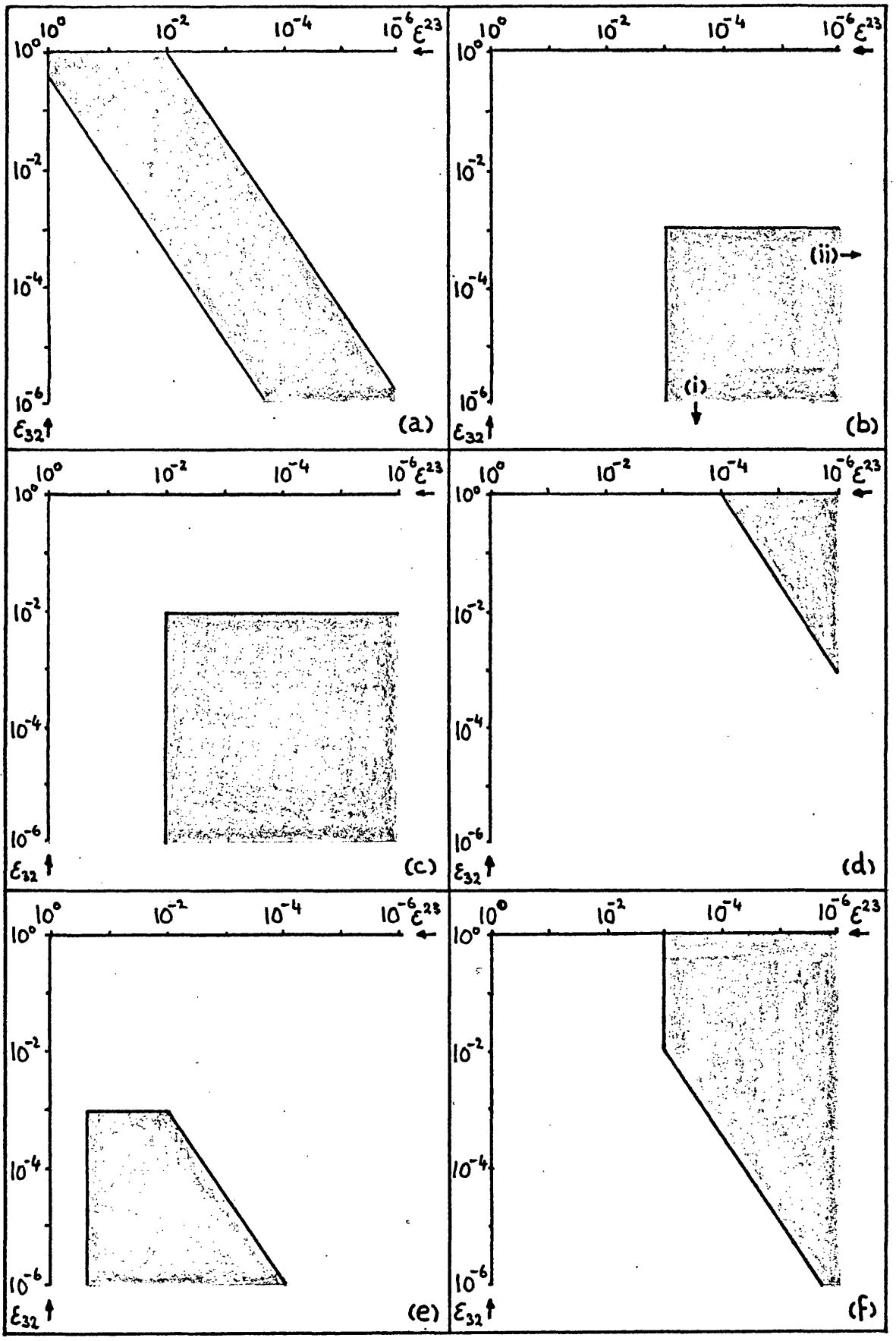

Figure 4.4 Regions in the ε^{23},ε_{32}-plane occupied by the following systems:

(a) Star-Star-Star
(b) Sun-Planet-Planet
(c) Planet-Satellite-Satellite
(d) Planet-Satellite-Sun
(e) Star-Star-Planet
(f) Star-Planet-Star

by the ε parameters, on each of the planets. Thus if we were to include only the most dominant perturber of each planet we would merely require to consider each planet with Jupiter in turn.

Similarly, for completeness, we include all possible combinations of triple sub-systems in Table 4.2 for satellites in orbit about their respective planets. However in their case it may be noted that in general there is no one body which dominates the system in the way Jupiter dominates the Solar System.

In Table 4.3 - systems of the type Planet-Satellite-Sun - it is seen in all cases that the mass of the satellite is negligible since α_{cr} does not vary from satellite to satellite of a system, to the limit of accuracy given. That is to say, ε^{23} is so small that the orbit of the mass-centre of the Planet-Satellite system about the Sun is essentially an undisturbed Keplerian ellipse as in the case of the motion of the Earth-Moon mass-centre about the Sun (cf. Brown, 1896). Although α_{cr} does not vary from satellite to satellite within a given satellite system the disturbance of the satellite by the Sun does, as demonstrated by the ε_{32} values. Clearly the closer the satellite is to the planet the smaller is the perturbation by the Sun and the smaller is ε_{32}.

Table 4.4 gives data on asteroids. As mentioned above the small mass of the asteroid results in small ε parameters (small ε^{23} for an inferior asteroid, small ε_{32} for a superior asteroid) characteristic of negligible disturbances on the planet's orbit. They are, of course, affected by the neighbouring planets and thus we give details for them as disturbed by Mars, Jupiter and Saturn. The next two tables (Tables 4.5 and 4.6) give data for numerical experiments by other authors, and Table 4.7 gives data for eight triple stellar systems taken from Szebehely and Zare (1977).

Figures 4.5 and 4.6 show respectively the distribution of the tabulated systems in the μ,μ_3-plane and $\varepsilon^{23},\varepsilon_{32}$-plane with respect to the contours of equal α_{cr}. It can be seen that the *cut off* of the $\alpha_{cr} = \alpha'(\varepsilon^{23},\varepsilon_{32})$ surface (see Section 4.4) does to a very large extent separate the stable systems (stable in the sense that they last for a great many revolutions without significant changes in their

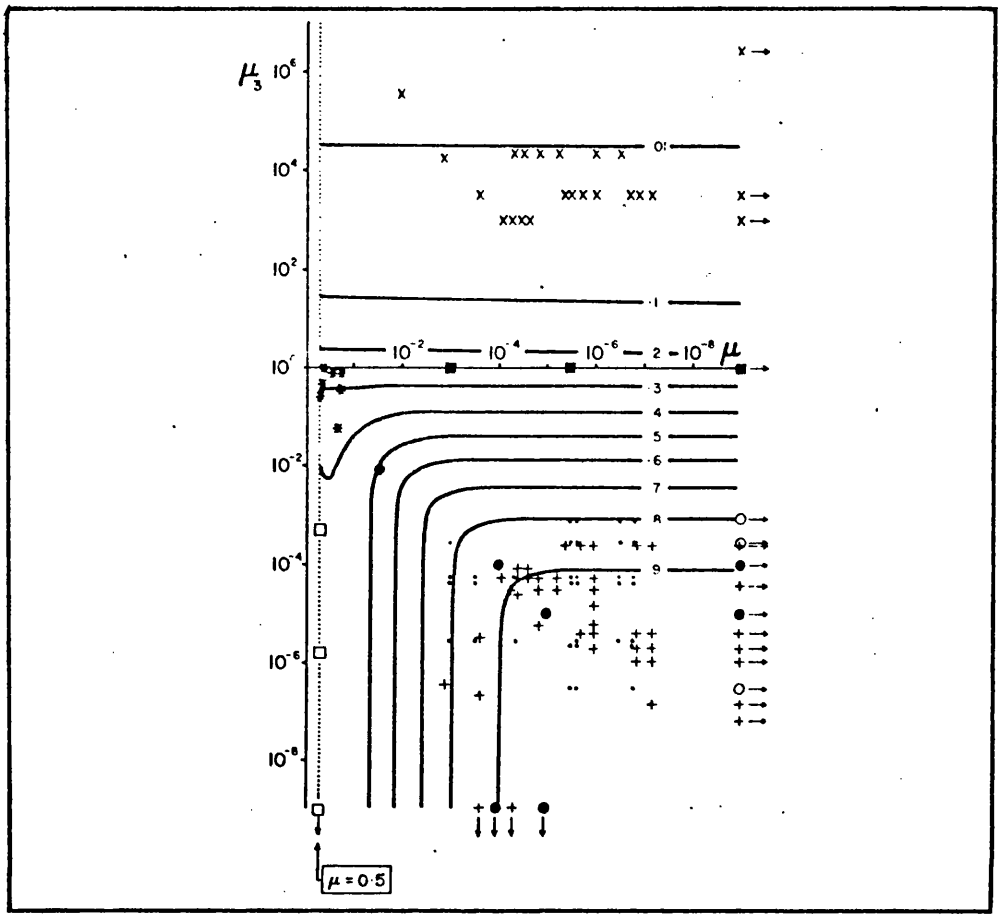

Figure 4.5 The critical stability surface displayed as contours in the μ,μ_3-plane where the symbols have the following meanings:

- • Group A1 - The Planetary System - planet disturbing planet
- + Group A2 - The Satellite Systems - satellite disturbing satellite
- × Group A3 - The Satellite Systems - Sun disturbing satellites
- O Group A4 - The Asteroid System - planet disturbing asteroids
- □ Group B1 - Superior planet of binary star system
- ■ Group B2 - Inferior planet of binary star system
- ● Group B3 - Simulated Planetary Systems - planet disturbing planet
- * Group C - Triple Stellar Systems

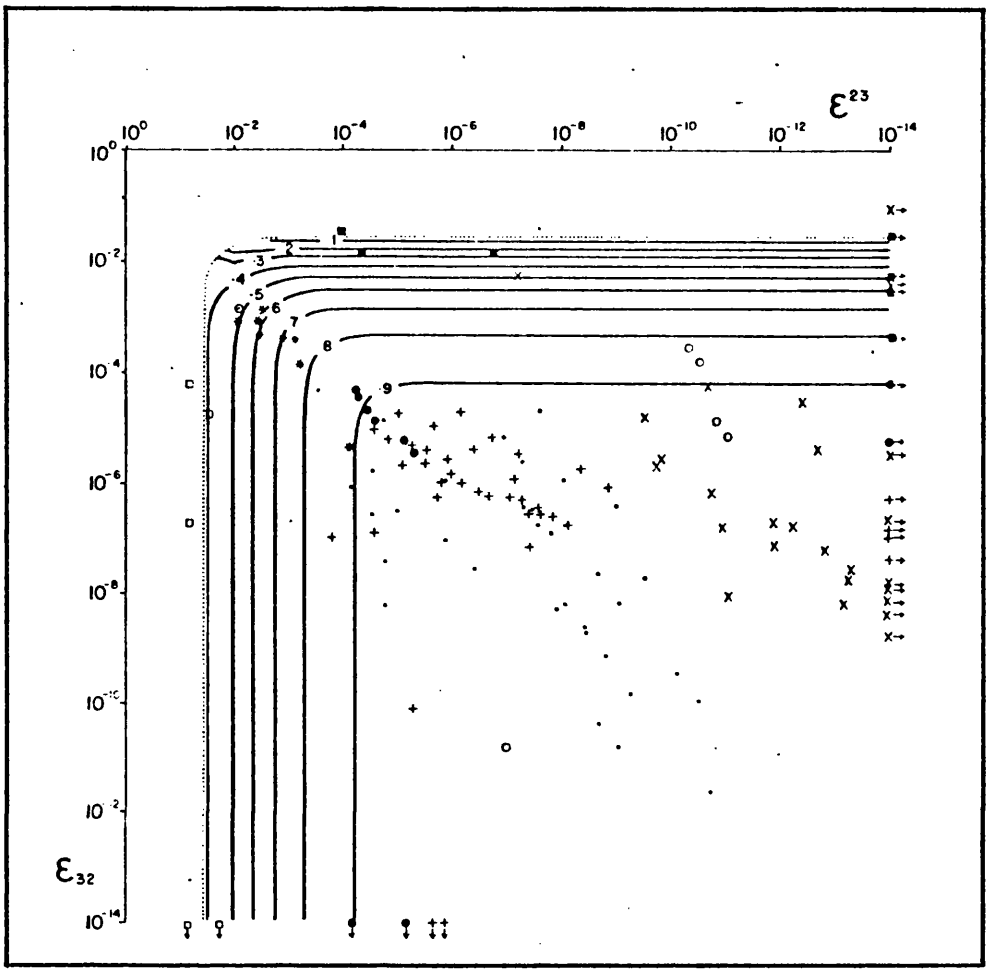

Figure 4.6 The critical stability surface displayed as contours in the $\varepsilon^{23},\varepsilon_{32}$-plane where the symbols have the same meanings as in Figure 4.5 and the dotted line denotes the "cut-off" of the critical stability surface viz. $\alpha_{cr} = 2(\varepsilon^{23})^{\frac{1}{2}}$.

constituent orbits) from the unstable: the present method therefore does allow a very simple criterion to be applied to decide the stability or instability of three-body systems.

At this point we note, however, a slight disadvantage of the (ε^{23}, ε_{32}) analysis. Whereas in the μ,μ_3 presentation, the value of α_{cr} above a point (μ',μ_3') in the μ, μ_3-plane was indeed the critical value of α for (μ',μ_3'), this relationship is lost in considering the $\alpha_{cr} = \alpha'(\varepsilon^{23},\varepsilon_{32})$ surface since ε^{23} and ε_{32} themselves depend on α, i.e. $\mu,\mu_3\alpha$ are orthogonal but $\varepsilon^{23},\varepsilon_{32},\alpha$ are not. This is *not* to say there is not a unique value of $\alpha = \alpha_{cr}$ such that $\alpha_{cr} = \alpha'(\varepsilon^{23},\varepsilon_{32})$ *but* merely to say for a given set $(\varepsilon^{23},\varepsilon_{32},\alpha)$ there are two possible values of α_{cr}: the first obtained from $\alpha_{cr} = \alpha'(\varepsilon^{23},\varepsilon_{32})$ and the second from $\alpha_{cr} = \alpha(\mu, \mu_3)$ where $\mu = \mu(\varepsilon^{23},\alpha)$ and $\mu_3 = \mu_3(\varepsilon_{32},\alpha)$. In every case, where the system is stable i.e. $\alpha < \alpha_{cr} = \alpha'(\varepsilon^{23},\varepsilon_{32})$ it is found that $\alpha < \alpha(\mu, \mu_3) < \alpha'(\varepsilon^{23},\varepsilon_{32})$. When a system is unstable i.e. $\alpha > \alpha_{cr} = \alpha'(\varepsilon^{23},\varepsilon_{32})$ then $\alpha > \alpha(\mu,\mu_3) > \alpha'(\varepsilon^{23},\varepsilon_{32})$. If $\alpha = \alpha_{cr} = \alpha'(\varepsilon^{23},\varepsilon_{32})$ then $\alpha_{cr} = \alpha'(\varepsilon^{23},\varepsilon_{32}) = \alpha(\mu, \mu_3)$. The following argument removes any disadvantage brought in by the lack of orthogonality of the set ε^{23}, ε_{32}, α.

Let $\varepsilon^{23},\varepsilon_{32}$ be the position of the real system (μ,μ_3,α_{act}) in the $\varepsilon^{23},\varepsilon_{32}$-plane. Let $\bar{\varepsilon}^{23}$, $\bar{\varepsilon}_{32}$ be the position of the critically stable system (μ,μ_3,α_{cr}) in the $\varepsilon^{23},\varepsilon_{32}$-plane where $\alpha_{cr} = \alpha(\mu,\mu_3)$.

Then by Equations (13)

$$\frac{\varepsilon^{23}}{\bar{\varepsilon}^{23}} = \left[\frac{\alpha_{act}}{\alpha_{cr}}\right]^2 ; \qquad \frac{\varepsilon_{32}}{\bar{\varepsilon}_{32}} = \left[\frac{\alpha_{act}}{\alpha_{cr}}\right]^3. \qquad (29)$$

There are three possible cases to consider depending on whether the system is (i) stable (ii) critically stable or (iii) unstable.

Case (i) $\dfrac{\alpha_{act}}{\alpha_{cr}} < 1$, thus $\varepsilon^{23} < \bar{\varepsilon}^{23}$ and $\varepsilon_{32} < \bar{\varepsilon}_{32}$, so that the stable system is moved, during the translation from the $O\mu\mu_3\alpha$ parameter space to the $O\varepsilon^{23}\varepsilon_{32}\alpha$ parameter space, relative to the critical stability surface, to a position where that surface is higher.

Case (ii) $\dfrac{\alpha_{act}}{\alpha_{cr}} = 1$, so that $\varepsilon^{23} = \bar{\varepsilon}^{23}$ and $\varepsilon_{32} = \bar{\varepsilon}_{32}$.

Therefore the stable system remains in the same position relative to the critical stability surface (as we would expect).

Case (iii) $\dfrac{\alpha_{act}}{\alpha_{cr}} > 1$, resulting in $\varepsilon^{23} > \bar{\varepsilon}^{23}$ and $\varepsilon_{32} > \bar{\varepsilon}_{32}$

so that here the unstable system is moved, relative to the critical stability surface, to a position where that surface is lower.

Hence it is seen that no system can change from one side of the critical stability surface to the other during the transformation from

$$\alpha_{cr} = \alpha(\mu,\mu_3) \quad \text{to} \quad \alpha_{cr} = \alpha'(\varepsilon^{23},\varepsilon_{32}).$$

Moreover it can be appreciated that there is some degree of sorting out of the systems depending upon how stable or unstable they are.

4.6 Discussion and Conclusions

In this chapter the aim has been to test the suitability of the ε parameters for a discussion of the stability of hierarchical many-body systems by considering the three-body problem which allows the application of the critical stability surface. This surface, although it is clearly only rigorous in the case of three bodies in initially circular, coplanar, co-rotational orbits, would still appear to have significance when there may be four or more bodies and small, but non-zero, inclinations and eccentricities. For such systems where there is an observable dynamical hierarchy in operation e.g. in the Solar System, it can surely be said that for the system as a whole to be stable, each of the three-body subsets of that system should satisfy (and preferably satisfy well) the critical stability criterion, i.e. $\alpha << \alpha_{cr}$. The justification for this is given in some measure by consideration of the expansion of the force function given earlier. Considering Equations (3.40) it can be seen that the disturbances on the Keplerian orbit of the ith mass about the mass-centre of the first i-1 masses are, to the order given, purely

additive. Further it is a feature of classical perturbation theory that to the first order the perturbations on any body due to any other bodies' actions are again purely additive. Thus it is contended that *to this extent* a many-body system *is* a set of three-body systems.

The ε representation of many-body systems (both real and from numerical integration studies) and their distribution with respect to the critical stability contours suggests that for a hierarchical system to be stable (in the sense of the hierarchy lasting, without any major change, for many orbits), then the ε's must, for the ith mass, be constrained in the fashion

$$\sum_{k} |\varepsilon^{ki}| + \sum_{\ell} |\varepsilon_{\ell i}| < E < 1 \qquad (30)$$

where $i = 2,\ldots,n$; $k = 2,\ldots,i-1$ $(i \geq 3)$; $\ell = i+1,\ldots,n$ $(i \leq n-1)$: cf. Equation (3.40). It is estimated that E is in the range $10^{-3} > E > 10^{-4}$, since it is in this range that the critical stability surface in the $0\varepsilon^{23}\varepsilon_{32}\alpha$ parameter space, for the three-body problem, is rising sharply to attain its highest values i.e. $\alpha_{cr} > 0.9$. This is interpreted in the following qualitative fashion: if the above condition is satisfied then it is statistically unlikely that the perturbations would build up sufficiently over an astronomically long period of time to result in the hierarchical ordering of the system being destroyed. We note however that in this present chapter we have plotted only the three-body subsets of many-body systems. Nevertheless it is clear that the vast majority of triple subsets satisfy the stability criterion of Szebehely and Zare well and also lie in the region of the plane where ε^{23} and ε_{32} are both less than 10^{-3}.

Clearly the stability is not solely dependant upon the values of ε^{23} and ε_{32} but will be affected by the α values. It can be seen from Fig. 4.6 that the majority of real systems congregate around ε values where the critical stability surface is high i.e. $\alpha_{cr} \gtrsim 0.8$. Thus, except for extreme $\alpha_{23} > 0.8$ it is sufficient for the stability of triple systems that ε^{23} *and* ε_{32} are both less than 10^{-3} or 10^{-4}. We note that this is in contrast to Fig.4.5 in which the systems are

plotted in the μ, μ_3-plane with respect to the contours of the $\alpha_{cr} = \alpha(\mu, \mu_3)$ surface. Here there is no clear arrangement of the systems with respect to the contours.

Although this crude criterion in α is probably sufficient in the case of three-body systems, we feel it better to modify it in the light of the following considerations.

If, in a three-body system, the critical stability criterion of Szebehely and Zare is satisfied, but only marginally, then it is possible that, although originally zero, the eccentricities of the osculating Keplerian orbits of the systems could build up significantly due to the perturbations which, although not resulting in the violation of the hierarchy of the three-body system, would put the stability of a many-body system, which included such a triple subset, at risk due to the possibility of orbits crossing. Further, if ε^{23} and ε_{32} are small then the perturbations on the Keplerian orbits within the system will be very small. Thus, it is felt that the system could exist close to the critical stability surface with very small overall changes occurring in the various Keplerian orbits of the system. On the other hand, if we consider larger ε^{23} and ε_{32} then the system will have to lie further from the critical stability surface to ensure that the overall changes in the Keplerian orbits of the bodies are kept minimal. The following criterion on the α_{23} value of each triple subset within a many-body system is suggested:

$$\frac{\alpha_{23}}{\alpha_{cr}} < A < 1 \qquad (31)$$

where α_{23} is the actual value of ρ_2/ρ_3 for the three-body subset, α_{cr} is the corresponding critical value for the three-body subset

and $A = A(\varepsilon^{23}, \varepsilon_{32}) : A \to 1$ as ε^{23} and $\varepsilon_{32} \to 0$.

Although the analysis was carried out for initially zero eccentricities of the two Keplerian orbits of the three-body system attention can be drawn to two remarkable systems. The first of these is the system Saturn-Titan-Hyperion (see Table 4.2, Number 70). There we see, that, for the masses given, and for circular orbits, the value

of α_{cr} is 0.8641. We may assume however, due to the considerable eccentricity of Hyperion's orbit (~ 0.1), that α_{cr} will be less than this value and indeed will be comparable to (and possibly less than) the actual value for the system. Alternatively, it might be considered reasonable that the parameter α_{23} should be given by

$$\alpha_{23} = \frac{\rho_{T\ max}}{\rho_{H\ min}} = \frac{a_T(1 + e_T)}{a_H(1 - e_H)} = 0.92$$

where suffices "T" and "H" denote Titan and Hyperion respectively. The orbits are almost coplanar and so by the critical stability criterion the system *could* show instability; but it exists. There is however an additional factor to be taken into account namely the critical argument θ arising from the 3:4 commensurability in mean motions n_H and n_T such that

$$\theta = 4\lambda_H - 3\lambda_T - \varpi_H \sim 180^\circ; \quad 4n_H - 3n_T - \dot{\varpi}_H \sim 0$$

where λ_H and λ_T are the longitudes of Hyperion and Titan, while ϖ_H is the longitude of Hyperion's apse. The amplitude of θ is about 36°. This critical argument ensures that the satellites' conjunction line librates about the moving aposaturnium of Hyperion so that the effective α_{23} is never more than about 0.78 which must be sufficiently below α_{cr} to ensure obedience of the critical stability criterion. Colombo and Franklin (1973) have argued that even if Goldreich's tidal mechanism is not the cause of the Titan-Hyperion resonance it may have arisen naturally. In other words, it is possible that Titan and Hyperion were formed at that resonance and, because it is stable, remained there. What is being said here in support of Colombo and Franklin's suggestion is that other pairs of satellites, formed as close together as Titan and Hyperion are but without the resonance, would have dispersed because of their inherently unstable set-up.

The second system of interest is Sun-Neptune-Pluto (see Table 4.8). It is well known that Pluto's perihelion distance is nearer the Sun than Neptune's mean radius vector. Up until ten years ago, because of

Table 4.8

SUN-NEPTUNE-PLUTO SYSTEM

Body	Semi-major axis (A.U.)	Eccentricity e	Mutual inclination	Mean motion (°/day)
Neptune	30.06	0.0096	~ 17°	0.005981
Pluto	39.44	0.2502		0.003979

the possibility of close approaches of Pluto to Neptune and of the possibility that $\alpha_{23} = \rho_N/\rho_P > 1$ when Pluto was at perihelion, standard expansion techniques - such as that dealt with in Chapter 3 in the Jacobi coordinate system - could not be applied to Neptune and Pluto because of the non-convergence of series involving $(\rho_N/\rho_P)^i$. In the context of the present study, we would say that the critical stability criterion for the Sun-Neptune-Pluto system would show the system to be unstable, since α_{23} can be greater than α_{cr} and indeed greater than unity.

It is now known, of course, from the work of Cohen and Hubbard (1965) that a critical argument

$$\theta = 3\lambda_P - 2\lambda_N - \varpi_P \sim 180^\circ$$

exists which librates about 180° with an amplitude of 76° and period 19670 years, thus ensuring that conjunctions avoid the region of Pluto's orbit which is closer to the Sun than Neptune. The maximum effective α_{23} is thus never more than 0.75. It is also possible that the argument of Pluto's perihelion also librates, a suggestion put forward by Brouwer (1966) who pointed out that a critical argument

$$\theta' = 3\lambda_P - 2\lambda_N - \Omega_P$$

should exist ensuring that $\omega = \theta' - \theta$ would librate. If so, then the high inclination of Pluto's orbit with respect to Neptune's could also increase the stability. Williams and Benson's study of 1971 showed that ω did indeed librate about 90° with an amplitude of approximately 24°.

We now proceed to consider the distribution of certain real cases of triple system in the $\epsilon^{23}, \epsilon_{32}$-plane together with the critical stability contours.

Thus far, the findings of this chapter are as follows: the region of $\epsilon^{23}, \epsilon_{32}$-plane such that

$$\epsilon^{23} \lesssim 10^{-3} \rightarrow 10^{-4}$$

and

$$\epsilon_{32} \lesssim 10^{-3} \rightarrow 10^{-4}$$

is a region of high stability in the many-body problem given suitable values of α_{23}.

In Fig.4.6 the available data for triple stellar systems were plotted. On this diagram one could superimpose the two diagonal lines shown in Fig.4.4(a) delimiting the area of the ε^{23} ,ε_{32}-plane within which triple star systems could exist according to the possible ranges for the mass-parameters μ and μ_3.

The region of high ε parameters would clearly always result in highly unstable triple systems. Furthermore, the high end of the α range would similarly produce unstable systems in a great many cases. The eight asterisks denote the positions of the eight triple systems given in Szebehely and Zare (1977) - see Table 4.7.

Apart from the fact that several of these systems are only marginally stable, the outstanding feature of the distribution is the complete lack of data for the region of maximum stability i.e. ε^{23} and ε_{32} both less than 10^{-3}. There are three possible explanations:

(i) All the available data are not plotted.

(ii) There is an observational selection effect making the observation of triples with relatively large ε parameters easier.

(iii) Such systems do not exist.

With respect to the first reason; it is certain that scattered throughout the literature lie additional data for triple stellar systems: a future search of the literature would harvest more points, possibly in the region of high stability. Since however the three masses making up a stellar system are generally of similar size any shift in the ε^{23} ,ε_{32}-plane towards smaller values necessitates finding stellar systems with small α_{23} values, possibly spectroscopic binaries with a third "visual" component.

There could well be an observational selection effect however. For stellar systems, as was mentioned above, any shifts in the ε^{23}, ε_{32}-plane are predominantly due to shifts in α_{23}. The stable region for triple stellar systems is thus one of low α_{23} values, and therefore if the system (m_1,m_2) is a visual binary this results in a large period of revolution for the third star, m_3, about the mass-centre of the binary. Thus for most visual binaries, possessing a third companion, two centuries of observation may not be long enough to detect the very

large number of triples which exist. The best hope of finding such highly stable systems probably lies in considering spectroscopic binaries with a third companion so that the period of the third mass is relatively short.

The third explanation - their non-existence - implies that for some reason, triples of this kind cannot exist. As mentioned in Section 3.4 this is undoubtedly the case for very widespread binaries themselves, let alone triples, since the central mass of the Galaxy itself plays the part of the third disturbing body rendering any binary star system unstable if the components are more widely separated than a certain limiting value. As an example we may take two solar masses whose separation r is α_{23} times the distance R of the binary from the galactic centre, taken to be 10^4 parsecs. The Galaxy's mass may be taken to be 10^{11} solar masses.

Now an ε parameter may be calculated to characterise the size of the disturbance of the central mass of the Galaxy on the binary viz.

$$\varepsilon_{32} = \frac{m_3}{M_2} \alpha_{23}^3$$

where $m_3/M_2 \simeq 10^{11}$ and $\alpha_{23} = r/R$. For stability it is required that $\varepsilon_{32} \leqslant 10^{-3}$ so that

$$\alpha_{23} = \left[\frac{M_2 \, \varepsilon_{32}}{m_3} \right]^{1/3} \sim 1/50{,}000.$$

Hence r for the limit of stability of binaries in the region of the Sun is of the order 0.2 parsecs or 40,000 A.U. If for example we are looking for a triple stellar system whose third body is of the order 40,000 A.U. from its binary and we wanted it to be in the region $\varepsilon^{23} = 10^{-6}$, $\varepsilon_{32} = 10^{-9}$ we would have $\alpha_{23} \sim 10^{-3}$ and the binary semi-major axis no more than 40 A.U. If the binary semi-major axis is reduced to 4 A.U., with the third body's distance again at the limit of 40,000 A.U., then $\alpha_{23} = 10^{-4}$ with $\varepsilon^{23} \sim 10^{-8}$ and $\varepsilon_{32} \sim 10^{-12}$. There is no way in which such systems could have been detected.

We now look at a similar set of systems, namely the planets of double stars (see Table 4.5). The points in Fig.4.6 given by numerical experiments by Harrington (1977) delineate very roughly the boundary of

the region where stability is assured given suitable α_{23} for low ε^{23} and ε_{32} i.e. less than 10^{-3}. As can be seen by considering Figs. 4.4 (e) and 4.4 (f) there is considerable scope for planets of binary stars to lie inside the stable region of the ε^{23},ε_{32}-plane. It may be noted here that, as shown by Figs. 4.4(e) and (f), the small mass of the planet results in, for an inferior planet, a low ε^{23} and high ε_{32}, while a superior planet gives high ε^{23} and low ε_{32}. That is to say the planet, in each case, barely disturbs the double star system's orbit.

Now the detection of planetary systems of stars other than the Sun is impossible except for the very nearest stars. It is not surprising then that no points have been plotted in the stable region for real systems. Some of the remarks made about the existence of highly stable triple systems carry over to this case. For example, if we are dealing with inferior planets in orbit about one component of a double star with the other component disturbing them, the limiting separation of the two stars is again 40,000 A.U. - imposed by the central mass of the Galaxy - in the Sun's neighbourhood. On the other hand a planet in a superior orbit about a double star may not be placed more than 40,000 A.U. distant from that binary.

It may therefore be concluded that as far as the ε diagram and the perturbation of the Galaxy is concerned, there is no reason why planetary systems should not exist in double star systems.

A further system which merits some closer attention is Sun-Jupiter-Saturn (see Table 4.1, Number 27). This real system has also been studied numerically by Nacozy (1976). It is found that, if we plot the real Sun-Jupiter-Saturn system in the $0\varepsilon^{23}$ $\varepsilon_{32}\alpha$ parameter space, it lies well below the critical stability surface, indicating a good measure of stability. If however, as was done by Nacozy, the masses of Jupiter and Saturn are increased and numerical integration tests carried out, it is found that the system remains stable until the masses are both multiplied by a factor greater than 29.25, whereupon secular trends appear in the orbital elements and the hierarchy of the system is broken. This system of augmented Jupiter and Saturn masses (see Table 4.1, Number 27N), if plotted on the ε^{23},ε_{32}-plane is found to be above its corresponding contour of the critical stability surface.

Furthermore, as noted in Section 4.5, a shift in the $\varepsilon^{23}, \varepsilon_{32}$-plane has occurred towards higher ε parameters than the real system. Thus no disagreement is found between the present treatment and that of Nacozy.

Clearly this situation implies that above the critical stability surface there lie zones of stability which are not obtainable in the analytical manner of Szebehely and Zare (1977), i.e. the criterion of Szebehely and Zare is a sufficient, but not necessary, condition for stability. The aim of further chapters of this thesis is to map out these zones of stability above the critical stability surface - in the three-body problem - for certain sets of initial conditions.

Lastly, attention is drawn to the numerical integrations of Horedt, Pop and Ruck (1977). Their numerical experiments involved work in the restricted and general four-body problem. The data and results of their four-body numerical integrations have been used by breaking their systems down into three-body subsets (see Table 4.6). It is then found that, in Numbers H5 - H13 in the above table, all the triple sub-systems give points that lie beneath the critical stability surface. It may be noted however that Horedt, *et al.* found that one of the systems underwent a violation of the hierarchy, in the sense that the eccentricities of the orbits built up sufficiently to allow the orbits within the four-body system to cross - an inherently unstable situation. It is tentatively suggested, at this stage, that this violation of the hierarchy was due to violation of the criteria on the ε parameters and α values presented earlier, (Equations (30) and (31)), whereby, although the triple subsets of a many-body system are individually stable, it is possible that taken overall the perturbations could build up statistically resulting in instability. Later chapters of this thesis will involve consideration of four-body systems.

In the next chapter, however, an improvement is made to the critical stability criterion of Szebehely and Zare in preparation for a numerical study of the coplanar general three-body problem in terms of the ε^{23} and ε_{32} parameters.

CHAPTER 5 REFINEMENT OF THE SUFFICIENT CONDITION FOR THE STABILITY OF COPLANAR HIERARCHICAL THREE-BODY SYSTEMS

5.1 Introduction

In Chapter 3 of this thesis parameters were derived which were considered to be physically meaningful for the discussion of the stability of hierarchical many-body systems. These parameters arose through an expansion of the force function of a many-body system, where the equations of motion are expressed in the Jacobian coordinate system. The force function was expanded in terms of the small quantities α_{ij} ($i = 2,\ldots,n-1$; $j = 3,\ldots,n$; $i < j$) where $\alpha_{ij} = \rho_i/\rho_j < 1$, $\rho_k = |\underset{\sim}{\rho}_k| = |M_{k-1}\overrightarrow{m_k}|$ and M_{k-1} is the position of the mass-centre of the subset of masses $m_1,\ldots,m_{k-1}$. For coplanar hierarchical three-body systems, referred to as CHT systems throughout the remainder of this chapter, two parameters arose from the analysis - ε^{23} and ε_{32} in the present notation.

The importance of the parameter c^2H in discussion of stability was demonstrated by the work of Zare (1976, 1977), summarised in Chapter 2. Further to this Szebehely (1977) and Szebehely and Zare (1977) showed how a simple criterion could be applied to assess a *measure of stability* for CHT systems. This idea was extended to the concept of the *critical stability surface* in Chapter 4 whereby, on this surface, the actual value of $c^2H - (c^2H)_{act}$ - of a system with given parameters μ, μ_3 and α or ε^{23}, ε_{32} and α_{23} (as previously defined) was equal to the critical value - $(c^2H)_{cr}$. If a system was represented by a point below the surface then that system could be said to be stable, inasmuch as an exchange between bodies was impossible; if above then the system might undergo an exchange of bodies*. The critical value $(c^2H)_{cr}$ was obtained, quite rigorously, from the appropriate collinear Lagrange configuration of the three-bodies; the

* This type of stability, where an exchange of bodies is prevented due to closure of the zero-velocity surfaces, may be referred to as *Hill-type stability*, since it was first employed by Hill in his study of the Moon's motion.

actual value $(c^2H)_{act}$ was obtained via a two two-body *approximation* to the three-body system in that the total angular momentum was taken to be the sum of the angular momenta contributed by m_2 in its orbit about m_1 and m_3 in its orbit about M_2, with a similar expression for the total energy.

In Chapter 4 the stability criterion, employing the above two two-body approximation, was presented as a surface in the $0\varepsilon^{23}\ \varepsilon_{32}\ \alpha_{23}$ parameter space. This surface, defined as $\alpha_{cr} \equiv \alpha'(\varepsilon^{23},\varepsilon_{32})$ such that if $\alpha \leqslant \alpha_{cr}$ the system is stable, was only examined in the case where the orbits are initially circular. In other words, the osculating orbit of m_2 relative to m_1 was taken to be a circle of radius a_2 while the osculating orbit of m_3 relative to M_2 was taken to be a circle of radius a_3 so that $\alpha_{23} = \alpha = a_2/a_3$, α_{cr} being the critical ratio of a_2/a_3 when $(c^2H)_{act} = (c^2H)_{cr}$.

Now, more exactly, we consider $\alpha_{23} = \rho_2/\rho_3$: ρ_2 and ρ_3 are functions, through the usual two-body expressions, of (a_2, e_2, f_2) and (a_3, e_3, f_3) - see Section 4.2, Equations(4.5) - where (a_2, a_3) are the osculating semi-major axes of what we may call the (m_1, m_2) and (M_2, m_3) subsystems respectively, (e_2, e_3) and (f_2, f_3) being the eccentricities of and true anomalies in these osculating orbits. The remaining orbital parameters are the osculating longitudes of pericentre - (ϖ_2, ϖ_3). The ε parameters themselves do not take account of any effect on the stability of (ϖ_2,ϖ_3). However, the angle θ, arising naturally during the derivation of the ε's, and defined by $\cos\theta = \underset{\sim}{\rho}_2 \cdot \underset{\sim}{\rho}_3/\rho_2\rho_3$, involves a combination of ϖ_2,ϖ_3, f_2 and f_3. Because the ε parameters appear to be significant in determining the likelihood of stability, the effects on the stability of CHT systems of varying ϖ_2,ϖ_3, f_2 and f_3 should be investigated. In other words, having obtained an exact expression for $(c^2H)_{act}$ in terms of $(a_i, e_i, \varpi_i, f_i;\ i = 2,3)$ it will be possible to locate accurately the opening and closing of the zero-velocity curves in any given problem in terms of the parameters of the osculating orbits of the CHT system.

An exact expression for the value of $(c^2H)_{act}$ is derived in Section 5.2 in order to allow the critical stability surface (the critical ratio of a_2/a_3 or ρ_2/ρ_3) to be determined with greater accuracy, for given values of the orbital parameters e_2, e_3, ϖ_2, ϖ_3, f_2, and f_3.

$(c^2H)_{act}$ is thus found to be dependant upon the masses (m_1, m_2, m_3) and the two sets of (osculating) orbital parameters. Further, in Section 5.3 the expression is used to determine, in a general fashion, the effects of the various orbital parameters on $(c^2H)_{act}$ and thus on the stability.

Numerical results are presented in Section 5.4 to 5.7. For given values of the masses (m_1, m_2, m_3) it is demonstrated how stability in terms of the maximum allowable values of the ratio a_2/a_3, such that the zero-velocity curves remain closed, is affected by variation of the orbital parameters e_2, e_3, ϖ_2, ϖ_3, f_2 and f_3 (see Section 5.4). The results are compared with those of Harrington (1972), which were derived from numerical integration experiments (see Section 5.5). In Sections 5.6 and 5.7 we consider two interesting real cases of CHT system viz. Sun-Jupiter-Saturn and Earth-Moon-Sun, the latter system being a borderline case of stability, in the sense of closure of the zero-velocity curves of the general three-body problem. The masses of these systems are varied in such a way as to investigate the degree of stability or instability of the real system (cf. Nacozy, 1976, 1977). The results are compared with those of Szebehely and McKenzie (1977 a,b) and those given in the above papers by Nacozy.

In Section 5.8 the results are discussed and certain conclusions drawn, attention being paid to some of the more important aspects of the analysis.

5.2 An Exact Expression for the Parameter c^2H in Coplanar Hierarchical Three-Body Systems.

Formulating the equations of motion of an n-body system in the Jacobian coordinate system it was found (see Section 3.5, Equation (3.29) and Figure 5.1) that

$$\frac{m_i M_{i-1}}{M_i} \ddot{\underset{\sim}{\rho}}_i = \underset{\sim}{\nabla}_i U \qquad i = 2,\ldots,n \qquad (1)$$

where, in the usual notation, m_i is the ith mass

$$M_i = \sum_{j=1}^{i} m_j$$

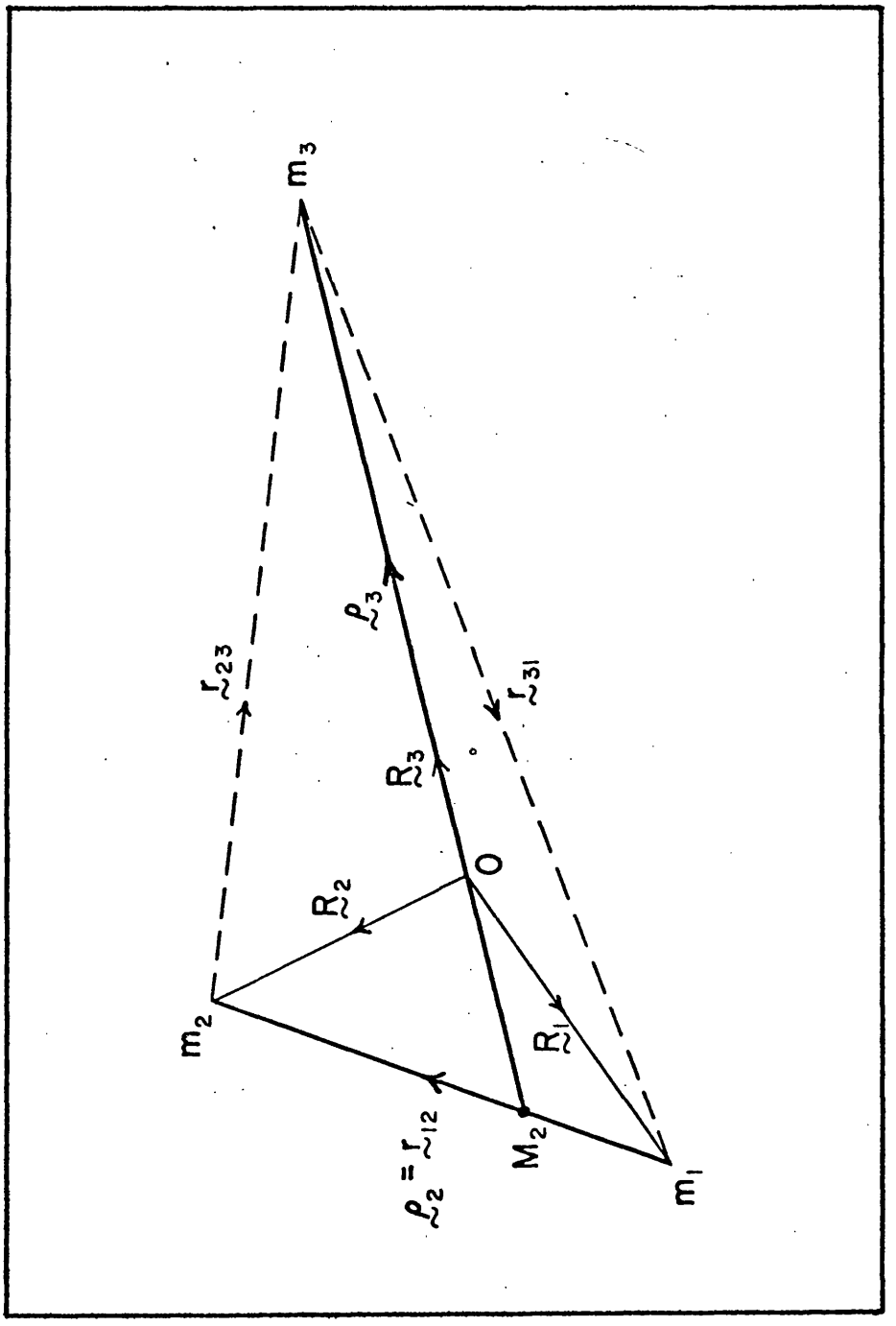

Figure 5.1 Definitions of quantities in Jacobian coordinate system and inertial reference frame with origin O at the centre of mass of the CHT system (see text for meaning of symbols).

$\underset{\sim}{\rho}_i = \overrightarrow{M_{i-1}\, m_i}$: M_{i-1} being the position of the mass-centre of the system of masses $m_1,\ldots,m_{i-1}$

$\underset{\sim}{\nabla}_i$ is the gradient operator with respect to $\underset{\sim}{\rho}_i$

$U = \frac{1}{2} \sum_{k=1}^{n} \sum_{\ell=1}^{n} \frac{m_k m_\ell}{r_{k\ell}}$ is the force function

$G = 1$

and $r_{k\ell} = |\overrightarrow{m_k\, m_\ell}|$.

To construct the energy integral, H, first form the scalar product of Equation (1) with $\dot{\underset{\sim}{\rho}}_i$, giving

$$\frac{m_i M_{i-1}}{M_i} \dot{\underset{\sim}{\rho}}_i \cdot \ddot{\underset{\sim}{\rho}}_i = \dot{\underset{\sim}{\rho}}_i \cdot \underset{\sim}{\nabla}_i U . \quad (i = 2,\ldots,n) \qquad (2)$$

Summing over all i then results in

$$\sum_{i=2}^{n} \frac{m_i M_{i-1}}{M_i} \dot{\underset{\sim}{\rho}}_i \cdot \ddot{\underset{\sim}{\rho}}_i = \sum_{i=2}^{n} \dot{\underset{\sim}{\rho}}_i \cdot \underset{\sim}{\nabla}_i U \qquad (3)$$

which, noting that

$$\dot{\underset{\sim}{\rho}}_i \cdot \ddot{\underset{\sim}{\rho}}_i = \frac{1}{2} \cdot \frac{d}{dt} (\dot{\underset{\sim}{\rho}}_i \cdot \dot{\underset{\sim}{\rho}}_i) \qquad (4)$$

and $U = U(\rho_i)$ is not explicitly dependant on the time (i.e. the R.H.S. of equation (3) is a perfect differential), results in

$$\sum_{i=2}^{n} \frac{m_i M_{i-1}}{M_i} \cdot \frac{d}{dt} (\dot{\underset{\sim}{\rho}}_i \cdot \dot{\underset{\sim}{\rho}}_i) = \frac{dU}{dt} . \qquad (5)$$

Integrating once, the energy integral, H, is obtained viz.

$$H = \frac{1}{2} \sum_{i=2}^{n} \frac{m_i M_{i-1}}{M_i} \dot{\underset{\sim}{\rho}}_i \cdot \dot{\underset{\sim}{\rho}}_i - U \qquad (6)$$

where U may be determined from the $\underset{\sim}{\rho}_i (i=2,\ldots,n)$ by use of Equation (3.37) which gives the $\underset{\sim}{r}_{k\ell}$ in terms of the $\underset{\sim}{\rho}_i$.

The integrals of angular momentum, $\underset{\sim}{c}$, may then be obtained by forming the vector product of Equation (1) with $\underset{\sim}{\rho}_i$ and summing over all i giving

$$\sum_{i=2}^{n} \frac{m_i M_{i-1}}{M_i} \underset{\sim}{\rho}_i \times \ddot{\underset{\sim}{\rho}}_i = \sum_{i=2}^{n} \underset{\sim}{\rho}_i \times \underset{\sim}{\nabla}_i U. \qquad (7)$$

Theorem:

$$\sum_{i=2}^{n} \frac{m_i M_{i-1}}{M_i} \underset{\sim}{\rho}_i \times \ddot{\underset{\sim}{\rho}}_i = \underline{0}$$

Proof: Now we have, by the definition of the $\underset{\sim}{\rho}_i$,

$$\underset{\sim}{\rho}_i = \underset{\sim}{R}_i - \bar{\underset{\sim}{R}}_{i-1} \qquad (8)$$

where $\underset{\sim}{R}_i$ is the position vector of the ith mass in an inertial coordinate system origin O viz. $\overrightarrow{Om_i}$, while

$$\bar{\underset{\sim}{R}}_i = \frac{1}{M_i} \sum_{j=1}^{i} m_j \underset{\sim}{R}_j \ , \qquad (9)$$

is the position vector of the mass-centre of the first i masses in the inertial coordinate system and

$$M_i = \sum_{j=0}^{i} m_j \qquad (10)$$

$m_o = 0$ being defined.

We may then write

$$m_i \underset{\sim}{R}_i = M_i \bar{\underset{\sim}{R}}_i - M_{i-1} \bar{\underset{\sim}{R}}_{i-1} \qquad (11)$$

and

$$m_i \underset{\sim}{\rho}_i = M_i(\bar{\underset{\sim}{R}}_i - \bar{\underset{\sim}{R}}_{i-1}) \qquad (12)$$

with similar expressions for their second derivatives.

Forming the quantities (cf. Plummer, 1918)

$$m_i \underset{\sim}{R}_i \times \ddot{\underset{\sim}{R}}_i = \frac{1}{m_i} \cdot (M_i \bar{\underset{\sim}{R}}_i - M_{i-1} \bar{\underset{\sim}{R}}_{i-1}) \times (M_i \ddot{\bar{\underset{\sim}{R}}}_i - M_{i-1} \ddot{\bar{\underset{\sim}{R}}}_{i-1}) \qquad (13)$$

and

$$\frac{m_i M_{i-1}}{M_i} \underset{\sim}{\rho}_i \times \ddot{\underset{\sim}{\rho}}_i = \frac{M_i M_{i-1}}{m_i} (\bar{\underset{\sim}{R}}_i - \bar{\underset{\sim}{R}}_{i-1}) \times (\ddot{\bar{\underset{\sim}{R}}}_i - \ddot{\bar{\underset{\sim}{R}}}_{i-1}) \qquad (14)$$

and then taking Equation (14) minus Equation (13) yields

$$\frac{m_i M_{i-1}}{M_i} \underset{\sim}{\rho}_i \times \ddot{\underset{\sim}{\rho}}_i - m_i \underset{\sim}{R}_i \times \ddot{\underset{\sim}{R}}_i = \frac{1}{m_i} (M_i M_{i-1} (\dot{\underset{\sim}{R}}_i - \dot{\underset{\sim}{R}}_{i-1}) \times (\ddot{\underset{\sim}{R}}_i - \ddot{\underset{\sim}{R}}_{i-1}) - (M_i \dot{\underset{\sim}{R}}_i - M_{i-1} \dot{\underset{\sim}{R}}_{i-1}) \times (M_i \ddot{\underset{\sim}{R}}_i - M_{i-1} \ddot{\underset{\sim}{R}}_{i-1}) \tag{15}$$

On expanding the vector products in Equation (15) and summing over i, from 1 to n, we obtain

$$\sum_{i=1}^{n} \left[\frac{m_i M_{i-1}}{M_i} \underset{\sim}{\rho}_i \times \ddot{\underset{\sim}{\rho}}_i - m_i \underset{\sim}{R}_i \times \ddot{\underset{\sim}{R}}_i \right] = \sum_{i=1}^{n} \left[M_{i-1} \dot{\underset{\sim}{R}}_{i-1} \times \ddot{\underset{\sim}{R}}_{i-1} - M_i \dot{\underset{\sim}{R}}_i \times \ddot{\underset{\sim}{R}}_i \right]. \tag{16}$$

Remembering that $M_o = m_o = 0$ was defined we then have

$$\sum_{i=2}^{n} \frac{m_i M_{i-1}}{M_i} \underset{\sim}{\rho}_i \times \ddot{\underset{\sim}{\rho}}_i - \sum_{i=1}^{n} m_i \underset{\sim}{R}_i \times \ddot{\underset{\sim}{R}}_i + M_n \dot{\underset{\sim}{R}}_n \times \ddot{\underset{\sim}{R}}_n = \underset{\sim}{0}, \tag{17}$$

which on noting that the second term is zero, since it is the time derivative of angular momentum expressed in an inertial reference frame, and the third is zero, since the mass-centre of the system moves with constant velocity, gives the required result viz.

$$\sum_{i=2}^{n} \frac{m_i M_{i-1}}{M_i} \underset{\sim}{\rho}_i \times \ddot{\underset{\sim}{\rho}}_i = \underset{\sim}{0}. \tag{18}$$

Q.E.D.

Now

$$\underset{\sim}{\rho}_i \times \ddot{\underset{\sim}{\rho}}_i = \frac{d}{dt} (\underset{\sim}{\rho}_i \times \dot{\underset{\sim}{\rho}}_i) \tag{19}$$

since $\dot{\underset{\sim}{\rho}}_i \times \dot{\underset{\sim}{\rho}}_i = \underset{\sim}{0}$, and using Equation (18), we have

$$\sum_{i=2}^{n} \frac{m_i M_{i-1}}{M_i} \frac{d}{dt} (\underset{\sim}{\rho}_i \times \dot{\underset{\sim}{\rho}}_i) = \underset{\sim}{0} \tag{20}$$

Integrating once yields the angular momentum integrals, $\underset{\sim}{c}$, viz.

$$\underset{\sim}{c} = \sum_{i=2}^{n} \frac{m_i M_{i-1}}{M_i} \underset{\sim}{\rho}_i \times \dot{\underset{\sim}{\rho}}_i . \tag{21}$$

Particularizing to the case n = 3 we then obtain

$$\underset{\sim}{c} = \frac{m_1 m_2}{(m_1+m_2)} \underset{\sim}{\rho}_2 \times \dot{\underset{\sim}{\rho}}_2 + \frac{m_3(m_1 + m_2)}{m_1 + m_2 + m_3} \underset{\sim}{\rho}_3 \times \dot{\underset{\sim}{\rho}}_3 \qquad (22)$$

and

$$H = \tfrac{1}{2} \left[\frac{m_1 m_2}{m_1+m_2} \dot{\underset{\sim}{\rho}}_2 \cdot \dot{\underset{\sim}{\rho}}_2 + \frac{m_3(m_1 + m_2)}{m_1 + m_2 + m_3} \dot{\underset{\sim}{\rho}}_3 \cdot \dot{\underset{\sim}{\rho}}_3 \right] - U \qquad (23)$$

where

$$U = \frac{m_1 m_2}{r_{12}} + \frac{m_2 m_3}{r_{23}} + \frac{m_3 m_1}{r_{31}} \; . \qquad (24)$$

By Equation (3.37), forming scalar products $(\underset{\sim}{r}_{k\ell} \cdot \underset{\sim}{r}_{k\ell})^{\frac{1}{2}}$,

$$r_{12} = \rho_2 \qquad (25a)$$

$$r_{23} = \left[\rho_3^2 + \frac{m_1^2}{(m_1+m_2)^2} \rho_2^2 - \frac{2m_1}{(m_1+m_2)} \underset{\sim}{\rho}_2 \cdot \underset{\sim}{\rho}_3 \right]^{\frac{1}{2}} \qquad (25b)$$

and

$$r_{31} = \left[\rho_3^2 + \frac{m_2^2}{(m_1+m_2)^2} \rho_2^2 + \frac{2 m_2}{(m_1+m_2)} \underset{\sim}{\rho}_2 \cdot \underset{\sim}{\rho}_3 \right]^{\frac{1}{2}} . \qquad (25c)$$

Equations (22) - (25) are general in nature, inasmuch as they are applicable to non-coplanar motions. If we now restrict the motion of the bodies to the ξ, η-plane then c_ξ and c_η vanish and we may put $c = |\underset{\sim}{c}| = c_\zeta$. Thus the angular momentum integral is given by the following

$$c = \frac{m_1 m_2}{m_1+m_2} \rho_2 V_2 \sin \psi_2 + \frac{m_3(m_1 + m_2)}{m_1 + m_2 + m_3} \rho_3 V_3 \sin \psi_3 \qquad (26)$$

where ψ_2, ψ_3 are the angles between $\underset{\sim}{\rho}_2, \dot{\underset{\sim}{\rho}}_2$ and $\underset{\sim}{\rho}_3, \dot{\underset{\sim}{\rho}}_3$ respectively, and $V_i = |\dot{\underset{\sim}{\rho}}_i| \quad i = 2,3.$

Then if we define osculating orbits for the orbit of m_2 relative to m_1 and m_3 relative to M_2 by the elements $(a_i, e_i, \varpi_i;\ i = 2,3)$ and the positions of the bodies in these orbits by f_i $(i = 2,3)$, we have the following standard expressions

$$\rho_i = \frac{a_i (1-e_i^2)}{1 + e_i \cos f_i} \qquad (27)$$

$$V_i = \left[\frac{M_i}{a_i} \frac{1 + 2 e_i \cos f_i + e_i^2}{1 - e_i^2}\right]^{\frac{1}{2}} \qquad i = 2,3 \quad (28)$$

and $$\sin \psi_i = \frac{1 + e_i \cos f_i}{(1 + e_i^2 + 2e_i \cos f_i)^{\frac{1}{2}}} \qquad (29)$$

If Equations (27) - (29) are substituted into Equation (26) we obtain

$$c = \frac{m_1 m_2}{(m_1+m_2)^{\frac{1}{2}}} a_2^{\frac{1}{2}}(1 - e_2^2)^{\frac{1}{2}} \pm \frac{m_3(m_1 + m_2)}{(m_1 + m_2 + m_3)^{\frac{1}{2}} a_3^{\frac{1}{2}}(1-e_3^2)^{\frac{1}{2}}} \qquad (30)$$

where the + or - sign in the equation depends on whether sin ψ_2 and sin ψ_3 are of similar or dissimilar sign i.e. whether the orbits are corotational or counter-rotational.

It is then immediately seen that the angular momentum does not in fact depend on any elements of the osculating orbit other than (a_2, e_2) and (a_3, e_3) nor does it depend upon the position in the orbit. This expression is identical to that obtained by Szebehely and Zare (1977) using the two two-body approximation to derive c.

Applying Equations (27) - (29) to the energy integral - Equations (23), (24) and (25) - we obtain, after some simplification,

$$H = \frac{1}{2}\left[- \frac{m_1 m_2}{a_2} + \frac{m_3(m_1+m_2)}{a_3} \cdot \frac{1+2e_3 \cos f_3 + e_3^2}{1 - e_3^2} \right]$$

$$- \frac{m_2 m_3}{a_3} \cdot \frac{1+e_3 \cos f_3}{1 - e_3^2} \cdot \frac{1}{\bar{r}_{23}} - \frac{m_3 m_1}{a_3} \cdot \frac{1+e_3 \cos f_3}{1 - e_3^2} \cdot \frac{1}{\bar{r}_{31}} \qquad (31)$$

where

$$\bar{r}_{23} = \left[1 + \frac{m_1^2}{(m_1+m_2)^2} \alpha_{23}^2 - \frac{2 m_1}{(m_1+m_2)} \alpha_{23} \cos \theta\right]^{\frac{1}{2}} \qquad (32a)$$

$$\bar{r}_{31} = \left[1 + \frac{m_2^2}{(m_1+m_2)^2} \alpha^2 23 + \frac{2 m_2}{(m_1+m_2)} \alpha_{23} \cos \theta\right]^{\frac{1}{2}} \qquad (32b)$$

$$\alpha_{23} = \frac{\rho_2}{\rho_3} = \frac{a_2}{a_3} \cdot \frac{1-e_2^2}{1-e_3^2} \cdot \frac{1+e_3 \cos f_3}{1+e_2 \cos f_2} \qquad (33)$$

and $\cos\theta = \dfrac{\underset{\sim}{\rho}_2 \cdot \underset{\sim}{\rho}_3}{\rho_2\ \rho_3}$ so that $\theta \quad (\varpi_2+f_2) - (\varpi_3+f_3)$.

We define θ as the phase angle of the system and also $\phi = \varpi_2 - \varpi_3$, the initial angular distance between the lines of apses.

Thus, using Equations (30), (31), (32) and (33) an exact expression for c^2H may be formed which allows for the dependance of c^2H, and thus the stability of the system, upon factors other than the semi-major axes and eccentricities of the osculating orbits for given masses. It may also be noted that, as in the analysis by Szebehely and Zare, the value of c^2H is not dependant upon the scale of the system, i.e. a_2 and a_3 only occur as the ratio $\alpha = a_2/a_3$.

5.3 The General Effects of Orbital Parameters on the Stability

In Section 5.2 an exact expression for c^2H was derived in terms of the osculating elements of a CHT system. It may be remarked that the value of c^2H will be a constant for any given system. c^2H may be obtained from the values of the osculating elements *at any instant*. Thus any results obtained in the following sections from initial values of c^2H will not be vitiated by the fact that the orbital parameters vary with time. Introducing normalised masses μ and μ_3 into Equations (30) and (31), we obtain

$$(c^2H)_{act} = \left[\mu(1-\mu)\ \alpha^{\frac{1}{2}}(1-e_2^2)^{\frac{1}{2}} \pm \frac{\mu_3}{(1+\mu_3)^{\frac{1}{2}}}\ (1-e_3^2)^{\frac{1}{2}}\ \right]^2 .$$
$$\cdot\tfrac{1}{2}\cdot\left[-\frac{\mu(1-\mu)}{\alpha} + \mu_3 \cdot \frac{1+2e_3\cos f_3}{1-e_3^2} - \frac{2\mu\mu_3}{\bar{r}_{23}} \cdot \frac{1+e_3\cos f_3}{1-e_3^2}\right.$$
$$\left. - \frac{2(1-\mu)\mu_3}{\bar{r}_{31}} \cdot \frac{1+e_3\cos f_3}{1-e_3^2}\ \right] \qquad (34)$$

where $1-\mu : \mu : \mu_3 = m_1 : m_2 : m_3$ without loss of generality

$(\mu: 0 < \mu \leq \tfrac{1}{2})$

$\alpha = a_2/a_3$

$$\bar{r}_{23} = (1 + (1-\mu)^2 \alpha_{23}^2 - 2(1-\mu)\ \alpha_{23} \cos\ \theta)^{\frac{1}{2}} \qquad (35a)$$

and $$\bar{r}_{31} = (1 + \mu^2 \alpha_{23}^2 + 2\mu\ \alpha_{23} \cos\ \theta)^{\frac{1}{2}}. \qquad (35b)$$

The quantities denoted $\bar{r}_{23}$ and $\bar{r}_{31}$ are dimensionless: they represent the distances r_{23} and r_{31} in units of ρ_3 i.e. $r_{23} = \rho_3 \bar{r}_{23}$ and $r_{31} = \rho_3 \bar{r}_{31}$.

It is clear from Equation (34) that if one of α, $\bar{r}_{23}$, $\bar{r}_{31}$ is small then $(c^2H)_{act} \lesssim 0$. This implies a likelihood of stability for the system, since this actual value of c^2H may be less than the critical value - $(c^2H)_{cr}$ - obtained from the collinear equilibrium configurations. The determination of the critical values of c^2H will be dealt with in more detail later in Section 5.4. At the moment we will only concern ourselves with stability in the case of small α, that is (m_1, m_2) forms a binary system with m_3 orbiting about their mass-centre, stability implying this hierarchical arrangement remains intact.

Any increase in e_2 or e_3 will generally decrease the stability of such an arrangement with given α(see Szebehely and Zare, 1977). The degree of dependance of the stability on e_2 and e_3 is largely dependant on the relative sizes of μ and μ_3.

The effect on $(c^2H)_{act}$ of changing the initial value of θ is now considered.

By Equations (34) and (35) it is seen that θ enters the expression for $(c^2H)_{act}$ in the form of a cosine function within the expressions for $\bar{r}_{23}$ and $\bar{r}_{31}$. The effect of θ on $(c^2H)_{act}$ may be obtained by partially differentiating Equation (34) with respect to θ. Noting that $c \neq c(\theta)$ we have, dropping the suffix "act",

$$\frac{\partial}{\partial\theta}\left[c^2H\right] = c^2 \frac{\partial H}{\partial \theta}. \qquad (36)$$

To examine the behaviour of c^2H with respect to θ we require to find those values of θ for which $\partial[c^2H]/\partial\theta = 0$. Clearly

$$\frac{\partial}{\partial\theta}\left[c^2H\right] = c^2\mu_3 \left(\frac{1 + e_3 \cos f_3}{1 - e_3^2}\right) \cdot \left(\frac{\mu}{\bar{r}_{23}^2} \frac{\partial \bar{r}_{23}}{\partial\theta} + \frac{1-\mu}{\bar{r}_{31}^2} \frac{\partial \bar{r}_{31}}{\partial\theta} \right). \qquad (37)$$

Upon deriving $\partial\bar{r}_{23}/\partial\theta$ and $\partial\bar{r}_{31}/\partial\theta$ and substituting in Equation (37) we find that we require

$$\mu(1-\mu)\ \alpha_{23}\ \sin\theta\left[\frac{1}{\bar{r}_{23}^{3}}-\frac{1}{\bar{r}_{31}^{3}}\right]=0, \tag{38}$$

so that *either* (i) $\theta = 0$ or π *or* (ii) $\bar{r}_{23} = \bar{r}_{31}$.

Case (i) In this case $\theta = 0$ or π and the three bodies are in a straight line i.e. $m_1m_2m_3$ $(\theta = 0)$ or $m_2m_1m_3(\theta = \pi)$

Case (ii) Using Equations (35) we find the angle θ_T, at the turning points, such that

$$1 + (1-\mu)^2\alpha_{23}^2 - 2(1-\mu)\ \alpha_{23}\cos\theta_T = 1 + \mu^2\ \alpha_{23}^2 + 2\mu\ \alpha_{23}\cos\theta_T \tag{39}$$

that is

$$\cos\theta_T = \tfrac{1}{2}(1 - 2\mu)\ \alpha_{23}. \tag{40}$$

It is a straightforward, but tedious, matter to evaluate $\partial^2[c^2H]/\partial\theta^2$ and show that case (i) results in minima of c^2H while case (ii) results in maxima of c^2H with respect to θ. We may therefore set up the case of least stability for any system with given (μ,μ_3) and given initial values $(\alpha, e_2, e_3, f_2, f_3)$ if we limit the configuration by Equation(40). This can be considered as a restriction on ϕ for given (f_2, f_3) values where

$$\phi = f_3 - f_2 \pm \cos^{-1}\left[\tfrac{1}{2}(1 - 2\mu)\ \alpha_{23}\right]. \tag{41}$$

Using Equation (40) to eliminate θ from Equation (35), we obtain the expression for the maximum value of $(c^2H)_{act} - (c^2H)_{max}$ - for a CHT system, within the range of 0 to 2π for θ, viz.

$$(c^2H)_{max} = \left[\mu(1-\mu)\ \alpha^{\frac{1}{2}}(1-e_2^2)^{\frac{1}{2}} \pm \frac{\mu_3}{(1+\mu_3)^{\frac{1}{2}}}\cdot(1-e_3^2)^{\frac{1}{2}}\right]^2 \cdot$$
$$\cdot\tfrac{1}{2}\cdot\left[-\frac{\mu(1-\mu)}{\alpha}+\mu_3\cdot\frac{1+2e_3\cos f_3+e_3^2}{1-e_3^2}\right.$$
$$\left.-2\frac{\mu_3}{\bar{r}}\cdot\frac{(1+e_3\cos f_3)}{1-e_3^2}\right] \tag{42}$$

where

$$\bar{r} = \bar{r}_{23} = \bar{r}_{31} = (1 + \mu(1-\mu)\,\alpha_{23}^2)^{\frac{1}{2}} \qquad (43)$$

The relative sizes of $(c^2H)_{act}$ at the turning values are relevant. In case (ii) it is clear that since $(c^2H)_{act}$ is an even-valued function of θ, the two maxima defined by Equation (40) have the same resulting value of $(c^2H)_{act}$.

Considering case (i), however, it is necessary to determine whether $[(c^2H)_{act}]$ is larger when $\theta = 0$ or $\theta = \pi$. Since θ only enters $(c^2H)_{act}$ in two terms within H we require to determine the larger of H_1 and H_2 where

$$H_1 = \left[\frac{-\mu}{\bar{r}_{23}} + \frac{(1-\mu)}{\bar{r}_{31}} \right]_{\theta = 0} \qquad (44)$$

and

$$H_2 = \left[\frac{\mu}{\bar{r}_{23}} + \frac{(1-\mu)}{\bar{r}_{31}} \right]_{\theta = \pi} \qquad (45)$$

Since $0 < \mu \leq \frac{1}{2}$ there are two possibilities:

(a) if $H_1 > H_2$ the configuration $m_1 m_2 m_3$ results in the larger value of $|(c^2H)_{act}|$

(b) if $H_1 < H_2$ the configuration $m_2 m_1 m_3$ results in the larger value of $|(c^2H)_{act}|$.

Now

$$H_1 = \frac{\mu}{1 - (1-\mu)\alpha_{23}} + \frac{1-\mu}{1 + \mu\alpha_{23}}$$

and

$$H_2 = \frac{\mu}{1 + (1-\mu)\alpha_{23}} + \frac{1-\mu}{1 - \mu\alpha_{23}}$$

so that

$$H_1 - H_2 = 2\mu(1-\mu)\,\alpha_{23} \left[\frac{1}{1-(1-\mu)^2\alpha_{23}^2} - \frac{1}{1-\mu^2\alpha_{23}^2} \right]. \qquad (46)$$

Hence $H_1 - H_2 > 0$ i.e. the configuration resulting in the more negative $(c^2H)_{act}$ value is $m_1m_2m_3$- unless $\mu = \frac{1}{2}$, in which case both configurations result in the same value.

As was stated by Zare (1977) the value of c^2H controls the opening and closing of the zero-velocity curves of the problem, and therefore its value can tell us whether an exchange between bodies is possible or not. The value of c^2H to ensure closure of the zero-velocity curves is again denoted $(c^2H)_{cr}$: this is purely a function of the masses. For any given CHT system to be stable, in the sense of no exchange of bodies being possible, the value $(c^2H)_{act}$ must be less than or equal to the prescribed critical value $(c^2H)_{cr}$ - equality implying critical stability. If we consider again the effect of phase angle on $(c^2H)_{act}$ we can see that there are five possible situations (Fig.5.2) for given initial orbital parameters (α, e_2, e_3, f_2, f_3) and given mass parameters (μ,μ_3) as follows:

(a) $(c^2H)_{act} < (c^2H)_{cr}$ $\forall\theta$: the system is stable for any given value of θ.

(b) $(c^2H)_{act} \leq (c^2H)_{cr}$: the situation is as in (a) above, except that at $\theta = \pm \theta_T$ the system is critically stable.

(c) $(c^2H)_{act} < (c^2H)_{cr}$ except for a small range in θ about $\theta = \pm\theta_T$ where $(c^2H)_{act} > (c^2H)_{cr}$ and where subsequently instability may set in.

There are four critically stable configurations.

(d) $(c^2H)_{act} > (c^2H)_{cr}$ except for a small range about $\theta = 0$ where stability is assured.

(e) $(c^2H)_{act} > (c^2H)_{cr}$ $\forall\theta$: the system may exhibit instability at all initial phase angles.

The parameter $(c^2H)_{act}$ is also dependant on the true anomalies f_2 and f_3, the degree to which they effect it being dependant upon the eccentricities e_2 and e_3. To examine the variation of $(c^2H)_{act}$ with respect to f_2 and f_3 we require to calculate $(\partial (c^2H)/ \partial f_2)_{f_3}$ and $(\partial (c^2H)/ \partial f_3)_{f_2}$ where in both these expressions (α, e_2, e_3, ϕ) are held constant.

After some reduction it is found that

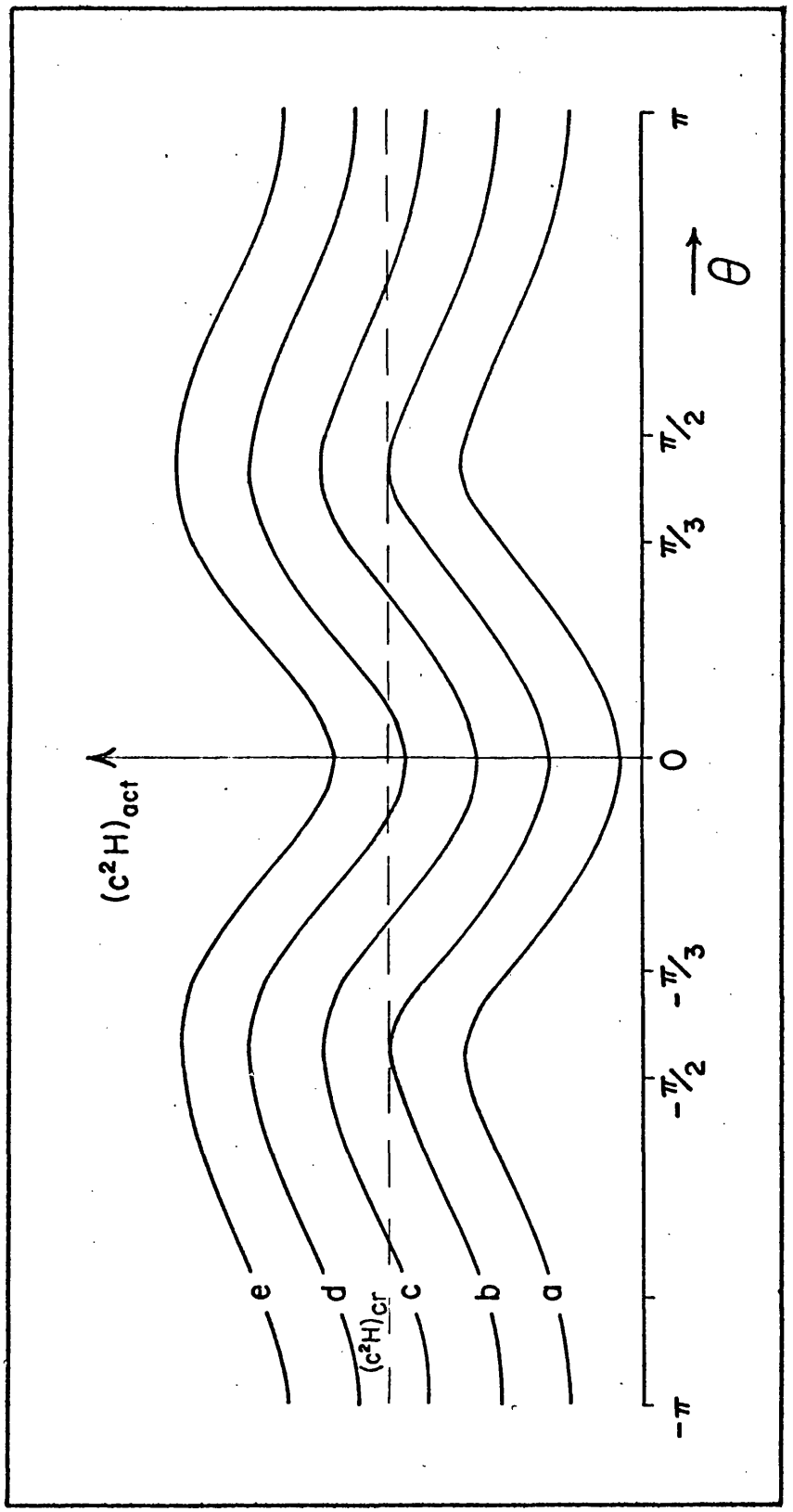

Figure 5.2 Effect of the phase angle θ on the stability in terms of the actual value of c^2H. The dotted line denotes the $(c^2H)_{cr}$ value for given μ,μ_3 and each curve gives the variation in $(c^2H)_{act}$ over the range $-\pi \leq \theta \leq \pi$ for certain initial values of orbital parameters (α, e_2, e_3, f_2, f_3): see text for description of curves (a) to (e).

$$\left[\frac{\partial(c^2H)}{\partial f_2}\right]_{f_3} = c^2\mu(1-\mu)\mu_3 \cdot \frac{1+e_3\cos f_3}{1-e_3^2} \cdot \left[\frac{\alpha_{23}^2}{\bar{r}_{23}^3} \cdot \frac{e_2 \sin f_2}{1+e_2\cos f_2} + \left\{\frac{1}{\bar{r}_{31}^3} - \frac{1}{\bar{r}_{23}^3}\right\}\right.$$

$$\left. \cdot \left\{ (\mu\alpha_{23}+\cos\theta)\,\alpha_{23}\frac{e_2 \sin f_2}{1+e_2\cos f_2} - \alpha_{23}\sin\theta \right\}\right] \qquad (47)$$

and

$$\left[\frac{\partial(c^2H)}{\partial f_3}\right]_{f_2} = -c^2\mu(1-\mu)\mu_3 \frac{1+e_3\cos f_3}{1-e_3^2} \cdot \left[\frac{\alpha_{23}^2}{\bar{r}_{23}^3} \frac{e_3 \sin f_3}{1+e_3\cos f_3} + \left\{\frac{1}{\bar{r}_{31}^3} - \frac{1}{\bar{r}_{23}^3}\right\}\cdot\right.$$

$$\left. \cdot \left\{(\mu\alpha_{23} + \cos\theta)\alpha_{23} \frac{e_3 \sin f_3}{1+e_3\cos f_3} - \alpha_{23}\sin\theta\right\}\right] -$$

$$- c^2\mu_3 \frac{e_3 \sin f_3}{1+e_3\cos f_3} \cdot \left[1 - \frac{\mu}{\bar{r}_{23}} - \frac{1-\mu}{\bar{r}_{31}}\right] . \qquad (48)$$

Examining these expressions it can be seen that if $\theta = 0, \theta_T, \pi$ (n.b. $\theta = \theta_T$ implies $\bar{r}_{23} = \bar{r}_{31}$) it follows that if f_2 and f_3 take the values 0 or/and π then $\left[\partial(c^2H)/\partial f_2\right]_{f_3}$ and $\left[\partial(c^2H)/\partial f_3\right]_{f_2}$ are both zero.

In Chapter 4 the procedure adopted to investigate the stability of any given system was, for given mass parameters (μ,μ_3), to find the value of the ratio $\alpha = a_2/a_3$ viz. α_{cr} such that $(c^2H)_{act} = (c^2H)_{cr}$. We may now introduce the parameters f_2, f_3 and θ and the eccentricities e_2 and e_3, which were neglected in Chapter 4, and use a similar procedure.

We have

$$(c^2H)_{act} = F(\mu, \mu_3, \alpha, e_2, e_3, f_2, f_3, \theta)$$

and

$$(c^2H)_{cr} = G(\mu, \mu_3),$$

so that we therefore require to find the value α_{cr} such that

$$F(\mu, \mu_3, \alpha_{cr}, e_2, e_3, f_2, f_3, \theta) = G(\mu,\mu_3).$$

If α_{act} is the value of the ratio a_2/a_3 for a given CHT system, defined by mass parameters μ and μ_3, then, for given values of

e_2, e_3, f_2, f_3, θ, if $\alpha_{act} \leq \alpha_{cr}$ then the system will be stable because the zero-velocity curves are closed. In this case the hierarchy (m_1, m_2) as binary with m_3 as external mass will remain intact. The case $\alpha_{act} = \alpha_{cr}$ is referred to as critical stability. If however $\alpha_{act} > \alpha_{cr}$ then stability is not assured and an exchange of bodies is possible. We then see that if $\alpha_{act}/\alpha_{cr} \ll 1$ this is analogous to $(c^2H)_{act} \ll (c^2H)_{cr}$ i.e. a very stable situation. As α_{act}/α_{cr} increases the system will become less stable until eventually, when $\alpha_{act}/\alpha_{cr} \gg 1$ the system is unstable.

Figure 5.3 demonstrates the effect of f_2 and f_3 on the value of α_{cr} for particular values of the mass parameters μ and μ_3 and orbital parameters (e_2, e_3, θ). It may be interpreted as follows.

The equal mass case is considered viz. $\mu = \mu_3 = \frac{1}{2}$, θ is taken to be zero and e_2 and e_3 both have values 0.1. Then over the possible range of f_2 and f_3 the largest α_{cr} value occurring is 0.340 and the smallest is 0.324. This range is split into ten and contours of α_{cr} are drawn on the f_2, f_3-plane at the intermediate heights. The contours are denoted 0.1, 0.2,... etc for increasing values of α_{cr}, for example α_{cr} of the 0.6 contour is

$$\alpha_{cr} = 0.324 + 0.6\ (0.340 - 0.324).$$

It is then seen that the greatest stability occurs at $f_2 = \pm\pi$ and $f_3 = 0$ i.e. when the (m_1, m_2) subsystem osculating orbit is at apocentre and the (M_2, m_3) subsystem is at pericentre. The least stability is found to be at $f_2 = 0$, $f_3 = \pm\pi$.

If the above calculations were repeated to obtain a diagram for $\theta = \theta_T$, the following situation arises: greatest stability occurs when the (m_1, m_2) subsystem is at pericentre with the (M_2, m_3) subsystem at apocentre i.e. $f_2 = 0$, $f_3 = \pm\pi$. Least stability is then found at $f_2 = \pm\pi$, $f_3 = 0$. The former case results in $\alpha_{cr} = 0.299$ and the latter $\alpha_{cr} = 0.293$ in the case with $\mu = \mu_3 = \frac{1}{2}$, $e_2 = e_3 = 0.1$ and $\theta = \theta_T$. The value $\theta = \pi$ results in a similar situation to $\theta = 0$ (excepting the α_{cr} values are reduced slightly) and it is found, admitting values of θ other than 0, θ_T, π, that the changes between the three situations vary continuously, i.e. the most stable (f_2, f_3) configurations vary continuously with θ .

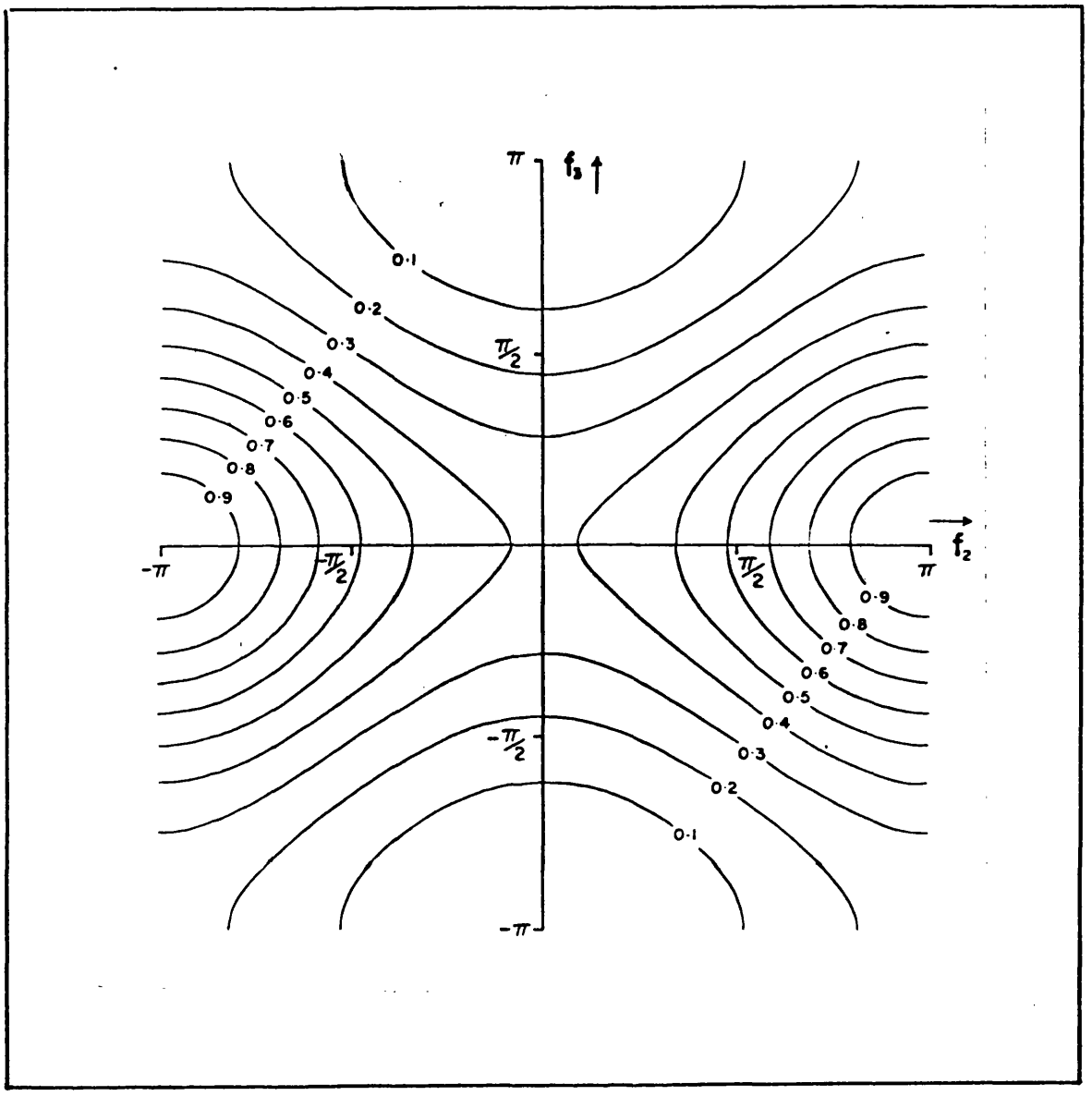

Figure 5.3 Effect of the true anomalies f_2, f_3 on the stability in terms of α_{cr}, the maximum allowable a_2/a_3 values. Contours are in units of the difference between $(a_2/a_3)\text{min}$ and $(a_2/a_3)\text{max}$ which have values 0.324 and 0.340 respectively.
($\mu = \mu_3 = \frac{1}{2}$; $e_2 = e_3 = 0.1$, $\theta = 0$)

It is clear that if, initially, $e_2 = e_3 = 0$, then θ is still well defined. It reduces to the difference in longitudes, ℓ_2 and ℓ_3 as measured from some reference direction. θ will then still affect the stability as demonstrated in the next section.

5.4 Results for Coplanar Hierarchical Three-Body Systems in General

As was remarked in Section 5.3 a large, negative value of $(c^2H)_{act}$ arises when one of α, $\bar{r}_{23}$ and $\bar{r}_{31}$ is small. This is equivalent to saying that the mutual distance of two of the bodies is small relative to the distance of either of these two from the third. Since an exact expression is used for $(c^2H)_{act}$ and it is not approximated by the use of two two-body approximations, it is possible that, with certain configurations, $(c^2H)_{act}$ is large and negative, but not in a manner which provides stability of (m_1, m_2) as binary and m_3 as the external mass.

We may define the initial motion of m_2 to be in an osculating orbit, with given $(a_2, e_2, \varpi_2; f_2)$ about m_1 and the motion of m_3 to be in an osculating orbit, with given $(a_3, e_3, \varpi_3; f_3)$, about M_2. However, it is to be expected that if α is large ($\simeq 1$) and $\theta \simeq 0$ i.e. $\bar{r}_{23}$ is small, the mutual attraction of m_2 and m_3 will be greater than m_1 and m_2. Thus we will have a situation where, in fact, m_2 and m_3 form the binary and m_1 is the external mass. Alternatively, if α is again large but $\theta \simeq \pi$, i.e. $\bar{r}_{31}$ is small, a similar situation arises: here m_1 and m_3 form the binary, m_2 being the external mass.

Thus it may be expected that in addition to the region of stability for $\alpha < 1$ and $0 \leq \theta < 2\pi$, we may find up to two other regions for which $(c^2H)_{act} \leq (c^2H)_{cr}$, implying stability when α is just less than unity and θ is within a small range of 0 or π. We must therefore consider how the correct $(c^2H)_{cr}$ value for each region should be chosen, as the choice will depend upon the relative sizes of the masses.

There are three possible arrangements of three masses in the collinear equilibrium configurations viz. $m_1m_2m_3$, $m_3m_1m_2$ and $m_2m_3m_1$. (In principle there are, of course, six, but the additional three are merely the "mirror images" of the above). These three arrangements give rise to three values of $(c^2H)_{cr}$ through a functional relationship which has already been described in Chapter 4; however, for reasons

which will become clear as we proceed, the topic is dealt with again, in greater detail, in Appendix A. Let these three values be denoted $(c^2H)_1$, $(c^2H)_2$, $(c^2H)_3$, where $(c^2H)_1 \leq (c^2H)_2 \leq (c^2H)_3$. These are respectively the primary, secondary and tertiary bifurcation values of c^2H.

For any three-body system, as c^2H rises from $-\infty$, we will obtain, after the manner of Zare (1976) (see Chapter 2), triply, doubly, simply and un-connected forbidden regions. The values $(c^2H)_i$ $i = 1,2,3$ above correspond respectively to the critical values of c^2H associated with the transitions from triply to doubly, doubly to simply and simply to un-connected forbidden regions. A triply connected forbidden region will always provide a sufficient condition that no exchange between bodies will occur in a three-body system and, under certain conditions, only a doubly connected region is necessary.

If we consider the masses above and let $m_1 > m_2 > m_3$ then the ordering, in the collinear configuration, to obtain the primary bifurcation value is $m_2m_3m_1$ (see Appendix A), $(c^2H)_2$ and $(c^2H)_3$ being obtained from the orders $m_1m_2m_3$ and $m_3m_1m_2$ respectively. We now consider the arrangement of the masses in a hierarchy. Letting (m_1, m_2) form the binary, m_3 being the external mass, with $m_1 > m_2 > m_3$, we require the largest possible value of $|(c^2H)_{cr}|$ to ensure endurance of this hierarchy. Since m_3 cannot lie between m_1 and m_2 the primary bifurcation is ruled out and we seek the secondary bifurcation so that $(c^2H)_{cr} = (c^2H)_2$.

If, however, $m_3 > m_1 > m_2$ or $m_1 > m_3 > m_2$ then the choice of the primary bifurcation is possible, and necessary, to ensure closure of the zero-velocity curves in the correct manner for stability.

In Figure 5.4 the procedure is again adopted of finding an α_{cr} value for given (μ,μ_3) and $(e_2, e_3, f_2, f_3,\theta)$ as described previously. The eccentricities e_2 and e_3, however, are set zero and therefore f_2 and f_3 are redundant. The remaining parameter is then θ , which is varied, α_{cr} values being determined such that $(c^2H)_{act} = (c^2H)_{cr}$. This results in pairs of values $(\alpha_{cr}, \theta_{cr})$ which may be plotted in polar diagram form to demonstrate the effect of θ on the stability. Each area of the diagram is now considered separately.

(i) <u>The central oval</u> encloses a region where $\alpha < 1$ and $0 \leq \theta < 2\pi$ i.e. the CHT system consists of (m_1,m_2) as binary and m_3 as external mass.

Within this region the pertinent, critical value of c^2H is given by

$$(c^2H)_{cr} = \begin{cases} (c^2H)_1 & \text{if } \mu < \mu_3 \\ (c^2H)_2 & \text{if } \mu > \mu_3 \end{cases},$$

$\mu = \mu_3$ resulting in $(c^2H)_1 = (c^2H)_2$. Therefore we seek pairs of values $(\alpha_{cr}, \theta_{cr})$ such that the system with such initial conditions is critically stable. These points form the central oval of the diagrams. If then a system with given initial configuration (α, θ) lies within this oval, the system will always remain in the form (m_1, m_2) as binary and m_3 as external mass since $(c^2H)_{act}$ will be less than $(c^2H)_{cr}$.

(ii) The right-hand lobe consists of an area where $\alpha \lesssim 1$ and $-\Delta\theta < \theta < +\Delta\theta$ where $\Delta\theta << \pi/2$ i.e. the hierarchy defined by the gravitational forces will be (m_2, m_3) as binary and m_1 as external mass. Within this region, since m_1 $(= 1 - \mu)$ is never the smallest mass, the primary bifurcation value of c^2H is appropriate viz.

$$(c^2H)_{cr} = (c^2H)_1.$$

In a similar fashion to the above we seek pairs of values $(\alpha'_{cr}, \theta'_{cr})$ which will give rise to $(c^2H)_{act} = (c^2H)_{cr}$. Once plotted these values will demarcate the region within which the above-mentioned hierarchy is stable.

(iii) The left-hand lobe is the area where $\alpha \lesssim 1$ and $\pi - \Delta\theta < \theta < \pi + \Delta\theta$ where $\Delta\theta << \pi/2$ i.e. the hierarchy defined by the gravitational forces will be (m_1, m_3) as binary and m_2 as the external mass. Within this region the $(c^2H)_{cr}$ value is given by

$$(c^2H)_{cr} = \begin{cases} (c^2H)_1 & \text{if } \mu > \mu_3 \\ (c^2H)_2 & \text{if } \mu < \mu_3 \end{cases}$$

which is the reverse of the situation in (i) above. Pairs of values $(\alpha'_{cr}, \theta'_{cr})$ are again sought, this time to delimit the region of stability for this hierarchy. Unlike case (ii) above this lobe may not

be present in all diagrams since for many pairs of (μ, μ_3), $\alpha'_{cr} > 1$ when $\theta \simeq \pi$ (see (iv) below).

(iv) The region $\alpha > 1$ is excluded since we are primarily interested in the stability of the hierarchy (m_1, m_2) as binary and m_3 as external mass, and in no case can there be such stability if $\alpha > 1$. The exterior circle on the diagrams denotes $\alpha = 1$.

(v) The region $\alpha < 1$ outwith the areas defined in (i), (ii) and (iii) above. Nothing can be said about stability in this area by the means used in this paper, recourse to numerical studies being appropriate.

Thus we have the result: if a CHT system, where (m_1, m_2) is taken to be the binary and m_3 the external mass, has an initial configuration such that it is defined by an (α, θ) point within the central oval then it is stable in the sense that an exchange of bodies is not possible. If, however, the initial configuration defines a point within the right-hand or left-hand lobes (or indeed $\alpha > 1$) then the given hierarchy is definitely not stable. Within the remainder of the diagram the question of stability is unanswered.

However, we now have not only an upper limit on α for stability (in the above-mentioned manner) but also limits on α for the region where stability is possible, but not assured by analytical means.

Figures 5.4 (a) - (f) present these regions for six pairs of values (μ, μ_3) in order to indicate the dependance of these regions on the masses of the system. Table 5.1 is complementary to Figures 5.3: it gives data on the critical values of α viz. α_{cr}, α'_{cr} for $\theta = 0$, $\pm \theta_T, \pi$ corresponding to these diagrams.

In Figures 5.5 (a) - (f) the equal mass case, viz. $\mu = \mu_3 = \frac{1}{2}$, is discussed, eccentricities being introduced in order to investigate the effects of f_2 and f_3. For example, in Figure 5.5(b) we set $e_2 = 0.3$, $e_3 = 0.0$, so that f_3 is indeterminate, f_2 being set equal to π. We then construct the (α, θ) polar diagram as above. Similarly in Figure 5.5 (e), we set $e_2 = 0.0$, $e_3 = 0.3$; f_2 is then indeterminate. The situation is restricted still further by allowing only straight line configurations $m_1 m_2 m_3$ i.e. $\theta = 0$, and an (α, f_3) polar diagram is constructed to show the regions of stability and instability for the hierarchy of interest.

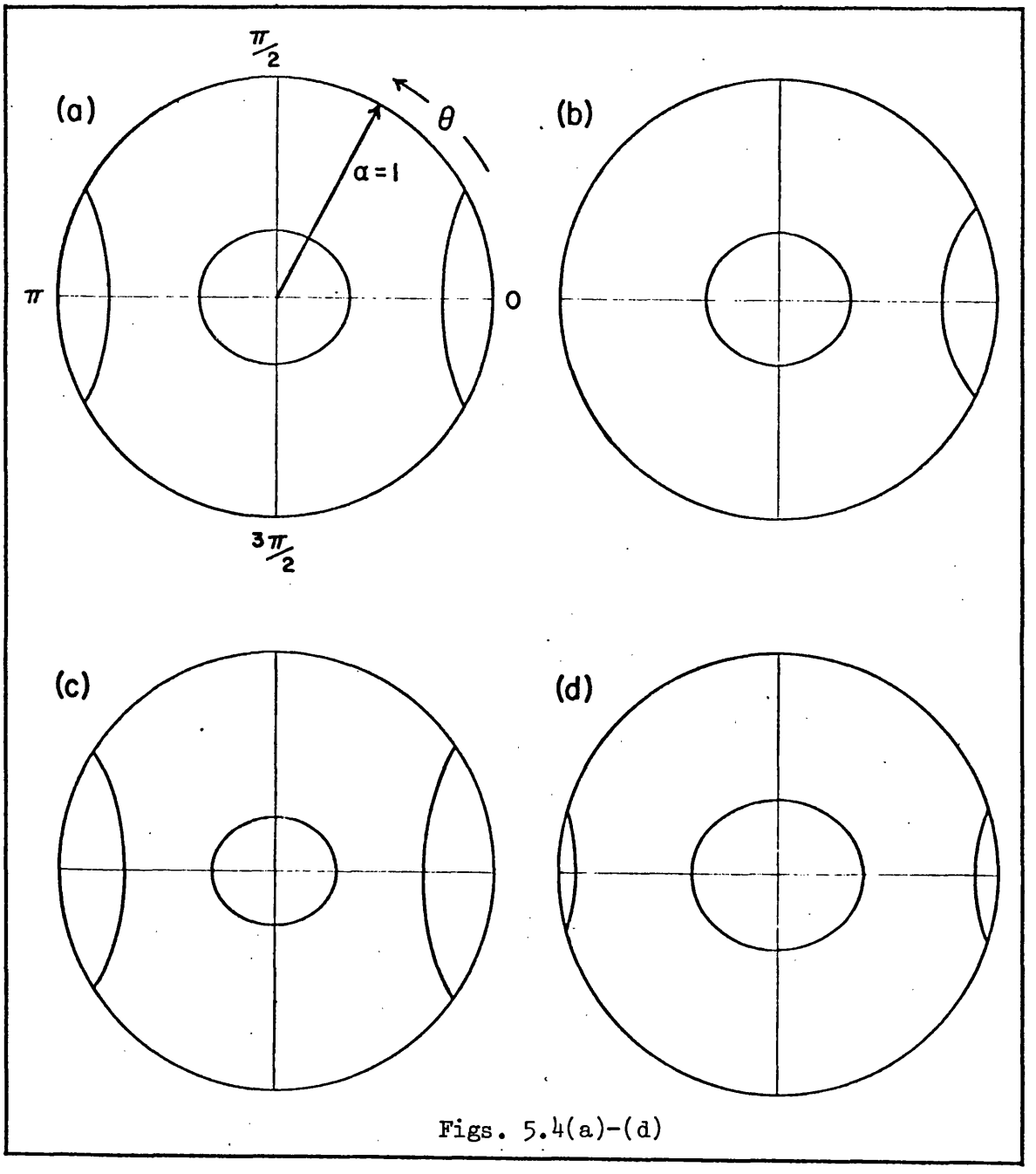

Figs. 5.4(a)-(d)

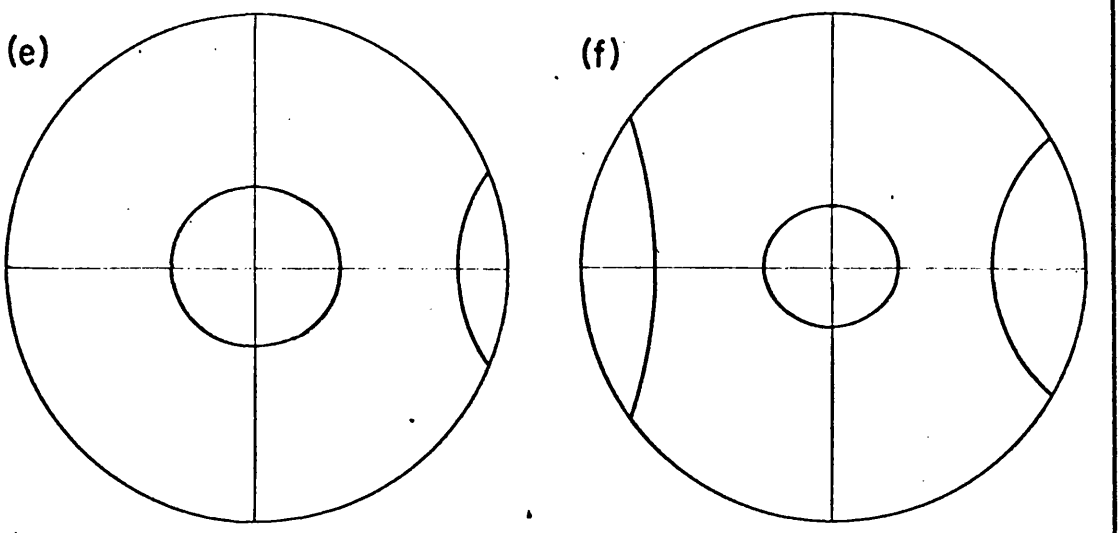

Figs. 5.4 (e) - (f)

Figures 5.4 Effect of phase angle θ on the stability in terms of α_{cr} and α'_{cr} for various sets of mass parameters μ, μ_3 as follows:

(a) $\mu = \frac{1}{2}$, $\mu_3 = \frac{1}{2}$
(b) $\mu = \frac{1}{3}$, $\mu_3 = \frac{1}{3}$
(c) $\mu = \frac{1}{2}$, $\mu_3 = 1$
(d) $\mu = \frac{1}{2}$, $\mu_3 = \frac{1}{4}$
(e) $\mu = \frac{1}{3}$, $\mu_3 = \frac{1}{4}$
(f) $\mu = \frac{1}{3}$, $\mu_3 = 1$

$\left.\begin{array}{l}\\\\\\\\\\\\\end{array}\right\}$ $e_2 = e_3 = 0$; f_2, f_3 indeterminate

°°

Table 5.1 - Critical values of α for Figures 5.4

Diagram	μ	μ_3	α_{cr} $\theta = 0$	α_{cr} $\theta = \pm \theta_T$	α_{cr} $\theta = \pi$	α'_{cr} $\theta = 0$	α'_{cr} $\theta = \pi$
a	$\frac{1}{2}$	$\frac{1}{2}$	0.333	0.305	0.333	0.757	0.757
b	$\frac{1}{3}$	$\frac{1}{3}$	0.326	0.306	0.323	0.764	0.984
c	$\frac{1}{2}$	1	0.286	0.260	0.286	0.674	0.674
d	$\frac{1}{2}$	$\frac{1}{4}$	0.375	0.346	0.375	0.917	0.917
e	$\frac{1}{3}$	$\frac{1}{4}$	0.341	0.320	0.337	0.815	-*
f	$\frac{1}{3}$	1	0.264	0.244	0.261	0.647	0.699

* where no value is given $\alpha'_{cr} > 1$.

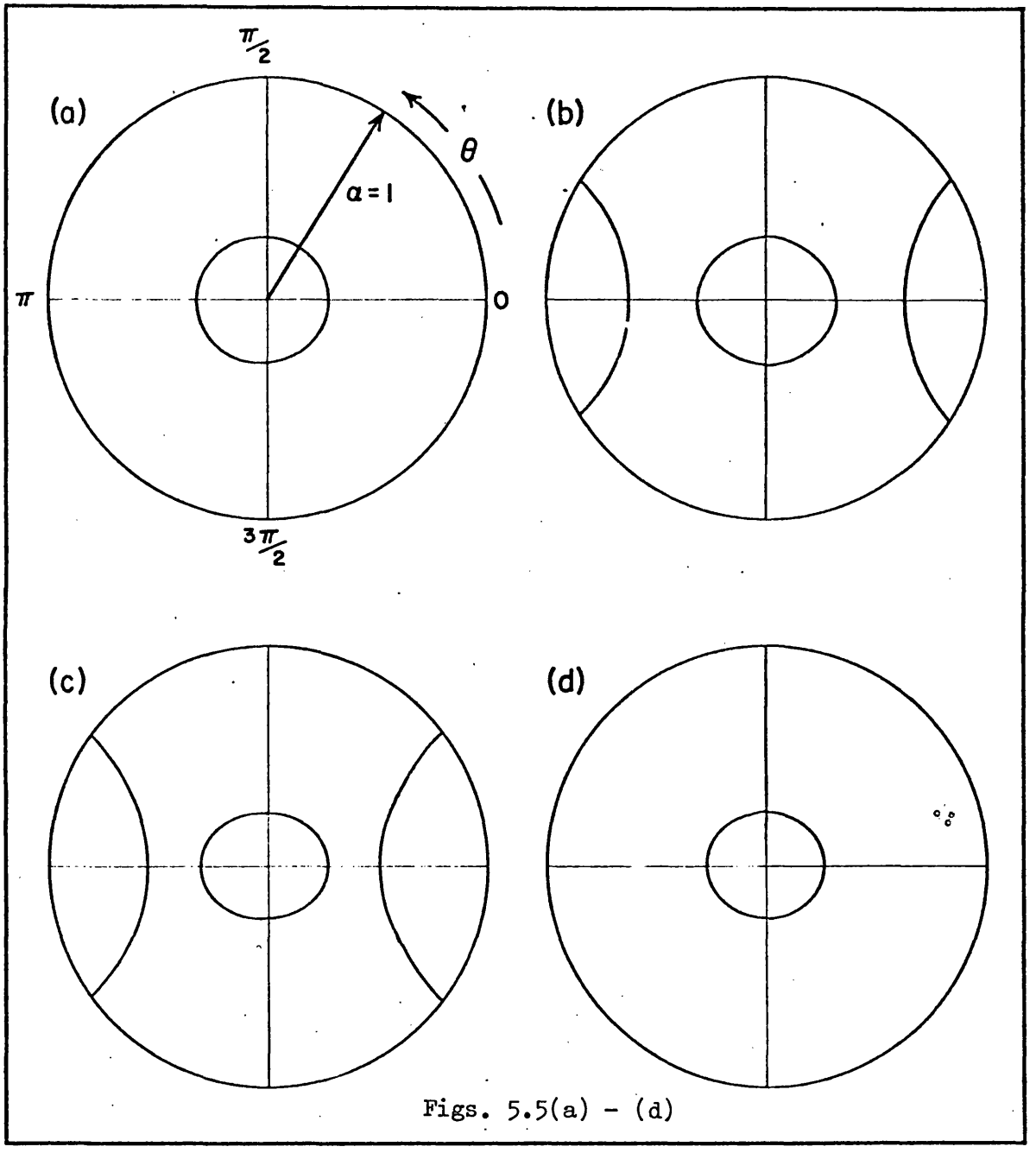

Figs. 5.5(a) - (d)

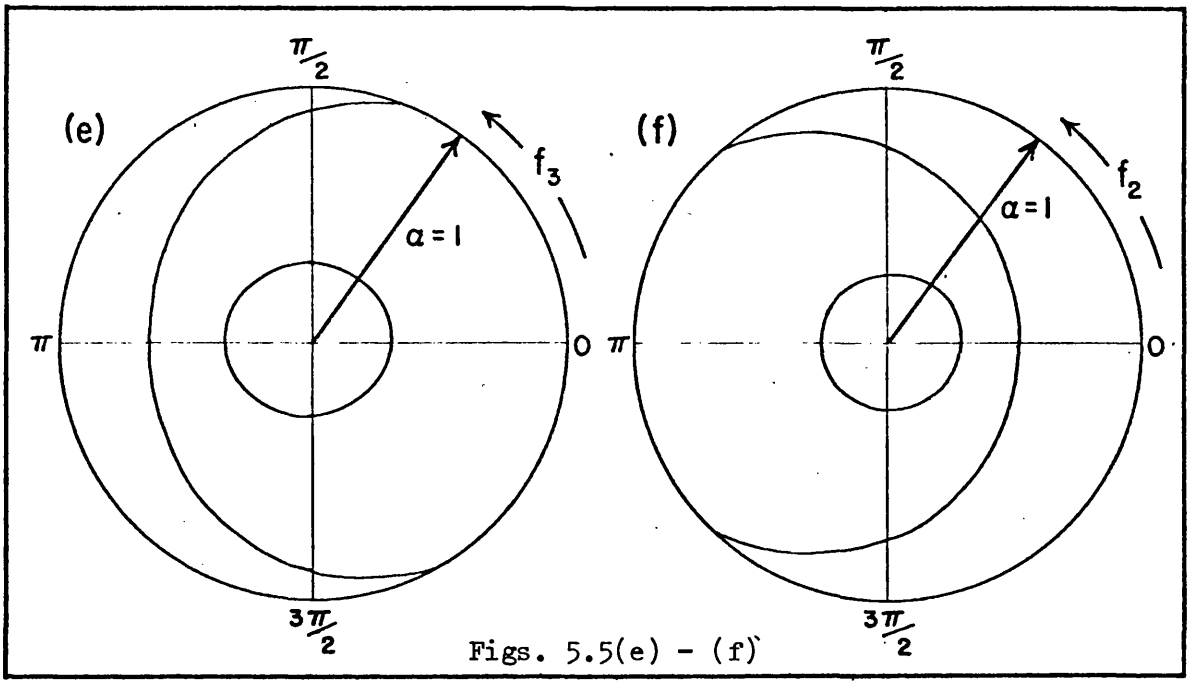

Figs. 5.5(e) - (f)

Figures 5.5 Effects of phase angle θ and true anomalies f_2, f_3 on the stability in terms of α_{cr} and α'_{cr} for equal mass systems.

(a) $e_2 = 0.3$, $e_3 = 0.0$; $f_2 = 0$, f_3 indeterminate; $\theta: 0 \leq \theta < 2\pi$
(b) $e_2 = 0.3$, $e_3 = 0.0$; $f_2 = \pi$, f_3 indeterminate; $\theta: 0 \leq \theta < 2\pi$
(c) $e_2 = 0.0$, $e_3 = 0.3$; f_2 indeterminate, $f_3 = 0$; $\theta: 0 \leq \theta < 2\pi$
(d) $e_2 = 0.0$, $e_3 = 0.3$; f_2 indeterminate, $f_3 = 0$; $\theta: 0 \leq \theta < 2\pi$
(e) $e_2 = 0.3$, $e_3 = 0.0$; $\theta = 0$; f_3 indeterminate, $f_2: 0 \leq f_2 < 2\pi$
(f) $e_2 = 0.0$, $e_3 = 0.3$; $\theta = 0$; f_2 indeterminate, $f_3: 0 \leq f_3 < 2\pi$

Table 5.2 - Critical values of α for Figures 5.5

Diagram	α_{cr} $\chi^{\dagger} = 0$	α_{cr} $\chi = \pi/2$	α_{cr} $\chi = \pi$	α'_{cr} $\chi = 0$	α'_{cr} $\chi = \pi$
a	0.299	0.290	0.299	- *	-
b	0.322	0.284	0.322	0.624	0.624
c	0.293	0.251	0.293	0.513	0.513
d	0.263	0.258	0.263	-	-
e	0.299	0.305	0.322	-	0.624
f	0.293	0.271	0.263	0.513	-

$\dagger\chi$ is to be interpreted as the appropriate angle i.e. one of θ, f_2, f_3 depending on which diagram is being considered

* where no value is given $\alpha'_{cr} > 1$.

We see that in each case of Figures 5.5 we obtain the familiar central oval which ensures the stability of the hierarchy, with either two, one or no other regions where the hierarchy is definitely unstable. These areas have the same interpretation as those of Figures 5.4. The shape of the lobe however, in the case of an $(\alpha, f_i)(i=2,3)$ polar diagram, will be different from the shape in an (α,θ) polar diagram. Table 5.2 gives data for critical values of α applicable to Figures 5.5 viz. α_{cr},α'_{cr} for $\theta = 0,\pm\theta_T,\pi$ where appropriate and $f_i = 0,\pi$ $(i=2,3)$ where appropriate.

5.5 Comparison of Results with Numerical Integrations

A numerical integration study of (equal mass) triple stellar systems by Harrington (1972) yielded maximum values of the ratio α possible to ensure the stability of the hierarchy (m_1,m_2) as binary and m_3 as external mass. Harrington used various sets of initial conditions for the purposes of his study. In the present notation these are:

$$\left.\begin{aligned} \mu &= \tfrac{1}{2} \\ e_2 &= 0.3,\ 0.5 \\ \varpi_2 &= 0,\ \pi/2 \\ f_2 &= 0 \end{aligned}\right\} \quad (m_1,m_2) \text{ subsystem}$$

$$\left.\begin{aligned} \mu_3 &= \tfrac{1}{2} \\ e_3 &= 0.25,\ 0.50,\ 0.75 \\ \varpi_3 &= 0,\ \pi/2 \\ f_3 &= \pi \end{aligned}\right\} \quad (M_2,m_3) \text{ subsystem}$$

where we have omitted any inclinations since the present criterion is only applicable to coplanar motions. We can however deal with a mutual inclination of 180° since this implies counter-rotational coplanar motion. Further, since we derive α_{cr} values for given masses and initial configurations we omit his α values chosen for use in his numerical investigation.

For the sake of completeness we also include the following

$$\begin{aligned} f_2 &= \pi/2,\ \pi \\ f_3 &= 0,\ \pi/2 \\ \varpi_2 &= \pi \\ \varpi_3 &= \pi \end{aligned}$$

although we may note that not all the possible sets of initial conditions to be derived from this data are independant. This redundancy arises from certain symmetries of the equal mass system and is also due to the occurrence of $(\varpi_2, \varpi_3, f_2, f_3)$ in combination to form θ within $(c^2H)_{act}$. In Table 5.3(a) we present, for corotational systems, maximal and minimal values of α_{cr}, and also minimal values of α'_{cr} over the possible ranges of ϖ_2, ϖ_3, f_2 and f_3. We also include, from Harrington's study, the values of α denoted α_s and α_u. These are respectively the largest of the α values chosen by Harrington which gave stability of the hierarchy and the smallest of his values which produced instability of the hierarchy. Table 5.3(b) presents similar data for counter-rotational systems.

Harrington (1972) defined stability of a system to mean "... *that there had been no significant change in the elements during the period of (numerical)integration, particularly in the semi-major axes or eccentricities; that is, the motion is that classified by Szebehely (1971) as Class 4 and termed revolution.*"

We would not therefore expect Harrington's limits on α for stability to be exactly the same as those derived in the present study. However, having said that, it may be seen from Tables 5.3(a) and (b) that in no case does Harrington's value α_u exceed our value $(\alpha'_{cr})_{min}$, that is, it appears that $(\alpha'_{cr})_{min}$ gives a useful limit outwith which numerical investigation of the stability of the hierarchy (m_1, m_2) as binary and m_3 as external mass is meaningless. Moreover, all his values α_s and α_u lie close to $(\alpha_{cr})_{min}$ and $(\alpha_{cr})_{max}$, in the case of corotational motion, indicating that there is not a significant region, not included within the central oval, where stability is possible numerically but not analytically by the present method. It is to be noted, however, that, in the case of counter-rotational motion, such a region of significant size does exist, as demonstrated by the fact that α_s and α_u are, in general, about a factor of 3 or 4 larger than $(\alpha_{cr})_{min}$ and $(\alpha_{cr})_{max}$. This is analogous to the case of the circular restricted three-body problem where, using periodic orbits to map out regions of stability, it is found that in the corotational case there is only a small region of stability outside that which is stable due to closure of the zero-velocity surfaces in comparison to the larger region in the case of counter-rotational motion.

Table 5.3(a) - Corotational Triple Stellar Systems (Equal Mass)

e_2	e_3	$(\alpha_{cr})_{min}$	$(\alpha_{cr})_{max}$	$(\alpha_{cr}')_{min}$	α_s*	α_u*
0.30	0.25	0.248	0.325	0.406	0.200	0.250
0.30	0.50	0.171	0.229	0.279	0.143	0.167
0.30	0.75	0.083	0.101	0.163	0.071	0.077
0.50	0.25	0.226	0.283	0.400	0.200	0.250
0.50	0.50	0.159	0.214	0.255	0.143	0.167
0.50	0.75	0.079	0.099	0.143	0.071	0.077

* α_s denotes the largest a_2/a_3 ratio found stable by Harrington and α_u the smallest a_2/a_3 ratio found unstable by Harrington.

Table 5.3(h) - Counter-rotational Triple Stellar Systems (Equal Mass)

e_2	e_3	$(\alpha_{cr})_{min}$	$(\alpha_{cr})_{max}$	$(\alpha'_{cr})_{min}$	α_s*	α_u*
0.30	0.25	0.0798	0.0799	-	0.250	0.286
0.30	0.50	0.0622	0.0624	0.726	0.200	0.250
0.30	0.75	0.0347	0.0349	0.354	0.100	0.143
0.50	0.25	0.0826	0.0829	0.943	0.250	0.286
0.50	0.50	0.0643	0.0647	0.611	0.200	0.250
0.50	0.75	0.0359	0.0362	0.297	0.100	0.143

* see footnote of Table III(a)

5.6 Sun-Jupiter-Saturn System

Considering Equation (34) we have (as in Section 5.3) a function F such that

$$(c^2H)_{act} = F(\mu,\mu_3,\alpha,\ e_2,e_3,f_2,f_3,\theta)$$

and further, since F is an even-valued function with respect to f_2,f_3 and θ, we can see that for given values of the remaining orbital parameters

$$\begin{aligned} F(f_2) &= F(-f_2) \\ F(f_3) &= F(-f_3) \\ F(\theta) &= F(-\theta) \end{aligned}$$

so that only the ranges $[0,\pi]$ of the variables need be studied, the ranges $(\pi, 2\pi)$ being neglected in what follows. Remembering that the critical value of c^2H is solely a function of the masses (see Appendix A), we have, as before,

$$(c^2H)_{cr} = G(\mu,\mu_3).$$

We defined μ and μ_3 above as follows,

$$\mu = \frac{m_2}{m_1 + m_2}, \quad m_1 \geq m_2$$

and $$\mu_3 = \frac{m_3}{m_1 + m_2}.$$

If we now introduce the factors γ_2 and γ_3 such that

$$\left.\begin{aligned} \mu' &= \frac{\gamma_2 m_2}{m_1 + \gamma_2 m_2} \\ \text{and} \quad \mu'_3 &= \frac{\gamma_3 m_3}{m_1 + \gamma_2 m_2} \end{aligned}\right] \qquad (49)$$

it becomes possible to solve for critical values of γ_2 and γ_3 such that

$$(c^2H)_{act} = (c^2H)_{cr}$$

or

$$F(\mu',\mu'_3,\alpha,\ e_2,e_3,f_2,f_3,\theta) = G(\mu',\mu'_3),$$

that is, to find mass parameters (μ', μ'_3) above which a given system defined by various orbital parameters *may* be unstable.

Nacozy (1976) presented a discussion on the stability of the Solar System based upon work by other authors and numerical experiments by himself. In that paper, and a subsequent one - Nacozy (1977), he studied the non-coplanar three-body problem of Sun-Jupiter-Saturn. For the analysis he presented, the masses of Jupiter and Saturn were augmented by the same factor γ. He studied the stability of the systems thus set up by integrating two sets of initial conditions for various γ values.

These sets of initial conditions were derived in the following manner from those given by Eckert *et al*.(1951) at the epoch of 1940. One group (set (1) in the notation of Nacozy, 1977) is obtained by holding the semi-major axes of Jupiter and Saturn fixed and varying γ ; the other (denoted set (2)) is obtained by holding the ratio of the mean motions of Jupiter and Saturn fixed and varying γ. In this way he hoped to gain insight into the validity of his results for many neighbouring sets of initial conditions.

By this means short-term numerical integrations of the Sun-Jupiter-Saturn systems, thus set up, may be used to discuss the stability of the Solar System over a longer time scale (see KNS theory, Nacozy, 1976). Two critical values of γ were found by Nacozy viz. 29.4 and 29.25 for sets (1) and (2) respectively. For values of γ larger than these values Saturn was ejected from the system in 10,000 years or less after the system had undergone an exchange of bodies.

Adapting Nacozy's method to the present treatment, we can derive values of γ for the onset of possible instability due to the opening of the zero-velocity curves. Values of $\gamma - \gamma_{crit}$ - may be found such that $(c^2H)_{act} = (c^2H)_{cr}$ i.e.

$$F(\mu', \mu'_3, \alpha, e_2, e_2, f_2, f_3, \theta) = G(\mu', \mu'_3)$$

where

$$\left.\begin{aligned} \mu' &= \frac{\gamma_{cr}\, m_J}{m_\odot + \gamma_{cr}\, m_J} \\ \mu'_3 &= \frac{\gamma_{cr}\, m_s}{m_\odot + \gamma_{cr}\, m_J} \end{aligned}\right] \qquad (50)$$

Table 5.4 - Nacozy type Sun-Jupiter-Saturn systems - Set 1

	γ_{crit}									
f_2		0			$\pi/2$			π		θ
f_3	0	$\pi/2$	π	0	$\pi/2$	π	0	$\pi/2$	π	
	21.52	20.79	20.22	22.20	21.24	20.53	23.15	21.87	20.97	0
	17.72	17.82	17.90	17.67	17.76	17.84	17.61	17.71	17.80	θ_T*
	(74.6)	(75.4)	(76.2)	(73.8)	(74.7)	(75.6)	(73.0)	(73.9)	(74.8)	
	17.83	17.89	17.95	17.78	17.85	17.91	17.74	17.81	17.88	$\pi/2$
	19.17	19.05	18.93	19.23	19.10	18.98	19.32	19.17	19.04	π

* θ_T is the value of θ at which c^2H is a maximum for given μ, μ_3, α_{23} (by Equation (40)). The values of θ_T are given in brackets in the line below in degrees.

Table 5.5 - Nacozy type Sun-Jupiter-Saturn systems - Set 2

γ_{crit}										θ
f_2	0			$\pi/2$			π			
f_3	0	$\pi/2$	π	0	$\pi/2$	π	0	$\pi/2$	π	
	22.47	21.68	21.08	23.17	22.17	21.43	24.16	22.83	21.88	0
	18.47	18.55	18.64	18.41	18.50	18.59	18.34	18.45	18.54	θ_T*
	(74.7)	(75.5)	(76.4)	(73.9)	(74.8)	(75.7)	(73.1)	(74.0)	(74.9)	
	18.57	18.63	18.70	18.53	18.60	18.67	18.48	18.56	18.63	$\pi/2$
	19.99	19.86	19.75	20.07	19.96	19.80	20.16	20.00	19.87	π

* see footnote for Table IV.

i.e. putting $\gamma_2 = \gamma_3 = \gamma$; $m_\odot$, m_J and m_S being the masses of the Sun, Jupiter and Saturn respectively. The real Sun-Jupiter-Saturn system (i.e. $\gamma = 1$) is defined by the following data:

$$\mu = 9.569.10^{-4}$$
$$\mu_3 = 2.865.10^{-4}$$
$$\alpha = 0.5454$$
$$e_2 = 4.8435.10^{-2}$$
$$e_3 = 5.5682.10^{-2}.$$

In Tables 5.4 and 5.5 are presented values of γ_{crit} for various sets of f_2, f_3 and θ for Nacozy's sets (1) and (2) respectively.

Two points must be stressed here. Firstly, we are assuming that the mutual inclination of the Jovian and Saturnian orbits is negligible. Secondly, any γ_{crit} value derived will necessarily be less than that derived by Nacozy since we would not expect instability to set in immediately upon the opening up of the zero-velocity curves.

Noting the above comments, it may be seen that the values of γ_{crit} derived above compare favourably with Nacozy's numerically obtained values. We obtain $17.61 \leqslant \gamma_{crit} \leqslant 23.15$ for set (1) and $18.34 \leqslant \gamma_{crit} \leqslant 24.16$ for set (2), the range resulting from the different sets of initial conditions. As in Sections 5.3 and 5.4 it is found that the straight line configuration ($\theta = 0, \pi$) results in the greatest stability, as revealed by the larger values for γ_{crit}. Furthermore it again demonstrates that the most stable straight line configuration occurs with $f_2 = \pi$ and $f_3 = 0$: that is, with the binary (m_1, m_2) at apocentre and the external mass m_3 at pericentre with respect to M_2. When θ equals θ_T it is found that (m_1, m_2) at pericentre and m_3 at apocentre with respect to M_2 gives rise to the most stable situation, although this situation is less stable than any of the straight line configurations.

5.7 Earth-Moon-Sun-System

The Earth-Moon-Sun system may be modelled in several different ways. We could follow Hill and consider it as a restricted three-body problem and hence neglect the mass of the Moon. In this case it is also essential

to neglect the eccentricity of the Earth's orbit about the Sun, since this eccentricity, however small, invalidates the use of the zero-velocity curves of the (circular) restricted problem (see Chapter 2 and Ovenden and Roy, 1960). Alternatively we could employ the zero-velocity curves of the general three-body problem. Using Equation (34) and the appropriate value of $(c^2H)_{cr}$ we could find several values of α_{cr}, given e_2 and e_3 for the Earth-Moon-Sun system, depending on f_2, f_3 and θ. If $\alpha_{act} \leq \alpha_{cr}$, where α_{act} is the real value of the ratio a_2/a_3, then the stability of the system would be assured in that the Moon would forever be confined to the zero-velocity oval about the Earth; on the other hand if $\alpha_{act} > \alpha_{cr}$ then the system is possibly unstable.

Furthermore, in a manner similar to that adopted in the previous section, we may solve for values γ_{crit} of the mass factor γ to examine the changes effected on the stability of the Earth-Moon-Sun system by altering the mass parameters defining the system.

The latter method is chosen since it appears, from the previous sections that γ_{cr} is more sensitive than α_{cr} to changes in the parameters defining the system. This is then applied to several different situations. For the real Earth-Moon-Sun system the following data have been assumed:

$$\begin{aligned} \mu &= 1.218.10^{-2} \\ \mu_3 &= 3.330.10^{5} \\ \alpha &= 2.570.10^{-3} \\ e_2 &= 5.49.10^{-2} \\ e_3 &= 1.6726.10^{-2}. \end{aligned}$$

We now multiply the masses of the Moon and the Sun by a factor γ to obtain (as in Section 5.6, Equation (50)),

$$\mu' = \frac{\gamma\mu}{1 + (\gamma-1)\mu} \quad ; \quad \mu'_3 = \frac{\gamma\mu_3}{1 + (\gamma-1)\mu} \quad .$$

It is found, throughout the possible ranges of f_2, f_3 and θ, that if $\gamma \lesssim 0.011$ then the system is stable. This is equivalent to $\mu' = 1.327.10^{-4}$ and $\mu'_3 = 3.628.10^{4}$, which is readily seen to approximate to a system of a Saturnian satellite disturbed by the Sun e.g. Saturn-Titan-Sun.

If we now keep μ constant and vary only μ_3 i.e. Equation (49) with $\gamma_2 = 1$, we obtain another value of γ_{crit} which is slightly higher than the previous at $\gamma_{crit} \lesssim 0.038$ ($\forall f_2, f_3, \theta$), which is in close agreement with Szebehely and McKenzie (1977b) who used the two two-body approximation to obtain $(c^2H)_{act}$. The resulting value of μ'_3 is $1.289.10^{-4}$, that is to say, if the Sun were reduced to a mass of $1.289.10^{-4}.(m_\odot + m_\oplus)$, then the Earth-Moon-Sun system would be stable according to the present method.

To examine the effect that the eccentricities have on the stability, we set $e_2 = e_3 = 0$. In this situation it is found, keeping other parameters fixed, that γ_{crit} will vary from 5 to 8 depending upon the value of θ. (n.b. Both lunar and solar masses are again multiplied by γ.) Similarly we may set μ very small, and therefore negligible, again neglect eccentricities, and thus set up a quasi-circular restricted problem using the general three-body treatment. The γ_{crit} values obtained are similar to the above, again falling in the range 4 to 8. If we then admit the use of the (small) e_2 value in both the above situations we derive not dissimilar γ_{crit} values and thus find this parameter to have little effect on the stability. Table 5.6 presents the data for these four models.

It is then seen that it is the introduction of the true value of e_3 which, though small, combined with the large μ_3 alters the value of γ_{crit} significantly, turning what was a borderline case of stability into an unstable situation. To demonstrate this effect we show in Figure 5.6 (curve (a)) how α_{cr} is affected by a variation in μ when $e_2 = 0$, $e_3 = 4.8435.10^{-2}$, $\mu_3 = 10^{-3}$: f_2 is then indeterminate and we take $f_3 = 0$ and $\theta = \theta_T$. This is then a system of the type Sun-Planet-Jupiter. We allow the planet's mass, defined by μ, to decrease and calculate critical values of α. As a means of comparison we also show the graph of α_{cr} when $e_3 = 0$ (curve (b)) - the other parameters being unchanged. It is then seen that whereas in the case of initially circular orbits the maximum allowable α for stability increases asymptotically to the value 0.796, the similar value, obtained when $e_3 \neq 0$, appears to tend to zero as $\mu \to 0$. A similar situation would arise if we were to set $e_2 \neq 0$ and let $\mu_3 \to 0$.

Table 5.6 - Earth-Moon-Sun System

System Parameters	γ_{crit}				
	θ	0	θ_T	$\pi/2$	π
$\mu = 1.218.10^{-2}$, $\mu_3 = 3.33.10^5$ $e_2 = 0$, $e_3 = 0$; f_2, f_3 indeterminate		7.609	5.051	5.051	7.599
$\mu = 1.218.10^{-2}$, $\mu_3 = 3.33.10^5$ $e_2 = 5.49.10^{-2}$, $e_3 = 0$; $f_2 = 0$, f_3 indeterminate		7.277	5.090	5.090	7.267
$\mu = 10^{-7}$, $\mu_3 = 3.33.10^5$ $e_2 = 0$, $e_3 = 0$; f_2, f_3 indeterminate		7.033	4.805	4.805	7.023
$\mu = 10^{-7}$, $\mu_3 = 3.33.10^5$ $e_2 = 5.49.10^{-2}$, $e_3 = 0$; $f_2 = 0$, f_3 indeterminate		6.750	4.849	4.849	6.740

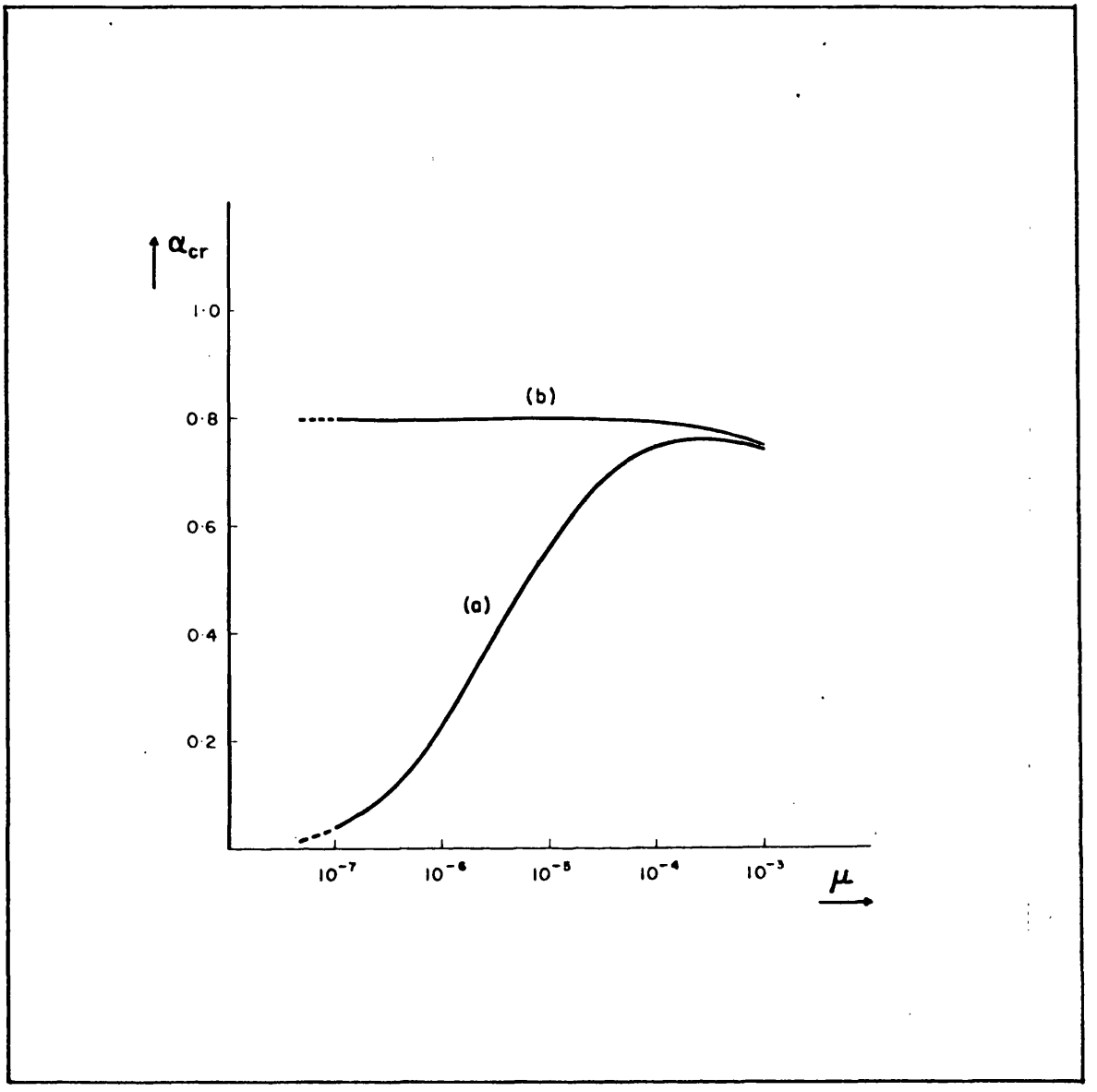

Figure 5.6 Effect of reduction in μ on α_{cr} for the cases (a) $\mu_3 = 10^{-3}$; $e_2 = 0$, $e_3 = 4.8435.10^{-2}$; $f_3 = 0$, $\theta = \theta_T$ (b) $\mu_3 = 10^{-3}$; $e_2 = 0$, $e_3 = 0$, $\theta = \theta_T$

This situation is analogous to the case of the circular versus the elliptic restricted three-body problems, where results obtained from the use of the zero-velocity curves of the circular restricted problem cannot be applied to the elliptic problem in any rigorous fashion for very small eccentricities of the primaries (see Ovenden and Roy, 1960).

5.8 Discussion and Conclusions

The aim of this chapter has been to investigate the effect of parameters neglected in Chapter 4 on the stability of CHT systems. The remaining parameters - f_2, f_3 and θ - which are pertinent to CHT systems, were introduced and their effect on the stability, in combination with e_2 and e_3, was investigated.

It is clear from the results obtained that any increase in e_2 or e_3 generally results in a decrease of stability (as would be expected) inasmuch as the maximum allowable value of the ratio a_2/a_2 for stability, α_{cr}, decreases. This is in agreement with Szebehely and Zare (1977). Further it was found in general that α_{cr} is affected up to the order of 20% by changes in the angular orbital parameters (f_2, f_3 and θ), the precise percentage change being dependant on the masses of the system and the eccentricities. It has also been shown that a worst possible configuration for stability exists which, it turns out, is very slightly more restrictive on the range of α for stability than the previous two two-body approximations of Chapter 4 and Szebehely and Zare (1977). At this particular configuration i.e. $\theta = \theta_T$ if, by way of example, we let $\mu = \mu_3 = \frac{1}{2}$ and $e_2 = e_3 = 0$, we would have, by the method described in Chapter 4 (cf. Equation (4.11)) $\alpha_{cr} = 0.311$ whereas, using Equation (42), α_{cr} reduces slightly to 0.305.

A further consequence is the introduction of another critical value of α viz. α'_{cr}. This value, taken at $\theta = 0$, will most likely provide a maximum value of the ratio α such that the hierarchy of interest, i.e. (m_1,m_2) as binary and m_3 as external mass, could be stable by numerical integration experiment. That is, if $\alpha > \alpha'_{cr}$ $(\theta = 0)$, then the above hierarchy is certainly *not* stable; the reasoning for this is as follows. Since the mutual gravitational effects of all three bodies are included in the present expression for $(c^2H)_{act}$ (Equation (34)), regions are found near $\theta \simeq 0$ and $\theta \simeq \pi$ where $\alpha \lesssim 1$ but the system can no longer be considered as hierarchical and of the above form. The hierarchy has in fact changed with (m_2,m_3) becoming the binary in the region about $\theta = 0$: while (m_1,m_3) is the binary in the region about $\theta \simeq \pi$.

It is now possible to further consider what might happen if $\alpha > \alpha'_{cr}$ $(\theta = 0)$ but we allow the actual value of θ to be different from zero.

If the existence of stability results in the relative constancy of the osculating elements of a CHT system, then α will remain almost constant for a stable system. If the "path" of a system in an (α,θ) plot is considered, it would, if the system were stable, tend to follow a circle. If $\alpha > \alpha'_{cr}$ (where α'_{cr} is again the value of α at $\theta = 0$ where $(c^2H)_{act} = (c^2H)_{cr}$ and $\alpha'_{cr} > \alpha_{cr}$) then such a circle would clearly intersect the area which is certainly unstable for the hierarchy with (m_1,m_2) as binary. It therefore seems reasonable to suppose that any system with $\alpha > \alpha'_{cr}$ is unstable no matter what value θ takes. The results derived in Section 5.5 with reference to numerical integration experiments by Harrington (1972) seem to bear out this point of view.

It is clear that contours of equal $(c^2H)_{act}$ could be drawn on an (α,θ) diagram - indeed the central oval and the two lobes, right and left, are examples of such contours. Since c^2H is a constant for any given system (once initial conditions have been defined), it follows that no system would be able to follow such a circular path described above, since it would in fact be crossing c^2H contours. The above point is considered merely to illustrate the probable instability for $\alpha > \alpha'_{cr}$ for all initial θ and not just small ranges about 0 and π. Further, it may be that a system could possibly be stable and show large variations in α, provided that these variations were periodic in nature. However throughout this thesis we are not considering such systems since they are not generally realised in nature.

It may now be remarked that it is possible to draw several critical stability surfaces in a manner similar to the previous chapter. The important surface, α_{cr}, giving an analytical limit on stability for (m_1,m_2) as binary and m_3 as external mass may be drawn for different sets of initial conditions - e_2, e_3, f_2, f_3, θ. These could be presented in *either* the $0\mu\mu_3\alpha$ parameter space *or* the $0\varepsilon^{23}\ \varepsilon_{32}\ \alpha_{23}$ parameter space - noting that $\alpha = a_2/a_3$ and $\alpha_{23} = \rho_2/\rho_3$. Furthermore, we could construct surfaces in either of these parameter spaces for α'_{cr} to give the limiting α outwith which the hierarchy of interest is certainly unstable for $\theta \simeq 0$ *or* $\theta \simeq \pi$ - and indeed probably unstable for the whole range of initial θ (see Appendix B). These surfaces however, in the case of initially non-zero eccentricities, are of dubious value due to the severe reduction in α_{cr} arising when μ and μ_3 are widely different (cf. Figure 5.6).

Let us now consider the real systems dealt with in this chapter. The γ_{crit} values obtained in the case of the Sun-Jupiter-Saturn system are all, not surprisingly, less than Nacozy's values of $\gamma = 29.25$ or $\gamma = 29.4$. They are however closer than the value of 13.65 obtained by Szebehely and McKenzie (1977a). This difference may be accounted for as follows. In the paper by Szebehely and McKenzie the orbits of Jupiter and Saturn were both taken to be about the Sun and the two two-body approximation to $(c^2H)_{act}$ was constructed accordingly. The present method considers the orbit of Jupiter to be about the Sun with Saturn in an orbit about the mass-centre of the Sun-Jupiter "binary", C_{SJ} say. Whereas it is clearly true that the real Saturn does effectively orbit the Sun, it is to be expected that if the masses of both planets were increased by a factor of 20 the discrepancy between the Sun-centred and C_{SJ}-centred orbit would increase and the latter would be the more appropriate. The difference between the two approaches is reflected in the discrepancy between the values of γ_{crit} obtained in this thesis and the previous value of 13.65.

In Table 5.7 we give approximate values for γ_{crit} for various methods of considering the Sun-Jupiter-Saturn system. The two two-body expressions for $(c^2H)_{act}$ have been used in the computation of these figures (as in Chapter 4, Equation (4.11)) to give a comparison between the figures obtained herein and those of Szebehely and McKenzie (1977a). (n.b. The values obtained may be slightly different from those of the above authors due to small differences in the data defining the system i.e. in $\mu, \mu_3, \alpha, e_2, e_3$.)

The system which most closely resembles those of Section 5.6 in Table 5.7 is Ref.No.1, the one resembling that of Szebehely and McKenzie being Ref. No.2. Thus it is seen that the alteration to a regime with the Saturnian orbit taken relative to the mass-centre of the Sun-Jupiter system results in an increase in γ_{crit} from about 14-15 to about 18-19. The latter figures are very close to the γ_{crit} values arising from the $\theta = \theta_T$ configurations in Tables 5.4 and 5.5. The remaining increase from 18-19 to 23 or 24 arises from the use of the exact expression for $(c^2H)_{act}$ and the straight line configuration $\theta = 0$.

Table 5.7 – Effect of Coordinate System on γ_{crit}

Ref. No.+	μ	μ_3	e_2	e_3	Focus of Saturnian Orbit *	γ_{crit}
1	$9.569.10^{-4}$	$2.865.10^{-4}$	$4.8435.10^{-2}$	$5.5682.10^{-2}$	C_{SJ}	18 - 19
2	$9.569.10^{-4}$	$2.865.10^{-4}$	$4.8435.10^{-2}$	$5.5682.10^{-2}$	S	14 - 15
3	$9.569.10^{-4}$	0	0	$5.5682.10^{-2}$	C_{SJ}	25 - 26
4	$9.569.10^{-4}$	0	0	0	C_{SJ}	26 - 27
5	$9.569.10^{-4}$	0	0	$5.5682.10^{-2}$	S	19 - 20
6	$9.569.10^{-4}$	0	0	0	S	19 - 20
7	$9.569.10^{-4}$	$2.865.10^{-4}$	0	0	C_{SJ}	20 - 21
8	$9.569.10^{-4}$	$2.865.10^{-4}$	0	0	S	15 - 16

+ in all cases $\alpha = 0.5454$ cf. Nacozy Set (1)

* this refers to whether Saturn is taken to orbit the Sun (S)
or is taken to orbit the mass-centre of the Sun-Jupiter system (C_{SJ})

Of the remaining systems in Table 5.7 Ref. Nos. 3-6 are quasi-restricted problems in the sense that μ_3 has been set negligibly small in the expressions for $(c^2H)_{act}$ and $(c^2H)_{cr}$, hence $e_2 = 0$ out of necessity. In systems Ref. Nos.7 and 8 the eccentricities have been set zero. We may see then from the former systems that neglect of the mass of Saturn (or the eccentricity of its orbit) and, by necessity, the eccentricity of Jupiter's orbit has a significant effect on γ_{crit} as would be the case in the use of the restricted three-body problem. Furthermore, we see that the neglect of eccentricities in the general three-body treatment also increases γ_{crit}, as found by Szebehely and McKenzie who obtained $\gamma_{crit} \simeq 15.08$ for such a system. This result agrees with our system Ref. No.8. Again the change to a C_{SJ}-centred Saturnian orbit increases this value by about 5 to 20-21 (Ref.No.7).

This sensitivity is again demonstrated in the application of this method to the Earth-Moon-Sun system, although the picture here is complicated by the large difference between μ and μ_3 which results in $(c^2H)_{act}$ being very sensitive to e_3. If we set $e_3 = 0$ then γ_{crit} will vary, as in the above case, by a factor somewhat less than 2 viz. $\gamma_{crit} \simeq 4\text{-}7$. The introduction of the true e_3 value causes the γ_{crit} value to decrease to about 10^{-2}. In other words the previously stable system ($\gamma_{crit} > 1$) has become unstable ($\gamma_{crit} < 1$) upon the introduction of e_3. In agreement with Szebehely and McKenzie (1977b), therefore, we cannot decide, on this basis, the stability or instability of the Earth-Moon-Sun system: all that may be said is that the real system is possibly unstable since $\alpha > \alpha_{cr}$.

Williams (1979), using the (circular) restricted problem of three-bodies as a model for the Earth-Moon-Sun system, found two values of γ for which stability was critical. This was considered a case of *double bifurcation*. If we now consider Figures 5.4(e) and (f) it is clear that if μ_3 is increased, μ remaining constant, the central oval will shrink whereas the right hand lobe will expand i.e. α_{cr} and α'_{cr} both decrease. It is now possible to envisage the meaning of the *double bifurcation*: ($\theta = 0$ being assumed at all times as in Williams, 1979) commencing with $\gamma << 1$ the system, with the Sun's mass much reduced, will be stable since the Moon will be contained in the central oval. Increasing γ the central oval will shrink until

$\alpha_{act} = \alpha_{cr}$ i.e. $\gamma = \gamma_{crit}$ and the system is critically stable. Further increase of γ will result in $\alpha_{cr} < \alpha < \alpha'_{cr}$ i.e. the system is possible unstable, the question of stability or instability being unanswered ($\gamma = 1$, the real system, lies in this range). γ may then be increased to γ'_{crit} where it is found that $\alpha = \alpha'_{cr}$, the hierarchy has now changed. *The Moon may no longer be considered to be in orbit about the Earth.* The zero-velocity curves are closed in such a way as to ensure that the *Moon and Sun* form a binary which cannot be disrupted by the Earth. When $\gamma > \gamma'_{crit}$ this situation is reinforced. The values obtained by Williams (1979) were $\gamma_{crit} \simeq 2.5$ and $\gamma'_{crit} \simeq 210$. The result $\gamma_{crit} > 1$, implying stability of the real system, arises through the use of the restricted three-body problem as a model.

It is admissable then to suggest that the Moon may have been captured by the Earth in the past or may escape in the future as was noted by Jeffrys and Szebehely (1978). In any event the applicability of a model involving only point-mass gravitational effects is thrown into question since the long-term evolution of the system is affected by other factors e.g. the effects of tidal friction.

CHAPTER 6 EMPIRICAL STABILITY REGIONS FOR COROTATIONAL COPLANAR HIERARCHICAL THREE-BODY SYSTEMS

6.1 Introduction

In the previous three chapters a set of stability parameters has been developed for hierarchical many-body systems arising from consideration of the dynamics of the problem (Chapter 3); the suitability of these parameters for a discussion of stability, in the three-body case, was examined by the use of an analytical stability criterion developed by Zare (1976, 1977), Szebehely (1977) and Szebehely and Zare (1977) (Chapter 4). Finally, by considering all the orbital parameters appropriate to the three-body case, the analytical stability criterion was refined and yielded some further information in the form of exact lower and probable upper bounds for the ratio ρ_2/ρ_3 within which it is necessary to seek stability of hierarchical three-body systems by numerical integration experiments (Chapter 5). It is the aim of this chapter to study, by means of the ε parameters, those regions of stability which are outwith the scope of the analytical critical stability surfaces studied in Chapters 4 and 5.

The $\varepsilon^{ki}, \varepsilon_{\ell i}$ parameters $\{ i = 2,\ldots,n;\ k = 2,\ldots,i-1\ (i \geq 3);\ \ell = i+1,\ldots,n\ (i \leq n-1) \}$, as has been previously stated, are taken to characterise the size of the disturbances on the various Keplerian orbits of the problem. These parameters are the coefficients of the leading (disturbing) terms in the expansion of the force function for a hierarchical many-body system where the arrangement of the bodies in *non-crossing* orbits of successively larger and larger semi-major axes allows the equations of motion to be properly written in Jacobian coordinates, thus permitting the expansion of the force function in terms of the ratio of the smaller radius vectors to the larger. Furthermore these parameters are dimensionless and are normalized to the appropriate central two-body force.

Now in the three-body case there are two Keplerian orbits defining the initial arrangement of a system: masses m_1 and m_2 are taken to move in disturbed Keplerian ellipses about their common

mass-centre, which as before is denoted by M_2; the mass m_3 is then found at a more remote distance such that its orbit is, at least in some initial phase, wholly outside the orbits of m_1 and m_2 relative to M_2 (i.e. the pericentre distance of m_3 from M_2 is greater than the apocentre distance of either m_1 or m_2 from M_2). In practice we may consider that $m_1 \geq m_2$, without loss of generality, so that in all cases the apocentre distance of m_1 from M_2 is less than the apocentre distance of m_2 from M_2 and we then need only consider the latter with respect to the pericentre distance of m_3. The ε^{23}, ε_{32} parameters then provide, respectively, a measure of the disturbance on the orbit of what may be called the (M_2, m_3) subsystem by m_1 and m_2 not being found at their common mass-centre, M_2, and a measure of the disturbance by m_3 on the orbit of the (m_1, m_2) subsystem.

Now if the ε parameters were zero for any given system then clearly the disturbance produced on the Keplerian orbits of the system would be nil. As the ε parameters are increased, *either* by an increase in the mass parameters $\mu[= m_2/(m_1 + m_2)]$ and $\mu_3[= m_3/(m_1 + m_2)]$ *or* by an increase in α_{23} (the ratio of, ρ_2, the radius vector of the (m_1, m_2) subsystem, to ρ_3, the radius vector of the (M_2, m_3) subsystem) *or both*, it would be expected that the variations on the elements of the Keplerian orbits of the system would also be increased. It is considered that the ε^{23}, ε_{32} terms characterise the major disturbances on the orbits of the system; the value of the α_{23} ratio is only of secondary importance. Hence to maintain a constant degree of perturbation systems are studied by holding fixed the ε^{23},ε_{32} values, and choosing an(initial) α_{23} value for the numerical experiment.

To reduce the number of parameters to an absolute minimum we only consider, at present, orbits which are coplanar, corotational and initially circular. We further restrict ourselves by considering only initial configurations such that m_1, m_2 and m_3 lie on a straight line in that order.

To delimit the regions of stability outwith the critical stability surface it is then necessary to find, for a given ε^{23},ε_{32} pair, the largest value of the ratio α_{23}, $(\alpha_{23})_o$ say, in order that the system defined by $(\varepsilon^{23}, \varepsilon_{32}, (\alpha_{23})_o)$ is just stable. That is to say, a system

with $\alpha_{23} > (\alpha_{23})_o$ will be unstable and a system with $\alpha_{23} < (\alpha_{23})_o$ will be stable. The unstable behaviour mentioned above may be exhibited in a number of ways, described in Section 6.2. Also in this section are defined the sets of initial conditions used to examine the empirical stability regions, how degrees of stability may be defined by which we may state whether one system is more or less stable than another and what results might be expected if the empirical stability regions do indeed exist.

In Section 6.3 the results of several hundred numerical integration experiments are presented in graphical form. It is shown how stability in general varies as the values of the ε^{23} ,ε_{32} parameters and the α_{23} ratio are varied; in Section 6.4 special cases of α_{23} where commensurabilities exist are studied. Finally in Section 6.5 the results are discussed, conclusions drawn and consideration given to systems containing four or more bodies.

6.2 Definitions and Description of the Numerical Experiments

The essential parameters for the stability of hierarchical three-body systems are considered to be ε^{23} and ε_{32}. If these parameters are small then it is to be expected that the variations on the Keplerian orbits of the (m_1, m_2) and (M_2, m_3) subsystems will also be small. The ε^{23} ,ε_{32} parameters were defined through the expression of the equations of motion of a hierarchical three-body system in the Jacobian coordinate system and an expansion of the force function viz.

$$\ddot{\underset{\sim}{\rho}}_2 = GM_2 \underset{\sim}{\nabla}_2 \left[\frac{1}{\rho_2} \{1 + \varepsilon_{32} P_2(C_{23}) + \text{higher order terms}\} \right] \quad (1)$$

$$\ddot{\underset{\sim}{\rho}}_3 = GM_3 \underset{\sim}{\nabla}_3 \left[\frac{1}{\rho_3} \{1 + \varepsilon^{23} P_2(C_{23}) + \text{higher order terms}\} \right] \quad (2)$$

where

$$\varepsilon^{23} = \frac{m_1 m_2}{(m_1+m_2)^2} \cdot \alpha_{23}^2 \quad (3)$$

$$\varepsilon_{32} = \frac{m_3}{(m_1+m_2)} \cdot \alpha_{23}^3 \quad (4)$$

and the other symbols have their usual meanings (see Chapter 4, Section 4.2).

It may be seen then that the $\varepsilon^{23}, \varepsilon_{32}$ parameters are the coefficients of the leading "disturbing" terms in the expansion of the force function; neglecting the higher order terms the only other term present represents the central two-body force, and thus, if the ε's are small, the motion will continue largely undisturbed given a suitably small value of α_{23}.

It may be conjectured that the disturbances, characterised by the ε parameters, are applied in a pseudo-random fashion. The question of whether a system with given $(\varepsilon^{23}, \varepsilon_{32}, \alpha_{23})$ is stable or not depends upon whether the variations on the orbit, due to these pseudo-random disturbances, are large enough to give rise to a situation where instability sets in. Clearly, of course, the disturbances, for any particular system are not applied in a random fashion since the variations in the semi-major axes and eccentricities will depend strongly on the fundamental frequencies of the system. However in a situation where we have no *a priori* knowledge of what the basic periods of the system will be, as defined by the masses and the initial values of the semi-major axes, it may loosely be considered that there is an element of randomness about the perturbations. Obviously cases may arise where a commensurability in mean motions exists which will alter the behaviour of the variations in the orbital elements of a system. This point will be discussed in greater depth in Section 6.4.

Summing up, it is considered that the size of the ε parameters may determine how far the semi-major axes and eccentricities defining the orbits in a system may depart from the initial values by what may be termed a "random walk" process. Instability or stability will then depend upon whether this random walk can or can not lead the system into an unstable configuration.

The systems are examined in terms of the ε parameters and the α_{23} value. We choose the ε's in preference to the masses, defined by μ and μ_3, since it appears, on the dynamical grounds outlined above, that the ε's are of more direct relevance to the variations on the orbits of a system than the actual size of the masses. Hence a numerical integration experiment will consist of the choosing of a set

of parameters (ε^{23},ε_{32}, α_{23}) for given eccentricities, longitudes of pericentre and phase angle (see Chapter 5, Section 5.2 for definitions), and carrying the numerical integration forward from these initial conditions over a specified time interval long enough to examine the system for possible stability or instability. By studying a group of systems of the same ε^{23},ε_{32} values we may then keep the perturbations on the orbits largely the same while varying the initial α_{23} value to find the largest α_{23} value, $(\alpha_{23})_o$ say, such that a system will be stable if (initially) $\alpha_{23} < (\alpha_{23})_o$. The value of $(\alpha_{23})_o$ is not to be confused here with α_{cr} or α_{23cr} as determined in Chapters 4 and 5. The value α_{23cr} gave a *sufficient but not necessary* condition that an exchange of bodies would not occur. As has been remarked previously it is not expected that instability would set in immediately upon the opening up of the zero-velocity curves. It may be remembered that Nacozy (1977) found his value γ, the factor by which the masses of Jupiter and Saturn must be multiplied, for the onset of instability to be around 30. However the largest value obtained analytically in Chapter 5 was around 25: this indicates the existence of a region of stability which is outwith the scope of the *analytical* critical stability surface, as would indeed be expected. The aim of the current investigation is to determine this region of stability in an empirical fashion using the ε parameters. The value $(\alpha_{23})_o$ is then a *necessary and sufficient* condition for stability.

The question of how the stability or instability of a system may be defined is now considered.

A stable situation may be defined to exist when the Keplerian orbits of the (m_1, m_2) and (M_2, m_3) subsystems continue to be executed throughout the duration of the particular numerical experiment exhibiting only periodic variations in the semi-major axes and eccentricities. Secular trends should be absent.

Instability may then occur in one of three ways:

(a) A close approach may occur between two of the bodies in the system, due to the variations on the initial orbital elements being sufficiently large, which may result in one of the bodies being thrown into a hyperbolic orbit and escaping the system: this is termed *break-up*.

(b) The orbits in the system may undergo secular changes [or possibly large (amplitude) periodic fluctuations] in their semi-major axes and eccentricities so that the pericentre distance of m_3 from M_2 becomes less than the apocentre distance of m_2 from M_2. The distance of m_1 from M_2 is always less than the distance of m_2 from M_2 if we prescribe that $m_1 \geq m_2$ i.e. $\mu \leq \frac{1}{2}$. Hence we need only consider the distances M_2m_3 and M_2m_2 to decide if this situation, called *cross-over*, occurs.

(c) The third possibility is similar to (a), but is not so severe: a close approach between bodies occurs resulting in significant non-reversible (i.e. non-periodic) changes in the semi-major axes and eccentricities of the orbits of the bodies. For example the mass m_3 may, upon a close approach to m_2, be thrown into an orbit with very long period and large eccentricity, this is clearly not a stable situation. This type of occurrence is termed a *close encounter*.

The degree of stability, which may be called the *durability*, of the system is then measured by considering the time it takes for one of the above possibilities (break-up, cross-over or close encounter) to occur. The longer the time required, the more durable the system. If no such occurrence arises the system is termed stable.

A "unit of time" is clearly required to measure the above. This unit must possess a definite significance for the system under consideration. Three units of time immediately come to mind: (i) the orbital period of the (m_1, m_2) subsystem (ii) the orbital period of the (M_2, m_3) subsystem and (iii) the synodic period of the (m_1, m_2) and (M_2, m_3) subsystems. Any other time unit is unsuitable since it would depend upon the values of the constant of gravitation and the masses. We choose (iii) above by consideration of the following example: suppose two planets are moving, in orbits of small eccentricity, about a central star i.e. μ and μ_3 are small. Further let us suppose α to be very large i.e. approaching unity. If we commence with the planets in a straight line on one side of the star and then set them off in their orbits they will come into conjunction one synodic period later. Now if this situation was unstable such that at the initial conjunction one of (a) - (c)

above occurred we would say that the situation is very unstable. However, if one of (a) - (c) occurred on the following conjunction, *one synodic period later*, then it might be remarked that the system is slightly more *durable*, it having survived over two conjunctions rather than just one. Measuring time in units of the periods of either the (m_1, m_2) or (M_2, m_3) subsystems will clearly not give a satisfactory picture of this since with α being large, one synodic period is composed of many (m_1, m_2) and (M_2, m_3) orbital periods (this factor between the synodic period and the other two tending to ∞ as α tends to one and μ and μ_3 tend to zero. Hence the situation when instability occurs on the second conjunction is better measured as being *one* synodic period later rather than what may be *many thousands* of (m_1, m_2) or (M_2, m_3) orbital periods. The synodic period gives directly information on how many conjunctions a system has survived without exhibiting some form of instability: this is clearly relevant since the grossest perturbation will occur around the time of conjunction. Hence we choose to measure time by the use of the synodic period.

For simplicity all the orbits in this study are taken to be coplanar, corotational and initially circular (i.e. $e_2 = e_3 = 0$; ϖ_2 , ϖ_3 , f_2 and f_3 are then not defined initially): furthermore the bodies always begin in the straight line configuration $m_1m_2m_3$ (i.e. $\theta = 0$ - see Chapter 5, Section 5.2 for definition of the orbital parameters). In other words the initial distance between m_1 and m_2 is a_2, their relative velocity, V_2, being the required value of circular velocity viz.

$$V_2 = \left[\frac{G(m_1 + m_2)}{a_2}\right]^{\frac{1}{2}} . \qquad (5)$$

Similarly, the distance between M_2 and m_3 is a_3, where $\alpha_{23} = a_2/a_3$, initially, their relative velocity being

$$V_3 = \left[\frac{G(m_1 + m_2 + m_3)}{a_3}\right]^{\frac{1}{2}} . \qquad (6)$$

In the notation of Chapter 5 the initial conditions for each numerical experiment are as follows:

a_2	$= \alpha_{23}$	a_3	$= 1$
e_2	$= 0$	e_3	$= 0$
ϖ_2	undefined	ϖ_3	undefined
f_2	undefined	f_3	undefined

and $\theta = 0$.

These initial conditions are then used to commence a numerical integration procedure, using a numerical method developed by the author, described and discussed in Appendices C and D, over a specified time interval. The length of the integration is determined by successive passages of the (m_1, m_2) subsystem through its initial sidereal direction, i.e. m_2 will commence at some longitude, ℓ_{20} say, with respect to a fixed reference direction ($\ell_{30} = \ell_{20}$ initially hence $\theta\{ = \ell_2 - \ell_3\} = 0$), and successive passages of the (m_1, m_2) subsystem through $\ell_2 = \ell_{20}$ will determine the time interval over which the integration is carried out. An experiment is continued for 100, 200, 400, etc. such successive passages depending upon requirements.

It was remarked earlier that systems are studied in terms of their ϵ parameters. To this end values are chosen of $\epsilon^{23} = 10^{-p}$ and $\epsilon_{32} = 10^{-q}$ where $p = 2, 3, 4, 5, 6$ and $q = 2, 3, 4, 5, 6$. A value of α_{23} is then chosen such that $\alpha_{23cr} < \alpha_{23} < \alpha'_{23cr}$ and the integration executed over the required time interval. Studying values of α_{23} outwith this range is not necessary since if $\alpha_{23} \leq \alpha^*_{23cr}$ then the system is stable. While if $\alpha_{23} \geq \alpha'^*_{23cr}$ the hierarchy which is being considered is definitely unstable (see Chapter 5).

It may be expected that as the initial value of α_{23} tends towards α'_{23cr} the durability of the system will diminish, resulting in the system becoming extremely unstable. On the other hand, when the initial value of α_{23} equals α_{23cr} then the system will definitely be stable. It is then required to determine $(\alpha_{23})_o$ (such that $\alpha_{23cr} < (\alpha_{23})_o < \alpha'_{23cr}$) where systems with initial $\alpha_{23} \leq (\alpha_{23})_o$ are stable. A gradual increase in durability is therefore expected as α_{23} is decreased from α'_{23cr} towards $(\alpha_{23})_o$.

*Both α_{23cr} and α'_{23cr} are calculated for $\theta = 0$.

It is not possible to determine the value of $(\alpha_{23})_o$ from a particular numerical experiment since this value is that which results in the system executing an infinite number of orbits before exhibiting instability. By use of the $\epsilon^{23}, \epsilon_{32}$ parameters, however, obvious trends may appear, enabling an accurate prediction of $(\alpha_{23})_o$ and possibly also the durability of any given system.

6.3 The Results

In this section are presented the results of almost 300 numerical integration experiments. In Figures 6.1 to 6.25 (see pages 172 to 196) graphs of number of synodic periods (N_s) until instability sets in versus initial α_{23} value are presented. The symbols on the graphs are defined as follows.

The abscissa α_{23} is the initial value of the ratio ρ_2/ρ_3 which, since the orbits are initially circular, is equal to a_2/a_3. The ordinate is N_s the number of synodic periods* until instability arises. A trial integration is run for a specific time interval to detect any instability, and the time the first instability occurs is noted, N_s is calculated and the point (α_{23}, N_s) plotted with one of the letters L, C, X, or B above it. These letters denote respectively that no instability has thus far been exhibited, a close encounter has occurred, a cross-over of orbits has arisen or the system has undergone break-up. The dashed line appearing to the left of the data points (on most graphs) denotes the value of α_{23cr}, the dashed line to the right denotes the position of α'_{23cr}.

*The number of synodic periods is calculated as follows. The real integration time, until one of break-up, cross-over and close encounter occurs (or the time limit on the integration is exceeded), is noted and using the value of the synodic period, *as calculated from the initial conditions*, the number of synodic periods is calculated. Note that the actual number of synodic periods is not considered since until instability sets in this is found to be little different from the value calculated above.

It is immediately apparent from the graphs that the durability of systems, as measured by N_s, decreases, as expected, as the initial value of α_{23} tends towards α'_{23cr}; furthermore as α_{23} approaches the value denoted $(\alpha_{23})_o$ it is seen that N_s climbs rapidly to large values indicating a good measure of durability. It is also apparent from the graphs that $\alpha_{23cr} < (\alpha_{23})_o$, the difference between the two decreasing as the ε values decrease, as is expected since $(\alpha_{23})_o$ is constrained to lie between α_{23cr} and α'_{23cr}.

All the graphs show a distinctive curve which steepens as $(\alpha_{23})_o$ is approached: this is especially clear in Figure 6.13. This trend is masked to a greater or lesser extent in certain other graphs by the appearance of peaks in the curves at certain values of α_{23}. In the next section these peaks are examined and it is shown that it is possible to ascribe them to the occurrence of commensurabilities in mean motion.

Neglecting these peaks, for the moment, it is possible to fit a curve to the points on each of these graphs. To achieve this we examined results by the use of different functions to predict values of N_s. In the absence of any analytical guidelines which might dictate the form of these functions it was felt that they should be kept as simple as possible. To this end two functions were studied viz.

$$N_s = \left[\frac{1 - (\alpha_{23})_o}{\alpha_{23} - (\alpha_{23})_o}\right]^{\beta} - 1 \qquad (7)$$

and

$$N_s = e^{\beta}\left[\frac{1 - \alpha_{23}}{\alpha_{23} - (\alpha_{23})_o}\right]^{\gamma} - 1 \,. \qquad (8)$$

The form of these was chosen to allow that as $\alpha_{23} \to 1^*$, then $N_s \to 0$

*It is sufficient to use 1 and not α'_{23cr} since, over the range of ε^{23} and ε_{32} being studied, α'_{23cr} differs so little from unity as to not alter the results significantly.

and as $\alpha_{23} \to (\alpha_{23})_o$ then $N_s \to \infty$. It may be noted here that the quantity $(1 - \alpha_{23})/(\alpha_{23} - (\alpha_{23})_o)$ could have been incorporated in other formulae of a more complex form: there would however have been no justification for the use of a more complex function. The parameters $(\alpha_{23})_o$ and β are then varied in Equation (7) to obtain the "best fit" curve to the data points. Similarly in Equation (8) $(\alpha_{23})_o$, β and γ are varied to find a best fit curve.

In this way one can determine *empirically* the values $(\alpha_{23})_o$ over the range of $\epsilon^{23}, \epsilon_{32}$ parameters studied (i.e. $\epsilon^{23} = 10^{-p}$, $\epsilon_{32} = 10^{-q}$ $p,q = 2,\ldots,6$). At non-integer values of p and q the value of $(\alpha_{23})_o$ may be obtained by interpolation since the surface $(\alpha_{23})_o = f(\epsilon^{23}, \epsilon_{32})$ is generally found to be smooth. Moreover it is also possible by this scheme to predict how durable a system will be. For those systems with initial $\alpha_{23} > (\alpha_{23})_o$ a number of synodic periods until instability sets in can be predicted by whichever of the above functions appears to be more appropriate.

By examination of a wide range of the parameters $(\alpha_{23})_o$ and β as appropriate to Equation (7) and $(\alpha_{23})_o$, β and γ as appropriate to Equation (8) it was found, by trial and error, that the latter yielded curves of a better fit.

Having chosen the appropriate formula - Equation (8) - values of $(\alpha_{23})_o$, β and γ to give curves which "best fit" the available data may be calculated. This was carried out as follows. Taking a set of data points for a given $(\epsilon^{23}, \epsilon_{32})$ pair, and a trial value of $(\alpha_{23})_o$, these were plotted on a graph in the form $\ln\left[\ln(N_s + 1)\right]$ versus $\ln\left(\frac{1 - \alpha_{23}}{\alpha_{23} - (\alpha_{23})_o}\right)$. It is found that the majority of the data points (generally those which lie away from commensurable values of the ratio α_{23}) fall in a line. If the value of $(\alpha_{23})_o$ is too small then this line will be *concave up*, if $(\alpha_{23})_o$ is too large the line will be *concave down*. The correct value of $(\alpha_{23})_o$ is the one which results in a straight line in this representation. The value of β may then be obtained from the intercept of this straight line with the $\ln\left[\ln(N_s + 1)\right]$ axis and the value of γ directly from the gradient of the line viz.

$$\ln\left[\ln(N_s + 1)\right] = \gamma \ln\left[\frac{1 - \alpha_{23}}{\alpha_{23} - (\alpha_{23})_o}\right] + \ln \beta. \quad (9)$$

In practice the "straight line" may be concealed by commensurabilities which allow values of N_s other than would be expected. This feature will be dealt with more fully in the next section.

Since the largest perturbation of the orbits occurs at conjunctions it is to be expected that any unstable behaviour will occur there. This will be (almost) an integral number of synodic periods from the initial time. Hence N_s can only assume approximately integral values. This results in the graph of $\ln\left[(\ln(N_s + 1)\right]$ versus $\ln\left(\frac{1 - \alpha_{23}}{\alpha_{23} - (\alpha_{23})_o}\right)$ being relatively smooth when N_s is large; however if N_s is small then the graph will have a "stepped" appearance since the difference between successive $\ln\left[\ln(N_s + 1)\right]$ values may be substantial. For this reason more weight was always given to the positions of data points at larger values rather than smaller values of N_s.

This procedure was carried out for each $(\varepsilon^{23}, \varepsilon_{32})$ pair and values of $(\alpha_{23})_o$, β and γ were determined: the results are presented in Table 6.1. The values in brackets denote trial values and not correct values since the data at these low values of ε^{23} and ε_{32} appeared to have been very largely affected by commensurabilities rendering it impossible to obtain good values for $(\alpha_{23})_o$, β and γ.

Table 6.1 - Curve Parameter Values

ε^{23}	ε_{32}	$(\alpha_{23})_o$	β	γ	α_{23cr}	α'_{23cr}
10^{-2}	10^{-2}	0.475	0.69	0.32	0.324	0.872
	10^{-3}	0.619	0.63	0.39	0.495	0.907
	10^{-4}	0.622	0.58	0.46	0.518	0.912
	10^{-5}	0.632	0.79	0.36	0.520	0.912
	10^{-6}	0.627	0.48	0.40	0.521	0.912
10^{-3}	10^{-2}	0.511	0.99	0.23	0.397	0.885
	10^{-3}	0.791	0.74	0.26	0.707	0.939
	10^{-4}	0.790	0.94	0.38	0.768	0.952
	10^{-5}	0.793	0.58	0.43	0.776	0.954
	10^{-6}	0.794	0.32	0.53	0.777	0.954
10^{-4}	10^{-2}	0.516	0.83	0.39	0.412	0.886
	10^{-3}	0.789	0.59	0.41	0.760	0.949
	10^{-4}	0.902	0.55	0.61	0.871	0.972
	10^{-5}	0.911	0.44	0.82	0.896	0.977
	10^{-6}	0.914	0.061	1.02	0.899	0.978
10^{-5}	10^{-2}	0.520	0.26	0.75	0.413	0.886
	10^{-3}	0.798	0.65	0.34	0.767	0.950
	10^{-4}	0.915	0.0097	1.87	0.894	0.977
	10^{-5}	(0.943)	(0.01)	(2.00)	0.942	0.987
	10^{-6}	(0.953)	(0.01)	(2.00)	0.952	0.989
10^{-6}	10^{-2}	0.519	0.12	1.02	0.413	0.887
	10^{-3}	0.800	0.38	0.39	0.767	0.950
	10^{-4}	0.917	0.15	0.78	0.897	0.977
	10^{-5}	(0.954)	(0.10)	(1.00)	0.953	0.989
	10^{-6}	(0.974)	(0.10)	(1.00)	0.973	0.994

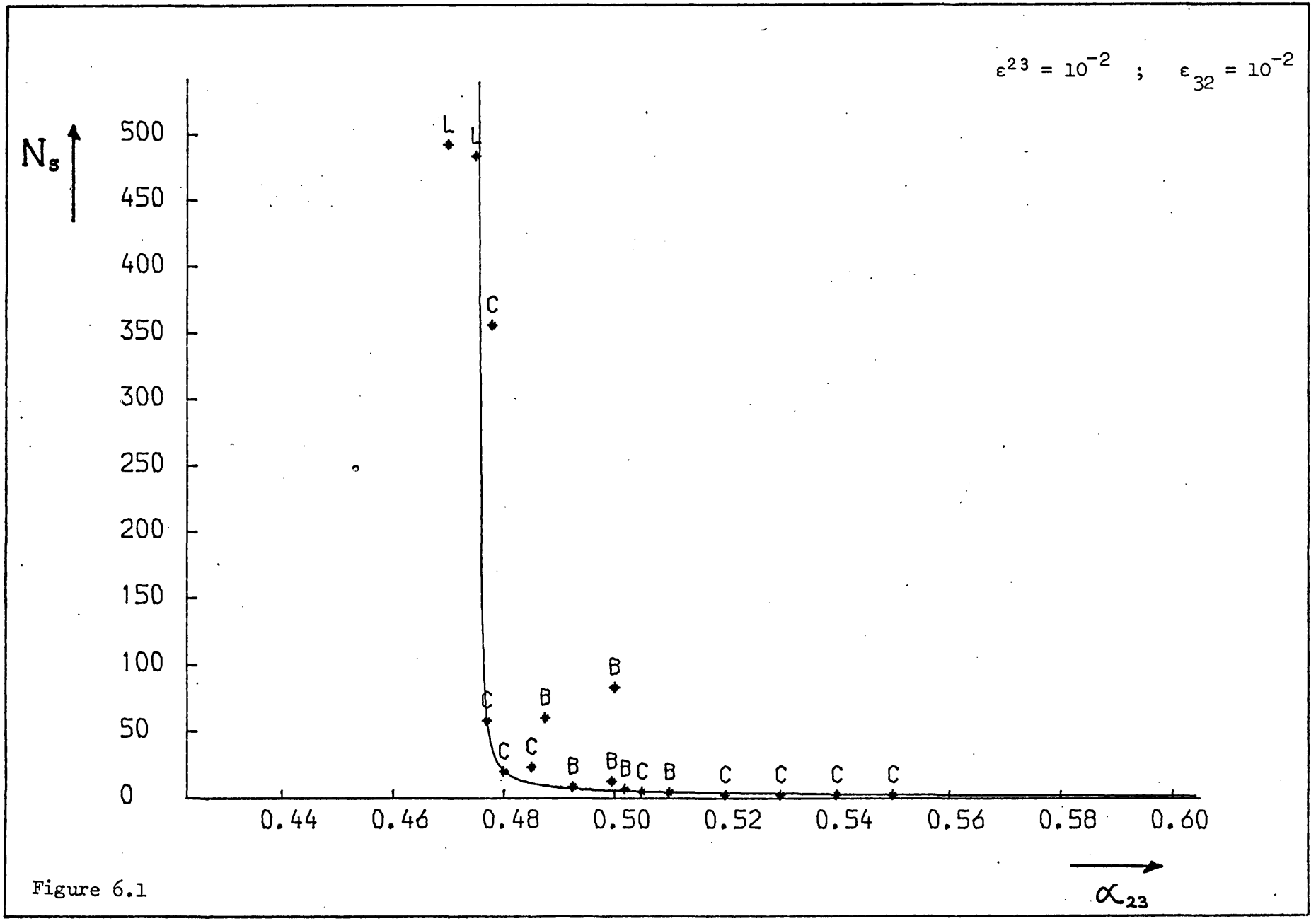
$\varepsilon^{23} = 10^{-2}$; $\varepsilon_{32} = 10^{-2}$
N_s
500
450
400
350
300
250
200
150
100
50
0
0.44
0.46
0.48
0.50
0.52
0.54
0.56
0.58
0.60
α_{23}

Figure 6.1

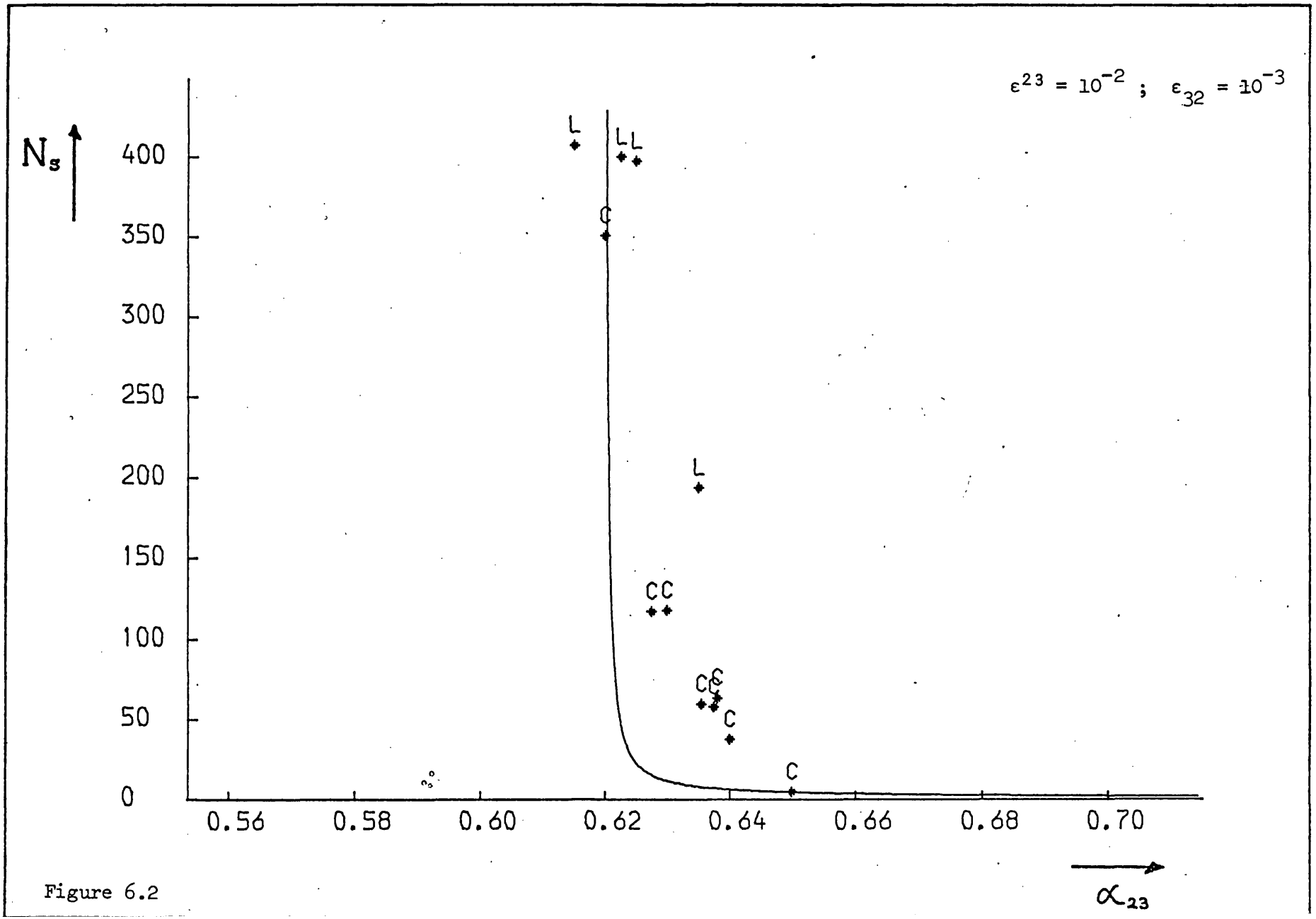
$\varepsilon^{23} = 10^{-2}$; $\varepsilon_{32} = 10^{-3}$
N_s
400
350
300
250
200
150
100
50
0
0.56
0.58
0.60
0.62
0.64
0.66
0.68
0.70
α_{23}
L
C

Figure 6.2

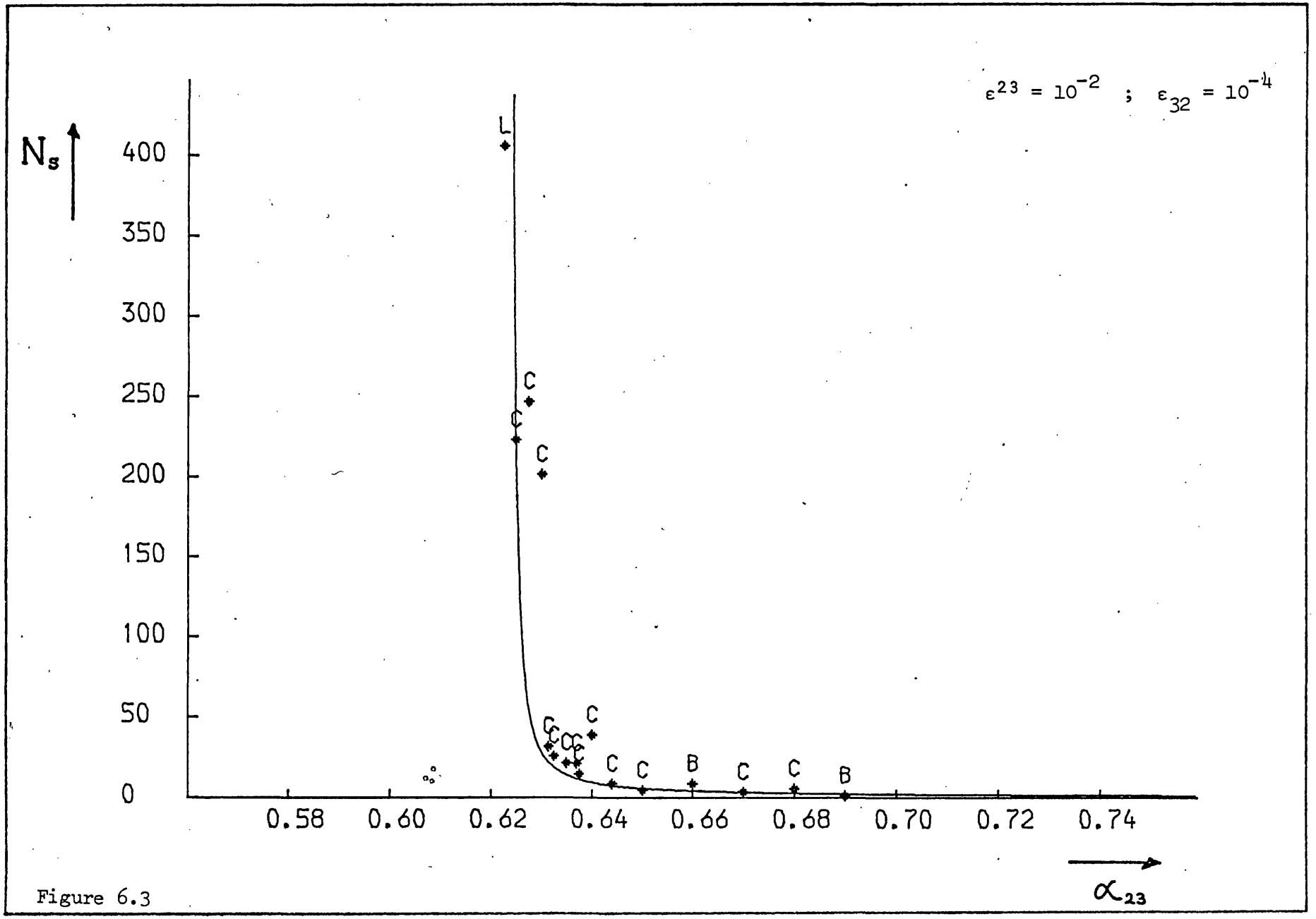
$\varepsilon^{23} = 10^{-2}$; $\varepsilon_{32} = 10^{-4}$
N_s
400
350
300
250
200
150
100
50
0
L
C
B
0.58
0.60
0.62
0.64
0.66
0.68
0.70
0.72
0.74
α_{23}

Figure 6.3

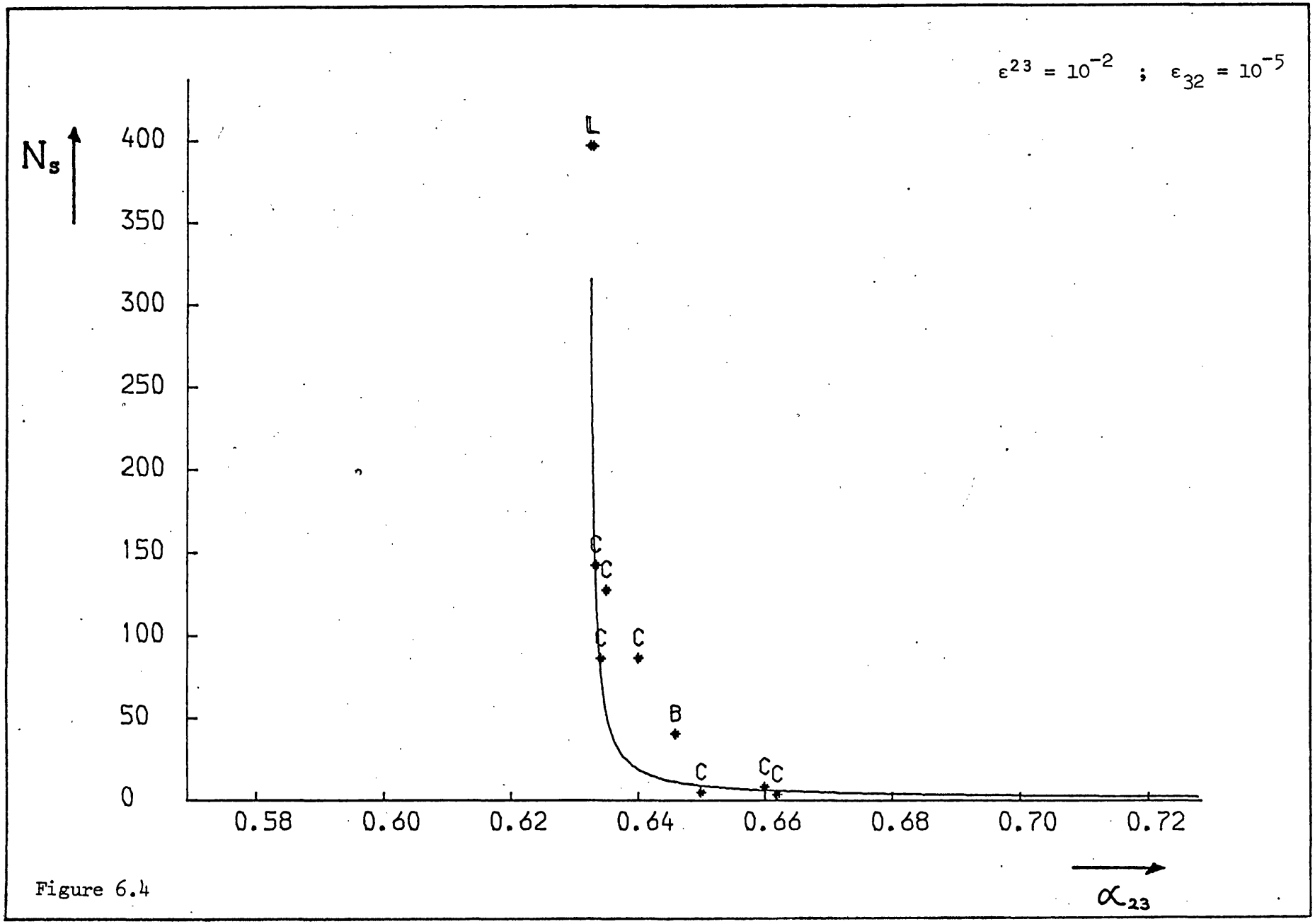
$\varepsilon^{23} = 10^{-2}$; $\varepsilon_{32} = 10^{-5}$
N_s
400
350
300
250
200
150
100
50
0
L
C
C
C
C
B
C
C
C
0.58
0.60
0.62
0.64
0.66
0.68
0.70
0.72
α_{23}

Figure 6.4

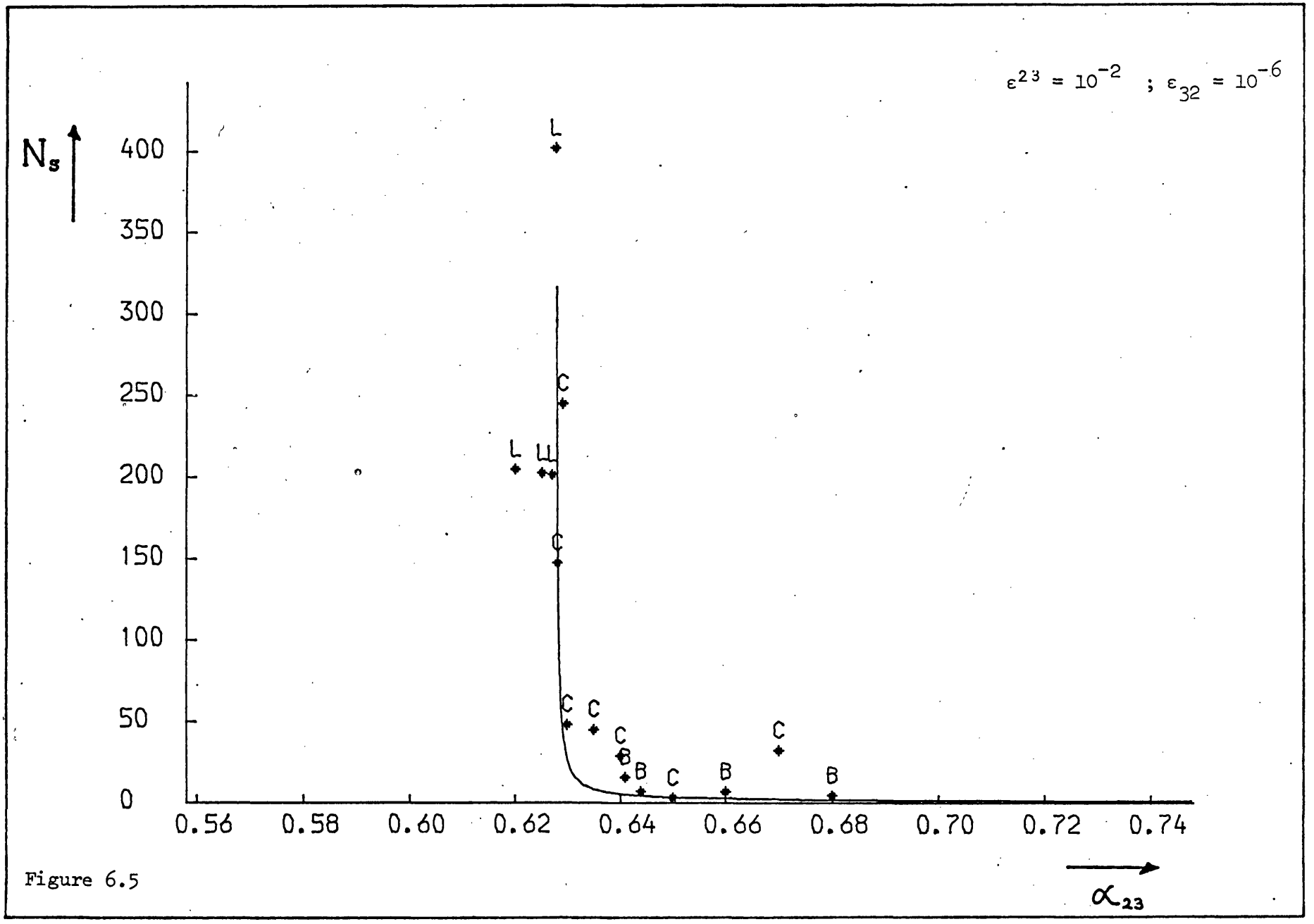
$\varepsilon^{23} = 10^{-2}$; $\varepsilon_{32} = 10^{-6}$
N_s
400
350
300
250
200
150
100
50
0
0.56
0.58
0.60
0.62
0.64
0.66
0.68
0.70
0.72
0.74
α_{23}

Figure 6.5

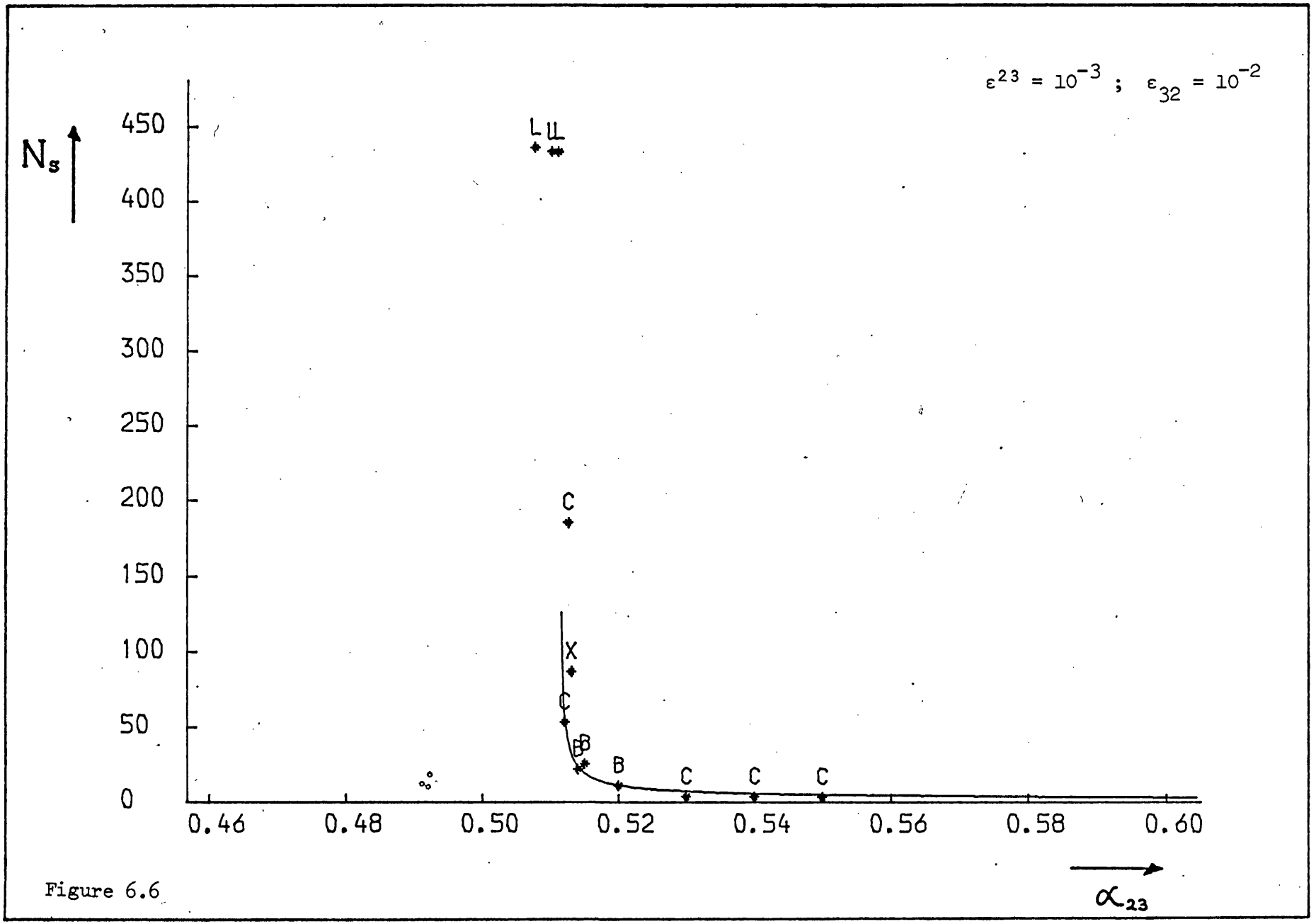
$\varepsilon^{23} = 10^{-3}$; $\varepsilon_{32} = 10^{-2}$
N_s
450
400
350
300
250
200
150
100
50
0
L L
C
X
C
B B B
B
C C C
0.46
0.48
0.50
0.52
0.54
0.56
0.58
0.60
α_{23}

Figure 6.6

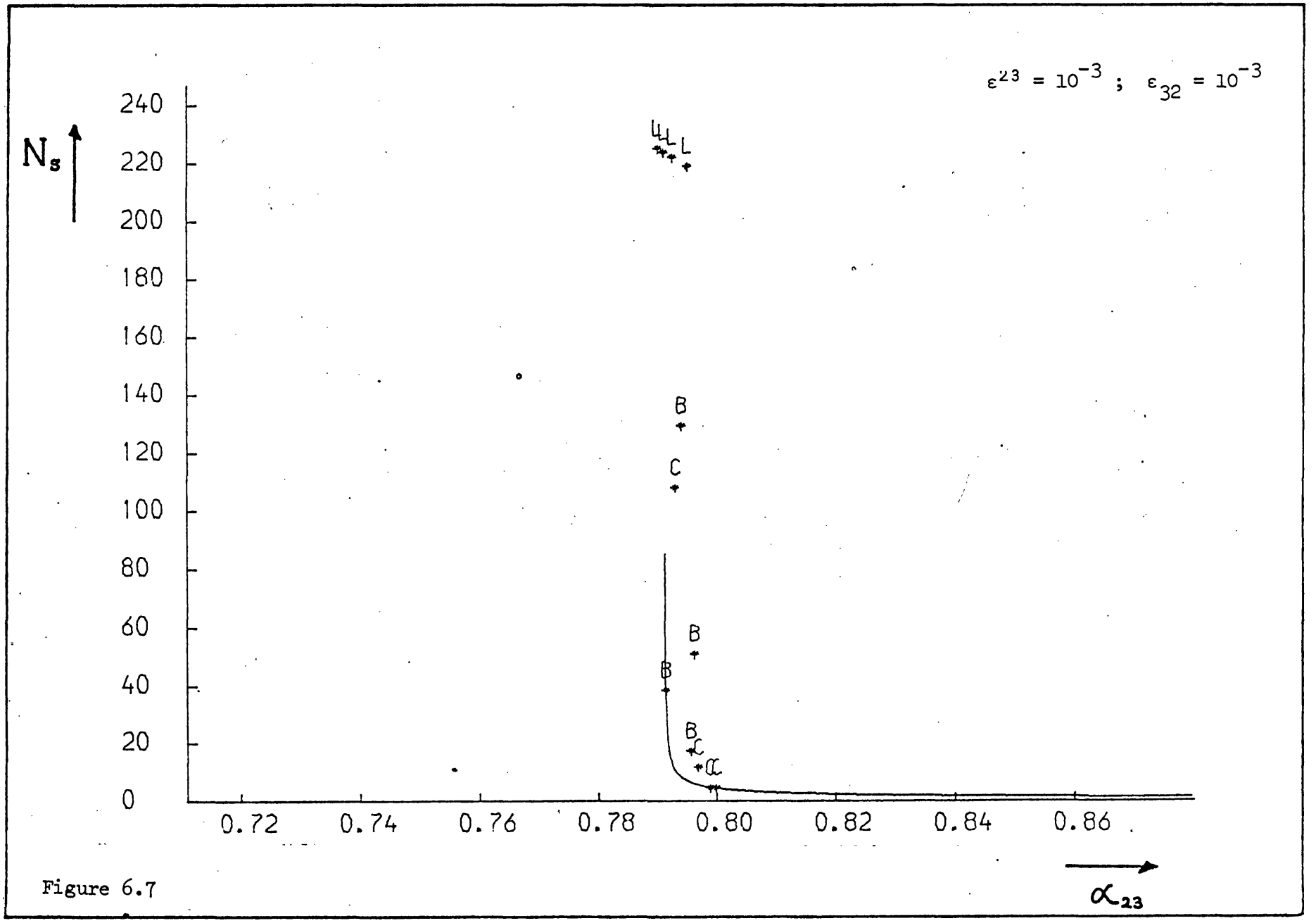
$\varepsilon^{23} = 10^{-3}$; $\varepsilon_{32} = 10^{-3}$
N_s
240
220
200
180
160
140
120
100
80
60
40
20
0
0.72
0.74
0.76
0.78
0.80
0.82
0.84
0.86
α_{23}

Figure 6.7

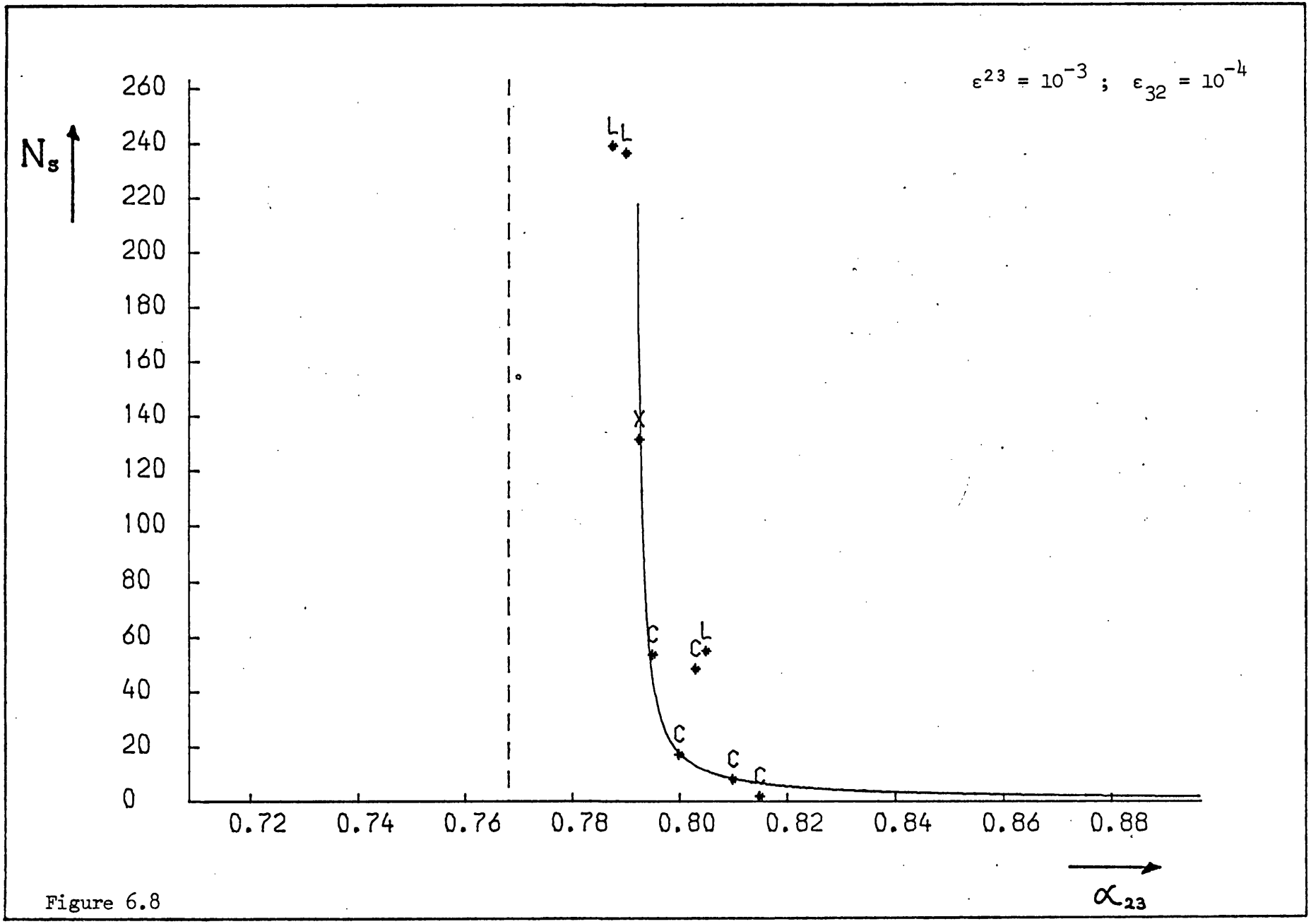
$\varepsilon^{23} = 10^{-3}$; $\varepsilon_{32} = 10^{-4}$
N_s
260
240
220
200
180
160
140
120
100
80
60
40
20
0
0.72
0.74
0.76
0.78
0.80
0.82
0.84
0.86
0.88
α_{23}
L
L
X
C
L
C
C
C
C

Figure 6.8

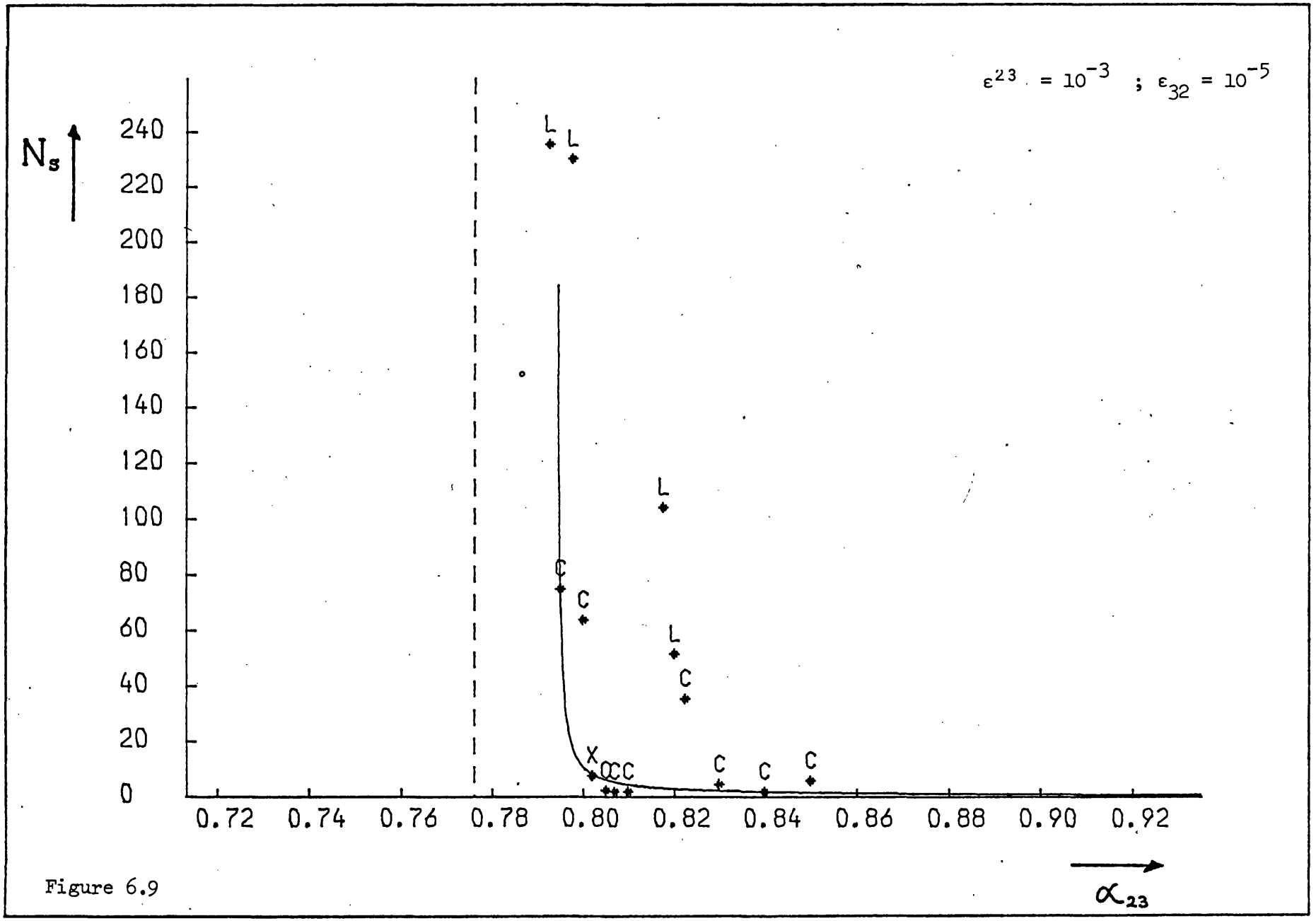
$\varepsilon^{23} = 10^{-3}$; $\varepsilon_{32} = 10^{-5}$
N_s
240
220
200
180
160
140
120
100
80
60
40
20
0
0.72
0.74
0.76
0.78
0.80
0.82
0.84
0.86
0.88
0.90
0.92
α_{23}

Figure 6.9

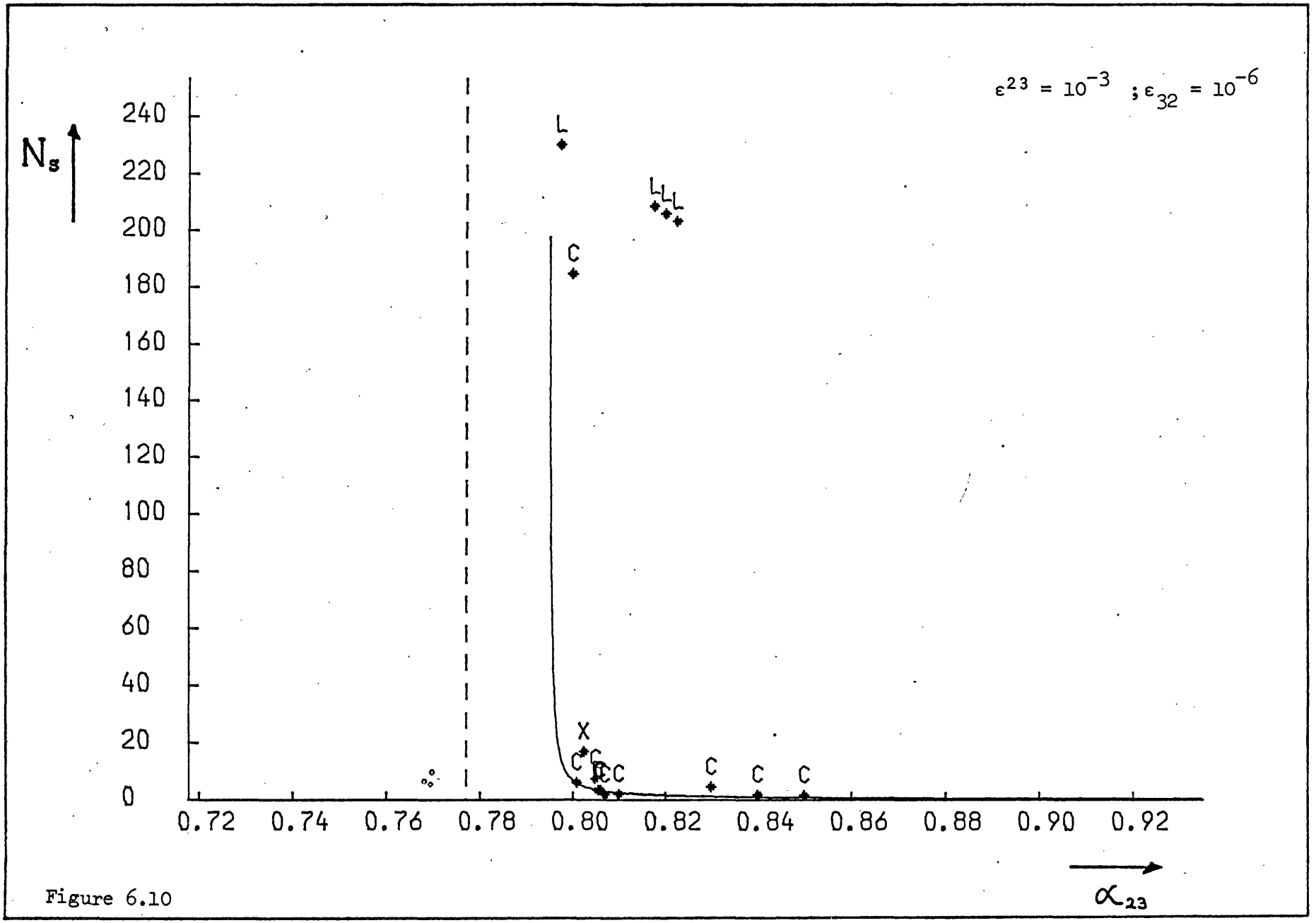
$\varepsilon^{23} = 10^{-3}$; $\varepsilon_{32} = 10^{-6}$
N_s
240
220
200
180
160
140
120
100
80
60
40
20
0
0.72
0.74
0.76
0.78
0.80
0.82
0.84
0.86
0.88
0.90
0.92
α_{23}

Figure 6.10

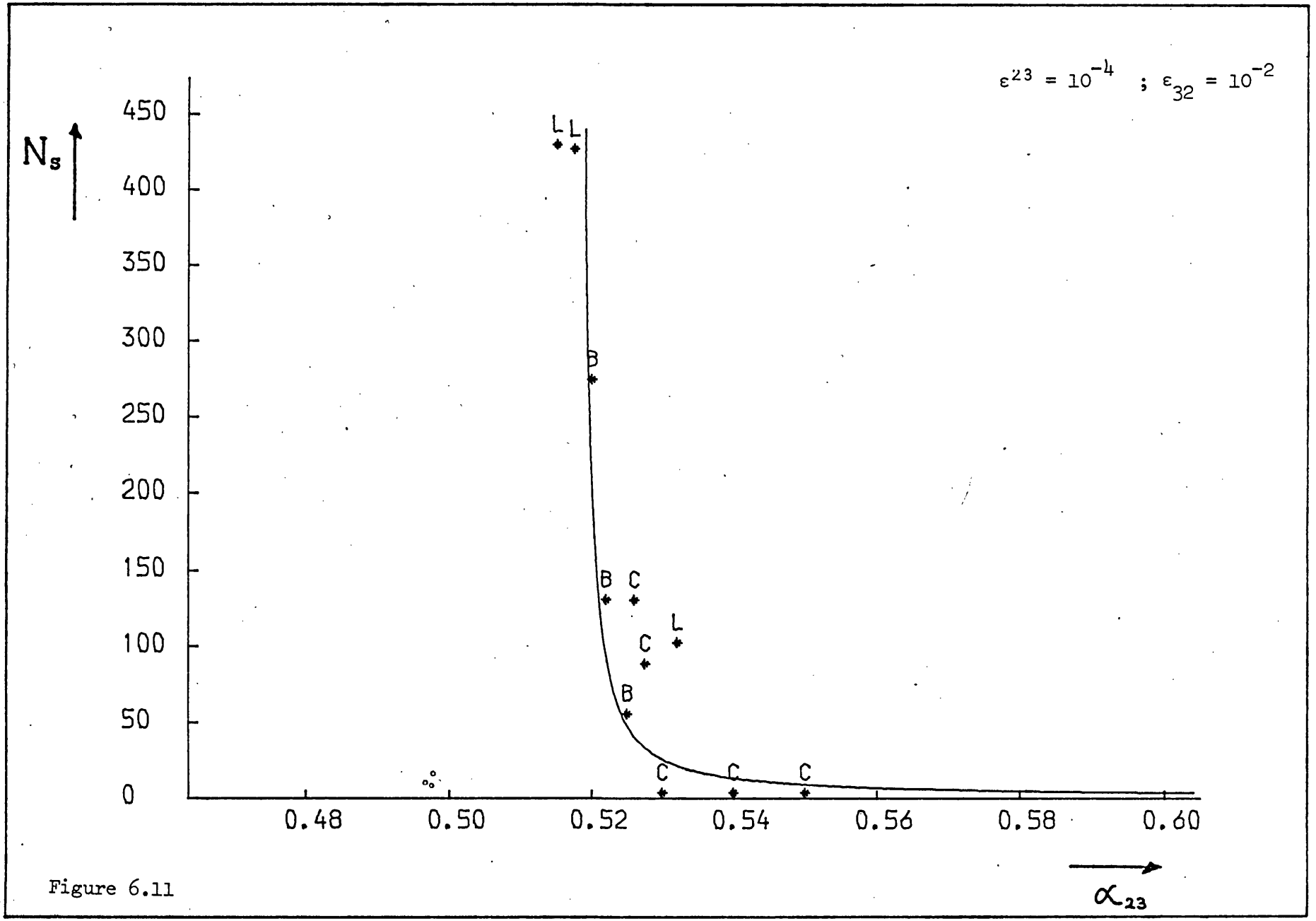
$\varepsilon^{23} = 10^{-4}$; $\varepsilon_{32} = 10^{-2}$
N_s
450
400
350
300
250
200
150
100
50
0
0.48
0.50
0.52
0.54
0.56
0.58
0.60
L L
B
B C
C
L
B
C C C
α_{23}

Figure 6.11

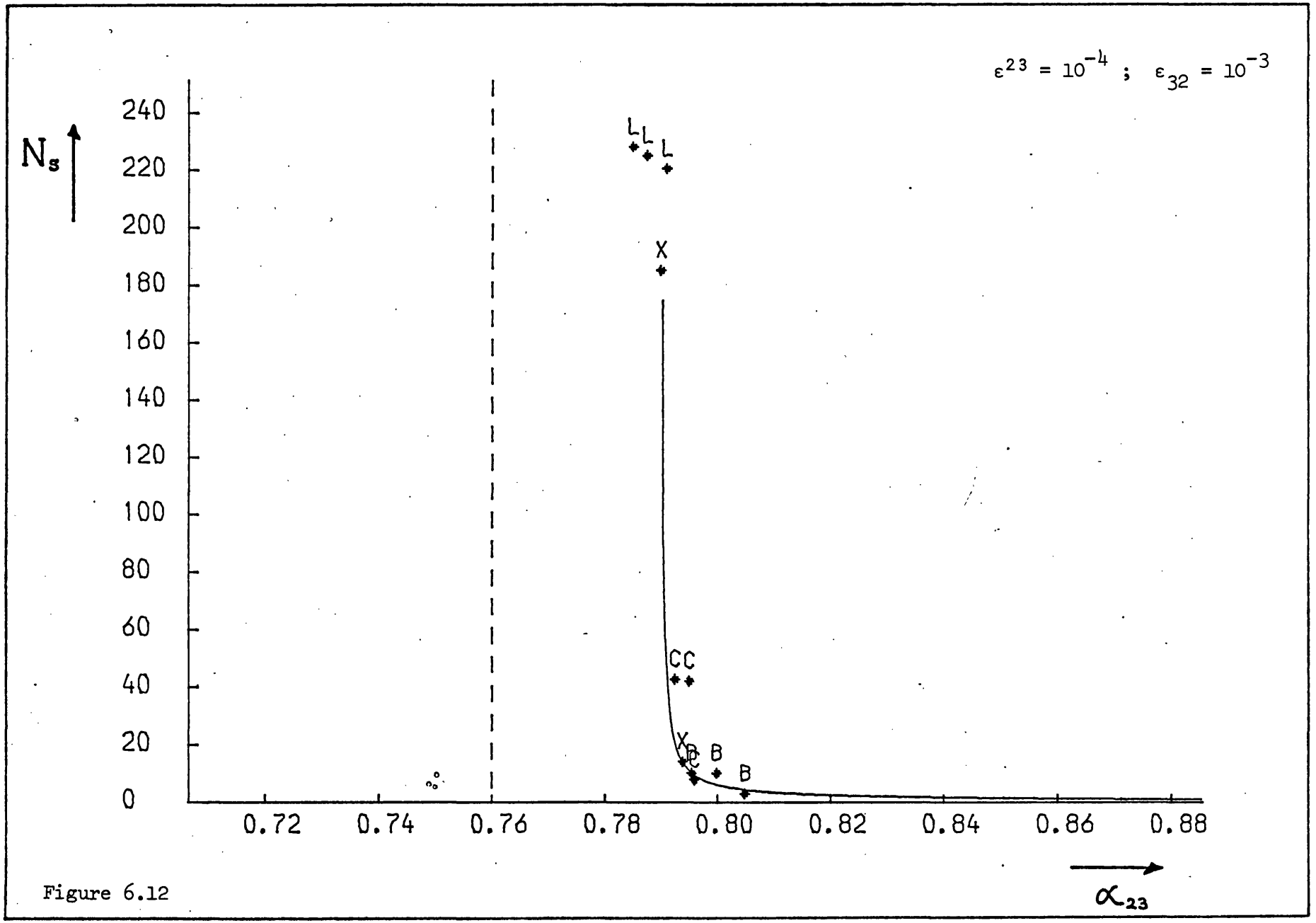
$\varepsilon^{23} = 10^{-4}$; $\varepsilon_{32} = 10^{-3}$
N_s
240
220
200
180
160
140
120
100
80
60
40
20
0
0.72
0.74
0.76
0.78
0.80
0.82
0.84
0.86
0.88
α_{23}

Figure 6.12

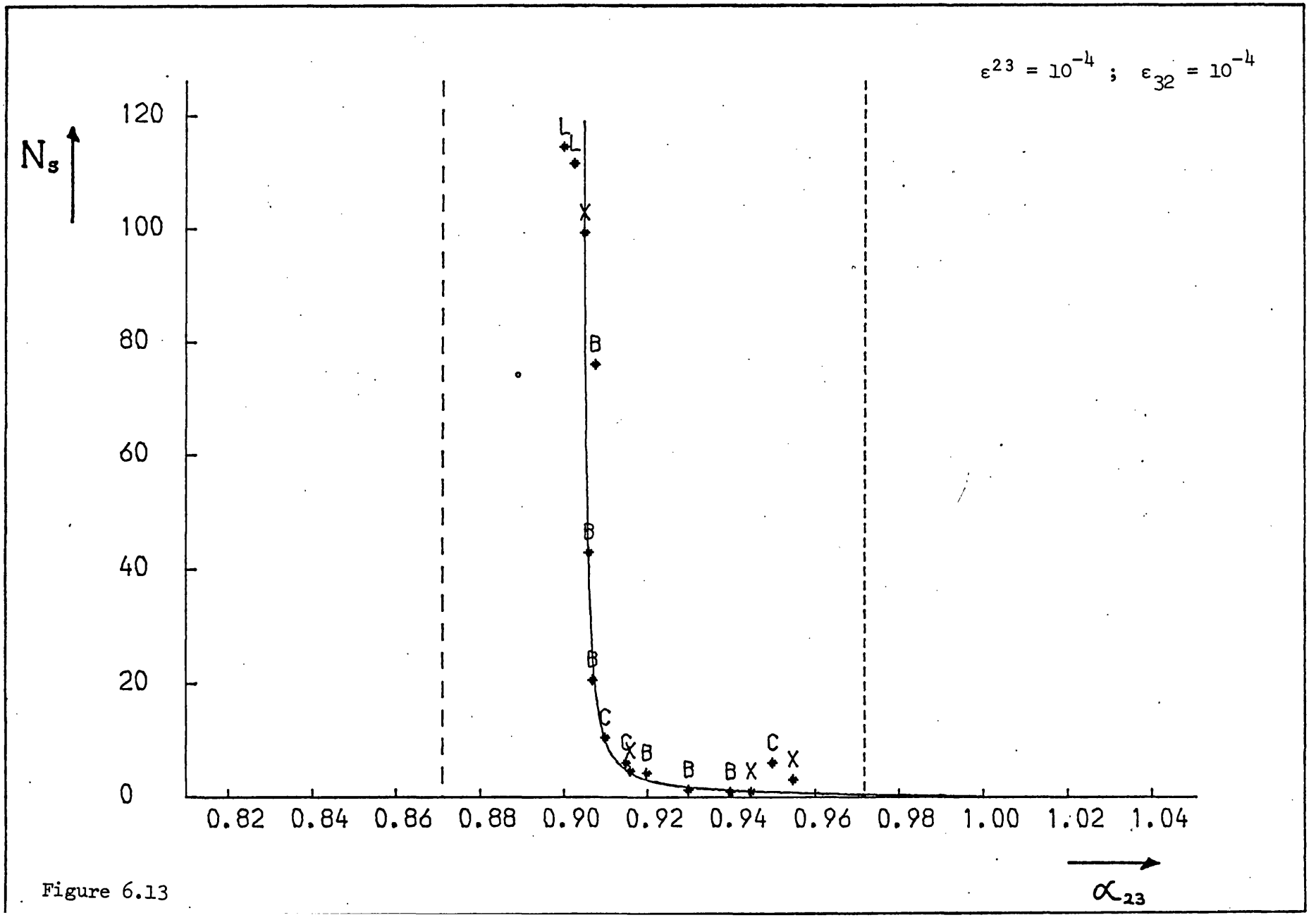
$\varepsilon^{23} = 10^{-4}$; $\varepsilon_{32} = 10^{-4}$
N_s
120
100
80
60
40
20
0
0.82
0.84
0.86
0.88
0.90
0.92
0.94
0.96
0.98
1.00
1.02
1.04
α_{23}

Figure 6.13

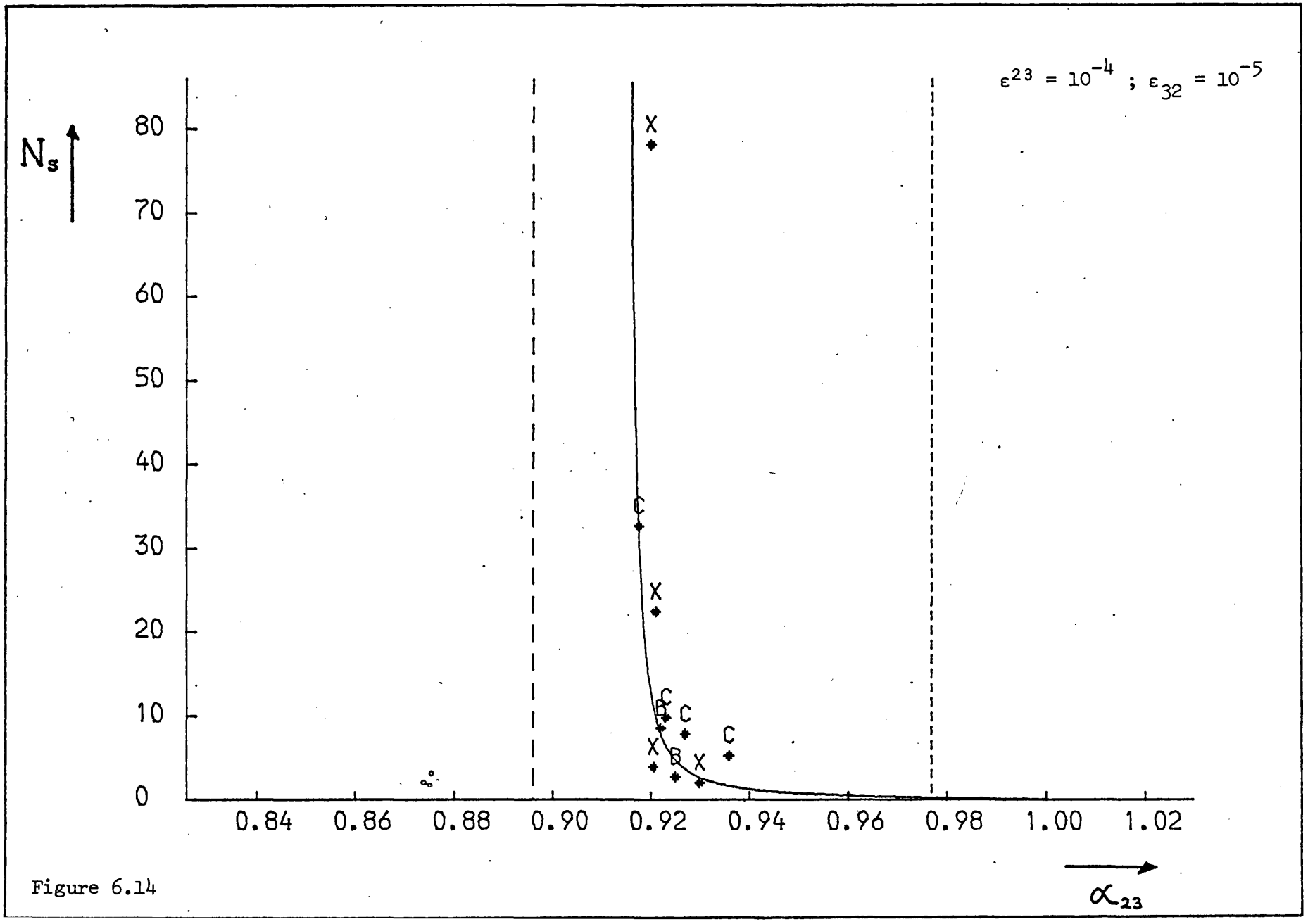
$\varepsilon^{23} = 10^{-4}$; $\varepsilon_{32} = 10^{-5}$
N_s
80
70
60
50
40
30
20
10
0
0.84
0.86
0.88
0.90
0.92
0.94
0.96
0.98
1.00
1.02
α_{23}

Figure 6.14

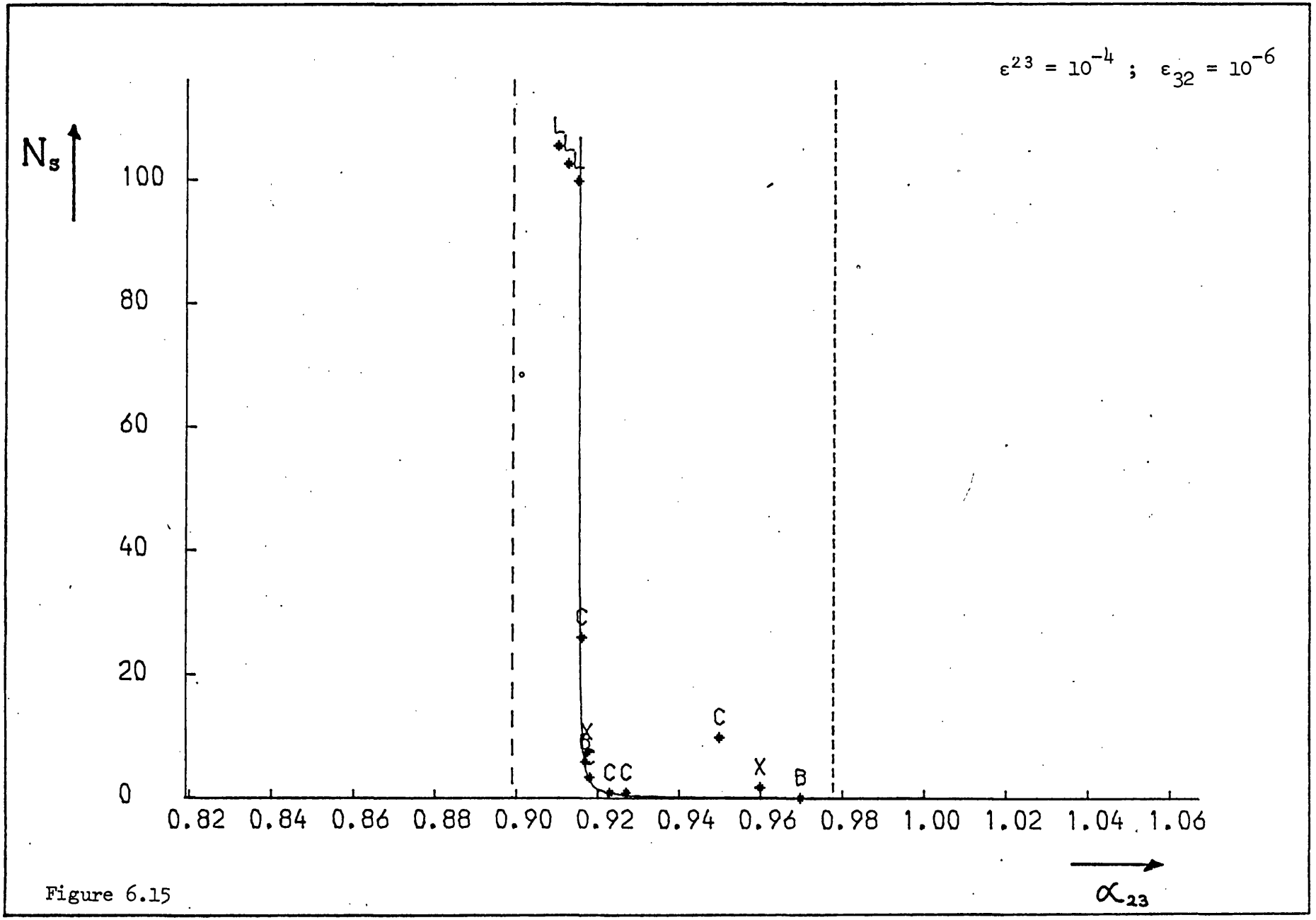
$\varepsilon^{23} = 10^{-4}$; $\varepsilon_{32} = 10^{-6}$
N_s
100
80
60
40
20
0
0.82 0.84 0.86 0.88 0.90 0.92 0.94 0.96 0.98 1.00 1.02 1.04 1.06
α_{23}
L
C
X
C C
C
X
B

Figure 6.15

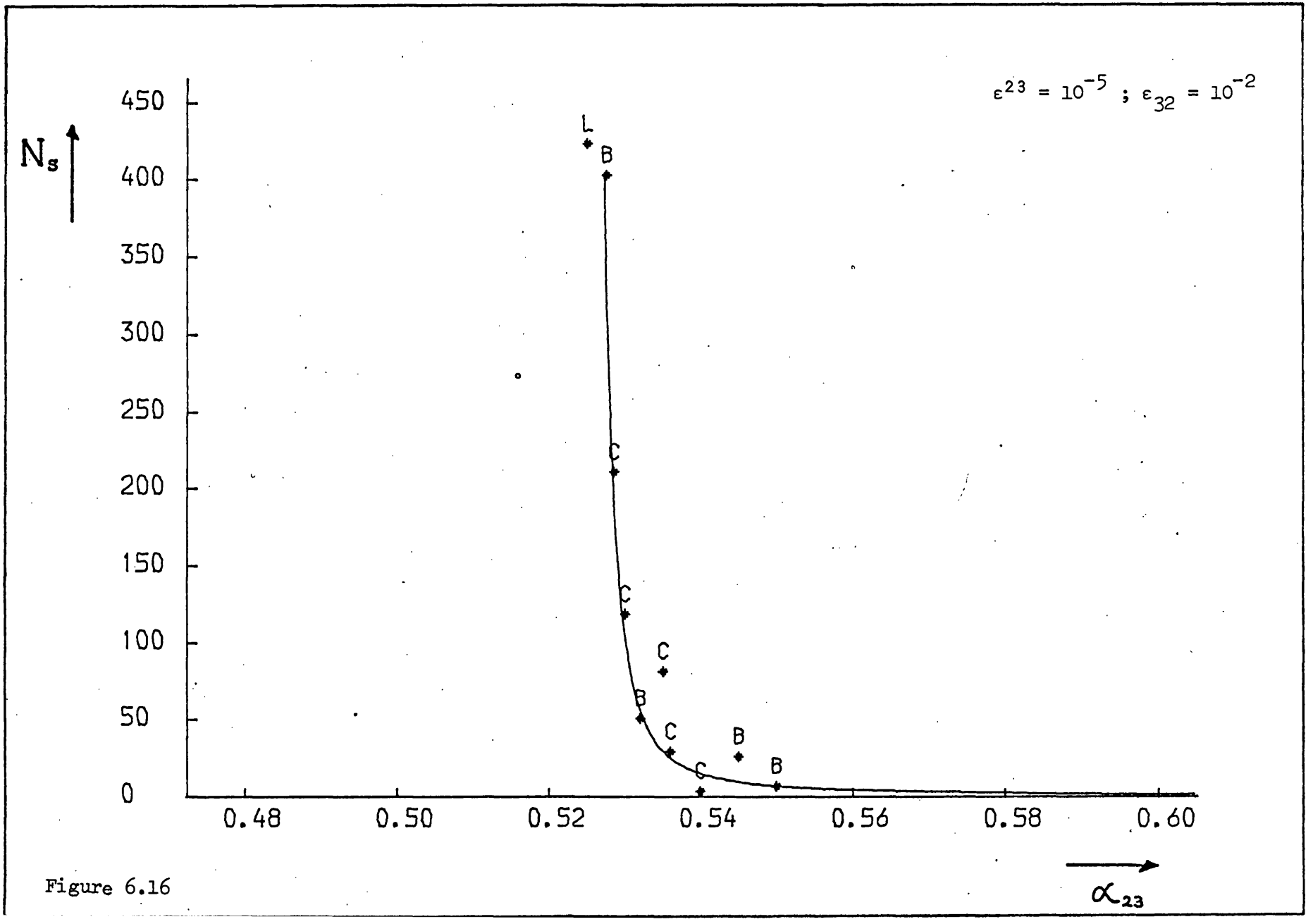
$\varepsilon^{23} = 10^{-5}$; $\varepsilon_{32} = 10^{-2}$
N_s
450
400
350
300
250
200
150
100
50
0
L
B
C
C
C
B
C
B
C
B
0.48
0.50
0.52
0.54
0.56
0.58
0.60
α_{23}

Figure 6.16

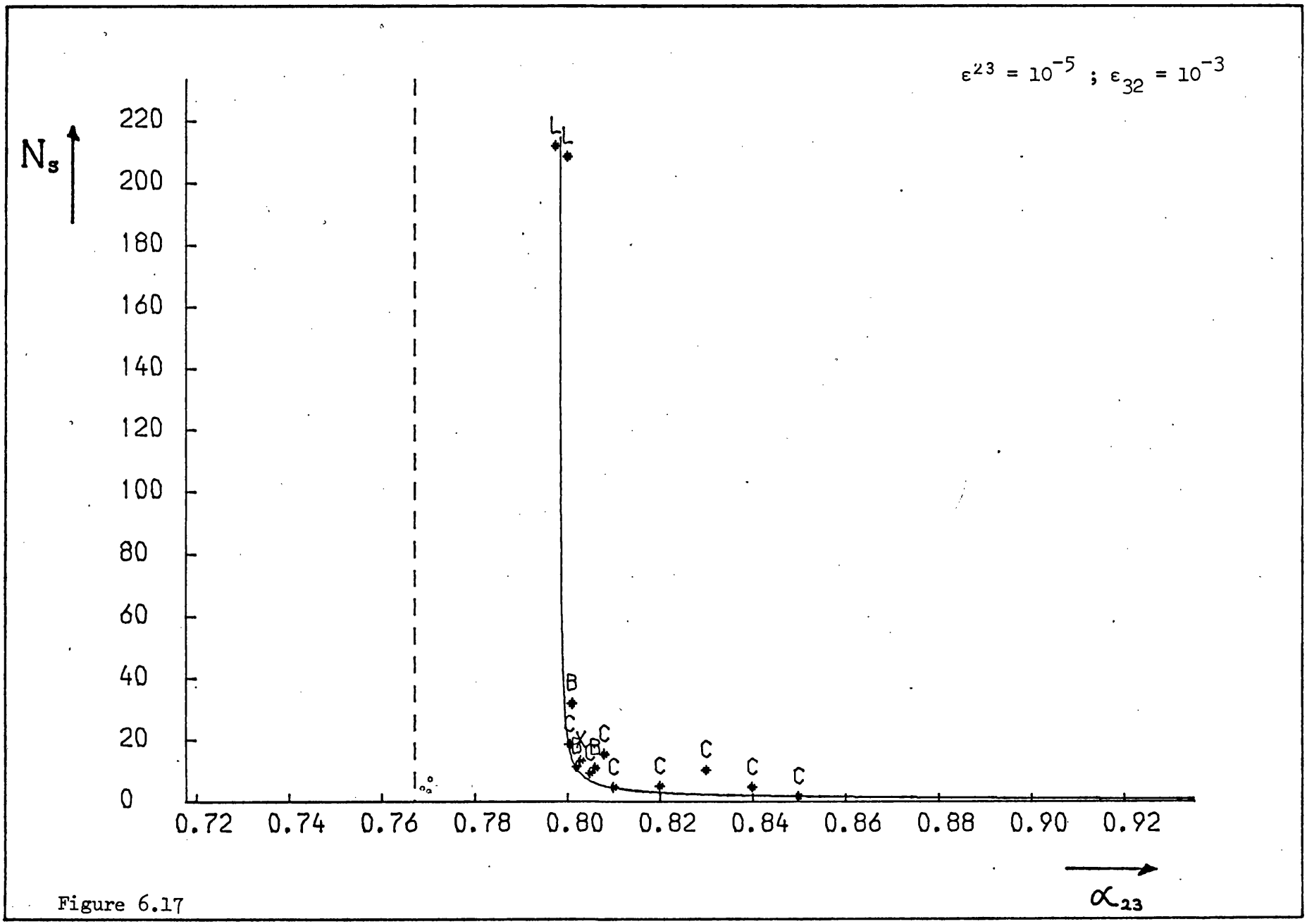
$\epsilon^{23} = 10^{-5}$; $\epsilon_{32} = 10^{-3}$
N_s
220
200
180
160
140
120
100
80
60
40
20
0
0.72
0.74
0.76
0.78
0.80
0.82
0.84
0.86
0.88
0.90
0.92
α_{23}

Figure 6.17

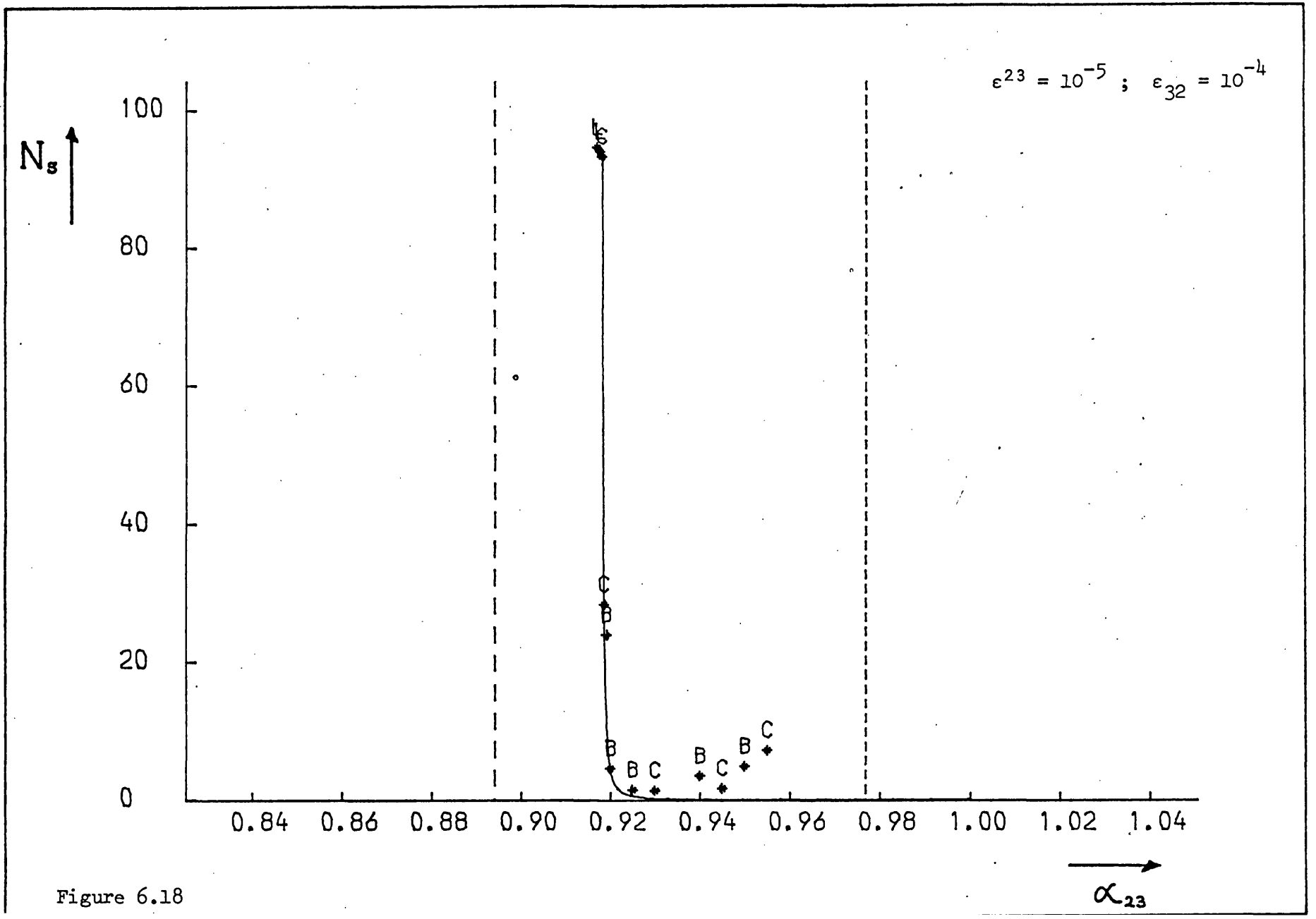
$\varepsilon^{23} = 10^{-5}$; $\varepsilon_{32} = 10^{-4}$
N_s
100
80
60
40
20
0
0.84
0.86
0.88
0.90
0.92
0.94
0.96
0.98
1.00
1.02
1.04
α_{23}
B
C

Figure 6.18

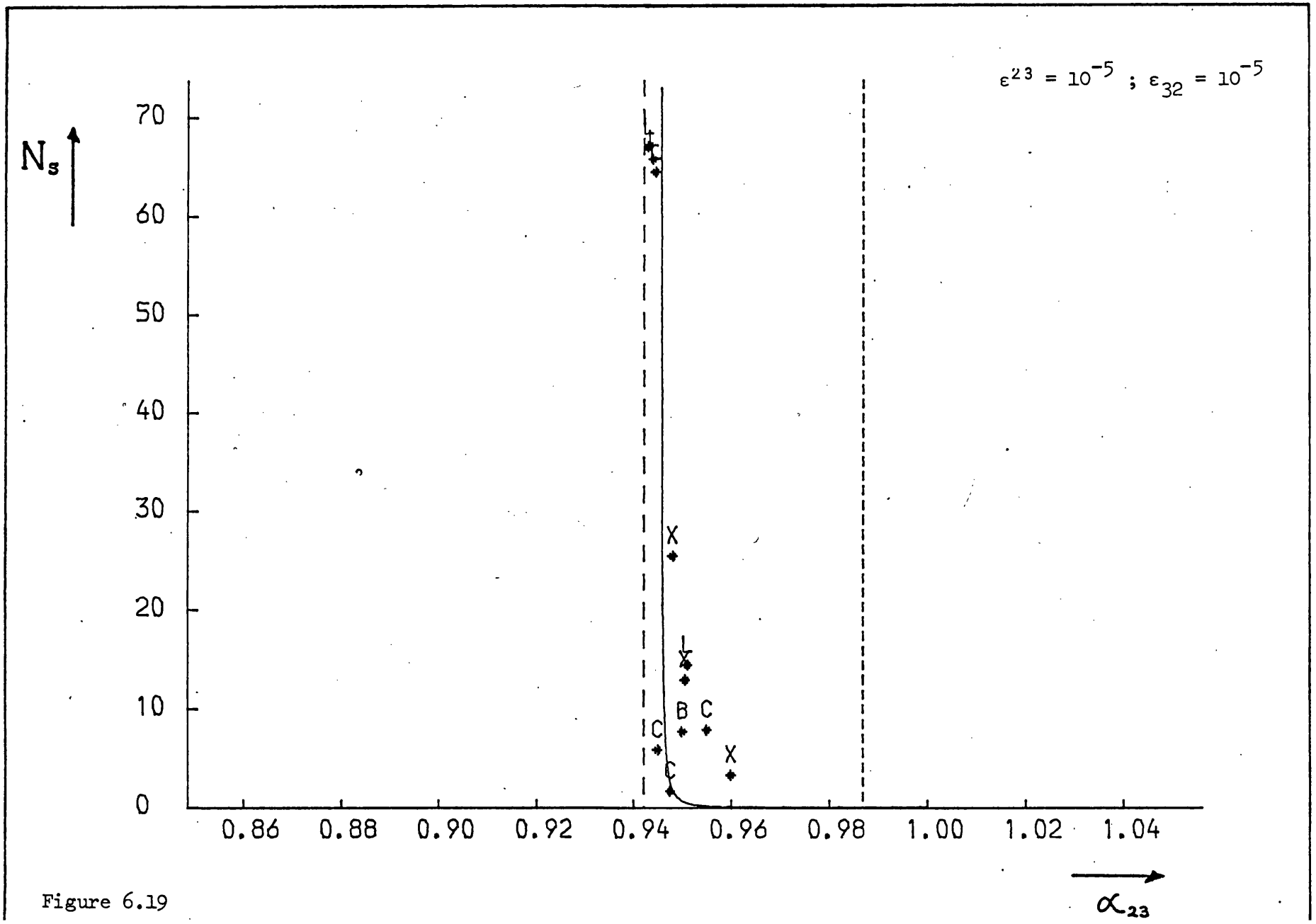
$\varepsilon^{23} = 10^{-5}$; $\varepsilon_{32} = 10^{-5}$
N_s
70
60
50
40
30
20
10
0
0.86
0.88
0.90
0.92
0.94
0.96
0.98
1.00
1.02
1.04
α_{23}
X
B
C

Figure 6.19

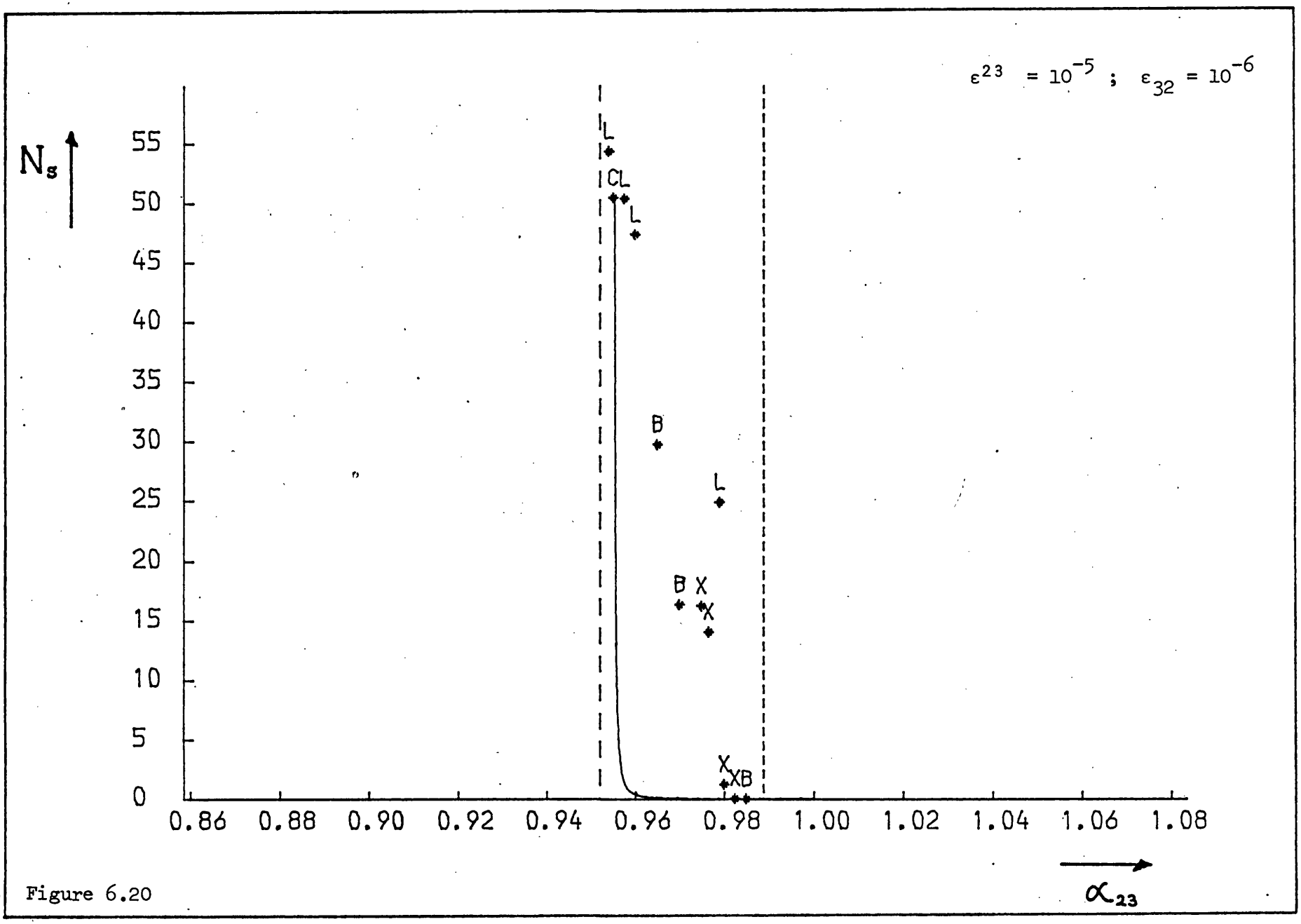
$\varepsilon^{23} = 10^{-5}$; $\varepsilon_{32} = 10^{-6}$
N_s
55
50
45
40
35
30
25
20
15
10
5
0
L
CL
L
B
L
B X
X
X
XB
0.86 0.88 0.90 0.92 0.94 0.96 0.98 1.00 1.02 1.04 1.06 1.08
α_{23}

Figure 6.20

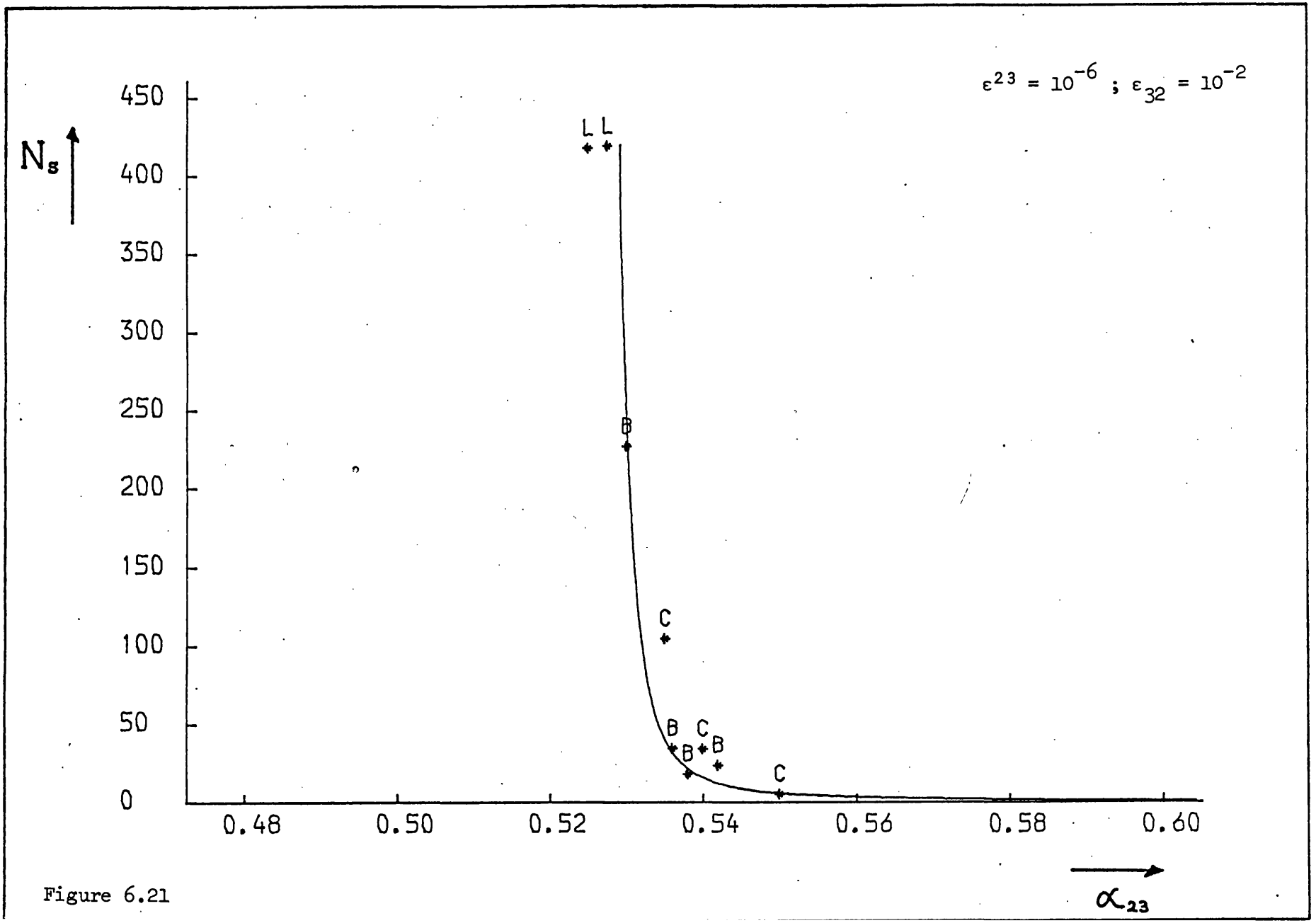
$\varepsilon^{23} = 10^{-6}$; $\varepsilon_{32} = 10^{-2}$
N_s
450
400
350
300
250
200
150
100
50
0
L L
B
C
B C B
B
C
0.48
0.50
0.52
0.54
0.56
0.58
0.60
α_{23}

Figure 6.21

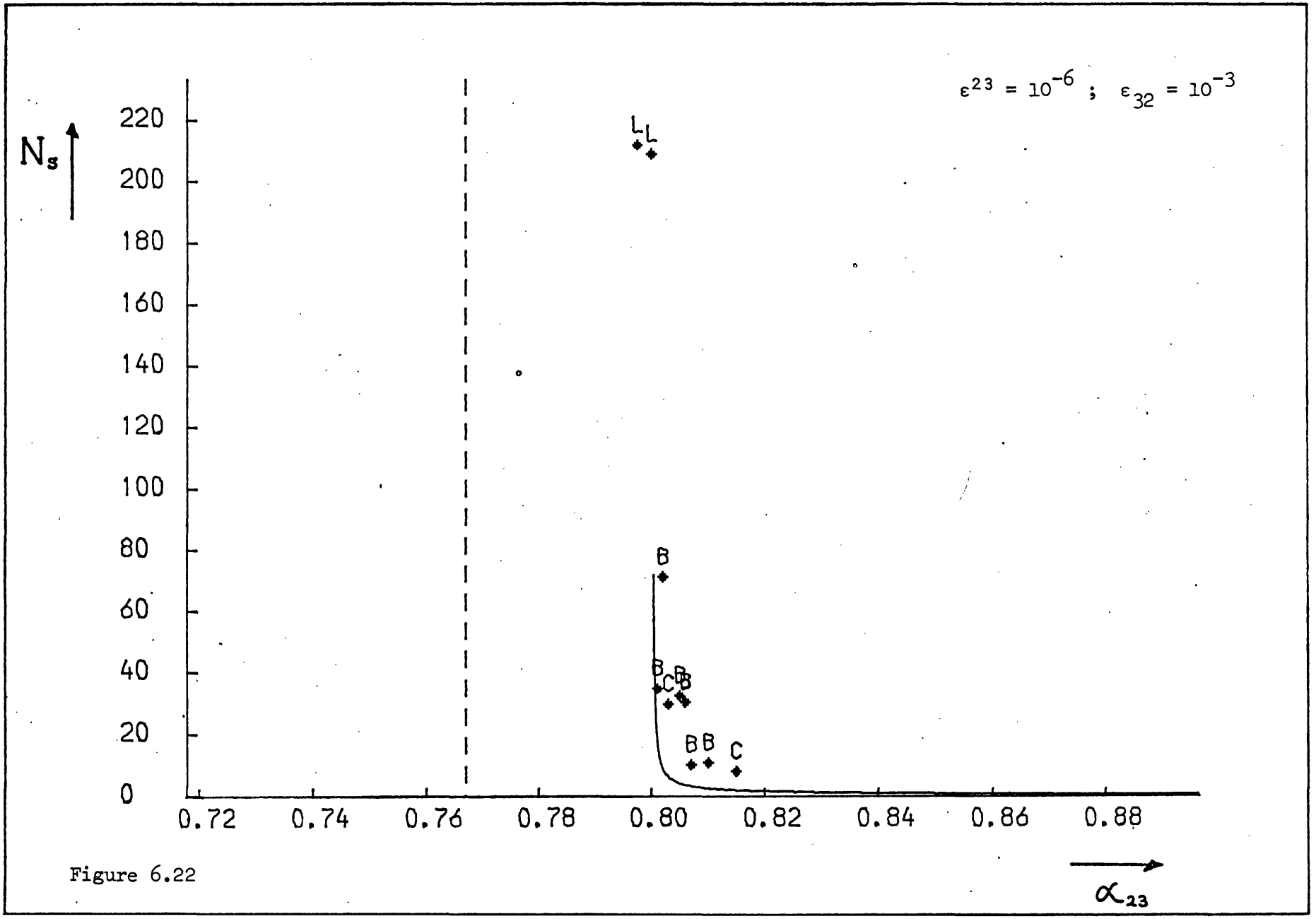
$\varepsilon^{23} = 10^{-6}$; $\varepsilon_{32} = 10^{-3}$
N_s
220
200
180
160
140
120
100
80
60
40
20
0
0.72
0.74
0.76
0.78
0.80
0.82
0.84
0.86
0.88
α_{23}
L L
B
B C B B
B B C

Figure 6.22

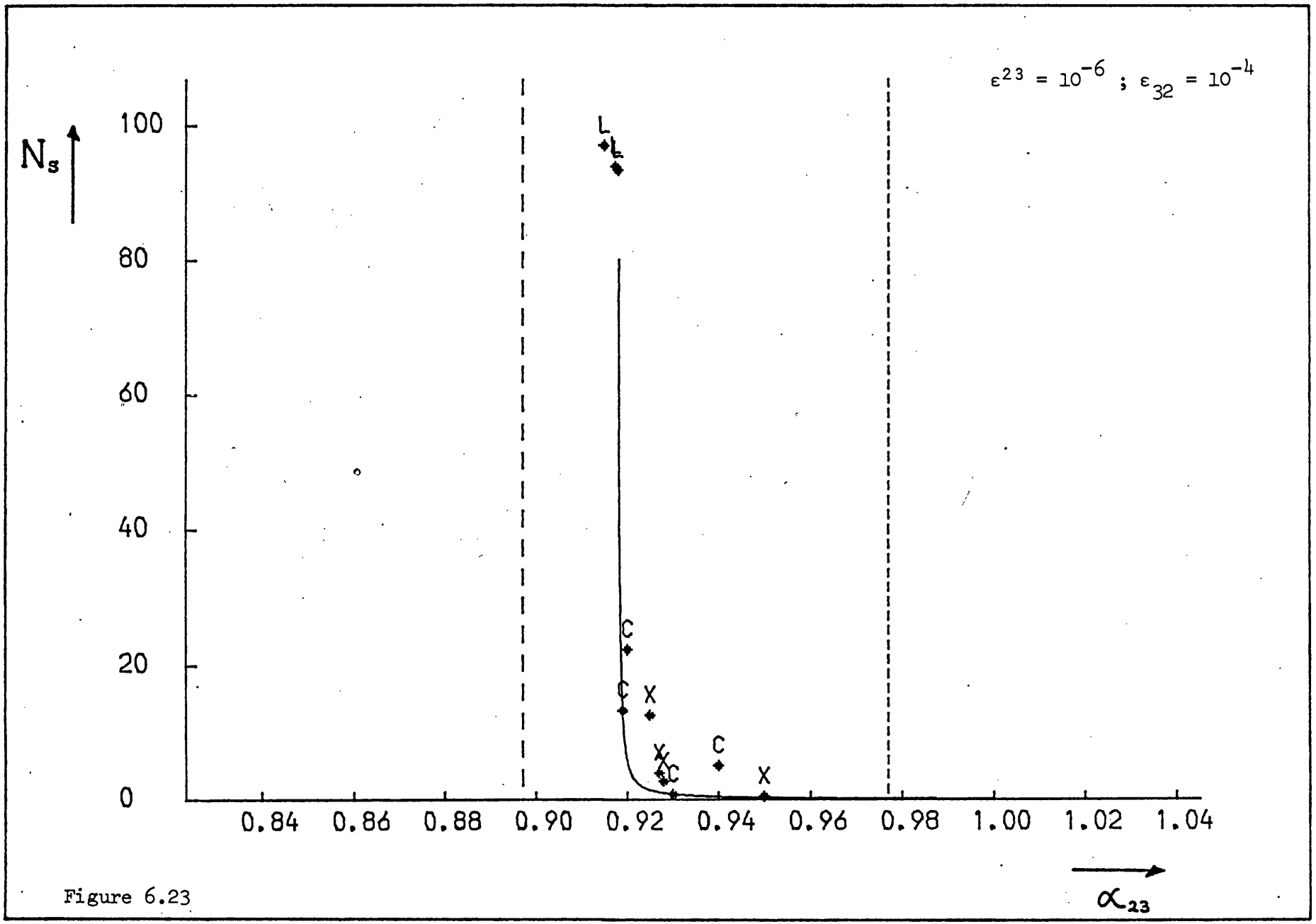
$\varepsilon^{23} = 10^{-6}$; $\varepsilon_{32} = 10^{-4}$
N_s
100
80
60
40
20
0
0.84
0.86
0.88
0.90
0.92
0.94
0.96
0.98
1.00
1.02
1.04
α_{23}

Figure 6.23

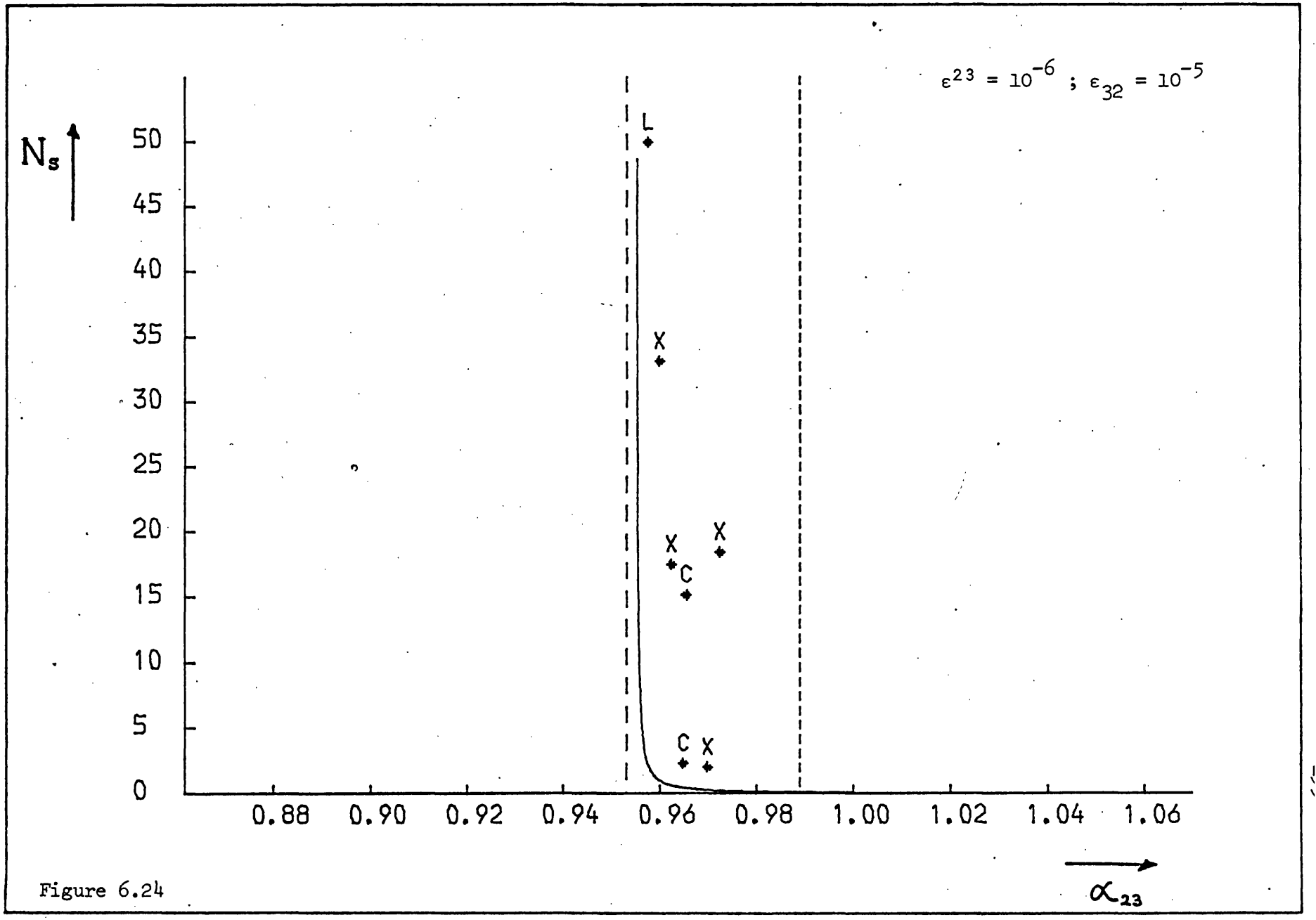
$\varepsilon^{23} = 10^{-6}$; $\varepsilon_{32} = 10^{-5}$
N_s
50
45
40
35
30
25
20
15
10
5
0
L
X
X
C
X
C
X
0.88
0.90
0.92
0.94
0.96
0.98
1.00
1.02
1.04
1.06
α_{23}

Figure 6.24

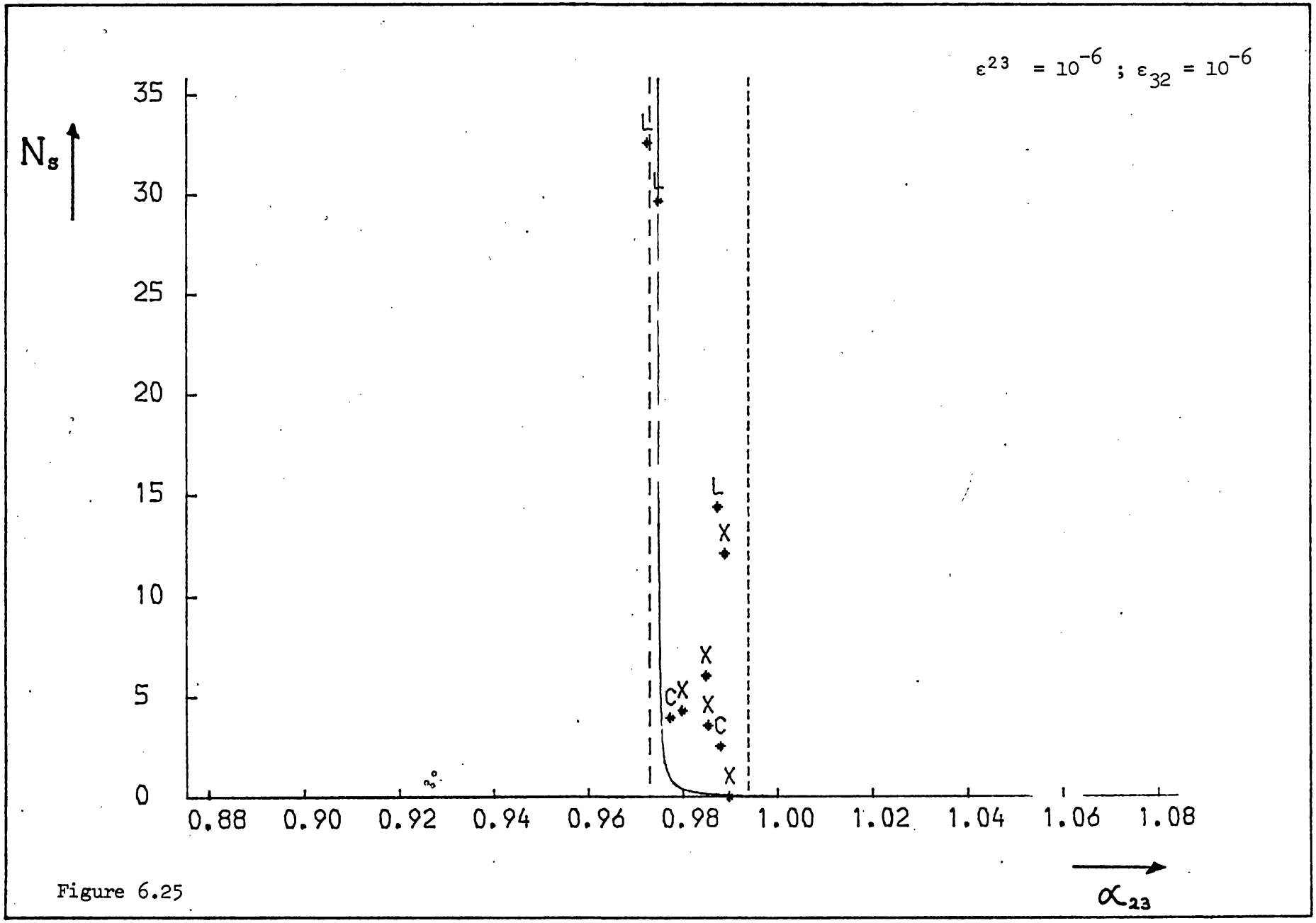
$\varepsilon^{23} = 10^{-6}$; $\varepsilon_{32} = 10^{-6}$
N_s
35
30
25
20
15
10
5
0
0.88
0.90
0.92
0.94
0.96
0.98
1.00
1.02
1.04
1.06
1.08
α_{23}

Figure 6.25

6.4 The Effect of Commensurabilities on the Degree of Stability

It is to be expected in the present numerical investigation that some sets of initial conditions will be found which give rise to commensurable situations during the time interval of the integration. As a rule - there are no exceptions - it is found that on commencing the numerical integration procedure (with the above mentioned initial conditions) the semi-major axes of the system change in a systematic fashion. The semi-major axis of the (m_1, m_2) subsystem always decreases, whereas that of the (M_2, m_3) subsystem increases. This tends to reduce the running or osculating value of α (the ratio $a_2 : a_3$). With these facts in mind we proceed to examine those features in Figures 6.1 - 6.25 where the number of orbits executed is found to be greater than the number predicted from the empirical stability curves.

In Table 6.2 are presented the notable features as they occur on the plots. The value of the $\varepsilon^{23}, \varepsilon_{32}$ parameters are given along with the initial α_{23} ratio which gives rise to the feature. Also given are commensurabilities which arise from α values immediately below (if possible) the α_{23} which appeared on the graph. This choice is due to the reduction in the running α value as commented on above. It is noted here that since we deal with initially circular orbits the initial α_{23} value is equal to the initial value of α. Excluded from this table are any results arising from Figures 6.19, 6.20, 6.24 and 6.25 i.e. ε pairs $(10^{-p}, 10^{-q})$ where $p = 5, 6$; $q = 5, 6$ for reasons which are discussed below.

The α values which give rise to commensurabilities in mean motion may be found in the following manner. Let n_2 and n_3 be the mean motions of the (m_1, m_2) and (M_2, m_3) subsystems respectively $(n_2 > n_3)$. n_2 and n_3 here may be defined from the set of initial conditions or any other set of osculating orbital parameters as follows

$$n_2^2 \; a_2^3 = G(m_1 + m_2) \qquad (10)$$

and

$$n_3^2 \; a_3^3 = G(m_1 + m_2 + m_3). \qquad (11)$$

Table 6.2 - Commensurabilities in Mean Motion

ϵ^{23}	ϵ_{32}	α_{23}	Commensurability/ Corresponding α
10^{-2}	10^{-2}	0.478 0.487 0.500	3:1 / 0.466
10^{-2}	10^{-3}	0.623 0.635	2:1 / 0.629
10^{-2}	10^{-4}	0.627 0.640	2:1 / 0.630
10^{-2}	10^{-5}	0.631 0.635	2:1 / 0.630
10^{-2}	10^{-6}	0.629	2:1 / 0.630
		0.670	11:6 / 0.668
10^{-3}	10^{-2}	0.513	11:4 / 0.496
10^{-3}	10^{-3}	0.792 0.795 0.796	10:7 / 0.787
10^{-3}	10^{-4}	0.805	7:5 / 0.799
10^{-3}	10^{-5}	0.818	11:8 / 0.809
10^{-3}	10^{-6}	0.797	10:7 / 0.788
		0.820	11:8 / 0.809
10^{-4}	10^{-2}	0.526	8:3 / 0.507
		0.532	5:2 / 0.531
10^{-4}	10^{-3}	0.795	10:7 / 0.787
10^{-4}	10^{-4}	0.908	7:6 / 0.902
		0.950	13:12/ 0.948
10^{-4}	10^{-5}	0.920	8:7 / 0.915
10^{-4}	10^{-6}	0.950	13:12/ 0.948
10^{-5}	10^{-2}	0.535	8:3 / 0.507
		0.545	5:2 / 0.531

Table 6.2 (continued)

ϵ^{23}	ϵ_{32}	α_{23}	Commensurability/Corresponding α
10^{-5}	10^{-3}	0.800	7:5 /0.799
		0.830	4:3 /0.825
10^{-5}	10^{-4}	0.955	14:13/0.952
10^{-5}	10^{-5}	-	- / -
10^{-5}	10^{-6}	-	- / -
10^{-6}	10^{-2}	0.535	8:3 /0.507
		0.540	5:2 / 0.531
10^{-6}	10^{-3}	0.810	11:8 / 0.808
10^{-6}	10^{-4}	0.926	9:8 / 0.924
		0.940	11:10/ 0.938
10^{-6}	10^{-5}	-	- / -
10^{-6}	10^{-6}	-	- / -

A commensurability is defined to occur when the ratio

$$\frac{n_2}{n_3} = \frac{A_2}{A_3} \qquad (12)$$

where A_2 and A_3 are integers. Now if we divide Equation (10) by Equation (11) we obtain, remembering $\alpha = a_2/a_3$,

$$\alpha = \left(\frac{n_3}{n_2}\right)^{2/3} \cdot \frac{1}{(1 + \mu_3)^{1/3}}. \qquad (13)$$

where, as usual, $\mu_3 = m_3/(m_1 + m_2)$. If we now let $n_2:n_3 = A_2:A_3$ then a value of α which gives rise to a commensurability can be defined to be

$$\alpha = \left(\frac{A_3}{A_2}\right)^{2/3} \cdot \frac{1}{(1 + \mu_3)^{1/3}}. \qquad (14)$$

The periods of revolution for the two subsystems, (m_1, m_2) and (M_2, m_3), may then be written as

$$T_2 = \frac{2\pi}{n_2} \quad \text{and} \quad T_3 = \frac{2\pi}{n_3} \qquad (15)$$

so that the expression for the osculating value of the synodic period, S, of the system may be written as

$$S = 2\pi A_2/\{n_2(A_2 - A_3)\}. \qquad (16)$$

From Equation (16) it is easily seen that straight line configurations of the three bodies can only occur along a finite number, ν, of sidereal directions where

$$\nu = A_2 - A_3 . \qquad (17)$$

This system of conjunction lines, somewhat like the spokes of a wheel, are fixed if the commensurability is exact. An inexact commensurability will result in the system of conjunction lines, or the "wheel", rotating.

The commensurability therefore causes the number of positions of conjunction lines to be limited: the conjunction line may not assume any sidereal direction. As in the case of Sun-Neptune-Pluto, conjunctions cannot occur in the direction of Pluto's perihelion: this could result in close approaches of the two planets and hence instability.

Now if during a numerical integration experiment a situation should arise giving a commensurability in mean motions this could enhance the durability of the system. Suppose during an experiment substantial eccentricities have built up on the osculating orbits of the (m_1, m_2) and/or (M_2, m_3) subsystems. Without a commensurability this system will tend to find itself rapidly in a conjunction where the (m_1, m_2) subsystem is around apocentre and/or the (M_2, m_3) subsystem is around pericentre. This will cause further drastic changes to the orbital elements possibly resulting in instability.

However, if a commensurability in mean motions were to exist then this would restrict the system to conjunctions in specific sidereal directions and hence specific regions of the orbits. The possibility arises that the system may avoid the "worst" conjunctions and survive a little longer until the inexactitude of the commensurability causes the "spokes on the wheel" to rotate allowing a conjunction to occur at a (m_1, m_2) apocentre /(M_2, m_3) pericentre type situation.

Clearly commensurabilities giving the "best chance of survival" are those which result in as few conjunction line directions as possible i.e. small ν, since this will sample the smallest number of all possible conjunction positions. Furthermore, it is probable that ν being odd is favourable since if the number of conjunction lines were even and one was placed at the most favourable position then automatically there would be a conjunction line at the least favourable position.

Of all the features noted in Figures 6.1 - 6.25 only five of these seem accountable to commensurabilities resulting in even values of ν. The probability of an event occurring r times in n trials is

$$ {}^{n}C_{r}\, p^{r}\, q^{n-r} $$

where

$$ {}^{n}C_{r} = \frac{n!}{(n-r)!\, r!} $$

p = probability of event occurring

and q = probability of event not occurring.

If it is then considered that it is an even chance (i.e. $p = q = \frac{1}{2}$) whether a commensurability with an odd or even number of conjunction lines, ν, should arise then it is readily calculated by the above formula that there is less than one chance in 100000 that only five of the thirty-six features which arise would be attributable to commensurabilities with even values of ν. It would seem that this is not a chance occurrence and that there is indeed a preference for commensurabilities resulting in odd values of ν.

In Table 6.3 are given the frequencies of the values of ν arising from the features of the curves noted in Table 6.2. It is seen that the values of ν are all small and even values are avoided.

Table 6.3 - Frequency of Numbers of Conjunction Lines

ν	1	2	3	4	5	6	7
Frequency	15	5	11	0	4	0	1

The "one spoked wheel" type of commensurability is clearly the most favourable of all since there is then only one possible direction for the conjunction line. Such commensurabilities i.e. 6:7, 7:8, 8:9, etc. are concentrated at α_{23} values greater than 0.9: it is felt that this explains the poor fit of curves at $(\varepsilon^{23}, \varepsilon_{32})$ pairs $(10^{-5}, 10^{-5})$, $(10^{-5}, 10^{-6})$, $(10^{-6}, 10^{-5})$, $(10^{-6}, 10^{-6})$ since at these values systems of $\alpha_{23} > 0.9$ are being studied.

6.5 Discussion and Conclusions

The aim of this chapter has been to examine, by means of the ε parameters, the stability of systems lying in the region outwith

the critical stability surfaces. In Section 6.3 it was shown that the durability of systems increased rapidly on approaching a certain value of α_{23} (which value being dependant on the ε parameters). This value was denoted $(\alpha_{23})_o$. The remaining parameters for each of the empirical stability curves were also determined viz. β and γ - these also being ε-dependant.

To examine the validity of the empirical stability curves for predicting the durability of systems three sets of numerical integration experiments were carried out. Each set consisted of one α_{23} value for each of the twenty-five $\varepsilon^{23}, \varepsilon_{32}$ pairs $[\ (10^{-p}, 10^{-q})$ $p = 2,\ldots,6;\ \ q = 2,\ldots,6\ ]$ as before.

Set (1) was taken at the value $\alpha_{23} = (\alpha_{23})_o$, for each $\varepsilon^{23}, \varepsilon_{32}$ pair, and hence should be stable - the results are given in Table 6.4. In this table N_2 denotes the number of passages the (m_1, m_2) subsystem made through its initial sidereal direction (see Section 6.2). N_3 is the corresponding data for the (M_2, m_3) subsystem. Hence if the orbits of the system were not disturbed N_2 and N_3 would be exactly the number of orbits executed by the (m_1, m_2) subsystem and (M_2, m_3) subsystem respectively. N_s is the number of synodic periods computed in the fashion described in Section 6.3. If no perturbation was suffered by the system then N_s would equal $N_s'(= N_2 - N_3)$. It may be noted, as we would expect, that N_s differs from N_s', that difference being greatest when the perturbation on the orbits is greatest i.e. $\varepsilon^{23} = 10^{-2}$ and $\varepsilon_{32} = 10^{-2}$. The difference between N_s and N_s' varies reasonably smoothly with the ε parameters.

Set (2) - see Table 6.5 - includes systems which, excepting those at small ε values, are predicted to run for several tens of synodic periods. Clearly the predictions will be affected by the errors contained within the curve parameters $(\alpha_{23})_o$, β and γ. It is therefore necessary to find out how sensitive the predictions are to errors in these parameters. To this end we differentiate N_s, as calculated by Equation (8), with respect to $(\alpha_{23})_o$, β and γ to obtain

Table 6.4 - Set (1): Experiments at Empirical Stability Limit

ϵ^{23}	ϵ_{32}	α_{23}	N_2	N_3	N'_s	N_s
10^{-2}	10^{-2}	0.475	400	121	279	241
	10^{-3}	0.619	400	179	221	201
	10^{-4}	0.622	400	182	218	203
	10^{-5}	0.632	400	183	217	199
	10^{-6}	0.627	400	182	218	201
10^{-3}	10^{-2}	0.511	400	130	270	216
	10^{-3}	0.791	400	255	145	111
	10^{-4}	0.790	400	262	138	118
	10^{-5}	0.793	400	263	137	117
	10^{-6}	0.794	400	263	137	116
10^{-4}	10^{-2}	0.516	400	133	267	214
	10^{-3}	0.789	400	261	139	111
	10^{-4}	0.902	400	329	71	56
	10^{-5}	0.911	400	339	61	52
	10^{-6}	0.914	400	340	60	50
10^{-5}	10^{-2}	0.520	400	134	266	212
	10^{-3}	0.798	400	263	157	105
	10^{-4}	0.915	400	339	61	48
	10^{-5}	0.943	400	362	38	33
	10^{-6}	0.953	400	367	33	27
10^{-6}	10^{-2}	0.519	400	134	266	212
	10^{-3}	0.800	400	263	137	104
	10^{-4}	0.917	400	340	60	47
	10^{-5}	0.954	400	358	42	26
	10^{-6}	0.974	400	382	18	15

Table 6.5 - Set (2): Predictions of Durability at $\alpha_{23} > (\alpha_{23})_o$

			Predicted Values		Actual Values		
ε^{23}	ε_{32}	α_{23}	N_s	$\pm \Delta N_s$	N_s	Time	Comments
10^{-2}	10^{-2}	0.4764	100	54	50C	$1.660.10^2$	151B
	10^{-3}	0.6213	100	39	200L	$1.216.10^3$	
	10^{-4}	0.6261	100	26	201L	$1.244.10^3$	
	10^{-5}	0.6337	100	30	87C	$5.578.10^2$	159B
	10^{-6}	0.6283	100	71	95C	$5.946.10^2$	100B
10^{-3}	10^{-2}	0.5116	100	88	89C	$3.422.10^2$	90X: 90B
	10^{-3}	0.7912	100	331	366C	$5.475.10^3$	380 X:380B
	10^{-4}	0.7931	100	28	78C	$1.184.10^3$	88X: 93B
	10^{-5}	0.7947	100	60	223L	$3.558.10^3$	
	10^{-6}	0.7953	100	92	118C	$1.809.10^3$	130 X:132B
10^{-4}	10^{-2}	0.5219	100	15	213L	$8.573.10^2$	
	10^{-3}	0.7904	100	68	221L	$3.303.10^3$	
	10^{-4}	0.9055	60	21	57C	$2.243.10^3$	
	10^{-5}	0.9168	50	14	41C	$1.846.10^3$	42B
	10^{-6}	0.9155	40	51	29C	$1.299.10^3$	36X
10^{-5}	10^{-2}	0.5301	100	17	96C	$4.000.10^2$	97B
	10^{-3}	0.7989	60	48	210L	$3.311.10^3$	
	10^{-4}	0.9183	50	56	79C	$3.646.10^3$	84B
	10^{-5}	0.9458	40	54	84X	$6.063.10^3$	
	10^{-6}	0.9559	10	9	26L	$2.345.10^3$	
10^{-6}	10^{-2}	0.5321	100	18	68C	$2.874.10^2$	70B
	10^{-3}	0.8004	80	184	43B	$6.871.10^2$	
	10^{-4}	0.9183	40	44	21C	$9.736.10^2$	
	10^{-5}	0.9556	15	13	13C	$1.158.10^3$	14X
	10^{-6}	0.9750	10	12	12C	$1.941.10^3$	

$$\frac{\partial N_s}{\partial (\alpha_{23})_o} = \beta\gamma \frac{(1-\alpha_{23})^\gamma}{(\alpha_{23}-(\alpha_{23})_o)^{\gamma+1}} \cdot e^{\beta\left[\frac{1-\alpha_{23}}{(\alpha_{23}-(\alpha_{23})_o}\right]^\gamma} \quad (18)$$

$$\frac{\partial N_s}{\partial \beta} = \left[\frac{1-\alpha_{23}}{\alpha_{23}-(\alpha_{23})_o}\right]^\gamma e^{\beta\left[\frac{1-\alpha_{23}}{\alpha_{23}-(\alpha_{23})_o}\right]^\gamma} \quad (19)$$

and

$$\frac{\partial N_s}{\partial \gamma} = \beta\left[\frac{1-\alpha_{23}}{\alpha_{23}-(\alpha_{23})_o}\right]^\gamma \cdot \ln\left[\frac{1-\alpha_{23}}{\alpha_{23}-(\alpha_{23})_o}\right] e^{\beta\left[\frac{1-\alpha_{23}}{\alpha_{23}-(\alpha_{23})_o}\right]} \cdot \quad (20)$$

These may be used to find the error in the predicted value of N_s due to an inaccuracy in each parameter - $(\alpha_{23})_o$, β and γ , e.g. $\Delta N_s = [\partial N_s/\partial\beta]\cdot\Delta\beta$. It is found, assuming an error half the size of the least significant digit in each parameter, that the predictions for set (2) are most sensitive to errors in $(\alpha_{23})_o$. These errors are presented in Table 6.5 along with the predicted value of N_s, the actual value of N_s obtained by numerical experiment and the details of the instability(s) the systems suffered (if they were unstable).

Set (3) is similar to set (2) except that the predictions are for a small number of synodic periods, ten or less. It is found here that errors due to an inaccuracy in any of $(\alpha_{23})_o$, β or γ are negligible. The data presented in Table 6.6 is similar in form to that of Table 6.5.

From the experiments of set (1) it was found that, over the time interval of the integrations, secular trends in the semi-major axes and eccentricities were absent. Only periodic variations in these were apparent.

Among the twenty-five predictions of set (2) 17 are correct inasmuch as the actual value for N_s is within the error bounds on the predictions. In fact the predicted value is generally close to the actual value. Of the remaining 8 experiments 7 have exceeded the maximum possible predicted values and are still executing their orbits with no sign of secular trends in the semi-major axes or

Table 6.6 - Set (3): Predictions of Durability at $\alpha_{23} > (\alpha_{23})_o$

			Predicted Values			Actual Values		
ε^{23}	ε_{32}	α_{23}	N_s	$\pm$	ΔN_s	N_s	Time	Comments
10^{-2}	10^{-2}	0.4855	10		0	125C	$4.274.10^2$	127B
	10^{-3}	0.6310	10		0	56C	$3.569.10^2$	76B
	10^{-4}	0.6385	10		0	13C	$8.806.10^1$	20B
	10^{-5}	0.6471	10		0	5C	$3.108.10^1$	
	10^{-6}	0.6336	10		0	38C	$2.409.10^2$	
10^{-3}	10^{-2}	0.5212	10		0	13C	$5.024.10^1$	14B
	10^{-3}	0.7932	10		1	198B	$3.013.10^3$	
	10^{-4}	0.8065	10		0	32C	$5.231.10^2$	56X:60B
	10^{-5}	0.8004	10		0	222C	$3.524.10^3$	225B
	10^{-6}	0.7985	10		1	229L	$3.586.10^3$	
10^{-4}	10^{-2}	0.5459	10		0	32C	$1.409.10^2$	33B
	10^{-3}	0.7957	10		0	12B	$1.876.10^2$	
	10^{-4}	0.9130	6		0	7C	$2.799.10^2$	9X
	10^{-5}	0.9246	5		0	2X	$1.057.10^2$	
	10^{-6}	0.9173	4		1	25C	$1.115.10^3$	
10^{-5}	10^{-2}	0.5436	10		0	15C	$6.675.10^1$	16B
	10^{-3}	0.8057	6		0	9C	$1.506.10^2$	11B
	10^{-4}	0.9199	5		2	5C	$2.143.10^2$	5X
	10^{-5}	0.9472	4		1	45X	$3.337.10^3$	
	10^{-6}	0.9580	1		0	6C	$5.654.10^3$	
10^{-6}	10^{-2}	0.5432	10		0	26C	$1.142.10^2$	32B
	10^{-3}	0.8022	8		1	112C	$1.808.10^3$	114B
	10^{-4}	0.9208	4		0	4X	$2.012.10^2$	
	10^{-5}	0.9578	2		0	49L	$4.661.10^3$	
	10^{-6}	0.9773	1		0	5X	$8.119.10^2$	

eccentricities. Referring back to Figures 6.1 - 6.25 it is possible to attribute these to the peaks which appear on the graphs and therefore they seem to be due to temporary commensurable situations arising during the integration experiment. One system has exhibited instability a little earlier than expected i.e. $\varepsilon^{23} = 10^{-6}$, $\varepsilon_{32} = 10^{-2}$. In Figure 6.26 these results are displayed in the form of a histogram to demonstrate the spread of the actual values about the predicted values. Along the x-axis are plotted the deviation of the actual values, N_{sact}, from the predicted values, N_{spre}, relative to the latter value i.e. $(N_{sact} - N_{spre})/N_{spre}$. This scale is divided into divisions of 0.2 and the number of systems which fall within each division is counted and displayed by a vertical bar. For example it is found that 3 systems lie within ± 10% of the predicted value of N_s, etc. The relatively good agreement of ε values 10^{-5} and 10^{-6} is probably fortuitous since the values of the curve parameters here were only chosen by comparison with neighbouring values.

The results for set (3) do not follow the predictions as closely. This however is not surprising since a temporary commensurability could arise in many of these systems causing the actual value of N_s to greatly exceed the *small* predicted value. Having said that it is worth noting that only 4 of this set of twenty-five actually accomplished a greater number of orbits than the corresponding experiment of set (2). Furthermore only 2 actually survived for a time less than that predicted. It appears then that the empirical stability curves give a good lower limit on the possible number of synodic periods a system will survive through. Figure 6.27 displays the results of Table 6.6 in the same way as Figure 6.26.

The empirical stability curves thus, in general, allow reliable predictions to be made of the durability of three-body systems. The value $(\alpha_{23})_o$ demonstrates the existence of a region of stability outwith the analytical stability region given by the critical stability surface. Furthermore, the division between the regions of stability and instability is sharp: the empirical stability curve climbs rapidly to obtain very high values of N_s over a small range in α_{23}. This is in agreement with Nacozy (1977) who found that secular trends were immediately apparent in the elements of Saturn's orbit when the masses

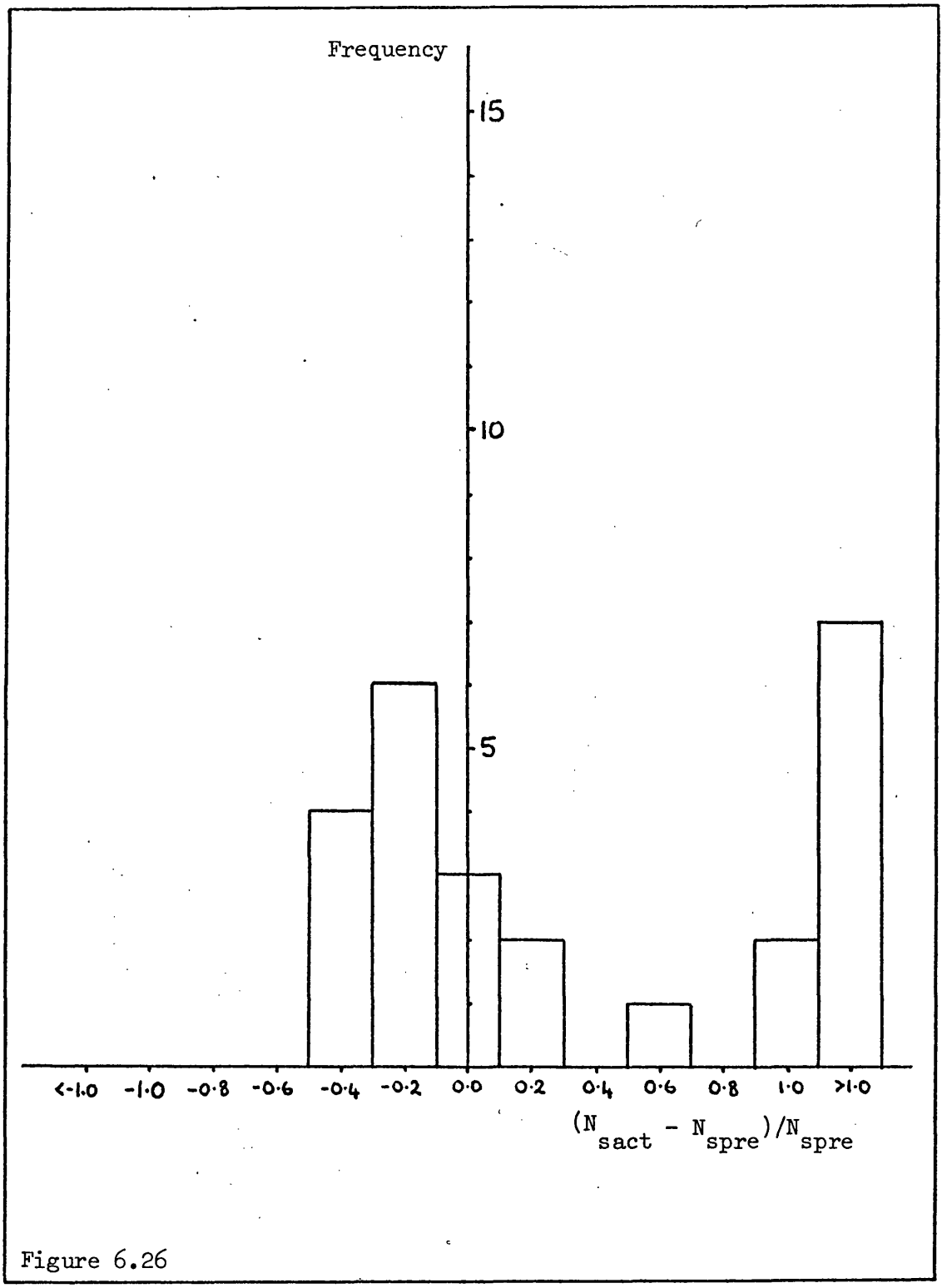
Frequency
15
10
5
<-1.0
-1.0
-0.8
-0.6
-0.4
-0.2
0.0
0.2
0.4
0.6
0.8
1.0
>1.0
(N sact - N spre)/N spre

Figure 6.26

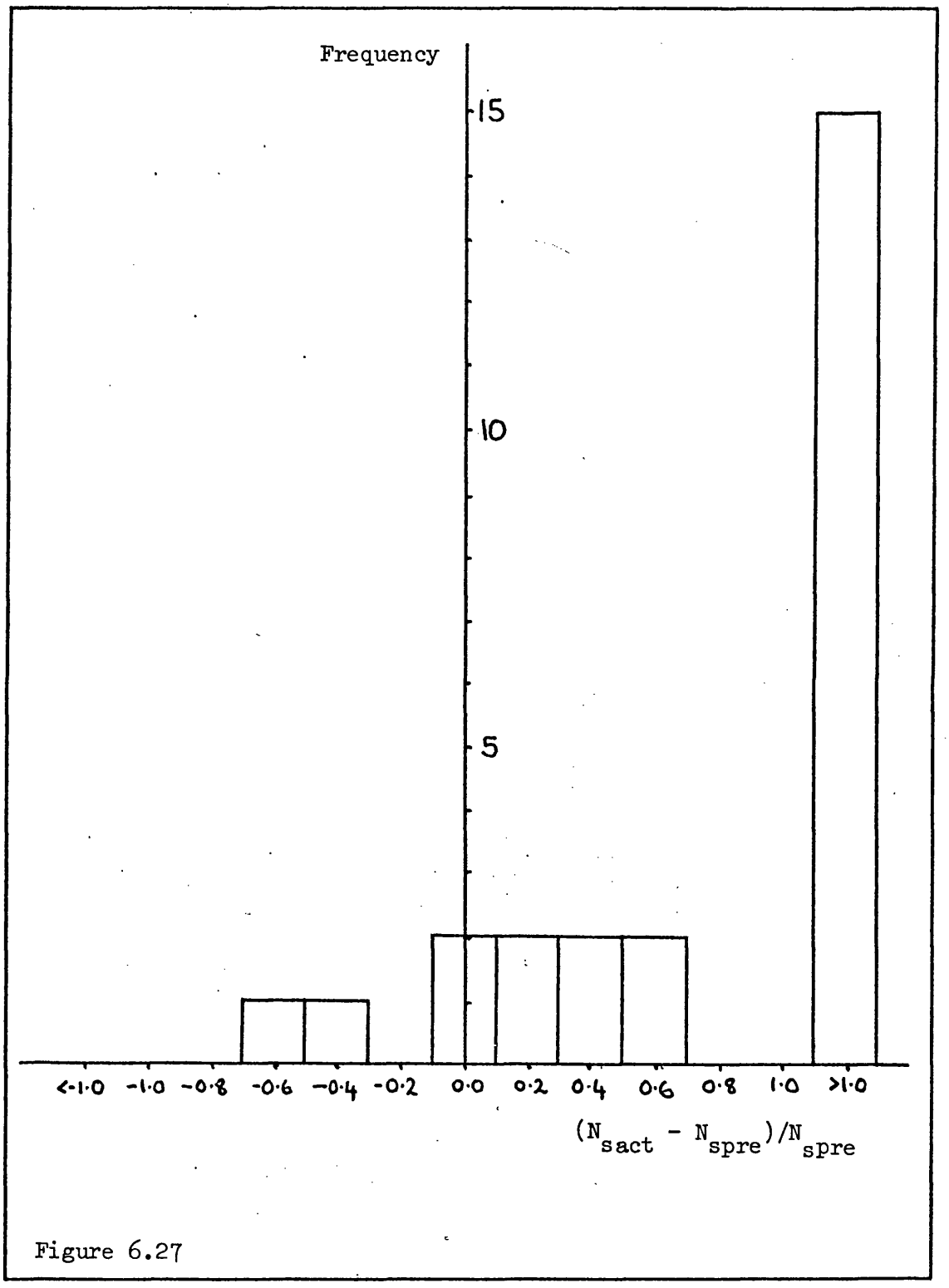
Frequency
15
10
5
<-1·0
-1·0
-0·8
-0·6
-0·4
-0·2
0·0
0·2
0·4
0·6
0·8
1·0
>1·0
$(N_{sact} - N_{spre})/N_{spre}$

Figure 6.27

of Jupiter and Saturn were multiplied by a factor beyond about 30. Below this value secular trends were apparently totally absent indicating a rapid transition from stability to instability. Nacozy's work will be referred to later.

It has been shown that only in cases where temporary commensurabilities arise does the actual value of N_s differ significantly from the predicted value. Clearly of course the $(\alpha_{23})_o$ value itself may be affected by commensurabilities. If the empirical stability curve should begin to rise close to an α_{23} value which can give rise to a commensurable situation then this will tend to increase $(\alpha_{23})_o$ and steepen the curve. This situation appears to have arisen when $\varepsilon^{23} = 10^{-3}$ and $\varepsilon_{32} = 10^{-3}$ since at these ε values $(\alpha_{23})_o$ is greater than the value at $\varepsilon^{23} = 10^{-3}$ and $\varepsilon_{32} = 10^{-4}$ or $\varepsilon^{23} = 10^{-4}$ and $\varepsilon_{32} = 10^{-3}$. Similarly at $\varepsilon^{23} = 10^{-2}$ and $\varepsilon_{32} = 10^{-5}$ $(\alpha_{23})_o$ is again anomalously high. The commensurabilities do indeed appear to be the reason for the peaks in the curves of the actual values of N_s. It would be unlikely, if they were chosen at random, that only *five* features would arise from commensurabilities giving an even number of conjunction line directions. The reasons for this were stated in Section 6.4.

It is an interesting feature of all the experiments conducted that in all the systems studied the body which was removed from the system was the one with smallest mass. This is reasonable since the smaller body will generally experience a larger disturbing force i.e. a larger ε value. This point will be discussed further in Chapter 7 where the relationship between the ε parameters and the variations imposed on the osculating Keplerian orbits of the (m_1, m_2) and (M_2, m_3) subsystems is examined.

As was mentioned previously Nacozy (1977) found that the Sun-Jupiter-Saturn system became unstable when the masses of Jupiter and Saturn were multiplied by a factor about 30. Saturn was ejected from the system in 10000 years or less. This increase in the Jovian and Saturnian masses results in ε values of $\varepsilon^{23} = 7.899.10^{-3}$ and $\varepsilon_{32} = 1.364.10^{-3}$(see Chapter 4, Table 4.1). Now if we consider the values of $(\alpha_{23})_o$ derived previously and interpolate, the appropriate value of $(\alpha_{23})_o$ for the system of augmented Jupiter and Saturn masses

may be obtained, viz. $(\alpha_{23})_o \sim 0.62$. This value is greater than the actual value of α_{23}, 0.55, and would suggest that Nacozy's system should be stable. However the effect of the eccentricities of the Jovian and Saturnian orbits has been neglected. It is reasonable to suppose that the value $(\alpha_{23})_o = 0.62$ should be compared with the value of α_{23} arising at a conjunction of Jupiter and Saturn occurring when Jupiter is at aphelion and Saturn is at perihelion viz.

$$\alpha_{23} = \frac{a_J}{a_S} \cdot \frac{1 + e_J}{1 - e_S} \qquad (21)$$

where suffix "J" denotes Jupiter and suffix "S" Saturn. Substituting values for $a_J/a_S = 0.55$, $e_J = 4.8.10^{-2}$ and $e_S = 5.6.10^{-2}$ we obtain $\alpha_{23} = 0.61$ at this configuration. This is remarkably good agreement. In fact we might expect, due to the large ε values of Nacozy's system, that the eccentricities of the orbits would be increased, due to the greater perturbation, allowing $\alpha_{23} > 0.62$ and hence resulting in instability. It is therefore expected that agreement with Nacozy's study would be possible if eccentricities were included in the present study. In the next chapter we proceed to examine the changes in the eccentricities and semi-major axes of the systems due to various ranges of perturbation.

CHAPTER 7 THE PREDICTION OF THE AMPLITUDE OF THE VARIATIONS IN SEMI-MAJOR AXES AND ECCENTRICITIES IN COPLANAR, COROTATIONAL, INITIALLY CIRCULAR, HIERARCHICAL THREE-BODY SYSTEMS

7.1 Introduction

Due to the way in which the ε parameters arise in the equations of motion, when the latter are expressed in the Jacobian coordinate system, it has been conjectured that they will be related to the changes imposed on the Keplerian orbits of a hierarchical system by perturbations from the other bodies of the system. In other words, the ε parameters are taken to characterise the magnitude of the disturbance on the Keplerian orbits of a system relative to the central two-body force: it is reasonable to suppose that these in turn are directly related to the changes in the osculating semi-major axes, eccentricities, etc. defining the orbits of the system. For example, it is reasonable to suppose that a system which results in ε parameters of the order of 10^{-3} will in general have its constituent orbits perturbed to a greater extent than one in which the ε parameters are around 10^{-6}.

Following the above argument it was decided to carry out a study to determine empirically, if possible, the relationship between the ε parameters and the changes in the osculating semi-major axes and eccentricities in the coplanar, co-rotational, initially circular, hierarchical three-body problem. The reasons for choosing to study three-body systems is again purely on the grounds of simplicity. Questions which this chapter will try to answer are:

For stable systems, are the amplitude of the periodic variations in the semi-major axes and eccentricities directly related, *in a simple way*, to the ε parameters?

Over what range in ε parameters and α ratio is the relationship valid?

In Section 7.2 a brief description is given of the numerical experiments which were used in the investigation; a fuller description of these has already been given in Chapter 6, Section 6.2. The results are given in this section in graphical form and enable us to draw attention to several interesting features arising from the graphs.

The effect commensurabilities have on the relationship between the ε parameters and the variations in the semi-major axes and eccentricities is also considered (see Section 7.3). Discussion of the results is presented in Section 7.4 along with some conclusions.

7.2 The Numerical Experiments and Results

As in Chapter 6 the systems are examined in terms of their ε parameters - ε^{23} ,ε_{32} - and initial α_{23} ratio. The ε parameters were allowed to take values in the range 10^{-i} where $i = 2,3,\ldots,6$ with the α_{23} value lying between $2(\varepsilon^{23})^{\frac{1}{2}}$ and unity; the former value being the lower limit for real systems as given in Chapter 4. Generally values were taken at steps of 0.05 in initial α_{23}.

Again our attention is restricted to considering only coplanar, corotational and initially circular orbits (i.e. $e_2 = e_3 = 0$; ϖ_2, ϖ_3, f_2, f_3 are then indeterminate initially): also only initially straight line configurations are studied where the bodies assume the order $m_1m_2m_3$ (i.e. $\theta = 0$ as defined in Chapter 5). These initial conditions were also described in Chapter 6 (see Section 6.2).

The time interval over which the numerical experiments were carried out was determined by the method as described in the above section. Each integration in this study was continued for 200 passages of the (m_1,m_2) subsystem through its initial sidereal direction, as referred to some fixed reference direction, or until one or other of the osculating eccentricities exceeded unity indicating that a break-up had occurred.

Some 454 experiments of the above type were carried out. In each the maximum deviations (from initial values) of the semi-major axes and eccentricities of the (m_1,m_2) and (M_2,m_3) subsystems, denoted (a_2,e_2) and (a_3,e_3) respectively, were determined. These variations in semi-major axes and eccentricities were denoted Δa_2, Δe_2, Δa_3 and Δe_3. (It may be noted that some of the values from the high range of α_{23} ($\alpha_{23} \gtrsim 0.8$) are omitted for certain pairs of ε parameters; this occurs since the system is so unstable that meaningful deviations from the original values of the semi-major axes and eccentricities are not obtainable).

Having obtained the maximum variation in the important orbital parameters - (a_2, e_2) and (a_3, e_3) - these were then plotted in the following fashion. The variations in the semi-major axes were first normalized i.e. $\Delta a_2/a_2$ and $\Delta a_3/a_3$ were formed. This done, the values of $\log_{10}(\Delta a_2/a_2)$, $\log_{10}(\Delta e_2)$, $\log_{10}(\Delta a_3/a_3)$ and $\log_{10}(\Delta e_3)$ were plotted against the initial α_{23} value, for a given pair of ε parameters. The graphs obtained are shown in Figures 7.1 - 7.20.

On each figure five curves are displayed: each curve is marked with a bracket of the form (i,j), where i and j are integers, this gives the values of the ε parameters for that curve viz. $\varepsilon^{23} = 10^{-i}$, $\varepsilon_{32} = 10^{-j}$.

The curves are arranged so that on each figure the ε parameter which is relevant to the variation being plotted goes through the range $10^{-2}, 10^{-3}, \ldots, 10^{-6}$ the other ε parameter remaining fixed. Thus there are five figures for each of the variations - $\Delta a_2/a_2$, Δe_2, $\Delta a_3/a_3$, Δe_3.

The other information presented on the graphs is the appropriate value of the ratio α for critical stability, i.e. α_{cr}, as calculated for $e_2 = e_3 = 0$ and $\theta = 0$. This is displayed as a short vertical bar crossing the appropriate curve.

The curve to the left of α_{cr} (i.e. $\alpha < \alpha_{cr}$) is shown as a solid line. This is the region of stability (i.e. no exchange of bodies is possible) where there indeed seems to be a relationship between the ε parameters and the variations on (a_2,e_2) and (a_3,e_3). To the right of α_{cr} the curve is shown as a dashed line except very close to the α_{cr} value where the above relationship seems to be maintained. This is a consequence of α being less than the empirical stability value $(\alpha_{23})_o$ (as derived in Chapter 6) and thus these systems will still be stable and exhibit only periodic variations in semi-major axes and eccentricities: secular trends are absent. The dashed part of the curves show no distinct relationship between the ε parameters and the changes in semi-major axes and eccentricity. This is due to two factors. Firstly the systems are unstable and hence we might expect the relationship to be lost at these high α_{23} values. It is also due, in part, to the integration experiments being terminated as the osculating eccentricity exceeds unity; the values of the variations plotted is then the highest value previous to when the osculating eccentricity of one of the orbits exceeded unity.

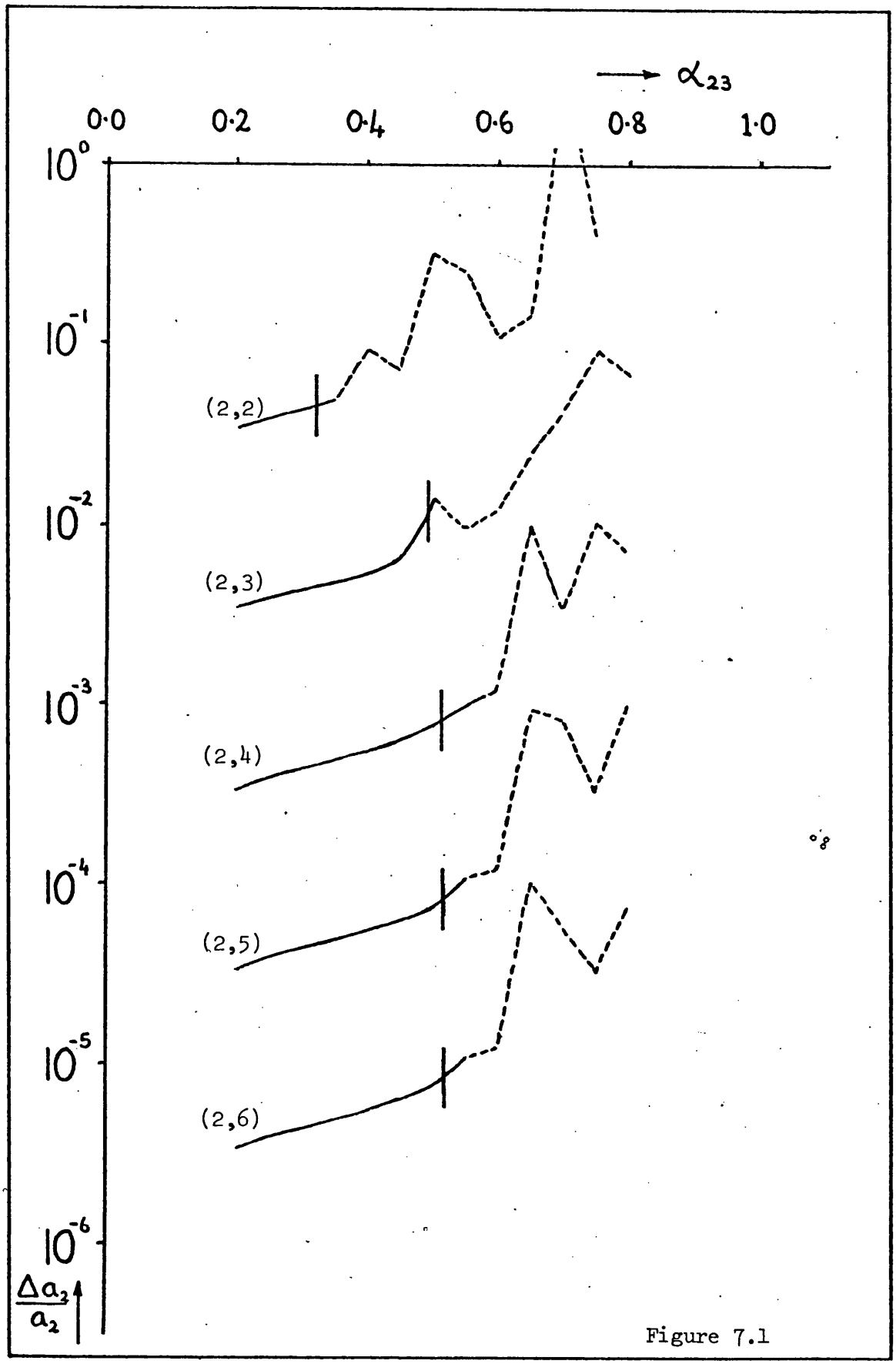
α_{23}
0·0
0·2
0·4
0·6
0·8
1·0
10^{0}
10^{-1}
10^{-2}
10^{-3}
10^{-4}
10^{-5}
10^{-6}
(2,2)
(2,3)
(2,4)
(2,5)
(2,6)
$\frac{\Delta a_2}{a_2}$

Figure 7.1

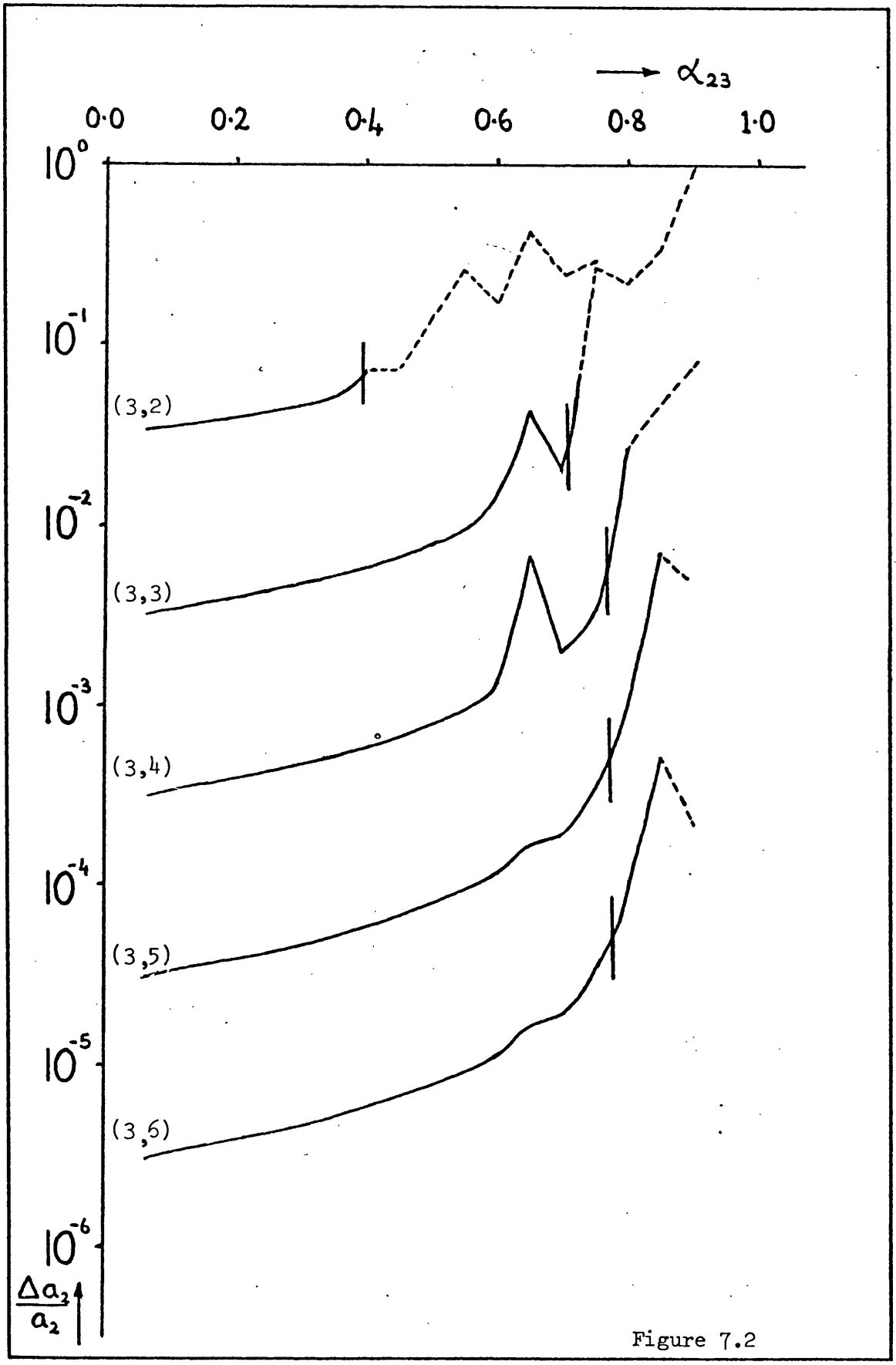
α_{23}
0·0
0·2
0·4
0·6
0·8
1·0
10^{0}
10^{-1}
10^{-2}
10^{-3}
10^{-4}
10^{-5}
10^{-6}
(3,2)
(3,3)
(3,4)
(3,5)
(3,6)
$\frac{\Delta a_2}{a_2}$

Figure 7.2

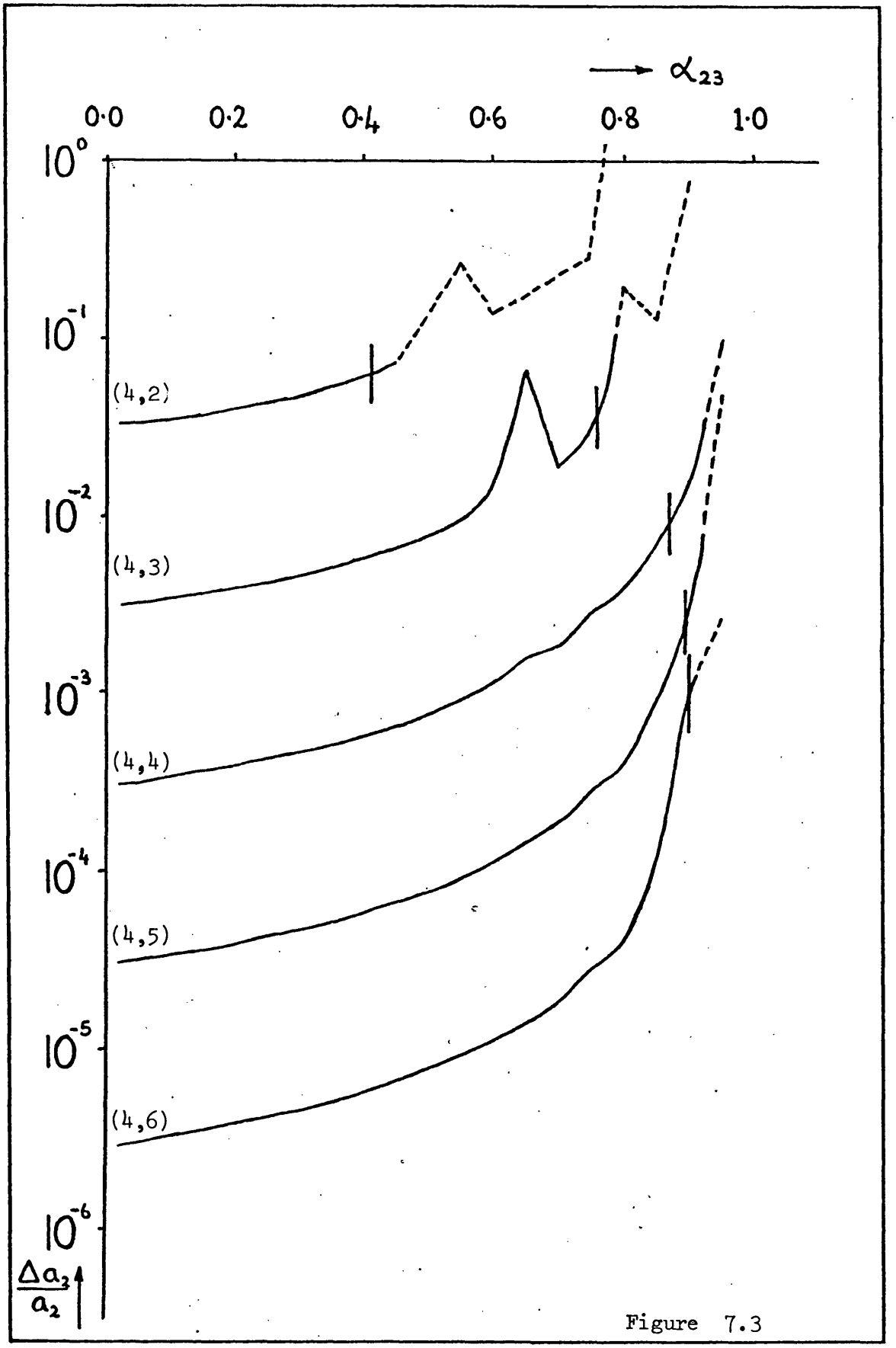
α_{23}
0·0
0·2
0·4
0·6
0·8
1·0
10^{0}
10^{-1}
10^{-2}
10^{-3}
10^{-4}
10^{-5}
10^{-6}
(4,2)
(4,3)
(4,4)
(4,5)
(4,6)
$\frac{\Delta a_3}{a_2}$

Figure 7.3

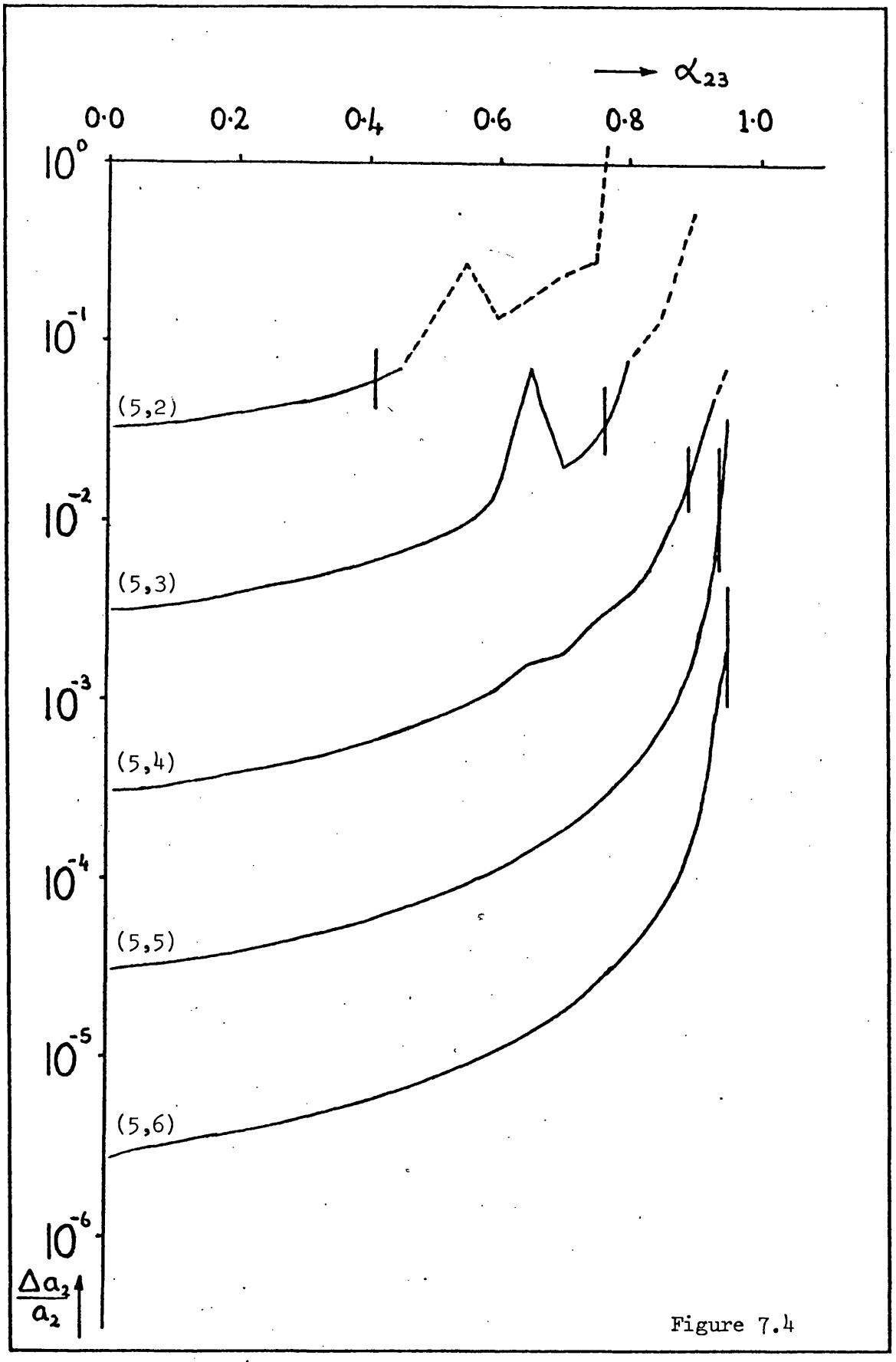
α_{23}
0·0
0·2
0·4
0·6
0·8
1·0
10^{0}
10^{-1}
10^{-2}
10^{-3}
10^{-4}
10^{-5}
10^{-6}
(5,2)
(5,3)
(5,4)
(5,5)
(5,6)
$\frac{\Delta a_2}{a_2}$

Figure 7.4

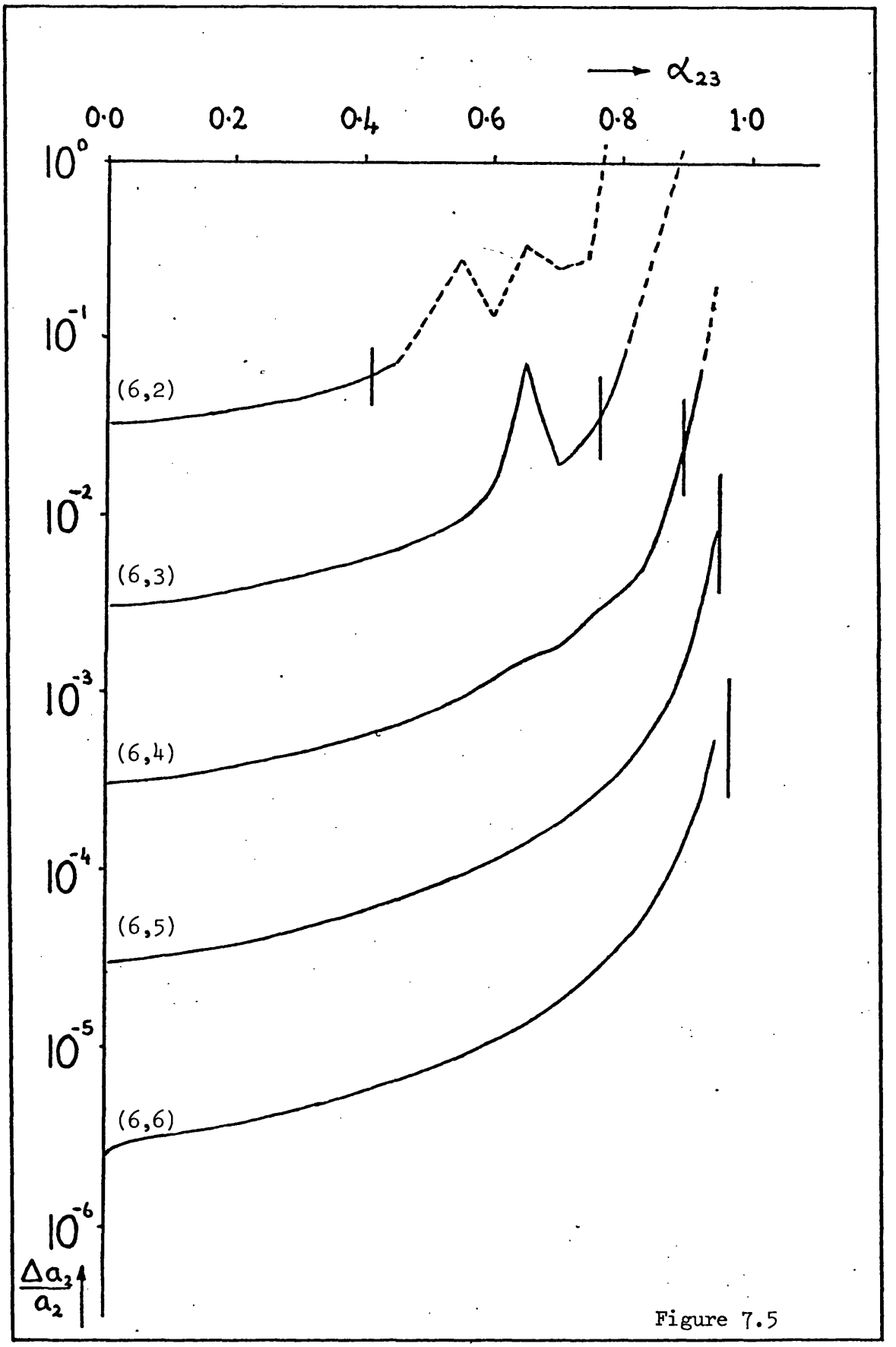
α_{23}
0·0
0·2
0·4
0·6
0·8
1·0
10^{0}
10^{-1}
10^{-2}
10^{-3}
10^{-4}
10^{-5}
10^{-6}
(6,2)
(6,3)
(6,4)
(6,5)
(6,6)
$\frac{\Delta a_2}{a_2}$

Figure 7.5

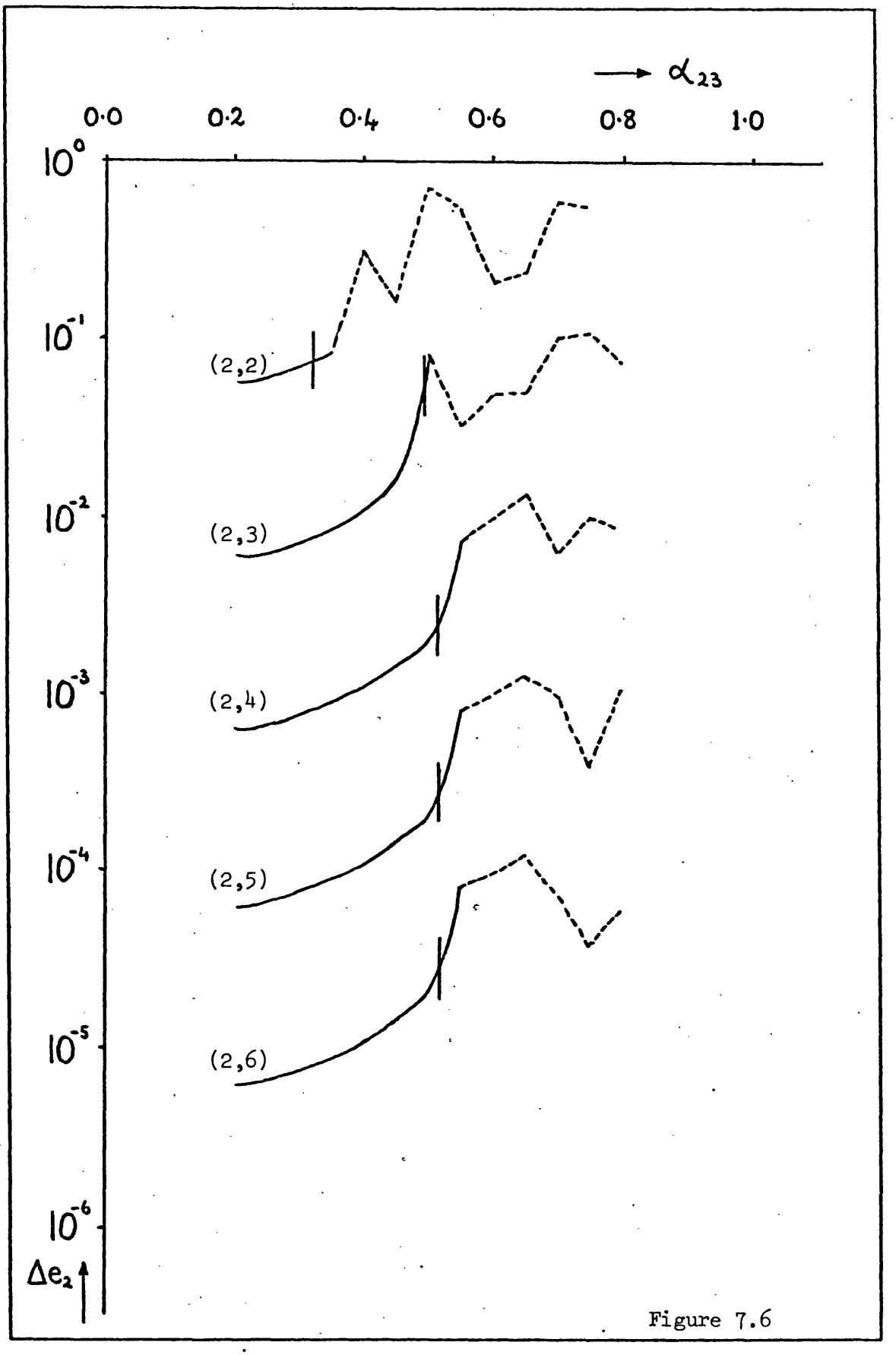
α_{23}
0·0
0·2
0·4
0·6
0·8
1·0
10^{0}
10^{-1}
10^{-2}
10^{-3}
10^{-4}
10^{-5}
10^{-6}
Δe_2
(2,2)
(2,3)
(2,4)
(2,5)
(2,6)

Figure 7.6

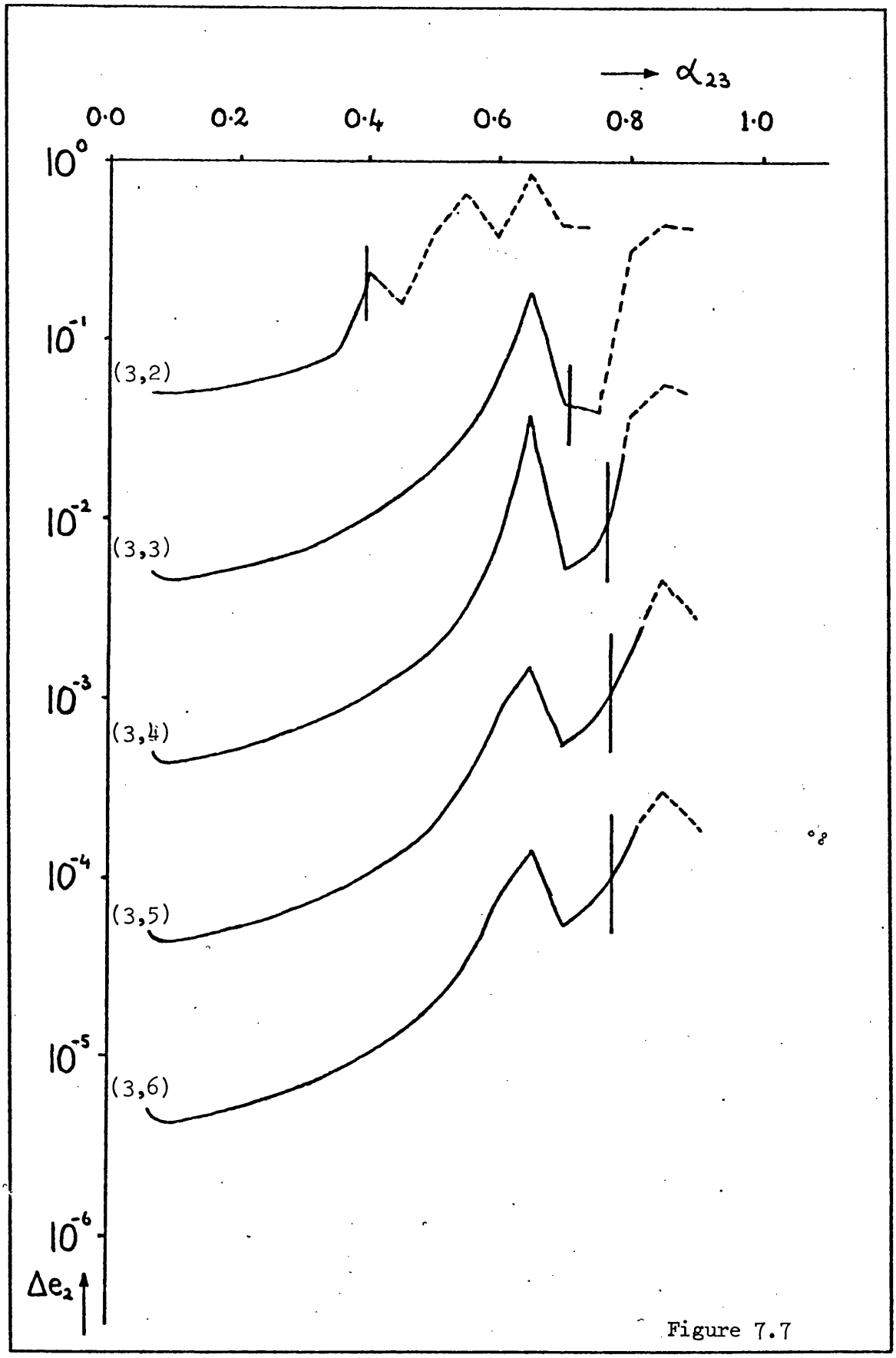
α_{23}
0·0
0·2
0·4
0·6
0·8
1·0
10^{0}
10^{-1}
10^{-2}
10^{-3}
10^{-4}
10^{-5}
10^{-6}
(3,2)
(3,3)
(3,4)
(3,5)
(3,6)
Δe_2

Figure 7.7

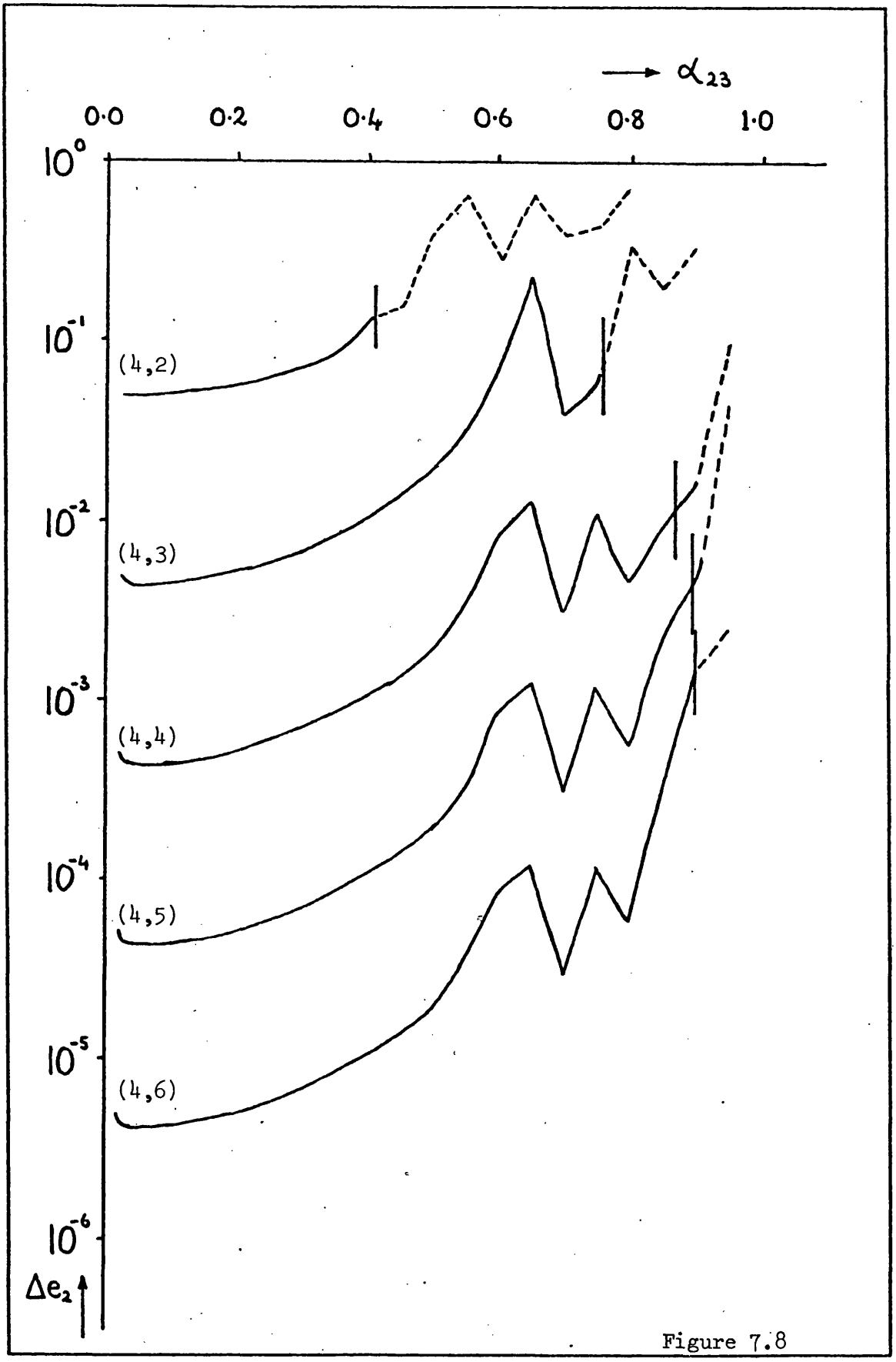
α_{23}
0·0
0·2
0·4
0·6
0·8
1·0
10^{0}
10^{-1}
10^{-2}
10^{-3}
10^{-4}
10^{-5}
10^{-6}
Δe_2
(4,2)
(4,3)
(4,4)
(4,5)
(4,6)

Figure 7.8

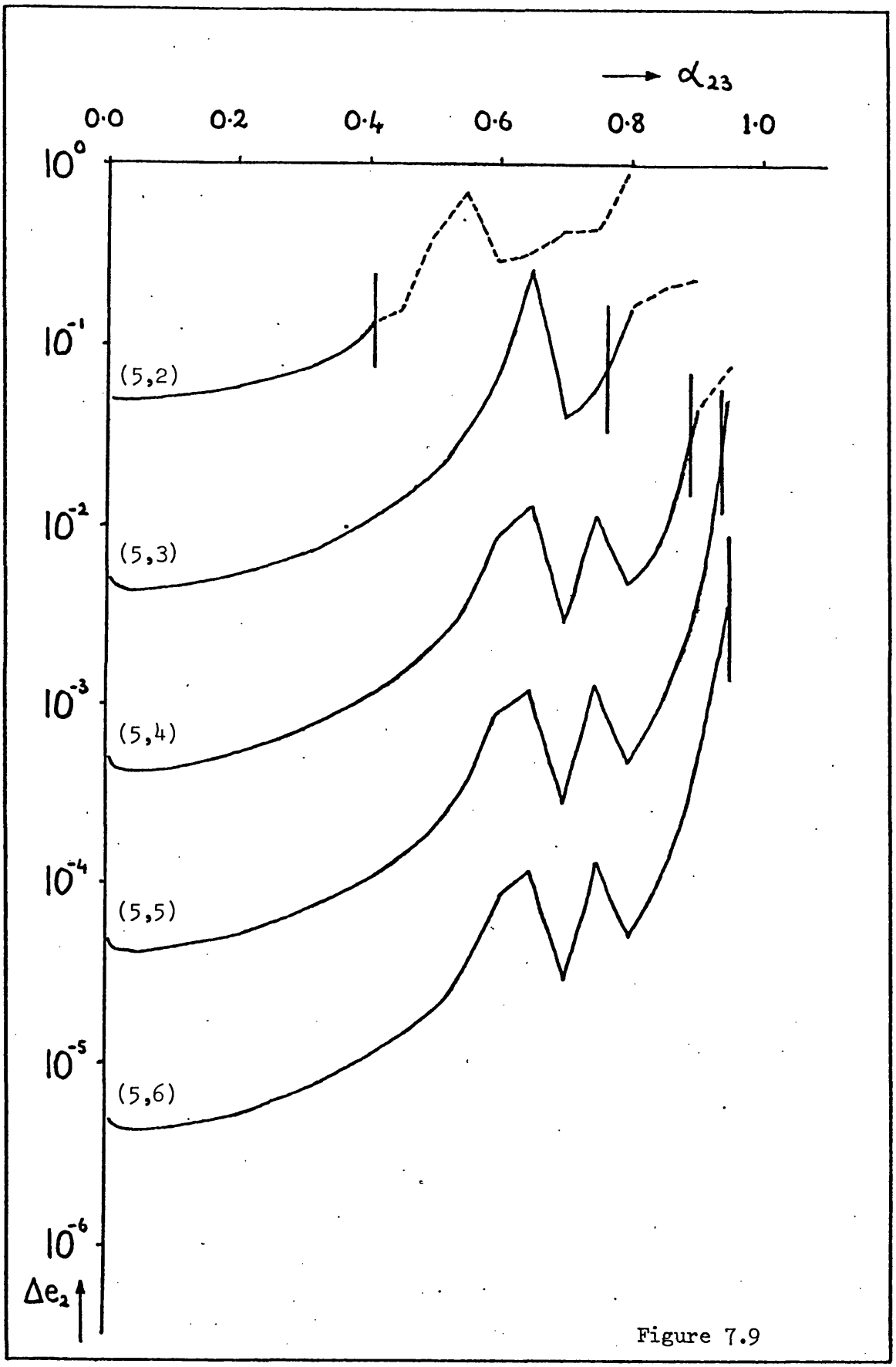
α_{23}
0·0
0·2
0·4
0·6
0·8
1·0
10^{0}
10^{-1}
10^{-2}
10^{-3}
10^{-4}
10^{-5}
10^{-6}
Δe_2
(5,2)
(5,3)
(5,4)
(5,5)
(5,6)

Figure 7.9

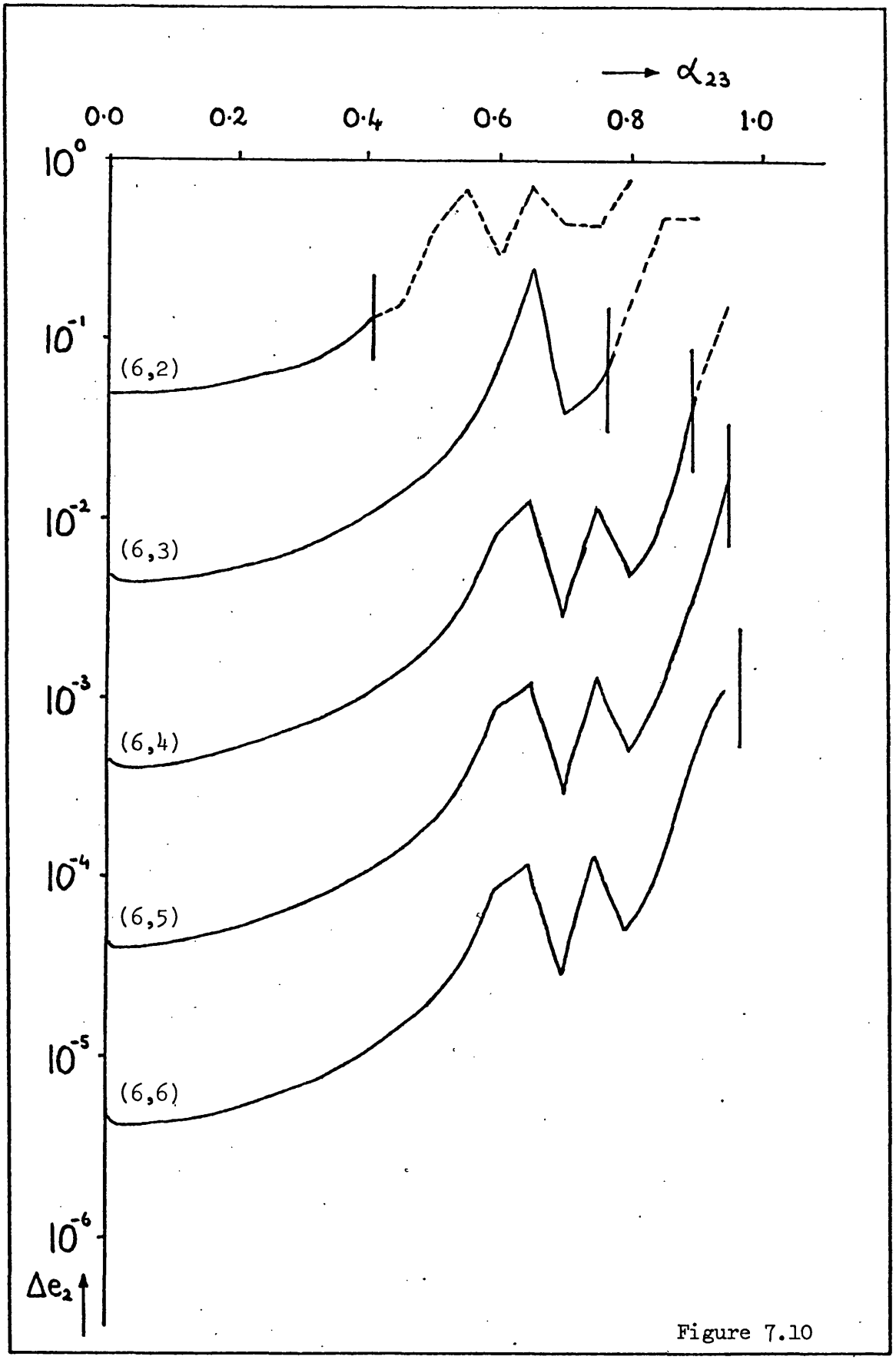
α_{23}
0·0
0·2
0·4
0·6
0·8
1·0
10^{0}
10^{-1}
10^{-2}
10^{-3}
10^{-4}
10^{-5}
10^{-6}
(6,2)
(6,3)
(6,4)
(6,5)
(6,6)
Δe_2

Figure 7.10

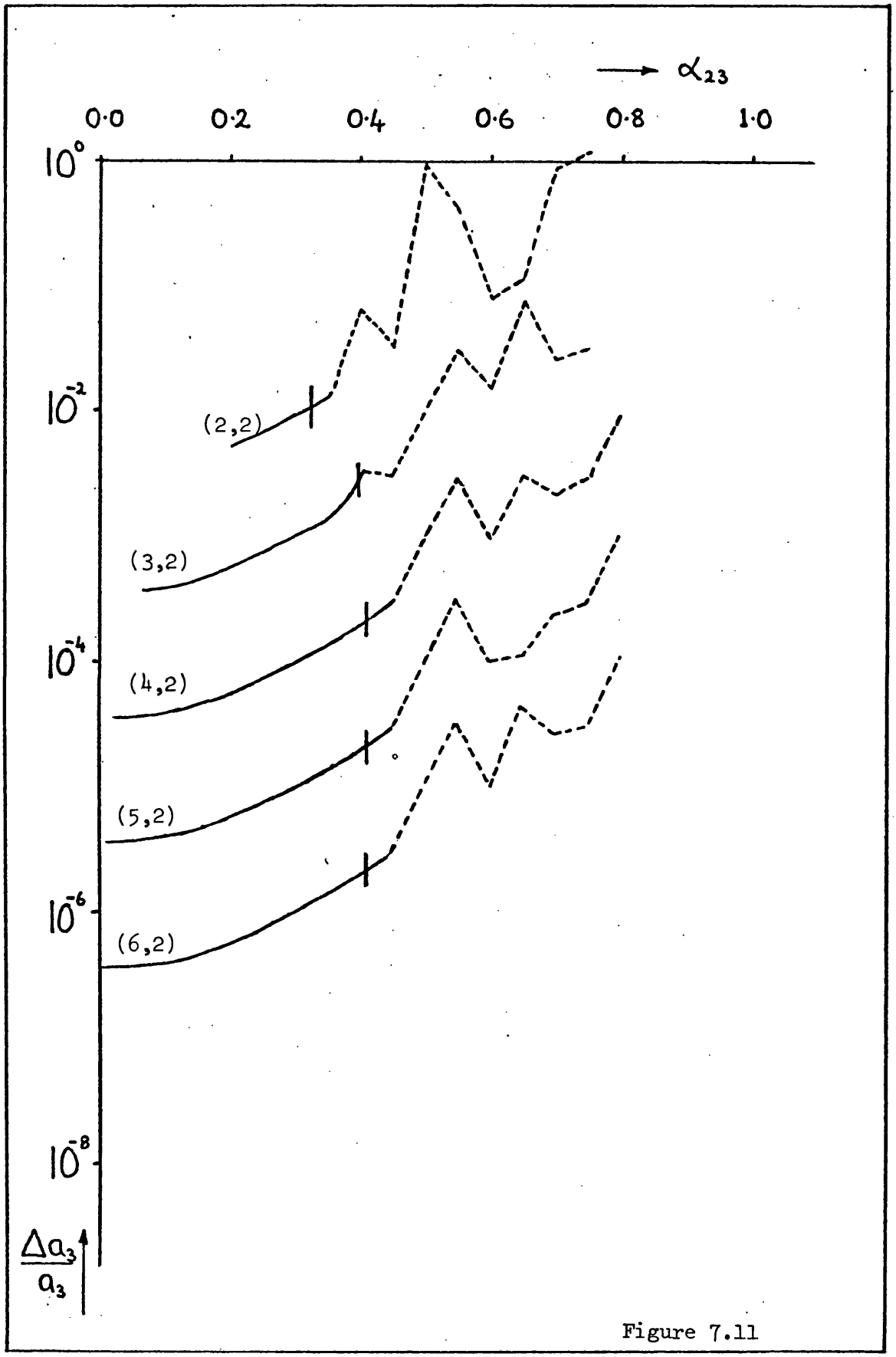
α_{23}
0·0
0·2
0·4
0·6
0·8
1·0
10^{0}
10^{-2}
10^{-4}
10^{-6}
10^{-8}
(2,2)
(3,2)
(4,2)
(5,2)
(6,2)
$\frac{\Delta a_3}{a_3}$

Figure 7.11

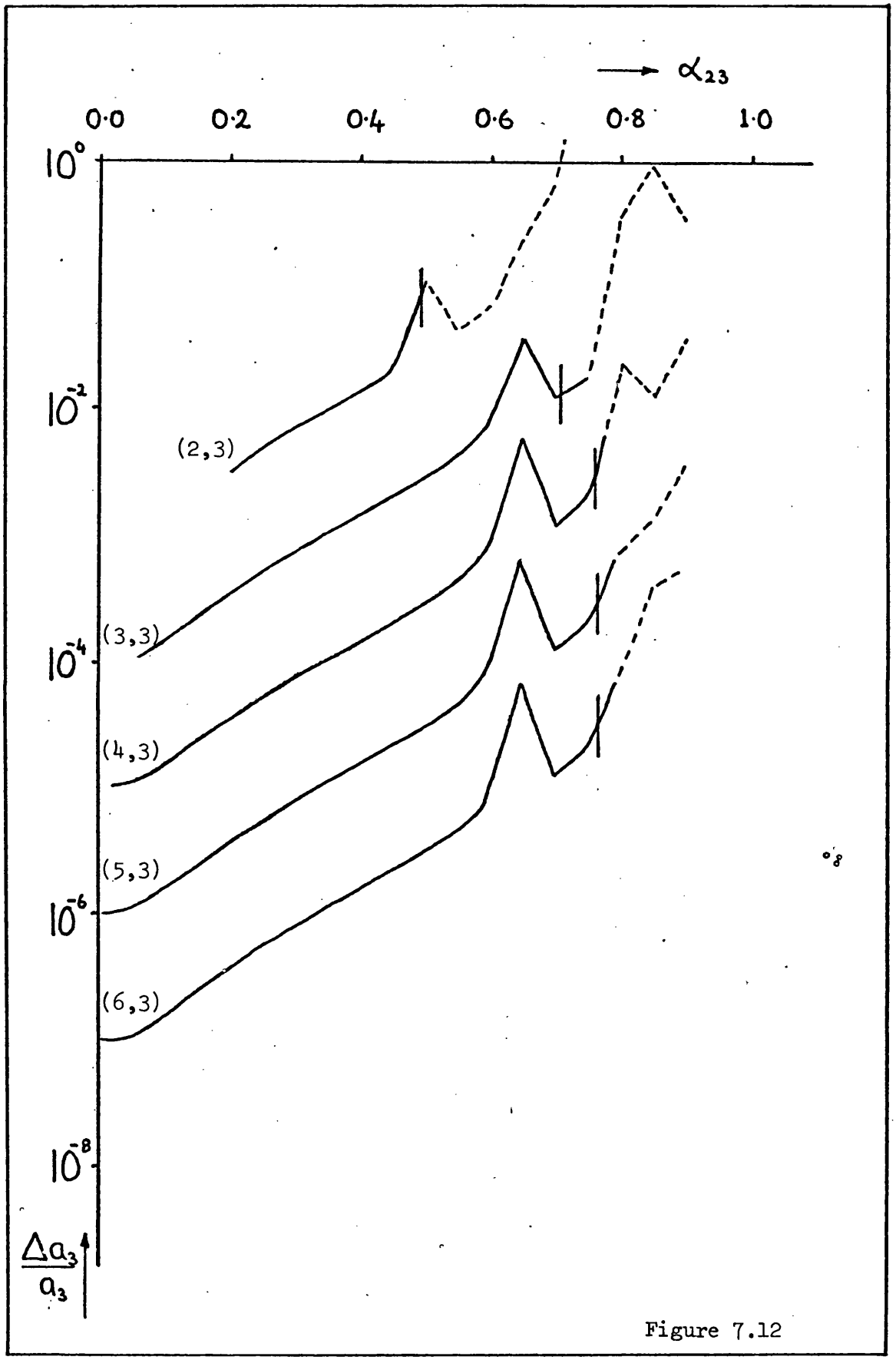
α_{23}
0·0
0·2
0·4
0·6
0·8
1·0
10^{0}
10^{-2}
10^{-4}
10^{-6}
10^{-8}
(2,3)
(3,3)
(4,3)
(5,3)
(6,3)
$\frac{\Delta a_3}{a_3}$

Figure 7.12

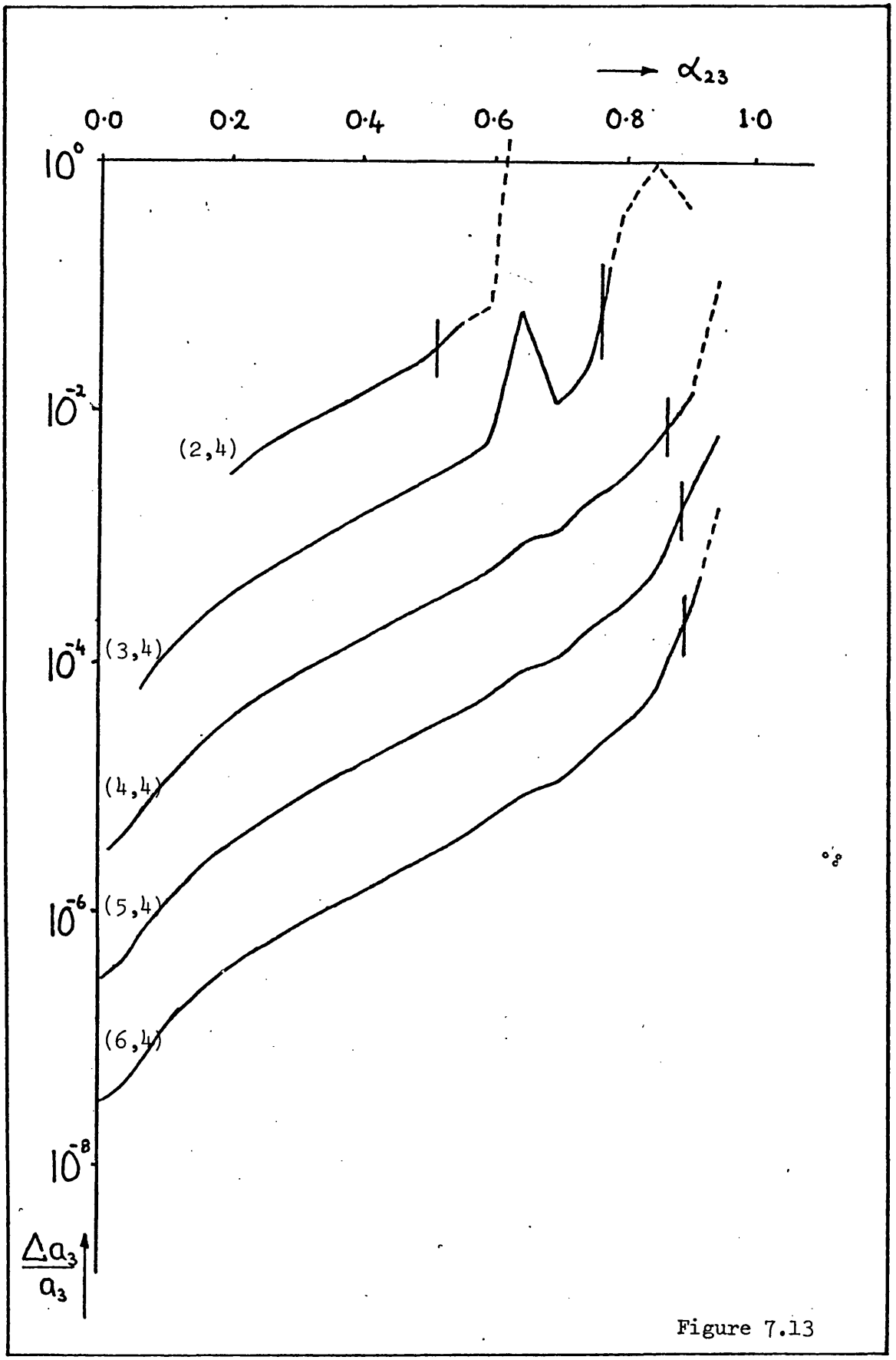
α_{23}
0·0
0·2
0·4
0·6
0·8
1·0
10^{0}
10^{-2}
10^{-4}
10^{-6}
10^{-8}
(2,4)
(3,4)
(4,4)
(5,4)
(6,4)
$\frac{\Delta a_3}{a_3}$

Figure 7.13

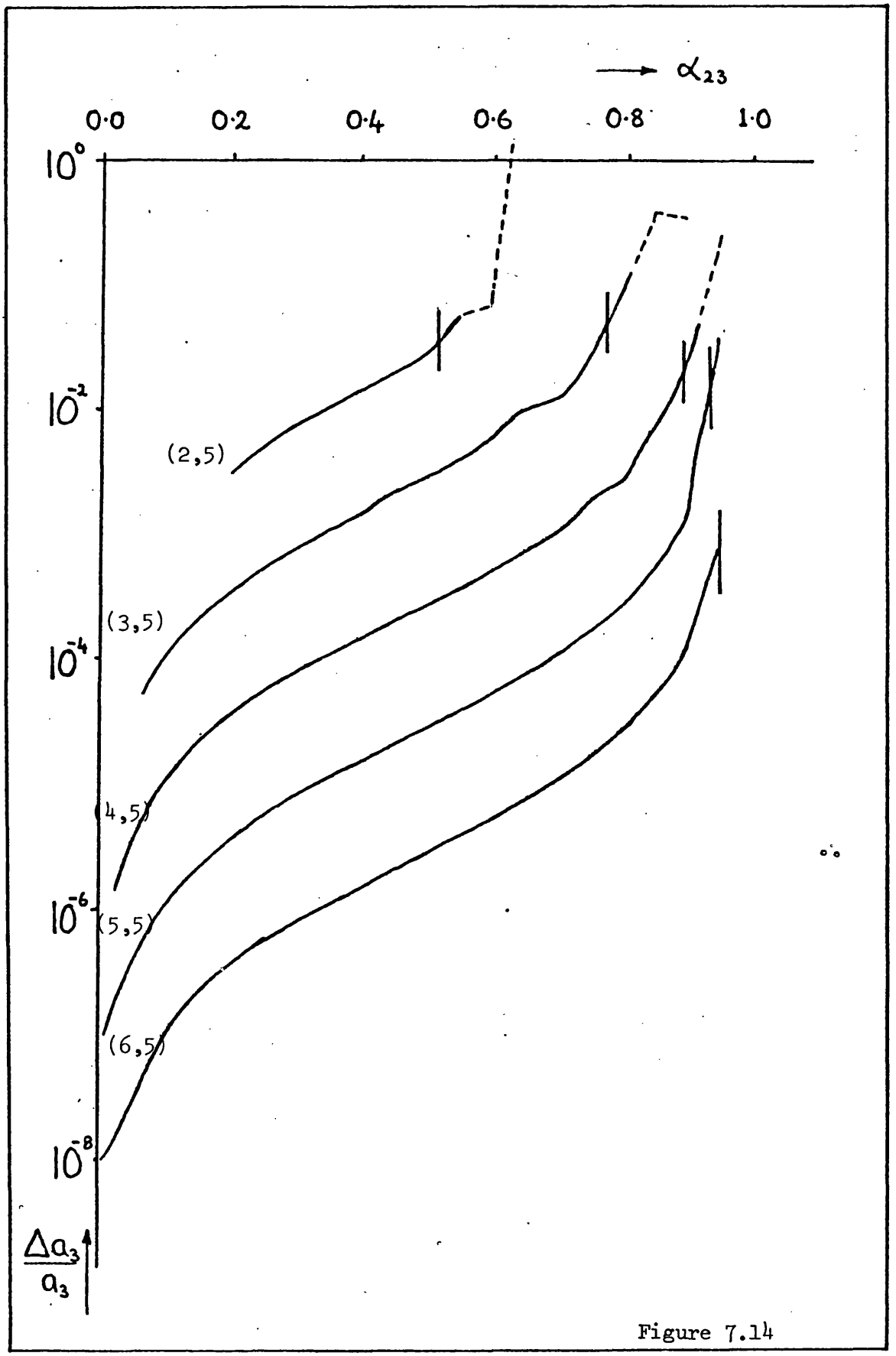
α_{23}
0·0
0·2
0·4
0·6
0·8
1·0
10^{0}
10^{-2}
10^{-4}
10^{-6}
10^{-8}
(2,5)
(3,5)
(4,5)
(5,5)
(6,5)
$\frac{\Delta a_3}{a_3}$

Figure 7.14

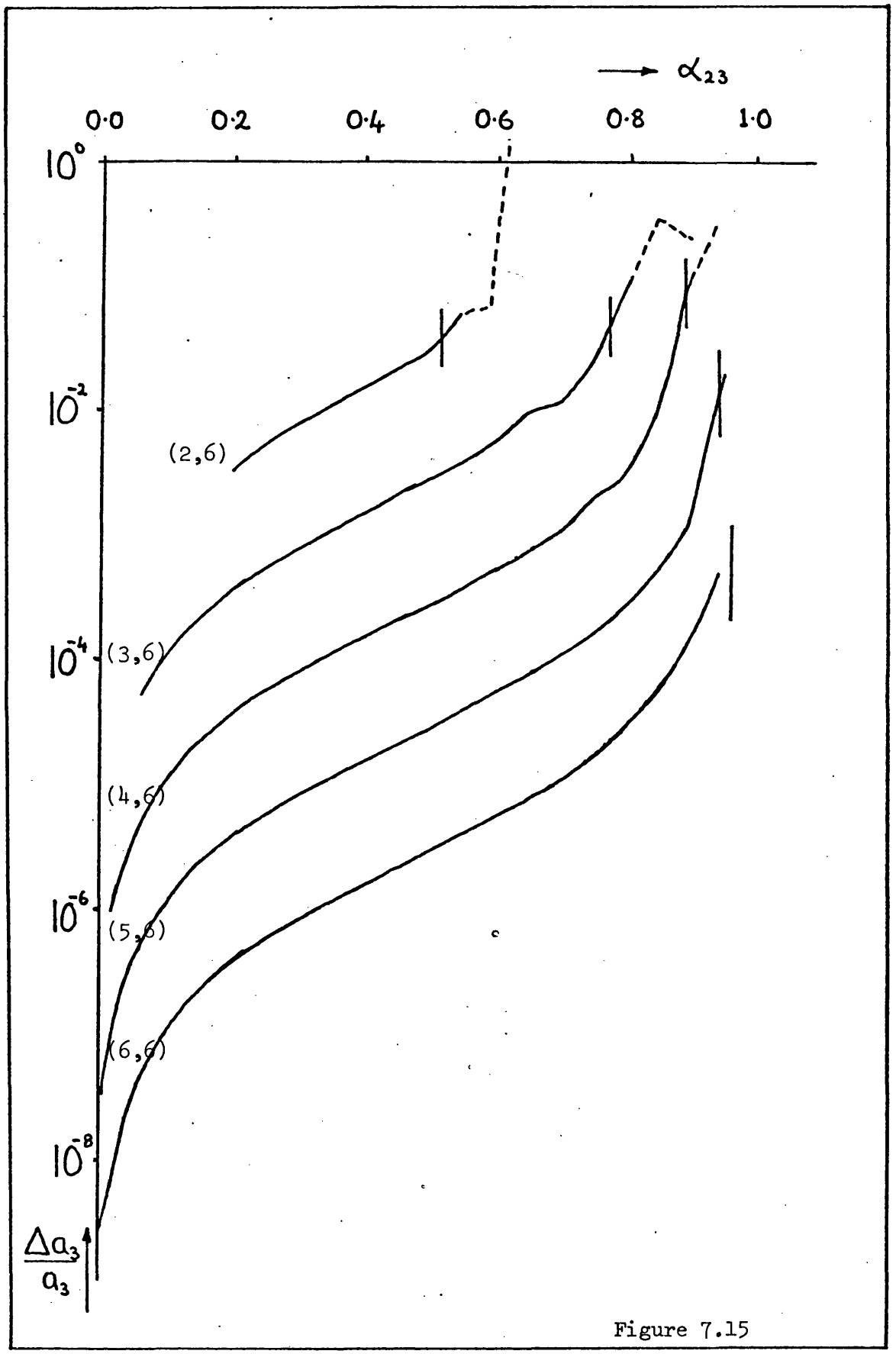
α_{23}
0·0
0·2
0·4
0·6
0·8
1·0
10^{0}
10^{-2}
10^{-4}
10^{-6}
10^{-8}
(2,6)
(3,6)
(4,6)
(5,6)
(6,6)
$\frac{\Delta a_3}{a_3}$

Figure 7.15

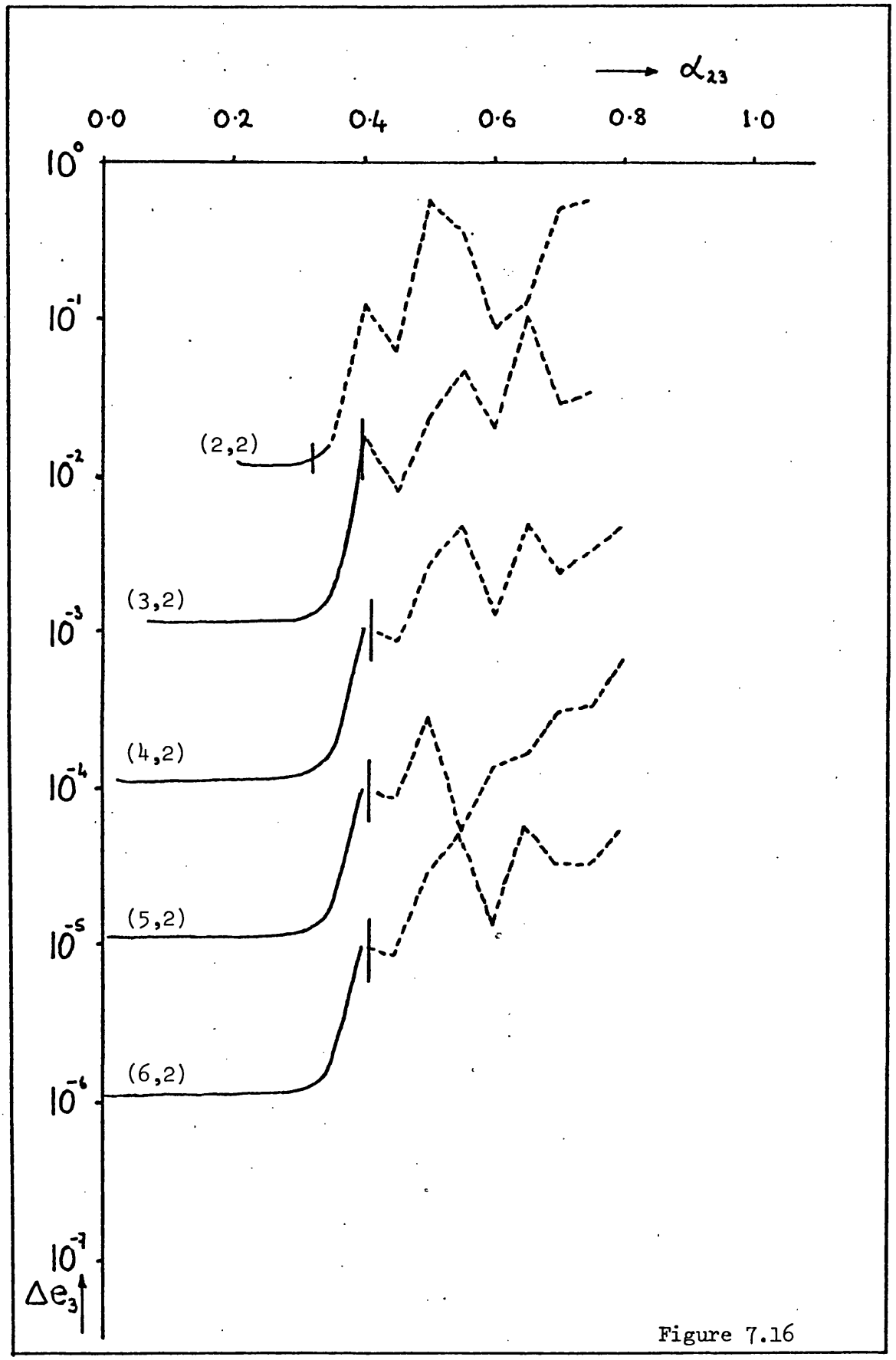
α_{23}
0·0
0·2
0·4
0·6
0·8
1·0
10^{0}
10^{-1}
10^{-2}
10^{-3}
10^{-4}
10^{-5}
10^{-6}
10^{-7}
Δe_3
(2,2)
(3,2)
(4,2)
(5,2)
(6,2)

Figure 7.16

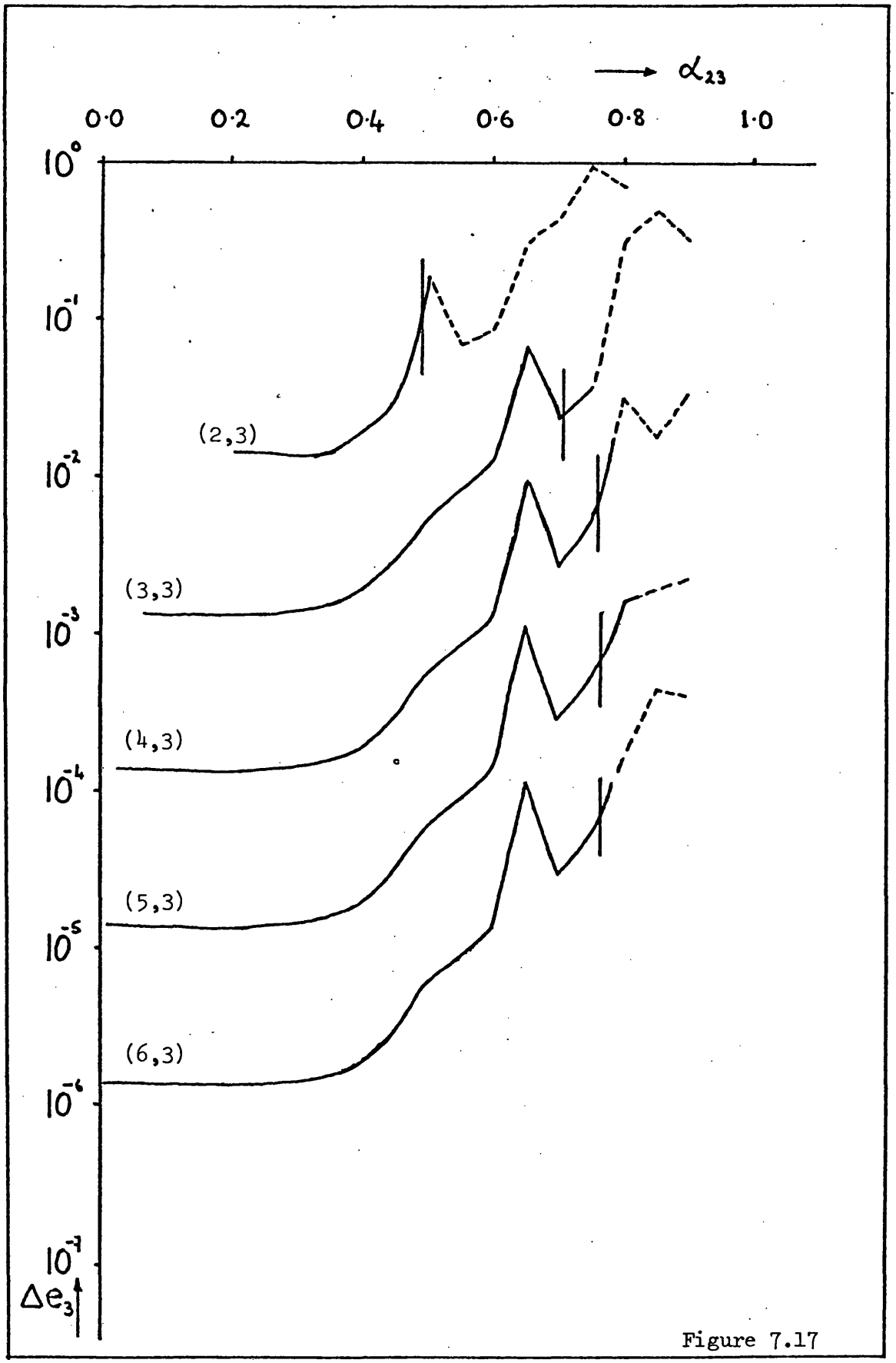
α_{23}
0·0
0·2
0·4
0·6
0·8
1·0
10^{0}
10^{-1}
10^{-2}
10^{-3}
10^{-4}
10^{-5}
10^{-6}
10^{-7}
Δe_3
(2,3)
(3,3)
(4,3)
(5,3)
(6,3)

Figure 7.17

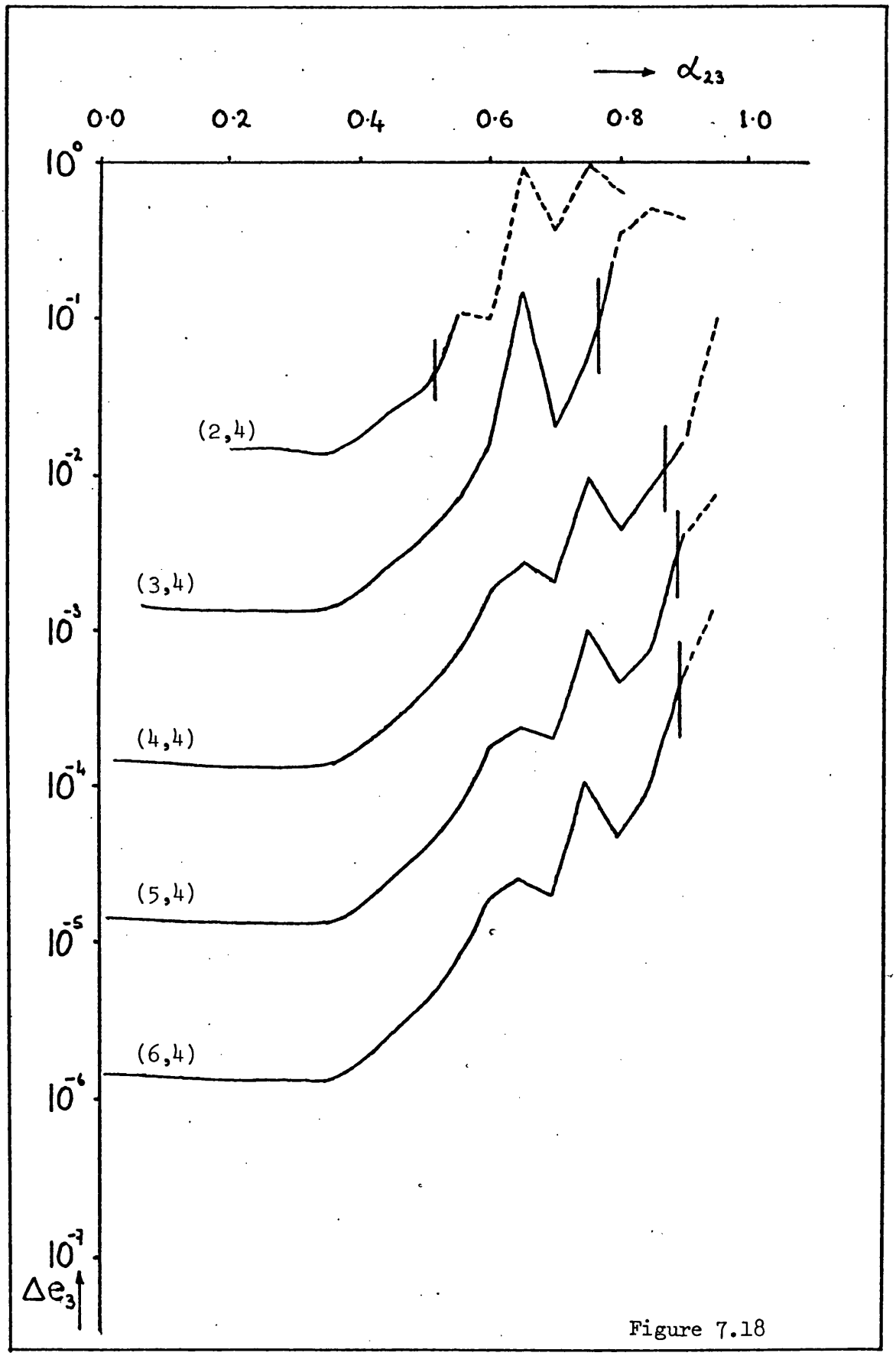
α_{23}
0·0
0·2
0·4
0·6
0·8
1·0
10^{0}
10^{-1}
10^{-2}
10^{-3}
10^{-4}
10^{-5}
10^{-6}
10^{-7}
Δe_3
(2,4)
(3,4)
(4,4)
(5,4)
(6,4)

Figure 7.18

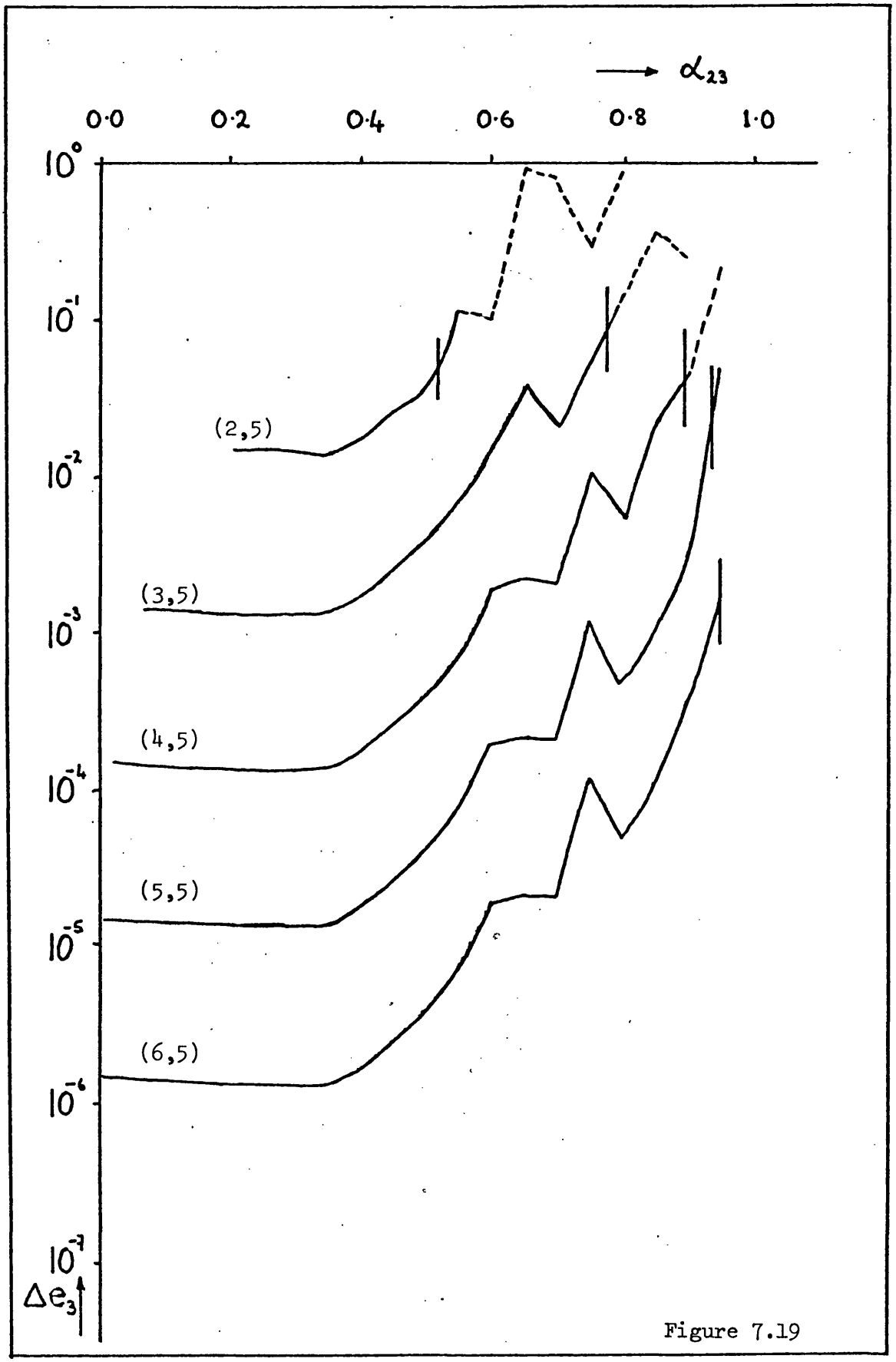
α_{23}
0·0
0·2
0·4
0·6
0·8
1·0
10^{0}
10^{-1}
10^{-2}
10^{-3}
10^{-4}
10^{-5}
10^{-6}
10^{-7}
Δe_3
(2,5)
(3,5)
(4,5)
(5,5)
(6,5)

Figure 7.19

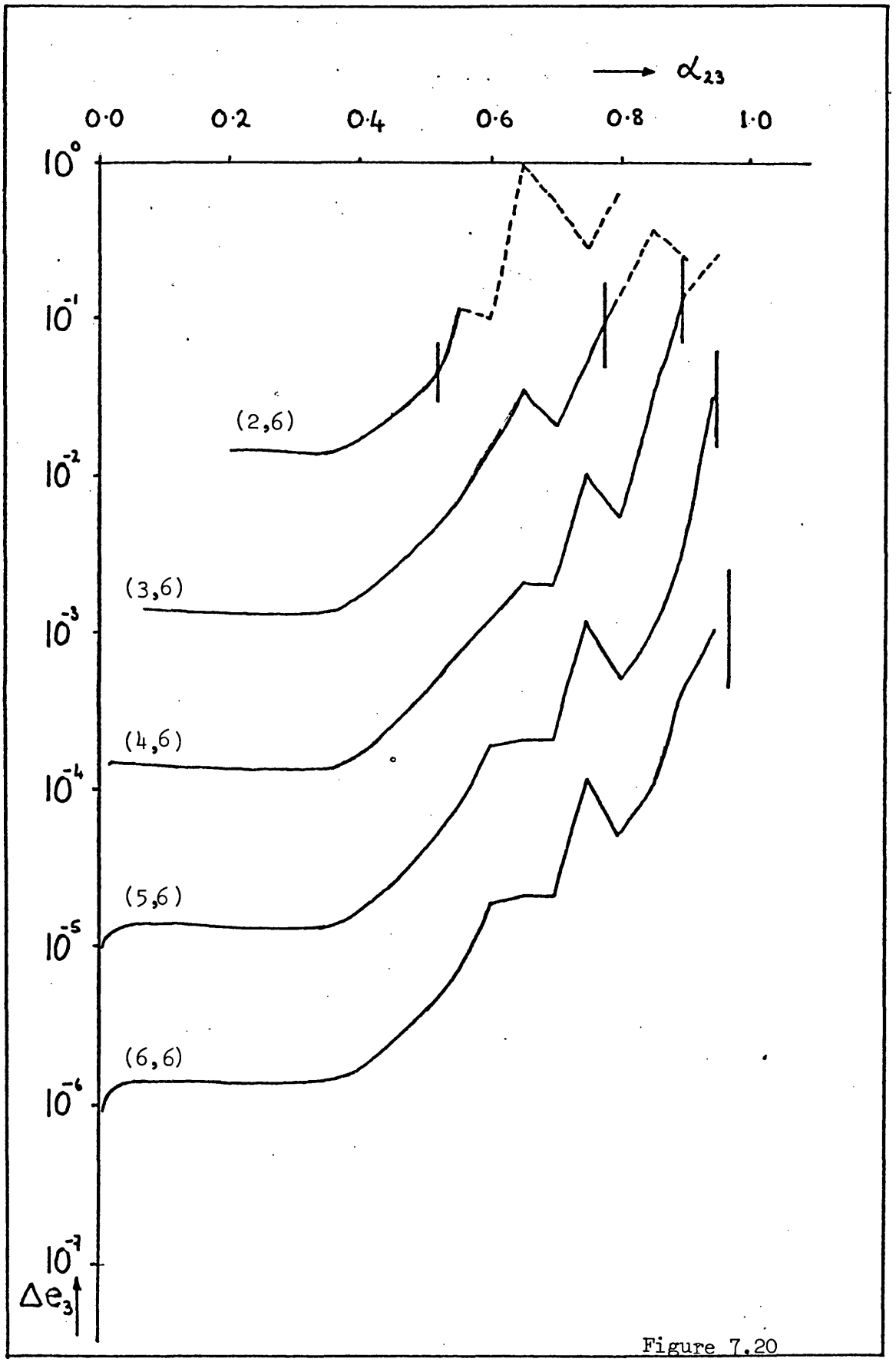
α_{23}
0·0
0·2
0·4
0·6
0·8
1·0
10^{0}
10^{-1}
10^{-2}
10^{-3}
10^{-4}
10^{-5}
10^{-6}
10^{-7}
Δe_3
(2,6)
(3,6)
(4,6)
(5,6)
(6,6)

Figure 7.20

7.3 The Effect of Commensurabilities on the Amplitude of the Variations

In the solution of the Lagrange planetary equations, correct to the first order in the masses, the expressions for the elements of a disturbed planetary orbit involve three types of term. These are (i) secular terms (ii) short-period inequalities* and (iii) long-period inequalities.

To ensure stability of a hierarchical system in the sense of maintaining the order within the hierarchy and the position of each orbit relative to the others it is essential that the expressions giving the semi-major axes, eccentricities and inclinations do not involve secular terms. The remaining angular elements may involve secular terms with no detriment to the stability of the system.

The short-period inequalities generally involve variations of the orbital elements of the orbit of the disturbed body which operate over a time scale which is comparable to the orbital periods of the system. The terms which arise in the expressions for the elements have divisors of the type $i_2n_2 + i_3n_3$ (i_2 and i_3 being integers); if one of these divisors is small, then the corresponding term in the expression for the element is enhanced giving a disturbance greater than might be expected.

The last type of term, the long-period inequalities, arise from the occurrence of approximate commensurabilities, in certain instances, of the mean angular motions n_2 and n_3 as discussed in Chapter 6, Section 6.4. The terms of this type constantly involve divisors of the type $i_2n_2 - i_3n_3$ (i_2 and i_3 being positive integers) which, if $n_2/n_3 \simeq i_3/i_2$, will be small, resulting in the corresponding term in the expression for the element being magnified and having a greater effect than would be expected *a priori*.

Thus in all the numerical experiments carried out it would be expected that there will be short period variations of the semi-major axes and eccentricities with long period variations showing up especially

*Inequality is used here to mean the deviation from purely elliptic motion i.e. the perturbation of an element due to the effects of other bodies.

about values of α where commensurabilities arise. In the numerical integrations where $\alpha_{23} < (\alpha_{23})_o$ there should be no secular trends apparent in the semi-major axes and eccentricities. This was always found to be the case.

If we now consider the diagrams, it is apparent that peaks occur on several of these. The most frequently occurring peak is at $\alpha_{23} = 0.65$ i.e. $\alpha = 0.65$ since initially circular orbits are dealt with here. The peaks only occur when $\alpha_{23cr} \geq 0.65$, that is, when the case $\alpha = 0.65$ is stable. This value of α, it may be remembered from Chapter 6 is very close to the 2:1 commensurability i.e. $\alpha = 0.630$ when $\mu_3 = 0$. When $\alpha_{23cr} > 0.75$ another peak arises in the graphs at $\alpha_{23} = 0.75$. This peak is close to the 3:2 commensurability i.e. $\alpha = 0.763$ when $\mu_3 = 0$.

Since the integration experiments are carried out at intervals of 0.05 in α_{23} the graphs contain no information as to the exact width of these peaks. Indeed the apparent "shoulder" on the peak at $\alpha_{23} = 0.65$, which occurs at $\alpha_{23} = 0.60$ on Figures 7.7 - 7.10 and 7.18 - 7.20, may be due to another commensurability and is not necessarily due to the effect of the 2:1 commensurability. To answer the question as to how wide the peaks are it would obviously be necessary to carry out further numerical integrations at intermediate initial α_{23} values. In general the height of the peaks in the curves giving the changes in semi-major axes is less than that of the curves giving the variations in eccentricity.

An interesting feature, not included in the graphs, occurred in the range of small ε_{32} on the curves pertaining to Δe_2. Between the values $\alpha_{23} = 0.01$ and $\alpha_{23} = 0.1$ a small peak appeared on each of these curves. The smooth curves were obtained by considering only the amplitude of the short-period variations at these values of initial α_{23}. The longer period trend which gave an increased degree of perturbation operated over a time scale comparable to the period of the orbit of m_3 relative to M_2- the mass-centre of m_1 and m_2. The systems in this region are generally of the type Star-Planet-Star i.e. inferior planets of binary star systems and it is possible that the larger perturbation due to the disturbance by the more massive m_3 (relative to m_2) in conjunction with the small value of n_3, relative to n_2, could cause a periodic trend in the elements of the orbit of the close pair i.e. the orbit of m_2, the planet, relative to

m_1 which is of longer period than the shortest period terms and possibly magnified due to the smallness of $i_2n_2 + i_3n_3$ as mentioned above.

At larger initial α_{23} ratios the orbital periods of the system are of the same order and hence the short period terms will all operate over similar time scales. When the initial α_{23} value is smaller then in this case the numerical experiments have not been carried over a real integration time comparable to the period of m_3 about the mass-centre of m_1 and m_2 and hence these trends, such as occur in the range $0.01 \lesssim \alpha_{23} \lesssim 0.1$, would not have sufficient time to manifest themselves.

If the integrations in this region were carried over a longer time scale then it is felt likely that although the curves might change in appearance slightly the overall simplicity of the relationship between the ε parameters, α_{23} ratio and variations in semi-major axes and eccentricities would not be lost.

7.4 Discussion and Conclusions

Although this brief examination of the relationship between the ε parameters, α ratio and the variations in the orbital elements (a_2, e_2) and (a_3, e_3) - the important ones for stability of coplanar hierarchical systems - has been carried out in a simple fashion, it is evident that such a relationship does exist. By simply considering the largest values of Δa_2, Δe_2, Δa_3 and Δe_3 obtained over a specified integration time - these being calculated only at specific sampling times - it is possible todemonstrate these relationships.

Excepting the occurrence of commensurabilities it is apparent that a main conclusion may be drawn: the order of size of the relevant ε parameter e.g. 10^{-2} or 10^{-5} etc. decides the order of size of the perturbations on the elements a and e of the osculating Keplerian orbit of the body being disturbed. The particular α_{23} value is of secondary importance inasmuch as it only modifies the magnitude of these perturbations.

It is probable that a better method of calculating the variations - Δa_2, Δe_2, Δa_3, Δe_3 - would have been to employ some type of time averaging scheme. For example calculate $\overline{\Delta a_2}$ as follows:

$$\overline{\Delta a_2} = \frac{1}{t_o} \int_o^{t_o} \{ a_2(t) - (a_2)_o \} \, dt$$

where t_o is the time of integration and $(a_2)_o$ is the initial a_2 value with similar expressions involving $\overline{\Delta e_2}$, $\overline{\Delta a_3}$ and $\overline{\Delta e_3}$. These values would give information on the mean deviation of the semi-major axes and eccentricities from their initial values.

The classical method of secular inequalities (see Smart, 1953) yields the amplitude of the long period variations in eccentricity and inclination in the planetary case of three-body systems, assuming that the changes in the semi-major axes are zero. The present treatment suggests that the changes in the semi-major axes are limited in a similar way to the changes in eccentricity and inclination (although clearly no variations in inclination have been obtained herein since only coplanar systems were considered). The results also suggest that relationships are obtainable, which would allow the calculation of these variations over a very large range of masses and α_{23} ratios. It would be an obvious extension of this present work to try to obtain *analytical* relationships which would positively identify the dependance of Δa_2, Δe_2, Δa_3, Δe_3 (and even Δi_2 and Δi_3, the variations in inclination) on the ε parameters and α_{23} ratio. This point will be discussed further in Chapter 10.

It was remarked in Chapter 6 that the smaller mass was always the one ejected from the three-body system if instability, in the form of break-up, occurred. Similarly when considering the variations imposed on the orbits of the (m_1,m_2) and (M_2,m_3) subsystems it is found that depending upon whether m_2 or m_3 is smaller then the larger variations will generally occur on the semi-major axis and eccentricity of the (m_1,m_2) or (M_2,m_3) subsystem respectively. Again it is observed that the larger variations are associated with the larger *disturbing* ε parameter . However it may be noted, in passing, that if ε^{23} and ε_{32} are the same magnitude then the variations imposed on the (m_1,m_2) subsystem are slightly larger than those imposed on the (M_2, m_3) subsystem.

CHAPTER 8 THE EMPIRICAL STABILITY PARAMETERS FOR THE HIERARCHICAL FOUR-BODY PROBLEM AND THEIR APPLICATION IN THE COPLANAR, COROTATIONAL, INITIALLY CIRCULAR CASE

8.1 Introduction

Thus far only hierarchical three-body systems have been considered in any depth. The justification for this is that it is the simplest case in which the use of the ε parameters may be tested. However it was remarked at the end of Chapter 4 that it might be possible to use the ε parameters to consider the stability in n-body hierarchical systems where $n \geq 4$. To this end it was proposed that the relevant stability parameter for any given orbit within a hierarchical system should be the sum of the ε parameters which operate on, i.e. disturb, that particular orbit (cf. Equation (4.30)). It was further recognised that there would also have to be a criterion on the α_{ij} ratios ($i=2,\ldots,n-1$; $j=3,\ldots,n$; $i < j$) for a given set of stability parameters (cf. Equation (4.31)).

The use of the four-body problem is the simplest case where the applicability of the summation of the ε parameters for each orbit as a stability parameter may be tested. It is also the simplest n-body case where no analytical stability criterion exists.

Considering the four-body case we require three osculating Keplerian orbits to define the motion of the system. Mass m_2 moves in a disturbed Keplerian ellipse relative to m_1, m_3 moves in a disturbed Keplerian ellipse relative to M_2 (the position of the mass-centre of m_1 and m_2) and m_4 moves in a disturbed Keplerian ellipse relative to M_3 (the position of the mass-centre of m_1, m_2 and m_3). There are therefore three two-body subsystems which may be denoted (m_1,m_2), (M_2,m_3) and (M_3,m_4).

Now these three orbits are disturbed by the other masses present. The orbit of (m_1,m_2) subsystem is disturbed by the masses m_3 and m_4. The (M_2, m_3) subsystem has its orbit perturbed by the masses m_1 and m_2 not being at their common mass-centre and by the mass m_4. Finally, the (M_3, m_4) subsystem's orbit is affected by m_1 and m_2 not being at their common mass-centre, also by M_2 (i.e. m_1 and m_2) and m_3 not being at their common mass-centre. Thus each orbit has a disturbance placed

on it from two sources: each of the three equations of motion for the system will therefore contain two ε parameters (see Section 8.2).

In Section 8.3 the numerical experiments which were carried out are described. The results derived from these experiments are given in the following two sections - Sections 8.4 and 8.5. A discussion of the results is given in Section 8.6.

8.2 The Empirical Stability Parameters Defined

In Chapter 3, Section 3.6, the equations of motion, in Jacobian coordinates, were used to derive the ε parameters. The relevant equation was Equation (3.40) with the form of the ε parameters being given by Equations (3.41). Let us now consider the case when n=4: there are three equations of motion, one for each of the two-body subsystems - (m_1, m_2), (M_2, m_3) and (M_3, m_4) - viz.

$$\ddot{\underset{\sim}{\rho}}_2 = G M_2 \nabla_{\underset{\sim}{2}} \left[\frac{1}{\rho_2} \{ 1 + \varepsilon_{32} P_2(C_{23}) + \varepsilon_{42} P_2(C_{24}) \} \right] \quad (1)$$

$$\ddot{\underset{\sim}{\rho}}_3 = G M_3 \nabla_{\underset{\sim}{3}} \left[\frac{1}{\rho_3} \{ 1 + \varepsilon^{23} P_2(C_{23}) + \varepsilon_{43} P_2(C_{34}) \} \right] \quad (2)$$

and

$$\ddot{\underset{\sim}{\rho}}_4 = G M_4 \nabla_{\underset{\sim}{4}} \left[\frac{1}{\rho_4} \{ 1 + \varepsilon^{24} P_2(C_{24}) + \varepsilon^{34} P_2(C_{34}) \} \right] \quad (3)$$

to the second order in the α's,

where
$$\left.\begin{aligned} \varepsilon_{32} &= \frac{m_3}{M_2}.\alpha_{23}^3 \quad ; \quad \varepsilon_{42} = \frac{m_4}{M_2} \cdot \alpha_{24}^3 \\ \varepsilon^{23} &= \frac{m_2}{M_2^2}\frac{M_1}{} \cdot \alpha_{23}^2 \quad ; \quad \varepsilon_{43} = \frac{m_4}{M_3} \cdot \alpha_{34}^3 \\ \varepsilon^{24} &= \frac{m_2^2 M_1}{M_2 M_3} \cdot \alpha_{24}^2 \quad ; \quad \varepsilon^{34} = \frac{m_3 M_2}{M_3^2}.\alpha_{34}^2. \end{aligned}\right\} \quad (4)$$

To form the empirical stability parameters for four-body systems we consider the straight line configuration $m_1\ m_2\ m_3\ m_4$, i.e. $C_{23} = C_{24} = C_{34} = 1$, so that $P_2(C_{23}) = P_2(C_{24}) = P_2(C_{34}) = 1$. This configuration is chosen since it is in this situation that the mutual perturbations among the bodies are at a maximum. The stability parameters Σ_2, Σ_3, Σ_4 may then be defined as follows:

$$\left.\begin{aligned} \Sigma_2 &= \varepsilon_{32} + \varepsilon_{42} \\ \Sigma_3 &= \varepsilon^{23} + \varepsilon_{43} \\ \Sigma_4 &= \varepsilon^{24} + \varepsilon^{34} \end{aligned}\right\} \qquad (5)$$

Thus Σ_i (i=2,3,4) is a measure of the disturbance placed on the orbit of m_i relative to M_{i-1} (the position of the mass-centre of the masses $m_1,\ldots,m_{i-1}$).

Alternatively we could have defined an "average" empirical stability parameter as follows:

$$\Sigma_2 = \frac{1}{T} \int_0^T \left[\varepsilon_{32} P_2(C_{23}) + \varepsilon_{42} P_2(C_{24}) \right] dt \qquad (6)$$

with similar expressions involving Σ_3 and Σ_4. In this expression the ε_{32}, C_{23}, ε_{42} and C_{24} are functions of the time, t. It would be sufficient, for the present purposes, to use the solution of the two-body problem to give these parameters their functional form. The time of integration T is given by considering the orbital periods of the system defined by the initial conditions. T is the shortest time interval such that

$$T = k.\, S_{23} = \ell.\, S_{34} \qquad (7)$$

where k and ℓ are positive integers, $S_{ij} = T_i T_j/(T_j - T_i)$ is the synodic period of the (M_{i-1},m_i) and (M_{j-1},m_j) subsystems (j > i) and T_i (i=2,3,4) are the orbital periods of the masses m_i relative to M_{i-1}.

Thus after a time T the system would return to its straight line initial configuration, assuming there to be no perturbation of the subsystems' orbits.

For the present investigation, however, the former definition of the Σ parameters is adopted for reasons of simplicity: there is no reason to believe at this stage that either definition is more appropriate than the other.

Following the same reasoning used for the ε parameters in Chapter 6, section 6.2, it may be assumed that the disturbances on the Keplerian orbits of the four-body system are applied in a pseudo-random fashion. The question of whether a *four-body* system with given $(\Sigma_2,\Sigma_3,\Sigma_4,\alpha_{23},\alpha_{34})$* is stable or not will then depend upon whether or not the resultant pseudo-random variations in the elements of the constituent Keplerian orbits of the system are large enough to cause some form of instability.

8.3 The Numerical Experiments

The numerical integration experiments in the four-body problem were carried out along the same lines as those in the three-body problem. The motion of the three constituent subsystems - (m_1, m_2), (M_2, m_3) and (M_3, m_4) is defined by three sets of osculating elements (a_i, e_i, ϖ_i) $\{i = 2,3,4\}$, for coplanar motion, along with three true anomalies f_i $\{i = 2,3,4\}$, giving the positions in these osculating Keplerian orbits. Since only the initially circular case of the problem is studied ϖ_i and f_i $\{i = 2,3,4\}$ are indeterminate initially and reduce to ℓ_i $\{i = 2,3,4\}$ the longitude of the body as measured with respect to some fixed reference direction i.e. if $\hat{\underset{\sim}{x}}$ is a unit vector in that reference direction then $\cos \ell_i = (\underset{\sim}{\rho}_i \cdot \hat{\underset{\sim}{x}})/\rho_i$.

The initial conditions of each integration are restricted still further by considering only the initially straight line configuration $m_1m_2m_3m_4$ i.e. $\ell_2 = \ell_3 = \ell_4$ $(= \ell_o$ say initially). We thus have the following initial conditions

$$\underset{\sim}{\rho}_i = (a_i, 0, 0) \quad ; \quad \dot{\underset{\sim}{\rho}}_i = (0, V_i, 0) \qquad (i = 2,3,4) \qquad (8)$$

where a_i are the semi-major axes of the subsystems (M_{i-1}, m_i) i=2,3,4 and V_i is the required "circular" velocity viz.

$$V_i = \left[\frac{G\,M_i}{a_i}\right]^{\frac{1}{2}} . \qquad (i = 2,3,4) \qquad (9)$$

*Only two initial α_{ij} parameters are required, although three arise in Equations (1)-(4), since α_{24} $[= \rho_2/\rho_4 = (\rho_2/\rho_3).(\rho_3/\rho_4)] = \alpha_{23} \cdot \alpha_{34}$.

The time interval over which the integration was carried out was determined by the successive passages of the (m_1, m_2) subsystem through its initial sidereal direction i.e. ℓ_o. The integrations in this chapter generally continued over 200 such passages. If the system exhibited instability by one of the eccentricities $e_i (i=2,3,4)$ becoming greater than unity then the integration experiment was terminated. Various data were noted from each experiment. The data include: the time up until the above instability, if any, occurred, the number of passages N_i {i=2,3,4} the subsystems (M_{i-1}, m_i) {i=2,3,4} respectively, made through their initial sidereal directions, the maximum deviation of the semi-major axes and eccentricities from initial values and which body, if instability occurred, was ejected from the system. The data is similar in form to that noted for the three-body systems excepting that no examination of the experiments has been made so far for evidence of close encounters. Also, although crossover of orbits was noted in several cases, no use was made of the time of this occurrence. *Only* break-up was considered as giving an indication of instability. (Clearly it will be necessary in future to examine the data of the numerical experiments for evidence of close encounters and cross-over and to note the time of their occurrence).

The systems were studied in terms of the parameters Σ_i (i=2,3,4) and $(\alpha_{23}, \alpha_{34})$; the other α value α_{24} is redundant since $\alpha_{24} = \alpha_{23} \cdot \alpha_{34}$. Then, fixing $a_3 = 1$ in all the experiments, we have $a_2 = \alpha_{23} \cdot \alpha_{34}$ and $a_3 = \alpha_{34}$. The last piece of information required, to obtain the initial conditions, the values for the masses m_i (i=1,...,4), is determined in the following fashion.

Let the ratio $m_1 : m_2 : m_3 : m_4$ be denoted by $1-\mu : \mu : \mu_3 : \mu_4$ where $\mu \leq \frac{1}{2}$ i.e. m_1 is always the larger of m_1 and m_2. The Σ and ε parameters for the four-body case are then

$$\Sigma_2 = \varepsilon_{32} + \varepsilon_{42} \qquad (10a)$$

$$\Sigma_3 = \varepsilon^{23} + \varepsilon_{43} \qquad (10b)$$

$$\Sigma_4 = \varepsilon^{24} + \varepsilon^{34} \qquad (10c)$$

where, from Equations (4),

$$\varepsilon_{32} = \mu_3 \alpha_{23}^3 \quad ; \quad \varepsilon_{42} = \mu_4 \alpha_{24}^3 \tag{11a}$$

$$\varepsilon^{23} = \mu(1-\mu) \alpha_{23}^2 \quad ; \quad \varepsilon_{43} = \frac{\mu_4}{1+\mu_3} \alpha_{34}^3 \tag{11b}$$

$$\varepsilon^{24} = \frac{\mu(1-\mu)}{1+\mu_3} \alpha_{24}^2 \quad ; \quad \varepsilon^{34} = \frac{\mu_3}{(1+\mu_3)^2} \alpha_{34}^2. \tag{11c}$$

Now by Equations (10a) and (11a)

$$\mu_4 = \frac{1}{\alpha_{24}^3} \cdot (\Sigma_2 - \mu_3 \alpha_{23}^3) \tag{12}$$

and by Equations (10b), (11b) and (12)

$$\mu(1-\mu) = \frac{1}{\alpha_{23}^2}\left[\Sigma_3 - \frac{1}{\alpha_{23}^3} \cdot \frac{(\Sigma_2 - \mu_3 \alpha_{23}^3)}{1+\mu_3}\right]. \tag{13}$$

Using Equations (12) and (13) in Equations (10) and (11) then gives

$$\Sigma_4 = \frac{\alpha_{34}^2}{1+\mu_3}\left[\Sigma_3 - \frac{1}{\alpha_{23}^3} \cdot \frac{(\Sigma_2 - \mu_3 \alpha_{23}^3)}{1+\mu_3}\right] + \frac{\mu_3}{(1+\mu_3)^2} \alpha_{34}^2 . \tag{14}$$

Upon multiplying Equation (14) through by $(1+\mu_3)^2$ we obtain a quadraticin μ_3 viz.

$$\Sigma_4 \mu_3^2 + (2\Sigma_4 - \alpha_{34}^2 \cdot [\Sigma_3 + 2])\mu_3 + \left(\Sigma_4 - \alpha_{34}^2\left[\Sigma_3 - \frac{\Sigma_2}{\alpha_{23}^3}\right]\right) = 0 \tag{15}$$

which may be solved, in the usual fashion, to give

$$\mu_3 = \frac{-(2\Sigma_4 - \alpha_{34}^2 [\Sigma_3 + 2]) \pm \left[(2\Sigma_4 - \alpha_{34}^2 [\Sigma_3 + 2])^2 - 4\Sigma_4 \left(\Sigma_4 - \alpha_{34}^2 \left[\Sigma_3 - \frac{\Sigma_2}{\alpha_{23}^3}\right]\right)\right]^{\frac{1}{2}}}{2\Sigma_4} \tag{16}$$

where the " - " sign is taken to give real values for the mass parameters. Having obtained μ_3 the value of μ_4 may be obtained by application of Equation (12) and also the value $\mu(1-\mu)$, and hence μ, from Equation (13). Thus the mass parameters μ, μ_3 and μ_4 are determined allowing the calculation of the initial velocities.

Thus far systems have been studied over the range 10^{-i} $(i=2,\ldots,6)$ in Σ_2, Σ_3 and Σ_4, resulting in one hundred and twenty-five triple sets $(\Sigma_2, \Sigma_3, \Sigma_4)$. At each of these points - $(\Sigma_2, \Sigma_3, \Sigma_4)$ - in the parameter space the ratios α_{23} and α_{34} have been taken over a spread from the lowest values* possible up to unity. This range of parameters is found to cover the complete range of 4-body hierarchical dynamical systems e.g. quadruple stellar systems, planetary or satellite systems, planets in multiple stellar systems, etc. The preliminary results of this investigation of the $(\Sigma_2, \Sigma_3, \Sigma_4, \alpha_{23}, \alpha_{34})$ parameter space in the corotational, coplanar, initially circular case of the four-body problem are presented in the following two sections.

8.4 Results - The Stability of Four-Body Systems

In examining the stability of coplanar, corotational hierarchical three-body systems with initially circular orbits the problem was made easier by the availability of analytical stability criteria in the form of α_{23cr} and α'_{23cr}. These values could be used to indicate the regions in $0\epsilon^{23}$ ϵ_{32} α_{23} parameter space where numerical investigation was required to decide the stability. Upon moving to the four-body problem we lose this advantage. There is no comparable analytical tool to use as a guideline. The following methods were adopted instead, utilising the three-body α_{23cr} values.

If we consider the structure of the hierarchical four-body system then we may break it down into three *three-body* subsystems (cf. the break down of the Solar System into three-body subsystems in Chapter 4).

*There is a restriction on the possible values of α_{23} and α_{34} for given values of Σ_2, Σ_3, Σ_4 in order that the values μ_1, μ_3 and μ_4 are real and positive in much the same way as $\alpha_{23} \geq 2(\epsilon^{23})^{\frac{1}{2}}$ in the three-body problem. In the present case however the exact analytical limits have not yet been determined. The systems investigated were chosen by finding by computer those sets of parameters $(\Sigma_2, \Sigma_3, \Sigma_4, \alpha_{23}, \alpha_{34})$ which resulted in "real" systems over specified ranges in Σ and α parameters.

The subsystems are (m_1, m_2, m_3), (m_1, m_2, m_4) and (m_1, m_3, m_4). Of these three it can be noted that (m_1, m_2, m_3) and (m_1, m_3, m_4) both contain two of the bodies which move in neighbouring orbits; the other subsystem (m_1, m_2, m_4) contains the two bodies which move in the innermost and outermost orbits. Therefore the triple subsystems which are *most* relevant to the stability of the four-body system are (m_1, m_2, m_3) and (m_1, m_3, m_4): because of the nature of the Jacobi coordinate system the latter of these is rewritten as (M_2, m_3, m_4) i.e. we "throw the mass of m_2 into m_1.*" The mutual perturbations of m_2 amd m_4 are smaller than those of m_2 and m_3 or m_3 and m_4 excepting in some special cases where a large value of m_2 or m_4 may alter this situation.

Having separated out the important triple subsystems we now proceed to calculate α_{23cr} - type values by two means:

(i) using the mass parameters μ, μ_3 and μ_4

and (ii) using the sigma parameters Σ_2, Σ_3 and Σ_4.

The procedures are described below.

(i) Here we use the critical stability values of α_{23} as determined by the masses for the initially circular, three-body case i.e. $\alpha_{23cr} = f(\mu, \mu_3)$ [this uses the two two-body approximation to the three-body motion as was described in Chapter 4, Section 4.3, since the following criteria are only approximate anyway.] Hence for the (m_1, m_2, m_3) triple subsystem we calculate

$$\alpha_{23cr} = f(\mu, \mu_3) \qquad (17)$$

and for the (M_2, m_3, m_4) triple subsystem we calculate

$$\alpha_{34cr} = f\left(\frac{\min(1, \mu_3)}{1 + \mu_3}, \frac{\mu_4}{1+\mu_3}\right). \qquad (18)$$

* This expression indicates that we add to the mass of m_1 that of m_2, the resultant mass being positioned at their common mass-centre i.e. M_2. The justification for so doing is that while neglecting the direct perturbations by m_2 on the rest of the system we do include the indirect perturbation by considering the orbit of m_3 relative to M_2 (see Danby, 1962).

Thus we obtain two *possible, approximate* limits outwith which these subsystems could be unstable, i.e. if $\alpha_{23} > \alpha_{23cr}$ as determined by Equation (17), then the (m_1, m_2, m_3) subsystem may be unstable and if $\alpha_{34} > \alpha_{34cr}$ then the (M_2, m_3, m_4) subsystem may be unstable.

(ii) Alternatively we may use the Σ parameters to determine the α_{23cr} and α_{34cr} values. The critical stability values used here are derived from the function $\alpha_{23cr} = f'(\varepsilon^{23}, \varepsilon_{32})$ for the three-body case, i.e. the critical value of α_{23} is determined from the ε values using the two two-body approximation for the three-body motion (cf. Chapter 4, Section 4.4). For the (m_1, m_2, m_3) subsystem we calculate

$$\alpha_{23cr} = f' (\Sigma_3, \Sigma_2) \qquad (19)$$

where Σ_3, being the parameter characterising the total perturbation of the (M_2, m_3) subsystem, takes the place of ε^{23} (cf. the effect of m_1 and m_2 on the (M_2, m_3) subsystem of the *three-body case*) and Σ_2, being the parameter characterising the total perturbation on the (m_1, m_2) subsystem, takes the place of ε_{32} (cf. the effect of m_3 on the (m_1, m_2) subsystem of the *three-body case*).

Similarly for the (M_2, m_3, m_4) subsystem we calculate

$$\alpha_{34cr} = f' (\Sigma_4, \Sigma_3) \qquad (20)$$

where Σ_4, being the parameter describing the total perturbation on the *outer* subsystem - (M_3, m_4) - of the three-body subsystem, takes the place of ε^{23} (cf. the effect on the *outer* subsystem of the three-body case) and Σ_3, being the parameter characteristic of the total perturbation on the *inner* subsystem - (M_2, m_3) - of the three-body subsystem, takes the place of ε_{32} (cf. the effect on the *inner* subsystem of the three-body case).

Then using the criteria of (i) *or* (ii) above we may say, *as a first approximation*, that hierarchical four-body systems where $\alpha_{23} \leq \alpha_{23cr}$ *and* $\alpha_{34} \leq \alpha_{34cr}$ will be stable and if either $\alpha_{23} > \alpha_{23cr}$ *or* $\alpha_{34} > \alpha_{34cr}$ then they *may* be unstable.

We could, of course, consider a value α_{24cr} derived by the methods outlined in (i) and (ii) above; however, if the subsystem (m_1, m_2, m_4)

was unstable then it is certainly true that either (m_1, m_2, m_3) or (M_2, m_3, m_4) would also be unstable. For example, consider that (m_1, m_2, m_4) is unstable due to m_4 being a large mass placed at an insufficiently large distance from the (m_1, m_2) subsystem i.e. the orbit of m_2 about m_1 will be unstable. Then consider the position of m_3: it will be between m_2 and m_4, even closer to m_4 than m_2 is, and hence its orbit about M_2 will also be unstable. The other case would arise in the following manner: if m_2 was large in comparison to m_4 and m_4 was not sufficiently far away for its orbit to be stable then it would follow that the orbit of m_3 would also be unstable. The converse arguments are not true: if either of the triple subsystems (m_1, m_2, m_3) or (M_2, m_3, m_4) is unstable then it does *not* follow that the system (m_1, m_2, m_4) would also be unstable. However it is probably a fair assumption that if both the (m_1, m_2, m_3) and (M_2, m_3, m_4) subsystems are stable then the (m_1, m_2, m_4) subsystem will also be stable, and hence the four-body system, as a whole, will be stable.

It will be remembered in Chapter 6 that, for three-body systems, if $\alpha_{23} \leq (\alpha_{23})_o$ then the systems were stable and showed no signs of secularity in the semi-major axes or eccentricities. On the other hand if α_{23} was close to unity this resulted in instability in all cases. If we now use the α_{23cr} and α_{34cr} values, derived in the above-mentioned manner, we may say that, as a first approximation, if $\alpha_{23} = \alpha_{23cr}$ then the (m_1, m_2, m_3) subsystem is stable and may be expected not to exhibit secularity in a_2 or e_2. Similarly if $\alpha_{34} = \alpha_{34cr}$ then the (M_2, m_3, m_4) subsystem is stable. If either α_{23} or α_{34} equals unity then the relevant subsystem - (m_1, m_2, m_3) or (M_2, m_3, m_4) - is *extremely* unstable. It may thus be reasoned that subsystems, of hierarchical four-body systems, of "equal instability" are those where the values $(\alpha_{23} - \alpha_{23cr})/(1 - \alpha_{23cr})$ or $(\alpha_{34} - \alpha_{34cr})/(1 - \alpha_{34cr})$ are equal, which one is considered depending on the subsystem under study [cf. the exponent in Equation (6.8)].

The situation for stable systems is slightly different. In this case if $\alpha_{23} = \alpha_{23cr}$ then the (m_1, m_2, m_3) subsystem is *just* stable: when $\alpha_{23} = 0$* then the system is as stable as it possibly can be.

*Such an α_{23} value may not be possible since the range is restricted by criteria similar to that obtained for the three-body problem (viz. $\alpha_{23} \geq 2(\varepsilon^{23})^{\frac{1}{2}}$) The maximum stability is merely chosen to be zero for convenience. Similar comments may be made as regards the α_{34} value.

Similarly, for the (M_2, m_3, m_4) subsystem the complete range of "degrees of stability" will occur between $\alpha_{34} = \alpha_{34cr}$ and $\alpha_{34} = 0$. Thus subsystems in which $(\alpha_{23} - \alpha_{23cr})/\alpha_{23cr}$ or $(\alpha_{34} - \alpha_{34cr})/\alpha_{34cr}$ (which one is used depends on the subsystem under consideration) are equal will be those of "equal stability".

To obtain an initial indication as regards the stability of hierarchical four-body systems the numerical integrations were plotted in the Oxy plane where the positive x coordinate is $(\alpha_{23} - \alpha_{23cr})/(1 - \alpha_{23cr})$, the positive y coordinate is $(\alpha_{34} - \alpha_{34cr})/(1 - \alpha_{34cr})$ and the negative x and y coordinates are respectively $(\alpha_{23} - \alpha_{23cr})/\alpha_{23cr}$ and $(\alpha_{34} - \alpha_{34cr})/\alpha_{34cr}$. It is to be hoped that hierarchical four-body systems of equal overall stability will be represented at the same point in such a diagram.

The results of such an initial investigation are shown schematically in Figure 8.1. The real systems, i.e. 4-body sub-sets taken from the Solar System's planets and satellites, eg. Sun-Mercury-Venus-Earth, were found to occupy the shaded region in the lower left quadrant of the Oxy plane. The numerical integrations were used to draw contours of "equal instability" in the remaining three quadrants. To measure the degree of instability the number of synodic periods accomplished by the most disturbed subsystem (i.e. S_{23} or S_{34}) of each four-body system was noted*. Approximate contours of equal numbers of synodic periods were then drawn among the points: this yielded a diagram of the type shown in Figure 8.1 for both the critical α ratios derived by the mass parameters (μ, μ_3, μ_4) (case (i) above) and the sigma parameters $(\Sigma_2, \Sigma_3, \Sigma_4)$ (case (ii) above).

Thus it is seen that real systems occupy the positions of greatest stability. Furthermore the stability increases as one moves to the bottom left of Figure 8.1. The contours which lie on the diagram could be drawn very simply; there were no areas of the diagram which involved contours of great complexity.

*It may be remarked here that the line x=y is the set of four-body systems in which the (m_1, m_2, m_3) and (M_2, m_3, m_4) subsystems have equal measures of stability or instability.

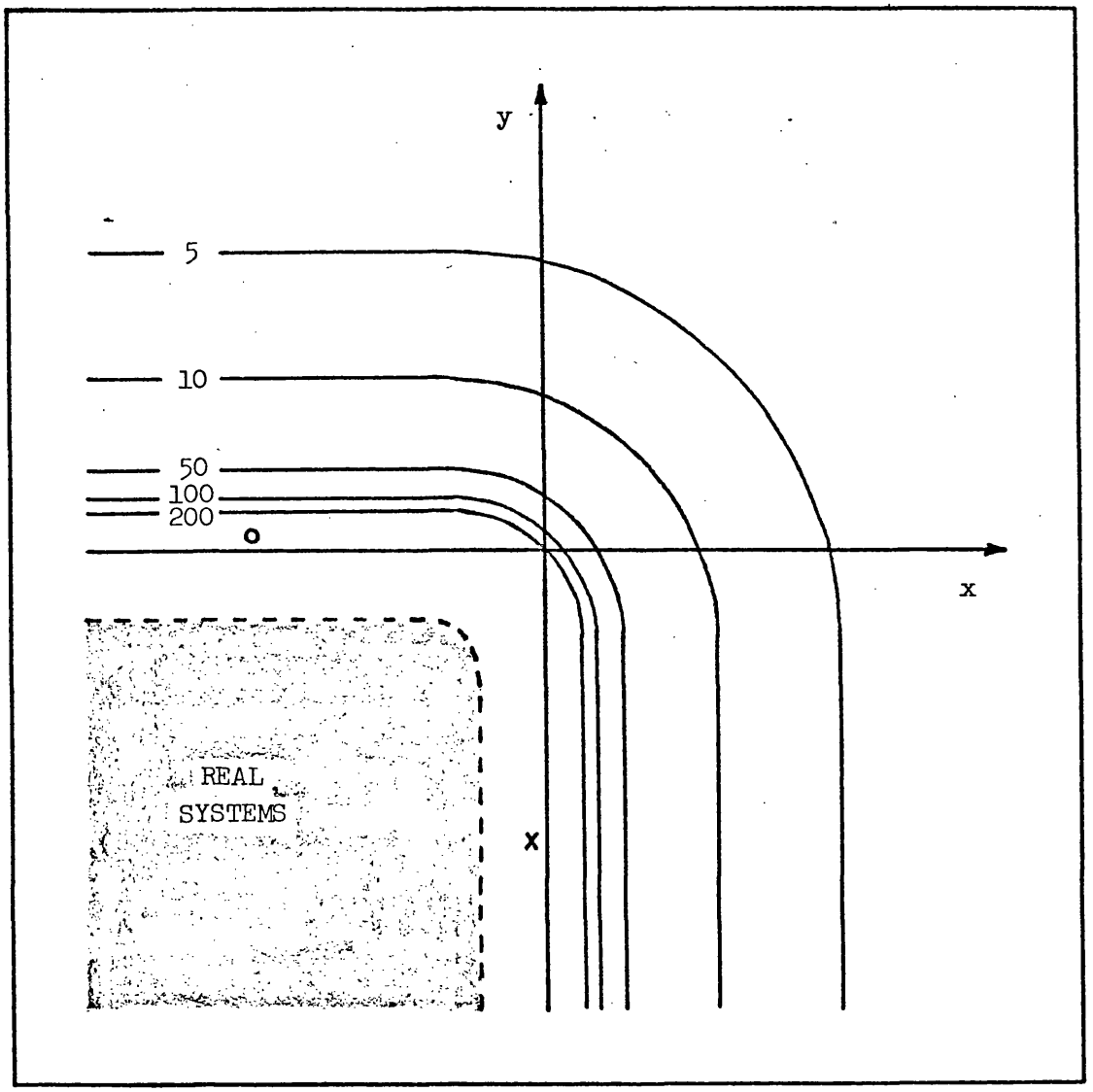

Figure 8.1 The stability of four-body systems in the x,y - plane where the coordinates are as follows:

$x(+ve) - (\alpha_{23} - \alpha_{23cr})/(1 - \alpha_{23cr})$; $x(-ve) - (\alpha_{23} - \alpha_{23cr})/\alpha_{23cr}$

$y(+ve) - (\alpha_{34} - \alpha_{34cr})/(1 - \alpha_{34cr})$; $y(-ve) - (\alpha_{34} - \alpha_{34cr})/\alpha_{34cr}$.

The contours represent lines of equal stability for four-body systems. They are only shown here in a very idealised form. However, from the numerical integrations it is clear that as the stable region is approached (lower left quadrant) the degree of stability, in the sense of the number of orbits completed before instability, climbs rapidly so that very stable systems are obtained over a short range in α_{23} and α_{34} [cf. Figs. 6.1-25 where, in the three-body case, the empirical stability curves rose steeply on approaching $(\alpha_{23})_o$].

This last result indicates that it should be possible to derive results for four-body systems similar to those of Chapter 6 for the three-body case. The results could be displayed as contours of S_{23} or S_{34} in the 0 α_{23} α_{34} plane for each set of Σ parameters (Σ_2, Σ_3, Σ_4) investigated.

Three cases of particular interest arose in this initial investigation: two were real systems, viz. Saturn-Titan-Hyperion-Iapetus and Saturn-Titan-Hyperion-Phoebe, the third being a numerical integration. The former are marked approximately on Figure 8.1 as "X", the latter as an "O".

It may be noted that the two real systems both including the triple subsystem Saturn-Titan-Hyperion are very much closer to the unstable region than are the other real systems considered. This is due to the relatively large α_{23} value: the (M_2, m_3, m_4), i.e. what may be called (Saturn + Titan) - Hyperion-Iapetus or (Saturn + Titan) - Hyperion - Phoebe subsystems, subsystem is stable in both cases. Here we may refer back to Chapter 4, Section 4.6, where the 4:3 commensurability in the mean motions of the Titan-Hyperion system was considered.

The numerical integration case was interesting from the point of view that it was unstable but was very close to the stable region. However, having said that, it only appeared in this position on the diagram which used the mass parameters (μ,μ_3,μ_4) to calculate the α_{23cr} and α_{34cr} values. The diagram, when using critical values of the α ratio derived from the use of the sigma parameters, was separated quite distinctly into two regions: the bottom left quadrant contained only stable systems (the real ones being well-away from the unstable region); all the unstable systems were in the other three quadrants. This suggests that the critical values of α_{23} and α_{34} derived from the use of the sigma parameters are a better indication of whether the four-body system will be stable than those derived from the mass parameters.

8.5 Results - The Prediction of the Amplitude of Variations on the Eccentricities

In the same manner as the maximum variations in semi-major axes and eccentricities were used in Chapter 7 to demonstrate the existence of simple relationships between the empirical stability parameters (ε^{23} ,ε_{32})

and these variations, relationships can be established between the $(\Sigma_2, \Sigma_3, \Sigma_4)$ parameters and the maximum variations in eccentricities in the four-body problem.

This is not unexpected since the ε terms in Equations (1) - (3) appear to be "additive". In other words if we consider the orbit of m_2 relative to m_1 i.e. Equation (1) then this orbit will have variations in semi-major axes and eccentricity. Due to the presence of m_3 we have amplitude of variations $da_2 = k_1 \varepsilon_{32}$ and $de_2 = \ell_1 \varepsilon_{32}$ and due to the presence of m_4 we have $\delta a_2 = k_2 \varepsilon_{42}$ and $\delta e_2 = \ell_2 \varepsilon_{42}$ where k_1, k_2 and ℓ_1, ℓ_2 are functions of the ε parameters and α ratios.

The total amplitude of these variations in semi-major axis and eccentricity will then be Δa_2, Δe_2 where

$$\Delta a_2 = da_2 + \delta a_2 = k_1 \varepsilon_{32} + k_2 \varepsilon_{42}$$

and

$$\Delta e_2 = de_2 + \delta e_2 = \ell_1 \varepsilon_{32} + \ell_2 \varepsilon_{42}$$

respectively. Similar arguments will hold for the other subsystems orbits.

Let us now consider a few examples of the amplitude of variation in eccentricity as they have been determined from the present preliminary investigation into the four-body problem. In Tables 8.1 - 8.9 are presented the amplitude of the variations in eccentricity for nine sets of sigma parameters. These tables fall into three groups Tables 8.1 - 8.3, 8.4 - 8.6 and 8.7 - 8.9

In these three sets we consider systems with the same α ratios but different Σ parameters. Specifically, the sigma parameters are reduced by an order of magnitude from table to table in the three sets. It may then be seen that when the order of magnitude of the Σ's changes then generally the corresponding Δe values also change by an order of magnitude. In particular, if the system is stable, then it is often found, to a fairly high degree of accuracy, that

$$\frac{(\Delta e_i)_1}{(\Sigma_i)_1} = \frac{(\Delta e_i)_2}{(\Sigma_i)_2} \qquad (i=2,3,4) \qquad (21)$$

i.e. with $\Sigma_i = (\Sigma_i)_1 = 10^{-b}$ giving an amplitude of variation in e_i of size $(\Delta e_i)_1 = a_1 . 10^{-(b+c)}$ then $\Sigma_i = (\Sigma_i)_2 = 10^{-d}$ results in an amplitude

of variation $(\Delta e_i)_2 = a_2.10^{-(d+c)}$ where a_1 and a_2 are positive real, with $a_1 \simeq a_2$, and b,c,d are positive integers. The more stable the systems become, i.e. the smaller the Σ values are for constant α ratios, then the better becomes the agreement of Equation (21). Indeed if an individual subsystem is more stable than the remaining parts of the system then the $\Sigma \sim \Delta e$ relationships for this subsystem will be more exact than those for the rest of the system. For example consider the systems denoted Ref.No.1 in Tables 8.1 - 8.3. It may be seen that the agreement between the Δe_4 values, along the lines of Equation (21), is very good. The Δe_3 values agree well except for the value at $\Sigma_3 = 10^{-4}$, while those for Δe_2 are slightly less good. It may then be noted from the critical values of α_{23} and α_{34} (as calculated from the sigma parameters) that the (m_1, m_2, m_3) subsystem is less stable than the (M_2, m_3, m_4) subsystem i.e. α_{23} is "closer" to α_{23cr} than α_{34} is to α_{34cr}. This type of relationship may break down when the instability of one part of a system affects the remaining stable orbits.

The same pattern shows up in Tables 8.4 - 8.6. In all cases the (m_1, m_2, m_3) subsystem is stable i.e. $\alpha_{23} \leq \alpha_{23cr}$, however when $\alpha_{34} = 0.5$, then the (M_2, m_3, m_4) subsystem becomes unstable i.e. $\alpha_{34} > \alpha_{34cr}$. This is reflected in the loss of the relationship of Equation (21). It may be noted however that the instability of the (M_2, m_3, m_4) subsystem (Table 8.4 - Ref.No.2) has resulted in an "unexpected" value for Δe_2; the unstable nature of the (M_2, m_3, m_4) subsystem's orbits has clearly affected the orbit of m_2 about m_1. The reason for the instability affecting the (m_1, m_2) subsystem's orbit is due to the fact that, of the two two-body subsystems in the (M_2, m_3, m_4) subsystem i.e. (M_2, m_3) and (M_3, m_4) it is the former which suffers the larger perturbation (cf. the large Σ_3 value). This subsystem, (M_2, m_3) is also a subsystem of the (m_1, m_2, m_3) triple subsystem and will tend to affect the orbit of the (m_1, m_2) subsystem. If it had been the case that the (M_3, m_4) subsystem's orbit was affected most by a larger value of Σ_4 then this instability would not have affected the (m_1, m_2) subsystem to such a large extent (see Table 8 .10).

Table 8.1 - $(10^{-4}, 10^{-4}, 10^{-4})$: $\alpha_{23cr} = 0.86$, $\alpha_{34cr} = 0.86$

Ref.No.	α_{23}	α_{34}	Δe_2	Δe_3	Δe_4
1	0.8000	0.6250	$7.20.10^{-3}$	$1.42.10^{-2}$	$6.87.10^{-3}$
2	0.8000	0.8125	$2.46.10^{-2}$	$1.27.10^{-2}$	$6.68.10^{-3}$
3	0.9500	0.6842	$2.97.10^{-1}$	$2.42.10^{-1}$	$2.77.10^{-2}$
4	0.9500	0.8421	$7.14.10^{-2}$	$7.59.10^{-2}$	$4.08.10^{-2}$

Table 8.2 - $(10^{-5}, 10^{-5}, 10^{-5})$: $\alpha_{23cr} = 0.94$, $\alpha_{34cr} = 0.94$

Ref. No.	α_{23}	α_{34}	Δe_2	Δe_3	Δe_4
1	0.8000	0.6250	$5.12.10^{-4}$	$1.19.10^{-3}$	$6.88.10^{-4}$
2	0.8000	0.8125	$6.59.10^{-4}$	$8.47.10^{-4}$	$8.37.10^{-4}$
3	0.9500	0.6842	$4.15.10^{-2}$	$4.00.10^{-2}$	$3.07.10^{-4}$
4	0.9500	0.8421	$2.75.10^{-2}$	$2.46.10^{-2}$	$1.11.10^{-3}$

Table 8.3 - $(10^{-6}, 10^{-6}, 10^{-6})$: $\alpha_{23cr} = 0.97$, $\alpha_{34cr} = 0.97$

Ref. No.	α_{23}	α_{34}	Δe_2	Δe_3	Δe_4
1	0.8000	0.6250	$4.85.10^{-5}$	$1.23.10^{-4}$	$6.80.10^{-5}$
2	0.8000	0.8125	$6.73.10^{-5}$	$8.88.10^{-5}$	$8.57.10^{-5}$
3	0.9500	0.6842	$1.09.10^{-3}$	$1.05.10^{-3}$	$1.23.10^{-5}$
4	0.9500	0.8421	$5.38.10^{-4}$	$4.87.10^{-4}$	$5.17.10^{-5}$

Table 8.4 - $(10^{-4}, 10^{-2}, 10^{-3})$: $\alpha_{23cr} = 0.50$, $\alpha_{34cr} = 0.35$

Ref. No.	α_{23}	α_{34}	Δe_2	Δe_3	Δe_4
1	0.2000	0.2500	$5.22.10^{-4}$	$2.79.10^{-2}$	$1.42.10^{-3}$
2	0.2000	0.5000	$2.12.10^{-3}$	$3.82.10^{-1}$	$2.00.10^{-2}$
3	0.3000	0.3333	$5.49.10^{-4}$	$2.92.10^{-2}$	$1.40.10^{-3}$

Table 8.5 - $(10^{-5}, 10^{-3}, 10^{-4})$: $\alpha_{23cr} = 0.76$, $\alpha_{34cr} = 0.74$

Ref. No.	α_{23}	α_{34}	Δe_2	Δe_3	Δe_4
1	0.2000	0.2500	$4.91.10^{-5}$	$2.77.10^{-3}$	$1.47.10^{-4}$
2	0.2000	0.5000	$5.04.10^{-5}$	$1.78.10^{-2}$	$3.03.10^{-4}$
3	0.3000	0.3333	$5.17.10^{-5}$	$2.75.10^{-3}$	$1.41.10^{-4}$

Table 8.6 - $(10^{-6}, 10^{-4}, 10^{-5})$: $\alpha_{23cr} = 0.89$, $\alpha_{34cr} = 0.88$

Ref. No.	α_{23}	α_{34}	Δe_2	Δe_3	Δe_4
1	0.2000	0.2500	$4.92.10^{-6}$	$2.76.10^{-4}$	$1.47.10^{-5}$
2	0.2000	0.5000	$5.07.10^{-6}$	$1.84.10^{-3}$	$3.27.10^{-5}$
3	0.3000	0.3333	$5.17.10^{-6}$	$2.72.10^{-4}$	$1.41.10^{-5}$

Table 8.7 - $(10^{-3}, 10^{-2}, 10^{-4})$: $\alpha_{23cr} = 0.48$, $\alpha_{34cr} = 0.36$

Ref. No.	α_{23}	α_{34}	Δe_2	Δe_3	Δe_4
1	0.4000	0.1250	$1.09.10^{-2}$	$4.97.10^{-2}$	$1.31.10^{-4}$
2	0.5000	0.1000	$1.89.10^{-2}$	$6.84.10^{-2}$	$1.46.10^{-4}$
3	0.5000	0.2000	$5.19.10^{-3}$	$4.17.10^{-2}$	$1.35.10^{-4}$

Table 8.8 - $(10^{-4}, 10^{-3}, 10^{-5})$: $\alpha_{23cr} = 0.75$, $\alpha_{34cr} = 0.74$

Ref. No.	α_{23}	α_{34}	Δe_2	Δe_3	Δe_4
1	0.4000	0.1250	$6.13.10^{-4}$	$4.45.10^{-3}$	$1.49.10^{-5}$
2	0.5000	0.1000	$1.16.10^{-3}$	$4.35.10^{-3}$	$1.47.10^{-5}$
3	0.5000	0.2000	$5.23.10^{-4}$	$4.11.10^{-3}$	$1.41.10^{-5}$

Table 8.9 - $(10^{-5}, 10^{-4}, 10^{-6})$: $\alpha_{23cr} = 0.88$, $\alpha_{34cr} = 0.89$

Ref. No.	α_{23}	α_{34}	Δe_2	Δe_3	Δe_4
1	0.4000	0.1250	$5.83.10^{-5}$	$4.72.10^{-4}$	$1.48.10^{-6}$
2	0.5000	0.1000	$1.16.10^{-4}$	$4.55.10^{-4}$	$1.48.10^{-6}$
3	0.5000	0.2000	$5.37.10^{-5}$	$4.02.10^{-4}$	$1.40.10^{-6}$

Table 8.10 - $\alpha_{23} = 0.4$, $\alpha_{34} = 0.8$

Σ_2	Σ_3	Σ_4	α_{23cr}	α_{34cr}	Δe_2	Δe_3	Δe_4
10^{-3}	10^{-3}	10^{-2}	0.68	0.48	$1.03.10^{-2}$	$1.71.10^{-2}$	$5.69.10^{-1}$
10^{-4}	10^{-4}	10^{-3}	0.86	0.75	$1.16.10^{-3}$	$8.06.10^{-3}$	$1.43.10^{-1}$

The remaining Tables 8.7 - 8.9 again show the familiar trends in Δe_2, Δe_3 and Δe_4 as the sigma parameters are changed.

8.6 Discussion

The aim of this chapter was to present a brief summary of preliminary results which have been obtained for the hierarchical four-body problem in the coplanar, corotational case with initially circular orbits. It would appear from these results that it is indeed possible to obtain results similar to those of the three-body case which were derived in Chapters 6 and 7.

Clearly the preliminary results only give a very incomplete survey of the whole picture. A very much larger number of numerical integrations will have to be used to obtain results comparable to those of the hierarchical three-body case. However it is hoped that the results gained in the latter will be useful in ensuring that only the minimum number of computer experiments will have to be used to examine the four-body case.

As yet it has not finally been decided how most effectively to measure the real time intervals of the various integrations. In the three-body case the number of synodic periods i.e. $S_{23} = T_2T_3/(T_3 - T_2)$ of the whole system was used to determine the degree of stability. We would then say that a system which executes 30 synodic periods before exhibiting instability is more stable than one which only accomplished 10. Moving on to the four-body problem we lose this convenient time unit. There are now three synodic periods viz.

$$S_{23} = \frac{T_2 T_3}{T_3 - T_2}$$

$$S_{24} = \frac{T_2 T_4}{T_4 - T_2} \qquad (22)$$

and

$$S_{34} = \frac{T_3 T_4}{T_4 - T_3}$$

A method of measuring time until instability in the four-body problem is now proposed. Remembering that the number of conjunctions which occur in the three-body problem is directly related to the number of synodic periods which have elapsed, we adopt the following method.

Suppose it is the orbit of the (m_1, m_2) subsystem which is disrupted most during the unstable behaviour. Then the time till this occurrence will be measured as t_2 where

$$t_2 = \frac{\varepsilon_{32} N_{s23} + \varepsilon_{42} N_{s24}}{\varepsilon_{32} + \varepsilon_{42}} \quad . \qquad (23)$$

and N_{sij} $(i < j)$ is the number of synodic periods elapsed between the (M_{i-1}, m_i) and (M_{j-1}, m_j) subsystems from the initial time up until the time of instability. Similar measures of the time will apply to the (M_2, m_3) and (M_3, m_4) subsystems if they are unstable so that finally the time will be measured as

$$t = \begin{cases} t_2 = \dfrac{\varepsilon_{32} N_{s23} + \varepsilon_{42} N_{s24}}{\varepsilon_{32} + \varepsilon_{42}} \text{ ; if } (M_1, m_2) \text{ is most unstable} \\ t_3 = \dfrac{\varepsilon^{23} N_{s23} + \varepsilon_{43} N_{s34}}{\varepsilon^{23} + \varepsilon_{43}} \text{ ; if } (M_2, m_3) \text{ is most unstable} \\ t_4 = \dfrac{\varepsilon^{24} N_{s24} + \varepsilon^{34} N_{s34}}{\varepsilon^{24} + \varepsilon^{34}} \text{ ; if } (M_3, m_4) \text{ is most unstable} \end{cases} \qquad (24)$$

Note that these time measures are essentially a combination of the number of synodic periods weighted with respect to the ε parameters, that is we have essentially weighted the conjunctions with respect to the relevant ε parameters.

Consider by way of example what happens to t_2 if one of the ε parameters is very small relative to the other. Suppose $\varepsilon_{32} >> \varepsilon_{42}$ then $t_2 \simeq N_{s23}$ and the time measure reduces, as it should with ε_{42} so small, to that of the three-body case.

It is hoped that by the use of these weighted time measurements and by considering close encounters, cross-over of orbits and break-ups (see Chapter 6, Section 6.2, for definitions), results in the four-body problem similar to those derived for the three-body case may be obtained.

The amplitude of variations in the semi-major axes and eccentricities should also be investigated. However, if it proves possible to derive these analytically (cf. Chapter 7, Section 7.4) by a method similar to the classical method of secular inequalities then this will substantially reduce the required amount of numerical investigation in this part of the work for hierarchical four-body systems.

CHAPTER 9 SPECIAL CASES OF HIERARCHICAL DYNAMICAL SYSTEM

9.1 Introduction

In Chapter 3 stability parameters were derived for many-body systems. These parameters were obtained through an expansion of the force function when the equations of motion are expressed in terms of the Jacobian coordinate system. The expansion was dependant upon the α_{ij} terms being less than unity where $\alpha_{ij} = \rho_i/\rho_j$ $(i < j)$ and ρ_i is the magnitude of the radius vector of the ith mass from the mass-centre of the first (i-1) masses. Certainly in the case of satellites being disturbed by the Sun this is valid since α ratios in this case can be very small e.g. about 1/400 for the Earth-Moon-Sun system. Also in the case of many stellar systems the α ratios can be sufficiently small: in fact since the masses are all of comparable size with the orbits being of generally substantial eccentricity and mutual inclination there are no other small quantities which would admit such an expansion. However in the case of planets (or indeed satellites) disturbing each other it is not always the case that the α ratios are small. Indeed the α ratios may be as close as we wish to unity and still result in stable systems by making the planetary masses sufficiently small. In fact the masses (of the planets) are *small* in comparison to the central mass i.e. the Sun. This fact may be made use of to carry out another expansion of the force function, along the lines of Chapter 3, but not assuming the α ratios to be small, in order to evaluate the applicability of the ε-parameters in the planetary case (see Section 9.2).

Having done this we will have sufficiently examined all types of naturally occurring system within the Solar System with respect to their ε values. The other remaining type of system lies outwith the Solar System, An example of the type was given by Evans (1968) in his "mobile diagrams" and was denoted Quadruple:Hierarchy 2. This is a system of a more general nature than those considered in the Jacobian system. Indeed this hierarchy may be extended so as to obtain octuple, 16-tuple, etc. systems.

Consider the following simple example. A star may be observed which appears, to the naked eye, as a single star: binoculars may reveal it to be a binary system. Employing a large telescope it may further be found that the components of the binary are in fact binaries themselves forming a quadruple system. Indeed we may suppose that each of the stars in the quadruple could, upon spectral examination, be shown to be a spectroscopic binary. This simple example gives a picture of how a generalised form of the Jacobian coordinate system could be formed. Each subsystem would consist of disturbed binary motion, the sizes of the binary orbits decreasing as we delve deeper and deeper into the system. This coordinate system, applicable to the above-mentioned general type of hierarchical system, is described in Section 9.3.

In Section 9.4 it is shown how an expansion of the force function in this coordinate system can yield ε-type parameters which provide, as in the Jacobian coordinate system, a measure of the disturbance of the system's orbits by all the other bodies in the system.

The results of this chapter are discussed in Section 9.5 and some conclusions are drawn.

9.2 The Planetary Case - A Re-evaluation of the "ε" Parameters

In the planetary case of the many-body problem, where several planets are considered to revolve about a central mass in disturbed Keplerian orbits, classical perturbation theories have made use of the relative smallness of the planetary masses compared to that of the central mass as an aid to expanding the disturbing function of the problem. Now in Chapter 3, Section 3.6, the expansion of the force function was carried out solely in powers of the α_{ij} terms where $\alpha_{ij} = \rho_i/\rho_j$ ($i=2,\ldots,n-1$; $j=3,\ldots,n$: $i < j$) and $\rho_i < \rho_j$. However in the planetary case it is possible for these α_{ij} ratios to assume values close to unity and it is therefore necessary to examine the validity of the ε parameters in this case. To do this another expansion of the force function is considered which takes account of the smallness of the planetary masses as compared to that of the central body.

Consider a system of n-1 planets in orbits about a central star. The star will be denoted m_1, the planets $m_2,\ldots,m_n$ in order of increasing distance from the star. Then in the Jacobian coordinate system we have, as in Chapter 3, Section 3.5,

$$\frac{m_i M_{i-1}}{M_i} \ddot{\underset{\sim}{\rho}}_i = \underset{\sim}{\nabla}_i U \qquad (i=2,\ldots,n) \qquad (1)$$

where $U = G \sum_{\ell=2}^{n} m_\ell B_\ell$ is the force function (2)

$$B_\ell = \sum_{k=1}^{\ell-1} \frac{m_k}{r_{k\ell}} \qquad (3)$$

m_i is the ith mass

$$M_i = \sum_{j=1}^{i} m_j \qquad (4)$$

$\underset{\sim}{\rho}_i = \overrightarrow{M_{i-1} m_i}$: M_{i-1} denoting the position of the mass-centre of the masses $m_1,\ldots,m_{i-1}$

$\underset{\sim}{\nabla}_i$ is the gradient operator with respect to $\underset{\sim}{\rho}_i$

and $r_{k\ell} = |\overrightarrow{\underset{\sim}{r}_{k\ell}}| = |\overrightarrow{m_k m_\ell}|$.

The expression for the $\underset{\sim}{r}^{\circ}_{k\ell}$ as a function of the $\underset{\sim}{\rho}_i$ is the same as Equation (3.37) i.e.

$$\underset{\sim}{r}_{k\ell} = \underset{\sim}{\rho}_\ell - \underset{\sim}{\rho}_k + \sum_{j=k}^{\ell-1} \frac{m_j}{M_j} \underset{\sim}{\rho}_j \qquad \forall k,\ell\ (k<\ell) \qquad (5)$$

where $\underset{\sim}{\rho}_1 = \underset{\sim}{0}$ was defined.

Thus to obtain U as a function of the $\underset{\sim}{\rho}_i$ we calculated $r^{-1}_{k\ell}$ by forming $(\underset{\sim}{r}_{k\ell} \cdot \underset{\sim}{r}_{k\ell})^{-\frac{1}{2}}$ viz.

$$\underset{\sim}{r}^{-1}_{k\ell} = \frac{1}{\rho_\ell}\left[1 + \alpha^2_{k\ell} - 2\alpha_{k\ell} C_{k\ell} + 2 \sum_{j=k}^{\ell-1} \frac{m_j}{M_j} \alpha_{j\ell}(C_{j\ell} - \alpha_{k\ell} C_{jk}) + \sum_{j=k}^{\ell-1} \sum_{h=k}^{\ell-1} \frac{m_j m_h}{M_j M_h} \cdot \alpha_{j\ell}\, \alpha_{h\ell}\, C_{jh}\right]^{-\frac{1}{2}}, \quad \forall k,\ell\ (k<\ell) \qquad (6)$$

where $\alpha_{ij} = \rho_i/\rho_j$

$$C_{ij} = \frac{\underset{\sim}{\rho}_i \cdot \underset{\sim}{\rho}_j}{\rho_i \rho_j}$$

and $\rho_i = |\underset{\sim}{\rho}_i|$.

Now whereas the expansion in Chapter 3, Section 3.6, was carried out in powers of the α_{ij}, neglecting powers of the α's greater than two, the present expansion will make use of the smallness of the m_i $(i=2,\ldots,n)$ as compared to m_1. Equation (6) may be rewritten as

$$r_{k\ell}^{-1} = \frac{S_{k\ell}}{\rho_\ell} \cdot \left[1 + S_{k\ell}^2 \cdot \left(2 \cdot \sum_{j=k}^{\ell-1} \frac{m_j}{M_j} \alpha_{j\ell} (C_{j\ell} - \alpha_{k\ell} C_{jk}) + \sum_{j=k}^{\ell-1} \sum_{h=k}^{\ell-1} \frac{m_j m_h}{M_j M_h} \alpha_{j\ell} \alpha_{h\ell} C_{jh} \right) \right]^{-\frac{1}{2}} \qquad (7)$$

where $$S_{k\ell} = \frac{1}{(1 + \alpha_{k\ell}^2 - 2\alpha_{k\ell} C_{k\ell})^{\frac{1}{2}}} \cdot \qquad (8)$$

Using the binomial expansion for $(1+x)^{-\frac{1}{2}}$ we will now expand out the square bracket of Equation (7) to the first order in the ratios m_i/m_1 $i=2,\ldots,n$. Thus we obtain

$$r_{k\ell}^{-1} = \frac{S_{k\ell}}{\rho_\ell} \left[1 - S_{k\ell}^2 \cdot \sum_{j=k}^{\ell-1} \frac{m_j}{m_1} \alpha_{j\ell} (C_{j\ell} - \alpha_{k\ell} C_{jk}) \right] \cdot \qquad (9)$$

In Equation (9) any contribution from the double summation of Equation (7) has been neglected since these terms are of order $m_i m_j / m_1^2$ and are therefore negligible. Further it is sufficient to approximate $m_j / M_j \simeq m_j / m_1$ since by the binomial expansion, using Equation (4),

$$\frac{m_j}{M_j} = \frac{m_j}{m_1} \cdot \left(1 + \sum_{g=2}^{j} \frac{m_g}{m_1} \right)^{-1} \qquad j=2,\ldots,n$$

$$= \frac{m_j}{m_1} - \frac{m_j}{m_1} \cdot \sum_{g=2}^{j} \frac{m_g}{m_1} + \ldots\ldots$$

$$= \frac{m_j}{m_1} + \quad 0\left[(m_i/m_1)^2\right] \qquad (i,j = 2,\ldots,n).$$

Note finally that there is no contribution from either summation in Equation (7) when j and/or h equals one since then, although m_j or m_h *is* m_1, ρ_j or ρ_h is zero, $\underset{\sim}{\rho}_1 = \underset{\sim}{0}$ being defined.

Substituting Equation (9) into Equation (3) the expression for the B_ℓ may be obtained viz.

$$B_\ell = \sum_{k=1}^{\ell-1} \frac{m_k}{\rho_\ell} \cdot S_{k\ell} \cdot \left[1 - \frac{S_{k\ell}^2}{m_1} \cdot \sum_{j=k}^{\ell-1} m_j\, \alpha_{j\ell}\,(C_{j\ell} - \alpha_{k\ell}\, C_{jk})\right]$$

$$= m_1\left[\sum_{k=1}^{\ell-1} \frac{m_k}{m_1} \frac{S_{k\ell}}{\rho_\ell} - \sum_{k=1}^{\ell-1}\sum_{j=k}^{\ell-1} \frac{S_{k\ell}^3}{\rho_\ell} \frac{m_k\, m_j}{m_1^2} \alpha_{j\ell}(C_{j\ell} - \alpha_{k\ell}\, C_{jk})\right]. \qquad (10)$$

Now in Equation (10) the first summation in the brackets contains one term of order unity i.e. k=1 and ℓ-2 terms of order m_k/m_1 (k=2,..., ℓ-1). The double summation contains ℓ-1 terms of order m_j/m_1, i.e. k=1 again, with j running from 1 to ℓ-1, and terms of order $m_k m_j/m_1$ (j=2,..., ℓ-1; k=2,...,ℓ-1:k $\leq$ j) which will be neglected. Noting that $S_{k\ell} = 1$ and $\alpha_{k\ell} = 0$ when k=1, i.e. $\rho_1/\rho_\ell = 0$ since $\underset{\sim}{\rho}_1 = \underset{\sim}{0}$ is defined, the final expression for B_ℓ is obtained:

$$B_\ell = \sum_{k=1}^{\ell-1} m_k \cdot \frac{S_{k\ell}}{\rho_\ell} - \sum_{j=1}^{\ell-1} \frac{m_j}{\rho_\ell}\, \alpha_{j\ell}\, C_{j\ell} \,. \qquad (11)$$

The Legendre polynomial of order r in x, i.e. $P_r(x)$, is defined as follows:

$$\frac{1}{(1 + a^2 - 2ax)^{\frac{1}{2}}} = \sum_{r=0}^{\infty} a^r P_r(x) \qquad (12)$$

where
$$P_0(x) = 1$$
$$P_1(x) = x$$
$$P_2(x) = \tfrac{1}{2}(3x^2 - 1)$$
$$P_3(x) = \tfrac{1}{2}(5x^3 - 3x)$$
$$\text{etc.....}$$

It is therefore possible using the relationship of Equation (12) to rewrite $S_{k\ell}$ in the form

$$S_{k\ell} = \sum_{r=0}^{\infty} \alpha_{k\ell}^r \, P_r(C_{k\ell}) \qquad (13)$$

which, on noting that $P_o(x) = 1$ and $P_1(x) = x$, yields

$$B_\ell = \sum_{k=1}^{\ell-1} \frac{m_k}{\rho_\ell} + \sum_{k=1}^{\ell-1} \frac{m_k}{\rho_\ell} \, \alpha_{k\ell} \, C_{k\ell} + \sum_{k=1}^{\ell-1} \frac{m_k}{\rho_\ell} \cdot \cdot \left\{ \sum_{r=2}^{\infty} \alpha_{k\ell}^r \, P_r(C_{k\ell}) \right\} - \sum_{j=1}^{\ell-1} \frac{m_j}{\rho_\ell} \, \alpha_{j\ell} \, C_{j\ell} \, . \qquad (14)$$

In the second and fourth terms of Equation (14) k and j are dummy suffices, thus

$$B_\ell = \frac{M_{\ell-1}}{\rho_\ell} + \sum_{k=1}^{\ell-1} \frac{m_k}{\rho_\ell} \, \alpha_{k\ell}^2 \cdot \left\{ \sum_{r=0}^{\infty} \alpha_{k\ell}^r \, P_{r+2}(C_{k\ell}) \right\} , \qquad (15)$$

which may be substituted into the force function, Equation (2), to give

$$U = G \sum_{\ell=2}^{n} \frac{m_\ell}{\rho_\ell} \cdot \left[M_{\ell-1} + \sum_{k=1}^{\ell-1} m_k \, \alpha_{k\ell}^2 \left\{ \sum_{r=0}^{\infty} \alpha_{k\ell}^r \, P_{r+2}(C_{k\ell}) \right\} \right] . \qquad (16)$$

Let us now rewrite Equation (1) thus

$$m_i \, M_{i-1} \, \ddot{\underset{\sim}{\rho}}_i = M_i \, \nabla_{\underset{\sim}{i}} \, U \, . \qquad i=2,\ldots,n$$

Substituting the expression for U - Equation (16) - into the above yields

$$m_i \, M_{i-1} \, \ddot{\underset{\sim}{\rho}}_i = G \, M_i \, \nabla_{\underset{\sim}{i}} \left[\sum_{\ell=2}^{n} \frac{m_\ell}{\rho_\ell} \left(M_{\ell-1} + \sum_{k=1}^{\ell-1} m_k \, \alpha_{k\ell}^2 \cdot \left\{ \sum_{r=0}^{\infty} \alpha_{k\ell}^r \, P_{r+2}(C_{k\ell}) \right\} \right) \right] .$$

Upon observing that all the $\underset{\sim}{\rho}_i$ are independent we then have

$$m_i M_{i-1} \ddot{\underset{\sim}{\rho}}_i = G M_i \underset{\sim}{\nabla}_i \left[\frac{m_i M_{i-1}}{\rho_i} + \frac{m_i}{\rho_i} \sum_{k=1}^{i-1} m_k \alpha_{ki}^2 \{ \sum_{r=0}^{\infty} \alpha_{ki}^r P_{r+2}(C_{ki}) \} \right.$$

$$\left. + m_i \sum_{\ell=i+1}^{n} \frac{m_\ell}{\rho_\ell} \alpha_{i\ell}^2 \{ \sum_{r=0}^{\infty} \alpha_{i\ell}^r P_{r+2}(C_{i\ell}) \} \right]$$

which on dividing through by $m_i M_{i-1}$ gives the result (cf. Equation (3.40))

$$\ddot{\underset{\sim}{\rho}}_i = G M_i \underset{\sim}{\nabla}_i \left[\frac{1}{\rho_i} \{ 1 + \sum_{k=1}^{i-1} \delta^{ki} S'_{ki} + \sum_{\ell=i+1}^{n} \delta_{\ell i} S'_{i\ell} \} \right]^* \qquad (17)$$

where $$\delta^{ki} = \frac{m_k}{m_1} \cdot \alpha_{ki}^2 \qquad (18)$$

$$\delta_{\ell i} = \frac{m_\ell}{m_1} \alpha_{i\ell}^3 \qquad (19)$$

and $$S'_{ij} = \sum_{r=0}^{\infty} \alpha_{ij}^r P_{r+2}(C_{ij}) . \qquad (20)$$

Comparing Equation (18) and (19) to the definitions of the ε parameters given in Equations (3.41) it may be seen that, correct to the first order in the masses m_i $(i=2,\ldots,n)$,

$$\delta^{ki} = \varepsilon^{ki} \quad \text{and} \quad \delta_{\ell i} = \varepsilon_{\ell i} .$$

*This expression, as it stands, also contains terms of second order in the planetary masses which should be neglected. These terms arise by considering the product of the masses $m_2,\ldots,m_i$ contained in M_i on the R.H.S. of the expression with the δ terms contained in the two summations. However, the terms arising from the product of M_i and $\underset{\sim}{\nabla}_i(1/\rho_i)$ (which represents the central two-body force) are all of first order in the masses, or greater, and should therefore be retained. It is thus seen that the use of the Jacobian coordinate system already includes several of the terms of first order in the masses.

Also if we neglect all but the lowest powers of the α_{ij} ratios i.e. $S'_{ij} = P_2(C_{ij}) \; \forall \; i,j$ then Equation (17) reduces to Equation (3.40) correct to the first order in the masses.

The difference between Equation (3.40) and the present Equation (17), for small masses m_i $i=2,\ldots,n$, is contained in the S'_{ij} terms. It may readily be seen that if the α_{ij} are close to (but less than) unity the S_{ij} terms may become large. This may significantly alter the magnitude of the disturbing terms in Equation (17).

For example consider a system of n-1 planets in the straight line configuration $m_1 \; m_2 \; m_3 \; \ldots . m_n$ i.e. $C_{ij} = 1 \; \forall \; i,j$: then we have

$$S'_{ij} = \sum_{r=0}^{\infty} \alpha_{ij}^{r}$$

since $P_r(1) = 1 \; \forall \; r$. It is a standard result that

$$\sum_{m=0}^{\infty} a^m = \frac{1}{1-a} \qquad (a < 1)$$

whence we have the result

$$S'_{ij} = \frac{1}{1 - \alpha_{ij}} \; . \qquad (21)$$

Substituting Equation (21) into Equation (17) we then find

$$\ddot{\underset{\sim}{\rho}}_i = G M_i \nabla_{\underset{\sim}{i}} \left[\frac{1}{\rho_i} \{ 1 + \sum_{k=1}^{i-1} \frac{\delta_{ki}}{1 - \alpha_{ki}} + \sum_{\ell=i+1}^{n} \frac{\delta_{\ell i}}{1 - \alpha_{i\ell}} \} \right]$$

whereupon it is seen, if any of the α_{ij} terms are close to unity they may very significantly alter the importance of their corresponding δ term.

However having said this it is clear that, if α_{ij} is less than 0.9 then the effective size of the mutual disturbing terms of the ith and jth planets will be altered by less than an order of magnitude when these two planets come into conjunction. Therefore it may be seen that, except for the very high range of α_{ij}, the δ parameters, and hence the ε's also, are indeed representative of the sizes of the perturbations on each orbit of the system by other members of the planetary system.

9.3 A Coordinate System for General Hierarchical Systems

Evans (1968) discussed, by means of "mobile diagrams", the different types of hierarchical arrangement of naturally occurring dynamical system. These were described in Chapter 3, Section 3.1. Thus far we have not considered the types of system denoted Quadruple: Hierarchy (2) by Evans (see Figure 3.1(c)). This is but one example of an arrangement common to many multiple stellar systems. For example in Chapter 3 the Castor system was described briefly. In this case there are six stars arranged in three binaries: these are further arranged into a close pair of binaries with the third at a more remote distance. The orbits of the system will be disturbed Keplerian ellipses as follows. Each of the stars in the three pairs will execute their orbits with respect to the mass-centre of their respective pairs. The close pair of binaries will execute their orbits such that their mass-centres revolve about the common mass-centre of the four bodies in this part of the system. The third pair will execute their orbit such their mass-centre moves in a disturbed Keplerian orbit about the mass-centre of the close pair of binaries.

Clearly we would expect that each part of the system, whether it be one single mass, a pair of masses *or more* will disturb the orbits of the other bodies in the system. For example we might expect from the analogy of a triple stellar system that the remote binary in the Castor system will tend to disturb the relative orbit of the close binaries in much the same way as the binary in a triple system has its orbit disturbed by the third mass. It is plain that such systems do not fall within the scope of the Jacobian coordinate system. Nevertheless a similar type of coordinate system may be arranged which uses the mass-centres of the various subsystems of such a hierarchy in the same way that the Jacobian system takes the position of each mass, m_i, relative to the mass-centre of the masses $m_1,\ldots,m_{i-1}$.

Consider a system of n bodies, where $n=2^m$ (m being an integer), and let the bodies be arranged hierarchically such that they are in 2^{m-1} binary subsystems which themselves pair up to form 2^{m-2} quadruple subsystems, etc. The situation is shown diagramatically in Figure 9.1 for the case n=8 i.e. m=3.

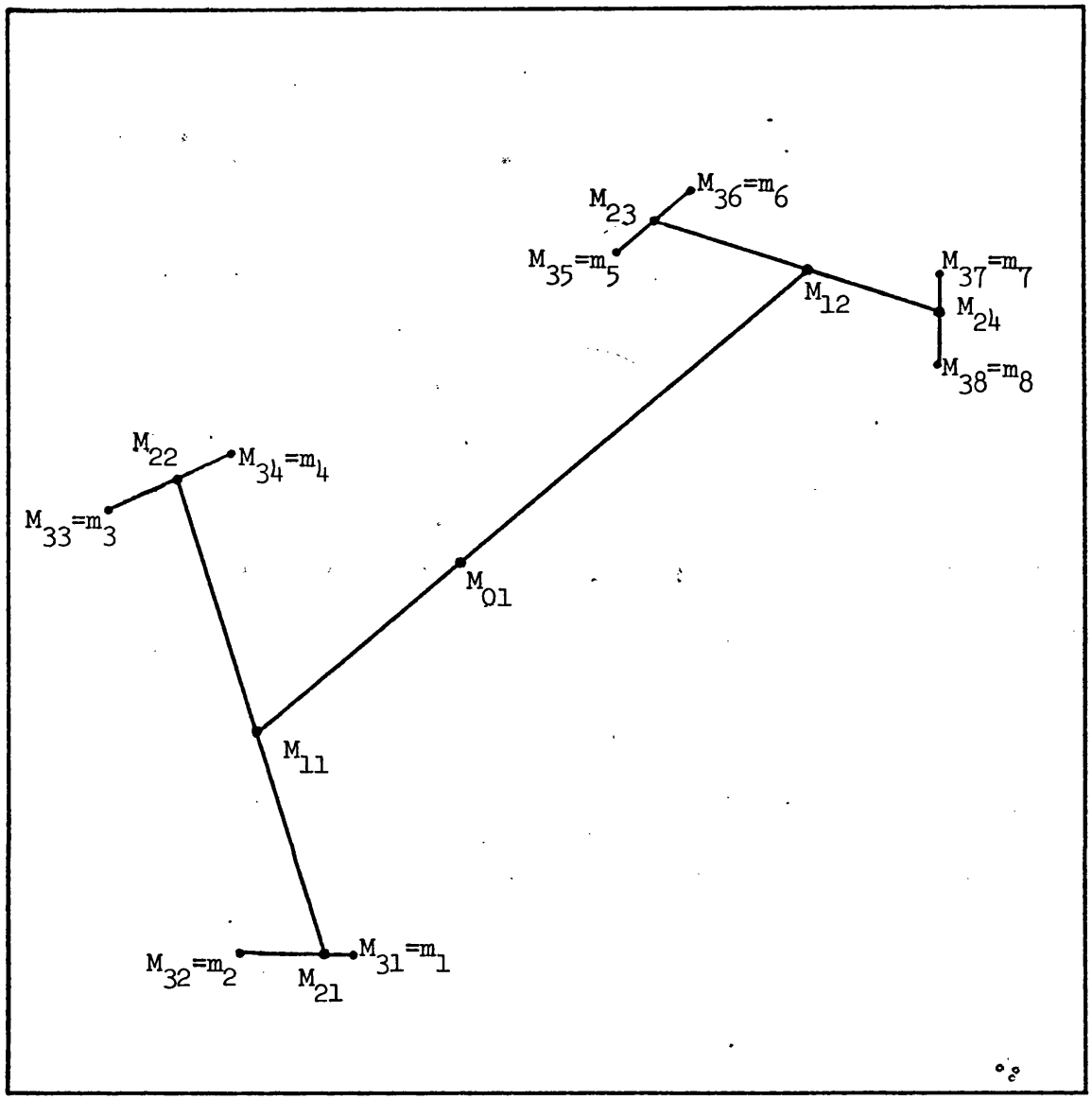

Figure 9.1 The hierarchical arrangement of an 8-body system along the lines of the arrangement observed in many naturally occurring dynamical systems. The positions marked M_{ij} are the mass-centres about which disturbed two-body motion occurs if the system is stable (see text for definitions of M_{ij} and description of the motion of the bodies).

Considering the masses to lie in the above-mentioned hierarchical arrangement, as shown in Figure 9.1, at least in some initial phase of the motion, the division of the $n(=2^m)$-body system into various subsystems may be carried out as follows.

The quantity

$$\left.\begin{aligned} M_{ij} &= \sum_{k=a}^{b} m_k \\ \text{where} \quad a &= (j-1).2^{m-i} + 1 \\ \text{and} \quad b &= j.2^{m-i} \end{aligned}\right\} \qquad (22)$$

denotes the *jth subsystem* in *level i* of the whole system. To explain this nomenclature let us again consider the case m=3. Here we find the following values of M_{ij} :

$$\left.\begin{aligned} M_{01} &= m_1 + m_2 + \ldots\ldots + m_8 \\ M_{11} &= m_1 + m_2 + m_3 + m_4 \\ M_{12} &= m_5 + m_6 + m_7 + m_8 \\ M_{21} &= m_1 + m_2 \\ M_{22} &= m_3 + m_4 \\ M_{23} &= m_5 + m_6 \\ M_{24} &= m_7 + m_8 \\ M_{3k} &= m_k \qquad (k=1,\ldots,8). \end{aligned}\right\} \qquad (23)$$

It can be seen readily that M_{01} is the sum of all the masses in the system; it is the zeroth level and contains $2^0(=1)$ subsystem i.e. the system itself. M_{01} will denote the position of the mass-centre of the system.

M_{11} and M_{12} occupy the first level which contains $2^1(=2)$ subsystems. The numbering of the masses is done in such a way that the masses in M_{11} and M_{12} constitute two separate quadruple systems. If we denote the positions of the mass-centres of these quadruple systems by M_{11} and M_{12} then they will, if the system is stable, execute disturbed Keplerian orbits about their common mass-centre, which has a position denoted by M_{01}.

Moving on to the second level we find $2^2(=4)$ subsystems, each $M_{2i}(i=1,..,4)$ being a distinct binary subsystem by using an appropriate numbering system for the masses. The M_{2i} $(i=1,...,4)$ will again denote the mass-centres of these binary systems. M_{21} and M_{22} will, if the system is stable, execute disturbed Keplerian ellipses relative to their common mass-centre M_{11}. Similarly M_{23} and M_{24} move relative to M_{12}.

In the third level we find $2^3(=8)$ subsystems which in this case are the masses themselves. The M_{3i} $(= m_i)$ are found to execute disturbed Keplerian ellipses relative to the mass-centre of their binary: e.g. m_1 and m_2 move relative to M_{21}, m_7 and m_8 relative to M_{24} etc.

In this way a system of n $(=2^m)$ bodies may be subdivided into its separate subsystems. In general there are (m+1) levels, denoted 0 to m, in a system, with level k containing 2^k subsystems. The subsystems in level k contain 2^{m-k} bodies e.g. if m=3 and k=2 then the subsystems are binaries, if m=5 and k=3 the subsystems are quadruples, etc.

In an inertial reference frame origin O let

$$\underset{\sim}{P}_{ij} = \overrightarrow{OM_{ij}} \quad . \tag{24}$$

where M_{ij} is the position of the mass-centre of the jth subsystem in level i (cf. Figure 9.1). The vectors $\underset{\sim}{P}_{ij}$ may be expressed in terms of the position vectors of the masses viz.

$$\underset{\sim}{P}_{ij} = \frac{1}{M_{ij}} \sum_{h=a}^{b} m_h \underset{\sim}{R}_h \tag{25}$$

where $a = (j-1)\, 2^{m-i} + 1$

$b = j.\, 2^{m-i}$ (26)

and $\underset{\sim}{R}_h = \overrightarrow{Om_h}$.

The vector $\underset{\sim}{\rho}_{ij}$ is defined to be $\overrightarrow{M_{i+1,2j-1}\, M_{i+1,2j}}$ i.e.

$$\underset{\sim}{\rho}_{ij} = \overrightarrow{O\, M_{i+1,2j}} - \overrightarrow{O\, M_{i+1,2j-1}}$$

$$\text{or } \underset{\sim}{\rho}_{ij} = \underset{\sim}{P}_{i+1,2j} - \underset{\sim}{P}_{i+1,2j-1} \qquad (27)$$

where the $\underset{\sim}{P}_{ij}$ are given by Equation (25). Differentiating Equation (27) twice with respect to time and using Equation (25) we then have

$$\ddot{\underset{\sim}{\rho}}_{ij} = \frac{1}{M_{i+1,2j}} \cdot \sum_{g=a}^{b} m_g \ddot{\underset{\sim}{R}}_g - \frac{1}{M_{i+1,2j-1}} \cdot \sum_{h=c}^{d} m_h \ddot{\underset{\sim}{R}}_h \qquad (28)$$

where
$$\left.\begin{aligned} a &= (2j-1).\,2^{m-i-1} + 1 \\ b &= (2j).2^{m-i-1} \\ c &= (2j-2).2^{m-i-1} + 1 \\ \text{and} \quad d &= (2j-1)2^{m-i-1} \,. \end{aligned}\right\} \qquad (29)$$

Now the equations of motion of an n-body system with respect to an inertial reference frame origin O are, in the usual notation

$$m_i \ddot{\underset{\sim}{R}}_i = \underset{\sim}{\nabla}_i U \qquad (i=1,2,\ldots,n) \qquad (30)$$

where
$$U = \tfrac{1}{2} G \sum_{k=1}^{n} \sum_{\ell=1}^{n} \frac{m_k m_\ell}{r_{k\ell}} \quad (k \neq \ell) \qquad (31)$$

is the force function

$\underset{\sim}{\nabla}_i$ is the gradient operator associated with $\underset{\sim}{R}_i$

m_i is the ith mass

$\underset{\sim}{R}_i$ is the position vector $\overrightarrow{Om_i}$

$r_{ij} = |\underset{\sim}{r}_{ij}| = |\underset{\sim}{R}_j - \underset{\sim}{R}_i|$

G is the gravitational constant

and a dot denotes differentiation with respect to time.

Thus we may recast Equation (28) as

$$\ddot{\underset{\sim}{\rho}}_{ij} = \frac{1}{M_{i+1,2j}} \cdot \sum_{g=a}^{b} \underset{\sim}{\nabla}_g U - \frac{1}{M_{i+1,2j-1}} \cdot \sum_{h=c}^{d} \underset{\sim}{\nabla}_h U.$$

i.e.

$$M_{i+1,2j} M_{i+1,2j-1} \ddot{\underset{\sim}{\rho}}_{ij} = M_{i+1,2j-1} \cdot \sum_{g=a}^{b} \underset{\sim}{\nabla}_g U - M_{i+1,2j} \cdot \sum_{h=c}^{d} \underset{\sim}{\nabla}_h U \qquad (32)$$

Supposing $\underset{\sim}{R}_i = (X_i, Y_i, Z_i)$ and $\underset{\sim}{\rho}_{ij} = (\xi_{ij}, \eta_{ij}, \zeta_{ij})$ in the inertial reference frame consider the x-component of Equation (32) viz.

$$M_{i+1,2j}\, M_{i+1,2j-1}\, \ddot{\xi}_{ij} = M_{i+1,2j-1} \cdot \sum_{g=a}^{b} \frac{\partial U}{\partial \xi_{ij}} \cdot \frac{\partial \xi_{ij}}{\partial X_g} -$$

$$- M_{i+1,2j} \sum_{h=c}^{d} \frac{\partial U}{\partial \xi_{ij}} \cdot \frac{\partial \xi_{ij}}{\partial X_h}$$

$$= \frac{\partial U}{\partial \xi_{ij}} \left[M_{i+1,2j-1} \cdot \sum_{g=a}^{b} \frac{\partial \xi_{ij}}{\partial X_g} - M_{i+1,2j} \sum_{h=c}^{d} \frac{\partial \xi_{ij}}{\partial X_h} \right] .$$

By Equations (25) and (27), noting that g and h are dummy suffices,

$$\frac{\partial \xi_{ij}}{\partial X_g} = \frac{m_g}{M_{i+1,2j}}$$

$$\frac{\partial \xi_{ij}}{\partial X_h} = \frac{-m_h}{M_{i+1,2j-1}}$$

thus

$$M_{i+1,2j}\, M_{i+1,2j-1}\, \ddot{\xi}_{ij} = \frac{\partial U}{\partial \xi_{ij}} \left[\frac{M_{i+1,2j-1}}{M_{i+1,2j}} \cdot \sum_{g=a}^{b} m_g + \frac{M_{i+1,2j}}{M_{i+1,2j-1}} \cdot \sum_{h=c}^{d} m_h \right]$$

which using Equations (22) and (29) gives

$$M_{i+1,2j}\, M_{i+1,2j-1}\, \ddot{\xi}_{ij} = M_{i,j} \frac{\partial U}{\partial \xi_{ij}} .$$

By considering similar results for the y and z components the equations of motion for the general hierarchical system are found to be

$$\frac{M_{i+1,2j}\, M_{i+1,2j-1}}{M_{i,j}}\, \ddot{\underset{\sim}{\rho}}_{ij} = \underset{\sim}{\nabla}_{ij} U \quad (i=0,\ldots,m-1;\ j=1,\ldots 2^i) \qquad (33)$$

where $\underset{\sim}{\nabla}_{ij}$ is the gradient operator with respect to $\underset{\sim}{\rho}_{ij}$. Equations (33) form a $6(2^m-1)^{th}$ order system, the reduction from the original $6(2^m)^{th}$ order system being effected by the use of the six centre-of-mass integrals (as in the case of the Jacobian Coordinate system). In the next section we consider an expansion of the force function analogous

to Chapter 3, Section 3.6, for the general hierarchical system. The expansion will be carried out in terms of the ratios $\rho_{ij}/\rho_{k\ell}$, where $i=0,\ldots,m-1$; $j=1,\ldots,2^i$: $k = 0,\ldots,m-1$; $\ell = 1,\ldots,2^k$: $k < i$, which are all less than unity.

9.4 The Expansion of the Force Function in the Case of General Hierarchical Systems

The equations of motion of an $n(=2^m)$-body system were derived in the previous section, in a coordinate system specially suited to the general hierarchical arrangements found in many multiple stellar systems. The equations are

$$\frac{M_{i+1,2j-1}\, M_{i+1,2j}}{M_{ij}}\, \ddot{\underset{\sim}{\rho}}_{ij} = \underset{\sim}{\nabla}_{ij} U \qquad \begin{matrix} i = 0,\ldots,m-1; \\ j=1,\ldots,2^i \end{matrix} \qquad (34)$$

where

$$U = \tfrac{1}{2} G \sum_{k=1}^{n} \sum_{\ell=1}^{n} \frac{m_k\, m_\ell}{r_{k\ell}} \qquad (k\neq\ell) \qquad (35)$$

is the force function of the problem. The other quantities in these equations are the same as in Section 9.3.

Clearly U, as it is found in Equation (35), has to be expressed in terms of the $\underset{\sim}{\rho}_{ij}$ instead of the $\underset{\sim}{r}_{k\ell}$; it is therefore necessary to obtain an expression for $\underset{\sim}{r}_{k\ell}$ as a function of the $\underset{\sim}{\rho}_{ij}$. Now

$$\underset{\sim}{r}_{k\ell} = \underset{\sim}{R}_\ell - \underset{\sim}{R}_k$$

thus

$$\underset{\sim}{r}_{k\ell} = \underset{\sim}{Q}_\ell - \underset{\sim}{Q}_k \qquad (36)$$

where

$$\underset{\sim}{Q}_\ell = \underset{\sim}{R}_\ell - \frac{1}{M_{01}} \sum_{g=1}^{n} m_g\, \underset{\sim}{R}_g \qquad (37)$$

is the position vector of m_ℓ with respect to M_{01} i.e. $\overrightarrow{M_{01}\, m_\ell}$. There is a similar expression for $\underset{\sim}{Q}_k$. To obtain an expression for $\underset{\sim}{Q}_k$ in terms of the $\underset{\sim}{\rho}_{ij}$ consider the 16-body system (i.e. m=4) of Figure 9.2. This has been drawn schematically to emphasise the ordering of the masses and the directions of the vectors $\underset{\sim}{\rho}_{ij}$.

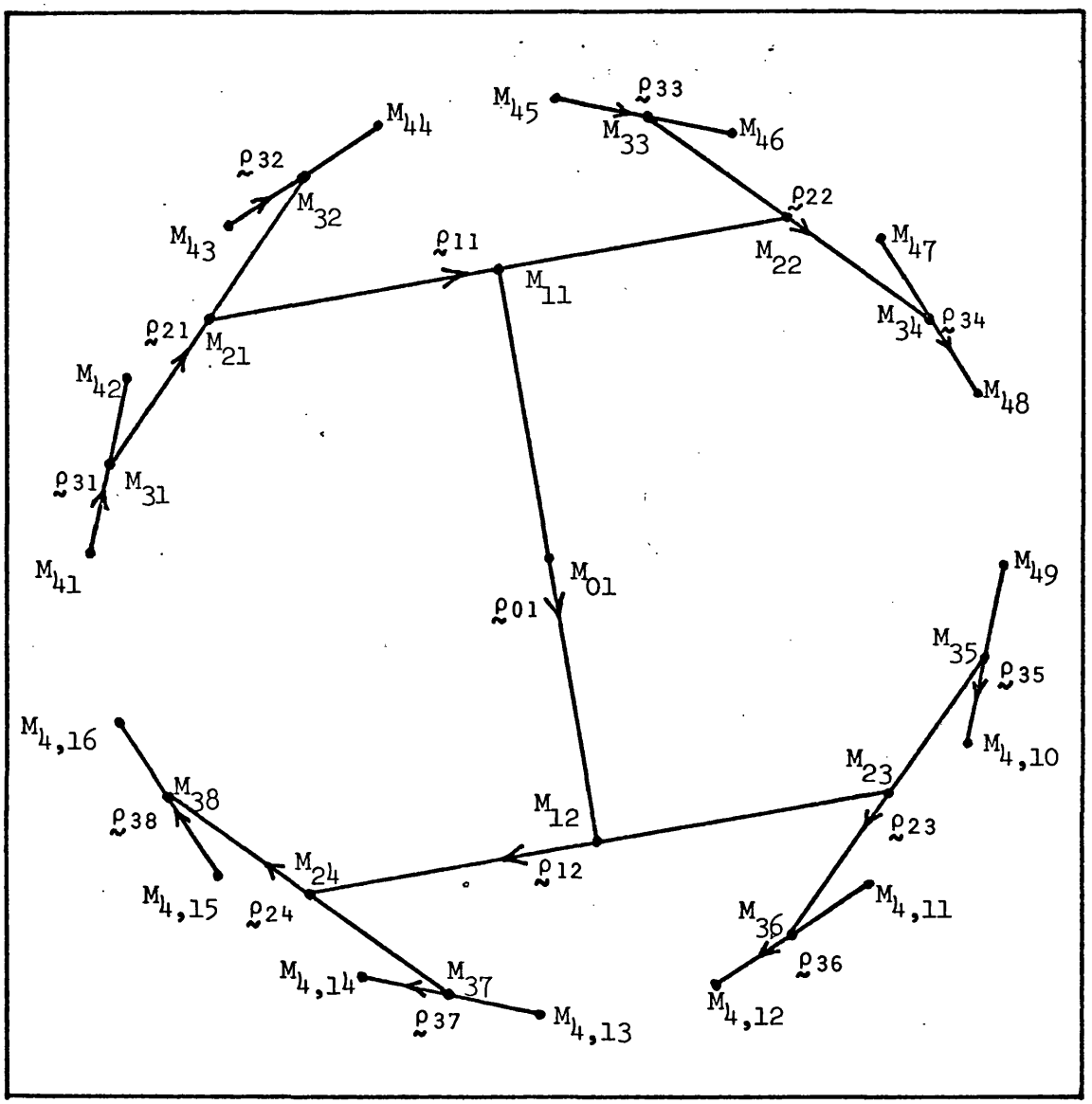

Figure 9.2 Schematic representation of a particular case of the general hierarchical coordinate system where m = 4 (see text for meanings of symbols used).

Firstly notice that

$$M_{ij} + M_{i,j-(-1)^j} = M_{i-1,\mathrm{int}(\frac{j+1}{2})}$$

where int(x) denotes the integer part of x.
Furthermore, M_{ij} and $M_{i,j-(-1)^j}$ are the mass-centres which move in disturbed Keplerian ellipses about the mass-centre $M_{i-1,\mathrm{int}(\frac{j+1}{2})}$.
Let us denote

$$f(j) = j - (-1)^j \tag{38}$$

and

$$g(j) = \mathrm{int}\,(\tfrac{j+1}{2}) \tag{39}$$

thus

$$M_{i,j} + M_{i,f(j)} = M_{i-1,g(j)}. \tag{40}$$

Now the $\underset{\sim}{\rho}_{ij}$ were defined so that

$$\underset{\sim}{\rho}_{i-1,g(j)} = \overrightarrow{M_{i,a}\, M_{i,b}} \tag{41}$$

$$\left.\begin{array}{l}\text{where} \quad a = \min(j,f(j)) \text{ is odd} \\ \text{and} \quad b = \max(j,f(j)) \text{ is even.}\end{array}\right\} \tag{42}$$

Consider now the vector, $\underset{\sim}{Q}'_{ij}$, from a mass-centre of a subsystem which is in level i i.e. M_{ij} to another mass-centre of a subsystem which is in level i-1 i.e. $M_{i-1,g(j)}$. Note that the former subsystem is itself a subsystem of the latter. Then it is readily seen, by considering the figure, that

$$\underset{\sim}{Q}'_{ij} = -(-1)^j \cdot \frac{M_{i,f(j)}}{M_{i-1,g(j)}}\, \underset{\sim}{\rho}_{i-1,g(j)}. \tag{43}$$

Furthermore this process may be continued as follows:

$$\left.\begin{array}{l}\underset{\sim}{Q}'_{i-1,g_1(j)} = -(-1)^{g_1(j)} \dfrac{M_{i-1,f(g_1(j))}}{M_{i-2,g_2(j)}}\, \underset{\sim}{\rho}_{i-2,g_2(j)} \\ \\ \underset{\sim}{Q}'_{i-2,g_2(j)} = -(-1)^{g_2(j)} \dfrac{M_{i-2,f(g_2(j))}}{M_{i-3,g_3(j)}}\, \underset{\sim}{\rho}_{i-3,g_3(j)}\end{array}\right\} \tag{44}$$

etc.....

where $g_i(j) = g(g_{i-1}(j)) \qquad (i > 1) \qquad (45)$

and $g_o(j) = j$ is defined.

By this process we may commence with $M_{m,k}$ and proceed to $M_{m-1,g_1(k)}$, thence to $M_{m-2,g_2(k)}$, eventually reaching M_{01}. Thus

$$\underset{\sim}{Q}_k = \sum_{h=0}^{m-1} (-1)^{g_h(k)} \cdot \frac{M_{m-h,f(g_h(k))}}{M_{m-1-h,g_{h+1}(k)}} \cdot \underset{\sim}{\rho}_{m-1-h,g_{h+1}(k)} \qquad (46)$$

There is a similar expression for $\underset{\sim}{Q}_\ell$ thus we may form $\underset{\sim}{r}_{k\ell}$ as follows:

$$\underset{\sim}{r}_{k\ell} = \sum_{h=o}^{m-1} (-1)^{g_h(\ell)} \cdot \frac{M_{m-h,f(g_h(\ell))}}{M_{m-h-1,g_{h+1}(\ell)}} \cdot \underset{\sim}{\rho}_{m-h-1,g_{h+1}(\ell)} - \\ - (-1)^{g_h(k)} \cdot \frac{M_{m-h,f(g_h(k))}}{M_{m-h-1,g_{h+1}(k)}} \cdot \underset{\sim}{\rho}_{m-h-1,g_{h+1}(k)} \qquad (47)$$

Notice that in Equation (47) it is sufficient to sum over h from 0 to a, where a is the value such that $g_{a+1}(\ell) = g_{a+1}(k)$. From h = a+1 to m-1 the terms in the summation cancel exactly. For example consider $\underset{\sim}{r}_{36}$ in Figure 9.2: the steps which make up $\underset{\sim}{r}_{36}$ are as follows

$$M_{43} \to M_{32} \to M_{21} \to M_{11} \; (\to M_{01} \to) M_{11} \to M_{22} \to M_{33} \to M_{46}.$$

Clearly we may omit the step in parentheses. This is essentially what is being done by summing over h from 0 to a.

Let us now, following Chapter 3, Section 3.6, obtain $r_{k\ell}^{-1}$ by forming $(\underset{\sim}{r}_{k\ell} \cdot \underset{\sim}{r}_{k\ell})^{-\frac{1}{2}}$. Firstly, however, let us rewrite Equation (47) as

$$\underset{\sim}{r}_{k\ell} = \underset{\sim}{\rho}_{m-a-1,g_{a+1}(\ell)} + \sum_{h=o}^{a-1} \left[F_{mh\ell} \, \underset{\sim}{\rho}_{m-h-1,g_{h+1}(\ell)} - F_{mhk} \, \underset{\sim}{\rho}_{m-h-1,g_{h+1}(k)} \right] \qquad (48)$$

where

$$F_{mh\ell} = (-1)^{g_h(\ell)} \cdot \frac{M_{m-h,f(g_h(\ell))}}{M_{m-h-1,g_{h+1}(\ell)}} \qquad (49)$$

and we may note that $\underset{\sim}{\rho}_{m-a-1,g_{a+1}(\ell)} = \underset{\sim}{\rho}_{m-a-1,g_{a+1}(k)}$.

Thus

$$r^{-1}_{k\ell} = \Bigg[\rho^{2}_{m-a-1,g_{a+1}(\ell)} + 2 \sum_{h=0}^{a-1} F_{mh\ell} \underset{\sim}{\rho}_{m-h-1,g_{h+1}(\ell)} . \underset{\sim}{\rho}_{m-a-1,g_{a+1}(\ell)}$$

$$- 2 \sum_{h=o}^{a-1} F_{mhk} \underset{\sim}{\rho}_{m-h-1,g_{h+1}(k)} . \underset{\sim}{\rho}_{m-a-1,g_{a+1}(k)}$$

$$+ \sum_{h=o}^{a-1} \sum_{j=o}^{a-1} F_{mh\ell} F_{mj\ell} \underset{\sim}{\rho}_{m-h-1,g_{h+1}(\ell)} . \underset{\sim}{\rho}_{m-j-1,g_{j+1}(\ell)}$$

$$+ \sum_{h=o}^{a-1} \sum_{j=o}^{a-1} F_{mhk} F_{mjk} \underset{\sim}{\rho}_{m-h-1,g_{h+1}(k)} . \underset{\sim}{\rho}_{m-j-1,g_{j+1}(k)}$$

$$- \sum_{h=o}^{a-1} \sum_{j=o}^{a-1} F_{mh\ell} F_{mjk} \underset{\sim}{\rho}_{m-h-1,g_{h+1}(\ell)} . \underset{\sim}{\rho}_{m-j-1,g_{j+1}(k)}$$

$$- \sum_{h=o}^{a-1} \sum_{j=o}^{a-1} F_{mj\ell} F_{mhk} \underset{\sim}{\rho}_{m-j-1,g_{j+1}(\ell)} . \underset{\sim}{\rho}_{m-h-1,g_{h+1}(k)} \Bigg]^{-\frac{1}{2}} \qquad (50)$$

where there is no contribution from any summation if a = 0*. In Equation (50) the last two double summations are equal, since j and h are dummy suffices, and thus may be combined. Realising that the first and second double summations are symmetrical in j and h, and separating out the terms where j=h, we have

$$r^{-1}_{k\ell} = \Bigg[\rho^{2}_{m-a-1,g_{a+1}(\ell)} + 2 \sum_{h=o}^{a-1} F_{mh\ell} \rho_{m-h-1,g_{h+1}(\ell)} \rho_{m-a-1,g_{a+1}(\ell)}$$

$$C^{m-h-1,g_{h+1}(\ell)}_{m-a-1,g_{a+1}(\ell)}$$

* n.b. In all the summations below there is no contribution from the summation when the lower limit is greater than the upper limit .

$$- 2 \sum_{h=o}^{a-1} F_{mhk}\, \rho_{m-h-1,g_{h+1}(k)}\, \rho_{m-a-1,g_{a+1}(k)}\, C^{m-h-1,g_{h+1}(k)}_{m-a-1,g_{a+1}(k)}$$

$$+ \sum_{h=o}^{a-1} \left(F^2_{mh\ell}\, \rho^2_{m-h-1,g_{h+1}(\ell)} + F^2_{mhk}\, \rho^2_{m-h-1,g_{h+1}(k)} \right)$$

$$+ 2 \sum_{h=o}^{a-1} \sum_{j=h+1}^{a-1} F_{mh\ell}\, F_{mj\ell}\, \rho_{m-h-1,g_{h+1}(\ell)}\, \rho_{m-j-1,g_{j+1}(\ell)} \cdot C^{m-h-1,g_{h+1}(\ell)}_{m-j-1,g_{j+1}(\ell)}$$

$$+ 2 \sum_{h=o}^{a-1} \sum_{j=h+1}^{a-1} F_{mhk}\, F_{mjk}\, \rho_{m-h-1,g_{h+1}(k)}\, \rho_{m-j-1,g_{j+1}(k)} \cdot C^{m-h-1,g_{h+1}(k)}_{m-j-1,g_{j+1}(k)}$$

$$- 2 \sum_{h=o}^{a-1} \sum_{j=o}^{a-1} F_{mh\ell}\, F_{mjk}\, \rho_{m-h-1,g_{h+1}(\ell)}\, \rho_{m-j-1,g_{j+1}(k)} \cdot C^{m-h-1,g_{h+1}(\ell)}_{m-j-1,g_{j+1}(k)} \Bigg]^{-\frac{1}{2}} \qquad (51)$$

where $$\rho_{i,j} = \left| \underset{\sim}{\rho}_{i,j} \right| \qquad (52a)$$

and $$C^{i,j}_{k,\ell} = \frac{\underset{\sim}{\rho}_{i,j} \cdot \underset{\sim}{\rho}_{k,\ell}}{\rho_{i,j}\, \rho_{k,\ell}} \,. \qquad (52b)$$

Defining

$$\alpha^{i,j}_{k,\ell} = \frac{\rho_{i,j}}{\rho_{k,\ell}} \qquad (< 1 \text{ when } k < i) \qquad (52c)$$

and noting that $\rho_{m-a-1,g_{a+1}(\ell)}$ may be freely interchanged with $\rho_{m-a-1,g_{a+1}(k)}$ (since $g_{a+1}(\ell) = g_{a+1}(k)$) we have

$$r^{-1}_{k\ell} = \frac{1}{\rho_{m-a-1,g_{a+1}(\ell)}} \cdot \Bigg[1 + 2 \sum_{h=o}^{a-1} \{ F_{mh\ell} \alpha^{m-h-1,g_{h+1}(\ell)}_{m-a-1,g_{a+1}(\ell)} C^{m-h-1,g_{h+1}(\ell)}_{m-a-1,g_{a+1}(\ell)} -$$

$$- F_{mhk} \alpha^{m-h-1,g_{h+1}(k)}_{m-a-1,g_{a+1}(k)} C^{m-h-1,g_{h+1}(k)}_{m-a-1,g_{a+1}(k)} \}$$

$$+ \sum_{h=o}^{a-1} \{ F^2_{mh\ell} (\alpha^{m-h-1,g_{h+1}(\ell)}_{m-a-1,g_{a+1}(\ell)})^2 + F^2_{mhk} (\alpha^{m-h-1,g_{h+1}(k)}_{m-a-1,g_{a+1}(k)})^2 \}$$

$$+2 \sum_{h=o}^{a-1} \sum_{j=h+1}^{a-1} F_{mh\ell} F_{mj\ell} \alpha^{m-h-1,g_{h+1}(\ell)}_{m-a-1,g_{a+1}(\ell)} \alpha^{m-j-1,g_{j+1}(\ell)}_{m-a-1,g_{a+1}(\ell)} C^{m-h-1,g_{h+1}(\ell)}_{m-a-1,g_{a+1}(\ell)} \cdot$$

$$\cdot C^{m-j-1,g_{j+1}(\ell)}_{m-a-1,g_{a+1}(\ell)}$$

$$+ 2 \sum_{h=0}^{a-1} \sum_{j=h+1}^{a-1} F_{mhk} F_{mjk} \alpha^{m-h-1,g_{h+1}(k)}_{m-a-1,g_{a+1}(k)} \alpha^{m-j-1,g_{j+1}(k)}_{m-a-1,g_{a+1}(k)} C^{m-h-1,g_{h+1}(k)}_{m-a-1,g_{a+1}(k)} \cdot$$

$$\cdot C^{m-j-1,g_{j+1}(k)}_{m-a-1,g_{a+1}(k)}$$

$$- 2 \sum_{h=o}^{a-1} \sum_{j=o}^{a-1} F_{mh\ell} F_{mjk} \alpha^{m-h-1,g_{h+1}(\ell)}_{m-a-1,g_{a+1}(\ell)} \alpha^{m-j-1,g_{j+1}(k)}_{m-a-1,g_{a+1}(k)} C^{m-h-1,g_{h+1}(\ell)}_{m-a-1,g_{a+1}(\ell)} \cdot$$

$$\cdot C^{m-j-1,g_{j+1}(k)}_{m-a-1,g_{a+1}(k)} \Bigg]^{-\frac{1}{2}},$$

which on application of the binomial expansion of $(1 + x)^{-\frac{1}{2}}$ gives, correct to the second order in the $\alpha^{i,j}_{k,\ell}$,

$$r^{-1}_{k\ell} = \frac{1}{\rho_{m-a-1,g_{a+1}(\ell)}} \cdot \Bigg[1 - \sum_{h=o}^{a-1} \{ F_{mh\ell} \alpha^{m-h-1,g_{h+1}(\ell)}_{m-a-1,g_{a+1}(\ell)} C^{m-h-1,g_{h+1}(\ell)}_{m-a-1,g_{a+1}(\ell)} -$$

$$- F_{mhk} \alpha^{m-h-1,g_{h+1}(k)}_{m-a-1,g_{a+1}(k)} C^{m-h-1,g_{h+1}(k)}_{m-a-1,g_{a+1}(k)} \}$$

$$+ \sum_{h=o}^{a-1} \{ F^2_{mh\ell} (\alpha^{m-h-1,g_{h+1}(\ell)}_{m-a-1,g_{a+1}(\ell)})^2 P_2(C^{m-h-1,g_{h+1}(\ell)}_{m-a-1,g_{a+1}(\ell)}) + F^2_{mhk} (\alpha^{m-h-1,g_{h+1}(k)}_{m-a-1,g_{a+1}(k)})^2 \cdot$$

$$\cdot P_2(C^{m-h-1,g_{h+1}(k)}_{m-a-1,g_{a+1}(k)}) \}$$

$$+ \sum_{h=o}^{a-1} \sum_{j=h+1}^{a-1} F_{mh\ell} F_{mj\ell} \alpha^{m-h-1,g_{h+1}(\ell)}_{m-a-1,g_{a+1}(\ell)} \alpha^{m-j-1,g_{j+1}(\ell)}_{m-a-1,g_{a+1}(\ell)} E^{m-h-1,g_{h+1}(\ell),\ m-j-1,g_{j+1}(\ell)}_{m-a-1,g_{a+1}(\ell),\ m-a-1,g_{a+1}(\ell)}$$

$$+ \sum_{h=o}^{a-1} \sum_{j=h+1}^{a-1} F_{mhk} F_{mjk} \alpha^{m-h-1,g_{h+1}(k)}_{m-a-1,g_{a+1}(k)} \alpha^{m-j-1,g_{j+1}(k)}_{m-a-1,g_{a+1}(k)} E^{m-h-1,g_{h+1}(k),\ m-j-1,g_{j+1}(k)}_{m-a-1,g_{a+1}(k),\ m-a-1,g_{a+1}(k)}$$

$$- \sum_{h=o}^{a-1} \sum_{j=o}^{a-1} F_{mh\ell} F_{mjk} \alpha^{m-h-1,g_{h+1}(\ell)}_{m-a-1,g_{a+1}(\ell)} \alpha^{m-j-1,g_{j+1}(k)}_{m-a-1,g_{a+1}(k)} E^{m-h-1,g_{h+1}(\ell),\ m-j-1,g_{j+1}(k)}_{m-a-1,g_{a+1}(\ell),\ m-a-1,g_{a+1}(k)} \Bigg] \qquad (53)$$

where $$E^{i,j,k,\ell}_{p,q,r,s} = 3\, C^{i,j}_{p,q}\, C^{k,\ell}_{r,s} - C^{i,j}_{k,\ell} \,. \qquad (54)$$

Consider the contribution, U_1 say, made to the force function by the terms of order $\alpha^{i,j}_{k,\ell}$ in Equation (53). Thus

$$U_1 = -\frac{1}{2} G \cdot \sum_{\ell=1}^{n} \sum_{k=1}^{n} \frac{M_{m\ell} M_{mk}}{\rho_{m-a-1,g_{a+1}(\ell)}} \cdot \sum_{h=0}^{a-1} \{F_{mh\ell} \alpha^{m-h-1,g_{h+1}(\ell)}_{m-a-1,g_{a+1}(\ell)} C^{m-h-1,g_{h+1}(\ell)}_{m-a-1,g_{a+1}(\ell)} - F_{mhk} \alpha^{m-h-1,g_{h+1}(k)}_{m-a-1,g_{a+1}(k)} \cdot C^{m-h-1,g_{h+1}(k)}_{m-a-1,g_{a+1}(k)} \}$$

which may be rewritten as

$$U_1 = -\tfrac{1}{2} G \sum_{\ell=1}^{n} \sum_{k=1}^{n} \frac{M_{m\ell} M_{mk}}{\rho_{m-a-1,g_{a+1}(\ell)}} \sum_{h=o}^{a-1} F_{mh\ell} \alpha^{m-h-1,g_{h+1}(\ell)}_{m-a-1,g_{a+1}(\ell)} \cdot C^{m-h-1,g_{h+1}(\ell)}_{m-a-1,g_{a+1}(\ell)}$$

$$+\tfrac{1}{2}G\sum_{\ell=1}^{n}\sum_{k=1}^{n}\frac{M_{m\ell}\,M_{mk}}{\rho_{m-a-1,g_{a+1}(\ell)}}\cdot\sum_{h=o}^{a-1}F_{mhk}\,\alpha^{m-h-1,g_{h+1}(k)}_{m-a-1,g_{a+1}(k)}\cdot$$

$$\cdot\,C^{m-h-1,g_{h+1}(k)}_{m-a-1,g_{a+1}(k)}\ .$$

On observing that $g_{a+1}(\ell) = g_{a+1}(k)$ and that k and ℓ are dummy suffices in these summations it is seen that $U_1 = 0$. This result is analogous to that of Lemma 1 in Chapter 3, Section 3.6.

Of the remaining terms in Equation (53) it may be shown quite readily in any particular case that the double summations do not make any contribution to the force function (see Appendix E). Thus it is found that

$$U = \tfrac{1}{2}\,G\sum_{\ell=1}^{n}\sum_{k=1}^{n}\frac{M_{mk}\,M_{m\ell}}{\rho_{m-a-1,g_{a+1}(\ell)}}\cdot\Bigg[1+$$

$$+\sum_{h=o}^{a-1}\Bigg[F^{2}_{mh\ell}\,(\alpha^{m-h-1,g_{h+1}(\ell)}_{m-a-1,g_{a+1}(\ell)})^{2}\,P_2(C^{m-h-1,g_{h+1}(\ell)}_{m-a-1,g_{a+1}(\ell)})+$$

$$+F^{2}_{mhk}\,(\alpha^{m-h-1,g_{h+1}(k)}_{m-a-1,g_{a+1}(k)})^{2}\,P_2(C^{m-h-1,g_{h+1}(k)}_{m-a-1,g_{a+1}(k)})\Bigg]\Bigg] \qquad (55)$$

Let us now particularize to the case m=2 i.e. the 4-body problem where the system consists of two close binaries which move around each other in disturbed Keplerian orbits (see Figure 9.3). The relevant equations are then

$$\frac{M_{i+1,2j-1}\,M_{i+1,2j}}{M_{i,j}}\,\ddot{\underset{\sim}{\rho}}_{ij} = \underset{\sim}{\nabla}_{ij}\,U \qquad i=0,1 \quad j=1,2^{i} \qquad (56)$$

where

$$U = G\Bigg[\frac{M_{21}\,M_{22}}{\rho_{11}}+\frac{M_{23}\,M_{24}}{\rho_{12}}+$$

$$+\frac{M_{11}\,M_{12}}{\rho_{01}}\Big\{1+\frac{M_{21}\,M_{22}}{M_{11}^{2}}\cdot(\alpha^{11}_{01})^{2}\,P_2(C^{11}_{01})+\frac{M_{23}\,M_{24}}{M_{12}^{2}}\cdot$$

$$\cdot(\alpha^{12}_{01})^{2}\,P_2(C^{12}_{01})\Big\}\Bigg] \qquad (57)$$

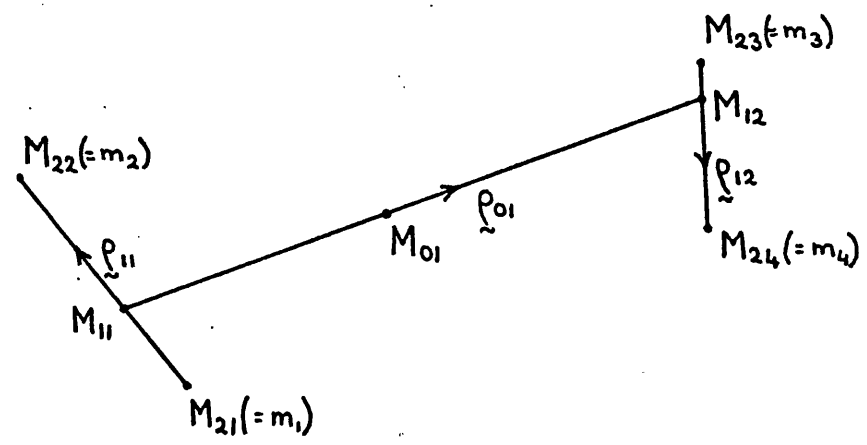

Figure 9.3

correct to the second order in the $\alpha_{k\ell}^{ij}$. Remembering that the $\underset{\sim}{\rho}_{ij}$ are all independant we then have

$$\ddot{\underset{\sim}{\rho}}_{01} = G M_{01} \frac{\partial}{\partial \underset{\sim}{\rho}_{01}} \left[\frac{1}{\rho_{01}} \{ 1 + \varepsilon_{01}^{11} P_2(C_{01}^{11}) + \varepsilon_{01}^{12} P_2(C_{01}^{12}) \} \right] \quad (58a)$$

$$\ddot{\underset{\sim}{\rho}}_{11} = G M_{11} \frac{\partial}{\partial \underset{\sim}{\rho}_{11}} \left[\frac{1}{\rho_{11}} \{ 1 + \varepsilon_{11}^{01} P_2(C_{01}^{11}) \} \right] \quad (58b)$$

$$\ddot{\underset{\sim}{\rho}}_{12} = G M_{12} \frac{\partial}{\partial \underset{\sim}{\rho}_{12}} \left[\frac{1}{\rho_{12}} \{ 1 + \varepsilon_{12}^{01} P_2(C_{01}^{12}) \} \right] \quad (58c)$$

where $$\varepsilon_{01}^{11} = \frac{M_{21} M_{22}}{M_{11}^2} (\alpha_{01}^{11})^2 \quad (59a)$$

$$\varepsilon_{01}^{12} = \frac{M_{23} M_{24}}{M_{12}^2} (\alpha_{01}^{12})^2 \quad (59b)$$

$$\varepsilon_{11}^{01} = \frac{M_{12}}{M_{11}} (\alpha_{01}^{11})^3 \quad (59c)$$

and $$\varepsilon_{12}^{01} = \frac{M_{11}}{M_{12}} (\alpha_{01}^{12})^3 \quad . \quad (59d)$$

In this simple case the meanings of the ε parameters defined in Equations (59a-d) are obvious.

ε_{01}^{11} is a measure of the disturbance produced on the orbit of M_{11} relative to M_{12} due to M_{21} and M_{22} not being positioned at their common mass-centre M_{11}. In other words a measure of the disturbance of m_1 and m_2 on the orbit of what may be called the (M_{11}, M_{12}) subsystem. Similarly ε_{01}^{12} is a measure of the disturbance of M_{23} and M_{24} (i.e. m_3 and m_4) on the orbit of the (M_{11}, M_{12}) subsystem. Note the ε notation: ε_{01}^{11} denotes the disturbance produced by the masses M_{21} and M_{22} *which lie on the vector* $\underset{\sim}{\rho}_{11}$ on the orbit of M_{11} and M_{12} *which lie on the vector* $\underset{\sim}{\rho}_{01}$. These two ε terms are similar in form to ε^{23} of the three-body case in Chapter 4.

ε_{11}^{01} is a measure of the disturbance produced on the orbit of the (M_{21}, M_{22}) subsystem *which lie on the vector* $\underset{\sim}{\rho}_{11}$ by the masses M_{23} and M_{24} which form the subsystem *which is positioned at* $\underset{\sim}{\rho}_{01}$ with respect to M_{11}. ε_{12}^{01} is then a measure of the disturbance by M_{21} and M_{22} on the orbit of the (M_{23}, M_{24}) subsystem. Note that these two ε terms are similar to ε_{32} of the three-body case. In fact we may recover the form of ε_{32} by setting one of the masses m_1 or m_2 zero in ε_{12}^{01} and m_3 or m_4 zero in ε_{11}^{01}.

The derivation of the ε parameters in this case and also the eight-body case (i.e. m=3) is considered more fully in Appendix F.

We will now, using the results for the eight-body case, derive ε parameters for the Castor system. The actual values derived will necessarily be approximate due to insufficient data for the system.

Firstly let us recapitulate the situation as regards this sextuple system. The following data were obtained from Heintz (1978) and Kopal (1959). The system consists of three binary systems which are denoted A, B and C: A and B are spectroscopic doubles with periods of 9.2 days and 2.9 days respectively while C is a close eclipsing binary of period 0.81 days. The subsystems A and B form a quadruple subsystem, the binaries revolving about their common mass-centre in a period of probably 450 to 500 years. Subsystem C revolves about the mass-centre of the quadruple subsystem consisting of A and B in a period estimated to be of the order of 2.10^4 years. The masses of the binary C are about equal: both are 0.64 times the mass of the Sun.

The masses of the larger components of binaries A and B may be obtained, with sufficient accuracy for present purposes, from their spectral classification. The primary in binary A is an A5 type star while that of binary B is an AlV. This results in masses of 2.09 and 3.23 times the mass of the Sun respectively (see Allen, 1973). The companions of these two stars both have low masses and no visible spectra: we will assume they are both around the lower limit for stellar masses and luminosity which results in a mass of 0.1 times the solar mass. The eccentricities of the orbits will be neglected in the following; these being unknown for most parts of the system except binaries A and B which have eccentricities of 0.5 and 0.002 respectively. The latter is negligible, the former will cause a change in the relevant ε parameter of a factor less than $(0.5)^2$ or $(0.5)^3$ depending on the ε type i.e. $\varepsilon^{ij}_{k\ell}$ or $\varepsilon^{k\ell}_{ij}$ $(i > k)$ respectively.

Now the equations of motion for the eight-body system, given in Appendix F (Equations (F.4)) are reduced to the six-body case in order to derive ε parameters for the Castor system. If we let ρ_{23} and ρ_{24} tend to zero then the equations of motion for these subsystems are removed and M_{35} and M_{36} "become one mass" viz. M_{23}: similarly M_{37} and M_{38} combine to form M_{24}. (Alternatively we could have set $m_6 = m_8 = 0$ and neglected the equations of motion for $\underset{\sim}{\rho}_{23}$ and $\underset{\sim}{\rho}_{24}$). The equations now become, remembering $\rho_{23} = \rho_{24} = 0$,

$$\ddot{\underset{\sim}{\rho}}_{01} = G M_{01} \frac{\partial}{\partial \underset{\sim}{\rho}_{01}} \left[\frac{1}{\rho_{01}} \{1 + \varepsilon^{11}_{01} P_2(C^{11}_{01}) + \varepsilon^{12}_{01} P_2(C^{12}_{01}) + \varepsilon^{21}_{01} P_2(C^{21}_{01}) + \varepsilon^{22}_{01} P_2(C^{22}_{01}) \} \right] \quad (60a)$$

$$\ddot{\underset{\sim}{\rho}}_{11} = G M_{11} \frac{\partial}{\partial \underset{\sim}{\rho}_{11}} \left[\frac{1}{\rho_{11}} \{ 1 + \varepsilon^{21}_{11} P_2(C^{21}_{11}) + \varepsilon^{22}_{01} P_2(C^{22}_{01}) + \varepsilon^{01}_{11} P_2(C^{11}_{01}) \} \right] \quad (60b)$$

$$\ddot{\underset{\sim}{\rho}}_{12} = G M_{12} \frac{\partial}{\partial \underset{\sim}{\rho}_{12}} \left[\frac{1}{\rho_{12}} \{ 1 + \varepsilon^{01}_{12} P_2(C^{12}_{01}) \} \right] \quad (60c)$$

$$\ddot{\underset{\sim}{\rho}}_{21} = G M_{21} \frac{\partial}{\partial \underset{\sim}{\rho}_{21}} \left[\frac{1}{\rho_{21}} \{ 1 + \varepsilon^{11}_{21} P_2(C^{21}_{11}) + \varepsilon^{01}_{21} P_2(C^{21}_{01}) \} \right] \quad (60d)$$

$$\ddot{\underset{\sim}{\rho}}_{22} = G M_{22} \frac{\partial}{\partial \underset{\sim}{\rho}_{22}} \left[\frac{1}{\rho_{22}} \{ 1 + \varepsilon^{11}_{22} P_2(C^{22}_{11}) + \varepsilon^{01}_{22} P_2(C^{22}_{01}) \} \right] \quad (60e)$$

where binary A is represented by the subsystem (M_{31}, M_{32})
binary B is represented by the subsystem (M_{33}, M_{34})
and binary C is represented by the subsystem (M_{23}, M_{24})

Equations (60 a,b,c,d,e) are respectively the equations of motion for: (a) the mass-centre of binary C relative to the mass-centre of the quadruple system of binaries A and B, (b) the mass-centre of binary A relative to that of binary B, (c) the masses of binary C relative to each other, (d) the masses of binary A relative to each other and (e) the masses of binary B relative to each other.

Referring to the data for the Castor system we may derive, using Kepler's third law (i.e. $n^2a^3 = \mu$), the following values for the semi-major axes of the system in astronomical units. (Since circular orbits are assumed the ρ_{ij} are the same as the semi-major axes values).

Then
$$\rho_{01} = 1400$$
$$\rho_{11} = 108 \quad ; \quad \rho_{12} = 0.0185$$
$$\rho_{21} = 0.112 \quad ; \quad \rho_{22} = 0.0594$$

with $M_{31} = 2.09$, $M_{32} = 0.1$, $M_{33} = 3.23$, $M_{34} = 0.1$, $M_{23} = 0.64$ and $M_{24} = 0.64$ (in terms of the solar mass). Then the ε parameters may be obtained by using Equations (F.5) of Appendix F. Thus

$$\left.\begin{aligned}
\varepsilon_{01}^{11} &= 1.42.10^{-3} \quad ; \quad \varepsilon_{01}^{12} = 4.37.10^{-11} \\
\varepsilon_{01}^{21} &= 1.11.10^{-10} \quad ; \quad \varepsilon_{01}^{22} = 3.16.10^{-11} \\
\varepsilon_{11}^{21} &= 4.69.10^{-8} \quad ; \quad \varepsilon_{11}^{22} = 8.81.10^{-9} \\
\varepsilon_{11}^{01} &= 1.06.10^{-4} \quad ; \quad \varepsilon_{12}^{01} = 9.95.10^{-15} \\
\varepsilon_{21}^{11} &= 1.70.10^{-9} \quad ; \quad \varepsilon_{21}^{01} = 2.99.10^{-13} \\
\varepsilon_{22}^{11} &= 1.09.10^{-10} \quad ; \quad \varepsilon_{22}^{01} = 2.94.10^{-14}
\end{aligned}\right\} \quad (61)$$

From these values it is plain that the three binaries - A, B and C - are each disturbed very little by the other components of the system. Furthermore, their binary nature does not disturb their arrangement as a triple system to any great extent. The major disturbance, i.e. ε_{01}^{11}, is that produced on the orbit of binary C relative to the mass-centre

of the quadruple system consisting of A and B by the binaries A and B not being found at their common mass-centre. Also, an order of magnitude less, ε_{11}^{01} , the effect of binary C on the relative orbit of binaries A and B. Thus we see that the most stable components of this sextuple system are the binaries themselves: C being the most stable and A the least stable. The least stable part of the system is the arrangement of the binaries as a triple system.

9.5 Discussion and Conclusions

It would appear from Section 9.2 that the ε parameters (derived in the *Jacobian* coordinate system) are a good measure of the disturbances on the orbits for the planetary case. Only in the high α range (greater than 0.9) are the perturbations, as characterised by the ε parameters, modified by more than an order of magnitude. For all the real cases arising in the Solar System the α values are less than 0.9 and thus it may be safely assumed that the ε values are a good measure of the disturbances on the orbits. Alternatively it would be possible to define a revised set of ε parameters $(\varepsilon'^{ki}, \varepsilon'_{\ell i})\{ i=2,\ldots,n;\ k=2\ldots, i-1\ (i \geq 3);\ \ell = i+1,\ldots,n\ (i \leq n-1)\}$ so that

$$\left.\begin{aligned} \varepsilon'^{ki} &= \frac{\varepsilon^{ki}}{1-\alpha_{ki}} = \frac{m_k M_{k-1}}{M_k M_{i-1}} \cdot \frac{\alpha_{ki}^2}{1-\alpha_{ki}} \\ \varepsilon'_{\ell i} &= \frac{\varepsilon_{\ell i}}{1-\alpha_{i\ell}} \quad \frac{m_\ell}{M_i} \cdot \frac{\alpha_{i\ell}^3}{1-\alpha_{i\ell}}, \end{aligned}\right\} \qquad (62)$$

the notation being the same as that of Chapter 3, Section 3.6. In the range of small α i.e. satellites of planets disturbed by the Sun, triple stellar systems, the $1/(1-\alpha)$ factor will not alter significantly the original ε parameter. In the range of ε's for planetary systems the parameters will then be suitably modified.

Turning our attention to the general hierarchical arrangement, found occurring naturally in many multiple stellar systems, a coordinate system was derived in Section 9.4 applicable to these systems. This coordinate system was used to derive a generalised set of ε parameters for two particular cases of the general hierarchical type of system i.e. the four- and eight-body cases.

The eight-body case was used, after a little reduction, to consider the stability of the Castor star system. The values of the ε parameters obtained suggested that the binaries of the system are *very* stable. The triple arrangement of the binaries is less stable. The generalised ε parameters may therefore be used to discuss the relative stability of various subsystems contained within a system. Indeed it could well be possible to decide which parts of a system may be unstable and which are stable.

Again considering the Castor system, it is noted that binary C lies a considerable distance from the mass-centre of binaries A and B. It is possible, using the coordinate system for the general hierarchical systems, to consider the disturbance imposed on the orbit of C relative to the mass-centre of A and B by the central bulge of the Galaxy.

Let ρ_{23}, ρ_{24} and ρ_{12} tend to zero i.e. masses $M_{35}, \ldots, M_{38}$ coalesce to form *one* mass M_{12}. Further let M_{12} denote the mass of the central bulge of the Galaxy i.e. about 10^{11} times the Solar mass. In the following, since the binaries A, B and C appear to be affected by and themselves effect their triple arrangement very little, we will neglect their binary nature and assume each of them to be one mass. Thus binary A is represented by M_{31} and binary B by M_{32}. The ρ_{22} value tends to zero and M_{22} represents the mass of binary C. The relevant equations of motion are then (see Appendix F)

$$\ddot{\underset{\sim}{\rho}}_{01} = G M_{01} \frac{\partial}{\partial \underset{\sim}{\rho}_{01}} \left[\frac{1}{\rho_{01}} \{1 + \varepsilon_{01}^{11} P_2(C_{01}^{11}) + \varepsilon_{01}^{21} P_2(C_{01}^{21})\} \right] \quad (63a)$$

$$\ddot{\underset{\sim}{\rho}}_{11} = G M_{11} \frac{\partial}{\partial \underset{\sim}{\rho}_{11}} \left[\frac{1}{\rho_{11}} \{1 + \varepsilon_{11}^{21} P_2(C_{11}^{21}) + \varepsilon_{11}^{01} P_2(C_{01}^{11})\} \right] \quad (63b)$$

$$\ddot{\underset{\sim}{\rho}}_{21} = G M_{21} \frac{\partial}{\partial \underset{\sim}{\rho}_{21}} \left[\frac{1}{\rho_{21}} \{1 + \varepsilon_{21}^{11} P_2(C_{11}^{21}) + \varepsilon_{21}^{01} P_2(C_{01}^{21})\} \right] \quad (63c)$$

where ε_{01}^{11} is a measure of the disturbance produced by the binary (A,B) and mass C on the orbit of the mass-centre M_{11} relative to the galactic mass M_{12}; ε_{01}^{21} is the effect of the binary nature of (A,B) on the same orbit; ε_{11}^{21} is a measure of the effect of binary (A,B) on the orbit of C relative to the mass-centre of (A,B); ε_{11}^{01} measures the disturbance of the central bulge of theGalaxy on the same orbit; ε_{21}^{11} and ε_{21}^{01} are

characteristic of the disturbance on the orbit of A relative to B by C and the central bulge of the Galaxy respectively. For data we have

$$\rho_{01} = 2.10^{9} \text{ A.U.}$$
$$\rho_{11} = 1400 \text{ A.U.}$$
$$\rho_{21} = 108 \text{ A.U.}$$
$$M_{31} = 2.19 \qquad M_{32} = 3.33$$
$$M_{22} = 1.28 \qquad M_{12} = 10^{11} \quad :$$

the masses being in terms of the solar mass. Thus

$$\left.\begin{aligned} \varepsilon_{01}^{11} &= 7.49.10^{-14} \quad ; \quad \varepsilon_{01}^{21} = 5.67.10^{-16} \\ \varepsilon_{11}^{21} &= 1.42.10^{-3} \quad ; \quad \varepsilon_{11}^{01} = 5.04.10^{-9} \\ \varepsilon_{21}^{11} &= 1.06.10^{-4} \quad ; \quad \varepsilon_{21}^{01} = 2.85.10^{-12} \ . \end{aligned}\right\} \qquad (64)$$

From these values we may see that the perturbation due to the central bulge of the Galaxy is several orders of magnitude lower than the mutual perturbations of the three binaries A,B and C. The effect the triple nature of the system has on the orbit of its mass-centre relative to the galactic centre is totally negligible (see ε_{01}^{11} and ε_{01}^{21} values). Comparing the two sets of ε parameters - Equations (61) and (64) - it is observed that the perturbation due to the Galaxy on the triple arrangement of the binaries A, B and C is of roughly the same order of magnitude as the perturbation due to the individual masses of the binaries on their triple arrangement.

It would have been possible, by deriving the equations of motion for the 16-body case, to include the binary nature of A,B and C and the galactic mass *in one system* . Then a direct comparison of the perturbations would have been possible. Indeed by the use of a system containing sufficient bodies (i.e. sufficiently large m) any hierarchical arrangement of bodies may be examined. For instance, if a planet was in revolution about one component of a multiple stellar system, it would readily be possible to consider the perturbations on the planet's orbit due to each subsystem of the stellar system. If the planet possessed satellites, they could be included: the disturbance on their orbits due

the presence of the stars in the system could then be measured. In this way many exotic types of system can be modelled, and their ϵ parameters examined.

CHAPTER 10 FUTURE WORK

10.1 Review

The aim of this thesis has been to introduce a set of parameters which have a physical meaning for the stability of hierarchical dynamical systems. These parameters were derived in Chapter 3 for systems of the type exemplified by triple stellar systems, planetary systems, satellite systems, etc. Throughout succeeding chapters these parameters have been examined in the case of the three-body problem - the simplest case available. The analytical stability criterion involving the zero-velocity curves of the general three-body problem was employed in the coplanar, corotational initially circular case to show that the ε parameters may be used to determine regions in the $\varepsilon^{23},\varepsilon_{32}$- plane where stability is assured, given a sufficiently small α_{23} ratio, and instability is certain (Chapters 4 and 5).

By the use of numerical experiments it was possible (in Chapter 6) to show that predictions of the durability of three-body systems could be made. The ε parameters could also be used to predict the amplitude of the periodic variations on the semi-major axes and eccentricities of the osculating Keplerian orbits of the system (Chapter 7).

The four-body problem was briefly examined in Chapter 8 and it was demonstrated that it is possible to obtain similar results for this type of system as for the three-body systems by defining the Σ parameters.

In Chapter 9 a set of ε parameters was derived which is applicable to systems of any type of hierarchy. The use of these ε parameters in a numerical investigation has not yet been considered.

10.2 The Extension to Non-Coplanar, Co/Counter-Rotational and Initially Non-Circular Orbits in the Hierarchical Three-Body Problem

All the numerical results obtained for hierarchical three-body systems and presented in this thesis cover a very restricted range of initial conditions. In every case the motion was coplanar and corotational, the osculating orbits were always initially circular with the initial

configuration such that the masses lay in the straight line $m_1 m_2 m_3$. Clearly the effect other orbital parameters have on the stability needs to be assessed.

In Chapter 6 the numerical integrations of the Sun-Jupiter-Saturn system by Nacozy (1976,1977) were considered. It was found that if we considered the largest α_{23} ratio which can occur in the system i.e. when Jupiter is at apocentre in its orbit and Saturn at pericentre, then this value,for the case Nacozy found tobe just unstable, gave remarkably good agreement with the values of $(\alpha_{23})_o$ which were derived from the present numerical investigation. It is therefore hoped that eccentricities may be introduced into the hierarchical three-body systems without greatly complicating the situation. The relevant value of α_{23} is probably that which arises at the time when the (m_1, m_2) subsystem is at apocentre and (M_2, m_3) subsystem is at pericentre.

The other orbital parameters, in the coplanar case, are ϖ_2, ϖ_3, f_2,f_3 and θ. Preliminary numerical investigations with non-zero values of θ, in the initially circular case, have confirmed the conclusions of Chapter 5 that the initial straight line configuration $m_1 m_2 m_3$, i.e. $\theta = 0$, is more stable than the configuration when the bodies are in the order $m_2 m_1 m_3$ i.e. $\theta = \pi$ which in turn is more stable than $\theta = \theta_T$, the value of θ which maximises the value of c^2H given that the other orbital parameters are held constant. The other parameters, being indeterminate in the initially circular case, have not yet been introduced. Using the analytical results of Chapter 5 we may choose the interesting cases to study. For instance, introducing values of e_2 and e_3 and setting $\theta = 0$ we know from the results of Chapter 5 that if the (m_1,m_2) subsystem is at apocentre and the (M_2, m_3) subsystem at pericentre then the stability, for this θ value, is at a *maximum* . Conversely if the (m_1, m_2) subsystem is at pericentre and (M_2, m_3) subsystem is at apocentre then analytically the system is at a *minimum* of stability. These types of initial configurations for the bodies of the system are the ones of interest for numerical studies.

Inclinations may also be introduced although there will be no analytical stability criterion since the stability criterion of Zare (1976, 1977) is only for planar motions.

These parameters, including the possibility of counter-rotational motion, permit a very large range of possible initial configurations of the bodies. Therefore a very large number of numerical integrations would be necessary to cover the whole range. It is hoped that by the use of the ε parameters definite trends will appear which will allow an easier and more rapid examination of all these cases. For instance if it is found that the value $(\alpha_{23})_o$ is related to the largest possible α_{23} value in a given system then this will significantly reduce the required amount of work since it will become largely unnecessary to examine the effects of f_2, f_3 and θ.

10.3 The Analytical Determination of the Amplitude of Variations in Semi-Major Axes, Eccentricities and Inclinations in the General n-Body Problem

The classical method of secular inequalities allows, for planetary systems, the calculation of the amplitude of the changes in eccentricities and inclinations, provided it is assumed that the changes in the semi-major axes are zero. The analysis uses the fact that in planetary systems the ratios of the planetary masses to the central mass are small, also that the eccentricities and inclinations are small. The orbits of the system are considered to be heliocentric i.e. centred on the central mass.

In Chapter 7 it was demonstrated by the use of numerical integrations that the ε parameters and α ratio for three-body systems, i.e. (ε^{23}, ε_{32}, α_{23}), are related in a simple way to the variations in semi-major axes and eccentricities in coplanar, corotational hierarchical three-body systems with initially circular orbits. The simplicity of the relationships suggests that it may be possible to derive the variations in the elements analytically for hierarchical n-body systems. The problem would involve a treatment similar to that of classical secular inequalities using the Jacobian coordinate system in place of the "heliocentric" type of coordinate system.

10.4 Numerical Investigation of n-Body ($n \geq 4$) Hierarchical Systems

When these types of system are considered it becomes necessary to consider a "sum of ε parameters" e.g. the Σ's as defined for 4-body systems in Chapter 8. This is an advance on the examination of the three-body problem since there the ε parameters appeared singly in the equations of motion. Also, as yet, there is no analytical stability criterion available for these systems. This allows us to test whether we may consider a sum of the ε parameters as relevant to the stability of each orbit of the system. The results for three-body systems may be used when considering the four (or more) body problem by splitting it into three-body subsets. For instance, in Chapter 8, the critical values of α_{23} in the three-body problem were used as a "stepping stone" for assessing the stability/instability of each triple subsystem of the four-body system.

The reason for this procedure is obvious if we consider the way in which the ε parameters arise in the equations of motion in the Jacobian coordinate system. Suppose all the masses in an n-body system are of the same order of magnitude (excepting the central mass, denoted m_1, which is larger). Then an ε parameter in the equation of motion for the orbit of m_i relative to M_{i-1} which arises due to the presence of the (superior) mass m_{i+1} contains an α ratio $\alpha_{i,i+1}$ raised to the third power i.e.

$$\varepsilon_{i+1,i} = \frac{m_{i+1}}{M_i} \alpha_{i,i+1}^3 \quad .$$

Considering the next mass, m_{i+2}, we have a disturbance on the orbit of the mass m_i characterised by

$$\varepsilon_{i+2,i} = \frac{m_{i+2}}{M_i} \alpha_{i,i+2}^3 \quad .$$

Comparing these two expressions we have the result, if $m_{i+1} \simeq m_{i+2}$,

$$\frac{\varepsilon_{i+1,i}}{\varepsilon_{i+2,i}} \simeq \left(\frac{\alpha_{i,i+1}}{\alpha_{i,i+2}} \right)^3$$

$$\simeq \left(\frac{1}{\alpha_{i+1,i+2}} \right)^3 > 1 \, .$$

That is, the disturbance due to the mass m_{i+2} is a factor $(\alpha_{i+1,i+2})^3$ down on the effect of m_{i+1}. A similar line of reasoning would apply to inferior bodies. Thus it may be seen that often only the disturbances due to the bodies immediately on either side of the body under examination need to be considered. Of these two dominant ε parameters the larger will allow the calculation of an approximate "α_{cr}" value by using the critical α value of the three-body problem. Thus we may use the three-body problem to aid progress in consideration of the four-body problem. Having obtained results for the four-body problem it would be possible to use these as an approximate model for the four-body subsystems of five-body systems. It is further to be expected that the predictions from four to five bodies would be more accurate than the predictions obtained for four-body system from the case of three-bodies.

It would also be interesting to investigate the stability of planetary orbits in multiple stellar systems and other hypothetical dynamical systems by means of the generalised ε parameters derived in Chapter 9. The systems may then be discussed in terms of which part is least stable or indeed unstable; if unstable then it may be predicted how many orbits it might be expected to exist for before instability would be exhibited. Which parts of the system might be expected to last through these catastrophic changes due to their great stability may also be predicted.

APPENDICES

APPENDIX A - Ordering of the Masses in Collinear Equilibrium Configurations to Obtain Primary, Secondary and Tertiary Bifurcation Values of c^2H

The three bifurcation values of c^2H are obtained from the collinear equilibrium solutions of the three-body problem. These are related to the primary, secondary and tertiary bifurcation points where the nature of the solutions to the motion of the three-body system may alter due to changes in the topology of the curves of zero-velocity. The method to locate the collinear configurations is described elsewhere (see Zare, 1976; Szebehely and Zare, 1977; Roy, 1978) but we outline it below, then proceed to demonstrate the required ordering of the masses to obtain each collinear configuration and hence a particular bifurcation value of c^2H, denoted $(c^2H)_{BV}$.

If masses m_A, m_B and m_C are positioned in collinear equilibrium configuration *in the order* $m_A\ m_B\ m_C$, and we let the ratio of the distances $|\overrightarrow{m_Bm_C}|\ :\ |\overrightarrow{m_Am_B}|$ be X:1 then X is obtained by solution of the quintic equation

$$F(m_A, m_B, m_C, X) = 0$$

where

$$\left.\begin{aligned} F(m_A, m_B, m_C, X) = {} & (m_A + m_B)X^5 + (3m_A + 2m_B)X^4 + (3m_A + m_B)X^3 \\ & -(3m_C + m_B)X^2 - (3m_C + 2m_B)X - (m_C + m_B). \end{aligned}\right\} \quad (1)$$

Having calculated X, we may obtain *a* bifurcation value of c^2H (the one obtained being dependant upon the relative sizes of m_A, m_B and m_C) by substitution of X into the equations

$$f(X) = m_Am_B + \frac{m_Am_C}{1+X} + \frac{m_Bm_C}{X} \quad (2)$$

$$g(X) = m_Am_B + m_Am_C(1 + X)^2 + m_Bm_CX^2 \quad (3)$$

from whence

$$(c^2H)_{BV} = -\frac{G^2f^2(X)\,g(X)}{2M} \quad (4)$$

where M is the sum of the masses.

If we now let

$$m_A = (1 + \varepsilon)^{\alpha} \; ; \quad m_B = (1 + \varepsilon)^{\beta} \; ; \quad m_C = (1 + \varepsilon)^{\gamma}$$

where α, β, γ take the values -1, 0, $+1$ only, then, supposing $\varepsilon << 1$, we have

$$m_A = 1 + \alpha\varepsilon; \quad m_B = 1 + \beta\varepsilon; \quad m_C = 1 + \gamma\varepsilon \quad \text{to } 0(\varepsilon).$$

We may substitute these values into Equation (1) to obtain

$$F(\varepsilon, X) = 0$$

for given α, β, γ values, and, noting that if $\varepsilon = 0$ (equal masses) then the solution of Equation (1) is $X = 1$, we may put

$$X = 1 - \frac{F(\varepsilon, 1)}{\left[\frac{\partial F(\varepsilon, X)}{\partial X}\right]_{X=1}} + \text{higher order} \qquad (5)$$

Substituting in the expressions from above we obtain

$$\left.\begin{aligned} X &= 1 + A\varepsilon \\ \text{where} \quad A &= \frac{7}{29}(\gamma - \alpha). \end{aligned}\right] \qquad (6)$$

Equation (2) may then be expressed in terms of $\varepsilon, \alpha, \beta, \gamma$

$$f(X) \quad 1 + \alpha\varepsilon + \beta\varepsilon + \frac{1 + \alpha\varepsilon + \gamma\varepsilon}{2 + A\varepsilon} + \frac{1 + \beta\varepsilon + \gamma\varepsilon}{1 + A\varepsilon}$$

which, upon application of the binomial expansion, gives

$$f(X) = \frac{5}{2}\left\{1 + \frac{1}{5}\left[3(\alpha+\gamma) + 4\beta\right]\varepsilon - \frac{1}{2}A\varepsilon\right\} + 0(\varepsilon^2). \qquad (7)$$

Similarly, we have

$$g(X) = 6.\left\{1 + \frac{1}{6}\left[5(\alpha+\gamma) + 2\beta\right]\varepsilon + A\varepsilon\right\} + 0(\varepsilon^2). \qquad (8)$$

Thus on substitution of Equations (7) and (8) into Equation (4) we obtain

$$(c^2H)_{BV} = -\left(\frac{5}{2}\right)^2 G^2_{\bullet}\left\{1 + \frac{1}{10}\left[17(\alpha+\gamma) + 16\beta\right]\varepsilon\right\} + 0(\varepsilon^2). \qquad (9)$$

Note that A does not appear in Equation (9), which is correct to $0(\varepsilon)$. This must be so since values of X arise in pairs (eg. if X results from the order $m_A m_B m_C$ then $1/X$ will result when considering the order

$m_C m_B m_A$) and each will result in the same $(c^2H)_{BV}$ value.

If we now consider possible arrangements and relative sizes of the masses, excepting the case $\alpha = \beta = \gamma$ when $X = 1$, we have nine possibilities as depicted in Table A.1.

This table shows that the primary bifurcation value of c^2H requires the smallest mass to assume the central position in the collinear configuration, the tertiary requiring the largest mass and the secondary the intermediate mass to be so positioned. We see further that, if there are two equal masses and the third is smaller, then the secondary and tertiary bifurcation points occur at the same c^2H value. In the same way we see that, if the third mass is larger, the primary and secondary bifurcation points have the same c^2H value. (When all masses are equal then the three bifurcation points occur at one value of c^2H).

We now consider a hierarchical system, with (m_1, m_2) as binary and m_3 as the external mass. Then, if the smallest mass is contained in the binary i.e. m_1 or m_2, we seek the primary bifurcation value of c^2H. If m_3 is the smallest mass then the configuration which results in the lowest bifurcation value of c^2H is not allowed since this would involve violation of the hierarchy by placing m_3 between m_1 and m_2. We instead use the secondary bifurcation value, obtained by placing the smaller of m_1 and m_2 in the centre of the collinear configuration.

Table A.1 - Bifurcation Points

α	β	γ	$(\frac{2}{5G})^2 . \lvert c^2 H \rvert$	Bifurcation
1	0	-1	1	Secondary
0	-1	1	$1 + \frac{\varepsilon}{10}$	Primary
-1	1	0	$1 - \frac{\varepsilon}{10}$	Tertiary
0	0	-1	$1 - \frac{17}{10}\varepsilon$	Secondary
0	-1	0	$1 - \frac{8}{5}\varepsilon$	Primary
-1	0	0	$1 - \frac{17}{10}\varepsilon$	Tertiary
1	0	0	$1 + \frac{17}{10}\varepsilon$	Secondary
0	0	1	$1 + \frac{17}{10}\varepsilon$	Primary
0	1	0	$1 + \frac{8}{5}\varepsilon$	Tertiary

APPENDIX B - The Surfaces of Critical Stability in the Initially Circular Case of the Coplanar, Corotational, Hierarchical Three-Body Problem.

If we consider the three masses m_1, m_2 and m_3 to be arranged hierarchically, at least in some initial phase of the motion, such that m_1 and m_2 form a binary system and m_3 is placed at a more remote distance then, as has been shown in Chapters 4 and 5, critical stability surfaces may be derived which determine whether exchanges between bodies are possible or not. In Chapter 4 the parameter controlling the opening and closing of the zero-velocity curves of the problem, i.e. c^2H, was determined by a two two-body approximation for the three-body system. Having derived the exact expression for c^2H in Chapter 5 the dependance of the critical stability surfaces on other orbital parameters could be assessed. Moreover, another critical value of the ratio α arose which was greater than the previous α_{cr}, but less than one. The aim of this Appendix is to show how the orbital parameter θ, as defined in Chapter 5, affects the critical stability surface and also to determine the other critical stability surface defined as $\alpha = \alpha'_{cr}$ in Chapter 5. The effects of e_2 and e_3 (and hence f_2 and f_3) are neglected since the introduction of eccentricities severely restricts the region of stability obtainable analytically when the mass parameters μ and μ_3 are widely different (see Chapter 5, Section 5.7).

In Figure B.1 are presented contours of the critical stability surface $\alpha_{cr} = \alpha(\mu, \mu_3, e_2, e_3, f_2, f_3, \theta)$, where (e_2, e_3) are zero, (f_2, f_3) are therefore indeterminate and $\theta = 0$, in the μ, μ_3-plane. We are therefore dealing with the case of the three bodies initially lying in a straight-line configuration. If we now let θ assume the value θ_T, i.e. the value of θ which maximises the value of $(c^2H)_{act}$ for a system (given that the other orbital parameters remain fixed), another surface may be determined: this is shown in Figure B.2. It may be noted that the surface resulting from the straight line configuration is slightly higher than that arising from the configuration $\theta = \theta_T$. This implies that the straight line configuration is stable, in the sense of no exchange between bodies being possible, over a larger range of α than the configuration $\theta = \theta_T$. The surface arising

from $\theta = \theta_T$ is very slightly lower than the original surface of Chapter 4 which was obtained using the two two-body approximations to the three-body motion to calculate c^2H.

The other important critical value of α derived in Chapter 5 was denoted α'_{cr}, and was calculated at $\theta = 0$. This is the value of α such that the system of the above mentioned hierarchy is definitely unstable. This arises since the zero-velocity curves are closed so that m_2 and m_3 are constrained to be the binary with m_1 as the external mass. The surface $\alpha'_{cr} = \alpha'(\mu,\mu_3,e_2, e_3, f_2, f_3,\theta)$, where (e_2, e_3) are zero, (f_2, f_3) are therefore indeterminate and $\theta = 0$, is shown as contours in the μ, μ_3-plane in Figure B.3.

These three surfaces may readily be transformed into the $0\varepsilon^{23}$ ε_{32} α_{23} parameter space, as was done in Chapter 4, and hence be displayed as contours in the ε^{23}, ε_{32}-plane. The surface arising from the straight line configuration is shown in Figure B.4; the configuration $\theta = \theta_T$ results in the surface shown in Figure B.5; the surface α'_{cr} is displayed in Figure B.6.

The dashed line in these three diagrams denotes the "cut-off" of the critical stability surfaces, as discussed in Chapter 4, Section 4.4. The 0.1 contours on Figures B.4 and B.5 and the 0.7, 0.6,..,0.1 contours on Figure B.6 are omitted for clarity as they all lie between the appropriate contour and the dashed line parallel to the ε^{23} axis.

Finally it may be noted that there are regions in the ε^{23}, ε_{32}-plane where the hierarchy of interest, as defined above, is definitely unstable*. If a system lies in the region outwith the dashed line in Figure B.6 then *a priori*, without consideration of the α value, the zero-velocity curves are closed so that m_2 and m_3 are constrained to form the binary with m_1 as the "external mass".

*Note however that since $\alpha < 1$ then $\varepsilon^{23} = \mu(1-\mu)\,\alpha^2 < 0.25$, for all real systems.

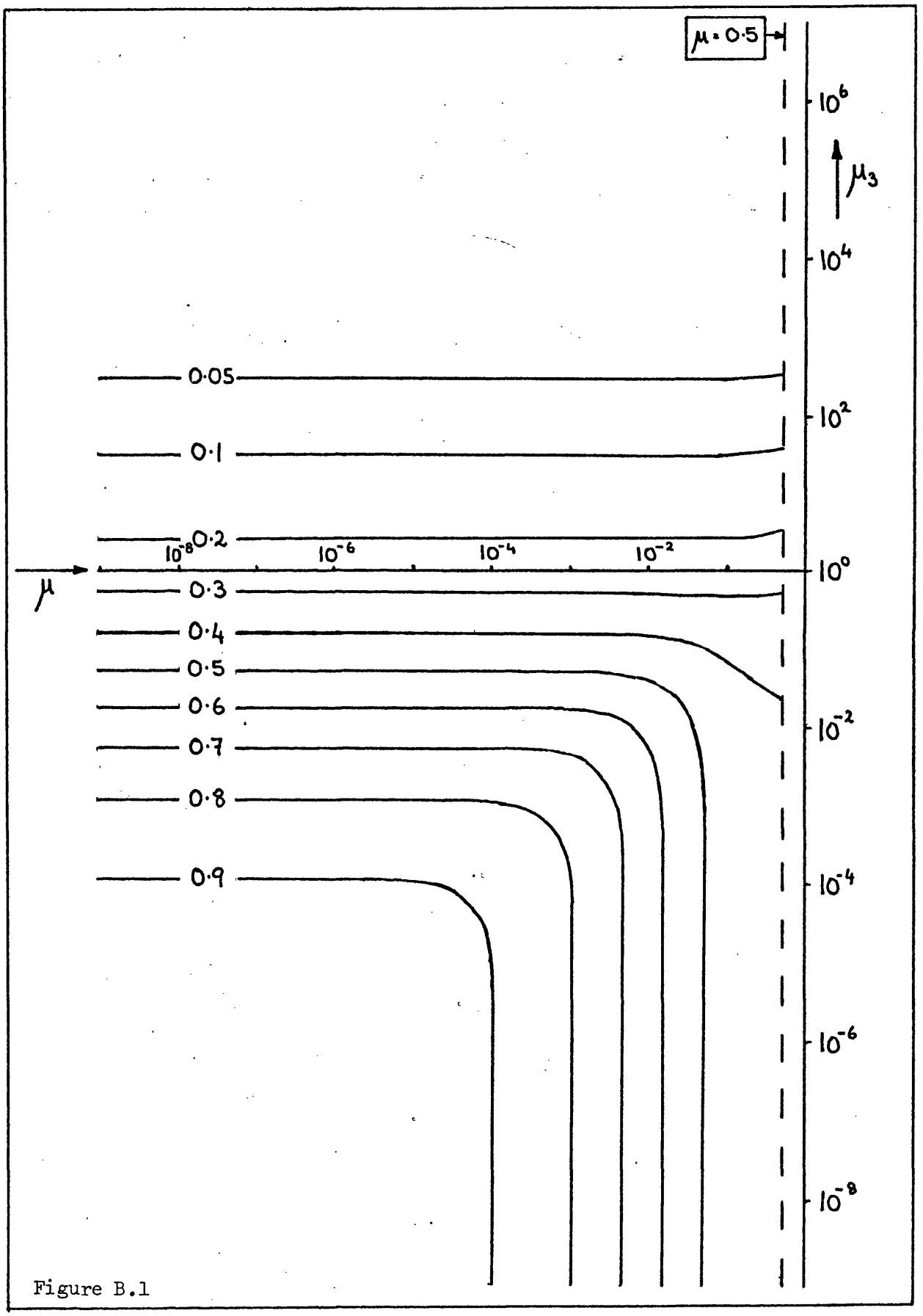
μ = 0·5
10^{6}
μ_3
10^{4}
0·05
10^{2}
0·1
0·2
10^{-8}
10^{-6}
10^{-4}
10^{-2}
10^{0}
μ
0·3
0·4
0·5
0·6
0·7
0·8
0·9
10^{-2}
10^{-4}
10^{-6}
10^{-8}

Figure B.1

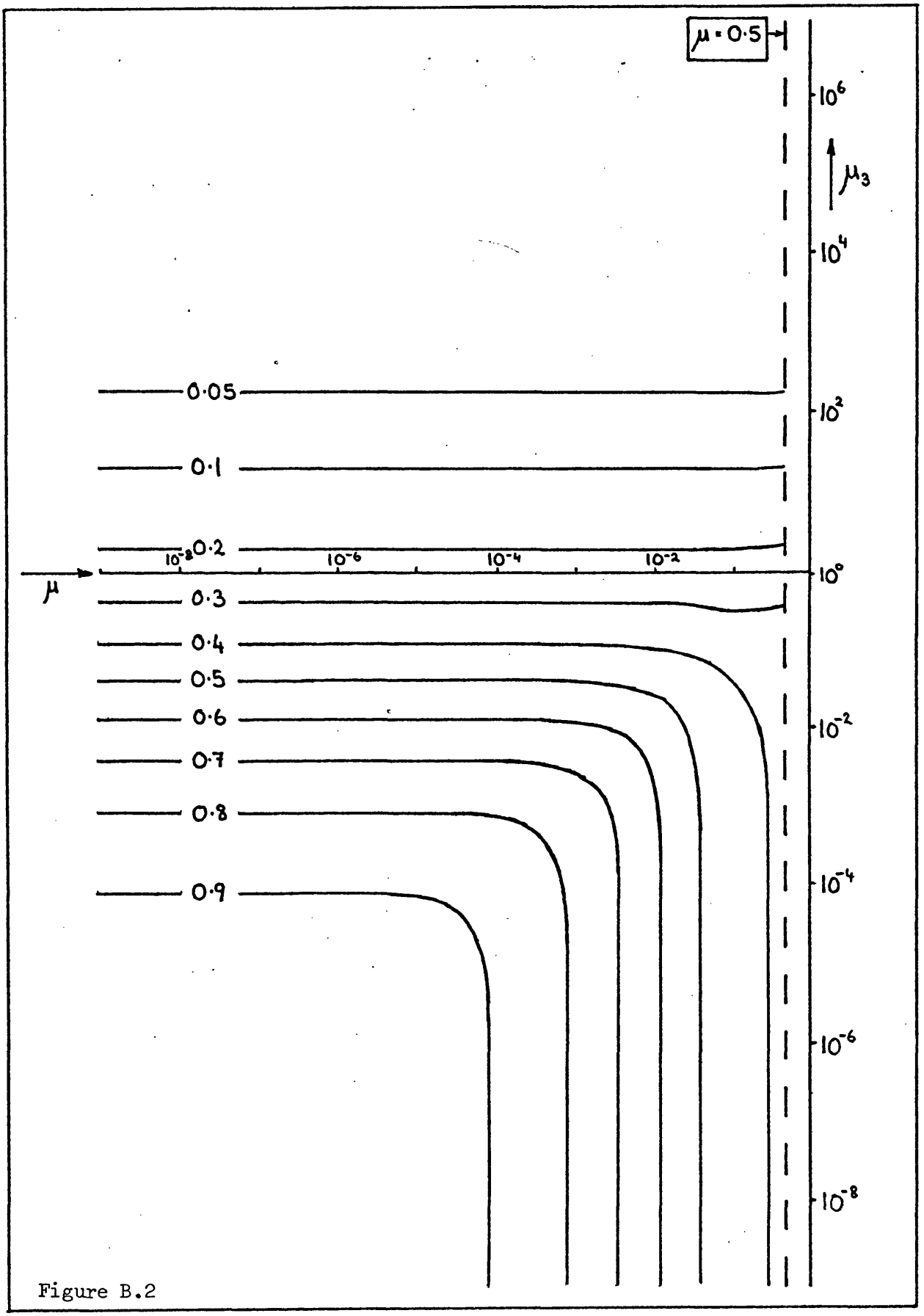
μ = 0·5
10^6
μ_3
10^4
0·05
10^2
0·1
0·2
10^{-8}
10^{-6}
10^{-4}
10^{-2}
10^0
μ
0·3
0·4
0·5
0·6
0·7
0·8
0·9
10^{-2}
10^{-4}
10^{-6}
10^{-8}

Figure B.2

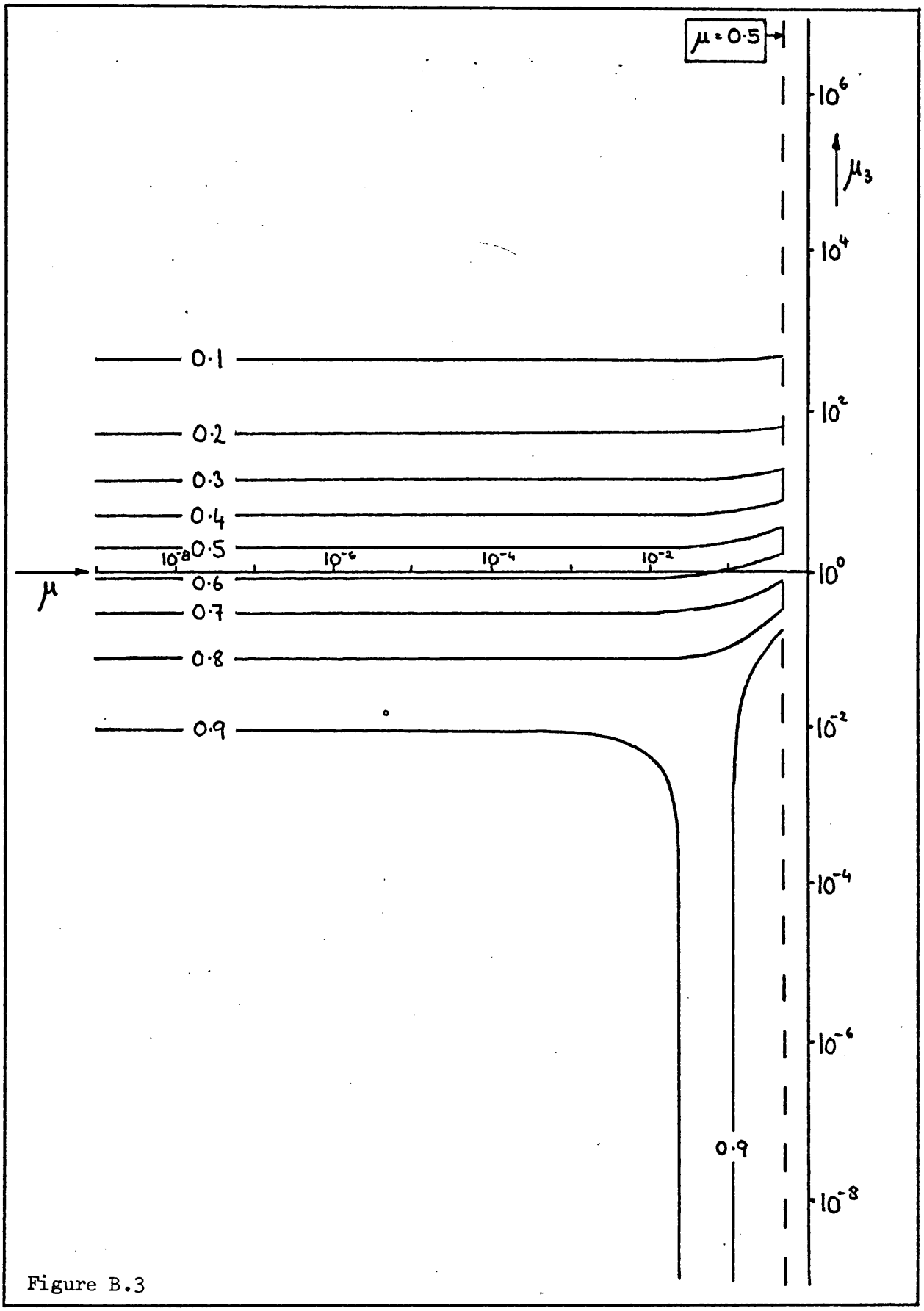
μ = 0·5
10^{6}
μ_3
10^{4}
0·1
10^{2}
0·2
0·3
0·4
0·5
10^{-8}
10^{-6}
10^{-4}
10^{-2}
10^{0}
μ
0·6
0·7
0·8
10^{-2}
0·9
10^{-4}
10^{-6}
0·9
10^{-8}

Figure B.3

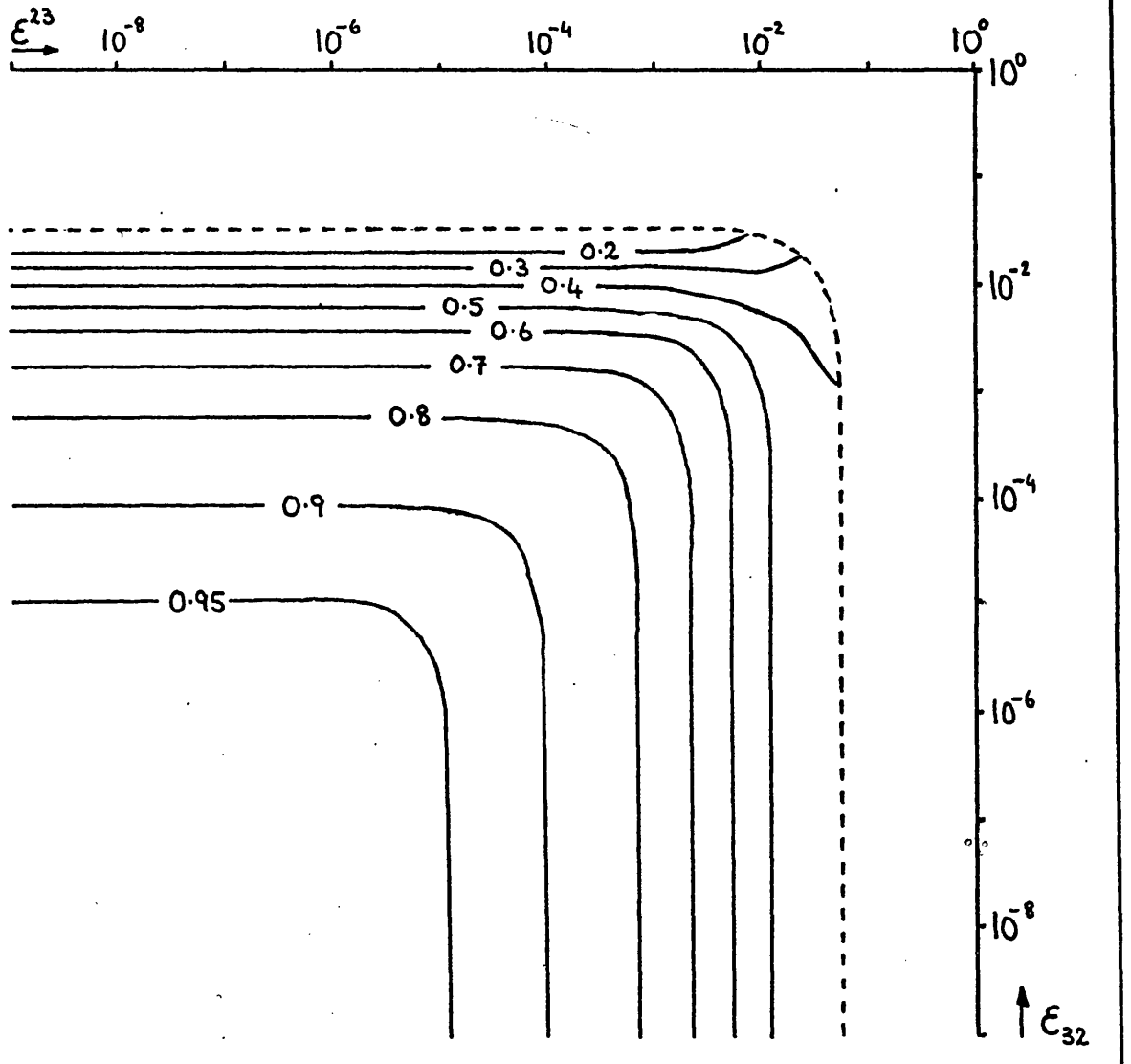
ε^{23}
10^{-8}
10^{-6}
10^{-4}
10^{-2}
10^{0}
10^{0}
10^{-2}
10^{-4}
10^{-6}
10^{-8}
ε_{32}
0·2
0·3
0·4
0·5
0·6
0·7
0·8
0·9
0·95

Figure B.4

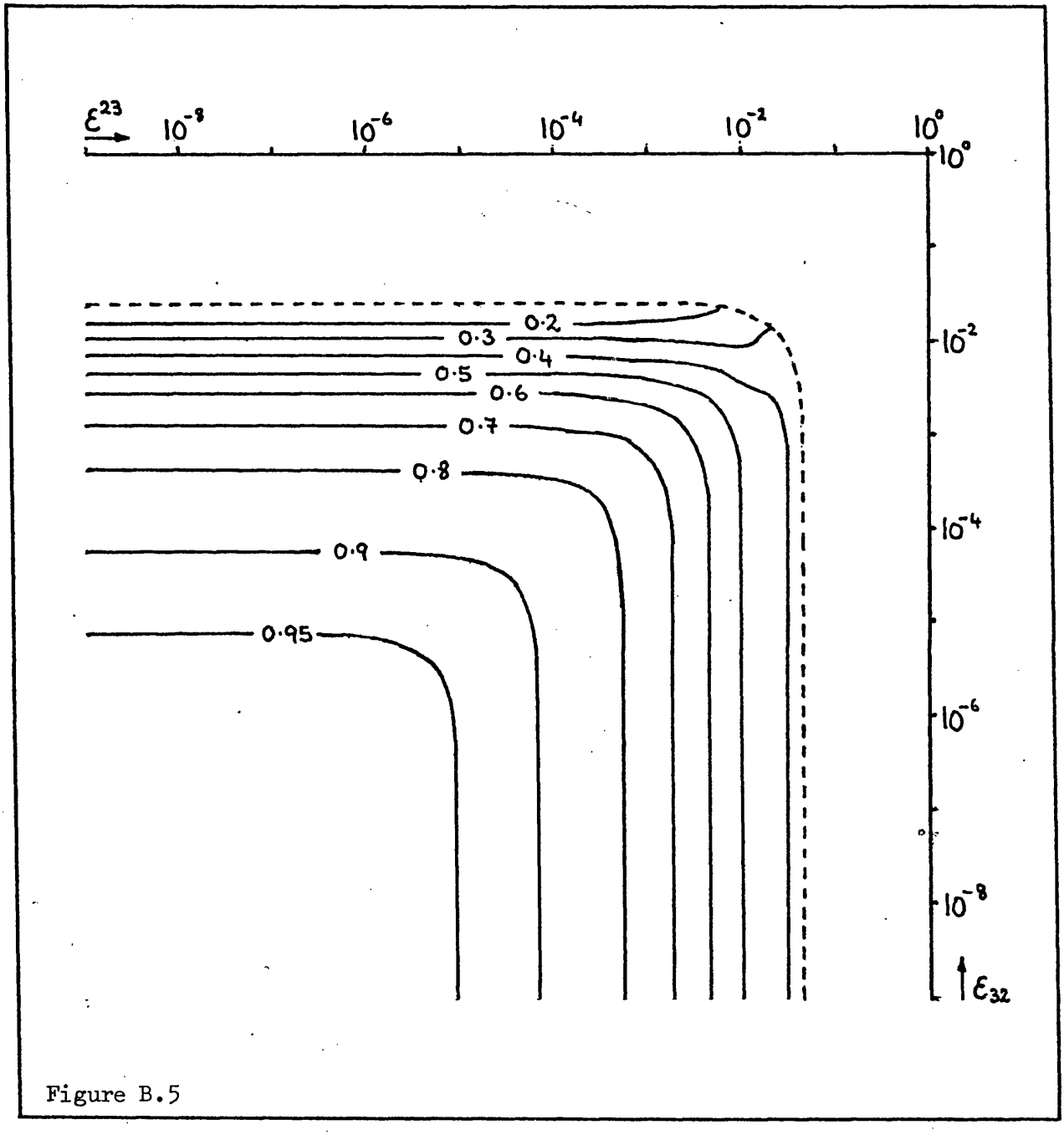
ε^{23}
10^{-8}
10^{-6}
10^{-4}
10^{-2}
10^{0}
10^{0}
10^{-2}
10^{-4}
10^{-6}
10^{-8}
ε_{32}
0·2
0·3
0·4
0·5
0·6
0·7
0·8
0·9
0·95

Figure B.5

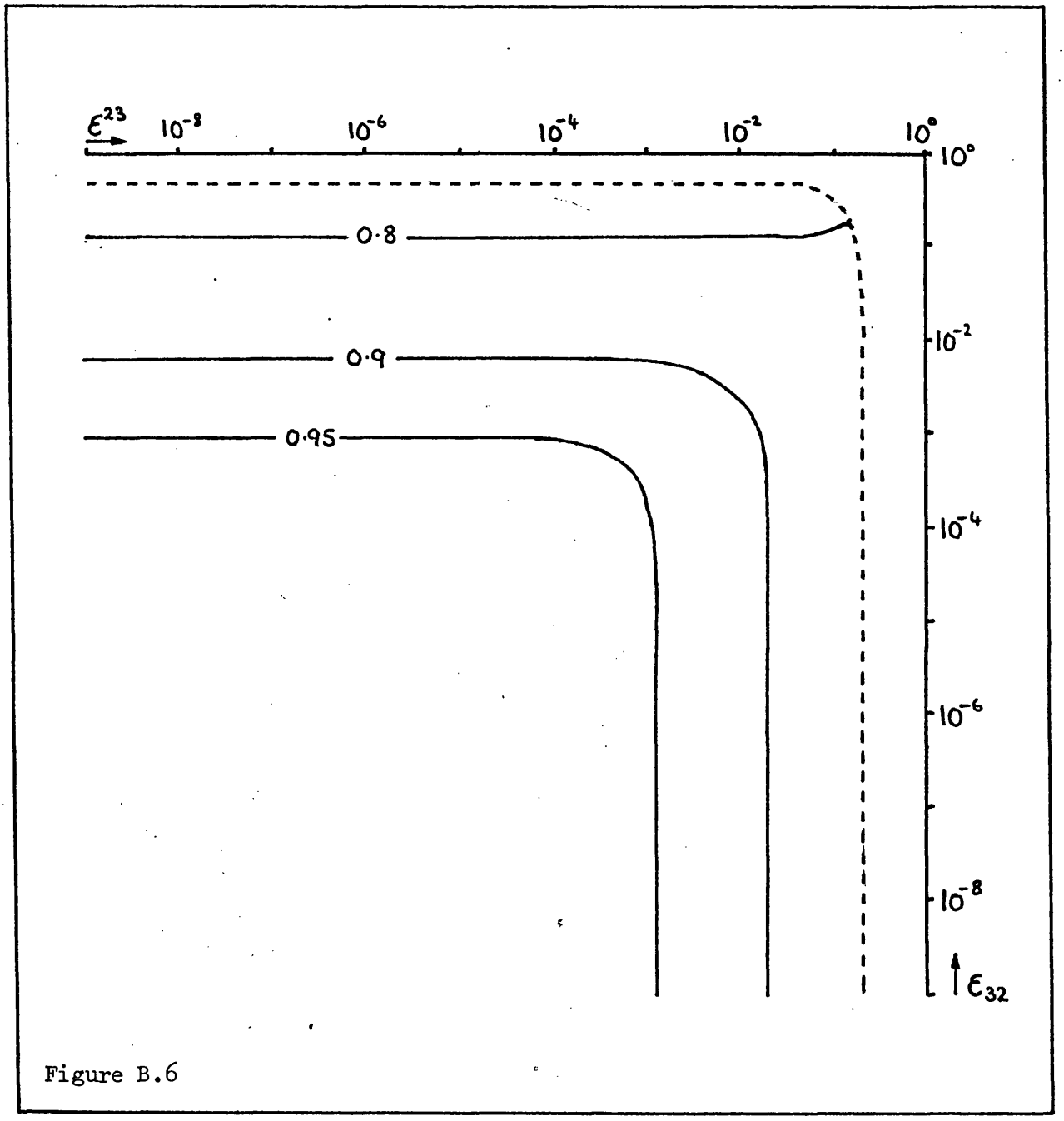
ϵ^{23}
10^{-8}
10^{-6}
10^{-4}
10^{-2}
10^{0}
10^{0}
10^{-2}
10^{-4}
10^{-6}
10^{-8}
ϵ_{32}
0·8
0·9
0·95

Figure B.6

APPENDIX C - A Description of the Recurrence Relation Scheme Used in the Numerical Integration of the Equations of Motion of the Many-Body Problem - Its Application to the Restricted Three-Body problem and Comparison with Similar Methods Used Previously

C.1 Introduction

The use of recurrence relations to compute the coefficients for an (explicit) Taylor series integration procedure was shown by Roy *et al.* (1972), in the simple example of the two-body problem, to be more efficient than the classical single-step integration procedure Runge-Kutta Four (RK4). In this context "efficiency" is a measure of how *quickly* any given problem can be carried out by a computer and how *accurate* is the resulting information. The use of recurrence relations as a tool in integrating various problems in celestial mechanics has been pursued by other authors (e.g. Myachin and Sizova, 1970; Broucke, 1971; Moran, 1972, 1973; Moran *et al.*, 1973; Black, 1973).

In particular Moran (1973) - see also Moran (1972) - applied recurrence relations to the three dimensional elliptic restricted three-body (ER3) problem in order to determine classes of orbit for which one or either of the standard Cowell or Encke formalisms of the equations of the problem (cf. Danby, 1962) was preferable. Due to the large amount of computer time currently spent on the (numerical) integration of many-body systems, e.g. the ER3 problem, it is advantageous to cut the required computing time to a minimum by a suitable choice of numerical integration method. We seek, in this present method, an improvement on the recurrence relation scheme of Moran (1973).

In Moran (1973), expressions for the Taylor series coefficients were derived using a set of four auxiliary variables (u, w, s and σ in the notation of the above paper) per relative position vector, each of these being represented by an infinite power series in the time t. In this way the differential equations of the system were reduced to quadratic form; substitution of the power series representation of

the variables and equating coefficients of powers of t then yielded the required recurrence relations. The integration step-length at each point in the orbit was automatically adjusted throughout the integration; this was accomplished by comparing the results of a single forward integration step with those obtained from two consecutive half-steps, subsequently halving, doubling or leaving unchanged the step-length, as appropriate, so as to keep the local truncation error (LTE) below a certain specified amount.

Instead of four auxiliary variables per relative vector we herein find that the introduction of only two is required (u and s in the notation of Moran, 1973). In our procedure, the recurrence relations are obtained by an application of Liebniz's Theorem rather than by equating coefficients in an infinite power series. This obviates the need for the basic differential equations of the system to be in quadratic form and so enables the above reduction in the required number of auxiliary variables to be effected. Moreover, this scheme would appear to possess a greater simplicity than schemes such as those of Myachin and Sizova (1970) whose treatment, although involving the same number of auxiliary variables , u and w^{-1} in the above notation, results in more complicated expressions for the Taylor series coefficients. Also, in the present treatment, the integration step-length is adjusted by comparing values of each position and velocity vector from before the integration step and after consecutive forward and reverse steps of the same step-length. This removes the need for the wasteful evaluation of derivatives at the halfway point (for approximately half the number of steps - see Section C.3) and also admits a much more accurately fitted step-length to be used throughout the orbit.

The above improvements all constitute substantial savings in machine time, and therein lies their importance. After establishing the recurrence relations, appropriate to the ER3 problem, in Section C.2, and presenting the method of step adjustment in Section C.3, the power of the new method is illustrated in Section C.4 by providing computational results which compare the efficiencies of the method Moran (1973) and the present method. In Section C.5 the results are summarized and some conclusions are drawn.

C.2 Equations and Recurrence Relations

In the ER3 problem, particles S, of mass $(1-\mu)$, and J, of mass μ, revolve around each other in a Keplerian ellipse, and we are concerned with the motion of a particle P, of negligible mass, in the combined gravitational field of S and J. In a reference frame, with its origin at S, the equations of motion are

$$\ddot{\underset{\sim}{r}} = -\left[(1-\mu)\frac{\underset{\sim}{r}}{r^3} + \mu\left\{\frac{\underset{\sim}{\Delta}}{\Delta^3} + \frac{\underset{\sim}{R}}{R^3}\right\}\right] \qquad (1)$$

and

$$\ddot{\underset{\sim}{R}} = -\frac{\underset{\sim}{R}}{R^3} \qquad (2)$$

where $\underset{\sim}{r} = (x,y,z)$ and $\underset{\sim}{R} = (X,Y,Z)$ are the vectors $\overrightarrow{SP}$ and $\overrightarrow{SJ}$ respectively,

$$\underset{\sim}{\Delta} = \underset{\sim}{r} - \underset{\sim}{R} \qquad (3)$$

and $r = |\underset{\sim}{r}|$, etc. The units of time and distance being chosen such that the constant of gravitation, G, is unity, with a dot denoting differentiation with respect to time.

We now proceed to set the above equations in recurrence relation form. Define the auxiliary variables a, A, α as follows:

$$a = r^{-3} \; ; \; A = R^{-3} \; ; \; \alpha = \Delta^{-3} \; . \qquad (4)$$

Equations (1) and (2) may be rewritten as

$$\ddot{\underset{\sim}{r}} = -\left[(1-\mu)\, a\underset{\sim}{r} + \mu(\alpha\underset{\sim}{\Delta} + A\underset{\sim}{R})\right] , \qquad (5)$$

and

$$\ddot{\underset{\sim}{R}} = -A\underset{\sim}{R}. \qquad (6)$$

We now apply Liebniz's Theorem on multiple derivatives of products to Equations (5) and (6) obtaining

$$\overset{(n)}{\underset{\sim}{r}} = -\left[(1-\mu)\cdot\sum_{i=0}^{n-2}\binom{n-2}{i}\overset{(i)}{a}\,\overset{(n-i-2)}{\underset{\sim}{r}} + \mu\sum_{i=0}^{n-2}\binom{n-2}{i}\overset{(i)}{\alpha}\,\overset{(n-i-2)}{\underset{\sim}{\Delta}} - \mu\overset{(n)}{\underset{\sim}{R}}\right] \qquad (7)$$

$$\overset{(n)}{\underset{\sim}{R}} = - \sum_{i=0}^{n-2} \binom{n-2}{i} \overset{(i)}{A} \overset{(n-i-2)}{\underset{\sim}{R}} \quad . \tag{8}$$

In the above $\overset{(n)}{\underset{\sim}{r}}$ denotes $d^n\underset{\sim}{r}/dt^n$, etc and $\binom{k}{\ell}$ is a binomial coefficient viz.

$$\binom{k}{\ell} = \frac{k!}{(k-\ell)!\ \ell!} \tag{9}$$

In order to use the relations (7) and (8) we clearly require expressions for the higher derivatives of a, A and α.

For a general function $g = r^{-q}$, where q is an integer, we see that, defining

$$b = \underset{\sim}{r}.\dot{\underset{\sim}{r}} \tag{10}$$

we obtain, successively,

$$\dot{g} = -q\, r^{-(q+1)}\, \dot{r} = -\, qr^{-(q+2)}\, b = \frac{-q}{r^2} gb$$

$$\ddot{g} = \frac{-q}{r^2}(\dot{g}b + g\dot{b}) + \frac{2q}{r^4} gb^2 = \frac{-1}{r^2}\left[(q+2)\dot{g}b + qg\dot{b})\right]$$

etc., from which it readily follows, by mathematical induction on the number of differentiations with respect to time, that

$$\overset{(i)}{g} = -\frac{1}{r^2} \sum_{j=1}^{i} \left[q \binom{i-1}{j-1} + 2\binom{i-1}{j} \right] \overset{(i-j)}{g}\ \overset{(j-1)}{b} \quad , \tag{11}$$

where we define $\binom{k}{\ell} = 0$ for $\ell > k$. Thus

$$\overset{(i)}{a} = -\frac{1}{r^2} \sum_{j=1}^{i} \left[3\binom{i-1}{j-1} + 2\binom{i-1}{j} \right] \overset{(i-j)}{a}\ \overset{(j-1)}{b} \quad , \tag{12}$$

with similar expressions for $\overset{(i)}{A}$ and $\overset{(i)}{\alpha}$, involving $B = \dot{\underset{\sim}{R}}.\underset{\sim}{R}$ and $\beta = \dot{\underset{\sim}{\Delta}}.\underset{\sim}{\Delta}$ respectively.

Finally it is required to calculate the higher order derivatives $\overset{(j)}{b}$, $\overset{(j)}{B}$ and $\overset{(j)}{\beta}$. From the definitions - Equation (10) - and again using Liebniz's Theorem, we obtain

$$\overset{(j)}{b} = \sum_{k=0}^{j} \binom{j}{k} \overset{(k)}{\underset{\sim}{r}}.\ \overset{(j-k+1)}{\underset{\sim}{r}} \tag{13}$$

with similar expressions for $\overset{(j)}{B}$ and $\overset{(j)}{\beta}$.

The relations given in Equations (7), (8), (12) and (13) enable us to compute derivatives of $\underset{\sim}{r}$ and $\underset{\sim}{R}$ up to any order we please, given the initial state vectors x_i (i=1,...,6) and $\dot{X}_i$(i=1,...,6). A suitable sequence of evaluation would be $\underset{\sim}{A}$, $\dot{\underset{\sim}{A}}$, {a}, {b}, $\ddot{\underset{\sim}{r}}$, $\ddot{\underset{\sim}{R}}$, $\ddot{\underset{\sim}{A}}$, $\dddot{\{a\}}$, $\dddot{\{b\}}$, $\dddot{\underset{\sim}{r}}$, $\dddot{\underset{\sim}{R}}$, $\dddot{\underset{\sim}{A}}$, etc., where {a} denotes the set (a, A, α), etc. These may then be combined with the appropriate factorial term to yield the desired Taylor series coefficients.

C.3 Adjustment of the Integration Step-length

Since it is required that the method be applicable to any set of initial conditions of the problem, including those in which there is a resulting close approach of P to either S or J, and/or a period during which P is at a great distance from both S and J, it is clearly necessary that the method employs an automatic scheme for adjusting the integration step-length to be used at any point in the orbit. In previous studies by Moran (1972, 1973), Myachin and Sizova (1970) and Roy *et al.* (1972) this adjustment is accomplished in the manner described below.

Let the trial step-length be h and integrate the configuration using (a) one integration step with step-length h and (b) two consecutive integration steps with step-length h/2. Then the difference in final configurations obtained by the two methods compared to some specified accuracy criterion gives insight into the suitability of the step-length h for the integration step under consideration. The step-length is then either kept the same, halved, or doubled, as appropriate before proceeding to the next step by means of the more accurate two half steps. This method is outlined in much more detail in Moran (1972).

This procedure is considered to be unsatisfactory for a number of reasons. Firstly, the derivatives have to be evaluated at the intermediate half-step point: this procedure is lengthy and wasteful of machine time if the result of the error comparison is other than a halving of the trial step-length. Secondly, the crude halving and doubling procedure results in truncation errors which can only be adjusted to within large factors of the acceptable error. This is

because the truncation error $\varepsilon \sim h^{n+1}$, where n is the order of the Taylor series employed: frequently, the value of n may be of the order of 10 for optimum efficiency of the method (cf. Section C.4), implying that ε can only be adjusted to within a factor $2^{11} \simeq 2000$. Thirdly, the optimum step-length for a particular integration step will not, in general, be equal to 2^p times the initial step (where p is an integer), thus time will be wasted running a portion of an orbit at a step-length h, when a step-length of say 1.9 h would yield sufficient accuracy. These last two points have also been raised by Barton *et al.* (1970) in their discussion of general Taylor series integration schemes.

A method of step-length adjustment is therefore now presented which removes all the above objections. The method is based on the consideration of the truncated terms in the Taylor series used, a technique studied by other authors (e.g. Barton *et al.*, 1970; Myachin and Sizova, 1970; Moran, 1972). Moran (1972) found that this technique yielded unfavourable results. This, it is felt, was due to insufficient rigour in his procedure which is remedied below by supplying a detailed error analysis of the method proposed herein. The method employs the device of consecutive forward and reverse integration steps with a trial step-length, followed by a comparison between the pre-integration and post-integration values of the position and velocity vectors in order to determine the necessary adjustment. The derivatives computed for the reverse step may then, under suitable conditions described later, be used for the next forward integration step. Thus their evaluation is not wasteful as in the doubling/halving methods of step adjustment. Furthermore, the method permits a much more refined step adjustment than a mere halving and doubling: this results in the local truncation error always remaining close to, but always less than, the specified allowable error. This latter point removes the second and third objections above.

Consider a function $\underset{\sim}{r}(t)$ and its Taylor series expansion about $t = t_o$, up to order n in the derivatives, viz.

$$\underset{\sim}{r}(t) = \sum_{i=0}^{n} \frac{\underset{\sim}{r}^{(i)}(t_o)\, h^i}{i!} , \qquad (14)$$

where $h = t - t_o$.

The (local) truncation error is clearly given by

$$\underset{\sim}{\varepsilon} = \frac{\overset{(n+1)}{\underset{\sim}{r}}(t_o)\, h^{n+1}}{(n+1)!} + O(h^{n+2}), \qquad (15)$$

where $O(h^n)$ means "terms of order h^n and higher".

Next consider the quantity $\underset{\sim}{r}'(t_o)$, obtained by *backward integration*, by Taylor series, from $\underset{\sim}{r}(t)$ with step-length $(-h)$, also up to order n in the derivatives, viz.

$$\underset{\sim}{r}'(t_o) = \sum_{i=0}^{n} (-1)^i \frac{\overset{(i)}{\underset{\sim}{r}}(t_o)\, h^i}{i!}. \qquad (16)$$

Using Equation (14) in Equation (16) we derive

$$\underset{\sim}{r}'(t_o) = \sum_{i=0}^{n} (-1)^i \frac{h^i}{i!} \left[\sum_{j=0}^{n-i} \frac{\overset{(i+j)}{\underset{\sim}{r}}(t_o) h^j}{j!} + \frac{\overset{(n+1)}{\underset{\sim}{r}}(t_o) h^{n-i+1}}{(n-i+1)!} + O(h^{n-i+2}) \right]. \qquad (17)$$

Reversing the order of summation over i and j in the double summation above we obtain

$$\underset{\sim}{r}'(t_o) = \sum_{j=0}^{n} \frac{h^j}{j!} \left[\sum_{i=0}^{n-j} (-1)^i \frac{\overset{(i+j)}{\underset{\sim}{r}}(t_o) h^i}{i!} \right] +$$

$$+ \sum_{i=0}^{n} (-1)^i \frac{\overset{(n+1)}{\underset{\sim}{r}}(t_o) h^{n+1}}{(n-i+1)!\, i!} + O(h^{n+2})$$

$$= \sum_{j=0}^{n} \left[\frac{\overset{(j)}{\underset{\sim}{r}}(t_o - h)\, h^j}{j!} - (-1)^{n-j+1} \cdot \frac{\overset{(n+1)}{\underset{\sim}{r}}(t_o) h^{n+1}}{(n-j+1)!\, j!} \right] +$$

$$+ \frac{\overset{(n+1)}{\underset{\sim}{r}}(t_o) h^{n+1}}{(n+1)!} \cdot \sum_{i=0}^{n} (-1)^i \binom{n+1}{i} + O(h^{n+2})$$

$$= \underset{\sim}{r}(t_o) - \frac{h^{n+1}}{(n+1)!}\left[\underset{\sim}{r}^{(n+1)} (t_o-h) + \right.$$

$$\left. + \underset{\sim}{r}^{(n+1)} (t_o) \cdot \sum_{j=0}^{n} \binom{n+1}{j} \left[(-1)^{n-j+1} - (-1)^{j} \right] \right] + O(h^{n+2}) \quad (18)$$

Now, using the identities

$$\sum_{j=0}^{n+1} (-1)^{j} \binom{n+1}{j} = \sum_{j=0}^{n+1} (-1)^{n-j+1} \binom{n+1}{j} = 0 , \quad (19)$$

obtained by expanding $(1-x)^{n+1}$ by the binomial theorem and letting $x \to 1$, we derive

$$\Delta \underset{\sim}{r} = \underset{\sim}{r}'(t_o) - \underset{\sim}{r}(t_o) = \begin{cases} \dfrac{-h^{n+1}}{(n+1)!}\left[\underset{\sim}{r}^{(n+1)} (t_o-h) - 2\, \underset{\sim}{r}^{(n+1)} (t_o) \right] + \\ \qquad + O(h^{n+2}), \quad n \text{ even} \\ \dfrac{-h^{n+1}}{(n+1)!}\, \underset{\sim}{r}^{(n+1)} (t_o-h) + O(h^{n+2}), \quad n \text{ odd.} \end{cases}$$

In either case, since $\underset{\sim}{r}^{(n+1)} (t_o-h) = \underset{\sim}{r}^{(n+1)} (t_o) + O(h)$, we see that

$$|\Delta \underset{\sim}{r}| = \frac{\left| \underset{\sim}{r}^{(n+1)} (t_o) \right| h^{n+1}}{(n+1)!} + O(h^{n+2}) , \quad (20)$$

which is exactly the same, to $O(h^{n+2})$, as $|\underset{\sim}{\varepsilon}|$ (see Equation (15)). Thus evaluation of $|\Delta \underset{\sim}{r}|$ by consecutive forward and reverse integration steps yields the size of the (local) truncation error, $|\underset{\sim}{\varepsilon}|$, for the forward step alone.

It will now be demonstrated how, by consideration of this local truncation error, the integration step-length may be adjusted at each point in the orbit so that the introduced error in the configuration after the integration step using the adjusted step-length is less than but close to, as denoted by the symbol $\underset{\sim}{<}$, some specified acceptable amount.

Let $\underset{\sim}{u}$ denote any one of the position or velocity vectors of the problem, and let the local truncation error determined, using the above procedure, for an integration step about $t = t_o$ using the trial step-length h be $\underset{\sim}{\varepsilon}$, i.e.

$$\underset{\sim}{\varepsilon} = \frac{h^{n+1}}{(n+1)!} \overset{(n+1)}{\underset{\sim}{u}}(t_o) + \frac{h^{n+2}}{(n+2)!} \overset{(n+2)}{\underset{\sim}{u}}(t_o) + O(h^{n+3}). \qquad (21)$$

Further, let $\underset{\sim}{u}$ be that vector, either position or velocity, such that $|\underset{\sim}{\varepsilon}|$ is a maximum. Then, letting the acceptable local truncation error be ε_o and denoting $|\underset{\sim}{\varepsilon}|$ by ε, etc. we clearly have two cases.

Case (a) $\varepsilon > \varepsilon_o$

Here we must clearly decrease h, to h' say, such that the resulting local truncation error $\varepsilon'(h') \lesssim \varepsilon_o$. Now

$$\underset{\sim}{\varepsilon}' = \frac{h'^{n+1}}{(n+1)!} \overset{(n+1)}{\underset{\sim}{u}}(t_o) + \frac{h'^{n+2}}{(n+2)!} \overset{(n+2)}{\underset{\sim}{u}}(t_o) + O(h'^{n+3}).$$

Let

$$h' = h.\left(\frac{\varepsilon_o}{\varepsilon}\right)^{1/(n+1)}, \qquad (22a)$$

(cf. the procedure outlined by Barton *et al.*(1970), except that here ε is *calculated*, and is not an *estimated* quantity); then

$$\underset{\sim}{\varepsilon}' = \frac{\varepsilon_o}{\varepsilon} \frac{h^{n+1} \overset{(n+1)}{\underset{\sim}{u}}(t_o)}{(n+1)!} \cdot \left[1 + \frac{\gamma h'}{n+2} + O(h'^2)\right], \qquad (23)$$

where $$\gamma \simeq \frac{\left|\overset{(n+2)}{\underset{\sim}{u}}(t_o)\right|}{\left|\overset{(n+1)}{\underset{\sim}{u}}(t_o)\right|}$$

is a quantity of order unity. Using Equation (21) in (23), we derive

$$\frac{\varepsilon'}{\varepsilon_o} = \frac{\frac{1}{h} + \left(\frac{\gamma}{n+2}\right)\left(\frac{\varepsilon_o}{\varepsilon}\right)^{1/(n+1)}}{\frac{1}{h} + \left(\frac{\gamma}{n+2}\right)} + O(h^2), \qquad (25a)$$

which, since $\varepsilon_o/\varepsilon < 1 << \frac{1}{h}$ means that $\varepsilon' \lesssim \varepsilon_o$ as required.

Case (b) $\varepsilon < \varepsilon_o$

Here we require to increase h, to h" say, but still such that $\varepsilon"(h") \lesssim \varepsilon_o$. Let

$$h" = h \left(\frac{\varepsilon_o}{\varepsilon}\right)^{1/(n+2)} . \qquad (22b)$$

(Note that if h" was defined along the lines of Equation (22a) $\varepsilon"$ would be slightly *greater* than ε_o by Equation (25a), this is clearly unacceptable).

Then by a similar procedure, we obtain

$$\frac{\varepsilon"}{\varepsilon_o} = \left(\frac{\varepsilon}{\varepsilon_o}\right)^{1/(n+2)} \left[\frac{\frac{1}{h} + \left(\frac{\gamma}{n+2}\right)\left(\frac{\varepsilon_o}{\varepsilon}\right)^{1/(n+2)}}{\frac{1}{h} + \left(\frac{\gamma}{n+2}\right)} \right] + O(h^2) \qquad (25b)$$

which is seen to be at most $\lesssim 1$, as required, upon neglect of the terms of first and higher order (since $h \lesssim 1$).

Although we have chosen to use Equation (22b) to control the local truncation error this is by no means a unique way to tackle the problem: an equally applicable method for increasing h would be

$$h" = h \left(\frac{\kappa\varepsilon_o}{\varepsilon}\right)^{1/(n+1)} \qquad (22c)$$

where the factor $\kappa(\lesssim 1)$ ensures the local truncation errors introduced by the step-length h" are acceptable. It is important to stress also that the revision of the step-length amounts to a *linear prediction* and it becomes apparent upon writing Equation (25(b)) in the form

$$\frac{\varepsilon"}{\varepsilon_o} = \frac{\left(\frac{\varepsilon}{\varepsilon_o}\right)^{1/(n+2)} \cdot \frac{1}{h} + \frac{\gamma}{n+2}}{\frac{1}{h} + \left(\frac{\gamma}{n+2}\right)} \qquad (25c)$$

that this prediction is not valid if h is not small and/or n is not large, as in such cases the first term in the numerator of Equation (25c) is no longer dominant. The allowances made for this shortcoming in the method will be discussed more fully in Section C.5.

It may be noted that the above errors refer to *vector magnitudes*.

This procedure is, in the opinion of the author, more appropriate than representing ε by expressions of the type (cf. Moran, 1972)

$$\varepsilon = \max_i \frac{2\,|q'_i - q_i|}{|q'_i| + |q_i|}, \qquad (26)$$

where q_i and q'_i are components of the state vectors x_i and X_i $(i=1,2,\ldots,6)$ obtained after one integration step and two half-steps respectively. Although this expression could be carried over into the present treatment (by taking q_i and q'_i to be the component values before and after consecutive forward and reverse integration steps) this would introduce artificially small step lengths when one of the q'_is is near zero. The definition of ε viz.

$$\varepsilon = \max \left(\frac{\Delta r}{r}, \frac{\dot{\Delta r}}{\dot r}, \frac{\Delta R}{R}, \frac{\dot{\Delta R}}{\dot R} \right) \qquad (27)$$

where, for example,

$$\Delta r = \left[(x' - x)^2 + (y' - y)^2 + (z' - z)^2 \right]^{\frac{1}{2}} \qquad (28)$$

and ε refers to the *relative* error in any vector, does not encounter this difficulty. It is clearly feasible to define a different ε_o value for each vector; Equation (27) then reduces to a set of conditions the appropriate one being that which produces the smallest step-length. Further we may also include in Equation (27) the relevant values for the relative errors in Δ and $\dot\Delta$.

The adjusted step-length, once obtained, is used in one of two ways as described below.

(a) $\varepsilon > \varepsilon_o$

Here we return to $t = t_o$ and compute a forward step with step-length h' (Equation (22a) which, by Equation (25a) results in an acceptable local truncation error. The procedure is then repeated using h' as the trial step-length for the next forward integration step.

(b) $\varepsilon < \varepsilon_o$

In this case we may take the results of the integration step with *trial* step-length h since $\varepsilon < \varepsilon_o$ in any case. Then using the derivatives, *previously calculated for the reverse integration step,* we carry out the next integration step with h" as the trial step-length. Hence, by not having to compute derivatives for the next forward step machine time is saved.

As a final comment in this Section it may be noted that we assume the knowledge of a fairly good approximation to the required step-length. While this is true as the integration proceeds, i.e. we may use the step-length of the integration step immediately previous to the current step as an approximate trial value, as described above, it is clear that initially, when commencing the integration, some iterative procedure will have to be adopted to ensure accuracy is not lost through the predictions of Equations (22(a), (b)) being erroneous due to an inaccurate approximation for the step-length of the first integration step.

The scheme adopted was as follows:

(i) Assume a trial step-length, h_o say, and calculate the local truncation error ε and adjust the step-length accordingly by one of Equations (22(a) and (b)).

(ii) Test the predicted step-length, h_1 say, against the original h_o. If $2\,|h_o - h_1| \,/\{\,|h_o| + |h_1|\}$ is greater than or equal to a specified amount δh then return to (i) above and repeat the procedure using h_1 as the new trial value. If less, then the required step-length has been found.

For this procedure δh was taken to be

$$\delta h = \frac{\delta}{(n+1)} \qquad (\delta < 1) \qquad (29)$$

by the following reasoning:

Suppose we have a trial step-length h_o which results in a truncation error ε and a correct step-length, h_1, which results in a truncation error ε_o then, neglecting $O(h^{n+2})$, we have

$$\varepsilon = \frac{\left| \underset{\sim}{r}^{(n+1)} \right|}{(n+1)!} h_o^{n+1} \qquad (30)$$

and

$$\varepsilon_o = \frac{\left| \underset{\sim}{r}^{(n+1)} \right|}{(n+1)!} h_1^{n+1} \qquad (31)$$

If we further suppose that $h_o = h_1 + \Delta h$, then Δh being positive and therefore $\varepsilon > \varepsilon_o$, then we have, dividing Equation (30) by Equation (31),

$$\frac{\varepsilon}{\varepsilon_o} = \left[\frac{h_1 + \Delta h}{h_1} \right]^{n+1} . \qquad (32)$$

or

$$\frac{\Delta h}{h_1} = \left(\frac{\varepsilon}{\varepsilon_o}\right)^{1/(n+1)} - 1 . \qquad (32)$$

Equation (32) forms the basis of an iterative procedure to find the correct initial step-length; a limit is required for the size of ε in terms of ε_o . Suppose we allow $\varepsilon = \varepsilon_o(1+\delta)$ for the first step-length, where $\delta < 1$, then the iteration will continue until

$$\frac{\Delta h}{h} = (1 + \delta)^{1/(n+1)} - 1$$

i.e.

$$\frac{\Delta h}{h} \simeq \frac{\delta}{n+1} \qquad (33)$$

since $\delta < 1$. Any discrepancy between ε and ε_o is so small now that any error introduced on the first integration step will be effectively $\leq \varepsilon_o$. The values taken for δ are generally less than 10^{-1}.

C.4 Computational Results

In this section it is demonstrated that the above improvements to the recurrence relation and step-length adjustment schemes do in fact constitute savings of machine time for given calculations. Clearly we must demonstrate that both improvements yield savings in

machine time, to this end we examine *three* methods of integration:

(a) the original method as described by Moran (1972)
(b) a "combination" method using the above recurrence relation scheme but retaining the halving/doubling step-length adjustment and
(c) the full method as described above.

In this way comparison of (a) and (b) shows the savings in time due to the reduction in the number of auxiliary variables and comparison of (b) to (c) the savings due to the refined step-length adjustment.

Using each of these methods a number of "interesting" orbits in the ER3 problem were computed with varying accuracy criterion ε_o and Taylor series order n. Table C.1 describes two of the orbits studied which yielded results representative of those obtained generally.

The total machine time (TMT) necessary for a given calculation is clearly a function of n*. We therefore require, to make a fair comparison among (a), (b) and (c), to optimise each with respect to n. This may be done by constructing graphs such as Figure C.1, of TMT versus n for a given method, orbit and accuracy criterion, and recording the value of n at the minimum turning point of the graph, which is denoted n_{opt}. For Figure C.1 n_{opt} takes the values 10, 10 and 8 for methods (a), (b) and (c) respectively. The minimum arises from the following considerations. As n is increased the required step-length for a given ε_o increases (cf. Equation (21)); this results in a shorter TMT necessary for a given (real) integration time. This trend prevails until the time required to compute the larger and larger number of derivatives begins to dominate the TMT and so the curve rises again.

Using the value n_{opt} orbits A and B (Table C.1) were integrated for the same length of (real)time by each of the methods, and for

*Note that n is kept fixed throughout any given integration as opposed to schemes such as that of Myachin and Sizova (1970) which use a *fixed* step-length and *adjust* n so that the local truncation error remains acceptable.

Table C.1 - Description of Orbits Studied

Orbit	μ		Initial Configuration $i = 1$	2	3	4	5	6	Remarks
A	0.5	x_{0i}	−1.14600	0.00000	0.00000	0.00000	0.55350	0.76127	Axisymmetric periodic orbit, family L_{3v} (Zagouras and Markellos, 1977). Integrated from $t = 0$ to $t = 40$ and then back to $t = 0$.
		X_{0i}	1.00000	0.00000	0.00000	0.00000	1.00000	0.00000	
B	0.99905*	x_{0i}	−0.03000	0.00000	0.00000	0.00000	−0.15000	0.00100	Initial orbit around J; escapes after 2 revolutions and thereafter orbits S. Integrated from $t = 0$ to $t = 25$ and then back to $t = 0$.
		X_{0i}	1.60000	0.00000	0.00000	0.00000	0.50000	0.00000	

* Sun-Jupiter case.

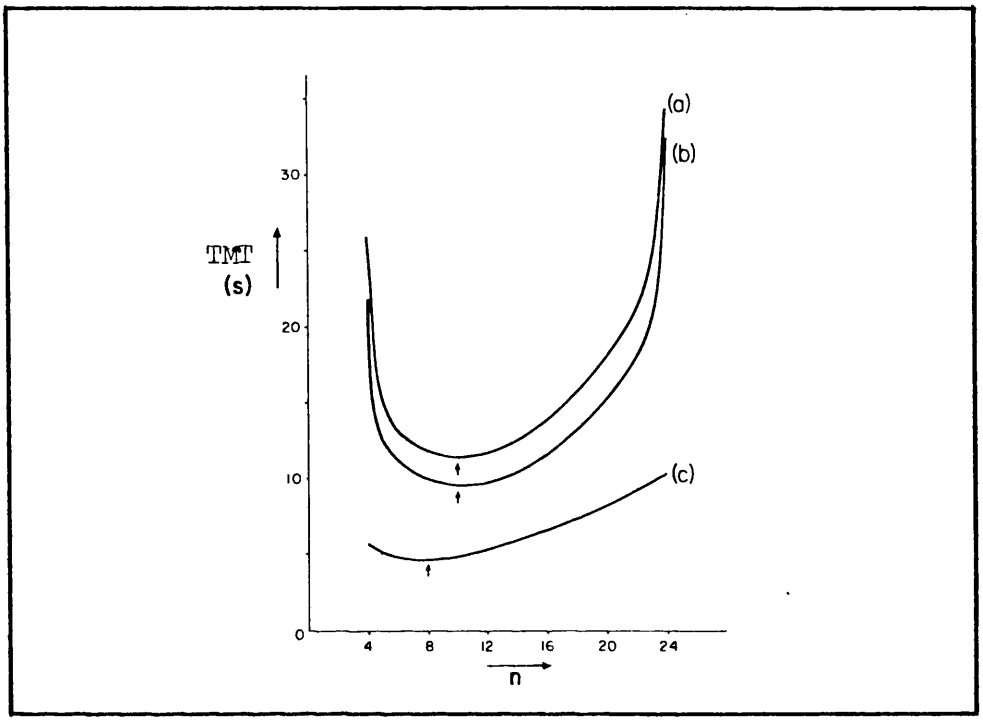

Figure C.1 The TMT required vs. Taylor series order n for methods (a), (b) and (c) for orbit A and $\varepsilon_o = 10^{-8}$. The optimum n-value, n_{opt}, for each method is shown arrowed (cf. Tables C.2 and C.3). Note the broad form of the curve for method (c) compared with those for methods (a) and (b); this is a consequence of the more refined step-adjustment procedure described in Section C.3.

Table C.2 - Comparison of integration methods for orbit A.

ε_0	Method and TMT (s)	n_{opt}	δ_{max}	$\overline{\delta}$
	(a) 7.46	8	4	1
10^{-6}	(b) 6.32	8	4	1
	(c) 2.82	4	10800	8030
	(a) 11.38	10	5	2
10^{-8}	(b) 9.63	10	5	2
	(c) 4.76	8	130	49
	(a) 17.41	12	1	1
10^{-10}	(b) 14.65	12	1	1
	(c) 7.29	10	66	26
	(a) 28.17	10	180	76
10^{-12}	(b) 22.53	10	170	72
	(c) 10.37	12	150	59

Table C.3 - Comparison of integration methods for orbit B.

ε_0	Method and TMT (s)	n_{opt}	δ_{max}	$\overline{\delta}$
	(a) 16.26	8	2040	870
10^{-6}	(b) 13.70	8	2040	870
	(c) 7.42	6	343000	147000
	(a) 26.13	10	680	280
10^{-8}	(b) 22.17	10	680	280
	(c) 12.21	8	90100	38200
	(a) 38.68	12	4500	1910
10^{-10}	(b) 32.34	12	4490	1910
	(c) 18.28	10	74900	31800
	(a) 71.65	10	69600	29600
10^{-12}	(b) 59.27	10	69400	29500
	(c) 25.56	12	29800	12700

accuracy criteria ε_o of 10^{-6}, 10^{-8}, 10^{-10}, 10^{-12}. The resulting TMT necessary, as well as δ_{max} and $\bar{\delta}$, the maximum and mean accumulated (truncation plus round-off) errors respectively (in units of ε_o), for each calculation are presented in Tables C.2 and C.3.

It is clear from the results of these tables (and also Figure C.1) that savings in machine time accrue from each of the modifications to the Moran (1972) method. These savings are discussed more fully in the next section.

C.5 Discussion and Conclusions

It has been demonstrated that it is possible to effect a reduction, over previous methods, in the number of auxiliary variables required to obtain the recurrence relations necessary for the generation of the coefficients for a Taylor series integration step in the ER3 problem. It is believed that these algorithms possess the maximum conciseness possible for a representation of the equations of motion in a recurrence relation form; there appear to be no gains in efficiency from the use of a single auxiliary variable. It has already been amply demonstrated by Roy *et al.* (1972) that recurrence relation techniques are faster and more accurate than implicit single-step methods such as RK4. Furthermore, Barton *et al.* (1970) concluded that the method of numerical integration of ordinary differential equations by Taylor series methods does not suffer from numerical instability over a wide range of required accuracies; thus it would appear that the present algorithm is an extremely effective single-step method for computing orbits in the ER3 problem, and as such provides an ideal standard with which to compare the multi-step methods e.g. Adam's method and the Gauss-Jackson method (cf.Merson, 1973), which are generally accepted to be the most efficient methods currently in use.

Moreover, we have seen that further savings in machine time result from the use of a continuously variable integration step-length, adjusted by comparison of pre-integration values with those after consecutive forward and reverse integration steps. This replaces the time-expensive halving and doubling method. However, slight caution is required in cases where the step-length, h, is large

and/or n is not very large since the method of linear prediction of the correct step-length, when h is being increased, breaks down. This problem could be circumvented by employing an iterative step-length adjustment scheme (cf. Barton *et al* ., 1970); this, however, would result in large increases in machine time requirements. At any rate when increasing h the result of the step using the trial h is accepted. Therefore, it is felt an iterative scheme is unnecessary (except for the initial step) providing any increase in step-length is limited to a factor 2 (cf. previous doubling method). By calculating *actual* values of the local truncation error as the integration proceeded for various sets of initial conditions it was in fact found that the value of ε always remained close to, but less than, ε_o.

Computationally it has been shown that the present integration method optimises for Taylor series of around order 10, at least for the orbits considered herein. The exact value of n_{opt} depends on the imposed accuracy criterion and is fairly independent of both the orbit being integrated and the method in use. Accumulated truncation plus roundoff errors (δ_{max}, $\bar{\delta}$) are, for large ε_o, larger for method (c) than for the halving/doubling methods (a) and (b); this trend diminishes, and is in fact reversed, as ε_o is reduced. The explanation for this is that for large ε_o truncation errors dominate the δ's; these are controlled more accurately by method (c) than by (a) or (b) which therefore result in unnecessarily small δ's (cf. Section C.3). It is expected, as ε_o is reduced and round-off errors begin to dominate, that the better conditioned method (c) will give lower accumulated errors. It is also evident from Tables C.2 and C.3 that even in the truncation error dominated regime the more stringent ε_o value required by method (c) to give δ values comparable to methods (a) and (b) still results in less TMT for a given calculation.

TMT savings of the present method (c) over the original Moran (1973) method are in excess of a factor of two and become larger as the allowable truncation error per step is reduced. Extension of the above scheme to the general three-body and many other types of dynamical system occurring in celestial mechanics is a straight-forward matter, due to the general nature of the terms in the basic equations of motion of such systems.

APPENDIX D - Applications of the Explicit Taylor Series Integration Scheme, Employing Recurrence Relations, and its Comparison with Classical Single-Step and Multi-Step Methods of Numerical Integration (as available on the Glasgow University ICL2976 Computer)

D.1 Introduction

In Appendix C the explicit Taylor series (TS) numerical integration scheme used throughout this thesis for numerical experimentation on many-body systems was described and compared to similar methods used previously; in particular, with the method of Roy *et al* . (1972). In that paper a comparison was made between the classical single-step (CSS) integration procedure Runge-Kutta Four, as described by Henrici (1963), and the TS scheme involving the use of four auxiliary variables to set up the required recurrence relations. It was this latter method which was used in Appendix C for comparison with the present TS scheme involving only two auxiliary variables. Combining the results of the paper by Roy *et al* ., where it was found that their TS scheme was of the order 6 to 15 times faster than Runge-Kutta Four, and Appendix C, which produced a further factor between 2 and 3 in saving of machine time, it can be appreciated that a saving up to a factor about 50 in machine time may accrue from the use of the present TS method as opposed to the CSS methods.

From several authors it appears that explicit TS schemes for numerical integration are more efficient i.e. *faster* and *more accurate* than CSS methods (see Deprit and Zahar, 1966; Barton *et al.*, 1970, Roy *et al.*, 1972). Moreover, among TS methods, that of Appendix C possesses a certain conciseness which makes it readily applicable to many of the differential equations arising in celestial mechanics.

Also, since it is generally accepted that classical multi-step (CMS) methods of numerical integration (e.g. Adam's, Gauss-Jackson methods, etc.) are among the most efficient currently in use (Merson, 1973) it is considered that the method of Appendix C is the ideal single-step method with which to compare the multi-step methods.

It is therefore the aim to give a comparison of three numerical methods: the TS method of Appendix C, a CMS method and CSS method are compared; the latter two being available on the Glasgow University ICL2976 computer (these being the obvious alternatives for use in the numerical experiments of this thesis).

The equations of motion and recurrence relationships for a few "common types" of dynamical systems are presented in Section D.2. In Section D.3, using the simple case of the two-body problem as an example, we outline the (numerical) integration procedures and ranges of parameters used. Data on machine time and errors for given numerical integration experiments are given in Sections D.4 and D.5; a summary and discussion of these results being given in Section D.6.

D.2 Applications - Equations of Motion and Recurrence Relationships

In this section, by way of example, the differential equations governing the motion of several dynamical systems are presented: also included are the appropriate set of auxiliary variables and hence the recurrence relationships which are set up to enable the calculation of the higher order derivatives of the position and velocity vectors. The systems treated are:

(i) The Two-Body Problem (which will be considered again later)
(ii) The Restricted Three-Body Problem (and the associated variational equations used in determining the stability of periodic orbits)
(iii) The General Three-Body Problem
(iv) The Motion of a Satellite about an Oblate Planet
(v) The Motion of a Satellite about a Planet with an Atmosphere

Example (i):

The equations of relative motion for a body of mass m_2 about a body of mass m_1 are

$$\ddot{\underset{\sim}{r}} = -G(m_1 + m_2) \frac{\underset{\sim}{r}}{r^3} \qquad (1)$$

where $r = |\underset{\sim}{r}|$

$\underset{\sim}{r} = \overrightarrow{m_1 m_2}$

and G is the constant of gravitation.

We introduce the auxiliary variables

$$a = r^{-3} \tag{2}$$

and

$$b = \underset{\sim}{r}.\dot{\underset{\sim}{r}} \tag{3}$$

and hence, by substitution of Equation (2) into Equation (1) and application of Leibniz's Theorem on multiple derivatives of products to the resultant expression we obtain (cf. Appendix C)

$$\overset{(n)}{\underset{\sim}{r}} = -G(m_1 + m_2) \sum_{i=0}^{n-2} \binom{n-2}{i} a^{(i)} \underset{\sim}{r}^{(n-i-2)} \tag{4}$$

where $\overset{(k)}{\underset{\sim}{r}}$ denotes the kth derivative (with respect to time) of $\underset{\sim}{r}$. Expressions to obtain the $a^{(i)}$ are thus required. These are (cf. Appendix C).

$$a^{(i)} = -\frac{1}{r^2} \sum_{j=1}^{i} \left[3\binom{i-1}{j-1} + 2\binom{i-1}{j} \right] a^{(i-j)} b^{(j-1)} \tag{5}$$

where

$$b^{(j-1)} = \sum_{k=0}^{j-1} \binom{j-1}{k} \underset{\sim}{r}^{(k)} \cdot \underset{\sim}{r}^{(j-k)} . \tag{6}$$

gives the required derivatives of b in terms of $\underset{\sim}{r}$ and its derivatives. The relations (4) to (6) enable us to successively calculate the higher order derivatives of $\underset{\sim}{r}$ i.e. given $\underset{\sim}{r}$ and $\dot{\underset{\sim}{r}}$, initially, we evaluate successively $\dot{a}$, $\dot{b}$, $\ddot{a}$, $\ddot{b}$, $\dddot{\underset{\sim}{r}}$, $\dddot{a}$, $\dddot{b}$, $\overset{(4)}{\underset{\sim}{r}}$, etc.

Example (ii):

As was seen in Section C.2 the equations of motion for the restricted three-body problem, involving massive bodies S and J and massless particle P, are

$$\ddot{\underset{\sim}{r}} = -\left[(1-\mu) \frac{\underset{\sim}{r}}{r^3} + \mu \left(\frac{\underset{\sim}{\Delta}}{\Delta^3} + \frac{\underset{\sim}{R}}{R^3} \right) \right] \tag{7}$$

and

$$\ddot{\underset{\sim}{R}} = -\frac{\underset{\sim}{R}}{R^3} \tag{8}$$

where the notation is as in Section C.2.

In studies of periodic orbits, and their stability, we are also interested in the variational equations of the problem. These are (cf. Zagouras and Markellos, 1977)

$$\frac{d}{dt}\left(\frac{\partial x_i}{\partial x_{oj}}\right) = \sum_{k=1}^{6} \frac{\partial \dot{x}_i}{\partial x_k} \cdot \frac{\partial x_k}{\partial x_{oj}} , \qquad (9)$$

where x_i $i = 1,\ldots,6$ is the state vector $(x,y,z,\dot{x},\dot{y},\dot{z})$ of the particle P with respect to S and the subscript zero refers to initial conditions. Denoting the variations $\partial x_i / \partial x_{oj}$ by v_{ij}, we readily derive from Equation (7)

$$\left.\begin{aligned} \dot{v}_{ij} &= v_{(i+3)_j} \qquad i = 1,2,3 \\ \dot{v}_{ij} &= \sum_{k=1}^{3} f_{ik}\, v_{kj} \qquad i = 4,5,6 \end{aligned}\right\} \; j = 1,\ldots,6 \qquad (10)$$

where we have denoted

$$f_{ik} = \partial \dot{x}_i / \partial x_k . \qquad (11)$$

In explicit form, in our inertial reference frame, the functions f_{ik}; $i = 4,5,6$; $k = 1,2,3$ are

$$\left.\begin{aligned} f_{41} &= -Q + R_1 x^2 + R_2 (x-X)^2 \; ; \\ f_{42} &= R_1 xy + R_2 (x-X)(y-Y) \; ; \\ f_{43} &= R_1 xz + R_2 (x-X)(z-Z) \; ; \\ f_{51} &= f_{42} \; ; \\ f_{52} &= -Q + R_1 y^2 + R_2 (y-Y)^2 \; ; \\ f_{53} &= R_1 yz + R_2 (y-Y)(z-Z) \; ; \\ f_{61} &= f_{43} \; ; \\ f_{62} &= f_{53} \; ; \\ f_{63} &= -Q + R_1 z^2 + R_2 (z-Z)^2 \end{aligned}\right\} \qquad (12)$$

where

$$Q = \frac{1-\mu}{r^3} + \frac{\mu}{\Delta^3} \; ; \quad R_1 = 3\frac{(1-\mu)}{r^5} \; ; \quad R_2 = \frac{3\mu}{\Delta^5} . \qquad (13)$$

Since the equations of motion - Equations (7) and (8) were set in recurrence relation form in Appendix C we will deal here with only the

equations of variation. In addition to the previously defined auxiliary variables

$$a = r^{-3} \; ; \qquad \alpha = \Delta^{-3} \qquad . \qquad . \qquad . \qquad . \qquad (14)$$

we now require also

$$d = r^{-5} \; ; \qquad \delta = \Delta^{-5} \; , \qquad (15)$$

giving

$$Q = (1-\mu)a + \mu\alpha \; ; \quad R_1 = 3(1-\mu)d; \quad R_2 = 3(1-\mu)\delta \; . \qquad (16)$$

We now apply Leibniz's Theorem to Equations (10) obtaining

$$\left.\begin{aligned} v_{ij}^{(n)} &= v_{(i+3)j}^{(n-1)} && i = 1,2,3 \\ v_{ij}^{(n)} &= \sum_{k=1}^{3} \sum_{\ell=1}^{n-1} \binom{n-1}{\ell} f_{ik}^{(\ell)} \, v_{kj}^{(n-\ell-1)} && i = 4,5,6 \end{aligned}\right\} j=1,\ldots,6 \qquad (17)$$

In order to apply Equations (17) we clearly require in addition to the higher derivatives of a and α, as given by Equation (C.12) using Equation (C.13), the higher derivatives of the f_{ik}, d and δ. The former are obtained easily from Equations (12) by application of Leibniz's Theorem and Equation (16), if expressions for the higher order derivatives of d and δ are available. These are (cf. Equation (C.11))

$$d^{(i)} = -\frac{1}{r^2} \sum_{j=1}^{i} \left[5 \binom{i-1}{j-1} + 2\binom{i-1}{j} \right] d^{(i-j)} \, b^{(j-1)} \qquad (18)$$

with a similar expression for $\delta^{(i)}$. The required expressions for $b^{(j)}$ and $\beta^{(j)}$ are as given in Equation (C.13).

Thus by the introduction of a further two auxiliary variables, d and δ, the variational equations of the restricted problem may be integrated along with the equations of motion.

Example (iii):

For the general three-body problem, defining normalized masses μ_1, μ_2, μ_3, such that $\mu_1 + \mu_2 + \mu_3 = 1$ and $\mu_1 : \mu_2 : \mu_3 = m_1 : m_2 : m_3$,

and letting G be unity (without loss of generality), the equations of motion are

$$\ddot{\underset{\sim}{r}}_k + \frac{\underset{\sim}{r}_k}{r_k^3} = \mu_k \cdot \sum_{\ell=1}^{3} \frac{\underset{\sim}{r}_\ell}{r_\ell^3} \qquad (k=1,2,3) \qquad (19)$$

where $\underset{\sim}{r}_1 = \overrightarrow{m_2 m_3}$

$\underset{\sim}{r}_2 = \overrightarrow{m_3 m_1}$

and $\underset{\sim}{r}_3 = \overrightarrow{m_1 m_2}$.

Again defining auxiliary variables

$$a_k = r_k^{-3} \quad \text{and} \quad b_k = \underset{\sim}{r}_k \cdot \dot{\underset{\sim}{r}}_k \qquad (k=1,2,3) \qquad (20)$$

we may derive the recurrence relationships

$$\overset{(n)}{\underset{\sim}{r}}_k = - \sum_{i=0}^{n-2} \binom{n-2}{i} a_k^{(i)} \, \underset{\sim}{r}_k^{(n-i-2)} + \mu_k \sum_{i=0}^{n-2} \sum_{\ell=1}^{3} \binom{n-2}{i} a_\ell^{(i)} \, \underset{\sim}{r}_\ell^{(n-i-2)} \qquad (21)$$

$$a_k^{(i)} = - \frac{1}{r_k^2} \sum_{j=1}^{i} \left[3\binom{j-1}{i-1} + 2\binom{j-1}{i} \right] a_k^{(i-j)} \, b_k^{(j-1)} \qquad (22)$$

and

$$b_k^{(j-1)} = \sum_{h=0}^{j-1} \binom{j-1}{h} \underset{\sim}{r}_k^{(h)} \cdot \underset{\sim}{r}_k^{(j-h)} \cdot \qquad (22)$$

Given initial values of $\underset{\sim}{r}_k, \dot{\underset{\sim}{r}}_k$ (k=1,2,3) we may then successively evaluate the derivatives viz. (a_k), (b_k), $(\dot{a}_k)$, $(\dot{b}_k)$, $(\ddot{\underset{\sim}{r}}_k)$, $(\ddot{a}_k)$, $(\ddot{b}_k)$, $(\dddot{\underset{\sim}{r}}_k)$, etc., where $(a_k) = a_k(k=1,2,3)$, etc.

Example (iv):

MacCullagh's Formula (cf. Roy, 1978) provides an expression for the potential, U, at a point P outside a body of arbitrary shape, where its centre of mass is taken as origin of the coordinate system Oxyz viz.

$$U = \frac{GM}{r} + \frac{G}{2r^3}(A + B + C - 3I) \qquad (23)$$

where M is the mass of the body

$\underset{\sim}{r} = |\overrightarrow{OP}|$

and A,B,C and I are respectively the moments of inertia of the body about the Ox, Oy, Oz and OP axes.

Suppose a satellite is in motion about a planet of arbitrary shape then its equations of motion will be

$$\ddot{\underset{\sim}{r}} = \underset{\sim}{\nabla} U \qquad (24)$$

where U is the potential function (Equation (23))

and $\underset{\sim}{\nabla}$ is the gradient operator with respect to $\underset{\sim}{r}$.

Expressing I in terms of A, B, C and $\underset{\sim}{r}$ [=(x,y,z)] we obtain, after some reduction,

$$\ddot{\underset{\sim}{r}} = -GM\frac{\underset{\sim}{r}}{r^3} + G(\underset{\sim}{F} - 3A')\frac{\underset{\sim}{r}}{r^5} - 5G(B'x^2 - B'y^2 + 3A'z^2)\frac{\underset{\sim}{r}}{r^7} \qquad (25)$$

where $A' = \frac{1}{2}(C - \frac{1}{2}(A+B))$

$B' = \frac{3}{4}(A-B)$

and $\underset{\sim}{F} = (-2B', 2B', -6A')$.

By defining the auxiliary variables $\alpha = r^{-3}$, $\beta = r^{-5}$, $\gamma = r^{-7}$ and differentiating Equation (25) n-2 times we obtain the recurrence relationships

$$\overset{(n)}{\underset{\sim}{r}} = -GM\sum_{i=0}^{n-2}\binom{n-2}{i}\overset{(i)}{\alpha}\overset{(n-i-2)}{\underset{\sim}{r}} + Gm(\underset{\sim}{F}-3A')\sum_{i=0}^{n-2}\binom{n-2}{i}\overset{(i)}{\beta}\overset{(n-i-2)}{\underset{\sim}{r}} - 5G\sum_{i=0}^{n-2}\binom{n-2}{i}\left[\left[\sum_{j=0}^{i}\binom{i}{j}\{B'\overset{(j)}{x}\overset{(i-j)}{x} - B'\overset{(j)}{y}\overset{(i-j)}{y} + 3A'\overset{(j)}{z}\overset{(i-j)}{z}\}\right]\cdot\left[\sum_{k=0}^{n-i-2}\binom{n-i-2}{k}\overset{(k)}{\gamma}\overset{(n-i-k-2)}{\underset{\sim}{r}}\right]\right], \qquad (26)$$

where $\overset{(i)}{\alpha}$, $\overset{(i)}{\beta}$, $\overset{(i)}{\gamma}$ may be obtained in the usual way by defining $b=\underset{\sim}{r}.\dot{\underset{\sim}{r}}$. The successive evaluation of derivatives is then carried out similarly to (i) and (iii) above.

Example (v):

The equations of motion for a satellite of mass m in orbit about a planet of mass M possessing an atmosphere are (cf. Roy, 1978)

$$\ddot{\underset{\sim}{r}} = - GM \frac{\underset{\sim}{r}}{r^3} - \tfrac{1}{2} C_D \frac{A}{m} \rho \, \dot{r} \, \dot{\underset{\sim}{r}} \qquad (27)$$

where $r = |\underset{\sim}{r}|$

C_D is the aerodynamic drag coefficient

A is the average cross-sectional area of the satellite

ρ is the air density at height $(r-R)$ above the planetary surface

and R is the radius of the planet.

Introducing the auxiliary variable "a" again we obtain, upon differentiating n-2 times,

$$\overset{(n)}{\underset{\sim}{r}} = - GM \sum_{i=0}^{n-2} \binom{n-2}{i} a^{(i)} \underset{\sim}{r}^{(n-i-2)} - \\ -\tfrac{1}{2} C_D \frac{A}{m} \rho \cdot \sum_{i=0}^{n-2} \binom{n-2}{i} r^{(i+1)} \underset{\sim}{r}^{(n-i-1)} \qquad (28)$$

where again the $a^{(i)}$ are obtained by the introduction of $b = \underset{\sim}{r}.\dot{\underset{\sim}{r}}$.

D.3 Numerical Integration Experiments

The main disadvantage of the application of a Taylor Series method to any given problem in celestial mechanics arises from the lack of any readily available computer programs for general application. In most cases it is used on an *ad hoc* basis, inasmuch as the computer program is written for one specific set of differential equations. From this apparent disadvantage however, one advantage is forthcoming: the algorithm when implemented should be the most economical in machine time since it was designed for a specific context.

It is for this reason that the present comparison is made between the TS method of Appendix C and the CSSand CMS methods of numerical integration available on the Glasgow University's own computer. It is felt appropriate that the TS method should be compared to alternatives which would *generally* be used.

The integration experiments were all carried out on an ICL2976 computer in double precision arithmetic (17 significant decimal digits). The integration procedures used, with appropriate references, were:

(a) TS method - as described in Appendix C

(b) CSS method - Merson's method, which is a Runge-Kutta type procedure, (see Mayers, 1962).

(c) CMS method - Krogh's method, which is a form of the Adams-Bashforth method with Krogh's step-length adjustment scheme (see Krogh, 1971).

The accuracy criteria (ε_o) imposed on all experiments to control local truncation error were $\varepsilon_o = 10^{-6}, 10^{-8}, 10^{-10}, 10^{-12}$. In the TS method these accuracy criteria are used so that the relative errors in $|\underset{\sim}{r}|$ and $|\dot{\underset{\sim}{r}}|$ after one integration step are both kept less than or equal to the chosen value ε_o. The CSS and CMS methods employ the criteria to control the absolute error in the individual components of $\underset{\sim}{r}$ and $\dot{\underset{\sim}{r}}$ after one integration step. This point will be considered further in Section D.4 when the errors in the numerical experiments are considered.

To examine the machine time used by the various methods, and the associated accumulated truncation and round-off errors, numerical trials were run using the two-body problem. This problem is chosen since it affords itself of analytical solution whereby the accuracy of the numerical solution may be readily examined. Using a range of values for the eccentricity (e = 0.00, 0.25, 0.50, 0.75, 0.95) we examine the way the solution is affected by the number of step-length changes required. The trial runs were all started at pericentre with the following initial conditions:

$$x = 1-e \quad ; \quad y = 0; \quad \dot{x} = 0; \quad \dot{y} = \left[(1+e)/(1-e)\right]^{\frac{1}{2}} ,$$

where $a = 1$.

Since, we may also set,

$$n^2a^3 = G(m_1 + m_2) = 1$$

we have $T = 2\pi$ in all cases.

Continuing any trial run through an integral number of periods

will result, in the absence of errors, in the values of $x, y, \dot{x}, \dot{y}$ returning to their initial values. Any discrepancy will arise from the accumulation of truncation and round-off errors.

D.4 Machine Time

Figures D.1 and D.2 display, by way of example, data on total machine time (TMT) taken by the TS method to accomplish one trial run for various orders of the TS expansion ($n = 4,6,8,\ldots,24$) and each of the four accuracy criteria. Also included are the data points for the CSS and CMS methods.

One trial run includes:

(a) the accessing of the program which is to be run from the computer "memory"
(b) the input of the required conditions and
(c) the numerical integration through ten orbital periods.

To obtain the machine time required to accomplish only the numerical integration it is necessary to subtract out the time taken for (a) and (b) above - this time was found to be three seconds, to a very high degree of accuracy, in all cases.

The graphs show that, for the TS method, a minimum in machine time occurs for a given $\varepsilon_o = 10^{-i}$ when n, the order of Taylor Series in use, lies in the range i to i + 2. These minima are independent of the eccentricity and arise solely from the trade-off between the required number of integration steps, which decreases as n increases, and the time to evaluate the derivatives at each step, which increases as n increases.

In order to compare the time taken by the TS method against those taken by the CSS and CMS methods, the relative efficiency is defined to be the ratio of the time taken by either the CSS or CMS methods to the time taken by the TS method for any given trial run. The results of this comparison are given in Table D.1. The machine times used are those required to accomplish ten orbits i.e. the observed time for a trial run less the above-mentioned three seconds.

It may be noted that as the accuracy requirement increases, the TS method gains over the CSS method. Whereas, as e is increased the

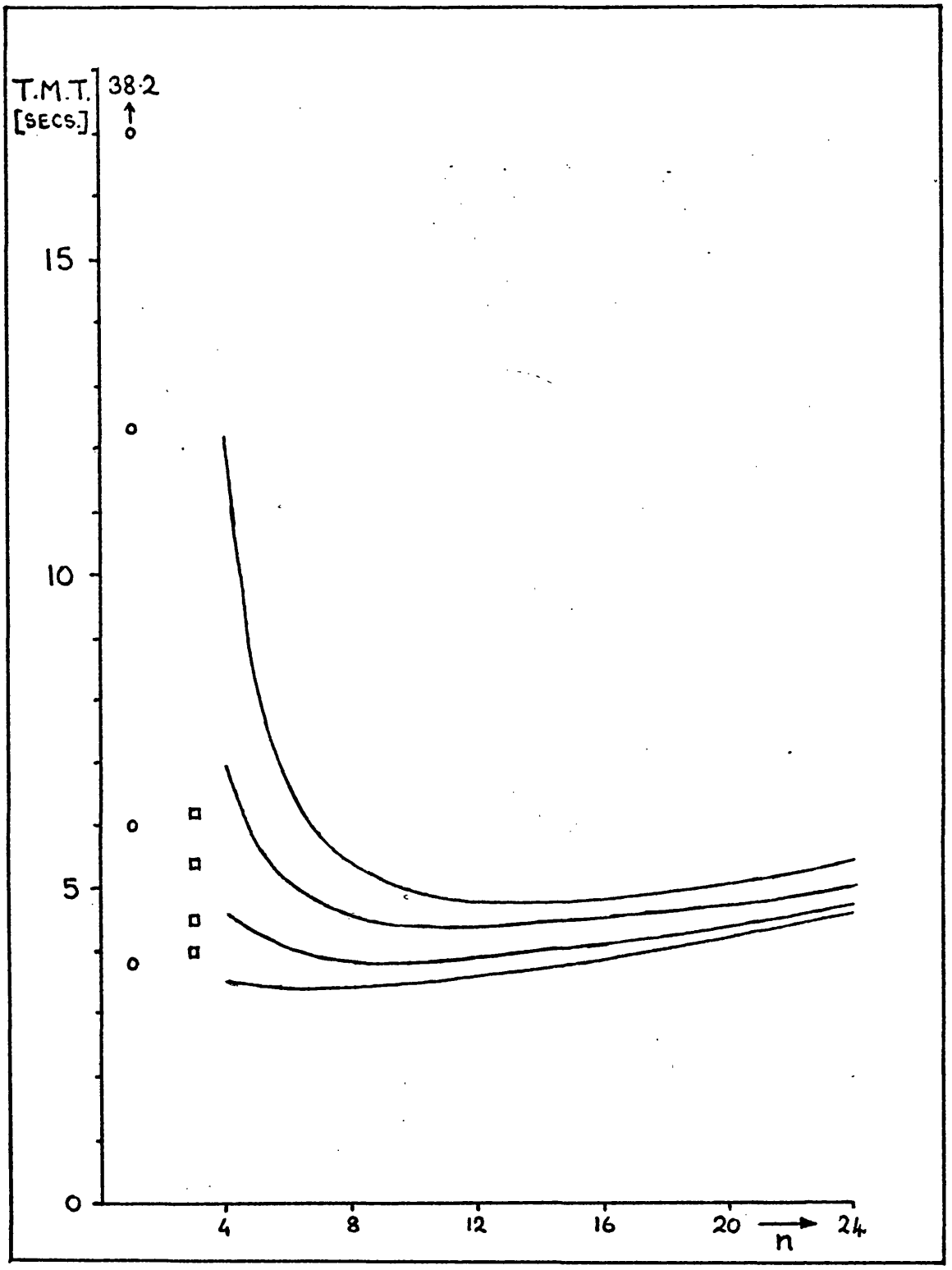

Figure D.1 Graph of total machine time (in seconds) taken by the TS method per trial run for varying n. The orbital eccentricity value is 0.25. The open squares and circles indicate the corresponding data for the CMS and CSS methods respectively. (n.b. For a given method the trial runs will take a longer time to execute as ε_o is decreased from 10^{-6} through 10^{-8} and 10^{-10} to 10^{-12}).

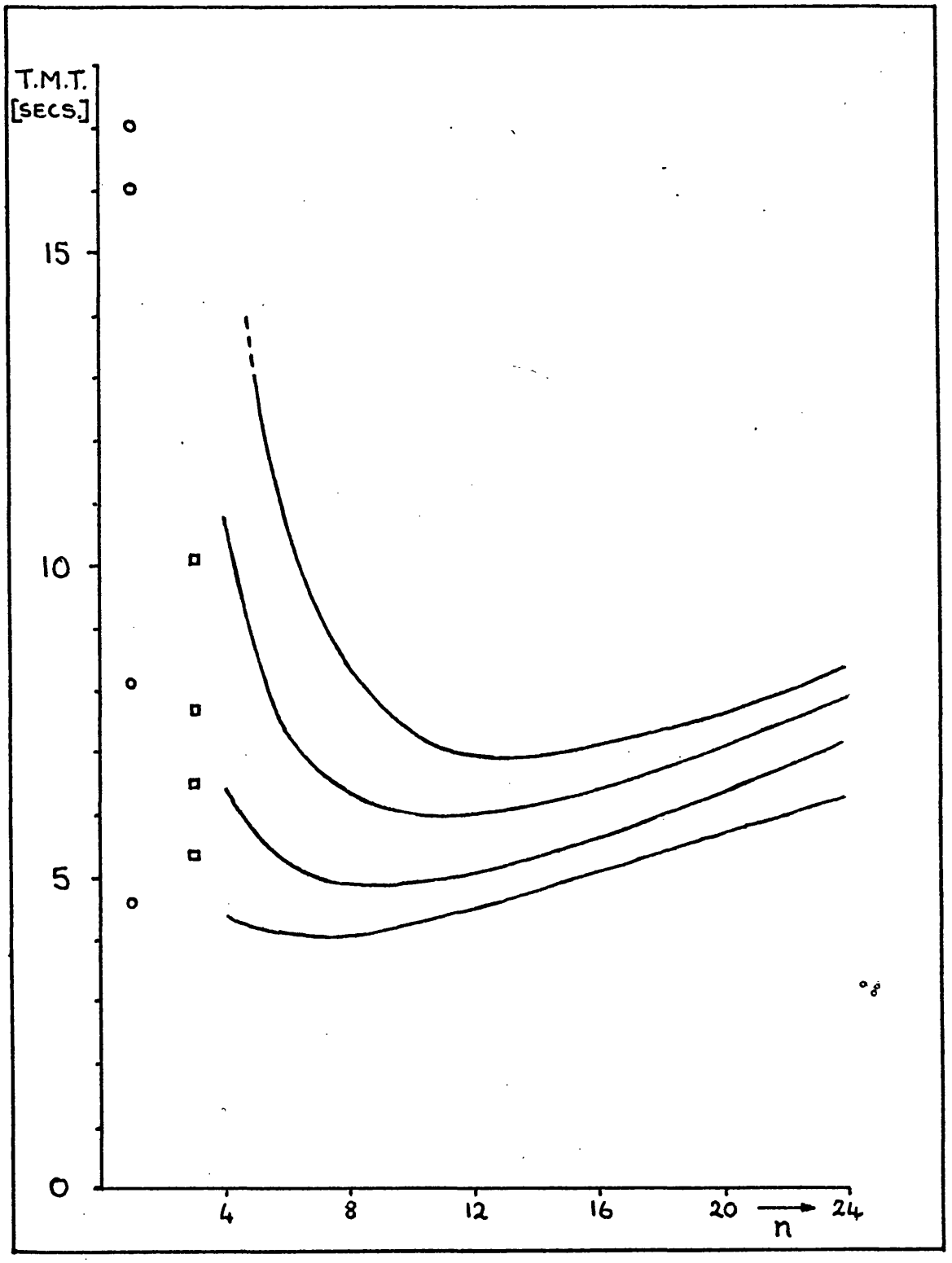

Figure D.2 Graph of total machine time (in seconds) taken by the TS method per trial run for varying n. The orbital eccentricity value is 0.75. The open squares and circles indicate the corresponding data for the CMS and CSS methods respectively. (n.b. For a given method the trial runs will take a longer time to execute as ε_o is decreased from 10^{-6} through 10^{-8} and 10^{-10} to 10^{-12}).

Table D.1 - Relative Efficiencies of CSS, CMS and TS Methods

ε_o	10^{-6}		10^{-8}		10^{-10}		10^{-12}	
Method	CSS	CMS	CSS	CMS	CSS	CMS	CSS	CMS
e = 0.00	2.4	1.1	4.0	1.1	7.2	1.3	21.2	1.9
e = 0.25	2.2	3.1	3.6°	1.9	6.8	1.8	19.6	1.9
e = 0.50	1.7	2.8	3.0	1.9	6.4	1.8	15.3	1.9
e = 0.75	1.5	2.0	2.7	2.0	5.8	1.8	14.3	1.9
e = 0.95	1.4	2.3	2.6	2.0	5.7	1.8	12.2	1.9

advantage of the TS method is decreased. When the CMS method is compared to the TS method it is found that at all e values, except 0.00, the gain in machine time is of the order of a factor of two. The different behaviour at e = 0.00 results from there being few, if any, step-length adjustments round a circular orbit; this will advantage the CMS method in which step-length changes are time consuming. In all cases however the TS method is faster.

D.5 Errors

In all the experiments the initial conditions were such that the two masses were at pericentre. This results in the components x and $\dot{y}$ being initially non-zero whereas $\dot{x}$ and y are both initially zero. The errors presented in Tables D.2 to D.6 below are therefore *relative* for x and $\dot{y}$ and *absolute* for $\dot{x}$ and y.

In no case was an accuracy criterion of less than 10^{-12} imposed on any trial run. This was to avoid the effect of round-off error on the result since the round-off will then generally be several orders of magnitude below the truncation error. The most obvious feature of these tables is the larger size of the errors in the initially zero as opposed to the initially non-zero components: the difference is often as much as three orders of magnitude. This was remarked upon by Roy *et al.* (1972).

Tables D.2 to D.6 show the accumulated errors in the components from an integration run for each of the eccentricity values and each of the accuracy criteria. The TS method was used at the particular value of n giving a minimum in machine time for the specified ε_o i.e. n_{opt}. However, it may be remembered that for an accuracy of 10^{-i} the curve of TMT versus n was approximately "flat" in the range of n from i to i+2. Therefore to *decrease* the accumulated truncation error by *decreasing* the required number of integration steps the order chosen should be the *largest* possible in the flat region i.e. $n_{opt} = i+2$ as a general rule.

For any given ε_o and e values, the errors for the three methods are comparable; although the TS method shows a slight improvement over the other two. This is attributable to the use of relative errors for the control of LTE in the TS method as against absolute

Table D.2 - Errors[+] after 10 orbits for e = 0.00

	ε_o	10^{-6}	10^{-8}	10^{-10}	10^{-12}
Method	Component				
CSS	x	4	0	0	1
	y	261	42	11	91
	$\dot{x}$	261	42	11	91
	$\dot{y}$	2	0	0	0
CMS	x	1	13	1	42
	y	46	542	29	1606
	$\dot{x}$	46	539	29	1605
	$\dot{y}$	1	7	0	22
TS	x	11	9	8	8
	y	466	438	400	361
	$\dot{x}$	466	438	400	361
	$\dot{y}$	4	5	4	4
n_{opt}		8	10	12	14

+Errors are given in units of ε_o. For the initially non-zero components $(x,\dot{y})$ the errors are proportional and for initially zero components $(y,\dot{x})$ the errors are absolute.

Table D.3 – Errors[+] after 10 orbits for e = 0.25

	ε_o	10^{-6}	10^{-8}	10^{-10}	10^{-12}
Method	Component				
CSS	x	5	1	7	6
	y	466	70	416	485
	$\dot{x}$	661	145	603	685
	$\dot{y}$	1	2	3	2
CMS	x	2	11	13	14
	y	709	16	676	791
	$\dot{x}$	987	22	932	1094
	$\dot{y}$	5	9	7	7
TS	x	4	8	6	2
	y	172	289	96	119
	$\dot{x}$	239	398	131	164
	$\dot{y}$	2	6	4	1
n_{opt}		8	10	12	14

+ as Table D.2

Table D.4 - Errors[+] after 10 orbits for e = 0.50

	ε_o	10^{-6}	10^{-8}	10^{-10}	10^{-12}
Method	Component				
CSS	x	5	9	5	7
	y	1258	1209	1065	1527
	$\dot{x}$	2935	2826	2503	3557
	$\dot{y}$	4	3	0	0
CMS	x	19	4	6	17
	y	891	609	1507	1795
	$\dot{x}$	2075	1408	3491	4168
	$\dot{y}$	9	1	1	7
TS	x	9	7	5	3
	y	498	27	275	139
	$\dot{x}$	1149	59	634	324
	$\dot{y}$	6	5	3	2
n_{opt}		8	10	12	14

+ as Table D.2

Table D.5 – Errors[+] after 10 orbits for e = 0.75

	ε_o	10^{-6}	10^{-8}	10^{-10}	10^{-12}
Method	Component				
CSS	x	46	4	3	12
	y	2943	3559	2524	4163
	$\dot{x}$	17830	21567	15296	25209
	$\dot{y}$	38	1	0	4
CMS	x	245	42	38	74
	y	6808	1189	3199	4264
	$\dot{x}$	41202	7179	19370	25827
	$\dot{y}$	197	25	20	39
TS	x	5	2	1	1
	y	342	620	627	713
	$\dot{x}$	2103	3724	3811	4302
	$\dot{y}$	2	1	1	0
n_{opt}		8	10	12	14

+ as Table D.2

Table D.6 - Errors[+] after 10 orbits for e = 0.95

	ε_o	10^{-6}	10^{-8}	10^{-10}	10^{-12}
Method	Component				
CSS	x	54466	546	8	15
	y	23026	22928	6424	50136
	$\dot{x}$	1402360	1468630	411503	3211320
	$\dot{y}$	51774	537	3	5
CMS	x	33750	1438	163	127
	y	18094	34985	39641	57495
	$\dot{x}$	1123360	2240710	2539130	3682690
	$\dot{y}$	32510	1161	57	62
TS	x	1247	156	24	24
	y	3447	11306	4952	8764
	$\dot{x}$	220739	724021	317327	561197
	$\dot{y}$	1204	119	12	12
n_{opt}		8	10	12	14

+ as Table D.2

Table D.7 - Required Number of Integration Steps per Orbit

Eccentricity	Accuracy Criterion (ε_o)			
	10^{-6}	10^{-8}	10^{-10}	10^{-12}
0.00	+12,441,157	14, 53,630	16, 74,2517	18, 81,5033
0.25	18, 84,221	20,102,630	22,160,1954	24,191,6934
0.50	26,125,275	30,161,832	32,212,2417	35,287,8483
0.75	37,167,370	42,223,1051	47,298,3488	51,396,11009
0.95	60,274,560	69,377,1684	76,462,5369	82,666,16843

+ The figures given are as follows: in a row ℓ, m, n, are respectively the number of steps per orbit taken by the TS, CMS, CSS methods

errors in the CSS and CMS methods. All components are generally of order unity or less. When $|\underset{\sim}{r}|$ and $|\dot{\underset{\sim}{r}}|$ always remain of order unity (i.e. a circular orbit) the absolute and relative error tests are essentially the same. However a highly eccentric orbit will result in small $|\underset{\sim}{r}|$ at pericentre and small $|\dot{\underset{\sim}{r}}|$ at apocentre: in these cases the relative error test is the more stringent and would be expected to give smaller accumulated truncation errors. as is indeed the case.

Accumulation of round-off error is dependant upon the required number of integration steps for any given problem. Table D.7 presents data on the approximate number of integration steps for each method. Generally the TS method is found to require fewer integration steps than either the CSS or CMS methods.

D.6 Conclusions

From the results of this Appendix it would appear that the use of an explicit TS method to integrate the differential equations of celestial mechanics can result in substantial savings of machine time while allowing computations of such an accuracy as to be eminently comparable to other methods.

Comparison has been made between the TS method and classical methods available to the author since these were the alternatives which could have been employed. It is noted that the TS method did not give the expected saving of a factor 50 in machine time over the CSS method, but "only" a factor of 20. This may be explained as follows: The Runge-Kutta method of Roy *et al.*(1972) used a halving and doubling method of step adjustment; this was found to be wasteful of time in Appendix C. Hence, since the CSS method used here employed a better step adjustment scheme it is expected that some saving in machine time would appear.

In comparing the TS and CMS methods, it appears that, in general, a factor two in machine time accrues from the use of the TS method. This factor is reduced however in the case of circular orbits which do not require time-expensive step-length changes to be made by the CMS method.

The contrast between the two methods is that, whereas the CSS

method gains on the TS method as e increases the CMS method is best in comparison to the TS method at small e values.

From the above results it may be finally noted that the present TS method offers considerable savings in machine time combined with high accuracy. The large integration step-lengths it allows will result in relatively less accumulation of error (truncation and round-off). It seems that the method, as written for a specific problem, possesses considerable advantages over currently available methods and does not involve the formulation of complex computer programs.

APPENDIX E - Derivation of Expressions for the Force Function in a General Hierarchical Many-Body System in terms of the ρ_{i-j} - The Four-Body and Eight-Body Cases

In Chapter 9, Section 9.4, the expression for $r_{k\ell}^{-1}$ was found to be, correct to the second order in the $\alpha_{k\ell}^{ij}$,

$$r_{k\ell}^{-1} = \frac{1}{\rho_{m-a-1,g_{a+1}(\ell)}} \cdot \Bigg[1 + \sum_{h=0}^{a-1} \Bigg\{ F_{mh\ell}^{2} \left(\alpha^{m-h-1,g_{h+1}(\ell)}_{m-a-1,g_{a+1}(\ell)}\right)^{2} \cdot P_2\left(C^{m-h-1,g_{h+1}(\ell)}_{m-a-1,g_{a+1}(\ell)}\right) + F_{mhk}^{2} \left(\alpha^{m-h-1,g_{h+1}(k)}_{m-a-1,g_{a+1}(k)}\right)^{2} P_2\left(C^{m-h-1,g_{h+1}(k)}_{m-a-1,g_{a+1}(k)}\right) \Bigg\}$$

$$+ \sum_{h=0}^{a-1} \sum_{j=h+1}^{a-1} F_{mh\ell} F_{mj\ell} \alpha^{m-h-1,g_{h+1}(\ell)}_{m-a-1,g_{a+1}(\ell)} \alpha^{m-j-1,g_{j+1}(\ell)}_{m-a-1,g_{a+1}(\ell)} \cdot E^{m-h-1,g_{h+1}(\ell),\ m-j-1,g_{j+1}(\ell)}_{m-a-1,g_{a+1}(\ell),\ m-a-1,g_{a+1}(\ell)}$$

$$+ \sum_{h=0}^{a-1} \sum_{j=h+1}^{a-1} F_{mhk} F_{mjk} \alpha^{m-h-1,g_{h+1}(k)}_{m-a-1,g_{a+1}(k)} \alpha^{m-j-1,g_{j+1}(k)}_{m-a-1,g_{a+1}(k)} \cdot E^{m-h-1,g_{h+1}(k),\ m-j-1,g_{j+1}(k)}_{m-a-1,g_{a+1}(k),\ m-a-1,g_{a+1}(k)}$$

$$- \sum_{h=0}^{a-1} \sum_{j=0}^{a-1} F_{mh\ell} F_{mjk} \alpha^{m-h-1,g_{h+1}(\ell)}_{m-a-1,g_{a+1}(\ell)} \alpha^{m-j-1,g_{j+1}(k)}_{m-a-1,g_{a+1}(k)} \cdot E^{m-h-1,g_{h+1}(\ell),\ m-j-1,g_{j+1}(k)}_{m-a-1,g_{a+1}(\ell),\ m-a-1,g_{a+1}(k)} \Bigg] \qquad (1)$$

where the notation is as described in Chapter 9.

The double summations can be shown not to contribute to the force function by considering any particular case. We will consider the cases where there are four bodies and eight bodies.

To obtain the expressions for each term arising from the double summations a short computer program was written in BASIC for use on the "Commodore PET" computer in the Department of Astronomy at Glasgow University. This program, a listing of which is included towards the end of this Appendix, generates the terms which arise from the double summations.

In the four-body case there are four such terms. These are:

$$-\frac{M_1 M_3}{P_{0,1}} \cdot \frac{M_{2,4}}{M_{1,2}} \cdot \frac{M_{2,2}}{M_{1,1}} \cdot A^{12}_{01} A^{11}_{01} \left[3C^{12}_{01} C^{11}_{01} - C^{12}_{11}\right] \quad (A)$$

$$+\frac{M_1 M_4}{P_{0,1}} \cdot \frac{M_{2,3}}{M_{1,2}} \cdot \frac{M_{2,2}}{M_{1,1}} \cdot A^{12}_{01} A^{11}_{01} \left[3C^{12}_{01} C^{11}_{01} - C^{12}_{11}\right] \quad (B)$$

$$+\frac{M_2 M_3}{P_{0,1}} \cdot \frac{M_{2,4}}{M_{1,2}} \cdot \frac{M_{2,2}}{M_{1,1}} \cdot A^{12}_{01} A^{11}_{01} \left[3C^{12}_{01} C^{11}_{01} - C^{12}_{11}\right] \quad (A)$$

$$-\frac{M_2 M_4}{P_{0,1}} \cdot \frac{M_{2,3}}{M_{1,2}} \cdot \frac{M_{2,2}}{M_{1,1}} \cdot A^{12}_{01} A^{11}_{01} \left[3C^{12}_{01} C^{11}_{01} - C^{12}_{11}\right] \quad (B)$$

The nomenclature may be most easily defined by considering one of the terms: for example the first term, if written in the nomenclature of Chapter 9 would be

$$-\frac{m_1 m_3}{\rho_{01}} \cdot \frac{M_{24}\ M_{22}}{M_{12}\ M_{11}}\ \alpha^{12}_{01}\ \alpha^{11}_{01}\ (3C^{12}_{01}\ C^{11}_{01} - C^{12}_{11}).$$

By noting the sign of each of the four terms above and the fact that $M_{2i} = m_i$ (i=1,2,3,4) in the 4-body case it is seen that the sum of these terms reduces to zero in the pairs denoted A and B. Hence the expression for U, in the four-body case, noting the symmetry of the region of (k,ℓ) summation, is

$$U = G \sum_{k=1}^{4} \sum_{\ell=k+1}^{4} \frac{M_{2k} M_{2\ell}}{\rho_{m-a-1,g_{a+1}(\ell)}} \left[1 + \sum_{h=0}^{a-1} \left[F^2_{mh\ell} \left(\alpha^{m-h-1,g_{h+1}(\ell)}_{m-a-1,g_{a+1}(\ell)} \right)^2 \cdot P_2 \left(C^{m-h-1,g_{h+1}(\ell)}_{m-a-1,g_{a+1}(\ell)} \right) + F^2_{mhk} \left(\alpha^{m-h-1,g_{h+1}(k)}_{m-a-1,g_{a+1}(k)} \right)^2 P_2 \left(C^{m-h-1,g_{h+1}(k)}_{m-a-1,g_{a+1}(k)} \right) \right] \right] \qquad (2)$$

where there is no contribution from a summation when the lower limit is greater than the upper.

Considering the eight-body problem we find 104 terms. These are:

$$-\frac{M_{1,3} M_{3,4} M_{3,2}}{P_{1,1} M_{2,2} M_{2,1}} \cdot A^{22}_{11} \cdot A^{21}_{11} \left[3C^{22}_{11} C^{21}_{11} - C^{22}_{21} \right] \quad (A)$$

$$+\frac{M_{1,4} M_{3,3} M_{3,2}}{P_{1,1} M_{2,2} M_{2,1}} \cdot A^{22}_{11} \cdot A^{21}_{11} \left[3C^{22}_{11} C^{21}_{11} - C^{22}_{21} \right] \quad (A)$$

$$+\frac{M_{1,5} M_{3,6} M_{2,3}}{P_{0,1} M_{2,3} M_{1,2}} \cdot A^{23}_{01} \cdot A^{12}_{01} \left[3C^{23}_{01} C^{12}_{01} - C^{23}_{12} \right] \quad (B)$$

$$+\frac{M_{1,5} M_{3,2} M_{2,1}}{P_{0,1} M_{2,1} M_{1,1}} \cdot A^{21}_{01} \cdot A^{11}_{01} \left[3C^{21}_{01} C^{11}_{01} - C^{21}_{11} \right] \quad (C)$$

$$-\frac{M_{1,5} M_{3,6} M_{3,3}}{P_{0,1} M_{2,3} M_{2,1}} \cdot A^{23}_{01} \cdot A^{21}_{01} \left[3C^{23}_{01} C^{21}_{01} - C^{23}_{21} \right] \quad (D)$$

$$-\frac{M_{1,5} M_{3,6} M_{2,3}}{P_{0,1} M_{2,3} M_{1,1}} \cdot A^{23}_{01} \cdot A^{11}_{01} \left[3C^{23}_{01} C^{11}_{01} - C^{23}_{11} \right] \quad (E)$$

$$-\frac{M_{1,5} M_{2,4} M_{3,2}}{P_{0,1} M_{1,2} M_{2,1}} \cdot A^{12}_{01} \cdot A^{21}_{01} \left[3C^{12}_{01} C^{21}_{01} - C^{12}_{21} \right] \quad (F)$$

```
  M 1 M 5 M 2 , 4  M 2 , 2   12  11      12  11     12
-------------------------. A  .A    [3C  C   - C   ]  (G)
  P 0 , 1 M 1 , 2  M 1 , 1   01  01      01  01     11

  M 1 M 6 M 3 , 5  M 2 , 3   23  12      23  12     23
-------------------------. A  .A    [3C  C   - C   ]  (B)
  P 0 , 1 M 2 , 3  M 1 , 2   01  01      01  01     12

  M 1 M 6 M 3 , 2  M 2 , 1   21  11      21  11     21
+------------------------. A  .A    [3C  C   - C   ]  (C)
  P 0 , 1 M 2 , 1  M 1 , 1   01  01      01  01     11

  M 1 M 6 M 3 , 5  M 3 , 3   23  21      23  21     23
+------------------------. A  .A    [3C  C   - C   ]  (D)
  P 0 , 1 M 2 , 3  M 2 , 1   01  01      01  01     21

  M 1 M 6 M 3 , 5  M 2 , 3   23  11      23  11     23
+------------------------. A  .A    [3C  C   - C   ]  (E)
  P 0 , 1 M 2 , 3  M 1 , 1   01  01      01  01     11

  M 1 M 6 M 2 , 4  M 3 , 2   12  21      12  21     12
-------------------------. A  .A    [3C  C   - C   ]  (F)
  P 0 , 1 M 1 , 2  M 2 , 1   01  01      01  01     21

  M 1 M 6 M 2 , 4  M 2 , 2   12  11      12  11     12
-------------------------. A  .A    [3C  C   - C   ]  (G)
  P 0 , 1 M 1 , 2  M 1 , 1   01  01      01  01     11

  M 1 M 7 M 3 , 8  M 2 , 4   24  12      24  12     24
-------------------------. A  .A    [3C  C   - C   ]  (H)
  P 0 , 1 M 2 , 4  M 1 , 2   01  01      01  01     12

  M 1 M 7 M 3 , 2  M 2 , 1   21  11      21  11     21
+------------------------. A  .A    [3C  C   - C   ]  (C)
  P 0 , 1 M 2 , 1  M 1 , 1   01  01      01  01     11

  M 1 M 7 M 3 , 8  M 3 , 4   24  21      24  21     24
-------------------------. A  .A    [3C  C   - C   ]  (I)
  P 0 , 1 M 2 , 4  M 2 , 1   01  01      01  01     21
```

```
  M 1 M 7 M 3 , 8  M 2 , 4   24  11     24  11     24
-------------------------. A  .A    [3C   C    - C    ]  (J)
  P 0 , 1 M 2 , 4  M 1 , 1   01  01     01  01     11

  M 1 M 7 M 2 , 3  M 3 , 2   12  21     12  21     12
+-------------------------. A  .A    [3C   C    - C    ]  (F)
  P 0 , 1 M 1 , 2  M 2 , 1   01  01     01  01     21

  M 1 M 7 M 2 , 3  M 2 , 2   12  11     12  11     12
+-------------------------. A  .A    [3C   C    - C    ]  (G)
  P 0 , 1 M 1 , 2  M 1 , 1   01  01     01  01     11

  M 1 M 8 M 3 , 7  M 2 , 4   24  12     24  12     24
+-------------------------. A  .A    [3C   C    - C    ]  (H)
  P 0 , 1 M 2 , 4  M 1 , 2   01  01     01  01     12

  M 1 M 8 M 3 , 2  M 2 , 1   21  11     21  11     21
+-------------------------. A  .A    [3C   C    - C    ]  (C)
  P 0 , 1 M 2 , 1  M 1 , 1   01  01     01  01     11

  M 1 M 8 M 3 , 7  M 3 , 4   24  21     24  21     24
+-------------------------. A  .A    [3C   C    - C    ]  (I)
  P 0 , 1 M 2 , 4  M 2 , 1   01  01     01  01     21

  M 1 M 8 M 3 , 7  M 2 , 4   24  11     24  11     24
+-------------------------. A  .A    [3C   C    - C    ]  (J)
  P 0 , 1 M 2 , 4  M 1 , 1   01  01     01  01     11

  M 1 M 8 M 2 , 3  M 3 , 2   12  21     12  21     12
+-------------------------. A  .A    [3C   C    - C    ]  (F)
  P 0 , 1 M 1 , 2  M 2 , 1   01  01     01  01     21

  M 1 M 8 M 2 , 3  M 2 , 2   12  11     12  11     12
+-------------------------. A  .A    [3C   C    - C    ]  (G)
  P 0 , 1 M 1 , 2  M 1 , 1   01  01     01  01     11

  M 2 M 3 M 3 , 4  M 3 , 2   22  21     22  21     22
+-------------------------. A  .A    [3C   C    - C    ]  (A)
  P 1 , 1 M 2 , 2  M 2 , 1   11  11     11  11     21
```

$$-\frac{M_{2}M_{4}}{P_{1,1}}\cdot\frac{M_{3,3}}{M_{2,2}}\cdot\frac{M_{3,2}}{M_{2,1}}\cdot {}^{A}_{11}\,{}^{22\ 21}_{A\ 11}\left[3C^{22}_{11}\ C^{21}_{11}-C^{22}_{21}\right] \quad (A)$$

$$+\frac{M_{2}M_{5}}{P_{0,1}}\cdot\frac{M_{3,6}}{M_{2,3}}\cdot\frac{M_{2,3}}{M_{1,2}}\cdot {}^{A}_{01}\,{}^{23\ 12}_{A\ 01}\left[3C^{23}_{01}\ C^{12}_{01}-C^{23}_{12}\right] \quad (B)$$

$$-\frac{M_{2}M_{5}}{P_{0,1}}\cdot\frac{M_{3,1}}{M_{2,1}}\cdot\frac{M_{2,1}}{M_{1,1}}\cdot {}^{A}_{01}\,{}^{21\ 11}_{A\ 01}\left[3C^{21}_{01}\ C^{11}_{01}-C^{21}_{11}\right] \quad (C)$$

$$+\frac{M_{2}M_{5}}{P_{0,1}}\cdot\frac{M_{3,6}}{M_{2,3}}\cdot\frac{M_{3,3}}{M_{2,1}}\cdot {}^{A}_{01}\,{}^{23\ 21}_{A\ 01}\left[3C^{23}_{01}\ C^{21}_{01}-C^{23}_{21}\right] \quad (D)$$

$$-\frac{M_{2}M_{5}}{P_{0,1}}\cdot\frac{M_{3,6}}{M_{2,3}}\cdot\frac{M_{2,3}}{M_{1,1}}\cdot {}^{A}_{01}\,{}^{23\ 11}_{A\ 01}\left[3C^{23}_{01}\ C^{11}_{01}-C^{23}_{11}\right] \quad (E)$$

$$+\frac{M_{2}M_{5}}{P_{0,1}}\cdot\frac{M_{2,4}}{M_{1,2}}\cdot\frac{M_{3,2}}{M_{2,1}}\cdot {}^{A}_{01}\,{}^{12\ 21}_{A\ 01}\left[3C^{12}_{01}\ C^{21}_{01}-C^{12}_{21}\right] \quad (F)$$

$$-\frac{M_{2}M_{5}}{P_{0,1}}\cdot\frac{M_{2,4}}{M_{1,2}}\cdot\frac{M_{2,2}}{M_{1,1}}\cdot {}^{A}_{01}\,{}^{12\ 11}_{A\ 01}\left[3C^{12}_{01}\ C^{11}_{01}-C^{12}_{11}\right] \quad (G)$$

$$-\frac{M_{2}M_{6}}{P_{0,1}}\cdot\frac{M_{3,5}}{M_{2,3}}\cdot\frac{M_{2,3}}{M_{1,2}}\cdot {}^{A}_{01}\,{}^{23\ 12}_{A\ 01}\left[3C^{23}_{01}\ C^{12}_{01}-C^{23}_{12}\right] \quad (B)$$

$$-\frac{M_{2}M_{6}}{P_{0,1}}\cdot\frac{M_{3,1}}{M_{2,1}}\cdot\frac{M_{2,1}}{M_{1,1}}\cdot {}^{A}_{01}\,{}^{21\ 11}_{A\ 01}\left[3C^{21}_{01}\ C^{11}_{01}-C^{21}_{11}\right] \quad (C)$$

$$-\frac{M_{2}M_{6}}{P_{0,1}}\cdot\frac{M_{3,5}}{M_{2,3}}\cdot\frac{M_{3,3}}{M_{2,1}}\cdot {}^{A}_{01}\,{}^{23\ 21}_{A\ 01}\left[3C^{23}_{01}\ C^{21}_{01}-C^{23}_{21}\right] \quad (D)$$

```
  M 2 M 6 M 3 , 5  M 2 , 3   23  11     23  11     23
+-------.-------.--------. A  .A    [3C  C   - C    ]  (E)
  P 0 , 1 M 2 , 3  M 1 , 1   01  01     01  01     11

  M 2 M 6 M 2 , 4  M 3 , 2   12  21     12  21     12
+-------.-------.--------. A  .A    [3C  C   - C    ]  (F)
  P 0 , 1 M 1 , 2  M 2 , 1   01  01     01  01     21

  M 2 M 6 M 2 , 4  M 2 , 2   12  11     12  11     12
-------.-------.--------. A  .A    [3C  C   - C    ]  (G)
  P 0 , 1 M 1 , 2  M 1 , 1   01  01     01  01     11

  M 2 M 7 M 3 , 8  M 2 , 4   24  12     24  12     24
-------.-------.--------. A  .A    [3C  C   - C    ]  (H)
  P 0 , 1 M 2 , 4  M 1 , 2   01  01     01  01     12

  M 2 M 7 M 3 , 1  M 2 , 1   21  11     21  11     21
-------.-------.--------. A  .A    [3C  C   - C    ]  (C)
  P 0 , 1 M 2 , 1  M 1 , 1   01  01     01  01     11

  M 2 M 7 M 3 , 8  M 3 , 4   24  21     24  21     24
+-------.-------.--------. A  .A    [3C  C   - C    ]  (I)
  P 0 , 1 M 2 , 4  M 2 , 1   01  01     01  01     21

  M 2 M 7 M 3 , 8  M 2 , 4   24  11     24  11     24
-------.-------.--------. A  .A    [3C  C   - C    ]  (J)
  P 0 , 1 M 2 , 4  M 1 , 1   01  01     01  01     11  %

  M 2 M 7 M 2 , 3  M 3 , 2   12  21     12  21     12
-------.-------.--------. A  .A    [3C  C   - C    ]  (F)
  P 0 , 1 M 1 , 2  M 2 , 1   01  01     01  01     21

  M 2 M 7 M 2 , 3  M 2 , 2   12  11     12  11     12
+-------.-------.--------. A  .A    [3C  C   - C    ]  (G)
  P 0 , 1 M 1 , 2  M 1 , 1   01  01     01  01     11

  M 2 M 8 M 3 , 7  M 2 , 4   24  12     24  12     24
+-------.-------.--------. A  .A    [3C  C   - C    ]  (H)
  P 0 , 1 M 2 , 4  M 1 , 2   01  01     01  01     12
```

$$-\frac{M_{2,1}\,M_{8,1}\,M_{3,1}}{P_{0,1}\,M_{2,1}\,M_{1,1}}\cdot A_{01}\,A_{01}\,[3C_{01}\,C_{01}-C_{11}]_{21}\,[3C_{11}\,C_{11}-C_{21}]_{11}\quad(C)$$

$$-\frac{M_{2,1}\,M_{8,4}\,M_{3,7}}{P_{0,1}\,M_{2,4}\,M_{2,1}}\cdot A_{01}\,A_{01}\,[3C_{01}\,C_{01}-C_{21}]_{24}\,[3C_{21}\,C_{21}-C_{24}]_{21}\quad(I)$$

$$+\frac{M_{2,1}\,M_{8,4}\,M_{3,7}}{P_{0,1}\,M_{2,4}\,M_{1,1}}\cdot A_{01}\,A_{01}\,[3C_{01}\,C_{01}-C_{11}]_{24}\,[3C_{11}\,C_{11}-C_{24}]_{11}\quad(J)$$

$$-\frac{M_{2,1}\,M_{8,3}\,M_{2,3}}{P_{0,1}\,M_{1,2}\,M_{2,1}}\cdot A_{01}\,A_{01}\,[3C_{01}\,C_{01}-C_{21}]_{12}\,[3C_{21}\,C_{21}-C_{12}]_{21}\quad(F)$$

$$+\frac{M_{2,1}\,M_{8,3}\,M_{2,2}}{P_{0,1}\,M_{1,2}\,M_{1,1}}\cdot A_{01}\,A_{01}\,[3C_{01}\,C_{01}-C_{11}]_{12}\,[3C_{11}\,C_{11}-C_{12}]_{11}\quad(G)$$

$$+\frac{M_{3,1}\,M_{5,3}\,M_{3,6}}{P_{0,1}\,M_{2,3}\,M_{1,2}}\cdot A_{01}\,A_{01}\,[3C_{01}\,C_{01}-C_{12}]_{23}\,[3C_{12}\,C_{12}-C_{23}]_{12}\quad(B)$$

$$-\frac{M_{3,1}\,M_{5,2}\,M_{3,4}}{P_{0,1}\,M_{2,2}\,M_{1,1}}\cdot A_{01}\,A_{01}\,[3C_{01}\,C_{01}-C_{11}]_{22}\,[3C_{11}\,C_{11}-C_{22}]_{11}\quad(K)$$

$$-\frac{M_{3,1}\,M_{5,3}\,M_{3,6}}{P_{0,1}\,M_{2,3}\,M_{2,2}}\cdot A_{01}\,A_{01}\,[3C_{01}\,C_{01}-C_{22}]_{23}\,[3C_{22}\,C_{22}-C_{23}]_{22}\quad(L)$$

$$+\frac{M_{3,1}\,M_{5,3}\,M_{3,6}}{P_{0,1}\,M_{2,3}\,M_{1,1}}\cdot A_{01}\,A_{01}\,[3C_{01}\,C_{01}-C_{11}]_{23}\,[3C_{11}\,C_{11}-C_{23}]_{11}\quad(E)$$

$$-\frac{M_{3,1}\,M_{5,4}\,M_{3,2}}{P_{0,1}\,M_{1,2}\,M_{2,2}}\cdot A_{01}\,A_{01}\,[3C_{01}\,C_{01}-C_{22}]_{12}\,[3C_{22}\,C_{22}-C_{12}]_{22}\quad(M)$$

```
  M 3 M 5 M 2 , 4  M 2 , 2   12  11     12  11     12
+-------.-------.-------. A  .A    [3C  .  C   - C   ]  (G)
  P 0 , 1 M 1 , 2  M 1 , 1   01  01     01  01     11

  M 3 M 6 M 3 , 5  M 2 , 3   23  12     23  12     23
-------.-------.-------. A  .A    [3C   C   - C   ]  (B)
  P 0 , 1 M 2 , 3  M 1 , 2   01  01     01  01     12

  M 3 M 6 M 3 , 4  M 2 , 2   22  11     22  11     22
-------.-------.-------. A  .A    [3C   C   - C   ]  (K)
  P 0 , 1 M 2 , 2  M 1 , 1   01  01     01  01     11

  M 3 M 6 M 3 , 5  M 3 , 3   23  22     23  22     23
+-------.-------.-------. A  .A    [3C   C   - C   ]  (L)
  P 0 , 1 M 2 , 3  M 2 , 2   01  01     01  01     22

  M 3 M 6 M 3 , 5  M 2 , 3   23  11     23  11     23
-------.-------.-------. A  .A    [3C   C   - C   ]  (E)
  P 0 , 1 M 2 , 3  M 1 , 1   01  01     01  01     11

  M 3 M 6 M 2 , 4  M 3 , 2   12  22     12  22     12
-------.-------.-------. A  .A    [3C   C   - C   ]  (M)
  P 0 , 1 M 1 , 2  M 2 , 2   01  01     01  01     22

  M 3 M 6 M 2 , 4  M 2 , 2   12  11     12  11     12
+-------.-------.-------. A  .A    [3C   C   - C   ]  (G)
  P 0 , 1 M 1 , 2  M 1 , 1   01  01     01  01     11

  M 3 M 7 M 3 , 8  M 2 , 4   24  12     24  12     24
-------.-------.-------. A  .A    [3C   C   - C   ]  (H)
  P 0 , 1 M 2 , 4  M 1 , 2   01  01     01  01     12

  M 3 M 7 M 3 , 4  M 2 , 2   22  11     22  11     22
-------.-------.-------. A  .A    [3C   C   - C   ]  (K)
  P 0 , 1 M 2 , 2  M 1 , 1   01  01     01  01     11

  M 3 M 7 M 3 , 8  M 3 , 4   24  22     24  22     24
-------.-------.-------. A  .A    [3C   C   - C   ]  (N)
  P 0 , 1 M 2 , 4  M 2 , 2   01  01     01  01     22
```

```
  M 3 M 7 M 3 , 8  M 2 , 4   24  11     24  11     24
+-------.-------.-------. A  .A    [3C   C    - C    ]  (J)
  P 0 , 1 M 2 , 4  M 1 , 1   01  01     01  01     11

  M 3 M 7 M 2 , 3  M 3 , 2   12  22     12  22     12
+-------.-------.-------. A  .A    [3C   C    - C    ]  (M)
  P 0 , 1 M 1 , 2  M 2 , 2   01  01     01  01     22

  M 3 M 7 M 2 , 3  M 2 , 2   12  11     12  11     12
-------.-------.-------. A  .A    [3C   C    - C    ]  (G)
  P 0 , 1 M 1 , 2  M 1 , 1   01  01     01  01     11

  M 3 M 8 M 3 , 7  M 2 , 4   24  12     24  12     24
+-------.-------.-------. A  .A    [3C   C    - C    ]  (H)
  P 0 , 1 M 2 , 4  M 1 , 2   01  01     01  01     12

  M 3 M 8 M 3 , 4  M 2 , 2   22  11     22  11     22
-------.-------.-------. A  .A    [3C   C    - C    ]  (K)
  P 0 , 1 M 2 , 2  M 1 , 1   01  01     01  01     11

  M 3 M 8 M 3 , 7  M 3 , 4   24  22     24  22     24
+-------.-------.-------. A  .A    [3C   C    - C    ]  (N)
  P 0 , 1 M 2 , 4  M 2 , 2   01  01     01  01     22

  M 3 M 8 M 3 , 7  M 2 , 4   24  11     24  11     24
-------.-------.-------. A  .A    [3C   C    - C    ]  (J)
  P 0 , 1 M 2 , 4  M 1 , 1   01  01     01  01     11

  M 3 M 8 M 2 , 3  M 3 , 2   12  22     12  22     12
+-------.-------.-------. A  .A    [3C   C    - C    ]  (M)
  P 0 , 1 M 1 , 2  M 2 , 2   01  01     01  01     22

  M 3 M 8 M 2 , 3  M 2 , 2   12  11     12  11     12
-------.-------.-------. A  .A    [3C   C    - C    ]  (G)
  P 0 , 1 M 1 , 2  M 1 , 1   01  01     01  01     11

  M 4 M 5 M 3 , 6  M 2 , 3   23  12     23  12     23
+-------.-------.-------. A  .A    [3C   C    - C    ]  (B)
  P 0 , 1 M 2 , 3  M 1 , 2   01  01     01  01     12
```

```
  M 4 M 5 M 3 , 3  M 2 , 2   22  11     22  11     22
+———————.———————.———————. A  .A    [3C  C   - C    ]  (K)
  P 0 , 1 M 2 , 2  M 1 , 1   01  01     01  01     11

  M 4 M 5 M 3 , 6  M 3 , 3   23  22     23  22     23
+———————.———————.———————. A  .A    [3C  C   - C    ]  (L)
  P 0 , 1 M 2 , 3  M 2 , 2   01  01     01  01     22

  M 4 M 5 M 3 , 6  M 2 , 3   23  11     23  11     23
+———————.———————.———————. A  .A    [3C  C   - C    ]  (E)
  P 0 , 1 M 2 , 3  M 1 , 1   01  01     01  01     11

  M 4 M 5 M 2 , 4  M 3 , 2   12  22     12  22     12
+———————.———————.———————. A  .A    [3C  C   - C    ]  (M)
  P 0 , 1 M 1 , 2  M 2 , 2   01  01     01  01     22

  M 4 M 5 M 2 , 4  M 2 , 2   12  11     12  11     12
+———————.———————.———————. A  .A    [3C  C   - C    ]  (G)
  P 0 , 1 M 1 , 2  M 1 , 1   01  01     01  01     11

  M 4 M 6 M 3 , 5  M 2 , 3   23  12     23  12     23
-———————.———————.———————. A  .A    [3C  C   - C    ]  (B)
  P 0 , 1 M 2 , 3  M 1 , 2   01  01     01  01     12

  M 4 M 6 M 3 , 3  M 2 , 2   22  11     22  11     22
+———————.———————.———————. A  .A    [3C  C   - C    ]  (K)
  P 0 , 1 M 2 , 2  M 1 , 1   01  01     01  01     11

  M 4 M 6 M 3 , 5  M 3 , 3   23  22     23  22     23
-———————.———————.———————. A  .A    [3C  C   - C    ]  (L)
  P 0 , 1 M 2 , 3  M 2 , 2   01  01     01  01     22

  M 4 M 6 M 3 , 5  M 2 , 3   23  11     23  11     23
-———————.———————.———————. A  .A    [3C  C   - C    ]  (E)
  P 0 , 1 M 2 , 3  M 1 , 1   01  01     01  01     11

  M 4 M 6 M 2 , 4  M 3 , 2   12  22     12  22     12
+———————.———————.———————. A  .A    [3C  C   - C    ]  (M)
  P 0 , 1 M 1 , 2  M 2 , 2   01  01     01  01     22
```

```
  M 4 M 6 M 2 , 4  M 2 , 2   12  11     12  11     12
+.-------.-------.-------. A  .A    [3C  C   - C    ]  (G)
  P 0 , 1 M 1 , 2  M 1 , 1   01  01     01  01     11

  M 4 M 7 M 3 , 8  M 2 , 4   24  12     24  12     24
-.-------.-------.-------. A  .A    [3C  C   - C    ]  (H)
  P 0 , 1 M 2 , 4  M 1 , 2   01  01     01  01     12

  M 4 M 7 M 3 , 3  M 2 , 2   22  11     22  11     22
+.-------.-------.-------. A  .A    [3C  C   - C    ]  (K)
  P 0 , 1 M 2 , 2  M 1 , 1   01  01     01  01     11

  M 4 M 7 M 3 , 8  M 3 , 4   24  22     24  22     24
+.-------.-------.-------. A  .A    [3C  C   - C    ]  (N)
  P 0 , 1 M 2 , 4  M 2 , 2   01  01     01  01     22

  M 4 M 7 M 3 , 8  M 2 , 4   24  11     24  11     24
+.-------.-------.-------. A  .A    [3C  C   - C    ]  (J)
  P 0 , 1 M 2 , 4  M 1 , 1   01  01     01  01     11

  M 4 M 7 M 2 , 3  M 3 , 2   12  22     12  22     12
-.-------.-------.-------. A  .A    [3C  C   - C    ]  (M)
  P 0 , 1 M 1 , 2  M 2 , 2   01  01     01  01     22

  M 4 M 7 M 2 , 3  M 2 , 2   12  11     12  11     12
-.-------.-------.-------. A  .A    [3C  C   - C    ]  (G)
  P 0 , 1 M 1 , 2  M 1 , 1   01  01     01  01     11  °ℯ

  M 4 M 8 M 3 , 7  M 2 , 4   24  12     24  12     24
+.-------.-------.-------. A  .A    [3C  C   - C    ]  (H)
  P 0 , 1 M 2 , 4  M 1 , 2   01  01     01  01     12

  M 4 M 8 M 3 , 3  M 2 , 2   22  11     22  11     22
+.-------.-------.-------. A  .A    [3C  C   - C    ]  (K)
  P 0 , 1 M 2 , 2  M 1 , 1   01  01     01  01     11

  M 4 M 8 M 3 , 7  M 3 , 4   24  22     24  22     24
-.-------.-------.-------. A  .A    [3C  C   - C    ]  (N)
  P 0 , 1 M 2 , 4  M 2 , 2   01  01     01  01     22
```

$$-\frac{M\,4\;M\,8\;M\,3\,,\,7\;M\,2\,,\,4}{P\;0\,,\,1\;M\,2\,,\,4\;M\,1\,,\,1}\;A^{24\;11}_{01\;01}\;[3C^{24\;11}_{01\;01}-C^{24}_{11}]\quad(J)$$

$$-\frac{M\,4\;M\,8\;M\,2\,,\,3\;M\,3\,,\,2}{P\;0\,,\,1\;M\,1\,,\,2\;M\,2\,,\,2}\;A^{12\;22}_{01\;01}\;[3C^{12\;22}_{01\;01}-C^{12}_{22}]\quad(M)$$

$$-\frac{M\,4\;M\,8\;M\,2\,,\,3\;M\,2\,,\,2}{P\;0\,,\,1\;M\,1\,,\,2\;M\,1\,,\,1}\;A^{12\;11}_{01\;01}\;[3C^{12\;11}_{01\;01}-C^{12}_{11}]\quad(G)$$

$$-\frac{M\,5\;M\,7\;M\,3\,,\,8\;M\,3\,,\,4}{P\;1\,,\,2\;M\,2\,,\,4\;M\,2\,,\,3}\;A^{24\;23}_{12\;12}\;[3C^{24\;23}_{12\;12}-C^{24}_{23}]\quad(O)$$

$$+\frac{M\,5\;M\,8\;M\,3\,,\,7\;M\,3\,,\,4}{P\;1\,,\,2\;M\,2\,,\,4\;M\,2\,,\,3}\;A^{24\;23}_{12\;12}\;[3C^{24\;23}_{12\;12}-C^{24}_{23}]\quad(O)$$

$$+\frac{M\,6\;M\,7\;M\,3\,,\,8\;M\,3\,,\,4}{P\;1\,,\,2\;M\,2\,,\,4\;M\,2\,,\,3}\;A^{24\;23}_{12\;12}\;[3C^{24\;23}_{12\;12}-C^{24}_{23}]\quad(O)$$

$$-\frac{M\,6\;M\,8\;M\,3\,,\,7\;M\,3\,,\,4}{P\;1\,,\,2\;M\,2\,,\,4\;M\,2\,,\,3}\;A^{24\;23}_{12\;12}\;[3C^{24\;23}_{12\;12}-C^{24}_{23}]\quad(O)$$

The terms above arising in the eight-body problem are again each denoted by a letter i.e. $A \to O$. Terms which are labelled with the same letter are factored by the same $\alpha^{ij}_{pq}\;\alpha^{k\ell}_{rs}\;(3\,C^{ij}_{pq}\,C^{k\ell}_{rs} - C^{ij}_{k\ell})$ terms.

By examination of the mass factors in front the terms denoted by the same letter it is readily found that the sum of all the above terms is zero: the terms reducing to zero in their groups denoted (A), (B), etc. as follows:

Group A:

$$(A) = \frac{1}{\rho_{11}} \cdot \frac{M_{32}}{M_{21}\ M_{22}} \{(m_1 - m_2)(-m_3 M_{34} + m_4 M_{33}) \}$$

On noting that $M_{33} = m_3$ and $M_{34} = m_4$ this is clearly zero.

Group B:

$$(B) = \frac{1}{\rho_{01}} \cdot \frac{1}{M_{12}} \cdot \{ (m_1 + m_2 + m_3 + m_4)(m_5 M_{36} - m_6 M_{35}) \} = 0$$

since $M_{35} = m_5$ and $M_{36} = m_6$.

Group C:

$$(C) = \frac{1}{\rho_{01}} \cdot \frac{1}{M_{11}} \{ (m_5 + m_6 + m_7 + m_8)(m_1 M_{32} - m_2 M_{31}) \} = 0$$

since $M_{31} = m_1$ and $M_{32} = m_2$.

Group D:

$$(D) = \frac{1}{\rho_{01}} \cdot \frac{M_{33}}{M_{23}\ M_{21}} \cdot \{ (m_1 - m_2)(-m_5 M_{36} + m_6 M_{35}) \} = 0$$

since $M_{35} = m_5$ and $M_{36} = m_6$.

Group E:

$$(E) = \frac{1}{\rho_{01}} \cdot \frac{1}{M_{11}} \cdot \{(m_3 + m_4 - m_1 - m_2)(m_5 M_{36} - m_6 M_{35}) \} = 0$$

(as Group B).

Group F:

$$(F) = \frac{1}{\rho_{01}} \cdot \frac{M_{32}}{M_{12}\ M_{21}} \{(m_1 - m_2) \cdot [-(m_5 + m_6)M_{24} + (m_7 + m_8)M_{23}] \}$$

which on noting that $M_{23} = m_5 + m_6$ and $M_{24} = m_7 + m_8$ is zero.

Group G:

$$(G) = \frac{1}{\rho_{01}} \cdot \frac{M_{22}}{M_{12}\, M_{11}} \{ (m_1 + m_2 - m_3 - m_4) \cdot [(m_7 + m_8)M_{23} - (m_5 + m_6)M_{24}] \} = 0$$

(as Group F).

Group H:

$$(H) = \frac{1}{\rho_{01}} \cdot \frac{1}{M_{12}} \{ (m_1 + m_2 + m_3 + m_4)(m_8 M_{37} - m_7 M_{38}) \} = 0$$

since $M_{37} = m_7$ and $M_{38} = m_8$.

Group I:

$$(I) = \frac{1}{\rho_{01}} \cdot \frac{M_{34}}{M_{24}\, M_{21}} \{ (m_1 - m_2)(m_8 M_{37} - m_7 M_{38}) \} = 0$$

(as Group H).

Group J:

$$(J) = \frac{1}{\rho_{01}} \cdot \frac{1}{M_{11}} \cdot \{ (m_1 + m_2 - m_3 - m_4)(m_8 M_{37} - m_7 M_{38}) \} = 0$$

(as Group H).

Group K:

$$(K) = \frac{1}{\rho_{01}} \cdot \frac{1}{M_{11}} \{ (m_5 + m_6 + m_7 + m_8)(m_4 M_{33} - m_3 M_{34}) \} = 0$$

(as Group A).

Group L:

$$(L) = \frac{1}{\rho_{01}} \frac{M_{33}}{M_{23}\, M_{22}} \{ (m_3 - m_4)(m_6 M_{35} - m_5 M_{36}) \} = 0$$

(as Group B).

Group M:

$$(M) = \frac{1}{\rho_{01}} \cdot \frac{M_{32}}{M_{12} M_{22}} \cdot \{ (m_3 - m_4) [(m_7 + m_8)M_{23} - (m_5 + m_6)M_{24}] \} = 0$$

(as Group F).

Group N:

$$(N) = \frac{1}{\rho_{01}} \cdot \frac{M_{34}}{M_{24}\, M_{22}} \{(m_3 - m_4)(m_8 M_{37} - m_7 M_{38})\} = 0$$

(as Group H).

Group O:

$$(O) = \frac{1}{\rho_{12}} \cdot \frac{M_{34}}{M_{24}\, M_{23}} \{(m_5 - m_6)(m_8 M_{37} - m_7 M_{38})\} = 0$$

(as Group H).

Another interesting feature of how the terms cancel can also be seen. If we consider the terms marked (A) we observe that they are similar to the 4-body case dealt with previously. In other words, the sum of these terms taken over the 4-body subset, consisting of $m_1 m_2 m_3 m_4$, is zero. A similar situation arises if we consider the four-body subset $m_5 m_6 m_7 m_8$. The terms arising from these masses are denoted (O) and are seen to cancel among themselves. If we let $[\Sigma\Sigma]$ denote the double summations of Equation (1) then the contribution to the force function from these terms, in the 8-body case, is U_2 where

$$U_2 = \tfrac{1}{2} G \sum_{k=1}^{8} \sum_{\ell=1}^{8} \frac{M_{3k}\, M_{3\ell}}{\rho_{m-a-1, g_{a+1}(\ell)}} \cdot \left(\left[\Sigma\ \Sigma \right] \right). \qquad (3)$$

Now we may separate out the two 4-body subsystems as follows

$$U_2 = \tfrac{1}{2} G \sum_{k=1}^{4} \sum_{\ell=1}^{4} \frac{M_{3k}\, M_{3\ell}}{\rho_{m-a-1, g_{a+1}(\ell)}} \left(\left[\Sigma\ \Sigma \right] \right) + \tfrac{1}{2} G \sum_{k=1}^{4} \sum_{\ell=5}^{8}$$

$$\frac{M_{3k}\, M_{3\ell}}{\rho_{m-a-1, g_{a+1}(\ell)}} \left(\left[\Sigma\ \Sigma \right] \right) + \tfrac{1}{2} G \sum_{k=5}^{8} \sum_{\ell=1}^{4} \frac{M_{3k}\, M_{3\ell}}{\rho_{m-a-1, g_{a+1}(\ell)}} \cdot$$

$$\left(\left[\Sigma\ \Sigma \right] \right) + \tfrac{1}{2} G \sum_{k=5}^{8} \sum_{\ell=5}^{8} \frac{M_{3k}\, M_{3\ell}}{\rho_{m-a-1, g_{a+1}(\ell)}} \cdot \left(\left[\Sigma\ \Sigma \right] \right). \qquad (4)$$

The first term in U_2 is merely the sum of terms arising from the 4-body subsystem $m_1m_2m_3m_4$ with the fourth term being the sum of terms arising from the $m_5m_6m_7m_8$ subsystem. These are both zero by considering the 4-body case. U_2 may then be rewritten, since k and ℓ are dummy suffices,

$$U_2 = G \sum_{k=1}^{4} \sum_{\ell=5}^{8} \frac{M_{3k}\, M_{3\ell}}{\rho_{m-a-1,g_{a+1}(\ell)}} \cdot \left(\left[\Sigma \; \Sigma \right] \right) . \qquad (5)$$

This result is general since an n-body system, where $n=2^m$, can clearly be divided into two systems of 2^{m-1} bodies each. These two subsystems can then be divided into four 2^{m-2} body subsets, etc.

The expression for U, in the eight-body case, may simply be written as,

$$U = G \sum_{k=1}^{8} \sum_{\ell=k+1}^{8} \frac{M_{3k}\, M_{3\ell}}{\rho_{m-a-1,g_{a+1}(\ell)}} \cdot \left[1 + \sum_{h=0}^{a-1} \left(F^2_{mh\ell}(\alpha^{m-h-1,g_{h+1}(\ell)}_{m-a-1,g_{a+1}(\ell)})^2 \cdot \right.\right.$$

$$\left.\left. \cdot P_2(C^{m-h-1,g_{h+1}(\ell)}_{m-a-1,g_{a+1}(\ell)}) + F^2_{mhk}\,(\alpha^{m-h-1,g_{h+1}(k)}_{m-a-1,g_{a+1}(k)})^2 P_2(C^{m-h-1,g_{h+1}(k)}_{m-a-1,g_{a+1}(k)}) \right) \right] \qquad (6)$$

where there is no contribution from a summation when the lower limit is greater than the upper. In Appendix F the terms arising from Equations (2) and (6) are derived explicitly and the equations of motion for the four-body and eight-body cases are formed, correct to the second order in the $\alpha^{ij}_{k\ell}$.

```
4 PRINT"□"
5 INPUT"▒▒▒M▒▒▒";M:N=2↑M
6 OPEN5,4
7 PRINT#5," THE NUMBER OF BODIES=2↑"M:PRINT#5:PRINT#5
10 FORK=1TON
20 K1=K+1
30 IF K1>N THEN GOTO985
40 FOR L=K1TON
50 KK=K:LL=L
60 GOSUB1000
65 XX=M-A-1
69 A1=A-1
70 FORJ=0TOA1
75 A2=J+1
76 IF A2>A1 THEN GOTO 345
80 FORH=A2TOA1
90 IF A1<0 THEN GOTO 345
100 IF J=H THEN GOTO 330
110 G0=L
120 FORII=0TOJ
130 IF II=0 THEN GOTO 150
140 G0=INT((G0+1)/2)
150 NEXTII
160 G1=INT((G0+1)/2)
170 F0=G0-(-1)↑G0
180 XA=M-J
190 YA=M-J-1
200 CA=(-1)↑G0
```

```
210 G2=L
220 FORII=0TOH
230 IF II=0 THEN GOTO 250
240 G2=INT((G2+1)/2)
250 NEXTII
260 G3=INT((G2+1)/2)
270 F2=G2-(-1)↑G2
280 XB=M-H
290 YB=M-H-1
300 CB=(-1)↑G2
309 A$="+"
310 IF CA*CB<0 THEN A$="-"
315 NO=A+10*L+100*L+1000*H+10000*J+100000*M
316 Q1=(M-J-1)*10+G1:Q2=(M-H-1)*10+G3:Q3=(M-A-1)*10+GA:Q4=(M-A-1)*10+GA
317 IFK<10ANDL<10THEN GOTO 318:GOTO320
318 PRINT#5,"  M"K"M"L"M"XA","F0" M"XB","G1" "Q1""Q2"   "Q1""Q2"  "Q1
319 GOTO324
320 IFK>10ANDL>10 THEN GOTO 321:GOTO323
321 PRINT#5,"M"K"M"L"M"XA","F0" M"XB","G1" "Q1""Q2"   "Q1""Q2"  "Q1
322 GOTO324
323 PRINT#5," M"K"M"L"M"XA","F0" M"XB",G1" "Q1""Q2"   "Q1""Q2"  "Q1
324 PRINT#5,A$"————————.————————.————————. A  .A    [3C   C   - C  / ]"
325 IF Q3<10 THEN GOTO 328
326 PRINT#5,"  P"XX","GA"M"YA","G1" M"YB","G3" "Q3""Q4"   "Q3""Q4"  "Q2
327 GOTO329
328 PRINT#5,"  P"XX","GA"M"YA","G1" M"YB","G3"  01  01""     01  01   "Q2
329 PRINT#5:PRINT#5
330 NEXTH
340 NEXTJ
345 GOSUB 2000
350 FOR J=0TOA1
360 FOR H=0TOA1
370 IF A1<0 THEN GOTO 970
390 G0=L
```

```
400 FOR II=0TOJ
405 IF II=0 THEN GOTO 420
410 G0=INT((G0+1)/2)
420 NEXTII
430 G1=INT((G0+1)/2)
440 F0=G0-(-1)↑G0
450 XA=M-J
460 YA=M-J-1
470 CA=(-1)↑G0
480 G2=K
490 FORII=0TOH
495 IF II=0 THEN GOTO 510
500 G2=INT((G2+1)/2)
510 NEXTII
520 G3=INT((G2+1)/2)
530 F2=G2-(-1)↑G2
540 XB=M-H
550 YB=M-H-1
560 CB=(-1)↑G2
570 A$="-"
580 IF CA*CB<0 THEN A$="+"
590 NO=A+10*L+100*K+1000*H+10000*J+100000*M
591 Q1=(M-J-1)*10+G1:Q2=(M-H-1)*10+G3:Q3=(M-A-1)*10+GA:Q4=(M-A-1)*10+GA
592 IFK<10ANDL<10THEN GOTO593:GOTO 595
593 PRINT#5,"  M"K"M"L"M"XA","F0" M"XB","G1" "Q1""Q2"   "Q1""Q2"  "Q1
594 GOTO599
595 IFK>10ANDL>10THEN GOTO 596:GOTO 598
596 PRINT#5,"M"K"M"L"M"XA","F0" M"XB","G1" "Q1""Q2"   "Q1""Q2"  "Q1
597 GOTO 599
598 PRINT#5," M"K"M"L"M"XA","F0" M"XB","G1" "Q1""Q2"   Q1""Q2"  "Q1
599 PRINT#5,A$"————————.————————.————————. A  .A    [3C   C   - C   ]"
620 IF Q3<10 THEN GOTO 623
621 PRINT#5,"  P"XX","GA"M""YA","G1" M"YB","G3" "Q3""Q4"   "Q3""Q4"  "Q2
622 GOTO 629
```

```
623 PRINT#5,"  P"XX","GA"M"YA","G1" M"YB","G3"  01  01""     01  01   "Q2
629 PRINT#5:PRINT#5
630 NEXTH
640 NEXTJ
970 NEXTL
980 NEXTK
985 CLOSE5
990 END
1000 GA=KK
1010 GB=LL
1020 TT=0
1030 TT=TT+1
1040 GA=INT((GA+1)/2)
1050 GB=INT((GB+1)/2)
1060 IF GA=GB THEN GOTO 1080
1070 GOTO1030
1080 A=TT-1
1090 RETURN
2000 REM K LOOP
2070 FORJ=0TOA1
2075 A2=J+1
2076 IF A2>A1 THEN GOTO 2345
2080 FORH=A2TOA1
2090 IF A1<0 THEN GOTO 2345
2100 IF J=H THEN GOTO 2330
2110 G0=K
2120 FORII=0TOJ
2130 IF II=0 THEN GOTO 2150
2140 G0=INT((G0+1)/2)
2150 NEXTII
2160 G1=INT((G0+1)/2)
2170 F0=G0-(-1)↑G0
2180 XA=M-J
2190 YA=M-J-1
```

```
2200 CA=(-1)↑G0
2210 G2=K
2220 FORII=0TOH
2230 IF II=0 THEN GOTO 2250
2240 G2=INT((G2+1)/2)
2250 NEXTII
2260 G3=INT((G2+1)/2)
2270 F2=G2-(-1)↑G2
2280 XB=M-H
2290 YB=M-H-1
2300 CB=(-1)↑G2
2309 A$="+"
2310 IF CA*CB<0 THEN A$="-"
2315 NO=A+10*L+100*L+1000*H+10000*J+100000*M
2316 Q1=(M-J-1)*10+G1:Q2=(M-H-1)*10+G3:Q3=(M-A-1)*10+GA:Q4=(M-A-1)*10+GA
2317 IFK<10ANDL<10THEN GOTO2318:GOTO2320
2318 PRINT#5,"  M"K"M"L"M"XA","F0" M"XB","G1" "Q1""Q2"   "Q1""Q2"  "Q1
2319 GOTO2324
2320 IFK>10ANDL>10THENGOTO2321:GOTO2323
2321 PRINT#5,"M"K"M"L"M"XA","F0" M"XB","G1" "Q1""Q2"   "Q1""Q2"  "Q1
2322 GOTO2324
2323 PRINT#5," M"K"M"L"M"XA","F0" M"XB",G1" "Q1""Q2"   "Q1""Q2"  "Q1
2324 PRINT#5,A$"————————.————————.————————. A  .A    [3C   C   - C   ]"
2325 IF Q3<10 THEN GOTO2328
2326 PRINT#5,"  P"XX","GA"M"YA","G1" M"YB","G3" "Q3""Q4"   "Q3""Q4"  "Q2
2327 GOTO2329
2328 PRINT#5,"  P"XX","GA"M"YA","G1" M"YB","G3"  01  01""     01  01   "Q2
2329 PRINT#5:PRINT#5
2330 NEXTH
2340 NEXTJ
2345 RETURN
```

APPENDIX F - Derivation of the Equations of Motion and Generalised ε Parameters for General Hierarchical Systems - The Four-Body and Eight-Body Cases

The expression for the force function, taking into account the symmetry of the region of (k,ℓ) summation, is

$$U = G \sum_{k=1}^{n} \sum_{\ell=k+1}^{n} \frac{M_{mk}\, M_{m\ell}}{\rho_{m-a-1,g_{a+1}(\ell)}} \cdot \left[1 + \sum_{h=0}^{a-1} \left\{ F^2_{mh\ell} \left(\alpha_{m-a-1,g_{a+1}(\ell)}\right)^2 \cdot P_2\left(C^{\,m-h-1,g_{h+1}(\ell)}_{m-a-1,g_{a+1}(\ell)}\right) + F^2_{mhk} \left(\alpha_{m-a-1,g_{a+1}(k)}\right)^2 P_2\left(C^{\,m-h-1,g_{h+1}(k)}_{m-a-1,g_{a+1}(k)}\right) \right\} \right] \qquad (1)$$

for the case n=4 and n=8. This expression was used, in a similar way to that of Appendix E, to set up a computer program in BASIC to calculate the terms arising from the triple summation. The program was run on the "Commodore PET" computer in the Department of Astronomy at Glasgow University. The program is included at the end of this Appendix.

In the four-body case eight terms arise from the triple summation. These are:

$$\frac{M_1 M_3 \left[M_{2,4} \right]^2 \left[{}^{12}A \right] \cdot \left[P\left(C^{12}_{01}\right) \right]}{P_{0,1} \left[M_{1,2} \right]} \qquad (A)$$

$$\frac{M_1 M_3 \left[M_{2,2} \right]^2 \left[{}^{11}A \right] \cdot \left[P\left(C^{11}_{01}\right) \right]}{P_{0,1} \left[M_{1,1} \right]} \qquad (B)$$

$$\frac{M_1 M_4 \left[M_{2,3} \right]^2 \left[{}^{12}A \right] \cdot \left[P\left(C^{12}_{01}\right) \right]}{P_{0,1} \left[M_{1,2} \right]} \qquad (A)$$

$$\frac{M_1 M_4 \left[M_{2,2} \right]^2 \left[{}^{11}A \right] \cdot \left[P\left(C^{11}_{01}\right) \right]}{P_{0,1} \left[M_{1,1} \right]} \qquad (B)$$

$$\frac{M_2 M_3}{P_{0,1}}\left[-\frac{M_{2,4}}{M_{1,2}}\right]_2 \cdot \left[A_{01}\right]_2 \cdot \left[P_2\left(C_{01}^{12}\right)\right] \qquad (A)$$

$$\frac{M_2 M_3}{P_{0,1}}\left[+\frac{M_{2,1}}{M_{1,1}}\right]_2 \cdot \left[A_{01}\right]_2 \cdot \left[P_2\left(C_{01}^{11}\right)\right] \qquad (B)$$

$$\frac{M_2 M_4}{P_{0,1}}\left[+\frac{M_{2,3}}{M_{1,2}}\right]_2 \cdot \left[A_{01}\right]_2 \cdot \left[P_2\left(C_{01}^{12}\right)\right] \qquad (A)$$

$$\frac{M_2 M_4}{P_{0,1}}\left[+\frac{M_{2,1}}{M_{1,1}}\right]_2 \cdot \left[A_{01}\right]_2 \cdot \left[P_2\left(C_{01}^{11}\right)\right] \qquad (B)$$

The notation in the above is explained by considering the first term by way of example. In the notation of Chapter 9 this is:

$$\frac{m_1 m_3}{\rho_{01}} \cdot \left[\frac{M_{24}}{M_{12}}\right]^2 \cdot \left(\alpha_{01}^{12}\right)^2 P_2\left(C_{01}^{12}\right) .$$

Thus, gathering terms together and including those arising from the double summation of Equation (1) , U is determined, correct to the second order in the $\alpha_{k\ell}^{ij}$ ratios, viz.

$$U = G\left[\frac{M_{21} M_{22}}{\rho_{11}} + \frac{M_{23} M_{24}}{\rho_{12}} + \frac{M_{11} M_{12}}{\rho_{01}}\left\{1 + \frac{M_{21} M_{22}}{M_{11}^2}\left(\alpha_{01}^{11}\right)^2 P_2\left(C_{01}^{11}\right) + \frac{M_{23} M_{24}}{M_{12}^2}\left(\alpha_{01}^{12}\right)^2 P_2\left(C_{01}^{12}\right)\right\}\right] \cdot \qquad (2)$$

Remembering that the $\underset{\sim}{\rho}_{ij}$ are all independent, the equations of motion may be formed as in Chapter 9 [Equations (9.58 a-c) and (9.59 a-d)].

Proceeding to the eight-body case the number of terms arising from the triple summation increases to 80 viz.

```
M 1 M 3 ┌  M 3 , 4 ┐2 ┌ 22 ┐2 ┌   22 ┐
────────.|-────────|.|A   |.|P (C  ) |   (A)
P 1 , 1 └  M 2 , 2 ┘  └ 11 ┘  └ 2  11 ┘

M 1 M 3 ┌  M 3 , 2 ┐2 ┌ 21 ┐2 ┌   21 ┐
────────.|-────────|.|A   |.|P (C  ) |   (B)
P 1 , 1 └  M 2 , 1 ┘  └ 11 ┘  └ 2  11 ┘

M 1 M 4 ┌  M 3 , 3 ┐2 ┌ 22 ┐2 ┌   22 ┐
────────.|+────────|.|A   |.|P (C  ) |   (A)
P 1 , 1 └  M 2 , 2 ┘  └ 11 ┘  └ 2  11 ┘

M 1 M 4 ┌  M 3 , 2 ┐2 ┌ 21 ┐2 ┌   21 ┐
────────.|-────────|.|A   |.|P (C  ) |   (B)
P 1 , 1 └  M 2 , 1 ┘  └ 11 ┘  └ 2  11 ┘

M 1 M 5 ┌  M 3 , 6 ┐2 ┌ 23 ┐2 ┌   23 ┐
────────.|-────────|.|A   |.|P (C  ) |   (C)
P 0 , 1 └  M 2 , 3 ┘  └ 01 ┘  └ 2  01 ┘

M 1 M 5 ┌  M 3 , 2 ┐2 ┌ 21 ┐2 ┌   21 ┐
────────.|-────────|.|A   |.|P (C  ) |   (D)
P 0 , 1 └  M 2 , 1 ┘  └ 01 ┘  └ 2  01 ┘

M 1 M 5 ┌  M 2 , 4 ┐2 ┌ 12 ┐2 ┌   12 ┐
────────.|-────────|.|A   |.|P (C  ) |   (E)
P 0 , 1 └  M 1 , 2 ┘  └ 01 ┘  └ 2  01 ┘

M 1 M 5 ┌  M 2 , 2 ┐2 ┌ 11 ┐2 ┌   11 ┐
────────.|-────────|.|A   |.|P (C  ) |   (F)
P 0 , 1 └  M 1 , 1 ┘  └ 01 ┘  └ 2  01 ┘

M 1 M 6 ┌  M 3 , 5 ┐2 ┌ 23 ┐2 ┌   23 ┐
────────.|+────────|.|A   |.|P (C  ) |   (C)
P 0 , 1 └  M 2 , 3 ┘  └ 01 ┘  └ 2  01 ┘

M 1 M 6 ┌  M 3 , 2 ┐2 ┌ 21 ┐2 ┌   21 ┐
────────.|-────────|.|A   |.|P (C  ) |   (D)
P 0 , 1 └  M 2 , 1 ┘  └ 01 ┘  └ 2  01 ┘
```

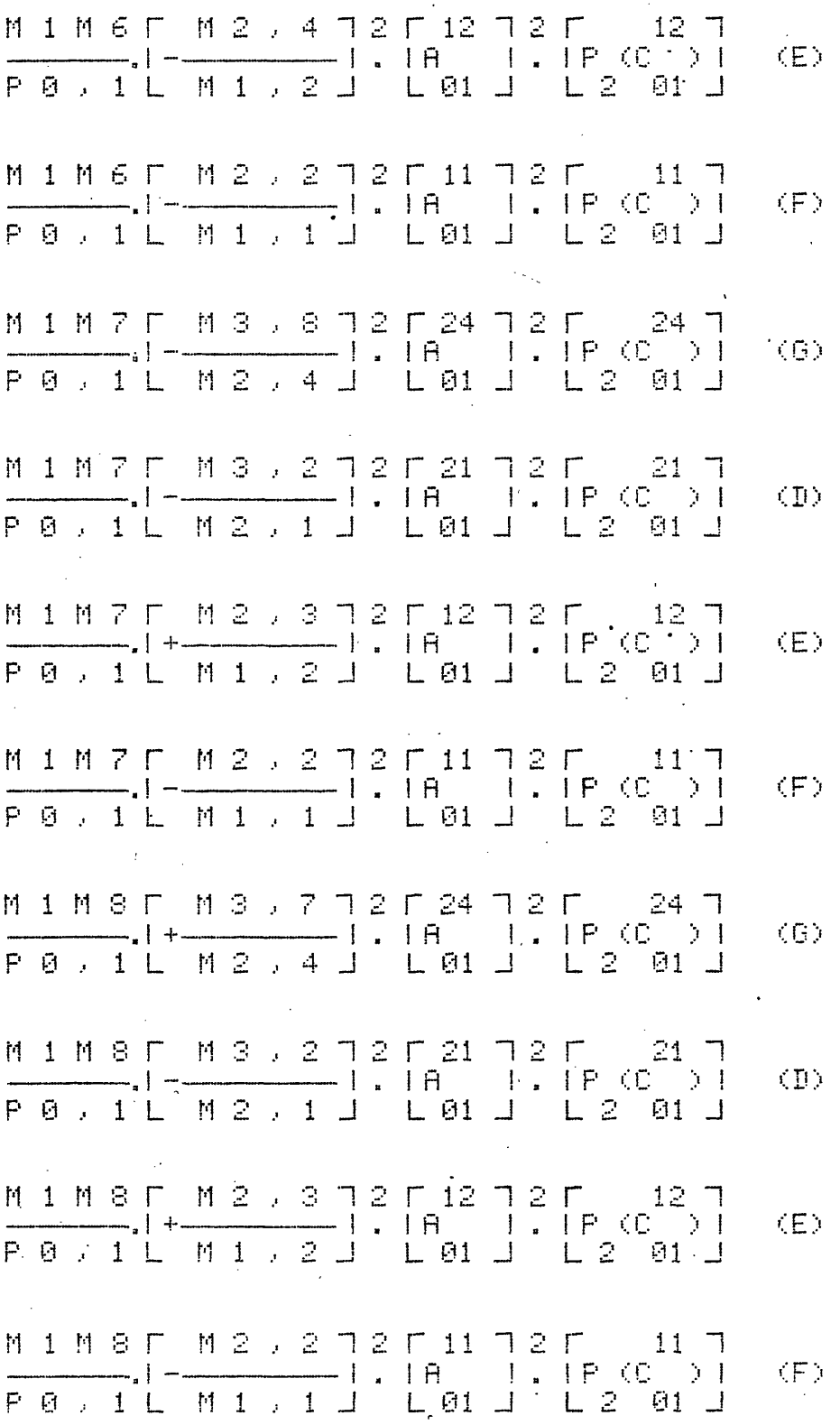
M 1 M 6 M 2 , 4 2 12 2 12
P 0 , 1 M 1 , 2 01 2 01
(E)
M 1 M 6 M 2 , 2 2 11 2 11
P 0 , 1 M 1 , 1 01 2 01
(F)
M 1 M 7 M 3 , 8 2 24 2 24
P 0 , 1 M 2 , 4 01 2 01
(G)
M 1 M 7 M 3 , 2 2 21 2 21
P 0 , 1 M 2 , 1 01 2 01
(D)
M 1 M 7 M 2 , 3 2 12 2 12
P 0 , 1 M 1 , 2 01 2 01
(E)
M 1 M 7 M 2 , 2 2 11 2 11
P 0 , 1 M 1 , 1 01 2 01
(F)
M 1 M 8 M 3 , 7 2 24 2 24
P 0 , 1 M 2 , 4 01 2 01
(G)
M 1 M 8 M 3 , 2 2 21 2 21
P 0 , 1 M 2 , 1 01 2 01
(D)
M 1 M 8 M 2 , 3 2 12 2 12
P 0 , 1 M 1 , 2 01 2 01
(E)
M 1 M 8 M 2 , 2 2 11 2 11
P 0 , 1 M 1 , 1 01 2 01
(F)

```
M 2 M 3 ┌ M 3 , 4 ┐2 ┌ 22 ┐2 ┌   22 ┐
────────.|-────────|.|A   |.|P (C  ) |   (A)
P 1 , 1 └ M 2 , 2 ┘  └ 11 ┘  └ 2  11 ┘

M 2 M 3 ┌ M 3 , 1 ┐2 ┌ 21 ┐2 ┌   21 ┐
────────.|+────────|.|A   |.|P (C  ) |   (B)
P 1 , 1 └ M 2 , 1 ┘  └ 11 ┘  └ 2  11 ┘

M 2 M 4 ┌ M 3 , 3 ┐2 ┌ 22 ┐2 ┌   22 ┐
────────.|+────────|.|A   |.|P (C  ) |   (A)
P 1 , 1 └ M 2 , 2 ┘  └ 11 ┘  └ 2  11 ┘

M 2 M 4 ┌ M 3 , 1 ┐2 ┌ 21 ┐2 ┌   21 ┐
────────.|+────────|.|A   |.|P (C  ) |   (B)
P 1 , 1 └ M 2 , 1 ┘  └ 11 ┘  └ 2  11 ┘

M 2 M 5 ┌ M 3 , 6 ┐2 ┌ 23 ┐2 ┌   23 ┐
────────.|-────────|.|A   |.|P (C  ) |   (C)
P 0 , 1 └ M 2 , 3 ┘  └ 01 ┘  └ 2  01 ┘

M 2 M 5 ┌ M 3 , 1 ┐2 ┌ 21 ┐2 ┌   21 ┐
────────.|+────────|.|A   |.|P (C  ) |   (D)
P 0 , 1 └ M 2 , 1 ┘  └ 01 ┘  └ 2  01 ┘

M 2 M 5 ┌ M 2 , 4 ┐2 ┌ 12 ┐2 ┌   12 ┐
────────.|-────────|.|A   |.|P (C  ) |   (E)
P 0 , 1 └ M 1 , 2 ┘  └ 01 ┘  └ 2  01 ┘

M 2 M 5 ┌ M 2 , 2 ┐2 ┌ 11 ┐2 ┌   11 ┐
────────.|-────────|.|A   |.|P (C  ) |   (F)
P 0 , 1 └ M 1 , 1 ┘  └ 01 ┘  └ 2  01 ┘

M 2 M 6 ┌ M 3 , 5 ┐2 ┌ 23 ┐2 ┌   23 ┐
────────.|+────────|.|A   |.|P (C  ) |   (C)
P 0 , 1 └ M 2 , 3 ┘  └ 01 ┘  └ 2  01 ┘

M 2 M 6 ┌ M 3 , 1 ┐2 ┌ 21 ┐2 ┌   21 ┐
────────.|+────────|.|A   |.|P (C  ) |   (D)
P 0 , 1 └ M 2 , 1 ┘  └ 01 ┘  └ 2  01 ┘
```


M 2 M 6 M 2 , 4 2 12 2 12
P 0 , 1 M 1 , 2 01 2 01
(E)
M 2 M 6 M 2 , 2 2 11 2 11
P 0 , 1 M 1 , 1 01 2 01
(F)
M 2 M 7 M 3 , 8 2 24 2 24
P 0 , 1 M 2 , 4 01 2 01
(G)
M 2 M 7 M 3 , 1 2 21 2 21
P 0 , 1 M 2 , 1 01 2 01
(D)
M 2 M 7 M 2 , 3 2 12 2 12
P 0 , 1 M 1 , 2 01 2 01
(E)
M 2 M 7 M 2 , 2 2 11 2 11
P 0 , 1 M 1 , 1 01 2 01
(F)
M 2 M 8 M 3 , 7 2 24 2 24
P 0 , 1 M 2 , 4 01 2 01
(G)
M 2 M 8 M 3 , 1 2 21 2 21
P 0 , 1 M 2 , 1 01 2 01
(D)
M 2 M 8 M 2 , 3 2 12 2 12
P 0 , 1 M 1 , 2 01 2 01
(E)
M 2 M 8 M 2 , 2 2 11 2 11
P 0 , 1 M 1 , 1 01 2 01
(F)

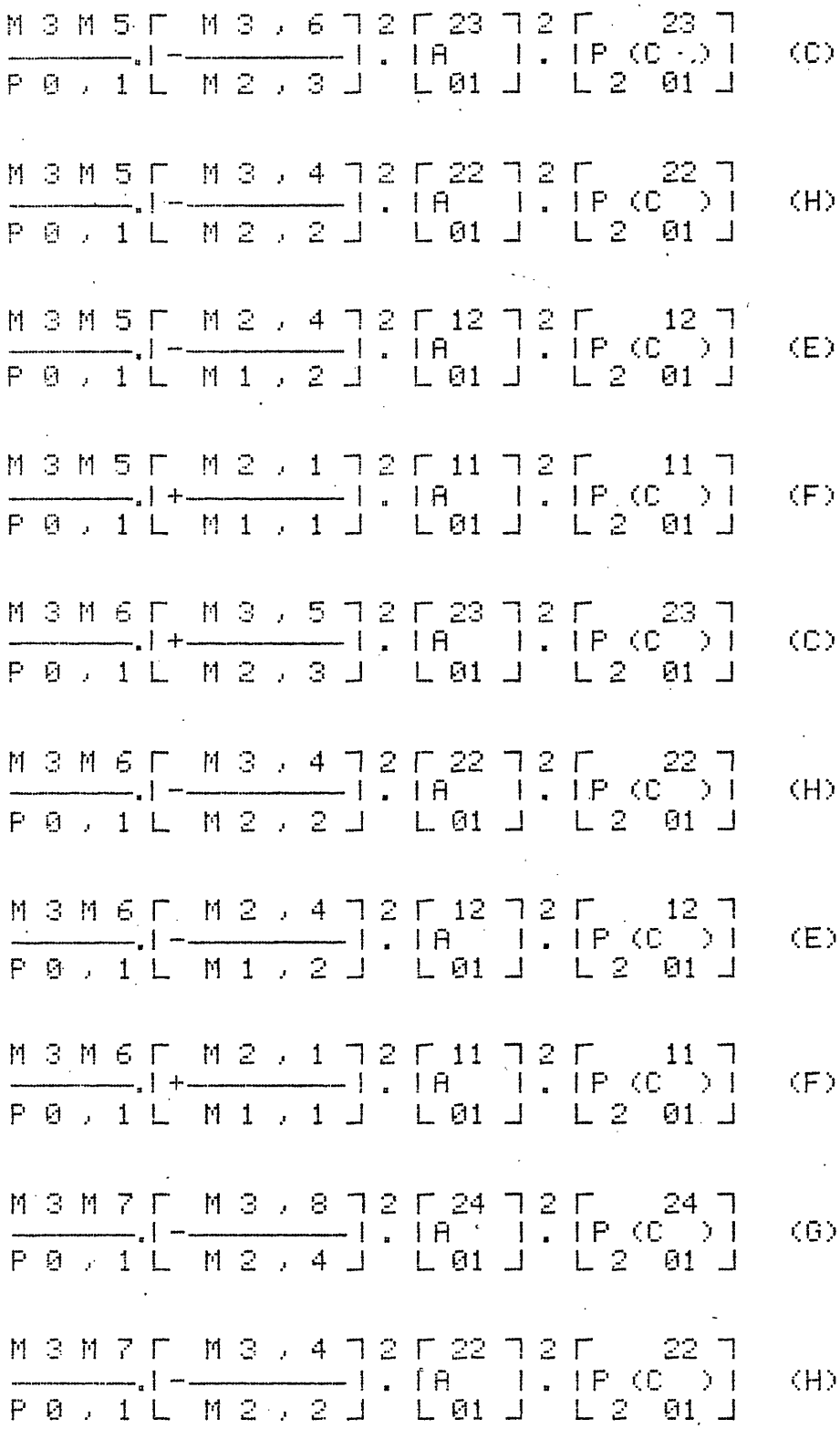
M 3 M 5 [M 3 , 6] 2 [23] 2 [23] (C)
P 0 , 1 [M 2 , 3] [01] [2 01]
M 3 M 5 [M 3 , 4] 2 [22] 2 [22] (H)
P 0 , 1 [M 2 , 2] [01] [2 01]
M 3 M 5 [M 2 , 4] 2 [12] 2 [12] (E)
P 0 , 1 [M 1 , 2] [01] [2 01]
M 3 M 5 [M 2 , 1] 2 [11] 2 [11] (F)
P 0 , 1 [M 1 , 1] [01] [2 01]
M 3 M 6 [M 3 , 5] 2 [23] 2 [23] (C)
P 0 , 1 [M 2 , 3] [01] [2 01]
M 3 M 6 [M 3 , 4] 2 [22] 2 [22] (H)
P 0 , 1 [M 2 , 2] [01] [2 01]
M 3 M 6 [M 2 , 4] 2 [12] 2 [12] (E)
P 0 , 1 [M 1 , 2] [01] [2 01]
M 3 M 6 [M 2 , 1] 2 [11] 2 [11] (F)
P 0 , 1 [M 1 , 1] [01] [2 01]
M 3 M 7 [M 3 , 8] 2 [24] 2 [24] (G)
P 0 , 1 [M 2 , 4] [01] [2 01]
M 3 M 7 [M 3 , 4] 2 [22] 2 [22] (H)
P 0 , 1 [M 2 , 2] [01] [2 01]

```
M 3 M 7 ┌  M 2 , 3 ┐ 2 ┌ 12 ┐ 2 ┌   12 ┐
────────.| +────────| . |A   | . |P (C  ) |   (E)
P 0 , 1 └  M 1 , 2 ┘   └ 01 ┘   └ 2  01 ┘

M 3 M 7 ┌  M 2 , 1 ┐ 2 ┌ 11 ┐ 2 ┌   11 ┐
────────.| +────────| . |A   | . |P (C  ) |   (F)
P 0 , 1 └  M 1 , 1 ┘   └ 01 ┘   └ 2  01 ┘

M 3 M 8 ┌  M 3 , 7 ┐ 2 ┌ 24 ┐ 2 ┌   24 ┐
────────.| +────────| . |A   | . |P (C  ) |   (G)
P 0 , 1 └  M 2 , 4 ┘   └ 01 ┘   └ 2  01 ┘

M 3 M 8 ┌  M 3 , 4 ┐ 2 ┌ 22 ┐ 2 ┌   22 ┐
────────.| -────────| . |A   | . |P (C  ) |   (H)
P 0 , 1 └  M 2 , 2 ┘   └ 01 ┘   └ 2  01 ┘

M 3 M 8 ┌  M 2 , 3 ┐ 2 ┌ 12 ┐ 2 ┌   12 ┐
────────.| +────────| . |A   | . |P (C  ) |   (E)
P 0 , 1 └  M 1 , 2 ┘   └ 01 ┘   └ 2  01 ┘

M 3 M 8 ┌  M 2 , 1 ┐ 2 ┌ 11 ┐ 2 ┌   11 ┐
────────.| +────────| . |A   | . |P (C  ) |   (F)
P 0 , 1 └  M 1 , 1 ┘   └ 01 ┘   └ 2  01 ┘

M 4 M 5 ┌  M 3 , 6 ┐ 2 ┌ 23 ┐ 2 ┌   23 ┐
────────.| -────────| . |A   | . |P (C  ) |   (C)
P 0 , 1 └  M 2 , 3 ┘   └ 01 ┘   └ 2  01 ┘

M 4 M 5 ┌  M 3 , 3 ┐ 2 ┌ 22 ┐ 2 ┌   22 ┐
────────.| +────────| . |A   | . |P (C  ) |   (H)
P 0 , 1 └  M 2 , 2 ┘   └ 01 ┘   └ 2  01 ┘

M 4 M 5 ┌  M 2 , 4 ┐ 2 ┌ 12 ┐ 2 ┌   12 ┐
────────.| -────────| . |A   | . |P (C  ) |   (E)
P 0 , 1 └  M 1 , 2 ┘   └ 01 ┘   └ 2  01 ┘

M 4 M 5 ┌  M 2 , 1 ┐ 2 ┌ 11 ┐ 2 ┌   11 ┐
────────.| +────────| . |A   | . |P (C  ) |   (F)
P 0 , 1 └  M 1 , 1 ┘   └ 01 ┘   └ 2  01 ┘
```

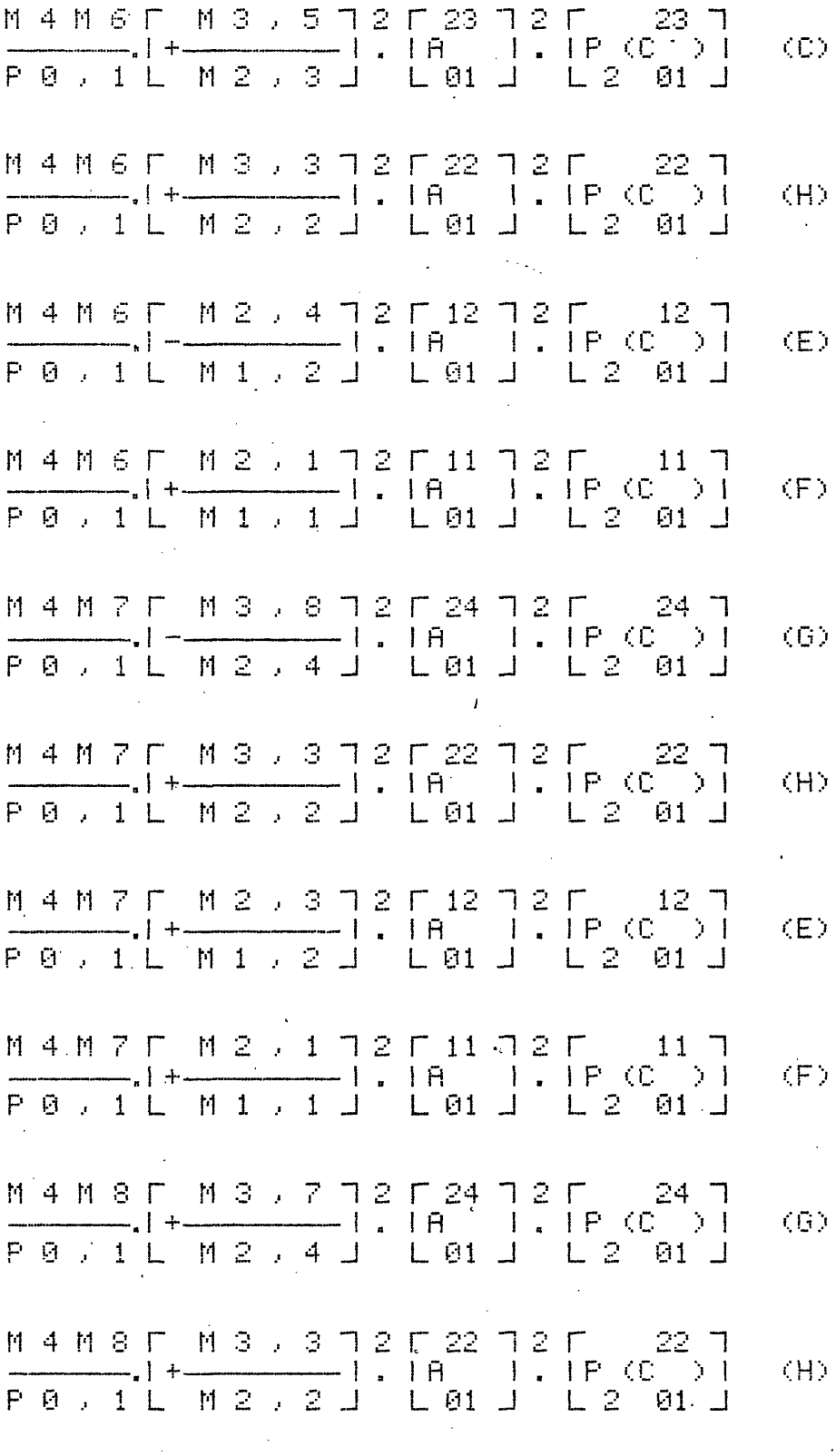
M 4 M 6 M 3 , 5 2 23 2 23
P 0 , 1 M 2 , 3 01 2 (C) 01 (C)
M 4 M 6 M 3 , 3 2 22 2 22
P 0 , 1 M 2 , 2 01 2 (C) 01 (H)
M 4 M 6 M 2 , 4 2 12 2 12
P 0 , 1 M 1 , 2 01 2 (C) 01 (E)
M 4 M 6 M 2 , 1 2 11 2 11
P 0 , 1 M 1 , 1 01 2 (C) 01 (F)
M 4 M 7 M 3 , 8 2 24 2 24
P 0 , 1 M 2 , 4 01 2 (C) 01 (G)
M 4 M 7 M 3 , 3 2 22 2 22
P 0 , 1 M 2 , 2 01 2 (C) 01 (H)
M 4 M 7 M 2 , 3 2 12 2 12
P 0 , 1 M 1 , 2 01 2 (C) 01 (E)
M 4 M 7 M 2 , 1 2 11 2 11
P 0 , 1 M 1 , 1 01 2 (C) 01 (F)
M 4 M 8 M 3 , 7 2 24 2 24
P 0 , 1 M 2 , 4 01 2 (C) 01 (G)
M 4 M 8 M 3 , 3 2 22 2 22
P 0 , 1 M 2 , 2 01 2 (C) 01 (H)

```
M 4 M 8 ┌  M 2 , 3 ┐ 2 ┌ 12 ┐ 2 ┌    12 ┐
────────.|+─────────|.  |A   |.  |P (C   )|   (E)
P 0 , 1 └  M 1 , 2 ┘   └ 01 ┘   └ 2  01 ┘

M 4 M 8 ┌  M 2 , 1 ┐ 2 ┌ 11 ┐ 2 ┌    11 ┐
────────.|+─────────|.  |A   |.  |P (C   )|   (F)
P 0 , 1 └  M 1 , 1 ┘   └ 01 ┘   └ 2  01 ┘

M 5 M 7 ┌  M 3 , 8 ┐ 2 ┌ 24 ┐ 2 ┌    24 ┐
────────;|--─────────|.  |A   |.  |P (C   )|   (I)
P 1 , 2 └  M 2 , 4 ┘   └ 12 ┘   └ 2  12 ┘

M 5 M 7 ┌  M 3 , 6 ┐ 2 ┌ 23 ┐ 2 ┌    23 ┐
────────.|--─────────|.  |A   |.  |P (C   )|   (J)
P 1 , 2 └  M 2 , 3 ┘   └ 12 ┘   └ 2  12 ┘

M 5 M 8 ┌  M 3 , 7 ┐ 2 ┌ 24 ┐ 2 ┌    24 ┐
────────.|+─────────|.  |A   |.  |P (C   )|   (I)
P 1 , 2 └  M 2 , 4 ┘   └ 12 ┘   └ 2  12 ┘

M 5 M 8 ┌  M 3 , 6 ┐ 2 ┌ 23 ┐ 2 ┌    23 ┐
────────.|--─────────|.  |A   |.  |P (C   )|   (J)
P 1 , 2 └  M 2 , 3 ┘   └ 12 ┘   └ 2  12 ┘

M 6 M 7 ┌  M 3 , 8 ┐ 2 ┌ 24 ┐ 2 ┌    24 ┐
────────.|--─────────|.  |A   |.  |P (C   )|   (I)
P 1 , 2 └  M 2 , 4 ┘   └ 12 ┘   └ 2  12 ┘

M 6 M 7 ┌  M 3 , 5 ┐ 2 ┌ 23 ┐ 2 ┌    23 ┐
────────.|+─────────|.  |A   |.  |P (C   )|   (J)
P 1 , 2 └  M 2 , 3 ┘   └ 12 ┘   └ 2  12 ┘

M 6 M 8 ┌  M 3 , 7 ┐ 2 ┌ 24 ┐ 2 ┌    24 ┐
────────.|+─────────|.  |A   |.  |P (C   )|   (I)
P 1 , 2 └  M 2 , 4 ┘   └ 12 ┘   └ 2  12 ┘

M 6 M 8 ┌  M 3 , 5 ┐ 2 ┌ 23 ┐ 2 ┌    23 ┐
────────.|+─────────|.  |A   |.  |P (C   )|   (J)
P 1 , 2 └  M 2 , 3 ┘   └ 12 ┘   └ 2  12 ┘
```

In the above each term has been marked with a letter between A and J: terms marked with the same letter are each factored by the same $(\alpha^{ij}_{k\ell})^2 \, P_2(C^{ij}_{k\ell})$ term. To simplify these terms the mass factors will be considered in the groups (A) to (J).

Group A:

$$(A) = m_1 m_3 \left(\frac{M_{34}}{M_{22}}\right)^2 + m_1 m_4 \left(\frac{M_{33}}{M_{22}}\right)^2 + m_2 m_3 \left(\frac{M_{34}}{M_{22}}\right)^2 + m_2 m_4 \left(\frac{M_{33}}{M_{22}}\right)^2$$

$$= M_{33} \, M_{34} \cdot \frac{M_{21}}{M_{22}}$$

Group B:

$$(B) = m_1 m_3 \left(\frac{M_{32}}{M_{21}}\right)^2 + m_1 m_4 \left(\frac{M_{32}}{M_{21}}\right)^2 + m_2 m_3 \left(\frac{M_{31}}{M_{21}}\right)^2 + m_2 m_4 \left(\frac{M_{31}}{M_{21}}\right)^2$$

$$= M_{31} M_{32} \cdot \frac{M_{22}}{M_{21}}$$

Group C:

$$(C) = m_1 m_5 \left(\frac{M_{36}}{M_{23}}\right)^2 + m_1 m_6 \left(\frac{M_{35}}{M_{23}}\right)^2 + m_2 m_5 \left(\frac{M_{36}}{M_{23}}\right)^2 + m_2 m_6 \left(\frac{M_{35}}{M_{23}}\right)^2$$

$$+ m_3 m_5 \left(\frac{M_{36}}{M_{23}}\right)^2 + m_3 m_6 \left(\frac{M_{35}}{M_{23}}\right)^2 + m_4 m_5 \left(\frac{M_{36}}{M_{23}}\right)^2 + m_4 m_6 \left(\frac{M_{35}}{M_{23}}\right)^2$$

$$= M_{35} \, M_{36} \cdot \frac{M_{11}}{M_{23}}$$

Group D:

$$(D) = m_1 m_5 \left(\frac{M_{32}}{M_{21}}\right)^2 + m_1 m_6 \left(\frac{M_{32}}{M_{21}}\right)^2 + m_1 m_7 \left(\frac{M_{32}}{M_{21}}\right)^2 + m_1 m_8 \left(\frac{M_{32}}{M_{21}}\right)^2$$

$$+ m_2 m_5 \left(\frac{M_{31}}{M_{21}}\right)^2 + m_2 m_6 \left(\frac{M_{31}}{M_{21}}\right)^2 + m_2 m_7 \left(\frac{M_{31}}{M_{21}}\right)^2 + m_2 m_8 \left(\frac{M_{31}}{M_{21}}\right)^2$$

$$= M_{31} \, M_{32} \cdot \frac{M_{12}}{M_{21}}$$

Group E:

$$(E) = m_1m_5\left(\frac{M_{24}}{M_{12}}\right)^2 + m_1m_6\left(\frac{M_{24}}{M_{12}}\right)^2 + m_1m_7\left(\frac{M_{23}}{M_{12}}\right)^2 + m_1m_8\left(\frac{M_{23}}{M_{12}}\right)^2$$
$$+ m_2m_5\left(\frac{M_{24}}{M_{12}}\right)^2 + m_2m_6\left(\frac{M_{24}}{M_{12}}\right)^2 + m_2m_7\left(\frac{M_{23}}{M_{12}}\right)^2 + m_2m_8\left(\frac{M_{23}}{M_{12}}\right)^2$$
$$+ m_3m_5\left(\frac{M_{24}}{M_{12}}\right)^2 + m_3m_6\left(\frac{M_{24}}{M_{12}}\right)^2 + m_3m_7\left(\frac{M_{23}}{M_{12}}\right)^2 + m_3m_8\left(\frac{M_{23}}{M_{12}}\right)^2$$
$$+ m_4m_5\left(\frac{M_{24}}{M_{12}}\right)^2 + m_4m_6\left(\frac{M_{24}}{M_{12}}\right)^2 + m_4m_7\left(\frac{M_{23}}{M_{12}}\right)^2 + m_4m_8\left(\frac{M_{23}}{M_{12}}\right)^2$$
$$= M_{23}\,M_{24}\cdot\frac{M_{11}}{M_{12}}$$

Group F:

$$(F) = m_1m_5\left(\frac{M_{22}}{M_{11}}\right)^2 + m_1m_6\left(\frac{M_{22}}{M_{11}}\right)^2 + m_1m_7\left(\frac{M_{22}}{M_{11}}\right)^2 + m_1m_8\left(\frac{M_{22}}{M_{11}}\right)^2$$
$$+ m_2m_5\left(\frac{M_{22}}{M_{11}}\right)^2 + m_2m_6\left(\frac{M_{22}}{M_{11}}\right)^2 + m_2m_7\left(\frac{M_{22}}{M_{11}}\right)^2 + m_2m_8\left(\frac{M_{22}}{M_{11}}\right)^2$$
$$+ m_3m_5\left(\frac{M_{21}}{M_{11}}\right)^2 + m_3m_6\left(\frac{M_{21}}{M_{11}}\right)^2 + m_3m_7\left(\frac{M_{21}}{M_{11}}\right)^2 + m_3m_8\left(\frac{M_{21}}{M_{11}}\right)^2$$
$$+ m_4m_5\left(\frac{M_{21}}{M_{11}}\right)^2 + m_4m_6\left(\frac{M_{21}}{M_{11}}\right)^2 + m_4m_7\left(\frac{M_{21}}{M_{11}}\right)^2 + m_4m_8\left(\frac{M_{21}}{M_{11}}\right)^2$$
$$= M_{21}\,M_{22}\cdot\frac{M_{12}}{M_{11}}$$

Group G:

$$(G) = m_1m_7\left(\frac{M_{38}}{M_{24}}\right)^2 + m_1m_8\left(\frac{M_{37}}{M_{24}}\right)^2 + m_2m_7\left(\frac{M_{38}}{M_{24}}\right)^2 + m_2m_8\left(\frac{M_{37}}{M_{24}}\right)^2$$
$$+ m_3m_7\left(\frac{M_{38}}{M_{24}}\right)^2 + m_3m_8\left(\frac{M_{37}}{M_{24}}\right)^2 + m_4m_7\left(\frac{M_{38}}{M_{24}}\right)^2 + m_4m_8\left(\frac{M_{37}}{M_{24}}\right)^2$$
$$= M_{37}\,M_{38}\cdot\frac{M_{11}}{M_{24}}$$

Group H:

$$(H) = m_3m_5\left(\frac{M_{34}}{M_{22}}\right)^2 + m_3m_6\left(\frac{M_{34}}{M_{22}}\right)^2 + m_3m_7\left(\frac{M_{34}}{M_{22}}\right)^2 + m_3m_8\left(\frac{M_{34}}{M_{22}}\right)^2$$
$$+ m_4m_5\left(\frac{M_{33}}{M_{22}}\right)^2 + m_4m_6\left(\frac{M_{33}}{M_{22}}\right)^2 + m_4m_7\left(\frac{M_{33}}{M_{22}}\right)^2 + m_4m_8\left(\frac{M_{33}}{M_{22}}\right)^2$$
$$= M_{33}\,M_{34}\cdot\frac{M_{12}}{M_{22}}$$

Group I:

$$(I) = m_5m_7\left(\frac{M_{38}}{M_{24}}\right)^2 + m_5m_8\left(\frac{M_{37}}{M_{24}}\right)^2 + m_6m_7\left(\frac{M_{38}}{M_{24}}\right)^2 + m_6m_8\left(\frac{M_{37}}{M_{24}}\right)^2$$
$$= M_{37}\,M_{38}\cdot\frac{M_{23}}{M_{24}}$$

Group J:

$$(J) = m_5m_7\left(\frac{M_{36}}{M_{23}}\right)^2 + m_5m_8\left(\frac{M_{36}}{M_{23}}\right)^2 + m_6m_7\left(\frac{M_{35}}{M_{23}}\right)^2 + m_6m_8\left(\frac{M_{35}}{M_{23}}\right)^2$$
$$= M_{35}\,M_{36}\cdot\frac{M_{24}}{M_{23}}$$

The expression for U (for the eight-body case) may then be written down, correct to the second order in the $\alpha_{k\ell}^{ij}$,

$$U = G\left[\frac{M_{31}\,M_{32}}{\rho_{21}} + \frac{M_{33}\,M_{34}}{\rho_{22}} + \frac{M_{35}\,M_{36}}{\rho_{23}} + \frac{M_{37}\,M_{38}}{\rho_{24}}\right.$$
$$+ \frac{M_{21}\,M_{22}}{\rho_{11}}\left\{1 + \frac{M_{31}\,M_{32}}{M_{21}^2}(\alpha_{11}^{21})^2\,P_2(C_{11}^{21}) + \frac{M_{33}\,M_{34}}{M_{22}^2}(\alpha_{11}^{22})^2\,P_2(C_{11}^{22})\right\}$$
$$+ \frac{M_{23}\,M_{24}}{\rho_{12}}\left\{1 + \frac{M_{35}\,M_{36}}{M_{23}^2}(\alpha_{12}^{23})^2\,P_2(C_{12}^{23}) + \frac{M_{37}\,M_{38}}{M_{24}^2}(\alpha_{12}^{24})^2\,P_2(C_{12}^{24})\right\}$$
$$+ \frac{M_{11}\,M_{12}}{\rho_{01}}\left\{1 + \frac{M_{21}\,M_{22}}{M_{11}^2}(\alpha_{01}^{11})^2\,P_2(C_{01}^{11}) + \frac{M_{23}\,M_{24}}{M_{12}^2}(\alpha_{01}^{12})^2\,P_2(C_{01}^{12})\right.$$

$$+ \frac{M_{31}\,M_{32}}{M_{11}\,M_{21}}(\alpha_{01}^{21})^2 P_2(C_{01}^{21}) + \frac{M_{33}\,M_{34}}{M_{11}\,M_{22}}(\alpha_{01}^{22})^2 P_2(C_{01}^{22})$$

$$+ \frac{M_{35}\,M_{36}}{M_{12}\,M_{23}}(\alpha_{01}^{23})^2 P_2(C_{01}^{23}) + \frac{M_{37}\,M_{38}}{M_{12}\,M_{24}}(\alpha_{01}^{24})^2 P_2(C_{01}^{24})\}\Bigg]. \qquad (3)$$

Using Equation (3) we may now form the individual equations of motion for the eight-body system remembering again that all the $\underset{\sim}{\rho}_{ij}$ are independant. From Chapter 9-Equations (9.34) and (9.35)-we have:

$$\ddot{\underset{\sim}{\rho}}_{01} = G M_{01} \frac{\partial}{\partial \underset{\sim}{\rho}_{01}}\left[\frac{1}{\rho_{01}}\{1 + \varepsilon_{01}^{11} P_2(C_{01}^{11}) + \varepsilon_{01}^{12} P_2(C_{01}^{12}) + \varepsilon_{01}^{21} P_2(C_{01}^{21}) + \varepsilon_{01}^{22} P_2(C_{01}^{22}) + \varepsilon_{01}^{23} P_2(C_{01}^{23}) + \varepsilon_{01}^{24} P_2(C_{01}^{24})\}\right] \qquad (4a)$$

$$\ddot{\underset{\sim}{\rho}}_{11} = G M_{11} \frac{\partial}{\partial \underset{\sim}{\rho}_{11}}\left[\frac{1}{\rho_{11}}\{1 + \varepsilon_{11}^{21} P_2(C_{11}^{21}) + \varepsilon_{11}^{22} P_2(C_{11}^{22}) + \varepsilon_{11}^{01} P_2(C_{01}^{11})\}\right] \qquad (4b)$$

$$\ddot{\underset{\sim}{\rho}}_{12} = G M_{12} \frac{\partial}{\partial \underset{\sim}{\rho}_{12}}\left[\frac{1}{\rho_{12}}\{1 + \varepsilon_{12}^{23} P_2(C_{12}^{23}) + \varepsilon_{12}^{24} P_2(C_{12}^{24}) + \varepsilon_{12}^{01} P_2(C_{01}^{12})\}\right] \qquad (4c)$$

$$\ddot{\underset{\sim}{\rho}}_{21} = G M_{21} \frac{\partial}{\partial \underset{\sim}{\rho}_{21}}\left[\frac{1}{\rho_{21}}\{1 + \varepsilon_{21}^{11} P_2(C_{11}^{21}) + \varepsilon_{21}^{01} P_2(C_{01}^{21})\}\right] \qquad (4d)$$

$$\ddot{\underset{\sim}{\rho}}_{22} = G M_{22} \frac{\partial}{\partial \underset{\sim}{\rho}_{22}}\left[\frac{1}{\rho_{22}}\{1 + \varepsilon_{22}^{11} P_2(C_{11}^{22}) + \varepsilon_{22}^{01} P_2(C_{01}^{22})\}\right] \qquad (4e)$$

$$\ddot{\underset{\sim}{\rho}}_{23} = G M_{23} \frac{\partial}{\partial \underset{\sim}{\rho}_{23}}\left[\frac{1}{\rho_{23}}\{1 + \varepsilon_{23}^{12} P_2(C_{12}^{23}) + \varepsilon_{23}^{01} P_2(C_{01}^{23})\}\right] \qquad (4f)$$

$$\ddot{\underset{\sim}{\rho}}_{24} = G M_{24} \frac{\partial}{\partial \underset{\sim}{\rho}_{24}}\left[\frac{1}{\rho_{24}}\{1 + \varepsilon_{24}^{12} P_2(C_{12}^{24}) + \varepsilon_{24}^{01} P_2(C_{01}^{24})\}\right] \qquad (4g)$$

where
$$\left.\begin{aligned}
\varepsilon_{01}^{11} &= \frac{M_{21}M_{22}}{M_{11}^2}\cdot(\alpha_{01}^{11})^2 \;;\; \varepsilon_{01}^{12} = \frac{M_{23}M_{24}}{M_{12}^2}\cdot(\alpha_{01}^{12})^2\\
\varepsilon_{01}^{21} &= \frac{M_{31}M_{32}}{M_{11}M_{21}}\cdot(\alpha_{01}^{21})^2 \;;\; \varepsilon_{01}^{22} = \frac{M_{33}M_{34}}{M_{11}M_{22}}\cdot(\alpha_{01}^{22})^2\\
\varepsilon_{01}^{23} &= \frac{M_{35}M_{36}}{M_{12}M_{23}}\cdot(\alpha_{01}^{23})^2 \;;\; \varepsilon_{01}^{24} = \frac{M_{37}M_{38}}{M_{12}M_{24}}\cdot(\alpha_{01}^{24})^2\\
\varepsilon_{11}^{21} &= \frac{M_{31}M_{32}}{M_{21}^2}\cdot(\alpha_{11}^{21})^2 \;;\; \varepsilon_{11}^{22} = \frac{M_{33}M_{34}}{M_{22}^2}(\alpha_{11}^{22})^2\\
\varepsilon_{11}^{01} &= \frac{M_{12}}{M_{11}}\cdot(\alpha_{01}^{11})^3 \;;\; \varepsilon_{12}^{23} = \frac{M_{35}M_{36}}{M_{23}^2}\cdot(\alpha_{12}^{23})^2\\
\varepsilon_{12}^{24} &= \frac{M_{37}M_{38}}{M_{24}^2}\cdot(\alpha_{12}^{24})^2 \;;\; \varepsilon_{12}^{01} = \frac{M_{11}}{M_{12}}\cdot(\alpha_{01}^{12})^3\\
\varepsilon_{21}^{11} &= \frac{M_{22}}{M_{21}}\cdot(\alpha_{11}^{21})^3 \;;\; \varepsilon_{21}^{01} = \frac{M_{12}}{M_{21}}\cdot(\alpha_{01}^{21})^3\\
\varepsilon_{22}^{11} &= \frac{M_{21}}{M_{22}}\cdot(\alpha_{11}^{22})^3 \;;\; \varepsilon_{22}^{01} = \frac{M_{12}}{M_{22}}(\alpha_{01}^{22})^3\\
\varepsilon_{23}^{12} &= \frac{M_{24}}{M_{23}}\cdot(\alpha_{12}^{23})^3 \;;\; \varepsilon_{23}^{01} = \frac{M_{11}}{M_{23}}\cdot(\alpha_{01}^{23})^3\\
\varepsilon_{24}^{12} &= \frac{M_{23}}{M_{24}}\cdot(\alpha_{12}^{24})^3 \;;\; \varepsilon_{24}^{01} = \frac{M_{11}}{M_{24}}\cdot(\alpha_{01}^{24})^3
\end{aligned}\right\} \quad (5)$$

If we let $i = 1,\ldots,m$; $k = 0,\ldots,m-1$; $j=1,\ldots,2^i$; $\ell = 1,\ldots,2^k$; $i > k$ then we may consider the meaning of the $\varepsilon_{k\ell}^{ij}$ individually. The ε_{01}^{11} term is a measure of the disturbance of two binaries M_{21} (i.e. m_1 and m_2) and M_{22} (i.e. m_3 and m_4) not being at their common mass-centre, M_{11}, on the orbit of M_{11} and M_{12} relative to each other. A similar meaning may be attached to ε_{01}^{12}. The disturbance of M_{31} and M_{32} not being at their common mass-centre on the orbit of M_{11} relative to M_{12} is measured by the ε_{01}^{21} terms: the ε_{01}^{22}, ε_{01}^{23}, ε_{01}^{24} terms characterise similar disturbances from the other three binaries of the eight-body system. ε_{11}^{21} and ε_{11}^{22} are measures of the disturbance on the orbit of

M_{21} relative to M_{22} by the binaries (M_{31}, M_{32}) and (M_{33}, M_{34}) respectively. In the other quadruple subsystem composed of binaries (M_{35}, M_{36}) and (M_{37}, M_{38}) the ε_{12}^{23} and ε_{12}^{24} play a similar role.

Turning our attention to the ε terms of the type $\varepsilon_{ij}^{k\ell}$ we will also consider these individually. The disturbance of the masses in the quadruple subsystem (M_{35}, M_{36}, M_{37}, M_{38}) not being at their common mass-centre on the orbit of M_{21} relative to M_{22} is characterised by ε_{11}^{01}. The term ε_{12}^{01} has similar meaning for the relative orbit of M_{23} and M_{24} which is affected by the masses $M_{31},\ldots,M_{34}$. The relative orbit of the binary subsystem (M_{31}, M_{32}) has disturbances imposed on it from other parts of the system: ε_{21}^{11} characterises the disturbance due to the masses of the binary subsystem (M_{33}, M_{34}) not being at their common mass-centre, and ε_{21}^{01} the disturbance due to the masses of the quadruple subsystem ($M_{35},\ldots,M_{38}$) not being at their common mass-centre. The other pairs of ε parameters viz. (ε_{22}^{11} , ε_{22}^{01}), (ε_{23}^{12} , ε_{23}^{01}) and (ε_{24}^{12} , ε_{24}^{01}) have similar roles to play in the(M_{33}, M_{34}), (M_{35}, M_{36}) and (M_{37}, M_{38}) binary subsystems respectively.

It may be noted in passing that the $\varepsilon_{k\ell}^{ij}$ terms are analogous to the ε^{ij} terms of the expansion of the force function in the Jacobian coordinate system where $i = 2,\ldots,n-1$; $j=3,\ldots,n$; $i < j$. Similarly the $\varepsilon_{ij}^{k\ell}$ terms are analogous to the ε_{ji} terms in the previous expansion. Further, the similarity between the sets of ε parameters in the quadruple subsystems of the eight-body system and those derived in the four-body case are obvious: the two sets of ε parameters (ε_{11}^{21}, ε_{11}^{22}, ε_{21}^{11}, ε_{22}^{11}) for the ($M_{31},\ldots,M_{34}$) subsystem and (ε_{12}^{23}, ε_{12}^{24}, ε_{23}^{12}, ε_{24}^{12}) for the ($M_{35},\ldots,M_{38}$) subsystem are directly comparable to the set (ε_{01}^{11}, ε_{01}^{12}, ε_{11}^{01}, ε_{12}^{01}) for the four-body case.

Lastly we may note that by setting various masses equal to zero or reducing particular α ratios to zero this general hierarchical eight-body system can be made to provide several different systems. For example we may recover the original Jacobian coordinate system, for the four-body case, if we let $\rho_{22} \to 0$, $\rho_{23} \to 0$, $\rho_{24} \to 0$ and $\rho_{12} \to 0$: this results in a four-body system with masses M_{31}, M_{32}, M_{22}, M_{12}.

Alternatively if we let $m_4 = m_6 = m_7 = m_8 = 0$ then a four-body system consisting of masses M_{31}, M_{32}, M_{33}, M_{35} will result. The equations of motion involving the zero magnitude masses i.e. $\ddot{\underset{\sim}{\rho}}_{22}$, $\ddot{\underset{\sim}{\rho}}_{23}$, $\ddot{\underset{\sim}{\rho}}_{24}$, $\ddot{\underset{\sim}{\rho}}_{12}$ are then neglected.

```
4 PRINT"□"
5 INPUT"■■■■■■■■";M:N=2↑M
6 OPEN5,4
7 PRINT#5," THE NUMBER OF BODIES=2↑"M:PRINT#5:PRINT#5
10 FORK=1TON
20 K1=K+1
30 IF K1>N THEN GOTO985
40 FOR L=K1TON
50 KK=K:LL=L
60 GOSUB1000
65 XX=M-A-1
69 A1=A-1
70 FORJ=0TOA1
90 IF A1<0 THEN GOTO 970
110 G0=L
120 FORII=0TOJ
130 IF II=0 THEN GOTO 150
140 G0=INT((G0+1)/2)
150 NEXTII
160 G1=INT((G0+1)/2)
170 F0=G0-(-1)↑G0
180 XA=M-J
190 YA=M-J-1
200 CA=(-1)↑G0
205 A$="+"
206 IF CA<0 THEN A$="-"
210 G2=K
220 FORII=0TOJ
230 IF II=0 THEN GOTO 250
240 G2=INT((G2+1)/2)
250 NEXTII
```

```
260 G3=INT((G2+1)/2)
270 F2=G2-(-1)↑G2
280 XB=M-J
290 YB=M-J-1
300 CB=(-1)↑G2
310 B$="+"
320 IF CB<0 THEN B$="-"
330 Q1=(M-J-1)*10+G1:Q2=(M-J-1)*10+G3
340 Q3=(M-A-1)*10+GA:Q4=(M-A-1)*10+GA
370 PRINT#5,"  M"K"M"L"┌  M"XA","F0"┐ 2 ┌"Q1"┐ 2 ┌   "Q1"┐"
380 PRINT#5,"  ──────.| "A$"──────── | . |A    | . |P (C  ) |"
390 IFQ3>10 THEN PRINT#5,"  P"XX","GA"└  M"YA","G1"┘   └"Q3"┘   └ 2 "Q3"┘"
392 IFQ3<10 THEN PRINT#5,"  P"XX","GA"└  M"YA","G1"┘   └ 01 ┘   └ 2  01 ┘"
395 PRINT#5:PRINT#5
396 PRINT#5,"  M"K"M"L"┌  M"XB","F2"┐ 2 ┌"Q2"┐ 2 ┌   "Q2"┐"
397 PRINT#5,"  ──────.| "B$"──────── | . |A    | . |P (C  ) |"
398 IFQ3>10 THEN PRINT#5,"  P"XX","GA"└  M"YB","G3"┘   └"Q3"┘   └ 2 "Q3"┘"
399 IFQ3<10 THEN PRINT#5,"  P"XX","GA"└  M"YB","G3"┘   └ 01 ┘   └ 2  01 ┘"
400 PRINT#5:PRINT#5
410 NEXTJ
970 NEXTL
980 NEXTK
985 CLOSE5
990 END
1000 GA=KK
1010 GB=LL
1020 TT=0
1030 TT=TT+1
1040 GA=INT((GA+1)/2)
1050 GB=INT((GB+1)/2)
1060 IF GA=GB THEN GOTO 1080
1070 GOTO1030
1080 A=TT-1
1090 RETURN
```

REFERENCES

REFERENCES

Allen, C.W.: 1973, Astrophysical Quantities, Athlone Press, University of London.

Arnol'd, V.I.: 1963, Usp. Mat. Nauk (Sov.Math - Usp) 18, No.6, 91; No.5,13.

Bailey, J.M.: 1971, Journal of Geophysical Research 76, 7827.

_____ 1972, Astron. J. 77, 177.

Barton, D., Willers, I.M. and Zahar, R.: 1970, in J.R. Rice (ed.) Mathematical Software, Academic Press, Lafayette, 369.

Batten, A.H.: 1973, Binary and Multiple Systems of Stars, Pergamon, Oxford.

Black, W.: 1973, Celest. Mech. 8, 357.

Bozis, G.: 1976, Astrophysics and Space Science 43, 355.

Broucke, R.: 1968, J.P.L. Tech. Rep. 32-1168.

_____ 1971, Celest. Mech. 4, 110.

Brouwer, D.: 1966, in G. Contopoulos (ed.) The Theory of Orbits in the Solar System and in Stellar Systems, Academic Press, New York.

Brouwer, D. and Clemence, G.M.: 1961, Methods of Celestial Mechanics, Academic Press, London.

Brouwer, D. and Van Woerkom, A.J.J.: 1950, Astron. Pap. Am. Ephemeris 13.

Brown, E.W.: 1896, An Introductory Treatise on the Lunar Theory, Cambridge University Press.

Cohen, C.J. and Hubbard, E.C.: 1964, Naval Weapons Laboratory Report, No.1945.

_____ 1965, Astron. J. 70, 10.

Cohen, C.J., Hubbard, E.C. and Oesterwinter, C.: 1967, Astron. J. 72, 973.

_____ 1972, Astron. Pap. Am. Ephemeris, 22.

Colombo, G. and Franklin, F.A.: 1973, in B. Tapley and V. Szebehely (eds.) Recent Advances in Dynamical Astronomy, Reidel, Dordrecht.

Danby, J.M.A.: 1962, Fundamentals of Celestial Mechanics, Macmillan, N.York.

Deprit, A. and Henrard, J.: 1965, Astron. J. 70, 271.

_____ 1967, Astron. J. 72, 158.

Deprit, A. and Zahar, R.: 1966, Z. Angew, Math. Phys. 17, 425.

Eckert, W.J., Brouwer, D. and Clemence, G.M.: 1951, Astron. Pap. Am. Ephemeris 12.

Evans, D.S.: 1968, Quarterly J. Roy. Astr. Soc. 9, 388.

Goldreich, P.: 1965, Mon. Not. Roy. Astr. Soc. 130, 159.

Golubev, V.G.: 1968, Doklady Akad. Nauk. SSSR. 180, 308.

Hagihara, Y.: 1952, Proc. Japan Acad. 28, 182.

_____ 1957, Stability in Celestial Mechanics, Pan-Pacific Press, Tokyo.

Harrington, R.S.: 1972, Celest. Mech. 6, 322.

_____ 1977, Astron. J. 82, 753.

Heintz, W.D.: 1978, Double Stars (Geophysics and Astrophysics Monographs), Reidel, Dordrecht.

Hénon, M.: 1965a, Ann. Astrophys. 28, 499.

_____ 1965b, Ann. Astrophys. 28, 992.

_____ 1966a, Bull. Astron. 1, part 1 p.57.

_____ 1966b, Bull. Astron. 1, part 2 p.49.

_____ 1969, Astron. Astrophys, 1, 223.

Henrici, P.: 1963, Discrete Variable Methods in Ordinary Differential Equations, New York. p.68.

Hill, G.: 1878, Am. J. Math. 1, 129, 245.

_____ 1905, Coll. Math. Works Vol.I, 284, Washington

Horedt, G.P., Pop, P. and Ruck, H.: 1977, Celest. Mech. 16, 209.

Huang, S-S.: 1960, P.A.S.P. 72, 106.

Hunter, R.B.: 1967, Mon. Not. Roy. Astr. Soc. 136, 245, 267.

Jacobi, C.G.J.: 1836, Compte Rendus de l'Acad. des Sciences III, 59, Paris.

Jeffrys, W.H. and Szebehely, V.G.: 1978, Comments on Astrophysics 8, 9.

Kolmogorov, A.N.: 1954, Doklady Akad. Nauk. SSSR (Sov.Phys-Doklady) 98,No.4

Kopal, Z.: 1956, Ann. Astrophys. 19, Part 6.

_____ 1959, Close Binary Systems Vol.5, p.484.

Krogh, F.T.: 1971, Algorithms for changing the stepsize used by a multi-step method. Jet Propulsion Laboratory Section 314, Tech.Memo. 275.

Kuiper, G.P.: 1956, Vistas in Astronomy, Vol.2, 1631, London.

Marchal, C. and Saari, D.: 1975, Celest. Mech. 12, 115.

Markellos, V.V.: 1974a, Celest. Mech. 9, 365.

_____ 1974b, Celest. Mech. 10, 87.

Mayers, D.F.: 1962, Methods of Runge-Kutta Type, Numerical Solution of Ordinary and Partial Differential Equations (Fox,L. (ed.)), Pergamon, pp.16-27.

Merson, C.H.: 1973, Numerical Integration of the Differential Equations of Celestial Mechanics, Royal Aircraft Establishment Report.

Message, P.J.: 1978, Proceedings of IAU Symposium No.41, Reidel, Dordrecht.

Moran, P.E.: 1972, Ph.D. Thesis, University of Glasgow.

_____ 1973, Celest. Mech. 7, 122.

Moran, P.E., Roy, A.E. and Black, W.: 1973, Celest. Mech. 8, 405.

Moser, J.: 1973, Stable and Random Motions in Dynamical Systems, Princeton University Press, Princeton, N.J.

Myachin, B.F. and Sizova, O.A.: 1970, Bull. Inst. Theo. Astr. Leningrad, 12, 138.

Nacozy, P.E.: 1976, Astron. J. 81, 787.

_____ 1977, Celest. Mech. 16, 77.

Newcomb, S.: 1876, Smithsonian Contribution to Knowledge 21.

Ovenden, M.W. and Roy, A.E.: 1960, Mon. Not. Roy. Astr. Soc. 123, 1.

Poincaré, H.: 1895, Les MéthodesNouvelles de la Méchanique Céleste, Gauthier-Villars, Paris.

Plummer, H.C.: 1918, An Introductory Treatise on Dynamical Astronomy, Cambridge University Press, London.

Rabe, E.: 1961, Astron. J. 66, 500.
_____ 1962, Astron. J. 67, 382.
Roy, A.E.: 1978, Orbital Motion, Adam-Hilger, Bristol.
_____ 1979, in V.G. Szebehely (ed.), Instabilities in Dynamical Systems, Reidel, Dordrecht.
Roy, A.E., Moran, P.E. and Black, W.: 1972, Celest. Mech. 6, 468.
Roy, A.E. and Ovenden, M.W.: 1954, Mon. Not. Roy. Astr. Soc. 114, 232.
_____ 1955, Mon. Not. Roy. Astr. Soc. 115, 296.

Siegel, C.L. and Moser, J.K.: 1971, Lectures on Celestial Mechanics, Springer-Verlag, Berlin.
Sinton, W.M.:1972, Sky and Telescope, 44, 304.
Smale, S.: 1970, Invent. Math. 11, 45.
Smart, W.M.: 1953, Celestial Mechanics, Longmans, London.
Strohmeier, W.: 1972, Variable Stars, International Series of Monographs on Natural Philosophy, Pergamon, Oxford.
Szebehely, V.G.: 1967, Theory of Orbits, Academic Press, New York.
_____ 1971, Celest. Mech. 4, 116.
_____ 1977, Celest. Mech. 15, 107.
_____ 1978, Celest. Mech. 18, 383.
Szebehely, V.G. and Evans, R.T.: 1980, Celest. Mech. 21, 259.
Szebehely, V.G. and McKenzie, R.: 1977a, Astron. J. 82, 79.
_____ 1977b, Astron. J. 82, 303.
Szebehely, V.G. and Zare, K.: 1977, Astron. Astrophys. 58, 145.

Tisserand, F.: 1889, Traité de la Méchanique Céleste, Gauthier-Villars, Paris.

Whittaker, E.: 1904, Analytical Dynamics, Cambridge University Press, London.
Wiesel, W.: 1980, Celest. Mech. 21, 265.
Williams, B.G.: 1979, Celest. Mech. 19, 357.
Williams, J.G. and Benson, G.S.: 1971, Astron. J. 76, 167.

Zagouras, C. and Markellos, V.V.: 1977, Astron. Astrophys. 59, 79.
Zare, K.: 1976, Celest. Mech. 14, 73.
_____ 1977, Celest. Mech. 16, 35.